UNIVERSIDAD COMPLUTENSE DE MADRID
FACULTAD DE VETERINARIA

TESIS DOCTORAL

Modelos in vitro de la infección por "Besnoitia besnoiti" y su empleo en estudios de patogenia molecular y cribado de fármacos

MEMORIA PARA OPTAR AL GRADO DE DOCTOR

PRESENTADA POR

Alejandro Jiménez Meléndez

Directora

Gema Álvarez García

Madrid

FACULTAD DE VETERINARIA

Departamento de Sanidad Animal

Modelos *in vitro* de la infección por *Besnoitia besnoiti* y su empleo en estudios de patogenia molecular y cribado de fármacos

TESIS DOCTORAL

D. Alejandro Jiménez Meléndez

Madrid, 2019

UNIVERSIDAD
COMPLUTENSE
MADRID

FACULTY OF VETERINARY SCIENCES

Animal Health Department

In vitro models of *Besnoitia besnoiti* infection and their application in molecular pathogenesis and drug screening studies

DOCTORAL THESIS

Mr. Alejandro Jiménez Meléndez

Madrid, 2019

DECLARACIÓN DE AUTORÍA Y ORIGINALIDAD DE LA TESIS PRESENTADA PARA OBTENER EL TÍTULO DE DOCTOR

D. Alejandro Jiménez Meléndez, estudiante en el Programa de Doctorado de Veterinaria, de la Facultad de Veterinaria de la Universidad Complutense de Madrid, como autor de la tesis presentada para la obtención del título de Doctor y titulada: "Modelos *in vitro* de la infección por *Besnoitia besnoiti* y su empleo en estudios de patogenia molecular y cribado de fármacos"

Y dirigida por: Dña. Gema Álvarez García

DECLARO QUE:

La tesis es una obra original que no infringe los derechos de propiedad intelectual ni los derechos de propiedad industrial u otros, de acuerdo con el ordenamiento jurídico vigente, en particular, la Ley de Propiedad Intelectual (R. D. legislativo 1/1996, de 12 de abril, por el que se aprueba el texto refundido de la Ley de Propiedad Intelectual, modificado por la Ley 2/2019, de 1 de marzo, regularizando, aclarando y armonizando las disposiciones legales vigentes sobre la materia), en particular, las disposiciones referidas al derecho de cita.

Del mismo modo, asumo frente a la Universidad cualquier responsabilidad que pudiera derivarse de la autoría o falta de originalidad del contenido de la tesis presentada de conformidad con el ordenamiento jurídico vigente.

En Madrid, a 4 de julio de 2019

Fdo.: Alejandro Jiménez Meléndez

Memoria presentada por **D. Alejandro Jiménez Meléndez** *para optar al grado de Doctor por la Universidad Complutense de Madrid.*

La presente tesis doctoral ha sido financiada por los proyectos AGL2013-44694-R y AGL2016-75202R del Ministerio de Economía y Competitividad, por el proyecto S2013/ABI2906 de la Comunidad de Madrid y por el Programa Nacional de Formación de Profesorado Universitario (FPU) del Ministerio de Educación, Cultura y Deporte (referencia FPU13-05481).

Dña. Gema Álvarez-García, Doctora en Veterinaria y Profesora Titular de Universidad adscrita al Departamento de Sanidad Animal de la Facultad de Veterinaria de la Universidad Complutense de Madrid,

CERTIFICA:

1) Que la tesis doctoral titulada **"Modelos *in vitro* de la infección por *B. besnoiti* y su empleo en estudios de patogenia molecular y cribado de fármacos"** presentada por el Licenciado en Veterinaria **D. Alejandro Jiménez Meléndez** para optar al grado de Doctor por la Universidad Complutense de Madrid ha sido realizada en las dependencias del **Departamento de Sanidad Animal** de la Facultad de Veterinaria de la Universidad Complutense de Madrid bajo su supervisión.

2) Que la presente tesis doctoral cumple con todas las condiciones exigidas para optar al grado de **Doctor por la Universidad Complutense de Madrid con Mención Internacional**.

De acuerdo con la normativa vigente, y como directora de la mencionada tesis doctoral, firmo el presente certificado por el que se autoriza su presentación.

En Madrid, a

Fdo. Dra. Gema Álvarez García

DOCTORADO CON MENCIÓN INTERNACIONAL

La presente tesis doctoral cumple con los requisitos exigidos por la Universidad Complutense de Madrid para obtener la mención de Doctor internacional:

1) Realización de una estancia mínima de tres meses en una institución de enseñanza superior o centro de investigación fuera de España:
   - Centro receptor: Instituto de Parasitología, Facultad de Veterinaria, UZH (Zürich, Switzerland)
   - Investigador principal: Dr. Adrian B. Hehl
   - Duración de la estancia: 3 meses (15/09/2017-14/12/2017).

2) Los apartados de resumen, justificación y objetivos, resultados, discusión y conclusiones de la tesis doctoral han sido redactados en una de las lenguas habituales para la comunicación científica en su campo de conocimiento, distinta a cualquiera de las lenguas oficiales en España (inglés).

3) La tesis doctoral ha sido evaluada por dos expertos pertenecientes a alguna institución de educación superior o instituto de investigación no español.

4) El tribunal evaluador de la tesis doctoral está compuesto por, al menos, un experto perteneciente a alguna institución de educación superior o centro de investigación no español.

AGRADECIMIENTOS

"*If a solution fails to appear ... and yet we feel success is just around the corner, try resting for a while. Like the early morning frost, this intellectual refreshment withers the parasitic and nasty vegetation that smothers the good seed. Bursting forth at last is the flower of truth*."
— Santiago Ramón y Cajal, Advice for a Young Investigator

Y por fin ha llegado este momento, en el que después de una intensa recta final, me encuentro escribiendo los agradecimientos de la tesis. Sé que estas páginas van a ser las más leídas de la misma y por ello, quiero estar a la altura. Siento que cada una de las decisiones que he tomado en mi vida han ido encaminadas a este momento, por lo que quiero agradecer a todos aquellos que, de una forma u otra, os hayáis cruzado en mi camino.

En primer lugar, quiero agradecer a mi directora y jefa, **Gema**. Porque esto no habría sido posible sin tu ayuda, gracias por estar al pie del cañón. Por estimularme y conseguir que me forme como proyecto de investigador y como persona, por hacerme ver cada nuevo reto con ilusión. Espero que estés tan orgullosa de este momento como lo estoy yo. Gracias por darme la oportunidad de poder conocer el mundo de la investigación y la curiosidad por descifrar alguno de los misterios de nuestra querida *Besnoitia*. También quiero agradecer al resto de la "cúpula" **Luis**, **Ignacio**, **Mercedes** y **Esther**. **Luis**, gracias por ser un ejemplo de investigador, de dedicación absoluta a una profesión tan vocacional y enriquecedora, por permitirme ser parte de este gran grupo de investigación que es SALUVET.

A los miembros de la "*Old generation*" **Iván**, **David**, **Paula** y **Dani**. Gracias por todo desde mis primeros momentos en el laboratorio, por compartir vuestra experiencia y conocimientos. **Dani**, gracias por ser un buen amigo, por las teorías de *GoT* (cualquier cosa es mejor que la 8ª temporada) y por ser mi mentor en el mundo de la besnoitia, las reglas de tres y gran parte de todo lo que aprendí en el laboratorio. **Iván**, te deseo lo mejor en esta nueva etapa saluvetiana 2.0, la vuelta a casa no puede ir mal. A mis compañeros de la "*New old generation*" y de la "*New generation*", a la base de la pirámide saluvetiana. Porque sin vosotros nada funcionaría, porque sois los responsables de que todos y cada uno de los experimentos que se plantean salga adelante y porque sin vosotros no habría llegado hasta aquí. A **Laura**, porque tras tantos años juntos y tantas experiencias vividas no sé que va a ser de mí ahora que nuestros caminos parece que se separan. Gracias por todo, sabes que aquí tienes un amigo y que los Jiménez llegaremos donde nos propongamos, ni más ni menos. Esto no es un final, vendrán nuevas temporadas de nuestras aventuras (desventuras espero que no). A **Marta**, muchas gracias por estar ahí, por capear los malos momentos con una sonrisa y por todo tu apoyo. A ver dónde nos lleva el camino ahora. A **Rober**, quién nos iba a decir hace tantos años cuando coincidimos en una clínica de pequeños animales que íbamos a acabar haciendo una tesis en el mismo grupo, porque teníamos que demostrar que los abulenses podemos llegar lejos. A **Laura Rico**, por ser una persona excelente, por los buenos ratos que hemos pasado en el laboratorio y porque me alegro de que consiguiese inculcarte algo de la pasión por la ciencia y el trabajo bien hecho. Porque tú lo vales (aunque Besnoitia se perdió una gran investigadora de momento).

A **Merche**, por las risas en momentos que hacen falta, porque sabes que siempre que lo necesites nos podemos tomar una doble (de las que te dejan doblada) y tirar para delante. A **María,** por haber traído una brisa de aire fresco al laboratorio, por tu buen carácter y tu disciplina. Porque ha sido un placer poder trabajar contigo, te deseo lo mejor. A **Alicia**, aunque hayamos coincidido menos sé que sacarás el trabajo adelante sin problema con tu gran paciencia, ¡mucho ánimo con los cultivos! También quería agradecer a los "*postdocs*", por toda su ayuda y aportar al grupo sus conocimientos y perspectivas vitales. A **Pili**, gracias por ayudarme en tantos ratos delante del equipo de PCR cuantitativa, por nuestras charlas sobre "*Walking dead* o *GoT*" y por demostrar que quien la sigue la consigue, sólo hay que tener paciencia y llegará. A **Rafa**, por ser un ejemplo de las cosas bien hechas, de tesón y de esfuerzo, por nuestras charlas nocturnas "arreglando el mundo". Te deseo lo mejor *bro*, no conozco a nadie que se lo merezca más. A **David**, por ser un ejemplo de tener las ideas claras, de que compaginar una vida personal llena de buenos momentos y una vida profesional es posible. Me alegro de haber podido coincidir contigo. Y a algunos que ya no están en SALUVET, como **Dani Rozas** (Dani Grande), por los buenos momentos y demostrar que tras un bache siempre hay que proseguir el camino.

A los miembros de *Saluvet-Innova*, con los que he compartido tantos momentos. **Javier Regidor**, gracias por compartir todos tus conocimientos, tu experiencia y tu saber hacer. A **Ángela**, porque eres una persona de las que quedan pocas, por tus consejos y los buenos momentos. A **Patri**, "la vasca", aunque más que ocho apellidos vascos lo que tienes es un corazón inmenso. Gracias por tu bondad y tu ayuda (y los viajes a Tineo, tu rodilla puede atestiguarlo). A las nuevas incorporaciones **Sheila** y **Sofía**, porque habéis caído en buen sitio, os deseo lo mejor. A **Raquel**, aunque hayas cambiado de destino gracias por todos los buenos momentos, por la expectación ante cada capítulo de GoT.

A **Lola**, por compartir tantas horas a mi lado, por preocuparse de la salud y el bienestar de la gente del 9 siendo como una madre (aunque no estemos de acuerdo en la temperatura del aire acondicionado, eso no tiene solución) y por animar cada mañana al entrar en el lab 9. A **Vane**, por enseñarme en mis primeros momentos en el laboratorio y por las risas que nos hemos echado (aunque sabes que tú y yo no nos podemos juntar, hablemos de lo que hablemos nos pillan jaja). También quería agradecer a las otras "secres" que he conocido durante esta tesis, **Ofe** y **Joaqui**, porque sin la parte administrativa un grupo tampoco puede funcionar.
A la otra "rama", los integrantes del mundo porcino. Muchas gracias **Cinta**, **Javier Lobo**, **Isabel** y **Chema**, por estar ahí y compartir vuestra inmensa experiencia. **Chema**, gracias por todas las charlas de cómo funciona el mundo de la investigación y cómo crecer profesionalmente.
A **Gustavo**, **Javier Carrión**, **Abel** y **Alicia**. Por echar un cable siempre que era necesario, por el buen rollo y toda la ayuda.

A todos los investigadores visitantes que he tenido la suerte de conocer en los más de cinco años que ha durado esta tesis. A los brasileños **Wagnner**, **Rinaldo**, **Larissa**, **Muller** y **Pomy**. Muchas gracias por todo, por llenar el laboratorio de alegría y sonrisas en cada visita. **Muller**, amigo. *Muito obrigado*. Por ser como un hermano al otro lado del charco, por los momentos que pasamos en el laboratorio y

fuera de él. Porque siempre nos quedará Río. **Pomy**, gracias por ser como eres, no cambies nunca. La chinegra más auténtica (y creo que la única) que he conocido en mi vida. Nunca olvidaré las lecciones de portuñol (camundongo, gambá y zarigüeya dieron para mucho). Gracias por ser tan buena anfitriona, por la feijoada y los sitios magníficos que conocimos. A los argentinos, **Lucy**, **Nacho, Marcelo** y **Yani**. Gracias por todos los buenos momentos. **Yani**, gracias por tu optimismo, tu fuerza. Y porque siempre que suene la bicicleta me acordaré de ti. También a vosotras **Alexandra**, **Lucy**, **Luca** y Cristina. Estoy convencido de que una de las mejores experiencias que brinda realizar la tesis es poder conocer gente de sitios tan distintos y que en tan corto plazo de tiempo se conviertan en gente importante en tu vida.

*I am deeply in debt to **Chandra** & **Adrian**. Thank you Chandra, because you made my stay to be fruitful and full of amazing scientific experiences. Also, to the rest of the members in Hehl´s group Rui, Lenka, Rahel, Florian and Carmen, for all the wonderful moments both inside the lab and outside, allowing me to discover the wonders of Switzerland. I would also like to acknowledge all the international collaborators that made possible all the research works included in this Doctoral thesis. Many thanks to you Andrew, Wes and Kayode, and all the persons involved in these works.*

A mi familia, a mis padres **Alejandro** y **Beatriz**. Gracias por haber posibilitado que llegue hasta aquí, porque este camino comenzó en casa. Espero que os sintáis orgullosos de mí. Porque la familia no se elige, pero no cambiaría nada. A mi hermano **Javier,** a mis tíos Ramón, Sonia y Piilar. A mis abuelos **Alejandro**, **Pilar**, **Ignacia** y **Carmelo.** Por estimularme la vocación de veterinario desde pequeño, cuando hacía la trashumancia desde el salón a la cocina.
A mis amigos **Arturo**, **Diego** y **Sergio**, por aguantar mis "chapas" de la tesis sin pestañear. Por todos los momentos que nos quedan juntos. También a mis amigos "de toda la vida", **Alba**, **Elena**, **Lidia** y **Raúl**. Porque aunque cada uno estemos en un sitio (parece que os ha gustado más Barcelona), cuando nos encontramos parece que no ha pasado el tiempo.
A Kris, por todo. Por seguir a mi lado y ser la mejor compañera en el viaje que emprendimos hace ya algún tiempo (y quién sabe dónde nos llevará). Por conseguir sacar lo mejor de mí. Porque juntos podemos con todo. Por seguir sumando. *"If you look into the distance, there's a house upon the hill. Guiding like a lighthouse to a place where you'll be safe to feel at grace 'cause we've all made mistakes. If you've lost your way I will leave the light on" Я тебя люблю*

A todos, mis más sinceras GRACIAS

The Road goes ever on and on
Down from the door where it began.
Now far ahead the Road has gone,
And I must follow, if I can,
Pursuing it with eager feet,
Until it joins some larger way
Where many paths and errands meet.
And whither then? I cannot say"

— J.R.R. Tolkien, The Fellowship of the Ring

ÍNDICE/TABLE OF CONTENTS

LISTA DE TABLAS/ LIST OF TABLES

INTRODUCCIÓN/INTRODUCTION

OBJETIVO 1/OBJECTIVE 1

OBJETIVO 2/OBJECTIVE 2

SUBOBJETIVO 2.2/SUBOBJECTIVE 2.2

SUBOBJETIVO 2.3/SUBOBJECTIVE 2.3

LISTA DE FIGURAS/LIST OF FIGURES

INTRODUCCIÓN/INTRODUCTION

OBJETIVO 1/OBJECTIVE 1

OBJETIVO 2/OBJECTIVE 2

SUBOBJECTIVO 2.1/SUBOBJECTIVE 2.1

SUBOBJETIVO 2.2/SUBOBJECTIVE 2.2

SUBOBJETIVO 2.3/SUBOBJECTIVE 2.3

LISTA DE ABREVIATURAS

SDS 1D/2 D	Electroforesis en 1 o 2 dimensiones
ABA	Ácido abscísico
ADAMTS1	Disintegrina y metaloproteasa con motivos de tromboespondina
ADN	Ácido desoxirribonucleico
ATP	Adenosín trifosfato
BEK	*Bovine Embryo Kidney*
BKIs	Fármacos inhibidores de las proteínas inhibidoras de calcio
BUVEC	*Bovine umbilical vein endothelial cells*
BVDV	Virus de la diarrea vírica bovina
Ca	Calcio
CCL2	Proteína quimiotáctica de monocitos 1
CD31	*Cluster of differentiation* 31
CD34	*Cluster of differentiation* 34
CD44	*Cluster of differentiation* 44
CDPK	Proteína quinasa dependiente de calcio
CI50	Concentración inhibitoria 50
CI99	Concentración inhibitoria 99
CRFK	*Crandal Ree Feline Kidney*
CRISPR	*Clustered Regularly Interspaced Polimophric Regions*
DHFR	Dihidrofolato reductasa
DHFS	Dihidrofolato sintasa
DIGE	*Differential in gel electrophoresis*
DMSO	Dimetil sulfóxido
EC	Célula endothelial
ELISA	*Enzyme Linked Immunosorbent Assay*
ENO	Enolasa
GAP	*Gliding associated protein*
GAPDH	Gliceraldehiído dehidrogenasa
Gly	Glicina
GRA	Proteínas de gránulos densos
HD	Hospedador definitivo
HFF	*Human Foreskin Fibroblasts*
HI	Hospedador intermediario
Hpi	Horas post-infección
HSP	*Heat shock protein*
ICAM1	Molécula de adhesión intercelular 1
ICW	*Inner cyst wall*
IFI	Inmunofluorescencia indirecta
IFNγ	Interferón γ
IL1A	Interleuquina 1A
IL6	Interleuquina 6
IMC	*Inner membrane complex*
IP3	Inositol trifosfato
IRG	GTPasas relacionadas con interferón
i-TRAQ	*Isobaric tag for relative and absolute quantitation*
ITS-1	*Internal trascriber spacer* 1
K	Potasio
KO	*Knock out*
LC	Cromatografía líquida
LDH	Lactato dehidrogenasa
MABs	Anticuerpos monoclonales
MAT	Aglutinación en placa

MDBK	Madin Darby Bovine Kidney
MetOH	Metanol
Mg	Magnesio
MIC	Proteína de micronemas
MLC	*Myosin light chain*
MS/MS	Espectrometría de masas
NaOH	Hidróxido sódico
NFkB	Factor de transcripción nuclear kB
OCW	*Outer cyst wall*
p.ej	Por ejemplo
PAC	Política agraria común
PCR	Reacción en cadena de la polimerasa
PDI	Proteína disulfuro isomarasa
PIP2	Fosfatidil inositol bifosfato
PLP1	*Perforin-like protein* 1
qPCR	PCR cuantitativa
RAPD	Amplificación aleatoria de ADN polimórfico
RON	*Rhoptry neck protein*
ROP	*Rhoptry protein*
SELE	E selectina
SRS	*SAG-1 related surface antigen*
TEM	Microscopía electrónica de transmisión
TGFβ	*Transforming growth factor* β
TNFa	Factor de necrosis tumoral a
URSS	Unión de Repúblicas Socialistas Soviéticas
VCAM1	Molécula de adhesión vascular 1
Vs	*versus*
WB	Western Blot
WGS	*Whole genome sequence*
XTT	Kit de proliferación celular basado en el cloruro de tetrazoliio

CAPÍTULO I:

RESUMEN/ABSTRACT

Resumen:

La besnoitiosis bovina es una enfermedad de curso crónico y debilitante ocasionada por el protozoo apicomplejo formador de quistes *Besnoitia besnoiti*. Esta enfermedad ocasiona considerables pérdidas económicas, fundamentalmente en las explotaciones de vaca nodriza. En la actualidad, dicha enfermedad se considera reemergente en Europa debido a su notable expansión geográfica desde zonas donde la enfermedad ha sido tradicionalmente endémica (como los Pirineos y la región del Alentejo en Portugal), y a un aumento de su prevalencia. Uno de los factores que ha contribuido en gran medida a esta diseminación es la ausencia de tratamientos o vacunas eficaces. Con estos antecedentes, el desarrollo de modelos *in vitro* es clave para estudiar la interacción patógeno-hospedador y para identificar posibles candidatos terapéuticos y vacunales. Por tanto, el objetivo de esta tesis doctoral fue el desarrollo y estandarización de nuevos modelos *in vitro* de infección por *B. besnoiti* y su empleo en estudios de patogenia molecular y cribado de fármacos.

En el Objetivo 1 de la presente tesis doctoral se han desarrollado nuevos modelos *in vitro* utilizando cultivos primarios procedentes del hospedador intermediario natural (el ganado bovino). En concreto, se han aislado células endoteliales (CE) y fibroblastos de aorta bovina, que son células diana del parásito durante la fase aguda y crónica de la enfermedad, respectivamente. Un hecho a destacar es que se analizó exhaustivamente el estado sanitario de los animales donantes y, a continuación, se monitorizaron los cultivos obtenidos para verificar la ausencia de patógenos del ganado bovino y contaminantes frecuentes de los cultivos celulares, como *Mycoplasma* spp. y el virus de la diarrea vírica bovina (VDVB), que pueden alterar la célula hospedadora. Posteriormente, mediante citometría de flujo, se estudió el perfil de expresión de una serie de marcadores de superficie (CD31, CD34, CD44) e intracelulares (citoqueratina y vimentina) para caracterizar los cultivos primarios aislados. Los resultados de morfología y citometría de flujo confirmaron el tipo celular. El marcador de superficie CD31, típico de CE, fue el que mayores diferencias de marcaje mostró entre las CE y los fibroblastos. Por el contrario, únicamente se detectó el marcador CD34 en las CE de pase bajo, y tanto en los fibroblastos como en las células endoteliales se detectaron los marcadores CD44, vimentina y citoqueratina. Posteriormente, se estudió el ciclo lítico de los taquizoítos del aislado de referencia Bb-Spain1 de *B. besnoiti* mediante el estudio de su capacidad para invadir y proliferar en ambos cultivos primarios. Los resultados mostraron que el ciclo lítico en CE y fibroblastos es muy similar al previamente descrito en las células epiteliales de mono Marc-145, con una baja tasa de invasión (en torno al 4%) hasta las 24 horas post-infección (hpi) y un crecimiento exponencial hasta las 72 hpi. Además, por primera vez, se ha estudiado la interacción de un protozoo Toxoplasmatinae con una cepa no citopática del VDVB en las CE, comprobándose que la invasión temprana de las células hospedadoras por parte del parásito se ve favorecida por VDBV.

Posteriormente, en el objetivo 2, se han empleado los modelos *in vitro* en estudios de patogenia molecular y cribado de fármacos.

En primer lugar, en el subobjetivo 2.1. se ha empleado el modelo *in vitro* puesto a punto en el objetivo 1 para estudiar la interacción parásito-célula hospedadora en CE de aorta bovinas (BAEC) a dos tiempos post-infección (pi): a las 12 hpi, cuando los taquizoítos han invadido las células hospedadoras, y a las 32 hpi, cuando los taquizoítos han realizado al menos dos rondas de replicación. Se emplearon células no infectadas como testigo negativo. Los análisis se realizaron con cuatro réplicas biológicas y en cada réplica se recogieron muestras para una validación adicional mediante PCR cuantitativa a tiempo real (qPCR). Se encontró un mayor número de genes diferencialmente expresados (GDE)

(*n*=446) cuando se compararon las BAEC infectadas en los dos tiempos pi estudiados. De ellos, 249 GDE se encontraron sobreexpresados a las 32 hpi. Los resultados han demostrado que la infección por *B. besnoiti* produce una activación de las BAEC, con la expresión de diversas citoquinas (IL6, IL1A), quimioquinas (CCL2, CCL24, CXCL1, CXCL2, CXCL3) y moléculas de adhesión para leucocitos (SELE, ICAM-1, VCAM-1), entre otras, fundamentalmente a las 12 hpi, mientras que a ambos tiempos pi se observó la expresión de genes implicados en angiogénesis (p. ej. diversos factores de crecimiento e integrinas) y la organización de la matriz extracelular (p. ej. metaloproteasas de matriz y ADAMTS), todo ello asociado al daño endotelial. Las principales rutas de señalización moduladas por el parásito fueron la ruta del factor de transcripción nuclear NF-κB, así como la ruta proinflamatoria del TNF-a. Dichos factores coordinarían la expresión de diversas moléculas efectoras responsables de un fenotipo proinflamatorio, de coagulación y pro-fibrótico en las células endoteliales, siendo responsables del reclutamiento de macrófagos y otros leucocitos que desencadenarían un proceso de inflamación y fibrosis, compatible con las lesiones histológicas descritas *in vivo* en los casos de besnoitiosis bovina, en las que se ha descrito una coexistencia de lesiones de fase aguda y crónica. Asimismo, se detectó la sobreexpresión de genes implicados en fases tempranas (p. ej. factores de crecimiento y metaloproteinasas de la matriz extracelular) y tardías (integrinas y vasohibina) de la angiogénesis. Además, se seleccionaron moléculas sobreexpresadas que juegan un papel clave en las rutas previamente señaladas (*n*=16) (p. ej. ICAM1, VCAM1, SELE, CCL2, IL6, ADAMTSL1) para la validación del transcriptoma mediante qPCR, confirmándose los resultados obtenidos. Adicionalmente, se estudió el transcriptoma de los taquizoítos de *B. besnoiti* a ambos tiempos pi, identificándose por primera vez numerosos genes ortólogos de *Neospora caninum* y *Toxoplasma gondii*, protozoos de la subfamilia Toxoplasmatinae al igual que *B. besnoiti*, que codifican proteínas implicadas en su ciclo lítico: proteínas de gránulos densos (GRA), proteínas de roptrias (RON y ROP), proteínas de micronemas (MIC), y de superficie (SRS), entre otras. En particular, destaca la sobreexpresión de genes que codifican proteínas de roptrias (ROP5B, ROP17, ROP40), micronemas (MIC2, MIC11), glideosoma (GAP80) y de superficie (SRS22A) a medida que progresa el ciclo lítico. Asimismo, se validó la expresión de un panel de genes (*n*=10) mediante qPCR corroborándose los resultados del transcriptoma. Por tanto, este estudio ha aportado información acerca de la interacción de los taquizoítos de *B. besnoiti* con sus células diana, mostrando la progresión de una activación endotelial con un fenotipo proinflamatorio y profibrótico tras la invasión y proliferación de los mismos, que se correlaciona con el daño vascular y las lesiones descritas *in vivo*.

No obstante, se optó por el empleo del modelo previamente puesto a punto por el grupo investigador en células epiteliales de riñón de mono Marc-145 para la evaluación de la seguridad y eficacia de diferentes fármacos (subobjetivos 2.2. y 2.3.), ya que: i) el ciclo lítico del aislado de referencia Bb-Spain1 es similar en los diferentes modelos *in vitro*; ii) existen dificultades inherentes a trabajar con los cultivos primarios y iii) puede existir variabilidad de los cultivos primarios en función del animal donador.

En el caso de las enfermedades ocasionadas por protozoos apicomplejos, así como en otras enfermedades comúnmente denominadas "enfermedades desatendidas", el reposicionamiento farmacológico es una aproximación muy empleada, ya que permite disponer de fármacos potencialmente eficaces que ya están comercializados. Por ello, en el subobjetivo 2.2. se estudió la seguridad y eficacia frente a la infección *in vitro* por taquizoítos de *B. besnoiti* de un panel de fármacos comercializados para su empleo en la especie bovina (decoquinato, diclazurilo, toltrazurilo, imidocarb, sulfadiazina y trimetoprim, sólo o en combinación con sulfadiazina). Los fármacos se administraron bien antes de la infección de las células hospedadoras (a las 0 hpi) o a las 6 hpi (cuando al menos el 50% de los taquizoítos ya han invadido la célula hospedadora). En primer lugar, se estudió el

posible efecto citotóxico de los fármacos mediante una prueba de viabilidad celular XTT. Posteriormente, se realizaron ensayos iniciales para optimizar el cribado farmacológico, que se llevó a cabo mediante la realización de inmunofluorescencia directa y el recuento posterior de eventos de invasión y proliferación (vacuolas parasitóforas o placas de lisis). Los compuestos que mostraron los mejores resultados (decoquinato y diclazurilo) fueron seleccionados para la determinación de sus concentraciones inhibitorias 50 (CI50) y 99 (CI99). Además, se estudió el efecto de los fármacos en la ultraestructura de los taquizoítos mediante microscopía electrónica de transmisión (TEM), así como el efecto post-tratamiento a largo plazo. Los resultados de citotoxicidad confirmaron que ninguno de los compuestos era citotóxico en el sistema *in vitro* empleado a las concentraciones utilizadas en el cribado. El decoquinato y el diclazurilo mostraron valores de inhibición de la invasión del parásito del 90 y 83% a las 0 hpi, y de 73 y 72% a las 6 hpi, respectivamente. El resto de los fármacos analizados mostraron una eficacia notablemente inferior y fueron descartados. Las CI99 obtenidas fueron de 100 nM para el decoquinato y 29,9 µM para el diclazurilo. Los resultados del TEM mostraron que el sitio de acción del decoquinato se encontraba en la mitocondria de los parásitos, mientras que el diclazurilo interfería con la citoquinesis de los zoítos hijos. Por tanto, el presente estudio ha demostrado la eficacia de ambos compuestos frente a la invasión y proliferación de *B. besnoiti in vitro*, si bien son necesarios futuros estudios en la especie de destino para valorar su seguridad y eficacia. Para el decoquinato, se han descrito concentraciones plasmáticas máximas superiores a la CI99 obtenida *in vitro*, mientras que en el caso del diclazurilo son necesarios estudios adicionales farmacocinéticos para mejorar su absorción y biodisponibilidad, ya que actualmente alcanza concentraciones plasmáticas máximas inferiores a la CI99 obtenida *in vitro*.

Por otra parte, en la búsqueda de nuevos candidatos terapéuticos, las proteínas quinasas dependientes de calcio (CDPKs) son dianas terapéuticas prometedoras en otros protozoos apicomplejos como *N. caninum*, *T. gondii*, *Plasmodium* spp. y *Cryptosporidium parvum*, debido a una serie de diferencias estructurales que han permitido el diseño selectivo de una clase de inhibidores conocidos como "*bumped kinase inhibitors*". Por ello, en el subobjetivo 2.3., se ha identificado y clonado el gen que codifica para la enzima *Bb*CDPK1 y se ha valorado la actividad enzimática de la proteína recombinante –rBbCDPK1- con un panel de nueve BKIs. Asimismo, se ha determinado la seguridad y eficacia de dichos compuestos frente a la infección por los taquizoítos de *B. besnoiti* en células Marc-145, tal y como se ha mencionado en el estudio anterior. Tras comprobar la seguridad de los nueve fármacos se realizó el cribado farmacológico empleando los fármacos a una concentración de 5 µM a los dos tiempos pi (0 y 6 hpi). Ocho de los compuestos estudiados mostraron valores de inhibición de la invasión y proliferación superiores al 80% al ser administrados a las 0 hpi. Los compuestos 1294, 1517, 1553 y 1571 fueron seleccionados para la determinación de sus CI99 (1294: 2,38µM; 1517: 2,20µM; 1553: 3,34µM; 1571: 2,78µM) mediante qPCR cuantitativa, al mostar los mejores resultados de eficacia en el cribado inicial y ser eficaces frente a otras especies de protozoos Toxoplasmatinae en otros estudios. No obstante, dichos tratamientos no fueron parasiticidas, hallazgo que fue corroborado mediante TEM, al confirmarse que el tratamiento con los BKIs interfería con la regulación del ciclo celular de los taquizoítos en división, dando lugar a la formación de complejos multinucleados que coexistían con parásitos viables dentro de las vacuolas parasitóforas. Se piensa que el tratamiento con BKIs en un animal infectado en combinación con una respuesta inmunitaria eficaz podrían controlar la infección. En resumen, los BKIs son herramientas terapéuticas prometedoras para controlar la besnoitiosis bovina, si bien son necesarios futuros ensayos *in* vivo en el ganado bovino. En este sentido, cabe destacar que para los BKIs 1294, 1517 y 1553 se han obtenido concentraciones plasmáticas superiores a 5 µM en terneros.

En su conjunto, esta tesis doctoral supone un avance al conocimiento de la biología de *B. besnoiti* con perspectivas al control de la infección. El desarrollo y estandarización de nuevos modelos *in vitro* basados en la obtención de células primarias diana del parásito procedentes de la especie bovina ha permitido estudiar la modulación de la célula endotelial por el taquizoíto de *B. besnoiti* y ha sentado las bases para la identificación de posibles biomarcadores de pronóstico y de posibles dianas terapéuticas o vacunales. Además, se ofrecen alternativas terapéuticas a corto-medio plazo para controlar la multiplicación y diseminación del parásito durante la fase aguda de la enfermedad, mediante el posible empleo del decoquinato y el diclazurilo, o a largo plazo mediante el empleo de cuatro posibles BKIs (1294, 1517, 1553 y 1571). No obstante, la seguridad y eficacia de estos compuestos deberá ser evaluada en la especie de destino (ganado bovino).

Abstract:

Bovine besnoitiosis is a chronic and debilitating disease caused by the cyst-forming apicomplexan parasite *Besnoitia besnoiti*. This disease is responsible for considerable economic looses, mostly in suckler-cow farms. Currently, this disease is considered as re-emerging in Europe due to its geographical expansion from areas where the disease has been considered as traditionally endemic (Pyrinees and Alentejo region in Portugal) together with an increase in its prevalence. One of the factors that has contributed greatly to this dissemination is the absence of efficient treatments and vaccines. With this background, the development of *in vitro* models of infection arises as a key tool in order to explore the parasite-host interaction, as well as to identify new therapeutic and vaccinal targets. Thus, the objective of the present doctoral thesis has been the development and standardization of novel *in vitro* models of *B. besnoiti* infection and their applications for molecular pathogenesis studies and drug screenings.

In the first objective of the present doctoral thesis, novel *in vitro* models have been developed employing primary cultures isolated from the natural intermediate host (cattle). Specifically, endothelial cells (EC) and fibroblasts have been isolated from bovine aorta, which represent target cells of the parasite during the acute and chronic stages of the disease, respectively. One key aspect considered is that the health status of donor animals was thoroughly checked, and primary cultures obtained were monitored to guarantee the absence of prevalent bovine pathogens and frequent contaminants of mammalian cell cultures such as *Mycoplasma* spp. and bovine viral diarrhea virus (BVDV), that can alter the host cells. Afterwards, the profile of expression of surface (CD31, CD34, CD44) and intracellular (vimentin, cytokeratin) markers was studied by flow cytometry in order to characterize the primary cultures obtained. Surface marker CD31, characteristic from ECs, was the marker which better discriminated between ECs and fibroblasts. On the other hand, expression of the marker CD34 was only detected in ECs with a low passage number, and in both fibroblasts and ECs CD44, vimentin and cytokeratin had high expression. Subsequently, the lytic cycle of tachyzoites from the Bb-Spain1 isolate of *B. besnoiti* was studied, addressing their capacities to invade and proliferate in both primary cultures. Results showed that the lytic cycle in both ECs and fibroblasts is remarkably similar to the one previously described in monkey epithelial kidney cells Marc-145, with low invasion rates (approximately 4%) up to 24 hpi and an exponential growth up to 72 hpi. Additionally, for the first time, the interaction of a Toxoplasmatinae parasite with a non-cytopathic strain of BVDV in ECs, showing that the early invasion of the host cells by tachyzoites is favoured.

Afterwards, in the second objective, *in vitro* models have been employed to perform molecular pathogenesis studies and drug screenings.

First, in the subobjective 2.1, the *in vitro* model developed in the objective 1 has been employed to study the host-parasite interaction in ECs from bovine aorta (BAEC) at two post-infection times: at 12 hpi, when tachyzoites have already invaded the host cells; and at 32 hpi, when tachyzoites have been subjected to at least two replicative rounds. Non-infected cells were employed as a negative control. Analyses were performed with four biological replicates, and in each replicate, additional samples were collected for further validation by qPCR. The highest number of differentially expressed genes (DEG) (n=446) were evidenced when both post-infection times were compared. From those, 249 DEG were overexpressed at 32 hpi. The results have shown that *B. besnoiti* infection is responsible for an activation of BAECs, with the expression of several cytokines (IL6, IL1A), chemokines (CCL2, CCL24, CXCL1, CXCL2, CXCL3) and leukocyte adhesion molecules (SELE, ICAM-1, VCAM-1), among others, predominantly at 12 hpi, Meanwhile at both post-infection times, the expression of genes involved in angiogenesis (growth factors and integrins) and the

organization of the extracellular matrix (i.e. matrix metalloproteinases and ADAMTS) were evidenced, all of them associated with endothelial damage. The most relevant signaling pathways modulated by the parasite were the nuclear transcription factor NFkB and the proinflammatory route of the tumor necrosis factor TNFa. These would be responsible for the expression of additional effector genes, that would unleash a proinflammatory, procoagulant and profibrotic phenotype in ECs, triggering the recruitment of macrophages and other leukocytes that would initiate an inflammatory and fibrotic process compatible with the histopathological lesions described *in vivo* for bovine besnoitiosis. The coexistence of lesions from both the acute and the chronic stage of bovine besnoitios has already been described. Besides, the overexpression of genes involved in early (growth factors and matrix metalloproteinases) and late (integrins and vasohibin) steps of angiogenesis has been described in the present work. Also, overexpressed molecules which play a key role in the previously mentioned pathways (*n*=16) (i.e. ICAM-1, VCAM-1, SELE, CCL2, IL6, ADAMTS1) were selected for further validation of the transcriptomic results by qPCR, corroborating the results. Additionally, the transcriptomic profile of *B. besnoiti* tachyzoites was studied at both post-infection times, identifying orthologues genes for other Toxoplasmatinae parasites, such as *N. caninum* and *T. gondii,* for the fisrst time. Among these, genes coding for proteins involved in the progression of the lytic cycle, such as dense granules proteins (GRA), rhoptry proteins (RON and ROP), microneme proteins (MIC) and surface (SRS) were described for the first time. In particular, it is noteworthy to remark the overexpression of genes that codify for rhoptry proteins (ROP5B, ROP17, ROP40), micronemes (MIC2, MIC11), glideosome (GAP80) and surface (SRS22A), among others, when the lytic cycle progresses. Also, the expression profile of a panel of *B. besnoiti* genes (*n*=10) by qPCR, corroborating transcriptomic results. Thus, this study has shed light on the interaction between *B.* besnoiti tachyzoites and their host cells, showing the progression of an endothelial activation with a proinflammatory and profibrotic profile after invasion and proliferation, which is correlated with the vascular damage and lesions described *in vivo*.

However, the *in vitro* model previously developed by the research group using monkey epithelial kidney cells Marc-145 has been employed in order to evaluate the safety and efficacy of a panel of drugs (subobjectives 2.2 and 2.3) since: i) the lytic cycle of the reference isolate Bb-Spain1 is similar in the *in vitro* models assayed so far; ii) there are inherent difficulties when working with primary cultures; iii) primary cultures may show variability depending on the donor animal.

In the context of diseases caused by apicomplexan protozoa, as it happens in other diseases known as neglected diseases, drug repurposing is a common approach, since it allows to have potentially effective drugs which are already in the marked. Thus, in the subobjective 2.2, the *in vitro* safety and efficacy against *B. besnoiti* tachyzoites of a panel of drugs already commercialized in cattle (decoquinate, diclazuril, toltrazuril, imidocarb, sulfadiazine and trimethoprim, alone or in combination with sulfadiazine) were studied. Drugs were administered either prior to the infection of the host cells (0 hpi) or at 6 hpi (when at least the 50% of the tachyzoites have invaded the host cell). First, potential toxic effects were evaluated using a proliferation XTT assay. Afterwards, preliminary assays were performed to optimize the subsequent drug screening, which was performed by direct immunofluorescences and counting of invasion and proliferation outcomes (parasitophorous vacuoles and lysis plaques). The compounds which showed the best results (decoquinate and diclazuril) were selected for the determination of the inhibitory concentrations 50 and 99 (IC50 and IC99) by qPCR. Besides, the effect of the drugs on the ultrastructure of the tachyzoites was studied by transmission electron microscopy (TEM), together with the long-term effects of the treatment. Citotoxycity results showed that none of the compounds was cytotoxic in the *in vitro* model employed at the concentrations used in the drug screening. Decoquinate and diclazuril showed values of inhibition of the parasite

invasion of 90 and 83% at 0 hpi, and 73 and 72% at 6 hpi, respectively. The rest of the drugs assayed showed less efficacy and were discarded. The IC99 obtained were of 100 nM for decoquinate and 29.9 µM for diclazuril. Results from the TEM assays showed that the site of action of decoquinate was in the mitochondria of the parasites, meanwhile diclazuril interfered on the cytokinesis of daughter zoites. Thus, the present study has shown the efficacy of both compounds against *B. besnoiti* invasion and proliferation. However, further studies are needed in the target species to assess their safety and efficacy. For decoquinate, maximum plasmatic concentrations above the IC99 obtained *in vitro* have been described, but for diclazuril further pharmacokinetic studies to improve their absortion and bioavailability are needed, since the maximum plasmatic concentrations described so far are below the IC99 obtained *in vitro*.

On the other hand, in the search of novel thereapeutic targets, the calcium dependent protein kinases (CDPKs) represent promising therapeutic targets in other apicomplexan parasites such as *N. caninum, T. gondii, Plasmodium* spp. or *Cryptosporidium parvum,* due to several structural differences that have allowed the development of a class of selective inhibitors known as bumped kinase inhibitors. Thus, in the subobjective 2.3, we have identified and cloned the gene that encodes for the enzyme *Bb*CDPK1 and the activity of the recombinant enzyme r*Bb*CDPK1 has been assayed with a panel of 9 BKIs. Besides, the safety and efficacy of those compounds have been assayed against *B. besnoiti* tachyzoites grown in Marc-145 cells as mentioned in the previous subobjective. After assessing that none of the compounds showed toxic effects in the *in vitro* system employed, the drug screening was performed employing the drugs at a concentration of 5 µM and at both pi times previously mentioned (0 and 6 hpi). Eight of the compounds showed values of inhibition of parasite invasion and proliferation greater than 80% when administered at 0 hpi. Compounds 1294, 1517, 1553 and 1571 were selected for the determination of their IC99 (1294: 2,38µM; 1517: 2,20µM; 1553: 3,34µM; 1571: 2,78µM) by qPCR since they showed the best results in the drug screening and being efficacious against other Toxoplasmatinae parasites in other studies. However, the treatments did not act in a parasiticidal way, finding that was corroborated by TEM, showing that BKI treatment interfered with the cell cycle regulation of dividing tachyzoites, leading to the formation of multinucleated complexes that coexisted with viable tachyzoites inside parasitophorous vacuoles. However, it is posible that, BKI-treatment in the face of an active immune response in infected animals, may clear the infection. To sum up, BKIs represent promising therapeutic tools to tackle bovine besnoitiosis, although future *in vivo* studies in cattle are needed. In this sense, for BKIs 1294, 1517 and 1553, maximum plasmatic concentrations above 5 µM have been described in calves.

As a whole, this doctoral thesis represents an advancement in the knowledge of *B. besnoiti* biology, with perspectives towards the control of the infection. The development and standardization of novel *in vito* models based on the obtention of primary target cells from the bovine host set the bases to study the modulation of the ECs by the tachyzoite stage of *B. besnoiti* and allowed to identify putative prognosis markers and therapeutic or vaccinal targets. Besides, therapeutic candidates are proposed for the short-medium run to control multiplication and dissemination of the parasite during the acute stage of the disease by the possible use of decoquinate and diclazuril, or in the long run by the use of four BKIs (1294, 1517, 1553 and 1571). However, the safety and efficacy of those compounds must be evaluated in the target species (cattle).

CAPÍTULO II: INTRODUCCIÓN

2.1. *Besnoitia besnoiti* y la besnoitiosis bovina

2.1.1. Revisión histórica

El protozoo apicomplejo *Besnoitia besnoiti* es el agente etiológico de la besnoitiosis bovina, una enfermedad crónica y debilitante del ganado bovino que cursa fundamentalmente con lesiones cutáneas en su fase crónica, así como con alteraciones sistémicas. El primer caso de besnoitiosis bovina en la literatura fue descrito en el sur de Francia en 1884 por Cadéac (1884), que denominó a la enfermedad como "*l'élephantiasis et l'anasarque du boeuf*". En 1912, Besnoit y Robin describieron la presencia de diversos casos en la zona del Pirineo Francés, y denominaron al agente etiológico *Sarcocystis* spp. (Besnoit y Robin, 1912). Sin embargo, hasta ese momento no se había descrito ninguna enfermedad similar en el ganado bovino y Marotel (1912) sugirió el término *Sarcocystis besnoiti* para referirse a su agente etiológico. En 1915, Franco y Borges describieron la presencia de casos clínicos de la enfermedad en Portugal, en la zona del Alentejo (Franco y Borges, 1915). Fue en este trabajo cuando, de forma definitiva, se denominó al agente etiológico como *B. besnoiti* y se introdujo el término besnoitiosis para referirse a la enfermedad producida por este parásito (Franco y Borges, 1915). No obstante, se piensa que esta enfermedad podría tener su origen en África, ya que se detectó la enfermedad en animales importados de Angola en Portugal (Leitao, 1949). Desde la primera descripción de la enfermedad en el continente africano, más concretamente en Sudáfrica (Hofmeyr, 1945), y hasta los años setenta, se obtuvieron en esta región los primeros aislados de *B. besnoiti* procedentes de ungulados infectados naturalmente, tanto domésticos (ganado bovino) como silvestres (impala y ñu). La obtención de estos primeros aislados, mantenidos mediante pases sucesivos en lagomorfos, permitió realizar las primeras infecciones experimentales en el ganado bovino, explorando las posibles rutas de transmisión, la cronobiología de la infección y las lesiones asociadas (Pols, 1960; Bigalke *et al.*, 1967; Bigalke, 1968; Basson *et al.*, 1970). En esos años también se comprobó que los bradizoítos pueden atravesar mucosas y que el parásito podría transmitirse de forma mecánica gracias a ciertos artrópodos hematófagos, como los tábanos y *Stomoxys* spp. Hay que destacar que los resultados obtenidos en estos trabajos no son comparables debido a la ausencia de un modelo experimental reproducible y de técnicas serológicas y moleculares para confirmar la infección, y además todos los autores coincidieron en señalar la dificultad de inducir signos clínicos característicos en bovinos infectados experimentalmente. Paralelamente, Basson *et al*. (1965, 1970) y McCully *et al.*, (1966) llevaron a cabo los primeros trabajos de distribución intra-orgánica del parásito. En sus estudios, describieron de forma detallada los signos clínicos de la enfermedad durante las fases aguda y crónica en infecciones naturales y experimentales, así como la distribución intra-orgánica de los quistes tisulares, destacando la detección de los mismos en el sistema cardiovascular (McCully *et al.*, 1966). También se describió, por primera vez, que los animales infectados desarrollaban una respuesta inmunitaria protectora frente a posteriores reinfecciones (Bigalke, 1968).

Por otra parte, tras la realización de infecciones experimentales se describió que los aislados procedentes de ñu (*Connochaetes taurinus*) originaban signos clínicos y lesiones menos graves en el ganado bovino que los aislados procedentes del ganado bovino. Esta menor virulencia de los aislados obtenidos de ñu posibilitó su uso posterior como vacuna viva, la cual evitó la aparición de signos clínicos en prácticamente la totalidad de los animales vacunados durante un periodo de cuatro años post-vacunación (Bigalke *et al.*, 1974).

A partir de los años setenta, hay que destacar varios estudios realizados en Israel en los que se estudiaron, por un lado, la distribución intra-orgánica del parásito mediante estudios histopatológicos en el aparato genital de hembras y machos infectados de forma natural (Neuman, 1972; Nobel *et al.*, 1977,1981), y realizando, por otro lado, los primeros estudios serológicos que pusieron de manifiesto la importancia de la enfermedad en este país (Neuman, 1972b, Frank *et al*., 1977; Goldman y Pipano, 1983). Cabe destacar también el trabajo realizado por Kumi-Diaka *et al*. (1981), donde se describieron las lesiones asociadas a la besnoitiosis crónica en el aparato genital de toros y en el cual se valoró el efecto de la infección en el espermiograma. También se realizaron estudios radiográficos para estudiar en profundidad las alteraciones testiculares en sementales infectados por *B. besnoiti*, observándose marcadas calcificaciones del parénquima testicular (Bargai *et al.*, 1984). Sin embargo, fue a finales de los años ochenta cuando, tras el mantenimiento de un aislado de *B. besnoiti* procedente de un toro naturalmente infectado en cultivo celular (Neuman, 1974), fue posible la realización de los primeros estudios de la ultraestructura del parásito mediante microscopía electrónica de transmisión, así como los primeros ensayos *in vitro* e *in vivo* para evaluar posibles tratamientos frente a la infección (Shkap *et al*., 1985,1987a). También se realizaron pruebas vacunales basadas en el empleo de un aislado de origen bovino avirulento en diversas especies animales (Shkap *et al.*, 1986; Shkap, 1987b). Esta vacuna viva, cuya seguridad todavía se desconoce, se utiliza en la actualidad de forma rutinaria en Israel para evitar el desarrollo de signos clínicos en los sementales importados.

En Europa, desde su primera descripción en los Pirineos y en Portugal (Cadéac, 1884; Franco & Borges, 1915) hasta finales de los años noventa, no se le prestó mucha atención a la enfermedad. Sin embargo, debido al número creciente de casos descritos en España (Juste *et al.*, 1990; Fernández-García *et al.*, 2009b; Fernandez-Garcia *et al.*, 2010; Diezma-Díaz *et al.*, 2017), en Portugal (Cortes *et al.*, 2004,2005,2006a,b,c,d) y en Francia (Alzieu, 2007), el aumento de la seroprevalencia junto con la descripción de nuevos brotes en otros países cercanos como Alemania, Croacia, Hungría, Italia, Suiza e Irlanda, la besnoitiosis bovina está considerada en la actualidad una enfermedad re-emergente en Europa (European Food Safety Authority, 2010; Álvarez-García *et al.*, 2013; Gutiérrez-Expósito *et al.*, 2017a). La descripción de nuevos casos ha permitido obtener nuevos aislados, lo cual ha posibilitado la realización de diversos estudios proteómicos (Fernández-García *et al.*, 2013; García-Lunar *et al.*, 2013a,2014;) y el desarrollo de numerosas técnicas de diagnóstico, tanto serológicas como moleculares (revisado por Gutiérrez-Expósito *et al.*, 2017a). Asimismo, se ha profundizado en la cronobiología de la infección durante las fases aguda y crónica en infecciones naturales (Langenmayer *et al.*, 2015a,b,c). En estos últimos años, el conocimiento de la prevalencia e incidencia de la enfermedad en zonas endémicas ha aumentado considerablemente (Álvarez-García *et al.*, 2014a; Gutiérrez-Expósito *et al.*, 2014), poniéndose de manifiesto que la enfermedad está ampliamente diseminada en el ganado bovino de carne en las regiones de los Pirineos y la Sierra de Urbasa-Andía (Navarra), describiéndose elevadas tasas de prevalencia, ya que las tasas de seroprevalencia intra-rebaño alcanzaron el 86,5% con valores de incidencia clínica y serológica de hasta el 20% en las granjas infectadas en ausencia de medidas de control adecuadas (Gutierrez-Exposito *et al.*, 2017b). Sin embargo, quedan aún muchas incógnitas por esclarecer relacionadas con la biología del parásito y su patogenia, que podrían facilitar el desarrollo de medidas de control, tanto quimioprofilácticas como vacunales.

2.1.2. Género *Besnoitia* spp.

Besnoitia besnoiti es un protozoo intracelular obligado perteneciente al subfilo Apicomplexa, familia Sarcocystidae y subfamilia Toxoplasmatinae, que incluye otros géneros de parásitos formadores de quistes de gran importancia tanto en medicina humana como veterinaria, tales como *Toxoplasma* y *Neospora* (Tenter *et al.*, 2002). Dentro del género *Besnoitia* spp. se han descrito diez especies hasta la fecha que afectan a diversas especies de mamíferos: *B. besnoiti, B. bennetti, B. caprae, B. tarandi, B. akadoni, B. jellisoni, B. darlingi, B. neotomofelis, B. oryctofelisi,* y *B. wallacei* (Olias *et al.*, 2011; Dubey & Yabsley, 2010), si bien tan sólo 4 de ellas (*B. besnoiti*, *B. bennetti, B. caprae* y *B. tarandi)* afectan a ungulados (Dubey *et al*., 2003a, 2004, 2005) (Tabla 1).

La otra especie incluida dentro del género *Besnoitia* que afecta a grandes rumiantes, *B. tarandi*, se describió originariamente en el reno (*Rangifer tarandus tarandus*) y en el caribú (*Rangifer tarandus caribou*) en la región ártica (Hadween, 1922), originando signos clínicos y lesiones muy similares a las originadas por *B. besnoiti* en el ganado bovino (Gutiérrez-Expósito *et al.*, 2012; Schares *et al.*, 2019). En el ganado caprino se han descrito infecciones parasitarias que cursan con los signos clínicos tradicionalmente asociados a la besnoitiosis bovina en países como Irán y Kenia y dichas infecciones han sido atribuidas a la especie *B. caprae* (Cheema y Toofanian, 1979; Bwangamoi *et al*., 1989; revisado por Olias *et al*., 2011). En équidos también se han descrito signos clínicos similares a la fase crónica de la besnoitiosis. La enfermedad se ha descrito principalmente en burros y, en menor medida, en caballos, si bien también existe la descripción de un caso en una cebra africana (Pols, 1960; Bigalke, 1968; Bigalke *et al.*, 2004). Recientemente, se ha descrito que la besnoitiosis equina puede ser considerada una enfermedad emergente en burros en EE.UU. (Dubey *et al.*, 2005; Elsheikha, 2007; 2008; Ness *et al.*, 2014). Además, la descripción más reciente de la enfermedad ha demostrado la existencia de burros infectados por *B. bennetii* en Europa, más concretamente en Bélgica (Liénard *et al.*, 2018), y de burros seropositivos a *Besnoitia* spp. en España (Gutiérrez-Expósito *et al.*, 2017b).

Debido a las similitudes que presentan las especies que infectan a los ungulados como i) el desconocimiento de los hospedadores definitivos (HD); ii) la ausencia de diferencias ultraestructurales; iii) la similitud en cuanto a los signos clínicos y lesiones desarrollados en los hospedadores intermediarios (HI) y iv) las intensas reacciones cruzadas serológicas observadas entre *B. besnoiti* y *B. tarandi* (Gutiérrez-Expósito *et al*., 2012), así como entre *B. besnoiti* y *B. bennetti* (Ness *et al*., 2012); se recurre al empleo de técnicas moleculares de genotipado para la identificación de la especie, ya que las secuencias del ADN ribosomal (ADRr) ITS1 son idénticas, al menos en el caso de *B. besnoiti* y *B. caprae* (Ellis *et al.*, 2000). Además, diversos estudios moleculares han demostrado que estas especies están muy relacionadas entre sí, ya que también poseen idénticas regiones 18S y 5,8S del ARNr y que, únicamente, una inserción de 2 pb en el segmento 28S diferencia *B. tarandi* de *B. besnoiti* (Ellis *et al.*, 2000; Schares *et al.*, 2009; Olias *et al.*, 2011). Por tanto, la técnica de caracterización genética que permite diferenciar *B. besnoiti*, *B. tarandi* y *B. bennetti* es el análisis microsatélites multilocus utilizando seis marcadores (BT5, BT6, BT7, BT9, BT20 y BT21) (Madubata *et al.*, 2012; Gutiérrez-Expósito *et al.*, 2016).

Tabla 1: Especies incluidas en el género *Besnoitia* spp.

Especie	Hospedador intermediario	Hospedador definitivo	Distribución geográfica	Referencias
B. akodoni	Ratón (*Akodon montensis*)	Desconocido	Brasil	Dubey *et al.*, 2003c
B. darlingi	*Lagartija metálica (Ameiva spp), Basilisco (Basiliscus* spp.*)* y Zarigüeya común (*Didelphis marsupialis)*	Gato/Lince rojo	Estados Unidos (EE.UU.)	Dubey *et al.*, 2002; Smith & Frenkel, 1977, 1984
B. jellisoni	Ratas canguro *(Dipodomys* spp.), Ratón ciervo (*Peromyscus maniculatus)*	Desconocido	EE.UU.	Frenkel *et al.*, 1976; Senaud *et al.*, 1974
B. neotomofelis	Rata montera norteña de México *(Neotoma micropus)*	Gato	Texas, EE.UU.	Dubey & Yabsley, 2010
B. oryctofelisi	Conejo (*Oryctolagus cuniculus*)	Gato	Argentina	Dubey & Lindsay, 2003; Dubey *et al.*, 2003b
B. wallacei	Ratas (*Rattus* spp.)	Gato	EE.UU. (Oahu, Hawaii), Japón, Kenia	Nganga *et al.*, 1994; Frenkel, 1977
B. bennetti	Burro (*Equus asinus*), caballo (*Equus caballus*) y cebra (*Equus zebra*)	Desconocido	EE.UU.	Elsheikha *et al.*, 2008; Elsheikha, 2007; Dubey *et al.*, 2005
B. besnoiti	Bovino (*Bos Taurus*) Kudu (*Tragelaphus strepsiceros*), impala (*Aepycerus melampus*) ñu azul (*Chonnochaetes taurinus*), corzo (*Capreolus capreolus*)	Desconocido	Europa, África Subsahariana, Oriente Medio, Corea	Alvarez-Garcia *et al.*, 2013; Dubey *et al.*, 2003a; Besnoit & Robin, 1912
B. caprae	Cabra (*Capra hircus*)	Desconocido	Irán, Kenia, Nigeria	Heydorn *et al.*, 1984; Oryan *et al.*, 2014; Oryan *et al.*, 2011; Oryan *et al.*, 2010; Oryan & Azizi, 2008
B. tarandi	Buey almizclero (*Ovibos moschatus)*, ciervo-mula *(Odocoileus hemionus*), caribú y reno (*Rangifer tarandus*)	Desconocido	Hemisferio norte (Finlandia, Canadá)	Hadween, 1922; Levine, 1961; Schares *et al.*, 2019

No obstante, sí que se han descrito diferencias entre las especies de *Besnoitia* que afectan a ungulados en cuanto al espectro de hospedadores intermediarios utilizados y en la diferente infectividad para animales de laboratorio (Pols, 1960; Njenga *et al.*, 1993; Nganga *et al.,* Dubey *et al*., 2003a, 2004, 2005; Oryan *et al*., 2010). De hecho, varias infecciones experimentales han demostrado que los gerbos de la especie *Meriones tristami* y los conejos son susceptibles a la infección por *B. besnoiti* pero no a la infección por *B. tarandi* (Pols, 1960; Neuman, 1962b; Bigalke, 1968, Shkap *et al*., 1987a; Dubey et al., 2004; Basso *et al.*, 2011), mientras que los ratones BALB/c son susceptibles a la infección por *B. caprae* (Oryan *et al.*, 2010, 2016; Namavari *et al.*, 2013) y parecen ser más resistentes a la infección por *B. besnoiti* (Kiehl *et al.*, 2010). No obstante, la variabilidad de los modelos experimentales empleados dificulta la comparación de los resultados obtenidos.

2.1.3. Ciclo biológico

Por analogía con otros protozoos pertenecientes a la subfamilia Toxoplasmatinae, como *N. caninum* o *T. gondii*, así como con otras especies pertenecientes al género *Besnoitia* spp., en las que se conoce el hospedador definitivo (HD), se presupone que *B. besnoiti* presenta un ciclo biológico heteroxeno (Figura 1). No obstante, hasta la fecha no se ha identificado la especie que actuaría como HD, y se presupone que podría ser un carnívoro.

Por su parte, se ha confirmado la presencia del parásito en varias especies de rumiantes (ganado bovino, corzo, impala, ñu, kudu) que actuarían como hospedador intermediario (HI) (Tabla 1). En Europa, el ganado bovino y el corzo (*Capreolus capreolus*) actúan como HI (Arnal *et al.*, 2017; Gutiérrez-Expósito *et al.*, 2016), siendo el ganado bovino el principal HI en el que se ha descrito la existencia de dos estadios asexuales e infectivos (taquizoíto y bradizoíto). Por otra parte, se ha detectado ADN del parásito en el ciervo (*Cervus elaphus*), por lo que su papel como HI no está claro y no se han detectado anticuerpos específicos anti-*B. besnoiti* en otras especies de pequeños rumiantes silvestres y domésticos, por lo que se piensa que su intervención en el ciclo biológico de *B. besnoiti* sería improbable (Arnal *et al.*, 2017)

Estudios recientes han explorado la posibilidad de que diversas especies de carnívoros presentes en la península ibérica presenten anticuerpos específicos frente a *B. besnoiti* (lobo, zorro, marta, garduña, tejón, gineta, gato silvestre, meloncillo, gato asilvestrado), obteniéndose resultados no concluyentes que no permiten demostrar el posible papel de ninguna de las especies analizadas en la transmisión de *B. besnoiti* en España (Millán *et al.*, 2012). En estudios realizados en Hungría (Hornok *et al.*, 2015a), se ha encontrado la presencia de ADN con un 99% de identidad con la región *Internal Transcriber Spacer* (ITS)-1 de *B. besnoiti* en muestras fecales de murciélago lagunero (*Myotis dasycneme*) procedentes de los Países Bajos, si bien se trata de una especie de murciélago migratoria y no se aisló al parásito. Además, no se debe descartar el posible papel de diversas especies como rumiantes silvestres, los roedores o incluso aves como reservorios del parásito en la transmisión (Bigalke, 1981; Mehlhorn *et al.*, 2009; Gutiérrez-Expósito *et al.*, 2013). De hecho, se han encontrado anticuerpos específicos frente a *Besnoitia* spp. en rumiantes silvestres en España (Gutiérrez-Expósito *et al.*, 2013, 2016), si bien los resultados obtenidos no sugieren un papel importante de los mismos en la epidemiología de la enfermedad. Por el contrario, se ha descrito la ausencia de anticuerpos específicos en rebaños de pequeños rumiantes domésticos (cabras y ovejas) localizados en zonas donde la besnoitiosis bovina es endémica (Gutiérrez-

Expósito *et al.*, 2017c). En otro estudio se analizó la presencia de anticuerpos específicos frente a *B. besnoiti* en seis especies de rumiantes silvestres y dos de carnívoros en Israel, si bien no se pudo confirmar la presencia de dichos anticuerpos mediante Western blot (WB) (Mazuz *et al.*, 2018).

Figura 1. Ciclo biológico y transmisión de *Besnoitia besnoiti*

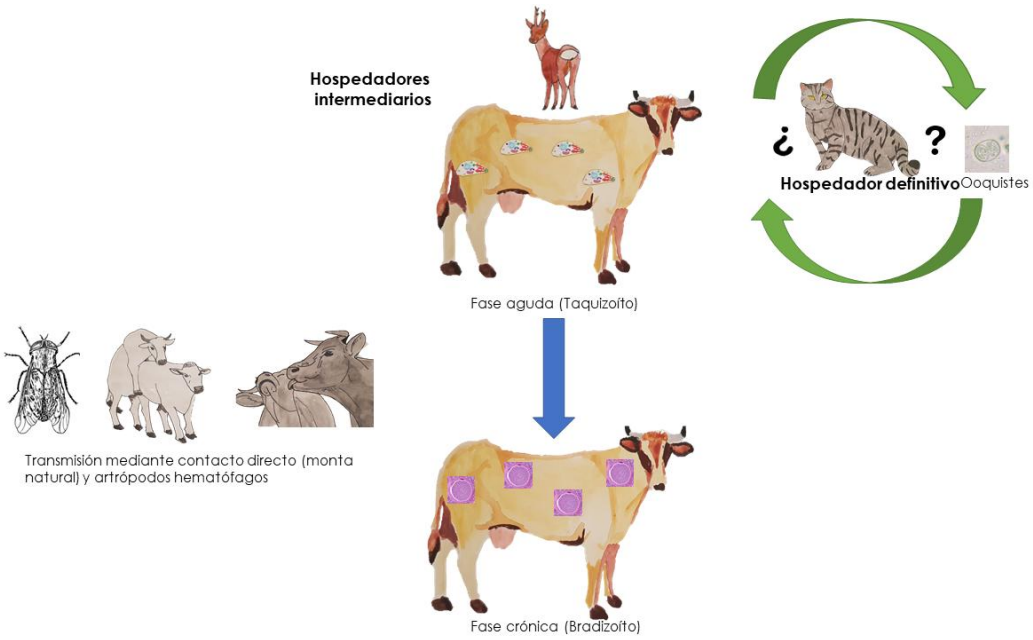

La microscopía electrónica de transmisión ha demostrado que los zoítos (taquizoítos y bradizoítos) de *Besnoitia* presentes en el HI tienen en común una ultraestructura característica de otros coccidios formadores de quistes, consistente en una película compuesta por tres capas, conoide, roptrias, micronemas, gránulos densos y un anillo polar anterior y posterior (Sheffield, 1966; Shkap *et al*., 1988; Dubey *et al.,* 2003; Reis *et al*., 2006). La red de microtúbulos subpelicular consiste en una fibra circular con una estructura helicoidal de 75 nm de diámetro, compuesta con dos filamentos en espiral de 30 nm de diámetro cada uno(Reis *et al.*, 2006).

Los taquizoítos (Figura 2) tienen un tamaño aproximado de 6-7,5 µm x 2,5-3,9 µm, una forma de luna creciente (o "banana") con un complejo apical que incluye un conoide, micronemas y roptrias, además de otras organelas secretoras también exclusivas de los apicomplejos, los gránulos densos, y la presencia de microporos en la superficie. El conoide, que se localiza en el polo apical, es una estructura de aproximadamente 6000 nm de longitud y 540 n m de ancho y sus dimensiones son menos variables que el tamaño de los propios taquizoítos (Reis *et al.*, 2006). El número de roptrias es variable y oscila entre 2 y 8 (Reis *et al.*, 2006). Además, los taquizoítos presentan también organelas típicas de células eucariotas (como el núcleo, retículo endoplásmico, aparato de Golgi y una mitocondria) (Figura 2).

Por otra parte, los bradizoítos se encuentran en el interior de quistes tisulares en el tejido conjuntivo de los HI, preferencialmente en piel y mucosas, aunque se han descrito en otras localizaciones como los tendones, los vasos sanguíneos, la esclerótica, el tracto respiratorio superior, el testículo y el epidídimo en los machos y vestíbulo vaginal en las hembras, entre otras localizaciones (Mbuthia *et al.*, 1993; Basso *et al.*, 2013; Frey *et al.*, 2013). Se desconoce cómo se inicia la formación del quiste (cistogénesis), pero se ha descrito que la aparición de los quistes tisulares es sincrónica y que van aumentando de tamaño con el tiempo (Bigalke, 1968), pudiendo alcanzar unas dimensiones de hasta

400 µm. Una diferencia importante con otros protozoos apicomplejos formadores de quistes como *N. caninum* o *T. gondii*, reside en el hecho de que la pared del quiste es gruesa y está constituida por dos capas: una capa externa (*outer cyst wall*; OCW) con múltiples fibras de colágeno entrelazadas; y una capa interna (*inner cyst wall*; ICW), con proteoglicanos y extensiones filamentosas que se proyectan hacia la membrana externa (Dubey *et al.*, 2003a; Langenmayer *et al.*, 2015b). El tamaño de los bradizoítos es similar al de los taquizoítos (6,0-7,5 por 1,9-2,3 µm) (Dubey *et al.*, 2003a), aunque se ha descrito que presentan una morfología más alargada y en el citoplasma, generalmente, existen un mayor número de gránulos de amilopectina que podrían constituir una reserva energética para este estadio. Los zoítos de las diferentes especies de *Besnoitia* son muy similares entre sí, y una de las pocas diferencias reseñables es la ausencia de cuerpos enigmáticos en los bradizoítos de las especies que infectan ungulados (*B. bennetti*; *B. besnoiti*; *B. caprae* y *B. tarandi*), si bien se desconoce el origen y función de dichas organelas (Dubey *et al*., 2003a, 2004, 2005).

Figura 2. Estadios asexuales de *B. besnoiti*: Taquizoítos (A) y Bradizoítos (C) (Fernández-García *et al*., 2009)**. B: esquema de la estructura típica de los zoítos de *B. besnoiti*.** Imágenes A y C obtenidas mediante microscopía electrónica de transmisión (TEM).

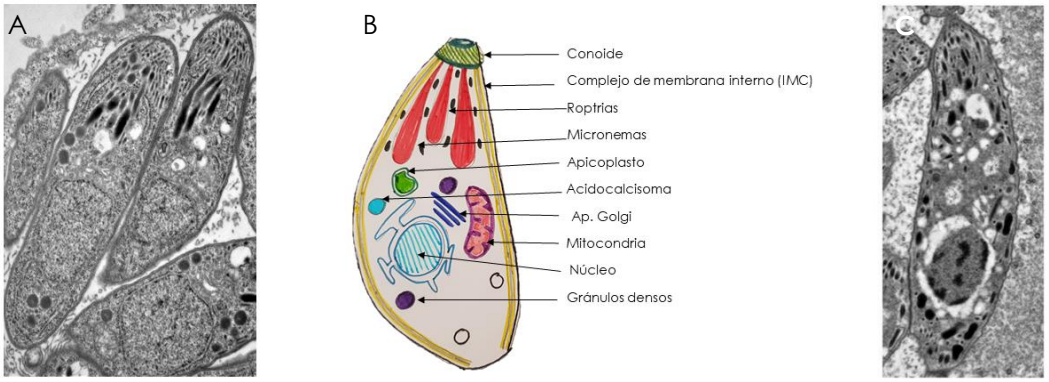

En relación a los ooquistes que eliminaría el HD en sus heces, éstos serían similares a los previamente descritos para otras especies del género *Besnoitia* que utilizan a los félidos como HD (*B. oryctofelisi; B. darlingi, B. wallacei, B. jellisoni*) (Frenkel, 1977; Dubey *et al.*, 2002, 2003b; Dubey & Lindsay, 2003; Dubey & Yabsley, 2010). Estos ooquistes tienen una morfología similar a los ooquistes de *T. gondii*, con unas dimensiones de 10x14 µm, se eliminan en las heces del HD sin esporular y, posteriormente, esporulan en el medio ambiente.

2.1.4. Transmisión y factores de riesgo

De acuerdo con los datos epidemiológicos disponibles hasta la fecha (sección 2.1.5.1), en los que se ha observado un aumento en la seroprevalencia con la edad de los animales, se piensa que el principal modo de transmisión de la infección por *B. besnoiti* es el horizontal, bien por contacto directo (monta natural, contacto estrecho entre animales sanos e infectados) o mediante vectores mecánicos (artrópodos hematófagos). En relación a la monta natural, se ha postulado que una posible rotura de los quistes superficiales localizados en el vestíbulo vaginal de las hembras durante la monta, debido a la fricción mecánica, facilitaría la transmisión de la infección de la

hembra a los sementales, y viceversa, ya que también se ha descrito la presencia de quistes en el pene del macho (Nieto-Rodríguez *et al.*, 2016). En 2015, Hornok *et al*, describieron que únicamente un 3% de las vacas cubiertas por un toro infectado desarrollaban anticuerpos específicos frente al parásito. No obstante, la situación de partida puede influenciar este resultado, ya que la seroprevalencia en el rebaño era baja (en torno al 5%). De hecho, posteriormente, Gazzonis *et al*. (2017) describieron un mayor riesgo para los toros de adquirir la infección tras la monta natural en un rebaño con un 41% de seroprevalencia intra-rebaño.

Ya desde los primeros estudios de transmisión realizados en 1960 se puso de manifiesto la capacidad del bradizoíto de atravesar las barreras mucosas (Bigalke, 1968), ya que la inoculación de bradizoítos por vía intranasal originó la aparición de fiebre, así como quistes tisulares en la esclerótica aproximadamente tres meses tras la infección, lo que sostiene la hipótesis del papel crucial de este estadio en la transmisión de la enfermedad.

Las observaciones realizadas en condiciones de campo por los franceses Cuillé y Chelle en 1937, así como los experimentos de cohabitación realizados posteriormente por Pols (1960), Schulz (1960), Bigalke (1968) y Gollnick *et al*. (2015) han puesto de manifiesto que la introducción de animales infectados en rebaños libres de la enfermedad originaba la aparición de brotes. Sin embargo, se ha descrito que la cohabitación no era el único factor implicado, ya que en ocasiones la mera introducción de animales infectados no era suficiente para el contagio y los casos únicamente aparecían con un marcado carácter estacional en verano y otoño (Bigalke 1968). En los experimentos de Bigalke se observó prácticamente un 100% de transmisión de la infección al cabo de un año.

Desde el primer momento, se ha descrito un papel importante en la estacionalidad y en la transmisión de la enfermedad por parte de artrópodos hematófagos, como moscas de los establos (*Stomoxys calcitrans*), tábanos o incluso moscas TseTse (*Glossina brevipalpis*), al alimentarse de animales infectados, ya que el aparato bucal de dichos dípteros es lo suficientemente potente para romper quistes tisulares con localización superficial. Ya en 1968, Bigalke describió que la transmisión era posible si bien eran necesario un gran número de picaduras. Posteriormente, Lienard *et al.* (2013) también realizaron experimentos para investigar la capacidad de *Stomoxys* spp. de transmitir *B. besnoiti*, especulándose con la posibilidad de que la transmisión ocurre cuando la alimentación del artrópodo se ve interrumpida por un comportamiento defensivo del animal y finaliza la ingesta de sangre en otro animal (Lienard *et al.*, 2013). Dicho estudio demostró la capacidad de *Stomoxys* spp. para transferir bradizoítos procedentes de quistes tisulares de un animal crónicamente infectado a un recipiente con sangre. No obstante, en dichos experimentos no se demostró la transmisión a animales sanos. Dichos estudios también demostraron la presencia de ADN del parásito en el contenido intestinal hasta 24 h post-ingestión de sangre infectada por PCR cuantitativa, si bien no se analizó la posible viabilidad de los parásitos. En los experimentos de cohabitación llevados a cabo por Gollnick (2015), se detectó ADN de *Besnoitia* spp. en una de las moscas recolectadas durante el estudio. Posteriormente, Sharif *et al*. (2019) han demostrado que *Stomoxys calcitrans* es capaz de transmitir la infección de un animal crónicamente infectado a conejos susceptibles de una forma más eficiente que lo que se pensaba hasta el momento. Tal y como se ha comentado, desde los trabajos realizados en Sudáfrica se ha descrito una estacionalidad de la enfermedad, ya que la mayor parte de los brotes o nuevos casos ocurriendo en meses cálidos cuando el ganado comparte pastos y artrópodos

hematófagos están en su periodo de máxima actividad (Gutierrez-Exposito *et al.*, 2017b; Fernandez-Garcia *et al.*, 2010; Alzieu, 2007; Bigalke, 1968)

Por el contrario, hasta la fecha no se ha demostrado la transmisión venérea ya que no se ha detectado ADN del parásito en el semen de sementales infectados (Esteban-Gil *et al.*, 2014).

Por otra parte, hasta la fecha no se ha podido confirmar la transmisión vertical vía transplacentaria o lactogénica, si bien parece poco probable, ya que se ha demostrado un descenso de los anticuerpos precalostrales en terneros nacidos de hembras crónicamente infectadas (Shkap *et al.*, 1994; Hornok *et al.*, 2015a,b), así como la ausencia de ADN del parásito en el calostro de vacas seropositivas (Hornok *et al.*, 2015b).

Por último, se ha estudiado la transmisión mediante el consumo de ooquistes en diversas ocasiones. Estudios realizados en la antigua URSS identificaron al gato como HD (Peteshev *et al.*, 1974), ya que los gatos infectados con tejidos de ganado bovino crónicamente infectado eliminaron ooquistes que fueron infectivos para marmotas, ratones, cabras, ovejas y terneros, si bien dichos estudios no han logrado ser reproducidos posteriormente (Diesing *et al.*, 1988; Basso *et al.*, 2011; Marcén-Seral, 2011). Diesing (1988) también realizó una infección experimental en 1988 utilizando hasta seis especies de víboras y 12 especies de carnívoros y no se observó la eliminación de ooquistes en las heces. En sus trabajos también exploró la posibilidad de que aves carroñeras, como buitres, pudieran actuar como HD, no obteniéndose resultados concluyentes.

Los factores de riesgo de la besnoitiosis descritos hasta la fecha están relacionados con la transmisión del parásito y, por tanto, con el sistema de manejo (extensivo *vs* intensivo) al que se ven sometidos los animales, siendo la besnoitiosis bovina más frecuente en explotaciones de vaca nodriza. Prácticas comúnmente asociadas al manejo de razas de aptitud cárnica, como la monta natural y el uso de pastos compartidos, favorecen el contacto directo entre animales sanos e infectados, así como la exposición a artrópodos hematófagos y a posibles reservorios silvestres. En los últimos años se ha visto que una de las claves para la diseminación y reemergencia de la enfermedad es el movimiento de animales infectados procedentes de zonas donde la enfermedad es tradicionalmente endémica (como el Pirineo Francés) a zonas libres.

Dentro de los factores de riesgo, se ha descrito un aumento de la seroprevalencia con la edad de los animales (Bigalke, 1968; Fernández-García *et al*., 2010; Gutiérrez-Expósito *et al*., 2014). En la literatura, los casos de besnoitiosis bovina en animales jóvenes son raros, si bien se ha descrito recientemente un caso clínico de besnoitiosis crónica en un animal menor de seis meses (Diezma-Díaz *et al.*, 2017), y la detección de anticuerpos específicos en animales con edades comprendidas entre los seis y los 12 meses (Hornok *et al.*, 2014). Ambos hallazgos podrían sugerir un cierto papel protector de los anticuerpos calostrales, así como una cierta resistencia de los animales jóvenes a la infección, de una forma análoga a lo que ocurre en infecciones por hemoparásitos como *Babesia bovis* (Brown *et al.*, 2006). Algunos autores afirman que los signos clínicos se suelen observar, principalmente, en animales de 2 a 4 años (Fouquet, 2009; Jacquiet *et al*., 2010). El sexo del animal no se ha descrito como un factor de riesgo, o existe cierta controversia al respecto, al haberse descrito similares valores de seroprevalencia en machos y hembras (Alvarez-Garcia *et al.*, 2014b) o mayores valores de seroprevalencia tanto en machos (Lee *et al.*, 2017b) como en hembras (Ashmawy & Abu-Akkada, 2014). Ciertos autores describen que en el caso de los sementales la aparición de signos clínicos y de mortalidad puede ser más frecuente (Bigalke, 1968;

Jacquiet *et al*., 2010), pero esto puede verse influenciado por el hecho de que los sementales son los animales más valiosos del rebaño y captan más la atención de los veterinarios. No obstante, los trabajos de Gazzonis *et al*. (2017) realizados en un brote de besnoitiosis bovina, encontraron que los machos presentaban un mayor riesgo de ser infectados. Por otra parte, todas las razas son susceptibles a la infección, pero se ha descrito principalmente en razas de aptitud cárnica (p. ej. Afrikaner, Aubrac, Charolesa, Limusina, Conjunto Mestizo, Parda Alpina, Pirenaica y Rubia de Aquitania), asociada a las prácticas de manejo que son más frecuentes en este tipo de explotaciones. En el ganado lechero apenas se han realizado estudios (Alshehabat *et al.*, 2016; Ryan *et al.*, 2016) y se ha señalado que la fase aguda febril puede ocasionar abortos en las hembras infectadas y descenso de la producción lechera. Por último, se desconoce si fenómenos fisiológicos (como la gestación) o patológicos (coinfecciones con patógenos bovinos, como el virus de la diarrea vírica bovina, o el virus respiratorio sincitial bovino) que cursan con una inmunosupresión podrían favorecer el desarrollo de signos clínicos. De hecho, en diversos experimentos se indujo una inmunosupresión transitoria con dexametasona o permanente mediante la esplenectomización de los animales (Bigalke, 1968) con el objetivo de favorecer el desarrollo de los signos clínicos obteniéndose resultados variables al realizarse infecciones empleando distintos diseños experimentales y no controlarse la calidad de los inóculos.

2.1.5. Impacto

Desde su descripción a principios del siglo XX, la besnoitiosis bovina ha pasado prácticamente desapercibida hasta los últimos 20 años. Por ello, para explicar las claves de su reemergencia hemos de considerar los mecanismos de transmisión descritos hasta la fecha y todas aquellas prácticas ligadas a los sistemas de manejo que se han considerado como factores de riesgo junto con aquellos cambios producidos recientemente que han afectado al sector del vacuno de carne. En relación a esto último, podemos destacar los cambios producidos por las políticas de la Unión Europea, dirigidas a aumentar el censo de explotaciones de ganado bovino de carne gracias a las ayudas de la Política Agraria Comunitaria (PAC), el comercio e introducción de animales procedentes de zonas donde la enfermedad ha sido tradicionalmente endémica (como el Pirineo Francés) para mejorar los caracteres productivos de razas bovinas autóctonas, fundamentalmente animales de razas Limusina y Charolesa; así como el cambio climático que podría favorecer un aumento de la actividad de artrópodos hematófagos y, por tanto, la transmisión mecánica durante un mayor número de meses al año al ampliarse el periodo estival.

2.1.5.1. Distribución geográfica, prevalencia e incidencia

La besnoitiosis bovina se ha descrito en varios países del África subsahariana, primero fue descrita en Sudáfrica y, posteriormente, en otros países (Angola, Botswana, Congo, Kenia, Namibia, Ruanda, Sudáfrica, Sudán, Tanzania, Uganda y Zimbabue) (revisado por Chatikobo *et al.*, 2013; Habarugira *et al*., 2019); en Asia (China, Corea del Sur, Israel, Kazajistán, Rusia y Uzbekistán)(revisado por Olias *et al.*, 2011), en el continente americano (Venezuela)(Vogelsgang y Gallo, 1941; Uzeda *et al.*, 2014) y en Europa (Portugal, España, Francia, Alemania, Suiza, Italia, Croacia, Hungría, Bélgica e Irlanda) (Ryan *et al.*, 2016; Álvarez-García *et al.*, 2016; Gutiérrez-Expósito *et al.*, 2017a). No

obstante, dada la falta de estudios, se desconoce la situación epidemiológica y la distribución geográfica actual de la misma en África, Asia y el continente americano.

En lo concerniente al continente europeo, la enfermedad se consideró restringida a zonas como el Alentejo portugués o el Pirineo francés, donde se realizaron las primeras descripciones de la misma (Besnoit & Robin, 1912; Franco & Borges, 1915). A partir de los años 90 esta enfermedad vuelve a cobrar importancia al diseminarse a lo largo del Alentejo portugués (Cortes *et al*., 2004; 2005; 2006; 2014), en España, Francia y en otros países limítrofes como Italia, Suiza o Alemania (Alzieu, 2007; Schares *et al.*, 2009; Fernandez-Garcia *et al.*, 2010; Gentile *et al.*, 2012; Basso *et al.*, 2013). Por último, en países como Alemania, Suiza, Croacia, Hungría y, más recientemente, Bélgica o Irlanda, las descripciones de la enfermedad son escasas y se limitan únicamente a la descripción de brotes epidémicos tras la introducción, posiblemente, de animales subclínicamente infectados procedentes de Francia (Schares *et al.*, 2009; Beck *et al.*, 2013; Basso *et al.*, 2013; Hornok *et al.*, 2014; Alvarez-Garcia, 2016; Ryan *et al.*, 2016).

En España, la primera descripción tuvo lugar en granjas localizadas en Navarra y Vizcaya por Juste *et al*. (1990), volviéndose a detectar posteriormente en animales de Navarra y el Pirineo Central (Irigoien *et al.*, 2000; Zacarias, 2009). Resultados posteriores de Álvarez-García *et al.* (2014a) han demostrado qué, en la Comunidad Foral de Navarra, la infección está diseminada en el ganado de carne en zonas de montaña (Pirineo y Sierra de Urbasa-Andía), donde la enfermedad se considera endémica (European Food Safety Authority, 2010; Álvarez-García *et al.*, 2013). La enfermedad hoy en día ya está presente de forma endémica también en otras zonas como la Sierra del Maestrazgo (Teruel), País Vasco, Castilla y León, La Rioja, Madrid, Guadalajara y Extremadura. Al igual que en el caso francés, se ha producido una notable diseminación hacia el centro y suroeste del país, con nuevos casos en Madrid, Castilla-La Mancha, Extremadura y Andalucía (Fernandez-Garcia *et al.*, 2010; Nieto-Rodríguez *et al.*, 2016; Diezma-Díaz *et al.*, 2017). En los estudios de prevalencia se han obtenido valores de seroprevalencia variables, hallándose prevalencias intra-rebaño superiores al 30% en la Sierra de Urbasa Andía (Zacarias, 2009). Posteriormente, Álvarez-García *et al*. (2014a) encontraron seroprevalencias individuales del 16% en ganado de carne frente a un 0% en ganado de leche en un estudio transversal realizado en Navarra. Recientemente, se han llevado a cabo estudios de prevalencia y dinámica de la infección en el Pirineo Central y la Sierra de Urbasa-Andía para conocer la situación actual en las zonas donde la enfermedad era tradicionalmente endémica. Dichos estudios han mostrado una alta prevalencia e incidencia de la infección, con un 87,3% de granjas seropositivas en el Pirineo y con una seroprevalencia individual en torno al 50% independientemente del sexo. En la Sierra de Urbasa Andía se han obtenido resultados similares, con una seroprevalencia intrarebaño que oscilaba entre el 35,6% y el 86,5% (Gutiérrez-Expósito *et al.*, 2017d). Además, Esteban-Gil *et al*. (2017) estudiaron el patrón epidemiológico en un rebaño con besnoitiosis endémica en los Pirineos, observándose una seroprevalencia individual del 38,34%, con un 18% de los animales seropositivos con signos clínicos. Recientemente, Garrido-Castañé *et al*. (2019) han detectado anticuerpos específicos en el ganado de aptitud cárnica en la región de los Pirineos catalanes, con una seroprevalencia individual del 25,1%, pero no detectaron anticuerpos en ganado de lidia o de aptitud lechera.

En cuanto a la incidencia, el único estudio realizado en España se ha llevado a cabo en la Sierra de Urbasa y Andía (zona en la que la enfermedad es endémica), describiéndose tasas de incidencia serológica y clínica del 22 y 12%, respectivamente, lo que indica una alta circulación del parásito en el rebaño (Gutiérrez-Expósito *et al.*, 2017d).

2.1.5.2. Patogenia, signos clínicos y lesiones

En un rebaño infectado, la gravedad y y los signos clínicos pueden variar en función de si se trata de una zona donde la enfermedad es endémica o estamos ante un brote epidémico, donde hasta un 40% del efectivo puede desarrollar signos clínicos variados y compatibles con una infección aguda o crónica. Se ha descrito que los signos clínicos pueden pasar desapercibidos si la carga parasitaria es baja. Las tasas de mortalidad descritas hasta el momento son bajas (inferiores al 10%) y pueden producirse tanto en la fase aguda como en la fase crónica de la enfermedad (Pols, 1960; Schulz, 1960; European Food Safety Authority, 2010; Álvarez-García *et al.*, 2014b).

A pesar de que en la actualidad se desconoce la ruta y el estadio responsables de la transmisión en los casos de infección natural, en diversos experimentos de transmisión se ha observado que el periodo de incubación es muy variable y que los primeros signos clínicos pueden aparecer entre 1 a 13 días post-infección, dependiendo de la ruta, con un tiempo medio de 13 días en infecciones naturales (Bigalke, 1968; Basson *et al.*, 1970; Bigalke *et al.*, 2004; Gollnick *et al.*, 2015)

Posteriormente, la enfermedad progresa de forma secuencial con dos fases bien diferenciadas: i) la fase aguda, durante la cual se observan signos clínicos inespecíficos originados por la multiplicación rápida de los taquizoítos en el interior de células endoteliales de los vasos (Langenmayer *et al.*, 2015c). Durante esta fase los animales desarrollan fiebre, edemas en zonas declives hasta 4-5 semanas post-infección (lo que en ocasiones se ha denominado fase de anasarca); y ii) la fase crónica, en la que se observan los signos clínicos cutáneos más característicos de la enfermedad, originados por el estadio de bradizoíto en el interior de quistes tisulares localizados preferentemente en el tejido subcutáneo de diversas localizaciones.

El desarrollo de los primeros quistes tisulares puede coincidir en el tiempo con signos clínicos de fase aguda, ya que se ha descrito el desarrollo de los mismos a partir de los 11 días post-infección (Basson *et al.*, 1970).

2.1.5.2.1. Fase aguda (febril):

Tras la infección, el primer signo clínico en aparecer suele ser la hipertermia, con temperaturas superiores a 39ºC que llegan a alcanzar 40,8 – 41,6 ºC (Pols, 1960; Bigalke, 1968, Givens y Marley, 2008; Gollnick *et al*., 2015) seguida de otros signos clínicos inespecíficos que frecuentemente pasan desapercibidos, tales como: depresión, linfadenomegalia de los linfonodos superficiales (p. ej. precrural, preescapular), pérdida de apetito y peso, fotofobia, descarga ocular y nasal así como taquicardia o taquipnea (Pols, 1960; Schulz, 1960; revisado por Álvarez-García *et al*., 2014b). La hipertermia puede ocasionar de forma indirecta abortos en hembras gestantes (Nobel *et al.*, 1981).

Durante esta fase aguda febril, que tiene una duración variable y puede extenderse entre 3 y 10 días, los taquizoítos, como parásitos intracelulares obligados, van a invadir y a proliferar en el interior de células endoteliales de los vasos sanguíneos, causando edemas, lesiones degenerativas y necróticas, vasculitis y trombosis que dan lugar a congestión, hemorragias y zonas infartadas (Pols, 1960; Basson *et al.*, 1970). Una vez se ha producido la replicación activa del parásito en el interior de las células diana se produce la egresión de los taquizoítos y rotura de la misma, lo que da lugar al daño tisular. Los taquizoítos se han observado en sangre circulante (parasitemia) desde el

tercer hasta el decimosegundo día desde la aparición de la reacción febril (Bigalke, 1968; Basson *et al.*, 1970; Diezma-Díaz *et al.*, 2017, 2018). Se ha sugerido también que la alteración de la permeabilidad de los vasos sanguíneos podría deberse a un efecto tóxico del parásito (Bigalke *et al.*, 2004). El edema se origina en las partes declives de cabeza y cuello y progresa a las extremidades y partes ventrales del cuerpo (Pols, 1960; Basson *et al.*, 1970). Los edemas en las articulaciones de las extremidades pueden ocasionar cojeras dolorosas y los animales infectados rehúsan moverse (Fernández-García *et al.*, 2010). En los casos más graves pueden aparecer signos respiratorios debido al desarrollo de edemas alveolares e intersticiales en el pulmón, que pueden ocasionar la muerte por fallo cardiorrespiratorio. La piel se encuentra tumefacta, engrosada y con dolor al tacto. El parásito también puede ocasionar una oftalmitis aguda, acompañada de lagrimeo y fotofobia (McCully *et al.*, 1966). Los sementales, durante la fase aguda, pueden desarrollar una orquitis dolorosa y con edema a nivel escrotal (Cortes *et al.*, 2005). La piel del escroto aparece caliente al tacto, engrosada y dolorosa a la palpación (Figura 3).

Las lesiones de fase aguda se han visto más frecuentemente asociadas con venas de pequeño-mediano calibre, así como arterias cutáneas y testiculares (McCully *et al.*, 1966; Basson *et al.*, 1970; Langenmayer *et al.*, 2015c). Por tanto, se asume que las células endoteliales y las lesiones vasculares en órganos diana tienen un papel crucial en la patogénesis de la besnoitiosis bovina. De hecho, Langenmayer *et al*. (2015), describieron la aparición de vacuolas parasitóforas conteniendo entre 2 y 5 zoítos en el interior de células endoteliales de los vasos sanguíneos en un animal durante sus experimentos de cohabitación. En el tracto respiratorio superior se ha descrito la aparición de hemorragias, necrosis, formación de pseudomembranas, edemas y erosiones. Además, aunque no se ha descrito en más ocasiones, en un semental infectado en Sudáfrica, que murió durante la fase aguda de la enfermedad, se describió un síndrome nefrótico acompañado de hipoalbuminemia, proteinuria y leucocitosis (Dubey *et al*., 2013).

Figura 3: Signos clínicos de las fases aguda (A,D) y crónica (B, C, E, F) de la besnoitiosis bovina (adaptado de Gutiérrez-Expósito *et al.*, 2017a).

A: orquitis durante la fase aguda de la besnoitiosis bovina; B: quistes tisulares macroscópicos en la conjuntiva ocular; C: degeneración testicular; D: Cojeras; E: Hiperqueratosis y zonas de alopecia; F: grietas y heridas en pezones.

2.1.5.2.2. Fase crónica

Al instaurarse una respuesta inmunitaria por parte del hospedador frente a la infección, los taquizoítos se convierten al estadio de multiplicación lenta o bradizoítos, que se localizan en el interior de quistes tisulares presentes en el tejido conectivo de diversas localizaciones, como la piel, el tracto respiratorio superior (cornetes nasales, epiglotis y tráquea) y el tracto genital. No obstante, los quistes tisulares también se han descrito en diversos órganos internos (McCully *et al.*, 1966; Nobel *et al.*, 1981; Frey *et al.*, 2013; Diezma-Díaz *et al.*, 2017). Se ha descrito que los quistes tisulares tienen como células diana histiocitos o miofibroblastos (Dubey *et al.*, 2013).

Durante la fase crónica, conocida como fase de escleroderma, se produce un deterioro gradual de la condición corporal, pérdida de peso y, ocasionalmente, mortalidad. Además, a partir de las 6-7 semanas post-infección, se pueden observar quistes tisulares macroscópicos que se visualizan inicialmente en las conjuntivas palpebral y esclerótica y, posteriormente, en el vestíbulo vaginal, los cuales muchas veces constituyen el único signo de enfermedad y son considerados patognomónicos de la misma (Pols, 1960; Bigalke, 1968,1981; Fernández-García *et al.*, 2010; Rostaher *et al.*, 2010; Gollnick *et al.*, 2015;). Éstos también se desarrollan en el endotelio, dermis, fascias, mucosa del tracto respiratorio superior, faringe, y en los machos, en el testículo y en el epidídimo, entre otras localizaciones. Curiosamente, se ha detectado recientemente la capacidad del parásito de atravesar la barrera hematoencefálica, con detección de ADN del mismo a nivel del sistema nervioso central (SNC) de bovinos en dos ocasiones (Basso *et al.*, 2013; Diezma-Díaz *et al.*, 2017). De hecho, Arnal *et al*. (2017) describieron quistes en el SNC de un corzo infectado con *B. besnoiti*.

Debido al desarrollo de los quistes tisulares (Figura 4) en el tejido subcutáneo de diversas localizaciones, se produce un engrosamiento, endurecimiento y formación de pliegues en la piel de los animales infectados, dando lugar a lo que se conoce como "piel de elefante" (Bigalke, 1981). En las zonas más parasitadas se produce alopecia e incluso necrosis de la epidermis. En los sementales, se han detectado quistes tisulares en diversas localizaciones del tracto genital, como las paredes vasculares del plexo pampiniforme (Kumi-Diaka *et al.*, 1981) o entre los túbulos seminíferos (Kumi-Diaka *et al.*, 1981; Dubey *et al.*, 2013). Por tanto, una disminución del aporte sanguíneo, junto con la necrosis del parénquima testicular y el engrosamiento de la piel del escroto podrían ser los responsables de la azoospermia (Bigalke, 1968,1981; Kumi-Diaka et al., 1981; Bigalke *et al.*, 2004). Además, en machos subclínicamente infectados, se ha descrito una peor calidad del semen descongelado, con peor motilidad de espermatozoides (Cortes *et al.*, 2006d). No obstante, no se describieron cambios en el semen fresco obtenido de los mismos animales.

Figura 4: Quistes tisulares con bradizoítos en su interior, presentes en un corte histológico de piel teñido con hematoxilina-eosina (H-E)

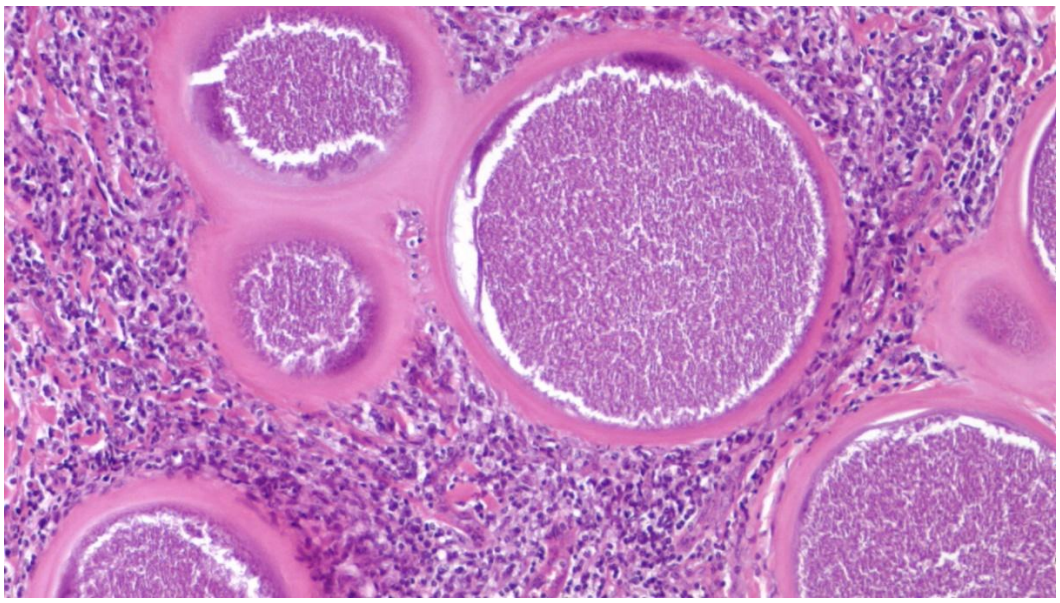

Por el contrario, en las hembras aparecen grietas y nódulos visibles en los pezones (Figura 3). A pesar de encontrarse crónicamente infectadas, las hembras pueden quedarse preñadas y los quistes tisulares se localizan de forma preferencial en el tracto genital distal (vestíbulo vaginal y vulva), aunque también se han descrito a nivel del miometrio y endometrio de cuernos uterinos (Nobel *et al.*, 1981; Frey *et al.*, 2013). Recientemente, se ha descrito la existencia de ADN de *B. besnoiti* a nivel de ovario (Diezma-Díaz *et al.*, 2017).

También se ha descrito la aparición de laminitis crónicas y úlceras en las pezuñas (Gollnick *et al.*, 2015). Con el tiempo, los animales crónicamente infectados pueden experimentar una aparente recuperación clínica y ser resistentes a las reinfecciones, pero permanecen infectados de por vida y su producción puede quedar mermada (Kumi-Diaka *et al.*, 1981; Nobel *et al.*, 1981; Frey *et al.*, 2013).

2.1.6. Diagnóstico

El diagnóstico clínico de la besnoitiosis aguda a veces es difícil, ya que los signos clínicos son inespecíficos y pueden pasar desapercibidos. Por otra parte, el diagnóstico serológico puede arrojar resultados falsos negativos ya que los animales tardan en seroconvertir al menos 3 semanas y el diagnóstico molecular tampoco es de ayuda, ya que la parasitemia es esporádica. En la fase crónica, la aparición de signos clínicos y lesiones más característicos permite orientar el diagnóstico. No obstante, el diagnóstico de la besnoitiosis bovina debe contemplar el diagnóstico epidemiológico, una exhaustiva inspección clínica y el diagnóstico laboratorial. Previamente a la visita a la explotación en la que han surgido los problemas, conocer la situación epidemiológica de partida es esencial, es decir, si la explotación está localizada en una zona donde la enfermedad es endémica o, por el contrario, en una zona libre y si se han introducido en el rebaño nuevos animales recientemente. A continuación, se realizará la inspección clínica en la que se tendrá en cuenta el diagnóstico diferencial con otras enfermedades que cursan con signos clínicos similares durante la fase aguda y crónica. (p.ej. lengua azul, dermatofitosis o sarna, entre otras (Cortes *et al.*, 2014). Durante la fase crónica, la detección macroscópica de quistes tisulares en la conjuntiva ocular tiene un gran valor

diagnóstico, ya que estos son patognomónicos de la enfermedad (Bigalke & Naude, 1962; Njagi *et al.*, 1998; Álvarez-García *et al.*, 2014b). En cualquier caso, el diagnóstico clínico siempre irá acompañado del diagnóstico laboratorial.

En la actualidad existen diferentes técnicas laboratoriales para la detección de la infección por *B. besnoiti*, tanto directas (basadas en la detección del parásito o su ADN) como indirectas (para la detección de anticuerpos específicos frente al mismo, como IFI, ELISA o WB) (revisado por Gutiérrez-Expósito *et al*., 2017a).

Dentro de las técnicas de diagnóstico directas cabe destacar la realización de una biopsia de piel de las zonas más afectadas para la observación mediante compresión entre dos placas de cristal ("placas de triquineloscopía") en búsqueda de quistes tisulares. También existen pruebas basadas en el empleo de la PCR comerciales y caseras, si bien su uso no es rutinario.

Las técnicas de diagnóstico indirecto desarrolladas hasta la fecha son pruebas serológicas basadas en la detección de anticuerpos específicos frente a *B. besnoiti* y son las que se utilizan para el diagnóstico rutinario de la besnoitiosis bovina, ya que permiten corroborar los resultados del diagnóstico directo así como detectar animales infectados de una forma subclínica, los cuales no presentan signos clínicos evidentes y en los que el número de quistes es bajo (Fernández-García *et al.*, 2010; Frey *et al.*, 2013). Se han desarrollado diferentes técnicas serológicas, como la inmunofluorescencia indirecta (IFI), la microaglutinación en placa (MAT), técnicas de enzimoinmuno ensayo (ELISA) y WB, siendo estas dos últimas las más utilizadas. La prueba ELISA es la técnica más utilizada a la hora de analizar un gran número de muestras, encontrándose disponibles varias pruebas ELISA comerciales (INGEZIM BES 12.BES.K1 INGENASA, ID Screen *Besnoitia* indirect 2.0, ID Screen *Besnoitia* milk, IDVET) y ELISAs caseros (García-Lunar *et al.*, 2013a, 2017). Recientemente, se ha desarrollado un ELISA indirecto basado en el uso de taquizoítos liofilizados (García-Lunar *et al.*, 2017), que mejora la sensibilidad y especificidad para el diagnóstico de la infección por *B. besnoiti* en el ganado bovino y en los rumiantes silvestres.

Si tras la realización de pruebas diagnósticas obtenemos un resultado positivo es importante adoptar medidas de manejo dirigidas a evitar la diseminación de la enfermedad. Si ambos resultados son negativos se considerará al animal como no infectado. No obstante, puede haber resultados discordantes entre las pruebas serológicas y el cuadro clínico que presenta el animal, en cuyo caso se recomendará re-muestrear al animal transcurrido un plazo de dos-tres semanas para confirmar el resultado mediante la prueba de WB.

2.1.7. Control

En la actualidad no existen fármacos disponibles frente a la besnoitiosis bovina ni vacunas autorizadas en Europa. Por lo tanto, las medidas de bioseguridad junto con un diagnóstico precoz juegan un papel crucial en el control de la misma.

2.1.7.1. Bioseguridad y Biocontención

Este control debería tener dos objetivos principales: por un lado, evitar la entrada de la infección al rebaño (bioseguridad) y, por otro, evitar su diseminación en el caso de un rebaño ya infectado (biocontención).

En las regiones libres se han de adoptar medidas para evitar la entrada de la infección en los rebaños. La mayoría de los brotes descritos en diferentes países europeos han ocurrido tras la introducción de animales portadores cuyo estado sanitario previo se desconocía. Por ello, realizar un diagnóstico clínico y serológico de los animales antes de su entrada al rebaño durante la cuarentena, así como evitar en la medida de lo posible prácticas de riesgo que favorecen la transmisión como la monta natural con machos de estado sanitario desconocido y el contacto con rebaños de estatus sanitario inadecuado, debe ser fundamental. Evitar la diseminación de la enfermedad en una granja ya infectada es más complejo. Una estrategia a largo plazo consiste en mantener un equilibrio entre el sacrificio selectivo y las producciones. Puesto que la seroprevalencia puede llegar a ser muy elevada en un rebaño infectado, el sacrificio de todos los animales seropositivos resulta inviable desde un punto de vista económico. Por ello, sólo los animales más gravemente afectados o improductivos deberían ser reemplazados por animales sanos y seronegativos, que se mantendrán aislados del resto del rebaño infectado y con un manejo separado en la medida de lo posible. En el grupo de hembras infectadas se recomienda el uso de la inseminación artificial ya que el riesgo de que un semental recién introducido adquiera la infección es elevado. Si esto no fuera posible, se empleará un semental seropositivo cuya calidad seminal se monitorizará regularmente. Un objetivo asumible sería tratar de evitar la aparición de signos clínicos en el rebaño a pesar de que la infección esté presente.

2.1.7.2. Immunoprofilaxis

Para el control de otras enfermedades ocasionadas por protozoos Toxoplasmatinae, la vacunación se ha considerado como una de las opciones más rentables y eficaces (Zhang *et al.*, 2013; Horcajo *et al.*, 2016;). En el caso de la besnoitiosis, en el pasado se desarrollaron dos vacunas vivas atenuadas en Sudáfrica e Israel (Bigalke *et al.*, 1974; Shkap, 1986), demostrándose que, tanto el empleo de un aislado atenuado procedente de ñu como de un bovino crónicamente infectado, evitaba la aparición de signos clínicos en prácticamente la totalidad de los animales vacunados. No obstante, no se han realizado estudios de seguridad ni controles exhaustivos de calidad del inóculo. En particular, la vacuna empleada en Israel consiste en la inoculación subcutánea de $2x10^8$ taquizoítos criopreservados en DMSO (Gutiérrez-Expósito, 2016).

2.1.7.3. Quimioprofilaxis

Al igual que en el caso de la vacunación, el empleo de tratamientos farmacológicos se considera una de las opciones más adecuadas para el control de enfermedades ocasionadas por protozoos apicomplejos teniendo en cuenta el binomio coste-beneficio (Sánchez-Sánchez *et al.*, 2018). No obstante, pese a los esfuerzos realizados hasta la fecha, en la actualidad no hay ningún fármaco que haya demostrado eficacia en la especie de destino frente a la besnoitiosis. Los estudios disponibles han analizado la posible eficacia tanto de fármacos ya comercializados frente a otras infecciones protozoarias como de fármacos de reciente generación frente a la infección por *B. besnoiti*.

2.1.7.3.1. Fármacos empleados hasta la fecha

Desde la aparición de la enfermedad se ha tratado de combatir los signos clínicos cutáneos de la fase crónica con sustancias de diversa procedencia y eficacia dudosa (Tabla 3), como el empleo de formol por vía intravenosa por los franceses Berthelon y Labeyre en 1938 (revisado por Franc & Cardiegues, 1999), formol al 10% durante las fases aguda y crónica de la enfermedad por Leitao en Portugal (1949) y Herin en Ruanda (1952) con supuestos efectos beneficiosos, e incluso aceite de motor y compuestos organoclorados por parte de ganaderos africanos descrito por Schulz (1960). También se postuló que el tratamiento tópico de las lesiones cutáneas típicas de la besnoitiosis bovina con un extracto procedente de un hongo (*Mycena chlorophos*) junto con la administración intravenosa de Lugol mejoraba los signos clínicos (Uvaliev & Baiagaziev, 1979). Posteriormente, otras experiencias llevadas a cabo en Francia con ganado naturalmente infectado demostraron que, por ejemplo, la administración parenteral de sulfametazina al 33% (30-50 mL/100 Kg peso vivo/48 h) era eficaz durante la fase aguda de la enfermedad; el tratamiento con toltrazuril diluido con agua y propilenglicol (po, 80 mL/100 Kg peso vivo) resultaba muy costoso y arrojaba resultados muy variables. Por otra parte, el uso de dos inyecciones de parvacuona (Clexon®) vía intramuscular a una dosis de 40 mg/Kg administradas con un intervalo de 48 h reducía los signos clínicos y eliminaba los quistes tisulares en un tercio de los animales tratados (Sahun, 1998).

Más recientemente, los datos obtenidos en animales infectados de forma natural y tratados con sulfonamidas han demostrado que, a pesar de ser comúnmente utilizadas para tratar de disminuir la gravedad de los signos clínicos, son incapaces de curar el ganado infectado y es frecuente la aparición de recidivas, incluso cuando el tratamiento se inicia al detectarse los primeros signos clínicos compatibles con la fase aguda (Jacquiet *et al.*, 2010). Asimismo, varios estudios han explorado la posible eficacia de la oxitetraciclina, tanto en animales infectados experimentalmente como en condiciones de campo. En animales naturalmente infectados, la administración de 3 inyecciones cada 48 h de oxitetraciclina a una dosis de 10 ml/100 kg durante la fase aguda de la enfermedad resultó beneficiosa (Franc & Cardiegues, 1999).

Tabla 2: Compuestos probados frente a *B. besnoiti in vivo*, tanto en ganado bovino como en animales de experimentación

Compuesto	Especie	Referencia
Formol	Ganado bovino, conejos	Pols, 1960; Franc & Cardiegues, 1999
Mycena clorophos	Ganado bovino	Uvaliev & Baigaziev, 1979
Lugol	Ganado bovino	Uvaliev & Baigaziev, 1979
Parvacuona	Ganado Bovino	Sahun, 1998
Sulfadiazina	Gerbos	Shkap *et al.*, 1987b
Sulfamerazina	Gerbos	Shkap *et al.*, 1987b
Sulfametazina	Gerbos, Ganado bovino	Shkap *et al.*, 1987b; Sahun, 1998
Sulfadoxina	Gerbos	Shkap *et al.*, 1987b
Pirimetamina	Gerbos	Pols, 1960; Shkap *et al.*, 1987b
Trimetoprim	Gerbos	Pols, 1960; Shkap *et al.*, 1987b
Aceturato de diminaceno	Gerbos	Shkap *et al.*, 1987b
Pentamidina		Shkap *et al.*, 1987b
Lactato de halofuginona	Gerbos	Shkap *et al.*, 1987b
Oxitetraciclina (OT) ; OT de acción larga	Gerbos, Conejos, Ganado bovino	Franc & Cardiegues, 1999; Shkap *et al.*, 1985, 1987b; Pols, 1960
Toltrazurilo	Ganado bovino	Sahun, 1998

Tabla 3: Compuestos probados frente a *B. besnoiti in vitro*.

Compuesto	Línea celular	Referencia
Oxitetraciclina	Vero	Shkap *et al.*, 1987b
Lactato de halofuginona	Vero	Shkap *et al.*, 1987b
Nitazoxanida, Tizoxanida	Vero	Cortes *et al.*, 2007a
Arilimidamides	Vero/HFF	Cortes *et al.*, 2011
Bifenillmidazotiazoles	HFF	Moine *et al.*, 2015
Buparvacuona	HFF	Müller *et al.*, 2018
Curcumina	BUVEC	Cervantes-Valencia *et al.*, 2018

Los tratamientos *in vivo* también han sido estudiados en animales de experimentación (conejos y gerbos) durante la fase febril de la enfermedad (Tabla 2). Pols (1960) investigó la eficacia de diferentes fármacos (formalina, pentamidinas, sulfamidas, trimetroprim, pirimetamina y oxitetraciclinas, entre otras) en conejos, sin obtener resultados satisfactorios. Por el contrario, Shkap *et al*. (1985) previno el desarrollo de orquitis en conejos con oxitetraciclina (30 mg/kg) por vía intramuscular tras el desafío con 10^6 taquizoítos de *B. besnoiti* por vía intraperitoneal. En el caso de los gerbos (*Meriones tristami*), la única droga efectiva fue la oxitetraciclina, capaz de reducir los signos clínicos de la fase aguda en 24-48 h tras la administración por vía intramuscular a una dosis de 200 mg/kg. Sin embargo, este mismo compuesto no fue efectivo durante el ensayo *in vitro* (Shkap *et al*., 1987b).

Además, la eficacia de varios compuestos ha sido estudiada *in vitro*, utilizando distintos modelos y con resultados variables (Tabla 3).

A pesar de todos los esfuerzos realizados, hoy en día no hay ningún fármaco comercializado eficaz frente a la infección por *B. besnoiti*. Sin embargo, se ha descrito que durante la fase crónica de la infección el tratamiento con antibióticos, antiinflamatorios y una buena alimentación tiene un cierto efecto beneficioso (Bigalke *et al.*, 2004).

El reposicionamiento farmacológico, es decir, el empleo de fármacos comercializados frente a otras infecciones en busca de su eficacia frente a otra enfermedad representa una alternativa económicamente viable y que permitiría disponer de fármacos eficaces para el control de la besnoitiosis bovina en un corto-medio plazo de tiempo. Esta estrategia ha sido empleada frente a otros parásitos relacionados, como *N. caninum* (Müller *et al.*, 2015), *T. gondii* (Dittmar *et al.*, 2016)) o *Cryptosporidium parvum* (Bessoff *et al.*, 2014), con resultados satisfactorios. En este contexto, la buparvacuona, que se emplea frente a la infección por *Theileria* spp. en EE.UU., ha demostrado buenos resultados *in vitro* frente a los taquizoítos de *B. besnoiti* (Müller *et al.*, 2018), pero su uso en especies destinadas a consumo humano no está autorizado en Europa. Además, los estudios realizados hasta la fecha demuestran la capacidad de los taquizoítos de adaptarse a concentraciones crecientes de este compuesto, si bien se desconoce el mecanismo de adaptación (Müller *et al.*, 2018). Recientemente, se ha demostrado la eficacia de extractos obtenidos de cúrcuma (*Curcuma longa*) frente a taquizoítos de *B. besnoiti in vitro,* reduciendo la viabilidad y motilidad de los mismos y mostrando una CI50 de 5,93 µM (Cervantes-Valencia *et al.*, 2018) (Tabla 3).

En la Tabla 4 se muestran los fármacos comercializados en bovino y que son eficaces frente a otras infecciones ocasionadas por protozoos apicomplejos.

Tabla 4. Compuestos comercializados en Europa para su empleo en el ganado vacuno y eficaces frente a infecciones ocasionadas por protozoos apicomplejos.

Familia química	Mecanismo de acción	Uso comercial			Eficacia *in vitro* frente a *N. caninum* /*T. gondii*/*B. besnoiti*	Referencias
		Parásito	Especie animal	Compuesto comercial		
Triazinonas						
Toltrazurilo	Inhibición de enzimas en la cadena respiratoria, Inhibición de la citoquinesis (endodiogénesis)	*Eimeria* e *Isospora* spp.	Aves, Ganado porcino, Ganado bovino	Baycox®, Bayer	Sí/Sí/ND	Darius *et al*., 2004
Diclazurilo	Apicoplasto, Inhibición de la citoquinesis (endodiogenesis)	Eimeria spp.	Aves, Ganado bovino	Vecoxan®, Elanco-Lilly	Sí/ND/ND	Lindsay & Blagburn, 1994; Lindsay *et al.*, 1995
Carbanilidas						
Imidocarb	Metabolismo del inositol y entrada en el eritrocito	*Babesia* spp.	Ganado bovino	Imizol®, MSD Animal Health	ND/ND/ND	Hines *et al.*, 2015
Inhibidores Dihibrofolatoreductasa (DHFR)-Dihidrofolato sintasa (DHFS)						
Sulfadiazina Trimetoprim	Síntesis de folatos, bloqueo secuencial (efecto sinérgico)	*T. gondii* (Toxoplasmosis humana)	Ganado bovino	Farcotrim®, CZV	Sí/Sí/Sí* (más eficaz frente a *T. gondii*)	Shkap et al., 1985, 1987b; Lindsay *et al.*, 1994
Quinolonas						
Decoquinato	Inhibición respiración celular mitocondrial (complejo bc1)	*Eimeria* spp.	Ganado bovino y caprino, avicultura	Deccox®, Zoetis	Sí/Sí/ND	Lindsay *et al.*, 1996, 1997

*Datos procedentes de intentos de tratamiento realizados en condiciones de infección natural *in vivo.*

ND: datos no disponibles

2.1.7.3.2. Fármacos de nueva generación

Actualmente, en la investigación de nuevas dianas y candidatos terapéuticos frente a protozoos apicomplejos, inicialmente el cribado de fármacos se lleva a cabo en modelos *in vitro*. Los estudios realizados hasta el momento han arrojado resultados prometedores en *B. besnoiti* utilizando varios fármacos de nueva generación como tiazolidas y arilimidamidas (Cortes *et al.*, 2011; Cortes *et al.*, 2007a)o bifenilimidazoazinas (Moine *et al.*, 2015). Las nitro-tiazolidas, nitazoxanida y derivados bromados han demostrado inhibir la proliferación de taquizoítos de *B. besnoiti* en células Vero a concentraciones de 5 y 10 µg por mL, pero estos compuestos no son capaces de inhibir la invasión de la célula hospedadora. En el caso de las bifenilimidazozoazinas, el compuesto 8e mostró una concentración inhibitoria (CI) 50 de 0,37 +/- 0,07 µM frente a *B. besnoiti* al ser administrado a monocapas de fibroblastos de prepucio humanos (HFF) infectadas con un aislado procedente del sur de Francia (Moine *et al.*, 2015).

En los últimos años se han realizado numerosos estudios con los fármacos inhibidores de las protein-quinasas dependientes de calcio (CDPKs), que pertenecen a la superfamilia de las serín-treonín-quinasas. Estas enzimas están conservadas en el subfilo Apicomplexa pero están ausentes en las células de mamíferos. Una característica estructural de la CDPK1 que se encuentra en protozoos apicomplejos reside en el hecho de que ésta presenta un aminoácido poco voluminoso (Glicina, Gly) en lugar de aminoácidos más voluminosos que se encuentran en las quinasas de mamíferos (p. ej. la metionina) y que se ubica en la entrada del bolsillo hidrofóbico de la unión al ATP en el sitio activo de la enzima. Esta diferencia estructural ha permitido el diseño de inhibidores selectivos de estas quinasas denominados "*bumped kinase inhibitors*" (Van Voorhis *et al.*, 2017), inhibidores competitivos del ATP que impiden la activación de la enzima al contener un anillo pirazolopirimidínico. Dichos inhibidores han demostrado una gran eficacia inhibiendo el crecimiento de protozoos estrechamente relacionados con *B. besnoiti* como *T. gondii*, *N. caninum*, *Babesia* spp., *Theileira* spp. *C. parvum*, *Plasmodium* spp., tanto *in vitro* como *in vivo* (Tabla 5) y la eficacia de algunos de estos compuestos se está valorando en estudios preclínicos, siendo el compuesto 1294 uno de los más prometedores (Van Voorhis *et al.*, 2017). En *T. gondii* se ha demostrado un papel esencial de la CDPK1 para el movimiento ("*gliding*"), así como en la invasión y egresión de la célula hospedadora, regulando procesos dependientes del calcio como la secreción de proteínas de los micronemas (Johnson *et al.*, 2012; Lourido *et al.*, 2012). Por su parte, la CDPK4 en *P. falciparum* juega un papel clave en los estadios sexuales, siendo importante para la exflagelación de los microgametos (Ojo *et al.*, 2012). La importancia de esta familia de proteínas en los diferentes parásitos y la actividad selectiva de los inhibidores hacen que éstos puedan ser potentes herramientas terapéuticas frente a la besnoitiosis bovina.

Tabla 5: Estudios de seguridad y eficacia realizados con los fármacos BKIs en infecciones por protozoos apicomplejos en modelos *in vitro*(a) e *in vivo*(b) (adaptado de Van Voorhis *et al.*, 2017).

Parásito apicomplejo	Enzima diana	Residuo "gatekeeper"	Experimentos realizados	Inhibición de cada compuesto (μM) y efectos observados *in vivo*					Referencias
				BKI-1	1294	1517	1553	1266	
Toxoplasma gondii	*Tg*CDPK1	Glicina (Gly)	Inhibición enzimática (IC50)[a]	0,003	0,003	0,002	0,001	0,5	Ojo *et al.*, 2010; Johnson *et al.*, 2012; Doggett *et al.*, 2014; Huang *et al.*, 2015; Winzer *et al.*, 2015; Vidadala *et al.*, 2016; Sánchez-Sánchez *et al.*, 2019
			Estudios *in vitro* (IC50)[a]	0,052	0,140	0,220	0,060	>3	
			Modelo murino[b]	ND	Curación	Curación	Curación	No curación	
			Modelo ovino[b]	ND	No curación (53% protección)	ND	ND	ND	
Cryptosporidium parvum	*Cp*CDPK1	Glicina (Gly)	Inhibición enzimática (IC50)[a]	0,0007	0,001	0,001	0,002	0,580	Castellanos-González et al., 2013, 2016; Lendner *et al.*, 2015; Schaefer et al., 2016; Hulverson *et al.*, 2017
			Estudios in vitro (IC50)[a]	ND	0,1	0,6	1,6	>80	
			Modelo neonatal murino (% reducción infección)[b]	ND	56	39	37	ND	
			Criptosporidiosis en ratón[b]	ND	Curación	Curación	No curación	ND	
			Criptosporidiosis en ternero[b]	ND	Curación	Curación	Curación	ND	
Plasmodium falciparum	*Pf*CDPK4	Serina (Ser)	Inhibición enzimática (IC50)[a]	0,004	0,009	0,037	ND	>3	Ojo *et al.*, 2012, 2014
			Exflagelación *P. falciparum*[a]	0,035	0,047	<0,3	ND	>3	
			Estadíos asexuales *P. falciparum*[a]	2	8	9,2	ND	>10	

Neospora caninum	*Nc*CDPK1	Glicina (Gly)	Inhibición enzimática (IC50)[a]	0,001	0,003	0,003	0,001	0,513	Ojo *et al*., 2014; Sánchez-Sánchez *et al*., 2018
			Estudios in vitro (IC50)[a]						
			Neosporosis en ratón[b]						
			Neosporosis ovina[b] (% reducción transmisión)	0,050	0,032	0,05	0,17	>2,5	
				ND	Curación	Curación	Curación	ND	
				ND	ND	ND	No Curación (23% protección)	ND	
Sarcocystis neurona	*Sn*CDPK1	Glicina (Gly)	Inhibición enzimática (IC50)[a]	ND	0,006	0,002	0,009	>2	Ojo *et al*., 2016
			Estudios in vitro (IC50)[a]						
			Sarcocistiosis en ratón[b]	ND	0,068	0,042	0,042	>10	
				ND	ND	ND	Curación	ND	

ND: datos no disponibles

[a] experimentos realizados *in vitro*; [b] experimentos realizados *in vivo*

2.2 Empleo de modelos *in vitro* en el estudio de protozoos Toxoplasmatinae

Las enfermedades producidas por protozoos parásitos pertenecientes a la subfamilia Toxoplasmatinae tienen un gran impacto socioeconómico en medicina veterinaria a nivel mundial (Müller & Hemphill, 2012; Sánchez-Sánchez *et al.*, 2018;) y, por ello, en la actualidad se están realizando numerosos estudios con el objetivo de desarrollar herramientas para su control, tanto terapéuticas como inmunoprofilácticas.

Al tratarse de parásitos intracelulares obligados, el estudio de su biología y la búsqueda de nuevas dianas terapéuticas requiere del empleo de modelos *in vitro,* basados en cultivos celulares, ya sean líneas celulares primarias o inmortalizadas. Actualmente, se mantienen en cultivo celular de forma rutinaria taquizoítos de *T. gondii*, *N. caninum*, *Hammondia* spp. y *Besnoitia* spp. (Müller & Hemphill, 2012). Gran parte de los conocimientos relativos a la biología de los protozoos formadores de quistes, así como de la interacción entre el parásito y el hospedador se han obtenido tomando como modelo a *T. gondii* (Kim & Weiss, 2004).

En el caso de *B. besnoiti*, el empleo de cultivos celulares ha permitido obtener numerosos aislados procedentes de animales infectados y, posteriormente, mantener y propagar el estadío de taquizoíto (Fernández-García *et al.*, 2009b; Schares *et al.*, 2009; ; Gentile *et al.*, 2012; Frey *et al.*, 2016; Diezma-Díaz *et al.*, 2017), el cual se ha empleado tanto para la obtención de antígeno y ADN para el desarrollo de pruebas diagnósticas (García-Lunar *et al.*, 2013a, 2017), como en los diferentes estudios de: i) descripción del ciclo lítico y caracterización de aislados (Frey *et al.*, 2016); ii) su interacción con la célula hospedadora con el objetivo de esclarecer los mecanismos moleculares responsables de la respuesta inmunitaria innata y el daño endotelial (Muñoz-Caro *et al.*, 2014a,b; Maksimov *et al.*, 2016; Taubert *et al.*, 2016); iii) el cribado de fármacos (Cortes *et al.*, 2011; Cortes *et al.*, 2007a, 2011; Müller *et al.*, 2018).

2.2.1 Ciclo lítico

El ciclo lítico es un proceso altamente conservado entre todos los parásitos Toxoplasmatinae (Blader *et al.*, 2015) que comprende una serie de eventos que acontecen de forma secuencial y programada, incluyendo las fases de desplazamiento mediante movimientos de deslizamiento y giro (denominado "*gliding motility*"), reorientación hacia la célula hospedadora, adhesión, invasión activa, establecimiento de la vacuola parasitófora, proliferación y egresión (Figura 5). Al egresar de la célula hospedadora, los taquizoítos extracelulares volverán a invadir las células vecinas, repitiéndose el ciclo y ocasionándose daño tisular. En su conjunto, el ciclo lítico permite que el taquizoíto pueda multiplicarse y diseminarse por diversos tejidos durante la fase aguda de la infección.

Las bases moleculares del ciclo lítico han sido estudiadas en detalle en *T. gondii* (Carruthers & Boothroyd, 2007; Blader *et al.*, 2015) y, en menor medida, en *N. caninum* (Hemphill *et al.*, 1996, 2004). En concreto, se ha descrito que las proteínas de la superficie del taquizoíto (SRS), así como aquellas secretadas desde los micronemas (MIC), el cuello y cuerpo de las roptrias (RON y ROP) y los gránulos densos (GRA), actúan coordinadamente y de forma secuencial a lo largo del ciclo lítico (Tabla 5). Hasta la fecha, no se han descrito dichas proteínas en los taquizoítos de *B. besnoiti*, pero dada la elevada homología que presentan las proteínas SRS, MIC, RON, ROP y GRA de *T. gondii* y *N. caninum*, se asume la existencia de genes ortólogos en *B. besnoiti* y que las proteínas codificadas puedan

compartir mecanismos de regulación similares (Müller & Hemphill, 2012). Pese a ello, debido a las notables diferencias en el espectro de hospedadores y las rutas de transmisión que utilizan los distintos protozoos, es posible que la interacción con las células hospedadoras presente diferencias (Hemphill & Gottstein, 2006; Innes *et al.*, 2007; Reid *et al.*, 2012). De hecho, se han descrito ciertas diferencias en los mecanismos moleculares implicados en el ciclo lítico de distintos protozoos apicomplejos (English *et al.*, 2015).

Recientemente, se han desarrollado una serie de anticuerpos monoclonales específicos del estadio de taquizoíto que reconocen distintos subcompartimentos celulares (Garcia-Lunar *et al.*, 2019). Concretamente, dos de los anticuerpos generados (MABs 3.10.8 y 5.5.11) se unen a la membrana del taquizoíto, tres marcan el extremo más apical (MABs 1.17.8 y 8.9.2) y muestran un patrón compatible con proteínas de micronemas (MIC), al desplazarse desde el extremo apical hacia el polo posterior de los taquizoítos durante la invasión, y dos tienen un patrón compatible con proteínas de gránulos densos (MABs 2GA, 2.A.12, 2.A.4), observándose su secreción temprana durante la invasión de la célula hospedadora al interior de la vacuola parasitófora, así como en la egresión. No obstante, la identidad molecular de las proteínas reconocidas por dichos anticuerpos monoclonales no se conoce hasta la fecha, por lo que serían necesarios más estudios.

Figura 5: Esquema del ciclo lítico de protozoos Toxoplasmatinae

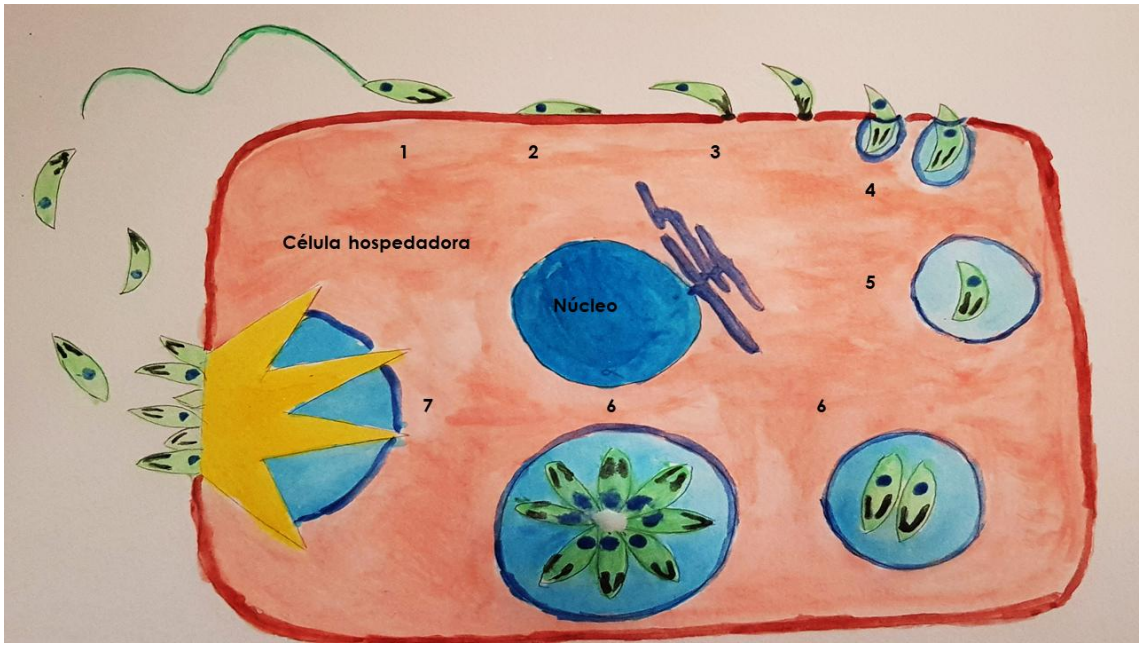

1: Motilidad mediante deslizamiento ("*gliding*"); 2: adhesión inicial mediada por proteínas de superficie (SRS); 3: Reorientación apical mediada por proteínas de micronemas (MIC); 4: Invasión activa de la célula hospedadora, secreción de proteínas de roptrias (RON,ROP); 5: Adaptación al ambiente intracelular, secreción de proteínas de gránulos densos (GRA); 6: Replicación intracelular; 7: Egresión.

2.2.1.1. Motilidad mediante deslizamiento o "gliding" y adhesión a la célula hospedadora:

Se considera que la motilidad activa de los taquizoítos de los protozoos apicomplejos es crítica, permitiendo la invasión de las células hospedadoras y el paso de barreras biológicas. Tanto en *T. gondii* (Barragán & Sibley, 2002) como en *N. caninum* (Collantes-Fernández *et al.*, 2012) se ha descrito que esta capacidad para atravesar barreras es dependiente del aislado utilizado, y que es responsable de un incremento en el

rango de hospedadores y en el tropismo tisular. Se han descrito tres tipos de motilidad: circular (círculos complejos), helicoidal (media circunferencia seguida de un giro) y giro del extremo apical mientras se sostiene sobre la base ("*twirling*") (Sibley *et al.*, 1998; Håkansson *et al.*, 1999). Una vez alcanzada la célula hospedadora, se produce inicialmente un contacto de baja afinidad mediado por las proteínas de superficie "*SAG1-related sequences*" (SRS). En concreto, en *N. caninum* se ha descrito la participación de las proteínas NcSAG1 y NcSRS2 (Hemphill & Gottstein, 1996; Howe *et al.*, 1998; Sonda *et al.*, 1998). Estudios recientes han demostrado que precisamente es en el perfil de expresión de proteínas SRS donde residen las mayores diferencias entre los taquizoítos de *T. gondii* y *N. caninum*, que podrían ser responsables de las diferencias existentes en el espectro de hospedadores (Reid *et al.*, 2012).

Para la motilidad de los taquizoítos es esencial la función del glideosoma, un complejo multiproteico formado por miosina A (MyoA) (Meissner *et al.*, 2002) junto con las proteínas asociadas al glideosoma "*gliding associated proteins*" GAP45 y GAP50 (Keeley & Soldati, 2004; Boucher y Bosch, 2015; Harding *et al.*, 2016).Además, el glideosoma contiene una cadena ligera de la miosina (MLC1) y dos cadenas esenciales (ELC1 y ELC2) con un papel regulador . El complejo motor de miosina se encuentra anclado en el complejo de membrana interno "*inner membrane complex*" (IMC)(Frenal *et al.*, 2010; Harding *et al.*, 2016).

2.2.1.2. Reorientación y fijación apical de los taquizoítos:

Tras la adhesión mediada por las proteínas SRS, los taquizoítos sufren una reorientación con el extremo apical de los mismos en oposición con la célula hospedadora. Este fenómeno está mediado por la secreción de moléculas de adhesión por los micronemas (MIC), que se anclan en la membrana plasmática del parásito, en el extremo apical. Esta secreción de las proteínas de los micronemas es dependiente de los niveles de Ca^{2+} intracelulares (Carruthers & Tomley, 2008). Se han descrito algunas diferencias entre las proteínas *Tg*MIC y *Nc*MIC, como el hecho de que en el caso de *T. gondii* se unen preferencialmente a residuos de heparán-sulfato y ácido siálico (Friedrich *et al.*, 2010), mientras que en el caso de *N. caninum* se unen a residuos de condroitín-sulfato (Naguleswaran *et al.*, 2002). Además, los dominios adhesivos "*lectin-like*" únicamente han sido descritos en las proteínas TgMIC (Friedrich *et al.*, 2010). Las proteínas MIC son ricas en residuos de cisteína (Keller *et al.*, 2004) y en su correcto posicionamiento y conformación es esencial la participación de la proteína disulfuro isomerasa (PDI), presente también en los micronemas y que, curiosamente, es la única proteína de *B. besnoiti* identificada y clonada (Marcelino *et al.*, 2011).

2.2.1.3. Invasión activa de la célula hospedadora

Durante el proceso de invasión activa de la célula hospedadora se forma una estructura conocida como unión móvil o "moving junction". Dicha unión está formada por la proteína de los micronemas AMA1 junto con proteínas del cuello de las roptrias RON2, RON4, RON5 y RON8 (Blader *et al.*, 2015), que interaccionan tanto con la membrana de la célula hospedadora como con el glideosoma del parásito. En *N. caninum* se han descrito ortólogos, por lo que el proceso de invasión podría ser similar al descrito para *T. gondii* (Marugán-Hernández *et al.*, 2011a) (Tabla 5).

Posteriormente, el taquizoíto se internaliza en el citoplasma de la célula hospedadora debido a un desplazamiento de la unión móvil hacia el polo posterior del taquizoíto y un estrangulamiento de la membrana plasmática, impidiendo la fusión con los lisosomas de la célula hospedadora (Mordue *et al.*, 1999a; Alexander *et al.*, 2005).

2.2.1.4. Adaptación al ambiente intracelular y replicación

La vacuola parasitófora, por analogía con *N. caninum* o *T. gondii*, se origina a partir de la membrana plasmática de la célula hospedadora y es modificada por parte del parásito (secreción de proteínas de los gránulos densos, GRA) para impedir su destrucción por fusión con los lisosomas (Hemphill *et al.*, 1996; Mordue *et al.*, 1999b). Además, la vacuola parasitófora es capaz de reclutar a las organelas de la célula hospedadora y de secuestrar su maquinaria metabólica en favor de la replicación del parásito (Nolan *et al.*, 2015). No obstante, se ha descrito que *T. gondii, N. caninum* y *B. besnoiti* presentan una serie de diferencias notables. En primer lugar, todos ellos reclutan el aparato de Golgi hacia la vacuola parasitófora, pero su estructura se ve alterada de distinta forma, ya que en el caso de *Besnoitia* se visualiza una compactación mientras que en *Toxoplasma* parece que se desintegra y en *Neospora* no sufre alteraciones evidentes (Cardoso *et al.*, 2018). Tanto en *N. caninum* como en *T. gondii* y *B. besnoiti* se ha visto un reclutamiento de la proteína Rab9A, que es un importante factor regulador del tráfico endosomal a la cercanía de la vacuola parasitófora. En el caso del centrosoma, *Toxoplasma* lo recluta hacia la vacuola parasitófora, pero esto no ocurre en *B. besnoiti* (Cardoso *et al.,* 2014). En el interior de la vacuola parasitófora, los taquizoítos experimentan ciclos sucesivos de replicación asexual por endodiogenia hasta desencadenarse la egresión del parásito al medio extracelular, lo que origina la lisis de la célula hospedadora y la posterior invasión de las células vecinas por los zoítos liberados, iniciándose un nuevo ciclo lítico (Frey *et al.*, 2016).

Una vez los zoítos son intracelulares, juega un papel crucial la secreción de proteínas que son capaces de inutilizar los mecanismos de defensa de la célula para asegurar la supervivencia del parásito. El ejemplo mejor estudiado en *T. gondii* es la inactivación de las GTPasas inducidas por interferón (IRG) por la tríada de proteínas de roptrias ROP5/ROP18 y ROP17 (Niedelman *et al.*, 2012; Hakimi *et al.*, 2017). Curiosamente, dichas proteínas son polimórficas entre distintos aislados del parásito y ROP5 es considerada un factor de virulencia clave en el ratón (Behnke *et al.*, 2011). Por el contrario, la información disponible acerca de estos efectores en *N. caninum* es más escasa (Tabla 5). No obstante, se han descrito numerosas proteínas *Nc*ROP que comparten un elevado porcentaje de identidad con sus ortólogos en *T. gondii* (Marugán-Hernández *et al.*, 2011a; Sohn *et al.*, 2011). Por ejemplo, se ha descrito que NcROP18 es un pseudogen y el número de copias de ROP5 es mucho menor en *N. caninum* (Reid *et al.*, 2012). De hecho, la incorporación del gen TgROP18 a una cepa de *N. caninum* incrementó su proliferación *in vitro* y su virulencia en el modelo murino (Lei *et al.*, 2014).

Entre las proteínas de gránulos densos, al igual que ocurre con las proteínas de roptrias, el número de trabajos disponibles en *N. caninum* es muy inferior a lo descrito en *T. gondii* (Tabla 5). Estas proteínas son capaces de modificar la membrana de la vacuola parasitófora y establecer una red microvesicular que asegura la supervivencia y aporte nutricional a los parásitos en división, generando un ambiente favorable para la replicación. Además, las proteínas de gránulos densos parecen estar involucradas en procesos de inmunomodulación (*Tg*GRA15, *Tg*GRA24, *Tg*GRA25) (Rosowski *et al.*, 2011; Braun *et al.*, 2013; Shastri *et al.*, 2014), de alteración de la expresión génica (*Tg*GRA16) (Bougdour *et al.*, 2013; Braun et al., 2013), de asociación con la mitocondria del

hospedador (*Tg*MAF1) (Pernas *et al.*, 2014) y regulando la propia egresión del parásito (*Tg*GRA22) (Okada *et al.*, 2013).

El número de proteínas de gránulos densos que han sido descritas hasta el momento en *N. caninum* es mucho menor (Tabla 5). *Nc*GRA6 y *Nc*GRA7 han sido relacionadas con los procesos de invasión del taquizoíto (Cho *et al.*, 2005; Aguado-Martínez *et al.*, 2010) y se ha demostrado que NcGRA7 es esencial para el inicio de la respuesta inmunitaria en el modelo murino (Nishikawa *et al.*, 2018), mientras que NcGRA6 también tiene un papel en la inducción de una respuesta inmunitaria protectora (Fereig *et al.*, 2019), aunque se desconoce la función del resto de las proteínas descritas.

2.2.1.5. Egresión

La egresión o salida de los taquizoítos al medio extracelular es similar a la invasión, siendo considerada en ocasiones como el primer paso del ciclo lítico (Blader *et al.*, 2015). Existen una serie de estímulos que son capaces de desencadenar la salida de los zoítos al exterior, que se pueden dividir en función de aquellos que se producen como consecuencia de una respuesta inmunitaria y aquellos que son independientes. Entre los primeros, destacan el daño a la célula hospedadora mediado por perforinas y la unión del receptor de muerte (Fas/FasL) tras una respuesta citotóxica mediada por linfocitos T CD8+ (Persson *et al.*, 2007). El daño a la membrana celular ocasiona un descenso en los niveles intracelulares de K^+ que origina la egresión (Moudy *et al.*, 2001).

En ausencia de una respuesta inmunitaria, la egresión se inicia mediante diversos mecanismos, como la producción de ácido abscísico (ABA), que se produce de forma continua durante la proliferación (Nagamune *et al.*, 2008a). Además, la replicación origina una acidificación de la vacuola parasitófora, y este descenso de pH puede reanudar la secreción de proteínas de micronemas por el K^+ (Roiko & Carruthers, 2013). Además, el cambio de pH es relevante para la proteína "p*erforin like protein* 1" (PLP1), que a bajos valores de pH se inserta en la membrana de la célula hospedadora y origina la formación de poros en la membrana.

Las señales que conducen a la egresión emplean dos segundos mensajeros: los niveles de Ca^{2+} citoplasmáticos y el GMP cíclico (GMPc). El papel del Ca^{2+} tanto en invasión como en la egresión ha sido estudiando a fondo (Nagamune *et al.*, 2008b), y se ha observado que el empleo de quelantes del $Ca2^+$ disminuye la motilidad y la secreción de micronemas, mientras que el aumento en los niveles de $Ca2^+$ (mediante el empleo de ionóforos) estimula la egresión, la descarga de micronemas y la motilidad, incrementando por tanto la capacidada de invasión (Wetzel *et al.*, 2004). En dicha señalización por Ca cobran un papel importante las proteínas quinasas dependientes de Ca (CDPKs), como TgCDPK1 (Lourido *et al.*, 2010; Lourido y Moreno, 2015) y TgCDPK3 (Treeck *et al.*, 2014). Por otra parte, el único efector conocido del cGMP en protozoos apicomplejos es la proteína quinasa G (PKG), cuya activación da lugar a la síntesis de fosfatidilinositol (4,5) bifosfato (PIP2), que es sustrato para la proteín-lipasa C que lo degrada a IP3. Este IP3 es capaz de desencadenar la liberación de Ca^{2+} de los depósitos intracelulares, produciéndose una interconexión entre los dos segundos mensajeros descritos hasta la fecha.

Tabla 6: Proteínas involucradas en el ciclo lítico descritas en *T. gondii* y *N. caninum*.

Eventos del ciclo lítico	Proteínas descritas en Tg	Proteínas descritas en Nc	Referencias
Motilidad mediante deslizamiento "*gliding*" y reorientación	MyoA GAP45, GAP50 Cadena ligera de la miosina (MLC1) ELC1, ELC2 Actina Proteasas romboidales	*Nc*GAP45 *Nc*ACT	Blader *et al.*, 2015; Regidor-Cerrillo *et al.*, 2015
Adhesión	Proteínas de superficie (SAGs)	*Nc*SAG1, *Nc*SRS2, *Nc*SRS67	Bezerra *et al.*, 2017; Blader *et al.*, 2015; Howe *et al.*, 1998; Sonda *et al.*, 1998; Hemphill & Gottstein, 1996; Hemphill, 1996
"*Moving junction*" e invasión activa	Proteínas de micronemas (AMA1, MIC) Proteínas de roptrias (ROP) Proteínas del cuello de las roptrias (RON)	*Nc*AMA1, *Nc*MIC1,2,3,4,6,817,19,26 AMA1 *Nc*RON2, *Nc*RON3, *Nc*RON4, *Nc*RON8 *Nc*ROP1, *Nc*ROP2Fam-1; *Nc*ROP4,5,8,9,30 *Nc*ROP40, *Nc*ROP1Fam *Nc*ROP16	Keller *et al.*, 2002; Naguleswaran *et al.*, 2002; Lovett *et al.*, 2000) Pastor-Fernández et al., 2016; Marugán-Hernández et al., 2011a Sohn et al., 2011
Establecimiento de la vacuola parasitófora y replicación intracelular	Proteínas de gránulos densos (GRA) Factores de transcripción ApiAP2 Proteínas quinasas dependientes de calcio (CDPKs) Proteínas quinasas estimuladas por mitógenos (MAPK) Complejo de membrana interno (IMC) GTPasas Rab	*Nc*GRA1,2,6,7,9,14 *Nc*CDPK1	Nishikawa et al., 2018; Blader et al., 2015; Ojo et al., 2014; Arranz-Solís et al., 2017; Reid et al., 2012; Dong et al., 2017; Pastor-Fernández, 2016 Leineweber et al., 2009
Egresión	Perforinas 1 (PLP1) NTPasas K+/Ca2 (CDPKs)	NcNTPasas CDPK1	Pastor-Fernández et al., 2016 Asai et al., 1998; Ojo et al., 2014

Para el estudio de la función específica de las proteínas involucradas en el ciclo lítico es esencial el desarrollo de metodologías de edición génica para la interrupción de la expresión y generación de parásitos defectivos "*knock out*". Recientemente, la implementación de la metodología de edición génica CRISPR-Cas9, ampliamente utilizada para el estudio de proteínas en *T. gondii* (Long *et al.*, 2016; Sidik *et al.*, 2016; Wang *et al.*, 2016; Shen *et al.*, 2017), ha sido implementada con éxito en *N. caninum* utilizando promotores de *T. gondii* (Arranz-Solís *et al.*, 2018), lo que podría facilitar la realización de estudios funcionales de muchas de estas proteínas en busca de su papel como posibles genes de virulencia. De hecho, Nishikawa *et al*. (2018) han explorado la función de tres proteínas de gránulos densos, demostrándose que GRA7 es esencial para desencadenar la respuesta inmunitaria en el modelo murino. Dicha metodología podría ser implementada también en *B. besnoiti*, lo que posibilitaría la realización de estudios comparativos de la función de proteínas importantes en el ciclo lítico de *T. gondii* y *N. caninum* con *B. besnoiti*.

Los resultados de Frey *et al*. (2016) mostraron que las etapas secuenciales del ciclo lítico previamente descritas para *N. caninum* y *T. gondii* (adhesión-invasión, proliferación intracelular y egresión) están presentes en los taquizoítos de *Besnoitia* spp. No obstante, ciertos aspectos son claramente diferentes, como por ejemplo la tasa de invasión (IRs). Los taquizoítos de *Besnoitia* muestran unas tasas de invasión bajas, entre el 5 y el 22%, lo que contrasta con las tasas de invasión descritas para *N. caninum* que oscilan entre el 20 y el 90% (Dellarupe *et al.*, 2014b). Además, los taquizoítos requieren más tiempo para invadir las células hospedadoras (Regidor-Cerrillo *et al.*, 2011; Dellarupe *et al.*, 2014b). A las 6 horas post-infección (hpi), únicamente se habían alcanzado el 50% de los eventos de invasión, mientras que en el caso de *N. caninum* a las 6 hpi ya se ha alcanzado la máxima tasa de invasión. Este hecho podría estar asociado a una mayor supervivencia extracelular de los taquizoítos de *Besnoitia*, ya que se ha descrito que la infectividad de los taquizoítos de *N. caninum* extracelulares desciende rápidamente en unas pocas horas. En el caso de *T. gondii*, la invasión es incluso más eficiente, con hasta un 75-80% de los taquizoítos intracelulares en los primeros 30 minutos pi (Naguleswaran *et al.*, 2003). Además, los resultados de Frey *et al*. (2016), corroborados posteriormente por Diezma-Díaz *et al*. (2017), mostraron que los taquizoítos del aislado Bb-Spain1 de *B. besnoiti* presentan una fase de adaptación (o "*lag phase*") a las condiciones intracelulares de aproximadamente 24 h, en las que no se observa aún la replicación del parásito, mientras que en el caso del aislado Bb-Italy2 esta fase se extiende durante 48 h. Por el contrario, en el caso de los taquizoítos de *N. caninum* se han descrito "*lag phases*" de entre 8 y 44 h (Regidor-Cerrillo *et al.*, 2011; Dellarupe *et al.*, 2014a) y para *T. gondii* de 8-10 h (Sundermann & Estridge, 1999). Además, los tiempos de duplicación, es decir, el tiempo que tardan los taquizoítos durante la fase de crecimiento exponencial en duplicarse es de entre 17,9-32 h en el caso de *Besnoitia*, mientras que para *N. caninum* y *T. gondii* se han descrito tiempos de duplicación inferiores (Sundermann & Estridge, 1999; Regidor-Cerrillo *et al.*, 2011; Jiménez-Pelayo *et al.*, 2017). La mayor supervivencia extracelular de los taquizoítos de *Besnoitia* podría favorecer su transmisión mediante artrópodos hematófagos. Diversos estudios han puesto de manifiesto que dicha supervivencia de los taquizoítos de *B. besnoiti* varía en función del artrópodo que podría actuar como vector, describiéndose supervivencias inferiores a 1 h en *Stomoxys calcitrans*, 3 h en moscas Tsetse y 24 h en tabánidos (revisado por Alvarez-Garcia *et al.*, 2014b).

Las diferencias encontradas entre los distintos aislados estudiados, tanto en invasión como en proliferación, sugieren que existe un cierto grado de variabilidad intraespecífica a nivel fenotípico. De acuerdo a sus tasas de invasión, los aislados se pueden clasificar en aislados con alta tasa de invasión (Bb-France, Bb-Evora03 y Bb-Israel), aislados con tasa de invasión media (Bb-Ger1) y aislados con baja tasa de invasión (Bb-Spain1, Bb-Spain2 and Bb-Italy2) (Frey *et al*., 2016). En dicho estudio, el aislado obtenido de *B. tarandi* presentó una tasa de invasión baja. Teniendo en cuenta los resultados de la proliferación, los aislados se clasifican en tres grandes grupos: con alta proliferación (Bb-Israel y *B. tarandi*); con proliferación intermedia (Bb-Ger1 y Bb-France) y aislados con baja tasa de proliferación (Bb-Italy2, Bb-Spain1, Bb-Spain2 y Bb-Evora03)(Frey *et al.*, 2016).

Finalmente, el ciclo lítico de *Besnoitia* spp., en contraposición a lo que ocurre en *T. gondii* y *N. caninum*, es asincrónico. Esto se debe probablemente al periodo de tiempo prolongado durante el cual los taquizoítos son capaces de infectar las células hospedadoras.

2.2.2. Líneas celulares

Para el desarrollo de modelos *in vitro* de infección, un componente crucial son las líneas celulares, ya sean cultivos primarios o líneas celulares inmortalizadas. Hoy en día los taquizoítos de *N. caninum*, *T. gondii* o *B. besnoiti* se pueden mantener y propagar en una gran variedad de líneas celulares (Muller & Hemphill, 2012), que crecen en monocapa bajo condiciones controladas de temperatura y CO_2. Además, en el caso de *B. caprae*, se ha visto que son capaces de proliferar en cultivos de macrófagos murinos en suspensión (Sadoughifar *et al.*, 2015). Se han empleado diversas líneas celulares primarias e inmortalizadas. Los cultivos primarios son aquellos que proceden de un tejido u órgano determinado y se pueden mantener durante un periodo de tiempo limitado gracias al empleo de medios de cultivo enriquecidos con factores de crecimiento específicos en función del tejido de procedencia. Por otro lado, las líneas celulares inmortalizadas son aquellas que proceden de un tejido u órgano en muchos casos de origen tumoral, o que son modificados genéticamente, para mantenerse en cultivo durante un tiempo ilimitado. A la hora de establecer un modelo *in vitro* es importante considerar así mismo la especie de procedencia, ya que puede afectar a la interacción parásito-hospedador (Müller & Hemphill, 2012) y el tejido de obtención, ya que se ha descrito una notable heterogeneidad en diversas poblaciones celulares como las células endoteliales (Aird, 2012) y los fibroblastos (Driskell & Watt, 2015). Además, el empleo de cultivos primarios presenta ventajas ya que permitiría reproducir de una manera más próxima lo que ocurre en condiciones *in vivo*, ya que la adaptación a condiciones *in vitro* ocasiona una serie de cambios fenotípicos que pueden producir una pérdida de las funciones específicas de cada tipo celular (Pan *et al.*, 2009).

El mantenimiento y la proliferación *in vitro* de taquizoítos de *T. gondii* y *N. caninum* se ha realizado en diferentes líneas celulares: células endoteliales, células epiteliales de riñón de mono (p. ej. células Marc-145 y células Vero), macrófagos, fibroblastos, células primarias de tejido cortical de cerebro de rata y queratinocitos epidérmicos murinos (revisado por Müller & Hemphill, 2012). Diversos estudios han demostrado que las condiciones de cultivo y criopreservación de los taquizoítos de *N. caninum* son, en general, similares a las empleadas en *T. gondii* (Müller & Hemphill, 2012). Del mismo modo, los taquizoítos de *B. besnoiti* se han mantenido en una gran variedad de líneas celulares, tanto primarias como inmortalizadas, tal y como se muestra en la Tabla 7, mediante protocolos muy similares a los descritos para *N. caninum* y *T. gondii* y con finalidades similares, como la obtención y caracterización de aislados y estudios farmacológicos. Sin embargo, hasta la fecha no se ha estudiado la transformación *in vitro* del estadio de taquizoíto al de bradizoíto y no se conoce mucho acerca de la biología del parásito desde un punto de vista molecular debido al escaso número de estudios genómicos, transcriptómicos y proteómicos realizados.

No obstante, en otros protozoos apicomplejos, se ha descrito un comportamiento diferencial en función de la célula hospedadora. Por ejemplo, en el caso de los bradizoítos de *B. jellisoni* obtenidos de quistes tisulares de rata canguro (*Dipodomys ordii*), se vio que se podrían multiplicar en varias líneas celulares, como cultivos embrionarios de bazo bovino ("*bovine embryonic spleen*", BES), cultivos embrionarios de tráquea bovina ("*embryonic bovine trachea*", EBTr) y cultivos de células renales bovinas ("*Madin Darvin bovine kidney*", MDBK), pero que el crecimiento en células BES o EBTr representaba unas mejores condiciones para la proliferación del parásito que la línea establecida MDBK (Fayer *et al.*, 1969). Además, en el caso de *Eimeria* spp. se ha descrito la formación de merontes de primera generación únicamente en células de origen bovino, tanto epiteliales como endoteliales (Hermosilla *et al.*, 2002). En *N. caninum*, dos aislados de distinta virulencia (Nc-Spain7 y Nc-Spain1H) no mostraron diferencias cuando su comportamiento fue estudiado

en células del trofoblasto bovino F3 en relación a lo previamente descrito para las células de riñón de mono Marc-145, con mayores tasas de invasión y proliferación del aislado más virulento (Nc-Spain7). Por el contrario, estos mismos aislados mostraron grandes diferencias cuando el comportamiento fue comparado con otra línea bovina, las células de carúncula materna BCEC, en las que ambos aislados mostraron tasas de invasión y proliferación muy inferiores, sugiriéndose una función de barrera para estas células (Jiménez-Pelayo *et al.*, 2017).

En el caso concreto de *B. besnoiti*, Schares *et al*. (2009) encontraron diferencias en función del tipo celular utilizado para el aislamiento, viéndose un mejor crecimiento de los taquizoítos en las líneas celulares KH-R y BHK21.

Tabla 7. Líneas celulares empleadas para el aislamiento y el mantenimiento de taquizoítos de *B. besnoiti in vitro*.

Línea celular	Tipo celular	Especie animal de origen	Tejido	Célula	Referencia
BHK; BHK21	Inmortalizada	Hámster	Riñón	Fibroblasto	Neuman, 1974 Schares *et al.*, 2009
CRFK	Inmortalizada	Gato	Riñón	Epitelial	Gobel *et al.*, 1985
HeLa	Inmortalizada	Humano	Cérvix	Epitelial	Neuman, 1974
Marc-145	Inmortalizada	Mono	Riñón	Epitelial	Fernández-García *et al.*, 2009b
NA42/13	Inmortalizada	Ratón	Tejido nervioso	Neuroblastoma	Schares *et al.*, 2009
RML-15 LSTH-RA-243	Inmortalizada	Garrapata		Células embrionarias/adultas	Samish *et al.*, 1988
Vero	Inmortalizada	Mono	Riñón	Epitelial	Shkap *et al.*, 1987b; Cortes *et al.*, 2007ª
BUVEC	Primaria	Bovino	Cordón umbilical	Endotelial	Maksimov *et al.*, 2016
HFF	Primaria	Humano	Prepucio	Fibroblasto	Frey *et al.*, 2016
KH-R	Primaria	Ternero	Corazón	Células embrionarias	Schares *et al.*, 2009
L929	Inmortalizada	Ratón	Tejido adiposo	Fibroblastos	Shkap *et al.*, 1987a
Cultivos primarios de riñón bovino embrionario ("*Bovine Embrio Kidney*", BEK)	Primaria	Bovino	Riñón	Epitelioide	Shkap *et al.*, 1987a
Cultivos primarios de riñón ovino embrionario ("*Fetal Lamb kidney*", FLK)	Primaria	Ovino	Riñón	Epitelioide	Bigalke & Naude, 1962
Células epiteliales de riñon bovino (*Madin-Darvy Bovine Kidney*, MDBK)	Inmortalizada	Bovino	Riñón	Epitelial	Shkap *et al.*, 1987ª
Células linfoblastoides bovinas (coinfectadas	Inmortalizada	Bovino	Tejido Linfoide	Linfocitos	Shkap *et al.*, 1987ª

con esquizontes de *Theileria annulata)* (BL)					
Cultivos tiroideos	Primaria	Ovino	Tiroides	Epitelial	Neuman, 1974

2.2.3. Aislados y variabilidad intra-específica

Otra de las aplicaciones de los modelos *in vitro* es la obtención de nuevas cepas o aislados procedentes de animales infectados.

En el caso de *T. gondii*, tradicionalmente se ha considerado el bioensayo en animales de laboratorio como la técnica de referencia o "*gold standard*" para la confirmación de la infección por dicho protozoo debido a la facilidad de producción de quistes tisulares en el modelo murino (Liu *et al.*, 2015). Para lograr una mayor tasa de éxito, se pueden utilizar ratones deficientes en IFN-gamma (IFN-γ) debido a su elevada susceptibilidad previamente al paso a cultivo celular. Gracias a esto, se han obtenido un gran número de aislados a nivel mundial. La estructura poblacional de *T. gondii* está muy bien definida, existiendo más de 15 haplogrupos pertenecientes a tres linajes clonales genéticamente diferenciados. Los aislados de tipo I (por ejemplo, RH) son aquellos que muestran una mayor virulencia en el modelo murino, generalmente procedentes de casos clínicos de toxoplasmosis humana. Los aislados de tipo II (ME49) y III (VEG) son menos virulentos en ratón y, generalmente, circulan en animales domésticos. En los últimos años, en el continente Sudamericano se están describiendo cepas "atípicas" que no pertenecen a ninguno de los linajes clonales descritos anteriormente y muestran una gran virulencia (Bertranpetit *et al*., 2017). No obstante, también se han descrito notables diferencias entre aislados pertenecientes al mismo linaje clonal, como entre los aislados TgSpSh1 y TgME49, ambos considerados tipo II y con un comportamiento diferente tanto *in vitro* como *in vivo* en modelos murinos y ovinos (Sánchez-Sánchez *et al*., 2019).

En el caso de *N. caninum*, hasta la fecha se han obtenido en torno a 100 aislados (Pastor-Fernández, 2016) procedentes tanto de hospedadores intermediarios (rumiantes como vaca, búfalo de agua, oveja, ciervo de cola blanca y bisonte europeo) como de hospedadores definitivos (perro, lobo) (Donahoe *et al.*, 2015; Dubey *et al.*, 2014; Dubey y Schares, 2011; Dubey *et al.*, 2011; Dubey *et al.*, 2011). La disponibilidad de este panel de aislados ha posibilitado el estudio comparativo de su variabilidad intraespecífica, tanto en modelos *in vitro* como *in vivo* (en modelos murinos, ovinos y bovinos). Los primeros estudios de variabilidad genética entre aislados de *N. caninum* se fundamentaron en el análisis del ARNr 18S, así como de la región ITS-1 (*Internal Transcribed Spacer*-1) y RAPD (*Randomly Amplified Polymorphic* DNA), y se indicó una menor variabilidad genética que la descrita para *T. gondii* (Beck *et al.*, 2009). Posteriormente, el desarrollo de marcadores basados en secuencias microsatélites evidenció una mayor diversidad genética tanto de aislados mantenidos *in vitro* (Regidor-Cerrillo *et al.*, 2006; Pedraza-Díaz *et al.*, 2009;) como de aislados de muestras de animales con infección natural (Regidor-Cerrillo *et al.*, 2008; Basso *et al.*, 2009,2010). Recientemente, se ha demostrado la existencia de mutaciones puntuales de un único nucleótido (SNP) en el genoma de *N. caninum* (Calarco *et al.*, 2018) encontrándose numerosas diferencias entre un aislado virulento (Nc-Liverpoll) y uno avirulento (Nc-Nowra). La variabilidad genética de los aislados de *N. caninum* se ve reflejada tanto en su comportamiento *in vitro* (Regidor-Cerrillo *et al.*, 2011; Dellarupe *et al.*, 2014b; Jiménez-Pelayo *et al.*, 2017) como en modelos *in vivo* murinos (Collantes-Fernández *et al.*, 2006) y bovinos (Rojo-Montejo *et al.*, 2009a,b).

En el caso de *B. besnoiti*, el aislamiento *in vitro* se ha realizado a partir de bradizoítos contenidos en el interior de quistes tisulares maduros procedentes de biopsias de piel o

vagina de animales infectados crónicamente. Para ello, es necesario liberar los bradizoítos del interior de los quistes tisulares, bien sea mediante una disrupción mecánica utilizando un homogeneizador tisular (tipo Potter-Elvehjem) o una disrupción enzimática con tripsina. Una vez se han roto los quistes, la suspensión resultante se inocula en monocapas de diversas líneas celulares como Marc 145 (Fernández-García *et al.*, 2009b; Gentile *et al.*, 2012; Frey *et al.*, 2016) o Vero (Schares *et al.*, 2009). Otra alternativa que se ha llevado a cabo, al igual que en el caso de *N. caninum* o *T. gondii*, consiste en la inoculación previa de ratones IFN-γ KO (p. ej. la estirpe B6.129S7-Ifngtm1Ts/J, Laboratorios Jackson) con el contenido de los quistes tisulares, generalmente utilizando una inoculación intraperitoneal (Schares *et al.*, 2009; Gentile *et al.*, 2012).

Tabla 8. Aislados de *B. besnoiti* obtenidos entre 1960 y 1980.

Aislado	País	Animal	Tipo de infección	Cultivo *in vitro*	Empleo en infecciones experimentales
Impala Strain	Sudáfrica	Antílope	Crónica	No	Conejo
Bb-Fuls Strain	Sudáfrica	Bóvido	Aguda	Sí	Bóvido, conejo y ratón
Bb-Schoeman Strain	Sudáfrica	Bóvido	Aguda	No	Conejo y ratón
Bb-Lamprechts A Strain	Sudáfrica	Bóvido	Aguda	No	Bóvido, conejo y ratón
Bb-Lamprechts B	Sudáfrica	Bóvido	Crónica	No	Bóvido, conejo y ratón
Bb-Wildebeest	Sudáfrica	Ñu	Crónica	Sí	Bóvido, conejo y ratón
Bb-Israel	Israel	Bóvido	Crónica	Sí	Bóvido y ratón

* Referencias: Shkap *et al.*, 1987a; Bigalke, 1968

El panel de aislados disponible de *B. besnoiti* en la actualidad es distinto respecto al panel existente en la década de los 60. (Tabla 8).

Entre los años 60 y 80 se obtuvieron diferentes aislados del parásito (Tabla 8) que fueron utilizados para la realización de infecciones experimentales en el ganado bovino y en diversas especies de animales de laboratorio. Al no disponer de modelos de infección en cultivos celulares, muchos de estos aislados se propagaban mediante pases sucesivos en conejos, dada la susceptibilidad de estos animales a desarrollar la fase aguda de la infección (Bigalke, 1968). Estos aislados se obtuvieron de animales con infección crónica, tanto antílopes (impala, ñu) como ganado doméstico en los cuales no se realizó ningún control sanitario, por lo que se desconoce si estos aislados estaban libres de otros patógenos frecuentes en el ganado bovino.

Posteriormente, se han obtenido nuevos aislados que se han mantenido *in vitro* en cultivos celulares. Los aislados bovinos obtenidos en Israel y, más recientemente, en Europa se aislaron directamente de ganado infectado crónicamente y dichos aislados están libres, al menos, de la infección por *Mycoplasma* spp. (Tabla 9).

Tabla 9. Aislados de *B. besnoiti* obtenidos *in vitro* a partir de 1980

Aislado*	País	Empleo en infecciones experimentales	Referencia
Bb1-Evora03	Portugal	No	Cortes *et al.*, 2006b
Bb1-Evora04	Portugal	No	Caro *et al.*, 2014
Bb-Lisbon14	Portugal	No	Ramakrishnan et al., No publicado
Bb-Spain1	España	No	Fernández-García *et al.*, 2009b
Bb-Spain2	España	No	No publicado
Bb-Spain3	España	Bóvido	Diezma-Díaz *et al.*, 2017
Bb-Spain4	España	Bóvido/Gato	Diezma-Díaz et al., enviado
Bb-Ger1	Alemania	Cobaya, gato, perro y ratón	Schares *et al.*, 2009
Bb-IPZ-2-GCH	Alemania	No	Basso *et al.*, 2013
Bb-France	Francia	Ratón	Lienard *et al.*, 2015
Bb-IPZ-1-GCH	Francia	No	Basso *et al.*, 2013
Bb-Italy1	Italia	No	Gentile *et al.*, 2012
Bb-Italy2	Italia	No	Frey *et al.*, 2016
Bb-IPZ-3-GCH	Suiza	No	Basso *et al.*, 2013

* Aislados procedentes de ganado bovino con una infección crónica.

Las técnicas moleculares desarrolladas hasta la fecha, como la PCR convencional de la región *Internal Transcriber Spacer* 1 (ITS-1) y la qPCR no permiten distinguir entre las especies de *Besnoitia* que infectan ungulados debido a la gran similitud existente en dicha región (Cortes *et al.*, 2007b ; Schares *et al.*, 2011b). Además, al contrario de lo que ocurre en *T. gondii* y en *N. caninum*, en *B. besnoiti* se ha descrito una variabilidad genética limitada mediante un panel de marcadores microsatélites, ya que dichos marcadores no diferencian entre aislados de *Besnoitia*. Únicamente, se han encontrado diferencias en uno de los marcadores (BT21) para un aislado procedente de Italia (Gutiérrez-Expósito *et al.*, 2016). No obstante, sí que permiten diferenciar entre las especies de *Besnoitia* que afectan a grandes herbívoros (Gutiérrez-Expósito *et al.*, 2016; Madubata *et al.*, 2012). A pesar de la escasa variabilidad genética encontrada hasta la fecha, sí que se han descrito diferencias fenotípicas en cuanto a las tasas de invasión y proliferación que presentan *in vitro* en células Marc-145 (Frey *et al.*, 2016).

2.2.4. Utilidad de los modelos *in vitro*

2.2.4.1. Estudios de la biología del parásito (Técnicas -ómicas).

En la búsqueda de una visión global de los distintos elementos implicados en la biología de protozoos apicomplejos desde una perspectiva molecular, las técnicas –ómicas (genoma, proteoma, transcriptoma, etc.) son esenciales. Su auge se ha producido tras la secuenciación y publicación del genoma de diversos patógenos eucariotas de importancia en salud pública y sanidad animal en la base de datos EuPathDB (*Eukaryotic Pathogen Database*, www.eupathdb.org) (Aurrecoechea *et al.*, 2016), que recoge información genómica, proteómica y transcriptómica de diversos géneros, especies y aislados de parásitos apicomplejos como *Cryptosporidium*, *Plasmodium*, *Eimeria*,

Hammondia, *Toxoplasma* y *Neospora*. Concretamente, la base de datos ToxoDB (www.toxodb.org) agrupa de forma libre y colaborativa la información *-ómica* disponible de estos últimos cuatro géneros, incluyendo varios aislados representativos de *T. gondii* (Gajria *et al.*, 2008). En *T. gondii* se realizaron las primeras descripciones de su genoma y transcriptoma y se emplearon técnicas de genética reversa para el estudio de diferentes factores de virulencia, y se ha usado comúnmente como un modelo para el estudio de otros protozoos apicomplejos (Kim & Weiss, 2004). Posteriormente, se han adaptado estas metodologías tanto para deleccionar como para expresar de forma constitutiva genes en *N. caninum* (Marugán-Hernández *et al.*, 2011a, b). Recientemente, la puesta a punto de la metodología de edición génica CRISPR-Cas9 en *N. caninum* utilizando promotores de *T. gondii* (Arranz-Solís *et al.*, 2018) facilitará el estudio de la función de genes y, posiblemente, podría ser adaptada para el estudio de *B. besnoiti*. A pesar de ser filogenéticamente muy cercanos, estos parásitos presentan diferencias notables en el rango de hospedadores que utilizan y en sus estrategias de transmisión, que podrían deberse a diferencias en los antígenos de superficie y diversos factores de virulencia secretados durante el ciclo lítico que jugarían un papel clave en la interacción con las células hospedadoras y la inducción de la respuesta inmunitaria (Hakimi *et al.*, 2017).

El empleo de múltiples técnicas -ómicas permite explorar los mecanismos moleculares que gobiernan las bases de la interacción parásito-hospedador y, por tanto, identificar posibles dianas para el control de las infecciones ocasionadas por dichos parásitos.

Tabla 10: Estudios realizados mediante el empleo de metodologías -ómicas en protozoos Toxoplasmatinae.

Parásito	Estadio (Tz/Bz/Sz/Oo)*	Técnica -ómica	Muestra	Metodología**	Principales hallazgos	Referencias
Toxoplasma gondii	Tz	Genómica	Taquizoítos del aislado RH (Tipo I)	WGS	Genoma de 69.35 Mb agrupado en 14 cromosomas con 111 genes únicos	Lau *et al.*, 2016
	Tz	Genómica/Transcriptómica	Taquizoítos del aislado ME49 (Tipo II)	WGS	Aproximadamente 62 Mb organizados en 14 cromosomas	Hassan et al., 2012
	Tz	Genómica/Transcriptómica	Taquizoítos del aislado VEG	WGS	Diferencias en el repertorio de genes expresados entre *T. gondii* y *N. caninum*, con una expansión de antígenos de superficie y la divergencia de factores de virulencia, como proteínas de roptrias, en *N. caninum*	Reid *et al.*, 2012
	Tz	Genómica/Transcriptómica	Taquizoítos del aislado VEG Tipo III)	WGS/RNA-Seq	Mejora de la anotación del genoma, corrigiendo hasta un tercio de los genes previametne anotados. Descripción de regions UTRs más largas de lo descrito para otros eucariotas. Identificación de *cis-natural antisense transcripts* (cis-NATs) y *long intergenic non-coding RNAs* (lincRNAs)	Ramaprasad *et al.*, 2015
	Oo/Sz/Tz/Bz	Transcriptómica	Muestas secuenciales durante el proceso de multiplicación *in vitro* desde ooquistes, esporozoítos (día 4), taquizoítos (dia 6 y 7), bradizoítos. Taquizoítos RH, ME49B7 y VEGmsj.	SAGE	Genes diferencialmente expresados durante el desarrollo *in vitro*. Marcadores de bradizoíto presentes en TgME49B7 y TgVEG pero ausentes en TgRH	Radke *et al.*, 2005
	Tz	Transcriptómica	Células epiteliales de riñon porcino (PK13) infectadas con taquizoítos del aislado TS-4	Microarray	Inducción de genes implicados en la transcripción, transducción de señales, respuesta inmunitaria, metabolism y apoptosis.	Okomo-Adhiambo et al., 2006

Tz	Transcriptómica	Monocitos de sangre periférica humanos diferenciados a macrófagos o células dendríticas infectados con taquizoítos del aislado RH	Microarray	Respuesta específica a distintos patógenos, y diferencias etnre macrófagos y células dendríticas. Inducción de genes implicados en la superfamilia del TNFa e IFN (solo en células dendríticas)	Chaussabel *et al.*, 2003
Tz	Transcriptómica	Fibroblastos de prepucio humanos (HFF) infectados con taquizoítos del aislado RH	Microarray	Sobreexpresión del receptor de transferrina y MacMARCKs (sustratos de la proteína quinasa C). Expresión de inmunomodulardores como IL-6.	Gail *et al.*, 2001
Tz	Transcriptómica	Cultivos sincronizados derivados de taquizoítos del aislado RH	Microarray	Descripción de dos subtranscriptomas distintos durante el ciclo lítico de los taquizoítos	Behnke *et al.*, 2010
Tz/Bz	Transcriptómica	Línea cellular humana Müller (MOI-M1) infectada con taquizoítos del aislado RH o bradizoítos del aislado Pru	Microarray	Sobreexpresión de citoquinas y quimioquinas como CCL2, IL-6, CXCL8 y CXCL2. No se detectó IFNγ ni IL-12	Knight et al., 2006
Sz/Tz	Transcriptómica	Células de epitelio intestinal de rata (IEC-18) infectadas con Sz o Tz del aislado M4	RNASeq	Sobreexpresión de genes asociados con la ruta proinflamatoria del TNFa via NFkB. Los esporozoítos muestran un transcriptoma intermedio entre ooquistes y taquizoítos	Guiton et al., 2017
Tz vs Sz	Transcriptómica	Merozoítos procedentes de enterocitos felinos y Taquizoítos del aislado CZ (Tipo II).	RNA-Seq	Metabolismo similar entre ambos estadios. 312 tránscritos exclusivos de los merozoítos frente a 453 exclusivos de los taquizoítos. Ausencia de expresión de la mayor parte de las proteínas GRA, MIC, y ROP descritas en los merozoítos, mientras que la familia SRS está ampliamente exxpresada.	Hehl et al., 2015
Tz	Transcriptómica/Proteómica	Taquizoítos sincronizados derivados del aislado TgRHΔKu80	RNA-Seq-ChIP	Unión cooperativa de los factores de transcripción ApiAP2X-5 y ApiAP2XI-5 para regular la progresión del ciclo celular	Lesage et al., 2018
Tz	Transcriptómica	Esplenocitos procedentes de ratones marsupiales (*Sminthopsis crassicaudata*)	RNA-Seq	Respuesta inmunitaria de tipo Th1 más potente que la generada por *N. caninum*, asociada a una menor morbilidad, cargas parasitarias y menores lesiones histopatológicas	Donahoe et al., 2017

			infectados con taquizoítos del aislado TaAuDg1			
	Tz	Proteómica	Taquizoítos	1-DE Gel LC-MS/MS; 2-DE Gel LC-MS/MS MudPIT	Descripción del proteoma de los taquizoítos	Bradley et al., 2005 Hu et al., 2006 Xia et al., 2008
	Ooquistes	Proteómica	Ooquistes esporulados de los aislados PYS y PRUS	iTRAQ LC-MS/MS	374 proteínas differencialmente expresadas, incluyendo factores de virulencia (GRA6, RON4, MIC3, ROP2A, GRA1, RON5, ROP18, MIC2, AMA1, MIC4, MIC6, ROP5 y GRA7) sobreexpresados en el aislado PYS	Zhou et al., 2017
	Tz	Proteómica	Taquizoítos de los aislados RH, PRU, TgQHO, TgC7 (tipo II)	DG DIGE + MS	110 manchas protéicas con una abundancia diferencial, correspondientes a 56 proteínas de T. gondii incluyendo SAG1, Hsp70, PDI, Hsp60.	Zhou et al., 2014
	Tz	Proteómica	Taquizoítos de los aislados GT1 (Tipo I), PTG (Tipo II),CTG (Tipo III).	2D-DIGE + MS	84 manchas proteicas correspondientes a 7 proteínasd de T. gondii con abundancia diferencial	Zhou et al., 2013
	Tz/Bz	Proteómica	Encéfalo de ratones infectados con quistes del aislado Pru (tipo II) a los 7, 14 y 21 días pi	2-DE MS/MS	60 manchas protéicas con expression diferencial, identificándose 45 proteínas del ratón, relacionadas con el metabolismo, la estructura celular, respuesta inmunitaria y transducción de señales.	Zhou et al., 2013
N. caninum	Tz	Genómica/Transcriptómica	Taquizoítos del aislado Nc-Liverpool	WGS	62 Mb organizados en 14 cromosomas. Aproximadamente 7500 genes que codifican para la síntesis de proteínas. Diferencias en el repertorio de genes expresados entre *T. gondii* y *N. caninum*, con una expansión de antígenos de superficie y la divergencia de factores de virulencia, como proteínas de roptrias, en N. caninum	Reid *et al.*, 2012
	Tz	Transcriptómica	Células del trofoblasto bovino (F3) infectadas con taquizoítos de aislados de alta (NcSpain7) y baja (NcSpain1H) virulencia.	RNA-Seq	Alteraciones en la organización de la matriz extracelular y la síntesis de colesterol. Expresión diferencial de genes característicos de apicomplejos entre los aislados con distinta virulencia	Horcajo *et al.*, 2017

Tz	Transcriptómica/Proteómica	Células epiteliales de riñón de mono Marc-145 infectadas con taquizoítos de alta (NcSpain7) y baja (NcSpain1H) virulencia	RNA-Seq/LC-MS-MS	Descripción de distintos proteomas a lo largo del ciclo lítico para ambos aislados. Los transcriptomas también mostraron diferencias notables, si bien eran inconsistentes con los datos del proteoma. Ambas aproximaciones mostraron un estado de pre-bradizoíto en el aislado menos virulento (NcSpain1H)	Horcajo *et al.*, 2018)
Tz	Transcriptómica	Ratones infectados con taquizoítos del aislado Nc-1	RNA-Seq	Sobreexpresión de 772 genes del ratón implicados en la respuesta inmunitaria del hospedador. Los genes que se correlaccionaban de forma positivaa con las cargas del parásito correspondían con la respuesta inmunitaria, mientras que los que tenían una correlación negativa estaban relacionados con la morfogénesis de neuronas y el metabolismo lipídico.	Nishimura et al., 2015
Tz	Transcriptómica	Macrófagos murinos infectados con taquizoítos KO para NcGRA7	RNA-Seq	NcGRA7 es capaz de modular la síntesis de citoquinas y quimioquinas por parte del hospedador, activando la respuesta inmunitaria	Nishikawa et al., 2018
Tz	Genómica/Transcriptómica	Taquizoítos del aislado NcLiverpool	WGS/RNA-Seq	Mejora de la anotación del genoma, corrigiendo hasta un tercio de los genes previametne anotados. Descripción de regions UTRs más largas de lo descrito para otros eucariotas. Identificación de *cis-natural antisense transcripts* (cis-NATs) y *long intergenic non-coding RNAs* (lincRNAs)	(Ramaprasad *et al.*, 2015)
Tz	Transcriptómica	Esplenocitos de ratones marsupials (*Sminthopsis crassicaudata*) infectados con taquizoítos del aislado Nc-Nowra	RNA-Seq	Respuesta inmunitaria de tipo Th1 no protectora, ya que se hayaan lesiones más graves que en el caso de ratones marsupiales infectados por *T. gondii*. Sobreexpresión de las rutas de señalización mediadas por TNFa e IFNγ	Donahoe et al., 2017
Tz	Proteómica	Taquizoítos aislado KBA2, JPA1	2DE	Descripción del proteoma del taquizoíto	Lee *et al.*, 2003, 2004
Tz/Bz	Proteómica	Taquizoítos y bradizoítos aislado Nc-Liv	2D-DIGE	Proceso de diferenciación hacia rutas anaeróbicas en bradizoítos, junto con la expresión de proteínas Hsp	Marugán-Hernández *et al.*, 2010

		Proteómica	Taquizoítos de aislados con diferente virulencia (Nc-Liv, Nc-Spain7, Nc-Spain1H)	DIGE – LC MS/MS	Mayor expresión de proteínas relacionadas con la motilidad, el estrés oxidativo y el ciclo lítico en los aislados más virulentos	Regidor-Cerrillo *et al.*, 2012
B. besnoiti	Tz/Bz	Proteómica	Tz/Bz	DIGE-MS/MS	Proteínas más abundantes en el estadio de bradizoíto (GAPDH, ENO1, LDH2, SOD y RNA polimerasa)	Fernandez-Garcia *et al.*, 2013
	Tz	Proteómica	Tz	2D-SDS + MS/MS	Descripción del inmunoma del Tz de *B. besnoiti*	Garcia-Lunar *et al.*, 2013b
	Tz	Proteómica	Tz *Besnoitia besnoiti* vs Tz *Besnoitia tarandi*	DIGE + MS	6 proteínas sobreexpresadas en *B. besnoiti* (LDH, Hsp90, fosforilasa nucleótidos de purina y 3 proteínas hipotéticas) y 6 proteínas sobre-expresadas en *B. tarandi* (G3PDH, LDH, PDI, mRNA *decapping* protein y 2 proteínas hipotéticas)	Garcia-Lunar *et al.*, 2014
	Tz	Genómica	Tz aislado Ger-1 (clon C6)	WGS	58.85 Mb organizados en 14 cromosomas, 8224 proteínas	Schares *et al.*, 2017
	Tz/Bz	Genómica/Transcriptómica	Tz/Bz aislado BbLISBON14	RNA-Seq	Genes diferencialmente expresados entre estadios	Ramakrishnan et al., comunicación personal

*Tz: Taquizoíto; Bz: Bradizoíto; Sz: Esporozoíto; Oo: ooquistes
**WGS: *Whole Genome Sequencing*; 1D/2D-SDS; Electroforesis en una dimensión/ dos dimensiones; DIGE; Electroforesis diferencial en gel; MS: espectrometría de masas; iTRAQ: *Isobaric tag for relative and absolute quantitation*; LC-MS/MS: cromatografía líquida acoplada a espectrometría de masas; ChIP: *chromatin immunoprecipitation*; SAGE: Serial analysis of gene expression; MudPit: *multidimensional protein identification technology*

2.2.4.1.1. Estudios genómicos

La genómica comprende la caracterización molecular de genomas completos mediante el estudio de su contenido, la organización y función de sus genes y la evolución de su información genética.

Los primeros estudios genómicos a gran escala en protozoos apicomplejos se basaron en el análisis de *Expressed Sequence Tags (*ESTs) (Ajioka, 1998; Howe, 2001; Ng *et al.*, 2002; Li *et al.*, 2003, 2004). Sin embargo, los avances tecnológicos pronto posibilitaron la secuenciación completa y la anotación de los genomas de *T. gondii* y de *N. caninum*, si bien la anotación del genoma de *T. gondii* es más completa y hasta la fecha se han secuenciado más de 17 aislados, cuyos genomas están disponibles en la base de datos ToxoDb (http://www.toxodb.org) (Gajria *et al.*, 2008). De ellos, tres: GT1 (tipo I); ME49 (tipo II) y VEG (tipo III) se consideran aislados tipo y han sentado las bases para la realización de estudios comparativos en busca de las bases moleculares de las diferencias en virulencia. Los genomas de *T. gondii* y *N. caninum* presentan aproximadamente 62 millones de pares de bases (Mb), divididos en 14 cromosomas y con aproximadamente 7500 genes que codifican proteínas. Debido a que el grado de homología que presentan los genomas de ambos parásitos es superior al 90%, tradicionalmente se ha utilizado a *T. gondii* como modelo a la hora de mejorar la anotación del genoma de *N. caninum*. De hecho, se ha demostrado que los genomas de ambos parásitos son ampliamente sinténicos y que han sufrido una escasa ganancia o pérdida de genes (Reid *et al.*, 2012). Por otro lado, la comparación del genoma de distintos géneros de apicomplejos ha definido la existencia de familias de genes que podrían estar asociadas a sus diferentes estrategias de evasión del sistema inmunitario del hospedador por su elevada tasa de mutación (Reid, 2015). En el caso de *T. gondii*, dichas familias incluyen las proteínas de superficie SRS (Tomavo, 2001; Reid *et al.*, 2012) y proteínas de las roptrias, con una función kinasa (ROP) (Talevich & Kannan, 2013). También se han realizado estudios para tratar de mejorar la anotación del genoma de *N. caninum* y reducir el número de proteínas hipotéticas en las bases de datos mediante análisis bioinformáticos (Calarco & Ellis, 2019).

En el caso concreto de *B. besnoiti*, el genoma del aislado Bb-Ger1 es el único secuenciado y publicado hasta la fecha, contando con 58 Mb, 14 cromosomas y más de 7000 genes codificantes de proteínas (Schares *et al.*, 2017) Bioproject PRJNA305615). En paralelo, también se ha secuenciado el genoma del aislado Bb-Lisbon14 (Bioproject PRJNA305615), revelando que contiene más de 50 Mbases y 6529 genes predichos (Ramakrishnan *et al*., *unpublished*).

Por otra parte, dado que el apicoplasto cuenta con su propio material genético y una maquinaria de expresión génica propia, se encuentra en el punto de mira de muchos estudios en busca de nuevas dianas terapéuticas. Por este motivo su genoma ha sido completamente secuenciado en *T. gondii* y *N. caninum*. Recientemente, el genoma del apicoplasto del aislado BbGer-1 de *B. besnoiti* también ha sido secuenciado y publicado (Schares *et al.*, 2017; Genbank ID CM008359.1)

2.2.4.1.2. Estudios transcriptómicos

La transcriptómica se encarga del estudio de los genes expresados en una etapa específica del desarrollo de un organismo mediante el análisis del ARN transcrito. La información obtenida de los estudios de transcriptómica sirve de nexo entre los hallazgos genómicos y proteómicos, aunque no tiene en cuenta los diferentes niveles de regulación

existentes entre la transcripción y la traducción, como son la maduración del ARN y su transporte al citoplasma. Al igual que ocurre en el caso del proteoma, a lo largo del ciclo lítico se pueden describir distintos sub-transcriptomas, estando asociados a la fase del ciclo celular (S/M o G1). Así, durante la fase G1 del ciclo celular predomina la expresión de genes conservados en eucariotas e importantes para la duplicación del material genético (como las ARN polimerasas, proteínas ribosomales y proteínas de replicación del ADN), mientras que en la fase S/M existe un predominio de genes específicos de apicomplejos (como SAG, MIC y ROP, entre otros) (Behnke *et al.*, 2010).

Los primeros análisis del transcriptoma del taquizoíto de *T. gondii* se realizaron mediante técnicas SAGE (*Serial Analysis Gene Expression*), ESTs, microarrays, MPSS (*Massively Parallel Signature Sequencing*) y TSSs (*Transcription Start Site*) (Radke *et al.*, 2005; Wastling *et al.*, 2009; Bahl *et al.*, 2010; Yamagishi *et al.*, 2010; Hassan *et al.*, 2012). Posteriormente, el desarrollo de nuevas metodologías de secuenciación masiva, como el RNA-seq ha facilitado la realización de estos estudios (Horcajo *et al.*, 2017). Además, muchos de los estudios de transcriptómica llevados a cabo hasta la fecha se han centrado en la determinación de los mecanismos de manipulación de las células hospedadoras tras la infección (Hakimi *et al.*, 2017).

Al contrario de lo que ocurre con *T. gondii*, existen pocos estudios transcriptómicos realizados en *N. caninum*. En primer lugar, se comparó a gran escala el perfil de expresión génico de taquizoítos de *N. caninum* con los datos disponibles de *T. gondii*, demostrándose que, si bien el contenido genético de ambos parásitos está muy conservado, existen notables diferencias (Reid *et al.*, 2012). Recientemente, el desarrollo de nuevas metodologías de secuenciación masiva, como la metodología RNA-Seq ha posibilitado la realización de estudios transcriptómicos de la infección por *N. caninum* tanto *in vivo* (Nishimura *et al*., 2015) como *in vitro* (Horcajo *et al.*, 2017).

Por el contrario, hasta la fecha no se ha realizado ningún estudio que aporte información sobre el perfil de expresión génico de los taquizoítos de *B. besnoiti* durante el ciclo lítico, la interacción de *B. besnoiti* con la célula hospedadora ni que compare el perfil de expresión génica entre diferentes aislados.

2.2.4.1.3 Estudios proteómicos

Durante los últimos años los abordajes proteómicos han surgido como herramientas muy útiles para el estudio de protozoos apicomplejos. La proteómica comprende el análisis global de las proteínas expresadas por un organismo en un momento determinado. Por ello, se pueden describir distintos proteomas a lo largo del ciclo lítico, y es esperable que las posibles diferencias en la interacción entre el parásito y distintas células hospedadoras se vean reflejadas en el proteoma. La integración de los datos genómicos, transcriptómicos y proteómicos permiten profundizar en las bases moleculares de la biología de los protozoos apicomplejos (Xia *et al.*, 2008; Wastling *et al.*, 2009; Krishna *et al.*, 2015; Horcajo *et al.*, 2018).

Los estudios realizados en *T. gondii* han tratado de determinar posibles factores de virulencia mediante la comparación del proteoma de aislados con diferente virulencia (Zhou *et al.*, 2013, 2014). Sin embargo, hasta el momento no se ha llevado a cabo ningún trabajo en el que se hayan determinado las diferencias existentes entre el proteoma de los taquizoítos y el de los bradizoítos. También se ha estudiado el proceso de modulación de las células infectadas en beneficio del parásito mediante el análisis de su proteoma antes y durante la infección (Nelson *et al.*, 2008; Zhou *et al.*, 2011), demostrándose, al igual que

en los estudios transcriptómicos, que *T. gondii* es capaz de alterar la expresión de proteínas estructurales y metabólicas, así como otras relacionadas con la respuesta inmunitaria del hospedador y con el control de la apoptosis.

La composición proteica de los taquizoítos de *N. caninum* fue definida por primera vez mediante técnicas de electroforesis bidimensional (Lee *et al.*, 2003, 2004). Posteriormente, la metodología 2D-DIGE (*Two Dimensional-DIfference Gel Electrophoresis*) ha permitido comparar el proteoma del taquizoíto y el bradizoíto, aportando datos cuantitativos de expresión y revelando que los bradizoítos sufren un proceso de diferenciación hacía rutas glicolíticas anaeróbicas y una mayor expresión de proteínas de respuesta al estrés (*Heat Shock Proteins*) (Marugán-Hernández *et al.*, 2010). Además, el DIGE junto con la espectrometría de masas (MS/MS) permitió realizar un estudio comparativo entre diversos aislados de *N. caninum*, encontrándose en los aislados virulentos una mayor abundancia de proteínas relacionadas con la motilidad, el estrés oxidativo y el ciclo lítico (Regidor-Cerrillo *et al.*, 2012). Recientemente, se ha realizado un estudio que combina la metodología RNA-Seq junto con la cromatografía líquida y espectrometría de masas (LC-MS/MS) para investigar diferencias en el proteoma y transcriptoma de dos aislados de *N. caninum* con distinta virulencia (Horcajo *et al.*, 2018).

En los últimos años se han realizado varios abordajes proteómicos para el estudio de *B. besnoiti*, de una forma análoga a cómo se han empleado las metodologías en *N. caninum*. No obstante, estos estudios han estado limitados por la ausencia del genoma, que no ha sido publicado hasta 2017 (Schares *et al.*, 2017), por lo que faltaba información acerca de muchas proteínas hipotéticas, no presentes en las bases de datos de *N. caninum* y *T. gondii*. Los estudios realizados se han centrado en el estudio de las diferencias en la composición proteica entre el estadio de taquizoíto y el de bradizoíto mediante la metodología 2D-DIGE junto con espectrometría de masas, identificándose cinco proteínas más abundantes en el estadio de bradizoíto (GA3PDH, Enolasa 1 (ENO1), Lactado deshidrogenasa (LDH), superóxido dismutasa (SOD) y RNA polimerasa) frente a cinco más abundantes en el estadio de taquizoíto (ENO2, lactato deshidrogenasa, *Heat shock protein* 70 (HSP70), PDI y ATP sintasa). Desafortunadamente, todas ellas son enzimas muy conservadas y no son exclusivas de protozoos del subfilo Apicomplexa (Fernández-García *et al.*, 2013). Posteriormente, también se caracterizó el proteoma y el inmunoma de los taquizoítos de *B. besnoiti* mediante la metodología 2D-SDS PAGE y espectrometría de masas, identificándose proteínas inmunógenas pero conservadas en eucariotas, relacionadas con el metabolismo energético, chaperonas y el metabolismo de radicales libres de oxígeno (García-Lunar *et al.*, 2014). También se ha realizado un abordaje proteómico para estudiar diferencias en la abundancia de proteínas y el perfil antigénico entre *B. besnoiti* y *B. tarandi*, observándose diferencias en la abundancia de proteínas conservadas en eucariotas como LDH, Hsp90, fosforilasa de nucleósidos de purina y tres proteínas hipotéticas aumentadas en *B. besnoiti* (GA3PDH, LDH, PDI, mRNA "*decapping protein*") y dos proteínas hipotéticas en *B. tarandi* (García-Lunar et al., 2014). Además, el perfil antigénico entre ambas especies es muy similar, lo que refuerza la idea de que ambas especies presentan importantes reacciones cruzadas a nivel serológico (Gutiérrez-Expósito *et al.*, 2012).

Hasta la fecha, únicamente se ha identificado y caracterizado una proteína conservada en organismos eucariotas (Tabla 10), la proteína disulfuro isomerasa (PDI) (Marcelino *et al.*, 2011), que por analogía con su ortólogo en *N. caninum* sería secretada por los micronemas y jugaría un papel importante en la invasión del parásito (Naguleswaran *et al.*, 2005). También se ha demostrado que el antígeno de bradizoíto BAG1 ("*heat shock*

protein Hsp30") reconoce a su ortólogo en *B. besnoiti* por inmunohistoquímica (IHQ) (Dubey *et al.*, 2003a).

Tabla 11: Proteínas identificadas en *B. besnoiti* hasta la fecha

Proteína	Estadio (Tz/Bz*)	Función	Referencia
BbPDI	Tz	Formación puentes disulfuro. Secretada por micronemas	Marcelino et al., 2011; García-Lunar et al., 2013
Peroxiredoxina dependiente de tioredoxina	Tz	Equilibrio redox	García-Lunar et al., 2013
Actina	Tz	Motilidad ("gliding")	García-Lunar et al., 2013
Factor de depolimerización de la actina	Tz	Motillidad ("gliding")	García-Lunar et al., 2013
Profilina	Tz	Motilidad e Invasión	García-Lunar et al., 2013
Tubulina (cadena b)	Tz	Citoesqueleto	García-Lunar et al., 2013
ENO2	Tz	Glicólisis	Fernández-García et al., 2013
LDH	Tz	Metabolismo	Fernández-García et al., 2013
HSP70	Tz	Chaperona	Fernández-García et al., 2013; García-Lunar et al., 2013
HSP60	Tz	Chaperona	García-Lunar et al., 2013
HSP90	Tz	Chaperona	García-Lunar et al., 2013
ATP sintasa	Tz	Metabolismo energético	Fernández-García et al., 2013
GA3PDH	Bz	Glicólisis	Fernández-García et al., 2013
ENO1	Bz	Glicólisis	Fernández-García et al., 2013
Superóxido dismutasa (SOD)	Bz	Equilibrio redox	Fernández-García et al., 2013
LDH2	Bz	Metabolismo	Fernández-García et al., 2013
RNA polimerasa	Bz	Síntesis RNA	Fernández-García et al., 2013

*Tz: Taquizoíto Bz: Bradizoíto

La identificación de proteínas clave para la progresión del ciclo lítico del parásito, y que puedan ser relevantes para la virulencia del mismo, es un punto clave en el desarrollo de nuevas estrategias de control, ya sean farmacológicas o vacunales.

2.2.4.2. Interacción parásito-hospedador:

2.2.4.2.1. Estudios de conversión de taquizoíto a bradizoíto in vitro

El proceso de conversión *in vitro* es muy eficaz en *T. gondii*, en el cual se han empleado diferentes agentes estresantes capaces de inducir la transformación del estadio de taquizoíto al de bradizoíto (revisado por Skariah *et al.*, 2010). Estos estudios han posibilitado el estudio de los mecanismos moleculares implicados en la conversión de taquizoíto al bradizoíto, la formación de la pared quística y el estudio de la funcionalidad de genes específicos de estadio. En el caso de *T. gondii*, la conversión puede ocurrir de forma

espontánea, dependiendo del aislado empleado (Sánchez-Sánchez et al., 2019) y, generalmente, se ha visto que dicha conversión espontánea es más frecuente en cultivos utilizando células musculares, tanto primarias como inmortalizadas, indicando una predilección por el tipo celular utilizado (da Fonseca Ferreira-da-Silva *et al.*, 2009; Guimarães *et al.*, 2008). No obstante, también se ha descrito la conversión espontánea al estadio de bradizoíto en células epiteliales intestinales de gato (de Muno *et al*., 2014). Además, es posible inducir la conversión mediante el empleo de factores estresantes abióticos como el pH alcalino, compuestos químicos o fármacos, choque térmico, deprivación de arginina y mediante la aplicación de IFN-γ y otras citoquinas proinflamatorias (Skariah *et al.*, 2010).

Por el contrario, en el caso de *N. caninum*, la conversión al estadio de bradizoíto de forma espontánea *in vitro* no se ha descrito hasta la fecha y su inducción es más difícil de conseguir, pareciendo tener más restricciones en cuanto a la célula hospedadora utilizada y los aislados del parásito (Weiss *et al.*, 1999). Además, el pH alcalino no es capaz de inducir la conversión a bradizoítos y es necesario el aporte de agentes donadores de óxido nítrico (nitroprusiato de sodio), que son agentes inductores de apoptosis, obteniéndose una eficiencia de conversión inferior a la que se obtiene en el caso de *T. gondii* (Vonlaufen *et al.*, 2002b; Risco-Castillo *et al.*, 2004;). En el caso de *Hammondia*, otro parásito perteneciente a la subfamilia Toxoplasmatinae, se ha descrito una conversión espontánea al estadio de bradizoíto *in vitro*, con una conversión prácticamente total a partir de los ocho días pi (Sokol et al., 2018; Gondim et al., 2015).

Hasta la fecha, se desconocen los factores capaces de desencadenar la conversión a bradizoíto en el caso de *B. besnoiti*, y la conversión espontánea no ha sido descrita hasta la fecha.

Además, para completar el ciclo biológico *in vitro* en condiciones reproducibles y controladas, sería esencial el desarrollo de un sistema capaz de reproducir las fases entero-epiteliales y la reproducción sexual que tiene lugar en el intestino de las especies que actúan como HD de *N. caninum* y *T. gondii*.

2.2.4.2.2. Interacción parásito-célula hospedadora

A la hora de estudiar la interacción parásito-hospedador, es deseable la realización de dichos estudios en un sistema *in vitro* que utilice células dianas del hospedador importante desde el punto de vista de la patogenia y la transmisión del parásito, ya que presumiblemente el sistema celular empleado va a condicionar el comportamiento del parásito. De hecho, se han llevado a cabo estudios en macrófagos (Olaffson et al., 2018) y células dendríticas (Weidner *et al.*, 2013), viéndose que *T. gondii* es capaz de inducir un fenotipo hipermigratorio, lo que soporta la hipótesis de que este parásito es capaz de modular el comportamiento de la célula hospedadora y utilizar células del sistema inmune como un "caballo de Troya", facilitando el cruce de las barreras biológicas y la diseminación por el organismo del hospedador (Weidner *et al.*, 2013). Del mismo modo, también se ha visto que *T. gondii* es capaz de activar las células de la microglía para inducir el fenotipo hipermigratorio, pero esto no ocurre en los astrocitos (Dellacasa-Lindberg et al., 2011). Se ha visto además que la inducción de este fenotipo hipermigratorio es dependiente de aislado, ya que la transmigración asociada a células dendríticas es mayor para los aislados de tipo II (TgME49), mientras que los aislados de tipo I (TgRH) tienen una mayor capacidad de transmigración cuando son extracelulares (Collantes-Fernández *et al.*, 2012). Se ha visto que en el fenotipo hipermigratorio son fenómenos importantes la

disolución de los podosomas de las células dendríticas, así como la secreción de metaloproteasas de matriz como TIMP1 (Ólafsson *et al.*, 2019).

En *N. caninum* también se ha visto que la infección de las células dendríticas facilita la diseminación de los taquizoítos *in vitro* a través de una barrera polarizada de células de coriocarcinoma humano BeWo. Asimismo, también se ha detectado una mayor carga parasitaria *in vivo* en un modelo murino al inocular células dendríticas infectadas por taquizoítos en comparación con la inoculación de taquizoítos (Collantes-Fernández *et al.*, 2012). También, dado que una de las manifestaciones clínicas más importantes de la neosporosis bovina es la aparición de abortos o el nacimiento de terneros congénitamente infectados en función de la fase de la gestación, recientemente se ha estudiado el comportamiento de dos aislados de *N. caninum* con diferente virulencia en modelos *in vitro*, en líneas celulares de placenta (tanto de carúncula como del trofoblasto) (Horcajo *et al.*, 2017), observándose un comportamiento diferencial de ambos aislados, con predilección por las células fetales (del trofoblasto), mientras que las células de la carúncula materna limitaban el crecimiento del parásito, lo que podría confirmar un efecto "barrera" para limitar la infección y evitar el paso de la infección al feto. Además, también se ha visto diferencias en la susceptibilidad de células del trofoblasto humano (BeWo) y del cuello de útero humanas (HeLa) a la infección por *N. caninum* (Carvalho *et al.*, 2010). En este estudio se vio que, si bien ambas células eran infectadas por los taquizoítos, existían diferencias y las células HeLa parecían más susceptibles. Concretamente, *N. caninum* producía un incremento en la síntesis del factor de inhibición de la migración de macrófagos (MIF) en las células HeLa, mientras que en las células BeWo producía un descenso en la síntesis del factor de crecimiento transformante TGF-β. También se ha visto que los taquizoítos de *N. caninum* producen una activación mediante fosforilación de la ruta de señalización celular p38 MAPK como un mecanismo de evasión de la respuesta inmunitaria en macrófagos murinos (Mota *et al.*, 2016). También se ha propuesto el uso de cultivos organotípicos del sistema nervioso central de ratas como una alternativa para el estudio de la interacción parásito-hospedador en *N. caninum* (Vonlaufen *et al.*, 2002a) simulando lo que ocurriría en condiciones naturales.

En células endoteliales bovinas obtenidas de la vena umbilical de terneros (BUVEC), se ha descrito que tanto *T. gondii* como *N. caninum* producen la transcripción de genes responsables de la activación del endotelio (como E-selectina, P-selectina, ICAM1, VCAM1), promoviendo la adhesión de leucocitos polimorfonucleares (Taubert *et al.*, 2006a, b). No obstante, la estimulación por parte de *T. gondii* de la adhesión de leucocitos era mayor que la de *N. caninum*. Además, se estudiaron las dinámicas de transcripción de otro panel de genes inmunomoduladores en células BUVEC infectadas con esporozoítos de *Eimeria bovis* o taquizoítos de *N. caninum* o *T. gondii*, midiéndose los niveles de quimioquinas (GROa, IL8, IP10, MCP-1 RANTES) y otros genes como GM-CSF, COX-2 e iNOS, viéndose un aumento de la transcripción en *T. gondii* y *N. caninum* comenzando a las 2-4 horas post-infección, mientras que la expresión bajaba a niveles del control negativo a las 12 hpi (Taubert *et al.*, 2006b). Por el contrario, los esporozoítos de *E. bovis* no producían un incremento en la transcripción de quimioquinas.

Además, se ha descrito que las trampas extracelulares de neutrófilos (NET) actúan como efectores tempranos en la respuesta inmunitaria innata frente a los taquizoítos de *N. caninum* tanto en células bovinas (Wei *et al*., 2018; Villagra-Blanco *et al*., 2017) como caprinas (Yang *et al*., 2018), caninas (Wei *et al*., 2016) o incluso de delfines (Villagra-Blanco *et al*., 2017b). Dichas trampas extracelulares consisten en una malla de ADN que contiene histonas y sustancias antimicrobianas, como elastasa, proteinasa 3, catepsina G o lactoferrina y es liberada por neutrófilos y otras células inmunes al espacio extracelular para atrapar microorganismos (Larrañaga *et al*., 2012).

En el caso de *B. besnoiti*, el único sistema *in vitro* empleando células de la especie de destino (bovino) que ha sido utilizado para el estudio de su biología consiste en el empleo de células BUVEC. En este sistema se han realizado estudios de los requerimientos metabólicos de los taquizoítos, viéndose que la proliferación del parásito va acompañada con la sobre-expresión de enzimas que están implicadas en rutas como la glutaminolisis y la glucólisis (Taubert *et al.*, 2016); así como estudios que han mostrado que la infección del parásito origina la transcripción de genes comúnmente asociados con la activación de células endoteliales que daría lugar a una respuesta inflamatoria, como P-selectina, molécula de adhesión intercelular 1 – ICAM-1-, quimioquinas -CXCL1, CXCL5, CCL5- y COX-2-, de una forma análoga a lo que se ha visto en *N. caninum* o *T. gondii* empleando el mismo sistema, que conllevan un incremento en la adhesión de leucocitos (Maksimov *et al.*, 2016).

También se han realizado un par de estudios para estudiar la respuesta inmunitaria innata frente a taquizoítos de *B. besnoiti*, observándose que la infección por los taquizoítos es capaz de inducir la formación de NET por parte de monocitos (Muñoz-Caro *et al.*, 2014a) y neutrófilos bovinos (Muñoz-Caro *et al.*, 2014b).

2.2.4.3. Identificación de nuevas dianas terapéuticas y cribado de fármacos

Otra utilidad de los modelos *in vitro* es la búsqueda y caracterización de los mecanismos de acción de posibles sustancias terapéuticas, permitiendo la realización de ensayos de pruebas de concepto de la utilidad de fármacos frente a estos parásitos (ensayos de seguridad y eficacia de fármacos) (ver Sección 2.1.7.3).

2.2.4.4. Limitaciones de los cultivos celulares

En la actualidad, el empleo de los modelos *in vitro* contribuye notablemente al estudio de la biología de protozoos apicomplejos y constituye un elemento esencial para la implementación de los principios de las 3R en experimentación animal (reemplazo, reducción y refinamiento), ya que proporciona un sistema en el que se pueden realizar pruebas de concepto antes de pasar a los modelos *in vivo*. Sin embargo, existen algunas limitaciones generales de los modelos *in vitro*, ya que son sistemas limitados incapaces de reproducir el efecto del microambiente y la interacción de diferentes tejidos y células, por lo que no sustituyen a los modelos *in vivo*; se trata de modelos relativamente estáticos y presentan dificultades en el estudio de las infecciones a largo plazo. Además, no existe una metodología uniforme en cuanto a los controles de calidad de los cultivos celulares, para garantizar la ausencia de coinfecciones que puedan alterar los resultados y la reproducibilidad de los mismos. Pero también presentan algunas limitaciones específicas asociadas al estudio de protozoos Toxoplasmatinae: i) incapacidad de reproducir el ciclo biológico completo del parásito (de momento no se han obtenido los estadios entero-epiteliales responsables del ciclo sexual *in vitro*); ii) no existe un modelo de cultivo celular estándar ni aislados parasitarios de referencia que permitan hacer comparables los diferentes estudios ; iii) generalmente se han empleado líneas celulares inmortalizadas y procedentes de tejidos diferentes a los tejidos diana del parásito, por lo que resultaría interesante contar con otros modelos *in vitro* más representativos de la infección natural.

En cuanto a los cultivos primarios empleados, para el estudio de la interacción parásito-hospedador es crucial tener en cuenta factores como la especie del animal donante, el tejido de obtención teniendo en cuenta la heterogeneidad de poblaciones celulares

descritas (Aird, 2012) y analizar el estado sanitario de los animales previamente a la obtención de los cultivos primarios para descartar infecciones concurrentes que puedan influir en el comportamiento *in vitro*. A la hora de establecer un modelo de estudio *in vitro* para realizar estudios de patogenia molecular, es imprescindible tratar de reproducir de una manera lo más próxima posible lo que ocurre en condiciones *in vivo*, por lo que sería deseable el empleo de cultivos primarios. De hecho, en el caso de las células endoteliales primarias disponibles comercialmente, las casas comerciales no recomiendan utilizar sus cultivos primarios más allá de un pase 16 (16 duplicaciones en condiciones *in vitro*), por la existencia de cambios fenotípicos debidos a la selección *in vitro*, que pueden dar lugar a la pérdida de funciones específicas del tejido de procedencia (Pan *et al.*, 2009). Por otra parte, dichos cultivos primarios presentan una inherente variabilidad, y aportan dificultades tanto desde el punto de vista técnico como económico al necesitar continuamente aislar nuevos cultivos primarios para la realización de nuevos experimentos.

Por otra parte, desde el punto de vista del parásito es importante monitorizar el número de pases *in vitro* al que se ve sometido para evitar su adaptación a las condiciones *in vitro*, como se ha visto en *N. caninum* (Bartley *et al.*, 2006) o *T. gondii*. (Nischik *et al.*, 2001). De hecho, en los experimentos realizados por Frey *et al*. (2016)), a pesar de tratar de evitar la adaptación a los cultivos celulares mediante un paso previo por un sistema celular en el que no se habían multiplicado los taquizoítos previamente, se desconocía el número de pases de los aislados que mostraron mayores capacidades invasivas y proliferativas (p. ej. Bb-Israel).

Por último, es crucial realizar controles de calidad de los reactivos comúnmente utilizados en cultivos celulares, como p. ej. del suero fetal bovino para garantizar la ausencia de contaminantes frecuentes como el virus de la diarea vírica bovina (BVDV) o *Mycoplasma* spp. La presencia de estos contaminantes puede alterar la interacción parásito-célula hospedadora y, por tanto, los resultados obtenidos. En el caso de BVDV, se sabe que este virus es capaz de alterar la respuesta inmunitaria tanto innata (Peterhans *et al.*, 2003) como adaptativa (Chase, 2013). No obstante, en la actualidad se desconoce la posible interacción entre *B. besnoiti* y BVDV en condiciones de campo.

CAPÍTULO III: JUSTIFICATION AND OBJECTIVES

Bovine besnoitiosis is caused by the apicomplexan protozoan *Besnoitia besnoiti.* This parasitic disease is gaining an increasing importance. It has been described in Central and Western Europe, including Spain, and goes on spreading in areas with extensive husbandry systems (European Food Safety Authority, 2010; Álvarez-García, 2016). This disease is responsible for diminishing productions and alters reproductive parameters in infected herds where natural mating is a common management practice (Álvarez-García *et al.*, 2014b). Indeed, acute infection may cause orchitis in bulls, which can lead to testicular atrophy and subsequent sterility during the chronic infection. Unfortunately, disease control is hampered by the absence of vaccines and/or effective treatments, which coupled with precise diagnosis and adequate management measures would represent the ideal control approach (Gutiérrez-Expósito *et al.*, 2017a). The development of a vaccine against *B. besnoiti* represents a long-term strategy, since there are still many gaps in the biology of the parasite. Particularly, the molecular mechanisms that govern the host-pathogen interactions still remain to be elucidated. On the other hand, drug repurposing (i.e. the use of commercialised drugs for cattle that are effective against other infectious diseases) represents a more realistic and cost beneficial approach. This objective could be reached in the short-medium run (Sánchez-Sánchez *et al.*, 2018). In the meantime, new drug targets should be also explored. An effective drug should target the tachyzoite stage, responsible for the acute stage, to avoid intra-organic dissemination, tissue damage and the establishment of the life-long chronic disease.

In this scenario, the development of suitable *in vitro* models of infection arise as valuable tools to study host-pathogen interactions and to identify drug or vaccine targets (Müller & Hemphill, 2012). For the development of *in vitro* models, we need to take into consideration both the parasite, since the tachyzoite stage must be able to invade and proliferate into the host cells, and the host, since ideal target cells should be isolated from the natural host free from other pathogens. Endothelial cells (ECs) and fibroblasts are *B. besnoiti* target cells during the acute and the chronic infection, respectively (Álvarez-García *et al.*, 2014b). Endothelial cells represent the first barrier in the lumen of blood vessels and, apart from their roles in hemostasis and the regulation of vascular tone, they play a key role as active regulators of innate immune responses, since they are able to express a range of innate pattern recognition receptors and secrete signaling molecules, such as cytokines and chemokines to induce white blood cells recruitment and extravasation to the focus of inflammation (Mai *et al.,* 2013). Fibroblasts are crucial for the extracellular matrix production and remodelation. Thus, fibroblasts are key mediators in fibrosis in conjunction with immune cells (Van Linthout *et al*., 2014).

Molecular pathogenesis studies in *in vitro* systems might lead us to explore the mechanisms responsible for the dissemination of the parasite and disease progression, both during the acute and the chronic stage. Previous studies carried out with ECs and fibroblasts infected with *B. besnoiti* have been restricted to the employment of either bovine umbilical vein endothelial cells (BUVEC) (Maksimov *et al.*, 2016; Taubert *et al.*, 2016) or Human Foreskin Fibroblasts (HFF) cells (Cortes *et al.*, 2007a). However, both cell lines do not fulfill both host species and tissue location requirements: i) BUVEC are unlikely to be infected in natural infections, since *B. besnoiti* vertical transmission has not been reported; ii) ECs show heterogeneity in structure and function depending on their localization; iii) the different host origin of HFFs does not make them the ideal system to dissect host-parasite interactions at the molecular level. Moreover, the absence of bovine pathogens, such as bovine viral diarrhea virus (BVDV), is crucial. This virus is a prevalent bovine pathogen, a frequent contaminant in foetal bovine serum (FBS) batches worldwide (Gagnieur *et al.*, 2014) and it is known to alter the transcriptomic profile of ECs *in vitro* (Neill *et al.,* 2008). Thus, primary ECs and fibroblasts of adult cattle circulatory system, free of BVDV, might be appropriate tools.

On the other hand, *in vitro* models allow to assess drug safety and efficacy as a proof of concept before switching to the target species. Thus, these models involve the implementation of the 3Rs principle of animal experimentation (replacement, reduction and refinement). As mentioned before, drug repurposing is considered as one of the viable alternatives nowadays, being economically affordable and allowing to tackle diseases caused by protozoan parasites. So far, both commercially available drugs, such as buparvaquone (Müller *et al.*, 2018), and new generation drugs, such as arylimidamides, thiazolides or biphenylimidazoazines (Moine *et al.*, 2015; Cortes *et al.*, 2007a, 2011) have been tested against *B. besnoiti in vitro*. However, it would be worth trying other commercially available compounds since buparvaquone is not licensed for cattle in Europe. In the search of novel therapeutic targets for the control of diseases caused by apicomplexan protozoa, the calcium dependent protein kinases (CDPKs) represent attractive drug targets since they are absent in mammalian cells and they have one key structural feature (a glycine gatekeeper in the active site of the enzyme), which has allowed the development of potent ATP-competitive inhibitors known as "bumped kinase inhibitors" (BKIs), which are effective against apicomplexan parasites both *in vitro* and *in vivo* (Van Voorhis *et al.*, 2017).

Accordingly, the general objective of the present Doctoral Thesis was to develop and employ *in vitro* models to perform molecular pathogenesis and drug screening studies in *B. besnoiti* infection". The general objective comprised two specific objectives:

Objective 1: Development of novel standardized *in vitro* models for the study of *B. besnoiti* infection using primary bovine target cells – aorta endothelial cells and fibroblasts – and studies on the parasite - bovine viral diarrhea virus interaction.

"Lytic cycle of *Besnoitia besnoiti* tachyzoites displays similar features in primary bovine endothelial cells and fibroblasts"

Novel *in vitro* models have been developed using primary cultures (ECs and fibroblasts) isolated from the natural host (cattle). Another key aspect considered was the health status of donor animals, since the absence of pathogens commonly found in cattle, such as BVDV, was checked. Moreover, the absence of BVDV was also monitored in the FBS employed in the cell cultures. Afterwards, the expression of surface and intracellular markers was assessed by flow cytometry to characterize both primary cell populations. Next, the lytic cycle of *B. besnoiti* tachyzoites was addressed in both cell cultures using Bb-Spain1 as a reference isolate. Besides, the interaction between BVDV and *B. besnoiti* tachyzoites was addressed for the first time in bovine aorta endothelial cells (BAEC).

Objective 2: Employment of *in vitro* experimental models in molecular pathogenesis and drug screening studies in *B. besnoiti* infection

Sub-objective 2.1.: Employment of BAEC in molecular pathogenesis studies of *B. besnoiti* infection

The present study aimed to unravel the molecular mechanisms that govern pathogenesis of *B. besnoiti* infection during acute bovine besnoitiosis. Thus, we have employed the previously developed *in vitro* model of infection based on BAEC. Next, host-parasite interactions were investigated by RNA-Seq at two time points post-infection (pi): 12 hpi, when tachyzoites have already invaded host cells, and 32 hpi, when tachyzoites have replicated for at least two generations. Non-infected cultures were also collected at 12 hpi. Samples were sequenced in an Illumina HiSeq 4000 sequencer and subjected for functional enrichment and pathway analyses. All analyses were performed with four biological replicates and samples were also collected for further transcriptome validation by real time quantitative PCR (qPCR). Additionally, the transcriptome of *B. besnoiti* tachyzoites was

studied at both time points pi in order to identify apicomplexan specific genes that may play a key role in the lytic cycle.

Sub-objective 2.2.: Drug screening of commercially available anti-coccidials against *B. besnoiti* infection.

Anticoccidial drugs commercialized in cattle and effective against other protozoan diseases (Sub-objective 2.2.) and new generation drugs (Sub-objective 2.3.) were screened in the immortalised Marc-145 cells. This *in vitro* model was employed as: i)the lytic cycle of tachyzoites from the BbSpain1 isolate in both BAEC and fibroblasts did not show remarkable differences either in invasion or proliferation parameters when compared to the immortalised Marc-145 cells; ii) there may be variability of primary cultures inherent to donors.

"Repurposing of commercially available anti-coccidials identifies diclazuril and decoquinate as potential therapeutic candidates against *Besnoitia besnoiti* infection."

In the present study the safety and efficacy of a panel of anti-coccidial drugs marketed for cattle (diclazuril, toltrazuril, decoquinate, imidocarb, sulfadiazine and trimethoprim, alone or in combination with sulfadiazine) was assessed against *B. besnoiti* tachyzoites using an *in vitro* model in Marc-145 cells. Next, the inhibitory concentrations 50 and 99 (IC50 & IC99) of the best candidates (diclazuril and decoquinate) were determined by qPCR. The effects of these selected drugs on the ultrastructure of the parasites were also determined by transmission electron microscopy (TEM) together with their long-term parasiticidal or parasitostatic activity.

Sub-objective 2.3.: Drug screening of new generation drugs (bumped kinase inhibitors) against *B .besnoiti* infection.

"*In vitro* efficacy of bumped kinase inhibitors against *B. besnoiti* tachyzoites."

In the present study, we identified and characterized BbCDPK1 and evaluated the efficacy of nine BKIs against *B. besnoiti* tachyzoites in a standardized *in vitro* assay model. First, BbCDPK1 was successfully identified and its enzymatic activity was corroborated with a panel of nine BKIs (1294, 1517, 1553, 1571, 1575, 1586, 1597, 1605, 1649). Next, these BKIs were screened for their safety and efficacy against *B. besnoiti in vitro* infection. Finally, the inhibitory concentrations 50 and 99 (IC50 & IC99) of the best candidates (1294, 1517, 1553 and 1571) were determined by qPCR. The effects of the selected drugs on the ultrastructure of the parasites were also determined by TEM together with their long-term parasiticidal or parasitostatic activity.

CAPÍTULO IV:

RESULTADOS/RESULTS

4.1. Objetivo 1: Desarrollo de nuevos modelos *in vitro* estandarizados para el estudio de la infección por *Besnoitia besnoiti* empleando cultivos primarios bovinos – células endoteliales y fibroblastos- y estudios de la interacción del parásito con el virus de la diarrea vírica bovina en células endoteliales.

En el presente estudio se han obtenido y estandarizado dos modelos *in vitro* para el estudio de la infección por *B. besnoiti* basados en el empleo de cultivos primarios de origen bovino, empleando células diana tanto de la fase aguda (células endoteliales de aorta, BAEC) como de la fase crónica de la enfermedad (fibroblastos). Para ello, se han tenido en cuenta dos aspectos clave: el empleo de cultivos primarios y la ausencia de *Mycoplasma* spp. y el virus de la diarrea vírica bovina (VDVB), un patógeno frecuente en el ganado bovino y que es un contaminante frecuente del suero fetal bovino empleado en cultivos celulares. Los resultados de morfología y citometría de flujo confirmaron el tipo celular. El marcador de superficie CD31, típico de CE, fue el que mayores diferencias de marcaje mostró entre las CE y los fibroblastos. Por el contrario, únicamente se detectó el marcador CD34 en las CE de pase bajo, y tanto en los fibroblastos como en las células endoteliales se detectaron los marcadores CD44, vimentina y citoqueratina.

A continuación, se caracterizó el ciclo lítico de los taquizoítos del aislado de referencia Bb-Spain1 de *B. besnoiti* en BAEC y fibroblastos. A pesar de que se encontraron bajas tasas de invasión (en torno al 3-4%) en ambos cultivos primarios, se observó una mayor invasión en las células BAEC a las 24 y 72 horas post-infección (hpi). Las cinéticas de proliferación no mostaron diferencias entre ambos cultivos primarios. Además, se estudiaron los efectos de una coinfección con VDBV, demostrándose que dicho virus favorece la invasión temprana de las células hospedadoras por parte de los taquizoítos en BAEC.

En conclusión, en este trabajo se han desarrollado y estandarizado dos modelos *in vitro* de células diana del parásito (BAEC y fibroblastos) procedentes del hospedador natural, y se ha demostrado la relevancia de las coinfecciones con el VDBV, que han de ser consideradas en futuros estudios con otros patógenos del ganado bovino.

Lytic cycle of *Besnoitia besnoiti* tachyzoites displays similar features in primary bovine endothelial cells and fibroblasts

Alejandro Jiménez-Meléndez[1]; María Fernández-Álvarez[1]; Alexandra Calle[2]; Miguel Ángel Ramírez de Paz[2]; Carlos Diezma-Díaz[1]; Patricia Vázquez-Arbaizar[1]; Luis Miguel Ortega-Mora[1]; Gema Álvarez-García[1*].

[1] SALUVET, Animal Health Department, Faculty of Veterinary Sciences, Complutense University of Madrid, Ciudad Universitaria s/n, 28040-Madrid, Spain.
[2] Departamento de Reproducción Animal, Instituto Nacional de Investigación y Tecnología Agraria y Alimentaria (INIA), Avenida Puerta de Hierro 12, local 10, 28040 Madrid, Spain

[*] Corresponding author: Tel: +34913944095. Fax: +34913944098. *E-mail*: gemaga@ucm.es

Envíado a la revista *Parasites & Vectors*

1. ABSTRACT

BACKGROUND: Bovine besnoitiosis, caused by the cyst-forming apicomplexan parasite *Besnoitia besnoiti,* is a chronic and debilitating cattle disease that continues to spread in Europe in the absence of control tools. In this scenario, *in vitro* culture systems are valuable tools to carry out safety and efficacy drug screenings and to unravel host-parasite interactions. However, studies performed in bovine target cells are scarce.

METHODS: Thus, the objective of the present study was to obtain primary bovine endothelial and fibroblast cell cultures, target cells during the acute and the chronic stage of the disease, respectively, from healthy bovine donors. Afterwards, expression of surface (CD31, CD34 and CD44) and intracellular markers (vimentin and cytokeratin) was studied to characterize both cell populations by flow cytometry. Next, the lytic cycle of *B. besnoiti* tachyzoites was studied in both target cells. Invasion rates were determined by counting parasitophorous vacuoles and lysis plaques by immunofluorescence at several post-infection times, and proliferation kinetics were studied by quantitative PCR (qPCR). Finally, the influence of BVDV co-infection on the host cell machinery, and consequently on *B. besnoiti* invasion and proliferation, was investigated in ECs.

RESULTS: Morphology and cytometry results confirmed the endothelial and fibroblast origins, as each cell culture showed a characteristic expression pattern of intracellular and surface markers. CD31 was the surface marker that best discriminated between BAECs and fibroblasts, since fibroblasts lacked CD31 labelling. In contrast, low levels of labelling or the absence of CD34 labelling was observed, and positive labelling for CD44, vimentin and cytokeratin was observed in both BAECs and fibroblasts. Regarding the lytic cycle of the parasite, although low invasion rates (approximately 3-4%) were found in both cell culture systems, more invasion was observed in BAECs at 24 and 72 hpi. The proliferation kinetics did not differ between the BAECs and fibroblasts. BVDV infection favoured early *Besnoitia* invasion and slightly influenced the proliferation kinetics, even though this increase was not statistically significant.

CONCLUSIONS: We have generated and characterized two novel standardized *in vitro* models for *Besnoitia besnoiti* infection based on bovine primary target BAECs and fibroblasts, and have shown the relevance of BVDV coinfections, which should be considered in further studies with other cattle pathogens.

Key Words: *Besnoitia besnoiti*, lytic cycle, aorta endothelial cells, fibroblasts, flow cytometry, bovine viral diarrhoea virus

2. BACKGROUND

Bovine besnoitiosis, caused by the cyst-forming apicomplexan parasite *Besnoitia besnoiti,* is a chronic and debilitating cattle disease characterized by both cutaneous and systemic clinical manifestations. This parasitic disease progresses in two sequential phases as a consequence of the development of the two asexual and infective stages of the parasite: tachyzoites, responsible for the acute infection, and bradyzoites, responsible for the chronic infection (Álvarez-Garcia *et al.*, 2014). Acutely infected animals may develop fever, oedema, orchitis and respiratory disorders. It has been postulated that endothelial and mononuclear cells are the parasite target cells during this stage. The tachyzoite lytic cycle results in host cell invasion, proliferation and egress from infected cells with subsequent tissue damage that may result in degenerative and fibroid necrotic lesions, vasculitis and thrombosis in parasitized tissues (Pols, 1960; Basson *et al.*, 1970; Langenmayer *et al.*, 2015). Next, tachyzoites switch into bradyzoites, which are packed inside tissue cysts to evade host immune responses. Tissue cysts are responsible for the characteristic skin lesions, such as hyperkeratosis, folding, alopecia and scars that occur during the chronic stage (Álvarez-García *et al.*, 2014). Previous studies have shown that tissue cyst formation occurs predominantly in cells of mesenchymal origin, such as fibroblasts and myofibroblasts (Dubey *et al.*, 2013).

Currently, this parasitic disease continues to spread in Europe in the absence of control tools (Gutiérrez-Expósito *et al.*, 2017). In this scenario, *in vitro* culture systems are essential tools to carry out safety and efficacy drug screenings and to unravel host-parasite interactions (Müller & Hemphill, 2012).

Tachyzoites of *B. besnoiti* can be successfully maintained in primary cultures and in immortalized cell lines from different host origins (tick, mouse, monkey, cat, hamster or human) (Neuman, 1974; Samish *et al.*, 1988; Schares *et al.*, 2009; Frey *et al.*, 2016). However, it has been reported that primary cells maintain many of the important markers and functions seen *in vivo* and better mimic the *in vivo* environment (Pan *et al.*, 2009). Moreover, the host species seems to be crucial when dissecting host-pathogen interactions (Müller &Hemphill, 2012). Studies performed so far with *B. besnoiti* in primary bovine cell lines have been restricted to the embryonic calf heart cells KH-R (Schares *et al.*, 2009), endothelial cells from umbilical veins (Maksimov *et al.*, 2016; Taubert *et al.*, 2016), as well as bovine monocytes and neutrophils (Muñoz-Caro *et al.*, 2014a, b). Nonetheless, BUVECs are unlikely to be infected in natural infections since vertical transmission has not been reported, and endothelial cell populations show heterogeneity in structure and function, depending on their localization (Aird, 2012). Thus, primary target ECs of the adult cattle circulatory system might be an appropriate tool. On the other hand, although *B. besnoiti* tachyzoites have been successfully maintained in human foreskin fibroblasts (Frey *et al.*, 2016), these cells are of a different host origin and thus are not the ideal system to dissect host-parasite interactions at the molecular level.

Another key issue to be considered regarding *in vitro* systems is the absence of cell culture contaminants, such as *Mycoplasma* spp. and viral infections to obtain reproducible and reliable data (Bürgi *et al.*, 2018). There are commercially available bovine ECs and fibroblasts, both as established and as primary cultures. However, the presence of bovine pathogens, such as bovine viral diarrhoea virus, a prevalent bovine pathogen and frequent contaminant in foetal bovine serum batches worldwide (Gagnieur *et al.*, 2014), is not routinely checked. In addition, established cell lines in repositories have been confirmed to be infected with BVDV (Bürgi *et al.*, 2018). Since BVDV is known to alter the transcriptomic profile of ECs *in vitro* ((Neill *et al.*, 2008), it may also influence the interaction of *B. besnoiti* with these target host cells.

Thus, the objective of the present study was to obtain and characterize primary bovine endothelial and fibroblast cell cultures from healthy bovine donors. Next, the *B. besnoiti* lytic cycle was studied in both target cells in terms of invasion and proliferation capabilities. Finally, the influence of BVDV co-infection was investigated in ECs.

3. RESULTS

3.1. Morphology and flow cytometry results show the endothelial and fibroblast origins of the isolated primary cell cultures from bovine aortas.

Recently isolated BAECs showed a polygonal morphology and grew in confluent monolayers with a cobble stone-like pattern. BAECs (Figure 1A) were not contaminated with other cell types, such as fibroblasts or smooth muscle cells, which are frequent contaminants after the chemical digestion of the endothelia. BAECs were viable and successfully passaged and maintained *in vitro* up to passage 30, without remarkable morphological changes, as shown in Figure 1B.

Bovine fibroblasts presented an elongated morphology and grew in non-overlapping monolayers, as shown in Figure 1C.

Flow cytometry analyses showed that low-passage BAECs were strongly positive for CD31, CD44, vimentin and cytokeratin, whereas they presented low expression of CD34 (Figure 2). The expression pattern of cellular markers showed by high passage BAECs was similar to that of low-passage BAECs for vimentin, CD44 and cytokeratin, but CD31 showed a lower fold-change in expression in high-passage BAECs (Figure 2). Additionally, high-passage BAECs were found to be negative for CD34. Fibroblasts were positive for cytokeratin, vimentin and CD44 and negative for CD31 and CD34 (Figure 2).

The pattern of expression of intracellular and surface markers for the bovine endometrial eMSCs 4H consisted of the high expression of vimentin, cytokeratin and CD44, but these cells remained negative for CD34 and CD31 (Figure 2).

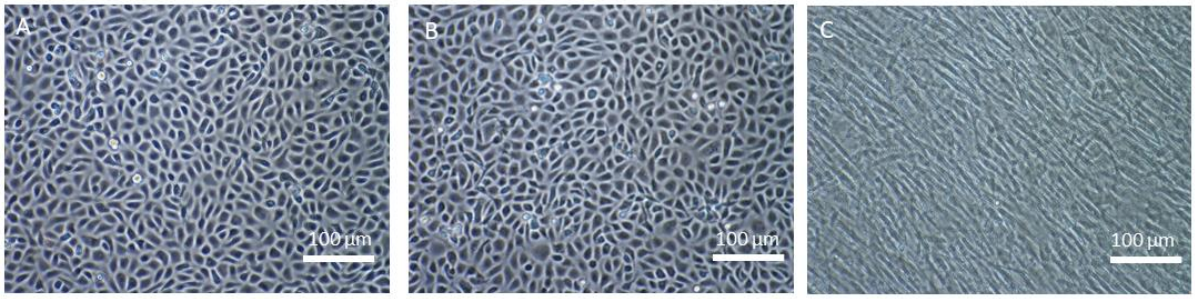

Figure 1: **Confluent monolayers of primary low-passage BAEC (A); high-passage BAECs (B) and bovine fibroblasts (C) at 100X magnification under an inverted light microscope.** Scale bars represent 100 µm.

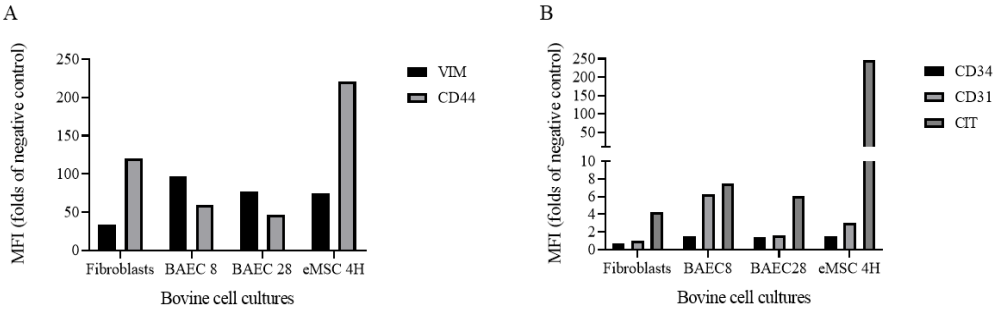

Figure 2: Intracellular and surface marker expression patterns in primary BAECs and fibroblasts by flow cytometry. CD44 and Vimentin labelling (A). CD31, CD34 and Cytokeratin labelling (B). Data correspond to the mean fluorescence intensity (fold-change compared to the negative control) for each sample.

3.2. Besnoitia besnoiti tachyzoites display higher invasion rates in BAECs at late invasion.

The total number of invasion events (LPs and/or PVs) at 72 hpi ranged from 18 in wells that were washed at 4 hpi to 39 in wells that were washed at 24 hpi in BAECs and from 17 in wells that were washed at 4 hpi to 32 in wells that were washed at 24 h pi in fibroblasts. A significant increase in the number of events per well was shown in both cell lines when the invasion times that were assayed were compared up to 24 hpi ($p<0.05$, Kruskal-Wallis) (Figure 3A). However, statistically significant differences between wells that were washed at 24 hpi and unwashed wells were not observed ($p>0.05$, Kruskal-Wallis).

When infected BAECs and fibroblasts were compared, statistically significant higher invasion rates were found in BAECs at 24 hpi and 72 hpi than in unwashed wells ($p<0.05$, Mann Whitney U test) (Figure 3A). The invasion rates were similar at 4, 8 and 12 hpi. Moreover, up to 50% of invasion events in both cell lines occurred between 4 and 8 hpi, as shown in Figure 3A.

Tachyzoites from the Bb-Spain 1 isolate showed exponential growth in both primary cell cultures assayed ($R^2>0,95$) (Figure 3B) from 12 hpi onwards, with a significant increase in the number of tachyzoites per well from 24 hpi onwards in both BAECs and fibroblasts ($p< 0,05$, Kruskal-Wallis). The doubling time during the exponential growth phase of the tachyzoites of the Bb-Spain-1 isolate was 13.15 ± 2.34 h in BAECs and 13.34 ± 2.17 h in bovine fibroblasts. No significant differences were found among BAECs and fibroblasts when tachyzoite yields (tachyzoites/β-actin) for each post-infection time point were compared ($p>0.05$, Mann-Whitney U test).

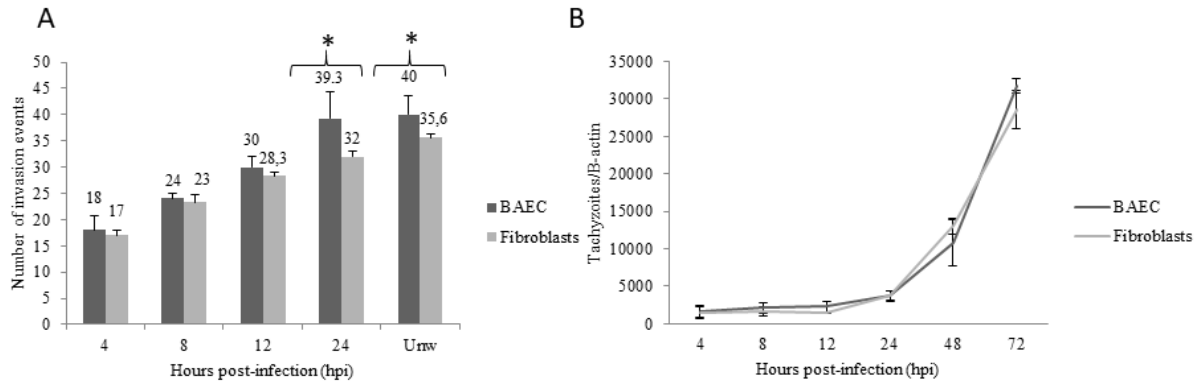

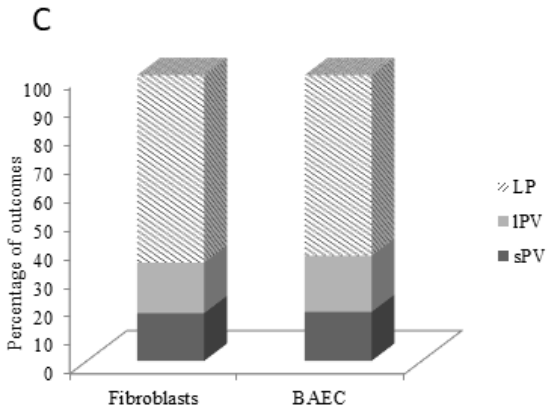

Figure 3: *Besnoitia besnoiti* tachyzoite invasion rates in BAECs and bovine fibroblasts (A). The total number of invasion events (parasitophorous vacuoles and lysis plaques) per well at the different time points pi. ***In vitro* proliferation kinetics of *B. besnoiti* tachyzoites in BAECs and bovine fibroblasts, as determined by qPCR (B). Invasion and proliferation outcomes (small and large parasitophorous vacuoles and lysis plaques) of *B. besnoiti* tachyzoites in BAECs and bovine fibroblasts in 24 hpi washed wells (C).** **s**PV: small parasitophorous vacuole; lPV: large parasitophorous vacuole; LP: lysis plaque.

The results from qPCR were in agreement with the immunostaining images captured at the same time points pi (Figure 4). Tachyzoites had already invaded host cells between 4 and 8 hpi, followed by a lag phase of up to 24 hpi. Then, proliferation began inside PVs that initially contained 2 tachyzoites (Figure 4), and at least two rounds of replication had been completed by 32 hpi. PVs continued to grow, and large PVs, as well as parasite egress and LPs, were observed from 48 hpi onwards in both BAECs and fibroblasts.

The parasite invasion and proliferation outcomes that were analysed at 72 hpi in 24 h washed plates mostly consisted of LP (around 65 %, Fig. 3C), rather than PVs, without statistically significant differences between the cell lines ($p>0.05$ X^2 test).

3.3. BVDV co-infection facilitates the early invasion of B. besnoiti tachyzoites in BAECs.

First, the BVDV-infection status was checked, showing BVDV RT-PCR Ct values ranging from 18 to 20 for BVDV-BAECs at every time point checked, while BAECs remained negative (Ct values over 38) (data not shown).

The total number of invasion events (LPs and/or PVs) at 72 hpi ranged from 26 in wells that were washed at 4 hpi to 48 in wells that were washed at 24 hpi in BVDV-BAECs. A significant increase in the number of invasion events was observed at 24 hpi compared to 4 hpi ($p<0.01$, Mann-Whitney U Test) (Figure 5A). The maximum number of invasion events was found in unwashed wells, although there were no significant differences compared with that of wells that were washed at 24 hpi ($p>0.05$, Mann-Whitney U Test). At 4 hpi, more than 50% of the invasion outcomes had already been produced (Figure 5A).

When BVDV-infected BAECs and BAECs were compared, statistically significant higher invasion rates were found in BVDV-infected BAECs than in BAECs in wells that were washed at 4 hpi ($p<0.01$, Mann-Whitney U test) (Figure 5A). The tachyzoite yield was similar between BVDV-infected BAECs and BAECs at 8 and 24 hpi. However, the tachyzoite yield was higher in BVDV-BAECs than in BAECs at 72 hpi, although the differences were not statistically significant (Fig. 5B; $p>0.05$, Mann-Whitney U test).

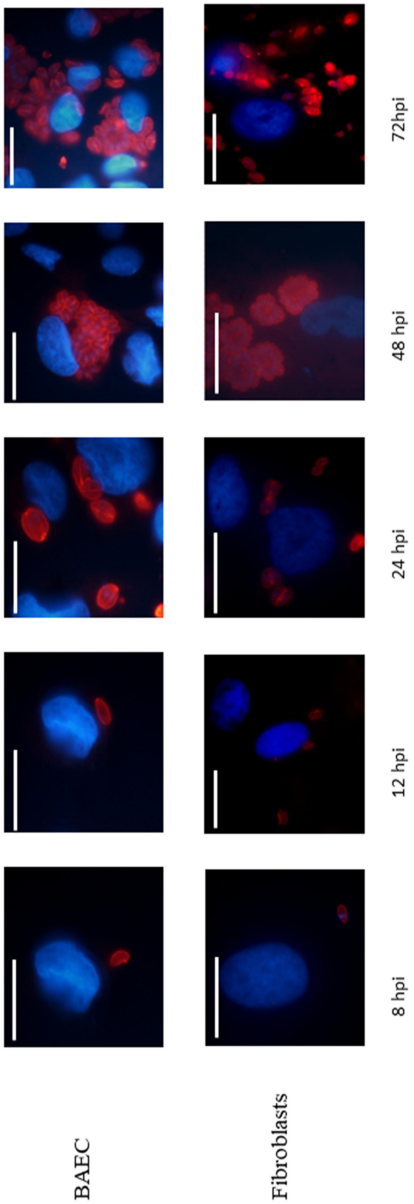

Figure 4: Lytic cycle of *Besnoitia besnoiti* tachyzoites, as monitored by immunofluorescence in primary BAECs and fibroblasts from 4 hpi up to 72 hpi. *Besnoitia besnoiti* tachyzoites are stained with a rabbit polyclonal antibody against *B. besnoiti* (red), and the nuclei of host cells are stained with

The parasite invasion and proliferation outcomes mostly consisted of LP (around 65 %, Fig. 5C), rather than PVs at all times assayed in both BAECs and BVD-infected BAECs, without statistically significant differences between the cell systems ($p>0.05$ X^2 test).

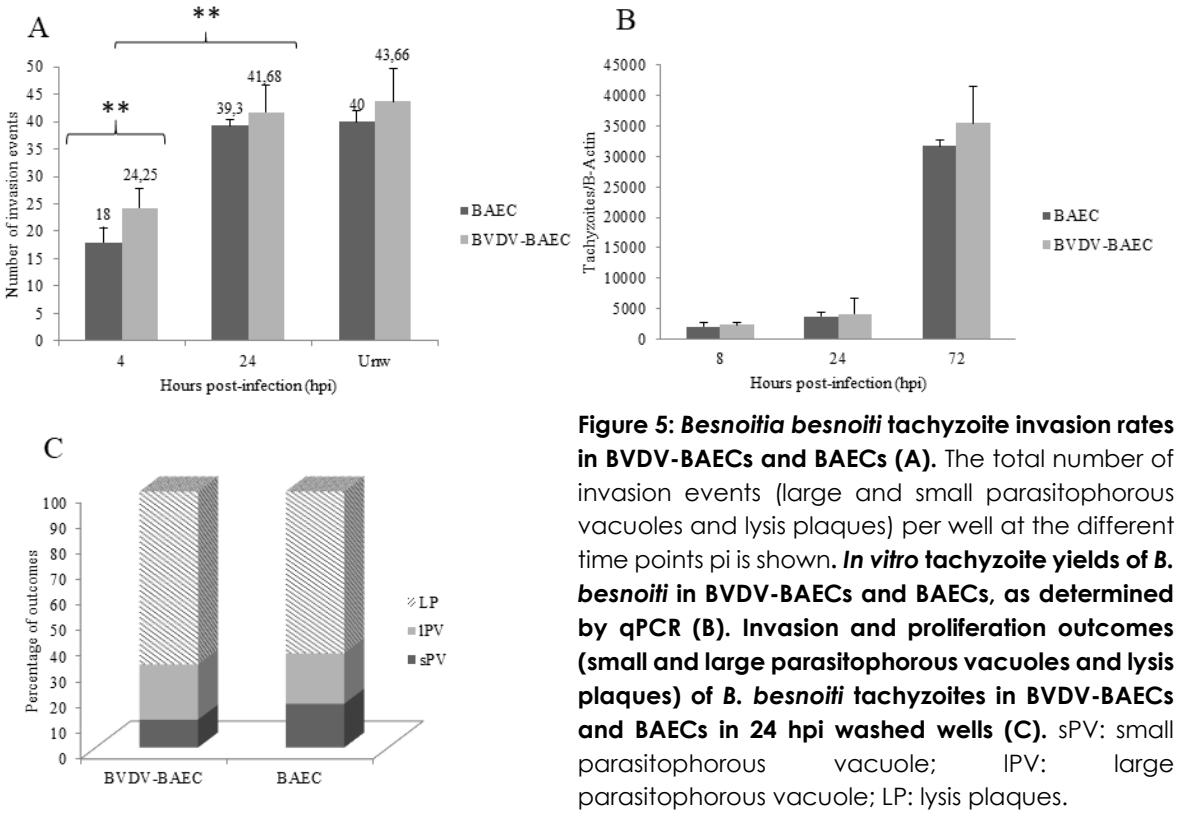

Figure 5: *Besnoitia besnoiti* tachyzoite invasion rates in BVDV-BAECs and BAECs (A). The total number of invasion events (large and small parasitophorous vacuoles and lysis plaques) per well at the different time points pi is shown. ***In vitro* tachyzoite yields of *B. besnoiti* in BVDV-BAECs and BAECs, as determined by qPCR (B). Invasion and proliferation outcomes (small and large parasitophorous vacuoles and lysis plaques) of *B. besnoiti* tachyzoites in BVDV-BAECs and BAECs in 24 hpi washed wells (C).** sPV: small parasitophorous vacuole; lPV: large parasitophorous vacuole; LP: lysis plaques.

4.DISCUSSION

Herein, two primary bovine cell lines, BAECs and fibroblasts, that were free from frequent cell culture contaminants were obtained and characterized by flow cytometry for the first time to study *B. besnoiti* infection in target cells.

The development of *in vitro* models for the study of obligate intracellular protozoa that utilize target primary cells is timely and essential (Müller & Hemphill, 2012), since immortalized cell lines show phenotypic modifications that are characteristic of tumour-like cells and, consequently, may lose the phenotypic traits and specific functions of their tissue of origin (Pan *et al.*, 2009). In addition, the host species origin and tissue localization are critical to better model *in vivo* environments. Previous studies carried out with ECs and fibroblasts infected with *B. besnoiti* have been restricted to either BUVECs (Maksimov *et al.*, 2016; Taubert *et al.*, 2016) or HFF cells (Frey *et al.*, 2016). However, both cell lines do not fulfil both the host species and tissue location requirements. Finally, another crucial requirement that was considered was the absence of widespread BVDV. Thus, herein, an exhaustive two-step quality control was performed. First, the health status of donors, which is usually unknown for primary and established bovine cell lines that are available in different repositories worldwide, was carefully checked (Bürgi *et al.*, 2018). Next, the foetal calf serum was shown to be free of BVDV, since it is widely known that non-cytopathic strains are usually present in the foetal bovine serum batches that are available worldwide (Uryvaev *et al.*, 2012).

When both cell lines were characterized, the morphology results and cytometry markers confirmed the endothelial and fibroblast origin. Endothelial cells from all vascular beds are aligned longitudinally *in vivo,* forming a single layer due to their anatomical location and laminar flow. However, this morphology may change as a result of *in vitro* conditions and is not considered a reliable indicator (Haudenschild C, 1984). BAECs grew as a single layer of cells

and presented a cobblestone pattern at confluence, as described for ECs from large vessels (Haudenschild C, 1984). In contrast, fibroblasts presented a flattened morphology and were spindle-shaped, as expected (Ehrlich, 2003). Moreover, each cell line showed a distinct expression pattern of intracellular and surface markers, and in agreement with previous reports, CD31 (or PECAM1) was the surface marker that best discriminated between BAECs and fibroblasts since fibroblasts lacked the expression of CD31. Additionally, differences in CD34 labelling were detected, and only low-passage BAECs were slightly positive. The CD31 and CD34 labelling of different ECs has been reported. CD31 is the most classical endothelial marker (Ataollahi *et al.*, 2014)and is expressed at cell junctions to maintain endothelial integrity and control permeability (Lertkiatmongkol *et al.*, 2016). In contrast, CD34 is a marker of pluripotency that is found only in circulating endothelial precursors (Valencia-Nuñez *et al.*, 2017). Interestingly, the CD31 and CD34 labelling also differed between low-passage and high-passage BAECs despite the homogeneous morphology shown by both cell lines at various passages. The lack of CD34 labelling may have been influenced by *in vitro* selection after 28 passages. This finding strengthens the hypothesis that the use of low-passage primary cells can avoid the phenotypic changes associated with *in vitro* selection. In agreement, the use of commercial primary ECs with a passage number higher than 16 is not recommended. In contrast, CD44, vimentin and cytokeratin labelling were observed regardless of the cell line origin and passage number. CD44 is a ubiquitous ligand that is important for the regulation of endothelial cell proliferation and apoptosis, modulating CD31 and VE-cadherin expression (Tsuneki & Madri, 2014), and for the regulation of vascular endothelial integrity via a CD31-dependent mechanism (Flynn *et al.*, 2013). In fibroblasts, CD44 mediates proliferation, apoptosis and migration (Tsuneki & Madri, 2016). Vimentin is an intermediate filament that provides mechanical integrity and structural support to fully differentiated endothelial cells (Helmke *et al.*, 2001). It has also been shown that vimentin is essential for the differentiation of endothelial cells from embryonic stem cells (Boraas & Ahsan, 2016). The network of cytoskeletal proteins is essential for the response of endothelial cells to mechanical stimuli, and the remodelling of this network may be important for the adhesion of motile tachyzoites to the endothelium, as has been shown for *T. gondii* tachyzoites under shear forces *in vitro*, where adhesion was enhanced (Harker *et al.*, 2014). In fibroblasts, vimentin is a key regulator of cell proliferation and keratinocyte differentiation in wound healing (Cheng *et al.*, 2016). Finally, cytokeratin is a marker that is commonly associated with epithelial cells, but early studies that were performed in endothelial cells from bovine aortas described a mixed population, composed of cells that were positive and negative for cytokeratin (Spanel-Borowski *et al.*, 1994). Cytokeratin-positive cells were more polygonal and grew in a cobblestone pattern that is commonly associated with endothelial cells, as observed in this study. In addition, the different phenotypes of endothelial cells have been described according to the cytokeratin pattern, and cytokeratin-positive cells in the microvasculature have been thought to be danger-sensing cells (Spanel-Borowski, 2011). In fibroblasts, cytokeratin expression is reported to be low, but some keratins have been shown to be present in fibroblasts *in vitro* (Katagata *et al.,* 2002*)*.

Regarding the *in vitro* parasite behaviour, tachyzoites were able to successfully invade and replicate within both of the target bovine cell lines that were assayed, as expected. Moreover, the parasites showed almost an identical lytic cycle to that previously described in Marc-145 cells (Frey et al., 2016; Diezma-Díaz *et al.*, 2017). Generally, our findings suggest that neither invasion nor proliferation are particularly favoured in both bovine target cells compared to a non-bovine cell line. According to these results and previous studies carried out with tachyzoites of the BbSpain-1 isolate, tachyzoites display lower invasion and proliferation rates than both *N. caninum* (Regidor-Cerrillo *et al.*, 2011) and *T. gondii* (Naguleswaran *et al.*, 2003) in all cell types that have been assayed thus far. Thus, this isolate was categorized as a low-invasion and low-proliferation isolate. However, slight differences between the invasive capabilities in BAECs and fibroblasts were found since the invasion rates at 24 hpi and in unwashed wells were higher in BAECs than in fibroblasts.

Accordingly, the maximum IR that was found in the present work was observed in BAECs and was not higher than 4.5%, in contrast with observations previously made (Taubert *et al.*, 2016), which showed IRs over 30% in BUVECs that were infected with tachyzoites from the Bb1Evora04 isolate. This result may have been influenced by several factors, such as differences in the isolate, MOI and passage number used. Moreover, higher MOIs were used, and the number of *in vitro* passages was not specified for the Evora04 isolate of *B. besnoiti* (Taubert *et al.,* 2016). In a previous study, differences in IRs were observed among different isolates, in which a Portuguese isolate showed higher IRs (approximately 20%) than the Spain1 isolate in Marc-145 cells (Frey *et al.*, 2016). It has been reported that prolonged *in vitro* culture can alter the phenotypic features and even the virulence of isolates of *N. caninum* (Bartley *et al.,* 2006) and *T. gondii* (Nischik *et al.,* 2001). Our results also showed that the tachyzoite invasion of the host cell can take place up to 24 hpi since there was an increase in the number of invasion events up to 24 hpi, confirming the prolonged extracellular survival of tachyzoites. However, most invasion events took place before 24 hpi, showing that the invasion kinetics that were observed in both bovine target cell lines were similar to those in Marc-145 cells, where most of the invasion outcomes occurred between 4 and 8 hpi. Again, exponential growth was observed, and replication was initiated from 24 hpi onwards, so the lag phase that is required for the parasite to adapt to the intracellular conditions extended up to 24 hpi. In addition, Td was in agreement with previous studies (Frey *et al.*, 2016; Diezma-Díaz *et al.*, 2017). The presence of both PVs and LPs at 72 hpi suggests asynchronous growth, which is most likely associated with the prolonged invasion capabilities of tachyzoites (Frey *et al.*, 2016).

However, the *in vitro* studies of the closely related apicomplexan parasites have shown host-type specific *in vitro* behaviour. The tachyzoite to bradyzoite switch seems to be favoured in differentiated cell types, such as keratinocytes for *N. caninum* (Vonlaufen *et al.,* 2002) or skeletal muscle cells in the case of *T. gondii* (da Fonseca Ferreira-da-Silva *et al.*, 2009). Additionally, in *Eimeria* spp., the formation of meronts I has only been described in cells with a bovine origin, both for epithelial and endothelial cells (Hermosilla *et al.*, 2002).In the cattle pathogen *N. caninum*, no striking differences were found when the behaviour of tachyzoites from high (NcSpain7) and low virulence (NcSpain1H) isolates was studied in cells with a different host origin (MARC-145 vs bovine trophoblast), but differences were found among two bovine cell lines from the placenta, foetal trophoblasts and maternal caruncular cells, since higher IRs and tachyzoite yields were found in trophoblast cells, suggesting that there was a barrier function for caruncular cells (Jiménez-Pelayo *et al.*, 2017). Considering the heterogeneity of both ECs and fibroblast populations (Aird, 2012; Nolte *et al.*, 2008), further refinement of the *in vitro* models that were standardized herein could be possible, including cell lines from target locations where parasite growth is favoured *in vivo*, such as the microvasculature from nasal turbinates, testis or skin.

Finally, this is the first study in which the *in vitro* interaction of BVDV with a protozoan belonging to the Toxoplasmatinae family has been studied. Interactions between *B. besnoiti* and BVDV could be relevant in the pathogenesis of bovine besnoitiosis, with consequences at the molecular level and in the clinical presentation of the disease under field conditions. In several regions of Spain, BVDV is frequently circulating in herds (Diéguez *et al.*, 2017), and its immunosuppressive properties are widely known since this virus is capable of altering both innate and adaptive responses in cattle (Chase, 2013; Peterhans *et al.*, 2003). However, the possible synergism of *B. besnoiti* and BVDV coinfections is unknown.

In the present work, BVDV infection favoured the early tachyzoite invasion of BAECs, which could explain the slight increase in the tachyzoite yield observed in BVDV-BAECs compared to BAECs. However, the total number of invasion events remained unchanged. These results may have been due to the immunosuppressive properties of this virus that have been described *in vitro* so far, mostly affecting the early recognition of pathogens that are related to TLR signalling; additionally, a decrease in Myeloid Differentiation factor 88 (MyD88) expression has been observed, which resulted in the impaired leukocyte function of myeloid cells (Schaut *et al.*, 2015). Interestingly, MyD88 has been shown to confer resistance in mice

against closely related Toxoplasmatinae parasites such as *T. gondii* (Scanga *et al.*, 2002) and *N. caninum* (Mineo *et al., 2009)*.

Although BVDV infection has been suggested to be a risk factor that may facilitate or exacerbate other infectious diseases, studies performed *in vivo* thus far have provided variable results. Several studies that have compared coinfections with BVDV and other closely related parasites, such as *N. caninum*, have found an association with BVDV and abortions due to *N. caninum* (Vanleeuwen *et al.*, 2009; Bjorkman *et al.*, 2000), while other studies claimed that there was no association (Mainar-Jaime *et al.*, 2001). Regarding *in vitro* co-infections, a recent study performed with the intracellular pathogen *Mycoplasma bovis* demonstrated that BVDV infection did not influence the *in vitro* behaviour of the bacteria, as assessed in bovine macrophages (Bomac) (Bürgi *et al.*, 2018). Thus, epidemiological studies addressing coinfections with *B. besnoiti* and BVDV are necessary to demonstrate the possible synergism that has been suggested *in vitro*.

In summary, we have standardized two *in vitro* models that employ the primary target bovine cells of acute and chronic *B. besnoiti* infection. The detailed description of the parasite lytic cycle in both cell lines could be used as the basis for further host-pathogen interaction studies at the molecular level. Moreover, the BVDV-BAEC model could be useful for other Toxoplasmatinae parasites and for other ruminant pathogens that replicate in ECs. One of the most relevant pathogens that is characterized by endothelial damage is Blue Tongue Virus, and numerous studies have been performed in bovine pulmonary artery endothelial cells without checking for the absence of pestivirus infection (Drew *et al.,* 2010).

5. MATERIALS AND METHODS

5.1. Ethics approval and consent to participate

All were approved by PROAE 25/2016. Spanish (Law 32/2007, R.D. 53/2013) and European (Council Directive 2010/63/EU) legal requirements and guidelines regarding experimentation and animal welfare were considered to carry out these experiments.

5.2. Donor animals

Heifers from the Asturiana de la Montaña breed that were approximately 24-months-old were selected based on the absence of pathogens that are commonly found in cattle, such as BVDV, infectious bovine rhinotracheitis, *Neospora caninum* and *Mycobacterium avium* subsp. *paratuberculosis* spp. based on ELISA techniques. The presence of specific antibodies against *B. besnoiti* and *N. caninum* was also ruled out by Western blotting (Álvarez-García *et al.*, 2003; García-Lunar *et al.*, 2013).

5.3. Isolation of primary endothelial cells and fibroblasts from bovine aortas

The selected animals were culled at a local slaughterhouse, and fresh bovine aortas were obtained and immediately clamped with sterilized plastic tie wraps. Next, the lumen was filled with wash medium consisting of Dulbecco´s modified Eagle´s medium(DMEM high glucose, Gibco, Life Technologies, Thermo Fisher Scientific, Waltham, MA, USA), 10% FBS (Gibco, Life Technologies, Thermo Fisher Scientific, Waltham, MA, USA) and a mixture of antibiotics (200 U/ml penicillin, 200 mg/ml streptomycin) (Lonza, Basel, Switzerland) (Ataollahi *et al.*, 2014). Afterwards, under a sterile hood, the aortas were dipped in ethanol and were cut into two or three 5-cm-long pieces, and each piece was opened with a longitudinal incision. The specimens were placed in separate sterile petri dishes with the endothelium facing up and covered with sterile filter paper to avoid further digestion of the tissue. Approximately 2 mL of 0.1% (wt/vol) collagenase type II solution was dripped onto each filter paper. Collagenase type II solution was prepared by dissolving 0.1 g of collagenase II (Gibco, Life Technologies, Thermo Fisher Scientific, Waltham, MA, USA) in 100 mL of Hank's balanced salt solution with calcium chloride ($CaCl_2$) and magnesium chloride ($MgCl_2$) (Gibco, Life Technologies, Thermo Fisher Scientific, Waltham, MA, USA). Samples were incubated at 37°C for 30 min, and the resulting fluid from the enzymatic digestion was centrifuged at 250 x *g* at 4°C for 5 min. The sample was then resuspended in specific medium for ECs, namely, M200(Gibco, Life Technologies, Thermo Fisher Scientific, Waltham, MA, USA), with plus 20% FBS and a specific supplement for large vessel ECs (LVES, Gibco, Life technologies, Life Thermo Fisher

Scientific, Waltham, MA, USA) prior to seeding the cells into T25 flasks. The medium was changed every 2-3 days until the cells were confluent and passaged.

To prevent fibroblast contamination, differential trypsinization was performed according to previously published protocols (OSullivan et al., 2003). Fibroblasts detach first in a mixed-cell culture when they are trypsinized. Briefly, when fibroblast contamination was detected, the cell culture medium was discarded, and the monolayer was gently rinsed with PBS. Prewarmed trypsin-EDTA was added, and the area of the culture containing both bovine aorta ECs and fibroblasts was observed under a light inverted microscope (Nikon Eclipse TS100) until the first fibroblasts started to detach. The cell culture supernatant containing fibroblasts was discarded, and fresh culture medium was added to the flask with BAECs.

In parallel, one flask was left undisturbed, without differential trypsinization, and fibroblasts slowly outgrew the ECs until the monolayer consisted only of fibroblasts. Afterwards, the fibroblasts were passaged, and a homogeneous culture was observed under the light microscope.

5.4. Parasites and cell cultures

Tachyzoites from the *B. besnoiti* Spain1 isolate (BbSpain1) were routinely maintained and propagated in the monkey kidney cell line Marc-145, according to previously published procedures (Frey *et al.*, 2016). Marc-145 cell cultures were passaged twice a week.

For *in vitro* assays, tachyzoites were harvested at three days post-infection, when most of the tachyzoites were still intracellular, by removing the infected cell monolayer with a cell scraper, followed by repeated passages through a 25-gauge needle and separation from cell debris on a disposable PD-10 column (Frey *et al.*, 2016). To avoid parasite adaptation to cell culture, only low-passage tachyzoites were included in the studies (passage numbers 10 to 21). Tachyzoite viability was confirmed by trypan blue exclusion followed by counting in a Neubauer chamber. Purified viable tachyzoites were used to infect confluent fibroblast or EC monolayers as described below for the lytic cycle characterization.

Newly obtained BAECs were maintained in a specific medium for ECs M200 (Gibco, Life Technologies, Thermo Fisher Scientific, Waltham, MA, USA) with 20% FBS, LVES (Gibco, Life Technologies, Thermo Fisher Scientific, Waltham, MA, USA) and a mixture of antibiotics (penicillin + streptomycin, Lonza, Basel, Switzerland) and passaged when confluent, approximately every 3-4 days. Bovine fibroblasts were cultured in DMEM with 15% FBS and antibiotics and passaged once a week using pre-mixed Trypsin EDTA (TrypLE®, Gibco, Life Technologies, Thermo Fisher Scientific, Waltham, MA, USA). High passage BAECs were maintained as described for low-passage BAECs. To avoid changes associated with the long-term *in vitro* maintenance of the cells, only low-passage BAECs and fibroblasts were used for the lytic cycle characterization.

The pattern of the expression of surface and intracellular markers by flow cytometry was performed in low-passage BAECs and fibroblasts (passage numbers 8 and 10, respectively). Additionally, high-passage BAECs were included (passage number 28).

Bovine pulmonary artery endothelial cells (CPAE, ATCC® CCL-209), that were persistently infected with a non-cytopathic strain of BVDV were maintained in DMEM high glucose plus 15% FBS and antibiotics (100 U/ml penicillin, 100 mg/ml streptomycin) and passaged twice a week. To avoid cross contamination, this cell line was kept in a different cell culture room with a separate incubator and laminar flow hood. This cell line was used as a source of infectious BVDV for further experiments.

Bovine immortalized endometrial cells (eMSC 4H) were employed as positive controls for the expression of the surface and intracellular markers that were analysed by flow cytometry. This cell line represents a cell population with markers that are characteristic of mesenchymal and epithelial cells (Calle et al., 2019). The eMSC 4H cells were maintained in RPMI 1640 with (Lonza, Basel, Switzerland), 10 % FCS and antibiotics (100 U/ml penicillin, 100 mg/ml streptomycin), and were passaged once a week.

The *B. besnoiti* isolate used for all *in vitro* assays tested negative for *Mycoplasma* spp. infection by PCR (Mycoplasma Gel Form

Kit®, Biotools, Madrid, Spain) following the manufacturer´s instructions, and BVDV by quantitative real-time PCR (RT-PCR) (Hoffmann *et al.*, 2006). The FCS used in all experiments was previously tested to confirm the absence of IgGs against *B. besnoiti*, *N. caninum* and *Toxoplasma gondii* by IFAT (Fernández-García *et al.*, 2009), and BVDV by RT-PCR (Hoffmann *et al.*, 2006).

5.5. Flow cytometry of surface and intracellular markers in bovine cell lines

The pattern of the expression of surface proteins (CD31, CD34, CD44) and intracellular molecules (vimentin and cytokeratin) were analysed in BAECs (both low and high passage cell lines), fibroblasts and endometrial cells by flow cytometry, essentially as previously described (Calle *et al.*, 2019).

The immunocytochemical analysis by flow cytometry was carried out following procedures previously described (Calle *et al.*, 2019). Briefly, for intracellular markers, first, cells were fixed with paraformaldehyde and then permeabilized with 0.4% Triton X100. Afterwards, appropriate dilutions, which were provided by the manufacturers, of the primary antibodies listed in Table 1 were added. Alexa Fluor 488-conjugated secondary antibodies (Jackson ImmunoResearch Laboratories, Cambridgeshire, UK) were added at a 1:500 dilution and incubated for 30 min at RT. For CD31, which was conjugated with allophycocyanin (APC), cells were washed with PBS, and the appropriate dilution of the conjugated primary antibody (1:50) in TNB was added to the cells. Subsequently, the cells were washed twice with PBS. Cells that were incubated with only the appropriate secondary antibodies were used as negative control samples. The analysis of the samples to determine the fold change of the expression, which was based on the fluorescence relative to that of the negative control cells, was performed with the Cell Lab Quanta SC system of Beckman Coulter using the FlowJo X software version 10.0.7r2 (Beckton Dickinson, Franklin lakes, NJ, USA).

5.6. Characterization of the lytic cycle of Besnoitia besnoiti tachyzoites in primary BAEC and bovine fibroblasts.

Invasion assays

Invasion assays were carried out essentially as previously described in Marc-145 cells (Frey *et al.*, 2016). Confluent monolayers of BAECs or fibroblasts (10^5 cells/well) were seeded on sterile coverslips in P24 cell culture plates and were infected with 10^3 viable tachyzoites/well (multiplicity of infection, MOI=0.01). Next, at 4, 8, 12 and 24 h post-infection, 3 washes with PBS were performed to remove non-adherent extracellular tachyzoites, and three infected wells were left undisturbed without washing for 72 h. Infected cultures were further incubated for 72 h at 37°C with 5% CO_2 in a humidified incubator. Then, the cells were fixed using ice-cold methanol for 20 min at RT, and immunostaining was performed. Afterwards, the number of invasion events per well, namely, small and large parasitophorous vacuoles (PVs) and lysis plaques (LPs), was counted as previously

Table 1: Markers employed to characterize primary BAEC and bovine fibroblasts by flow cytometry.

Marker	Location	Primary antibody			Secondary Antibody		Labelled cell*	References
		Clone	Isotype	Dilution	Isotype (Alexa fluor 488)	Dilution		
Vimentin	Intracellular	LN-6[a]	Mouse monoclonal IgM	1:100	Anti Mouse IgG	1:500	ECs/Fb	Cheng *et al.*, 2016; Helmke et al., 2001
Cytokeratin	Intracellular	C-11[a]	Mouse monoclonal IgG1	1:100	Anti Mouse IgG	1:500	ECs/Fb	Katagata *et al.*, 2002; Spanel-Borowski, 1994, 2011
CD34**	Surface	NA[b]	Rabbit polyclonal IgG	1:100	Anti Rabbit IgG	1:500	ECs	Valencia-Núñez *et al.*, 2017
CD44	Surface	IM7[c]	Rat monoclonal IgG2b	1:50	Anti Rat IgG	1:500	ECs/Fb	Tsuneki & Madri, 2014, 2016
CD31	Surface	CO.3E-1D4[d]	Mouse monoclonal IgG2a-APC***	1:50	//	//	ECs	Ataollahi *et al.*, 2014; Lertkiatmongkol *et al.*, 2016

* ECs: Endothelial cells / Fb: Fibroblasts
** CD34: marker for hematopoietic stem cells (Valencia-Núñez et al., 2017)
*** CD31 conjugated to Allophycocyanin (APC) (direct staining)
[a] supplied by Sigma-Aldrich; [b] supplied by Biorbyt; [c]: supplied by Bio-Rad; [d]: supplied by NovusBio

described (Frey *et al.*, 2016). The invasion of a single tachyzoite was assumed to result in one invasion event. All conditions were tested in triplicate in at least three independent experiments.

Proliferation assays

P24 cell culture plates with confluent BAECs or fibroblast monolayers (10^5 cells/well) were infected with 10^6 purified viable tachyzoites/well (MOI=10) (Frey *et al.*, 2016). After 4 h, the wells were washed 3 times with PBS to remove non-adhered extracellular tachyzoites, and the infected culture plates were further incubated at 37ºC in a humidified 5% CO_2 incubator. At 4, 8, 12, 24, 48 and 72 hpi, supernatants were discarded, and samples were collected according to the manufacturer´s instructions from a Rapid Lyse Kit (Mackerey-Nagel, Düren, Germany) and stored at -80ºC until DNA extraction. In parallel, cell culture replicates were seeded on coverslips, infected as described above and fixed with a mixture of 3% paraformaldehyde and 0.05% glutaraldehyde in PBS at the pi times selected (4, 8, 12, 24, 32, 48 and 72 hpi) for immunofluorescence staining. Three coverslips were photographed for each condition using an inverted fluorescence microscope at 600x magnification (Nikon Eclipse TE 200, Chiyoda, TYO, JP).

Proliferation assays were carried out in triplicate and repeated in three independent experiments.

5.7. Besnoitia besnoiti invasion and proliferation in BAEC infected with BVDV.

To study the possible influence of BVDV on *B. besnoiti* tachyzoite *in vitro* behaviour, BAECs were infected with a non-cytophatic strain of BVDV using supernatants obtained from persistently infected CPAE cells (ATCC® CCL-209™) (BVDV RT PCR Ct values 18-20) (Hoffmann *et al.*, 2006). Briefly, 1 mL of the supernatant from confluent CPAE cells was added to a confluent T25 flask of 90% confluent BAECs, incubated for 1 h at 37ºC and 5% CO_2 and replaced with fresh culture medium. Infection was confirmed by RT-PCR (Hoffmann *et al.*, 2006) after two consecutive passages and at the end of the study.

This cell line, named BVD-BAEC, was kept under the same conditions but was physically separated from BVD-free cells, using a different incubator and a flow hood that were located in a separate room.

Afterwards, the effect of BVDV co-infection on the early (4 hpi) and late invasion (24 and 72 hpi) of *B. besnoiti* tachyzoites was studied. PD10-purified tachyzoites of the BbSpain1 isolate were inoculated into confluent BVDV-infected BAECs at a parasite MOI of 0.01, and at 4 and 24 hpi, non-invaded tachyzoites were removed with three washes with PBS. Three wells were left undisturbed without washing, and plates were fixed at 72 hpi. Proliferation assays were performed essentially as described for the lytic cycle characterization, with a MOI of 10, and samples were collected for subsequent DNA extraction and qPCR at 8, 24 and 72 hpi. In parallel, cultures that had been seeded on sterile coverslips were infected under the same conditions and fixed at the post-infection times previously mentioned. All conditions were tested in triplicate in three independent assays.

5.8. Immunofluorescence staining

For immunofluorescence staining, supernatants of the cell cultures were discarded at 72 hpi. Next, cells were washed 3 times with PBS for 5 min each and then fixed by the addition of ice-cold methanol for 10 min. After another wash with PBS, cells were permeabilized with 300 µl/well of 0.2% Triton-X 100 in PBS for 30 min at 37ºC, followed by 3 additional washes with PBS. Primary polyclonal rabbit-anti tachyzoite BbSpain1 polyclonal antiserum (Gutiérrez-Expósito *et al.*, 2013) was added at a dilution of 1:1000 in PBS and incubated for 1 h at 37ºC. After 3 additional washes with PBS, Alexa Fluor® 594 goat anti-rabbit IgG (H+L), (Life technologies, Thermo Fisher Scientific, USA) was added to each well at a dilution of 1:1000 in PBS. The plates were incubated for 45 min at RT in the dark and washed 3 times with PBS. During the final wash, nuclei were labelled with DAPI staining. Finally, the plates were washed with distilled water, and the total number of invasion events per well was counted using an inverted fluorescence microscope (Nikon eclipse TE200) at 200X magnification.

5.9. DNA extraction and quantitative real-time PCR (qPCR)

The harvested cell culture samples were incubated for 10 min at 56ºC, and DNA was purified using the spin column protocol for

cultured cells according to the manufacturer's instructions in the Rapid Lyse kit (Mackerey Nagel, Düren, Germany). DNA was eluted in 100 µl elution buffer. The DNA content and purity of each sample were measured by UV spectrometry using a Biotek Multiplate Reader (Biotek, Winooski, VT, USA).

A BbRT2 qPCR assay was carried out for the specific detection of *Besnoitia* spp. DNA from ungulates (i.e., *B. besnoiti*, *B. tarandi, B. caprae*, and *B. bennetti*) and was performed as previously described (Schares *et al.*, 2011b). Herein, the GoTaq (Promega, Madison, WI, USA) system was used. Briefly, each 25 µl reaction contained 12.5 µl of GoTaq master mix® (Promega, Madison, WI, USA), 0.5 µl of primer Bb3 (5'-CAA CAA GAG CAT CGC CTT C-3'; 20 µM), 0.5 µl of primer Bb 6 (5'-ATT AAC CAA TCC GTG ATA GCA G-3'; 20 µM), and 6.5 µl water. The qPCRs were run on a 7500 Fast Real-Time PCR System® (Applied Biosystems, Thermo Fisher Scientific, Waltham, MA, USA). Twenty-one hundred nanograms of DNA in a volume of 5 µl was added to each reaction.

The DNA positive control was extracted from *B. besnoiti* tachyzoites cultured *in vitro*. The product of the DNA extraction process using water instead of cells was used as a negative control. In each qPCR, 10-fold serial dilutions of genomic DNA corresponding to 0.1–100,000 Bb-Spain1 tachyzoites were included. The cycling conditions were 10 min at 95°C, followed by 40 cycles at 95°C for 15 s and at 60°C for 1 min. Fluorescence emission was measured during the 60°C step. A dissociation stage was added at the end of each run, and the melting curves were analysed. The threshold cycle values (Ct-values) obtained for positive samples in the BbRT2-PCR are also expressed as tachyzoites per reaction using the standard curve included in each run.

To normalize the quantification of the parasites and account for variations in the DNA content in the samples, a bovine ß-actin standard curve was designed ranging from 64 ng of DNA per µl to 0.2 ng per µl. The results are expressed as the ratio between the amount of parasites and bovine ß-actin.

5.10. Data analyses

To assess the differences in parasite invasion and proliferation among the different time points pi studied for each cell line, Kruskal-Wallis followed by a Dunn´s post-test was performed. Additionally, differences among the cell lines were explored using a Mann-Whitney *U* test.

The doubling time (Td) was defined as the period of time required for a tachyzoite to duplicate during the exponential multiplication period, excluding the lag phase (when there is not parasite multiplication) and the egression phase. The doubling time was determined by using non-linear regression analysis and an exponential growth equation, as previously described (Jiménez-Pelayo *et al.*, 2017).

Finally, a chi-square test was used to address possible differences regarding the percentages of the different invasion and proliferation outcomes between BAECs and fibroblasts and among BVDV-infected BAECs and non-infected BAECs.

Statistical analyses were performed with GraphPad statistics software 6.0 (San Diego, CA, USA).

ACKNOWLEDGEMENTS

This work was financially supported through research projects from the Spanish Ministry of Economy and Competitiveness (Ref. AGL2013-04442; AGL2016- 75202-R), Community of Madrid (Ref. P2018/BAA-4370, PLATESA2-CM). Alejandro Jiménez-Meléndez was supported by a grant from the Spanish Ministry of Education, Culture and Sports (grant nº FPU13/05481). Carlos Diezma-Díaz was supported by a grant from the Spanish Ministry of Economy and Competitiveness (BES-2014-069839). Patricia Vázquez was a holder of a Juan de la Cierva-Formación post-doctoral contract (FJCI-2014-20982) from the Spanish Ministry of Economy and Competitiveness. We also would like to acknowledge members from SALUVET research group for their excellent support.

The funders had no role in study design, data collection and analysis, decision to publish, or preparation of the manuscript.

Authors' contributions

LMO and GAG conceived the study and participated in its design; AJM and MFA wrote

the manuscript, with interpretation of results and discussion inputs from MAR, AC, LMO, GAG; AJM, MFA and CDD performed *in vitro* infection of the cultures, collection of the samples and ELISA assays; AJM and MFA designed and performed PCR analyses; AJM, AC and MAR performed flow cytometry analysis; AJM and PV isolated bovine endothelial and fibroblast primary cultures used in the assays. AJM carried out statistical analyses and interpreted the results. All authors read and approved the final manuscript.

REFERENCES:

Aird, W.C., 2012. Endothelial cell heterogeneity. Cold Spring Harbor perspectives in medicine 2 (1), a006429.

Álvarez-García, G., Collantes-Fernández, E., Costas, E., Rebordosa, X., Ortega-Mora, L.M., 2003. Influence of age and purpose for testing on the cut-off selection of serological methods in bovine neosporosis. Vet. Res. 34 (3), 341-352.

Álvarez-García, G., García-Lunar, P., Gutiérrez-Expósito, D., Shkap, V., Ortega-Mora, L.M., 2014. Dynamics of *Besnoitia besnoiti* infection in cattle. Parasitology 141 (11), 1419-1435.

Ataollahi, F., Pingguan-Murphy, B., Moradi, A., Abas, Wan Abu Bakar Wan, Chua, K.H., Osman, N.A.A., 2014. New method for the isolation of endothelial cells from large vessels. Cytotherapy 16 (8), 1145-1152.

Bartley, P.M., Wright, S., Sales, J., Chianini, F., Buxton, D., Innes, E.A., 2006. Long-term passage of tachyzoites in tissue culture can attenuate virulence of *Neospora caninum in vivo*. Parasitology 133, 421-432.

Basson, P., McCully, R., Bigalke, R., 1970. Observations on the pathogenesis of bovine and antelope strains of *Besnoitia besnoiti* (Marotel, 1912) infection in cattle and rabbits. Onderstepoort J Vet Res. 37(2),105-126

Bjorkman, C., Alenius, S., Manuelsson, U., Uggla, A., 2000. *Neospora caninum* and bovine virus diarrhoea virus infections in Swedish dairy cows in relation to abortion. Vet. J. 159 (2), 201-206.

Boraas, L.C., Ahsan, T., 2016. Lack of vimentin impairs endothelial differentiation of embryonic stem cells. Scientific reports 6, 30814.

Bürgi, N., Josi, C., Bürki, S., Schweizer, M., Pilo, P., 2018. *Mycoplasma bovis* co-infection with bovine viral diarrhea virus in bovine macrophages. Vet. Res. 49 (1), 2.

Calle, A., López-Martín, S., Monguió-Tortajada, M., Borràs, F.E., Yáñez-Mó, M., Ramírez, M.Á., 2019. Bovine endometrial MSC: mesenchymal to epithelial transition during luteolysis and tropism to implantation niche for immunomodulation. Stem Cell Res. Ther. 10 (1), 23.

Caro, T.M., Hermosilla, C., Silva, L.M., Cortes, H., Taubert, A., 2014. Neutrophil extracellular traps as innate immune reaction against the emerging apicomplexan parasite *Besnoitia besnoiti*. PloS one 9 (3), e91415.

Chase, C.C., 2013. The impact of BVDV infection on adaptive immunity. Biologicals 41 (1), 52-60.

Cheng, F., Shen, Y., Mohanasundaram, P., Lindstrom, M., Ivaska, J., Ny, T., Eriksson, J.E., 2016. Vimentin coordinates fibroblast proliferation and keratinocyte differentiation in wound healing via TGF-beta-Slug signaling. Proc. Natl. Acad. Sci. U. S. A. 113 (30), E4320-7.

da Fonseca Ferreira-da-Silva, M., Takács, A.C., Barbosa, H.S., Gross, U., Lüder, C.G., 2009. Primary skeletal muscle cells trigger spontaneous *Toxoplasma gondii* tachyzoite-to-bradyzoite conversion at higher rates than fibroblasts. Int. J. Med. Microbiol. 299 (5), 381-388.

Diéguez, F.J., Cerviño, M., Yus, E., 2017. Bovine viral diarrhea virus (BVDV) genetic diversity in Spain: A review. Spanish Journal of Agricultural Research 15 (2), 05-01.

Diezma-Díaz, C., Jiménez-Meléndez, A., Fernández, M., Gutiérrez-Expósito, D., García-Lunar, P., Ortega-Mora, L., Pérez-Salas, J., Blanco-Murcia, J., Ferre, I., Álvarez-García, G., 2017. Bovine chronic besnoitiosis in a calf: Characterization of a novel *B. besnoiti* isolate from an unusual case report. Vet. Parasitol. 247, 10-18.

Drew, C.P., Heller, M.C., Mayo, C., Watson, J.L., MacLachlan, N.J., 2010. Bluetongue virus infection activates bovine monocyte-derived macrophages and pulmonary artery endothelial cells. Vet. Immunol. Immunopathol. 136 (3-4), 292-296.

Dubey, J.P., van Wilpe, E., Blignaut, D.J., Schares, G., Williams, J.H., 2013. Development of early tissue cysts and associated pathology of *Besnoitia besnoiti* in a naturally infected bull (*Bos taurus*) from South Africa. J. Parasitol. 99 (3), 459-466.

Ehrlich P (2003). The fibroblast-populated collagen. A model of fibroblast collagen interactions. In: Methods in molecular medicine. Vol. 78. Wound healing: methods and protocols. DiPietro L and Burns AL (eds) (2003). Springer, New York.

Fernández-García, A., Risco-Castillo, V., Pedraza-Díaz, S., Aguado-Martínez, A., Alvarez-García, G., Gómez-Bautista, M., Collantes-Fernández, E., Ortega-Mora, L.M., 2009. First isolation of *Besnoitia besnoiti* from a chronically infected cow in Spain. J. Parasitol. 95 (2), 474-476.

Flynn, K.M., Michaud, M., Canosa, S., Madri, J.A., 2013. CD44 regulates vascular endothelial barrier integrity via a PECAM-1 dependent mechanism. Angiogenesis 16 (3), 689-705.

Frey, C.F., Regidor-Cerrillo, J., Marreros, N., García-Lunar, P., Gutiérrez-Expósito, D., Schares, G., Dubey, J.P., Gentile, A., Jacquiet, P., Shkap, V., Cortes, H., Ortega-Mora, LM., Álvarez-García, G., 2016. *Besnoitia besnoiti* lytic cycle *in vitro* and differences in invasion and intracellular proliferation among isolates. Parasites & vectors 9 (115).

Gagnieur, L., Cheval, J., Gratigny, M., Hébert, C., Muth, E., Dumarest, M., Eloit, M., 2014. Unbiased analysis by high throughput sequencing of the viral diversity in fetal bovine serum and trypsin used in cell culture. Biologicals 42 (3), 145-152.

García-Lunar, P., Ortega-Mora, L.M., Schares, G., Gollnick, N.S., Jacquiet, P., Grisez, C., Prevot, F., Frey, C.F., Gottstein, B., Álvarez-García, G., 2013. An Inter-Laboratory Comparative Study of Serological Tools Employed in the Diagnosis of *Besnoitia besnoiti* Infection in Bovines. Transbound Emerg. Dis. 60 (1), 59-68.

Gutiérrez-Expósito, D., Ortega-Mora, L.M., Marco, I., Boadella, M., Gortazar, C., San Miguel-Ayanz, J.M., García-Lunar, P., Lavin, S., Álvarez-García, G., 2013. First serosurvey of *Besnoitia* spp. infection in wild European ruminants in Spain. Vet. Parasitol. 197 (3-4), 557-564.

Gutiérrez-Expósito, D., Ferre, I., Ortega-Mora, L.M., Álvarez-García, G., 2017. Advances in the diagnosis of bovine besnoitiosis: current options and applications for control. Int. J. Parasitol. 47 (12), 737-751.

Harker, K.S., Jivan, E., McWhorter, F.Y., Liu, W.F., Lodoen, M.B., 2014. Shear forces enhance *Toxoplasma gondii* tachyzoite motility on vascular endothelium. MBio 5 (2), e01111-13.

Haudenschild C (1984) Morphology of vascular endothelial cells in culture. In: Biology of endothelial cells, Jaffe E (1984). Springer, New York.

Helmke, B.P., Thakker, D.B., Goldman, R.D., Davies, P.F., 2001. Spatiotemporal analysis of flow-induced intermediate filament displacement in living endothelial cells. Biophys. J. 80 (1), 184-194.

Hermosilla, C., Barbisch, B., Heise, A., Kowalik, S., Zahner, H., 2002. Development of *Eimeria bovis in vitro*: suitability of several bovine, human and porcine endothelial cell lines, bovine fetal gastrointestinal, Madin–Darby bovine kidney (MDBK) and African green monkey kidney (VERO) cells. Parasitol. Res. 88 (4), 301-307.

Hoffmann, B., Depner, K., Schirrmeier, H., Beer, M., 2006. A universal heterologous internal control system for duplex real-time RT-PCR assays used in a detection system for pestiviruses. J. Virol. Methods 136 (1-2), 200-209.

Jiménez-Pelayo, L., García-Sánchez, M., Regidor-Cerrillo, J., Horcajo, P., Collantes-Fernández, E., Gómez-Bautista, M., Hambruch, N., Pfarrer, C., Ortega-Mora, L.M., 2017. Differential susceptibility of bovine caruncular and trophoblast cell lines to infection with high and low virulence isolates of *Neospora caninum*. Parasit.Vectors. 10 (1), 463.

Katagata, Y., Takeda, H., Ishizawa, T., Hozumi, Y., Kondo, S., 2002. Occurrence and comparison of the expressed keratins in cultured human fibroblasts, endothelial cells and their sarcomas. J. Dermatol. Sci. 30 (1), 1-9.

Langenmayer, M.C., Gollnick, N.S., Majzoub-Altweck, M., Scharr, J.C., Schares, G., Hermanns, W., 2015c. Naturally Acquired Bovine Besnoitiosis: Histological and Immunohistochemical Findings in Acute, Subacute, and Chronic Disease. Vet. Pathol. 52 (3), 476-488, 0300985814541705.

Lertkiatmongkol, P., Liao, D., Mei, H., Hu, Y., Newman, P.J., 2016. Endothelial functions of platelet/endothelial cell adhesion molecule-1 (CD31). Curr. Opin. Hematol. 23 (3), 253-259, 10.1097/MOH.0000000000000239.

Mainar-Jaime, R., Berzal-Herranz, B., Arias, P., Rojo-Vázquez, F., 2001. Epidemiological pattern and risk factors associated with bovine viral-diarrhoea virus (BVDV) infection in a non-vaccinated dairy-cattle population from the Asturias region of Spain. Prev. Vet. Med. 52 (1), 63-73.

Maksimov, P., Hermosilla, C., Kleinertz, S., Hirzmann, J., Taubert, A., 2016. *Besnoitia besnoiti* infections activate primary bovine endothelial cells and promote PMN adhesion and NET formation under physiological flow condition. Parasitol. Res. 115 (5), 1991-2001.

Mineo, T.W., Benevides, L., Silva, N.M., Silva, J.S., 2009. Myeloid differentiation factor 88 is required for resistance to *Neospora caninum* infection. Vet. Res. 40 (4), 1-12.

Müller, J., Hemphill, A., 2012. *In vitro* culture systems for the study of apicomplexan parasites in farm animals. Int. J. Parasitol. , 10.1016/j.ijpara.2012.08.004; 10.1016/j.ijpara.2012.08.004.

Muñoz-Caro, T., Silva, L.M., Ritter, C., Taubert, A., Hermosilla, C., 2014. *Besnoitia besnoiti* tachyzoites induce monocyte extracellular trap formation. Parasitol. Res. 113 (11), 4189-4197.

Naguleswaran, A., Muller, N., Hemphill, A., 2003. *Neospora caninum* and *Toxoplasma gondii*: a novel adhesion/invasion assay reveals distinct differences in tachyzoite-host cell interactions. Exp. Parasitol. 104 (3-4), 149-158.

Neill, J.D., Ridpath, J.F., Lange, A., Zuerner, R.L., 2008. Bovine viral diarrhoea virus infection alters global transcription profiles in bovine endothelial cells. Dev. Biol. (Basel) 132, 93-98.

Neuman, M., 1974. Cultivation of *Besnoitia besnoiti* Marotel, 1912, in cell culture. Tropenmed. Parasitol. 25 (2), 243-249.

Nischik, N., Schade, B., Dytnerska, K., Dlugonska, H., Reichmann, G., Fischer, H.G., 2001. Attenuation of mouse-virulent *Toxoplasma gondii* parasites is associated with a decrease in interleukin-12-inducing tachyzoite activity and reduced expression of actin, catalase and excretory proteins. Microbes Infect. 3 (9), 689-699.

Nolte, S.V., Xu, W., Rennekampff, H.O., Rodemann, H.P., 2008. Diversity of fibroblasts--a review on implications for skin tissue engineering. Cells Tissues Organs 187 (3), 165-176.

OSullivan F. Meleady P, McBride S, Clynes M. Primary culture. In: Animal cell culture techniques. Edited by Martin Clynes. 2003. Elsevier.

Pan, C., Kumar, C., Bohl, S., Klingmueller, U., Mann, M., 2009. Comparative proteomic phenotyping of cell lines and primary cells to assess preservation of cell type-specific functions. Mol. Cell. Proteomics 8 (3), 443-450.

Peterhans, E., Jungi, T.W., Schweizer, M., 2003. BVDV and innate immunity. Biologicals 31 (2), 107-112.

Pols, J.W., 1960. Studies on bovine besnoitiosis with special reference to the aetiology. Onderstepoort Jour Vet Res 28 ((3)), 265-356.

Regidor-Cerrillo, J., Gómez-Bautista, M., Sodupe, I., Aduriz, G., Álvarez-García, G., Del Pozo, I., Ortega-Mora, L.M., 2011. *In vitro* invasion efficiency and intracellular proliferation rate comprise virulence-related phenotypic traits of *Neospora caninum*. Vet. Res. 42 (1), 41, 10.1186/1297-9716-42-41.

Samish, M., Shkap, V., Bin, H., Pipano, E.M., 1988. Cultivation of *Besnoitia besnoiti* in four tick cell lines. Int. J. Parasitol. 18 (3), 291-296.

Scanga, C.A., Aliberti, J., Jankovic, D., Tilloy, F., Bennouna, S., Denkers, E.Y., Medzhitov, R., Sher, A., 2002. Cutting edge: MyD88 is required for resistance to *Toxoplasma gondii* infection and regulates parasite-induced IL-12 production by dendritic cells. The Journal of Immunology 168 (12), 5997-6001.

Schares, G., Maksimov, A., Basso, W., More, G., Dubey, J.P., Rosenthal, B., Majzoub, M., Rostaher, A., Selmair, J., Langenmayer, M.C., Scharr, J.C., Conraths, F.J., Gollnick, N.S., 2011b. Quantitative real time polymerase chain reaction assays for the sensitive detection of *Besnoitia besnoiti* infection in cattle. Vet. Parasitol. 178 (3-4), 208-216.

Schares, G., Basso, W., Majzoub, M., Cortes, H.C., Rostaher, A., Selmair, J., Hermanns, W., Conraths, F.J., Gollnick, N.S., 2009. First *in vitro* isolation of *Besnoitia besnoiti* from chronically infected cattle in Germany. Vet. Parasitol. 163 (4), 315-322.

Schaut, R.G., McGill, J.L., Neill, J.D., Ridpath, J.F., Sacco, R.E., 2015. Bovine viral diarrhea virus type 2 in vivo infection modulates TLR4 responsiveness in differentiated myeloid cells which is associated with decreased MyD88 expression. Virus Res. 208, 44-55.

Spanel-Borowski, K., 2011. Five different phenotypes of endothelial cell cultures from the bovine corpus luteum: present outcome and role of potential dendritic cells in luteolysis. Mol. Cell. Endocrinol. 338 (1-2), 38-45.

Spanel-Borowski, K., Ricken, A.M., Patton, W.F., 1994. Cytokeratin-positive and cytokeratin-negative cultured endothelial cells from bovine aorta and vena cava. Differentiation 57 (3), 225-234.

Taubert, A., Hermosilla, C., Silva, L., Wieck, A., Failing, K., Mazurek, S., 2016. Metabolic signatures of *Besnoitia besnoiti*-infected endothelial host cells and blockage of key metabolic pathways indicate high glycolytic and glutaminolytic needs of the parasite. Parasitol. Res. 115 (5), 2023-2034.

Tsuneki, M., Madri, J.A., 2016. CD44 influences fibroblast behaviors via modulation of cell–cell and cell–matrix interactions, affecting survivin and hippo pathways. J. Cell. Physiol. 231 (3), 731-743.

Tsuneki, M., Madri, J.A., 2014. CD44 regulation of endothelial cell proliferation and apoptosis via modulation of CD31 and VE-cadherin expression. J. Biol. Chem. 289 (9), 5357-5370.

Uryvaev, L., Dedova, A., Dedova, L., Ionova, K., Parasjuk, N., Selivanova, T., Bunkova, N., Gushina, E., Grebennikova, T., Podchernjaeva, R., 2012. Contamination of cell cultures with bovine viral diarrhea virus (BVDV). Bull. Exp. Biol. Med. 153 (1), 77-81.

Valencia-Nuñez, D.M., Kreutler, W., Moya-Gonzalez, J., Alados-Arboledas, P., Muñoz-Carvajal, I., Carmona, A., Ramirez-Chamond, R., Carracedo-Añon, J., 2017. Endothelial vascular markers in coronary surgery. Heart Vessels 32 (11), 1390-1399.

Vanleeuwen, J.A., Haddad, J.P., Dohoo, I.R., Keefe, G.P., Tiwari, A., Tremblay, R., 2009. Associations between reproductive performance and seropositivity for bovine leukemia virus, bovine viral-diarrhea virus, *Mycobacterium avium* subspecies *paratuberculosis*, and *Neospora caninum* in Canadian dairy cows. Prev. Vet. Med. 94(1-2):54-64.

Vonlaufen, N., Muller, N., Keller, N., Naguleswaran, A., Bohne, W., McAllister, M.M., Bjorkman, C., Muller, E., Caldelari, R., Hemphill, A., 2002b. Exogenous nitric oxide triggers *Neospora caninum* tachyzoite-to-bradyzoite stage conversion in murine epidermal keratinocyte cell cultures. Int. J. Parasitol. 32 (10), 1253-1265.

OBJETIVO 2: Empleo de modelos experimentales *in vitro* para la realización de estudios de patogenia molecular y cribado farmacológico en la infección por *B. besnoiti*.

Resumen

En la actualidad se desconoce la patogénesis de la besnoitiosis bovina, así como las bases moleculares responsables de la progresión de la enfermedad. Por ello, en el subobjetivo 2.1. se han empleado las células endoteliales de aorta bovina (BAEC) obtenidas en el objetivo 1 de la presente tesis doctoral para investigar la interacción parásito-célula hospedadora mediante la metodología de secuenciación masiva RNA-Seq a dos tiempos post-infección (pi): a las 12 h pi, cuando los taquizoítos ya han invadido las células hospedadodas y a las 32 hpi, cuando los taquizoítos han realizado dos rondas de replicación. Además, se ha estudiado el perfil global de expresión génica de los taquizoítos a ambos tiempos pi.

Se han detectado 446 genes bovinos con una expresión diferencial entre ambos tiempos pi, 249 se encuentraron sobreexpresados y 197 infraexpresados a las 32 hpi. Destacó la sobreexpresión de diferentes citoquinas, quimioquinas y moléculas de adhesión de leucocitos a las 12 hpi, y de genes implicados en la angiogénesis y la organización de la matriz extracelular a ambos tiempos pi, demostrándose una activación de las células endoteliales asociada al daño endotelial. La infección moduló las rutas de señalización del factor de transcripción NFkB y el TNF-a, las cuales coordinan la expresión de varias proteínas efectoras responsables de un fenotipo proinflamatorio y profibrótico. Estos mediadores serían responsables de la atracción y reclutamiento de macrófagos, que desencadenarían los fenónemos de inflamación crónica y fibrosis observados durante la fase crónica de la enfermedad. Finalmente, la infección también ha modulado la angiogénesis, detectándose la sobreexpresión de genes implicados tanto en una fase temprana (p. ej. factores de crecimiento y metaloproteinasas de matriz) como tardía (integrinas y vasohibina). Estos resultados se confirmaron tras seleccionar y validar por qPCR un panel de genes clave implicados en los mecanismos anteriormente citados (p. ej. ICAM1, VCAM1, SELE, CCL2, IL6 y ADAMTS1, entre otros) y que presentaron los mayores cambios de expresión. Por otra parte, se han identificado ortólogos de *Besnoitia* implicados en el ciclo lítico de otros protozoos Toxoplasmatinae, y que estuvieron sobreexpresados a las 32 hpi (p.ej. ROP40, ROP5B, MIC1, MIC10, entre otros). Asimismo, de nuevo se validó un número representativo de genes identificados mediante qPCR.

Además, se han empleado los modelos *in vitro* en los estudios de cribado farmacológico. En el subobjetivo 2.2., se ha utilizado la estrategia de reposicionamiento farmacológico, analizando un panel de fármacos ya disponibles en el mercado y con eficacia demostrada frente a otras especies de protozoos apicomplejos en búsqueda de potenciales candidatos terapéuticos frente la besnoitiosis bovina. Para ello, taquizoítos de *B. besnoiti* fueron expuestos a diferentes concentraciones de toltrazurilo, diclazurilo, imidocarb, decoquinato, sulfadiazina y trimetoprim, sólo o en combinación con sulfadiazina. Los fármacos se añadieron a dos tiempos pi seleccionados: justo antes de la infección de las células Marc-145 (0 hpi) o a las 6 hpi. Además, se estudió su posible toxicidad en las células mediante la realización de una prueba de viabilidad celular XTT. Los compuestos que mostraron los resultados más prometedores en el cribado fueron seleccionados para la determinación de las concentraciones inhibitorias 50 (CI50) y 99 (CI99) mediante qPCR. Además, se estudió el impacto de los fármacos en la ultraestructura de los taquizoítos mediante microscopía electrónica de transmisión (TEM), y se realizaron estudios a largo plazo para estudiar si el efecto de los mismos era parasitostático o

parasiticida. Los ensayos de citotoxicidad mostraron que ninguno de los compuestos afectaba a las células a las concentraciones empleadas en el cribado. El decoquinato y el diclazurilo mostraron tasas de inhbición de la invasión del parásito del 90 y 83%, al ser administrados a las 0 hpi, y del 73 y 72% al ser administrados a las 6 hpi, respectivamente. El resto de los fármacos fueron descartados por su toxicidad o por presentar una eficacia inferior. El decoquinato y el diclazurilo presentaron CI99 de 100 nM y 29,9 µM, respectivamente. Los ensayos de TEM mostraron que el decoquinato afectaba principalmente a la mitocondria de los taquizoítos, mientras que el diclazurilo interfería con la citoquinesis y división de los mismos.

Finalmente, en el subobjetivo 2.3., en lo concerniente a la búsqueda de nuevas dianas terapéuticas frente a la besnoitiosis bovina, se identificó el gen codificante de la enzima CDPK1 de *B. besnoiti*. A continuación, se comprobó la disminución de la actividad enzimática de la proteína recombinante con un panel de nueve BKIs mediante un ensayo luciferasa. Posteriormente, se analizó la seguridad y eficacia de dichos compuestos frente a taquizoítos de *B, besnoiti* en células Marc-145. Los resultados del cribado farmacológico, utilizando los fármacos a una concentración de 5 µM, mostraron que ocho de los compuestos mostraron valores de inhibición de la invasión y proliferación del parásito superiores al 80%. Los compuestos 1294, 1517, 1553 y 1571 fueron seleccionados y se determinaron sus concentraciones inhibitorias 99 (CI99) (1294: 2,38 µM; 1517: 2,20 µM; 1553: 3,34 µM; 1571: 2,78 µM) mediante qPCR. No obstante, la exposición de los taquizoítos a las CI99 no mostró un efecto parasiticida. Dicho efecto fue confirmado mediante microscopía electronica de transmisión (TEM), al demostrarse que el tratamiento con BKIs interfería con la regulación del ciclo celular produciéndose alteraciones en la división de los taquizoítos que daban lugar a la formación de grandes complejos multinucleados que coexistían con taquizoítos viables en el interior de las vacuolas parasitóforas.

En resumen, se ha estudiado la interacción a nivel molecular entre *B. besnoiti* y las BAEC, demostrándose la progresión de una activación del endotelio de tipo II a consecuencia de la invasión y proliferación del parásito y se han identificado posibles biomarcadores de pronóstico y posibles dianas terapéuticacs o vacunales. Además, se ha demostrado la eficacia del decoquinato, el diclazurilo y los BKIs 1294, 1517, 1553 y 1571 frente a la infección por *B. besnoiti in vitro*. Es posible que *in vivo*, una respuesta inmunitaria activa junto con el tratamiento farmacológico sean capaces de eliminar la infección, si bien son necesarios estudios de seguridad y eficacia en la especie de destino.

RNA-Seq analyses reveal that endothelial activation and fibrosis are early and progressively induced by *Besnoitia besnoiti* host cell invasion and proliferation

Alejandro Jiménez-Meléndez[1], Chandra Ramakrishnan[2], Adrian B. Hehl[2], Gema Álvarez-García[1]

[1] SALUVET, Animal Health Department, Faculty of Veterinary Sciences, Complutense University of Madrid, Ciudad Universitaria s/n, 28040-Madrid, Spain.

[2] Institute of Parasitology, University of Zurich, Winterthurerstrasse 266a, 8057 Zurich, Switzerland

* Corresponding author: Tel: +34913944095. Fax: +34913944098. *E-mail*: gemaga@vet.ucm.es.

Manuscrito en preparación

Repurposing of commercially available anti-coccidials identifies diclazuril and decoquinate as potential therapeutic candidates against *Besnoitia besnoiti* infection.

Alejandro Jiménez-Meléndez[1], Laura Rico-San Román[1], Vreni Balmer[2], Andrew Hemphill[2], Luis M. Ortega-Mora[1], Gema Álvarez-García[1]

[1] SALUVET, Animal Health Department, Faculty of Veterinary Sciences, Complutense University of Madrid, Ciudad Universitaria s/n, 28040-Madrid, Spain.

[2] Institute of Parasitology, Vetsuisse Faculty, University of Berne, Länggass-Strasse 122, CH-3012 Berne, Switzerland.

* Corresponding author: Tel: +34913944095. Fax: +34913944098. *E-mail*: gemaga@vet.ucm.es

Manuscript published in *Vet. Parasitol.,* 2018 Sep 15;261:277-85.
doi:10.1016/j.vetpar.2018.08.015. Epub 2018 Aug 31.

Presented as oral communication in the Apicomplexa in farm animals Congress 2017.
(11-13th October, Madrid, Spain).

ABSTRACT

Repurposing of currently marketed compounds with proven efficacy against apicomplexan parasites was used as an approach to define novel candidate therapeutics for bovine besnoitiosis. *Besnoitia besnoiti* tachyzoites grown in MARC-145 cells were exposed to different concentrations of toltrazuril, diclazuril, imidocarb, decoquinate, sulfadiazine and trimethoprim alone or in combination with sulfadiazine. Drugs were added either just prior to infection of MARC-145 cells (0 hours post infection, hpi) or at 6 hpi. A primary evaluation of drug effects was done by direct immunofluorescence staining and counting. Potential effects on the host cells were assessed using a XTT kit for cell proliferation. Compounds displaying promising efficacy were selected for IC_{50} and IC_{99} determination by qPCR. In addition, the impact of drugs on the tachyzoite ultrastructure was assessed by TEM and long-term treatment assays were performed. Cytotoxicity assays confirmed that none of the compounds affected the host cells. Decoquinate and diclazuril displayed invasion inhibition rates of 90 and 83 % at 0 h pi and 73 and 72 % at 6 h pi, respectively. The remaining drugs showed lower efficacy and were not further studied. Decoquinate and diclazuril exhibited IC_{99} values of 100 nM and 29.9 µM, respectively. TEM showed that decoquinate primarily affected the parasite mitochondrium, whilst diclazuril interfered in cytokinesis of daughter zoites. The present study demonstrates the efficacy of diclazuril and decoquinate against *B. besnoiti in vitro* and further assessments of safety and efficacy of both drugs should be performed in the target species.

Key Words: *Besnoitia besnoiti*; tachyzoite; commercial drugs; decoquinate; diclazuril; *in vitro* assays.

1. INTRODUCTION

Besnoitia besnoiti is a cyst-forming apicomplexan protozoan belonging to the Toxoplasmatinae subfamily and closely related to *Neospora caninum* and *Toxoplasma gondii*. *B. besnoiti* causes bovine besnoitiosis, a debilitating disease of cattle characterized by non-specific clinical signs such as fever or oedemas at the acute stage and skin manifestations during the chronic stage that may end up with sterility in bulls (Gutiérrez-Expósito *et al.*, 2017). In the absence of effective treatments or vaccines for disease control, the last 20 years have witnessed a steady increase in the number of infected herds, and the disease appeared in countries where it had not been described before. Thus, the European Food and Safety Authority (EFSA) has considered bovine besnoitiosis as re-emerging in Europe (European Food Safety Authority, 2010). Recent outbreaks have been described in Central Europe or even Ireland (Álvarez-García, 2016; Ryan *et al.*, 2016)

Due to assumed similarities with other Toxoplasmatinae parasites, *B. besnoiti* is suspected to have a heteroxenous life cycle, but the definitive host is still elusive (Basso *et al.*, 2011). In Europe, cattle act as the main intermediate host, where two asexual and infective stages of the parasite develop: tachyzoites, responsible for the acute stage of the disease, and bradyzoites, found inside tissue cysts and responsible for the characteristic skin lesions during the chronic stage.

Currently, there are no effective therapeutics for the treatment of bovine besnoitiosis. An effective drug should target the tachyzoite stage and affect the dissemination of the parasite into different organs during the acute disease stage, and should preferentially also impact on the tissue cysts that contain bradyzoites. In the past, the effects of a wide range of compounds were assessed in naturally infected bovines, as well as in experimentally infected rabbits and gerbils (Pols, 1960; Shkap *et al.*, 1985a, 1987b). However, results have remained inconclusive due to fact that these assays were performed under variable experimental conditions, and there was a lack of well-established and reproducible *in vivo* models to study bovine besnoitiosis.

Previous *in vitro* studies demonstrated that thiazolides (Cortes *et al.*, 2007a), arylimidamides (Cortes *et al.*, 2011), and bumped kinase inhibitors (BKIs) (Jiménez-Meléndez *et al.*, 2017) exhibited promising *in vitro* activities against *B. besnoiti*. However, arylimidamides and thiazolides are not commercially available for ruminants in Europe and BKIs are "new generation drugs" in a pre-clinical stage of development (Van Voorhis *et al.*, 2017). Thus, they may represent

valuable therapeutical tools only in the long run. In contrast, repurposing of drugs with well characterized activities, and which are already on the market for other indications, might be a valuable strategy for a speedier implementation of novel treatments against besnoitiosis. The same approach has also been exploited for other closely related parasites such as *N. caninum* (Müller *et al.*, 2016), *T. gondii* (Dittmar *et al.*, 2016) or *Cryptosporidium parvum* (Bessoff *et al.*, 2014). Thus, in this study decoquinate, diclazuril, toltrazuril, imidocarb, sulfadiazine and trimethoprim, were assessed for *in vitro* activity against *B. besnoiti*, as these drugs are commercialised in cattle for the treatment of relevant diseases caused by apicomplexan parasites.

Decoquinate is an anticoccidial quinolone initially developed for poultry in 1967 (Williams, 2006) and approved as an additive in feed to prevent intestinal coccidiosis in cattle and goats. Decoquinate affects the parasite mitochondrium and acts as a cytochrome *bc1* inhibitor, thus it impairs the transfer of electrons from ubiquinone to cytochrome C (Fry & Williams, 1984). The compound is also active against *N. caninum* tachyzoites (Lindsay *et al.*, 1997) and also affects the proliferation of *T. gondii* (Lindsay *et al.*, 1998). The coccidicides toltrazuril and diclazuril are triazinone derivatives and are effective against intracellular stages of *Eimeria* and *Isospora* spp. The exact mechanism of action is not well understood, but several studies have shown that these drugs affect enzymes of the respiratory chain, and also target other enzymes such as dihydrofolate reductase (DHFR) (Stock *et al.*, 2017). Imidocarb is a dicationic diamidine of the carbanilide series of antiprotozoal compounds and currently the drug of choice for the treatment of bovine babesiosis caused by *Babesia* spp. (Vial & Gorenflot, 2006). The mode of action is uncertain, but it is supposed to interfere with the production and/or utilization of polyamines or the prevention of the entry of inositol into the erythrocytes. The antibiotics sulfadiazine and trimethoprim are used in cattle for the treatment of colibacillosis, metritis and pneumonia (Kaartinen *et al.*, 1999), and they are also commonly applied for prophylaxis and treatment of toxoplasmosis in humans (Torre *et al.*, 1998). They act synergistically by sequentially blocking dihydropteroate synthase (DHPS) and dihydrofolate reductase (DHFR), both of which are crucially involved in the folate biosynthesis pathway and essential for nucleoside biosynthesis and nucleic acid formation. Moreover, sulfadiazine can be used to treat coccidiosis (Daugschies & Najdrowski, 2005).

Thus, the objective of the present study was to evaluate the safety and efficacy of these six commercially available drugs against *B. besnoiti* tachyzoites *in vitro*.

2. MATERIALS AND METHODS

2.1. Parasite maintenance and cell cultures

The monkey kidney cell line Marc-145 and human foreskin fibroblasts (HFF), as well as tachyzoites from the *B. besnoiti* Spain1 (Bb Spain 1) isolate, were maintained according to previously published procedures (Jiménez-Meléndez *et al.*, 2017). Marc-145 cell cultures were passaged twice a week, whilst HFF cultures only once a week. The *B. besnoiti* isolate used for all *in vitro* assays was tested negative to *Mycoplasma* spp. infection by PCR (Mycoplasma Gel Form Kit®, Biotools, Spain) following the manufacturer´s instructions and bovine viral diarrhea virus (BVDV) by quantitative real-time PCR (qPCR) (Hoffmann *et al.*, 2006). The fetal calf serum (FCS) used in all the experiments was previously checked for the absence of IgGs against *B. besnoiti*, *N. caninum* and *T. gondii* by IFAT (Fernández-García *et al.*, 2009a). For drug assays, tachyzoites were harvested three days post infection (dpi), when most of them were still intracellular, by recovering the infected cell monolayer with a cell scraper, followed by repeated passages through a 25-gauge needle at 4 °C and separation from cell debris on a PD-10 column (Frey *et al.*, 2016). Tachyzoite viability was confirmed by trypan blue exclusion followed by counting in a Neubauer chamber. Purified viable tachyzoites were used to infect Marc-145 cell monolayers.

2.2. Cytotoxicity in Marc-145 cells

The potential toxicity of the compounds against Marc-145 cells was assessed by a XTT cell viability assay (Panreac-AppliChem, Barcelona, Spain). Marc-145 cells in the exponential phase of growth were seeded in

96-well flat-bottom plates at a density of 2×10^4 cells/well containing compounds at the maximum concentration employed in our assays and grown for 72 h at 37 °C in a 5% CO_2 humidified incubator. Afterwards, 50 µL of XTT reagent was added to each well and further incubated for 4 h. Fluorescence was measured at the respective excitation and emission wavelengths of 475 nm and 660 nm in a Biotek Multiplate Reader (Biotek, Winooski, VT, USA) and specific OD values were determined according to the instructions from the manufacturer. The compounds were tested in quadruplicate in three independent assays.

2.3. Primary drug assays on B. besnoiti-infected MARC-145 cells

In preliminary experiments, dose- finding studies were carried out with at least 4 concentrations for each drug, following the procedure described by Jiménez-Meléndez et al. (2017). Each concentration was tested in triplicate in two or more independent assays. Briefly, monolayers of Marc-145 cells ($5x10^4$ cells per well) were incubated in culture medium at 37 °C / 5% CO_2 and grown to confluence in 24-well plates. Treatments were initiated by adding the compounds to the cell cultures just prior to infection (0 hours post infection, hpi) or 6 h after cells were infected (6 hpi). The drug concentrations employed in these experiments are outlined in Table 1, and were selected based on previous *in vitro* studies on *N. caninum*, *T. gondii* or other apicomplexan parasites (e.g *Babesia* spp., *Theileria* spp.). Depending on the compound, the solvents Dimethyl Sulfoxide or a mixture of NaOH/MetOH (Lindsay *et al.*, 2013) were added to negative control wells at equal volumes (see Table 1). Cultures were infected with 10^3 purified tachyzoites of *B. besnoiti* Bb Spain-1 when the compounds were already present, or compounds were administered 6 hpi. In the latter case, infected monolayers were gently rinsed 3 times with Phosphate Buffered Saline (PBS) prior to the addition of the compounds in order to remove non-invaded tachyzoites. Drugs were kept in the medium of cell culture until immunofluorescence staining was performed at 72 hpi. Once the optimal concentrations for each compound were identified, the assays were repeated employing the same procedure under optimized conditions. In some experiments employing sulfadiazine and trimethoprim, alone or in combination, longer treatments of 6 days, involving at least two lytic cycles of the parasite, were carried out (Lindsay *et al.*, 1994). Each condition was assessed in triplicate and all experiments were carried out in three independent assays.

2.4. Immunofluorescence staining

For immunofluorescence staining, supernatants of the cell cultures were discarded at 72 hpi, cells were washed 3 times with PBS and were fixed by the addition of ice-cold methanol for 10 min. After another wash in PBS, cells were permeabilized with 300 µl/ well of 0.2% Triton-X 100 in PBS for 30 min at 37 °C, followed by 3 additional washes with PBS. A primary polyclonal rabbit-anti tachyzoite Bb-Spain1 polyclonal antiserum (Gutiérrez-Expósito *et al.*, 2013) was added at a dilution of 1:1000 in PBS and incubated for 1 h at 37°C. After 3 additional washes with PBS, Alexa Fluor® 488 Goat Anti-Rabbit IgG (H+L), (Life technologies, Thermo Fisher Scientific, USA) were added per well at a dilution of 1:1000. The plates were incubated for 45 min at room temperature in the dark, and washed 3 times with PBS. In the final wash, DAPI stain was included to stain the nuclei. Finally, the plates were washed with distilled water and the total number of invasion events per well was counted using an inverted fluorescence microscope (Nikon eclipse TE200) at 200X magnification. Two categories of plaque forming tachyzoites were distinguished: parasitophorous vacuoles (PVs) and lysis plaques, as described by (Frey *et al.*, 2016).

2.5. IC_{50} and IC_{99} determination

Those compounds that showed the highest values of both parasite invasion and proliferation inhibition were selected for IC_{50} and IC_{99} determination (the effective concentrations to reduce proliferation by 50% or 99%, respectively). Marc-145 cells

Tabla 1: Compounds tested in all *in vitro* assays and results obtained in the preliminary experiments carried out to determine the best concentrations for the subsequent drug screening.

Compound (Company)	Solvent	Drug Stock Solution	Drug Concentration used in assays			References**
			Previous trials (Effect observed in treated cell cultures)	Subsequent experiments	IC_{50} and IC_{99} determinations	
Decoquinate (Zoetis™)	NaOH 0.1N–MetOH 90%	2.4 mM	240, 200, 100, 50 nM (No lysis plaques, PV*)	240 nM	240 nM – 0.24 nM	Lindsay et al., 2013
Diclazuril (Elanco-Lilly™)	DMSO	10 mM	100 µM (Cytotoxicity)	30 µM	40 µM – 0.04 µM	Lindsay et al., 1995
			70, 50 µM (No lysis plaques or PV)			
			30 µM (No lysis plaques, PV)			
			10 µM (PV)			
Toltrazuril (Bayer™)	DMSO	10 mM	100, 70, 50 µM (Cytotoxicity)	30 µM		Darius et al., 2004
			30 µM (No lysis plaques, PV)			
			10 µM (Lysis plaques and PV)			
Imidocarb (MSD Animal Health™)	DMSO	10 mM	70, 50, 30, 10 µM (Lysis plaques and PV)	30 µM		Hines et al., 2015
Sulfadiazine (CZV™)	DMSO	50 mM	200, 100, 70, 50 µM (Lysis plaques and PV)	100 µM		Lindsay et al., 1994
Trimethoprim (CZV™)	DMSO	50 mM	200, 100, 70, 50 µM (Lysis plaques and PV)	100 µM		Lindsay et al., 1994
Sulfadiazine + Trimethoprim (CZV™)	DMSO		100-100; 100-50; 100-30; 100-10 (Lysis plaques and PV)	100 µM – 10 µM		Lindsay et al., 1994

*PV: parasitophorous vacuoles

** Previous studies done with these compounds and other apicomplexan parasites in order to select appropriate doses to be tested.

were grown to confluency in 24 well plates. Just prior to infection, drugs were added at final concentrations ranging between 40 µM and 4 nM for diclazuril and 240 nM and 0.24 nM for decoquinate. Bb-Spain 1 tachyzoites were added at a parasite: host cell ratio of 1:100 (10^3 tachyzoites per well). Control wells containing the drug solvents were also included in each culture plate. After 72 hpi, samples were collected using a lysis solution (100 µL PBS, proteinase K and AL Buffer) and stored at -80 °C until further DNA extraction according to the manufacturer´s instructions (DNeasy Blood and Tissue, Qiagen, Valencia, CA, USA). Each condition was assessed in triplicate and the experiments were carried out in three independent assays.

2.6. DNA extraction and quantitative real-time PCR (qPCR)

The harvested cell culture samples were incubated for 10 min at 56°C, and DNA was purified using the spin column protocol for cultured cells according to the manufacturer's instructions contained in the DNeasy Blood and Tissue kit (Qiagen, Valencia, CA, USA). DNA was eluted in 200 µl elution buffer. DNA content and purity of each sample was measured by UV spectrometry using a Biotek Multiplate Reader (Biotek, Winooski, VT, USA).

The BbRT2 qPCR assay for the specific detection of *Besnoitia* spp. DNA from ungulates (i.e., *B. besnoiti*, *B. tarandi, B. caprae*, and *B. bennetti*) was performed according to Schares *et al.*, (2011b). Herein the SYBR Green system was used. Briefly, each 20 µl reaction contained 10 µl of Power SYBR Green master mix® (Applied Biosystems, Foster City, CA, USA), 0.5 µl of primer Bb3 (5'-CAA CAA GAG CAT CGC CTT C-3'; 20 µM), 0.5 µl of primer Bb 6 (5'-ATT AAC CAA TCC GTG ATA GCA G-3'; 20 µM), and 4 µl water. The qPCRs were run on a 7500 Fast Real-Time PCR System® (Applied Biosystems, Thermo Fisher Scientific, USA). 20-100 ng of DNA in a volume of 5 µl was added to each reaction. The DNA positive control was extracted from *B. besnoiti* tachyzoites cultured *in vitro*. The product of the DNA extraction process using water instead of cells was used as a negative control. In each qPCR, 10-fold serial dilutions of genomic DNA corresponding to 0.1–100,000 Bb-Spain1 tachyzoites were included. The cycling conditions were 10 min at 95 °C followed by 40 cycles of 95 °C for 15 s and 60 °C for 1 min. Fluorescence emission was measured during the 60 °C step. A dissociation stage was added at the end of each run, and the melting curves were analysed. BbRT2-PCR was run in duplicate for each sample. The threshold cycle values (Ct-values) obtained for positive samples in the BbRT2-PCR were also expressed as tachyzoites per reaction using the standard curve included in each run.

2.7. Studies on the impact of decoquinate and diclazuril on the viability of B. besnoiti tachyzoites

Tachyzoites from Bb-Spain 1 strain were grown as previously stated and decoquinate or diclazuril were added just prior to infection at the previously established IC_{99} concentrations. Drugs were kept for 6, 24 or 48 h. Drug containing medium was discarded and fresh culture medium was added. Cell cultures were evaluated until 10 days post treatment (dpt), by daily visual inspection by light microscopy. Samples were collected at 1, 3 and 5 dpt for subsequent qPCR analysis. IFAT at 8 and 10 dpt were also performed to assess whether any tachyzoites were able to re-infect host cells (Winzer *et al.*, 2015). Each assay was done in triplicate and at least three independent experiments were carried out.

2.8. Transmission Electron Microscopy

HFF cell cultures were maintained in T25 tissue culture flasks and were infected with 10^7 Bb-Spain1 tachyzoites (parasite: host cell ratio of 10:1). After allowing the tachyzoites to invade the host cells for 3 h, monolayers were washed three times with PBS and treated with decoquinate or diclazuril at the previously stated EC_{99} for each compound. Control flasks without drugs contained the corresponding amounts of either DMSO or NaOH/MetOH. Samples were processed for TEM analysis at different time points of treatment (1, 3 and 6 days) as described elsewhere (Müller *et al.*, 2017b).

2.9. Data analyses

Values for cytotoxicity of compounds are depicted in percentage (%) in relation to the respective vehicle, and were statistically evaluated using Student's-*t*-

test using the raw data from the specific ODs calculated as explained in section 2.2.

To determine the percentage of inhibition of parasite growth, the invasion rates (IRs) were calculated by counting all the events per well, IRs were then related to the respective negative vehicle control to determine the relative growth (RG) of the parasite for each drug experiment. The percentage of inhibition was determined as follows:

% RG = (IR drug / IR vehicle) x 100

% Inhibition = 100 - %RG

For IC_{50} and IC_{99} calculations based on qPCR, the amount of DNA was quantified by spectrophotometry in each sample and adjusted. The RG in each drug concentration was determined relative to the vehicle control using the tachyzoite yield per ng of DNA. IC_{50} and IC_{99} values were calculated using the ED50 plus sheet for Microsoft Excel after a logarithmic transformation of the data.

Kruskal-Wallis test was performed to compare the efficacy of the 6 compounds against *B. besnoiti* in the drug screening, and a two-way ANOVA test followed by a Tukey post-test for multiple comparisons was employed to compare the different treatment durations. All statistical analyses were performed using the software GraphPad Prism 6.0 (GraphPad Software, San Diego, CA, USA).

3. RESULTS

3.1. Cytotoxicity assessments in uninfected Marc-145 cells

At the concentrations used here, none of the compounds exhibited significant cytotoxicity when compared to their respective vehicle controls (DMSO or NaOH/MetOH) as shown by the results from the XTT assay ($p>0.05$; *t*-test). Percentages of cytotoxicity of the screened compounds compared to the solvent-treated negative control wells were as follows: diclazuril: 3.2%; toltrazuril: 6%; imidocarb: 2.8%; decoquinate: 2.3%; sulfadiazine: 3%; trimethoprim: 3.1%; sulfadiazine + trimethoprim: 3.3%. Moreover, upon inspection by light microscopy, no alterations in the Marc-145 cells morphology were detected.

3.2. Primary drug assessments using immunofluorescence-based read-outs

The criteria employed to select the drug concentrations for the screening assays were the absence of cytotoxicity and the presence of an effect on *B. besnoiti* growth on the preliminary assays performed. In those assays, we found that toltrazuril was cytotoxic in the *in vitro* system employed for concentrations higher than 30 µM (50, 70 and 100 µM), leading to the detachment of the hosts cells (Table 1).

Table 2: Percentage of inhibition of parasite growth in the drug screening when compounds were administered at 0 or at 6 h pi.

Drugs		Decoquinate	Diclazuril	Toltrazuril	Imidocarb	Sulfadiazine	Trimethoprim	SDZ + TM
Time of administration	0 hpi	90	83.2	82.3	40	43	41	50
	6 hpi	74	72,8	69	36	19	31	35

In the initial drug treatments, initiated either during invasion (0 hpi) or at 6 hpi, decoquinate, diclazuril and toltrazuril were the most efficient drugs and inhibited parasite growth by more than 65% (Table 2). In general, the efficacy was higher when compounds were administered concomitantly to infection at 0 h pi, except for imidocarb (Kruskal-Wallis test, $p<0.05$).

Parasitic growth was markedly inhibited in wells treated with decoquinate, diclazuril and toltrazuril, since only PVs but not lysis plaques were found. In contrast, in cultures treated with the other compounds and in the control wells, distinct lysis plaques were clearly visible, indicating that parasites had completed the lytic cycle. Decoquinate and diclazuril were the most efficacious, and were consequently selected for further studies (Table 2). In contrast, sulfadiazine administered at 6 h pi was the least effective compound (19 % of parasite growth inhibition, Kruskall-Wallis test, $p<0.01$) (Table 2). When sulfadiazine or trimethoprim, alone or in combination, were kept in the cultures for up to 6 days, tachyzoites were still able to replicate and proliferate, as seen by the presence of confluent lysis plaques visualized by immunofluorescence, similar to non-treated control wells (data not shown).

As previously published for the isolate employed, 80% of the invasion events observed at 72 hpi consisted of lysis plaques in non-treated wells (Frey et al. 2016).

3.3. IC_{50} & IC_{99} determinations of decoquinate and diclazuril

For both, decoquinate and diclazuril, dose-dependent effects on parasite proliferation were observed (Kruskal Wallis, $p<0.01$). When administered concomitantly to infection at concentrations higher than 0.24 nM, exposure of infected cells to decoquinate led to a significant reduction in parasite growth, and the IC_{50} was calculated to be 10 nM.

For diclazuril, higher concentrations were needed: parasitic growth was markedly inhibited when the compound was administered at concentrations higher than 40 nM, and the IC_{50} was 135 nM (Fig.1). To reach 99% inhibition, 120 nM of decoquinate and 29.5 µM of diclazuril were required.

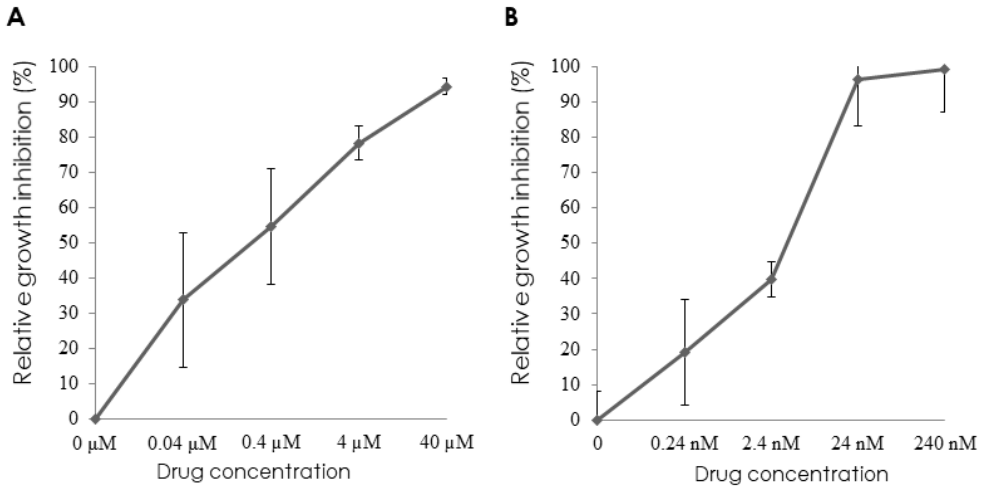

Figure 1: Relative inhibition of *B. besnoiti* tachyzoite proliferation (in & with respect to the vehicle negative control). Decoquinate (A) and diclazuril (B) were administered at 0 h pi. Tachyzoite proliferation was assessed by qPCR.

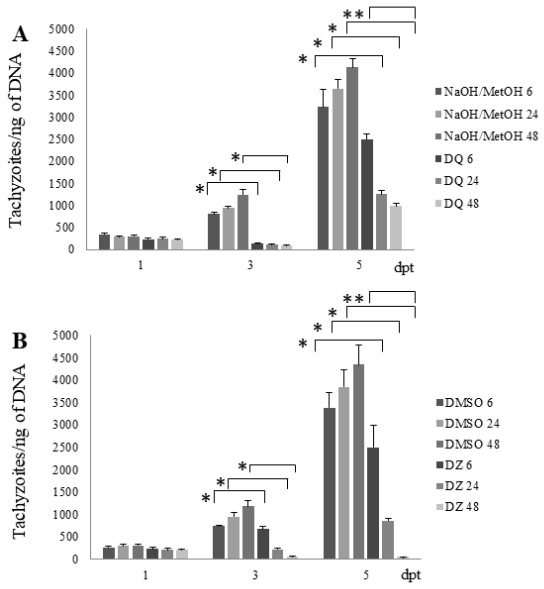

Figure 2: Tachyzoite yield expressed as tachyzoites per ng of DNA from *B. besnoiti* infected Marc-145 cells, which were treated with decoquinate (A) or diclazuril (B) for 6, 24 or 48 h, and further cultured without drugs. Samples were collected at 1, 3 & 5 dpt.

***** Statistically significant differences between treated wells and their corresponding control wells at 3 and at 5 dpt for any treatment durations ($p<0.001$).

** Statistically significant differences among the different treatment durations (6, 24 and 48 h) for both drugs at 5 dpt ($p<0.001$).

3.4. Decoquinate and diclazuril treatments do not act parasiticidal

Infected cultures were treated with decoquinate or diclazuril with concentrations corresponding to the IC_{99} for a maximum period of 48 h, and drugs were removed and the culture continued, this in order to study the long term effects of the treatments. Parasitic growth was hardly detected until 3 dpt, regardless which drug was used and how long the treatment had lasted. Subsequently, higher inhibition rates corresponded to longer treatments of up to 48 h (Fig. 2). Statistically significant differences between treated wells and their corresponding control wells were observed at 3 and at 5 dpt for any treatment durations ($p<0.001$, Two-Way ANOVA), with a lowest parasitic load in treated wells. Differences were also found among the different treatment durations (6, 24 and 48 h) for both drugs at 5 dpt and higher inhibition rates corresponded to longer treatments ($p<0.001$, Two-Way ANOVA) (Fig. 2).

Short treatments for 6 and 24 h with decoquinate were more effective since the tachyzoite yields obtained at 3 dpt in decoquinate treated wells were significantly lower than in diclazuril-treated wells. Further analysis by IF at 8 and 10 dpt showed that tachyzoites remained viable and were able to re-infect host cells even after treatments of 48 h with decoquinate. Lysis plaques were present at 10 dpt in all treated wells. However, in wells treated with diclazuril for 48 h, the parasitic load was clearly diminished both at 3 d pt and at 5 dpt, showing the lowest tachyzoite yield. Shorter treatments for up to 24 h were less effective and failed to inhibit parasite proliferation completely. This finding was also corroborated upon inspection in the light microscope and by IF, since lysis plaques were absent in wells treated with diclazuril for 48 h at 7 or 10 d pt, but present in wells treated for 6 h or 24 h at both post-infection time points (7 and 10 d pt) (data not shown).

3.5. Ultrastructural alterations in B. besnoiti tachyzoites induced by decoquinate and diclazuril treatments

B besnoiti tachyzoites obtained from drug solvent treated controls exhibited the hallmarks of apicomplexan parasites and closely resembled *T. gondii* and *N. caninum* tachyzoites. A negative control culture treated with decoquinate solvent (NaOH/MetOH) is shown in Fig. 3A. Tachyzoites were located within a PV that was filled with a granular matrix, and the apically located secretory organelles such as micronemes, rhoptries, as well as dense granules were evident. In addition, tachyzoites contained one mitochondrium, of which only segments were seen on a given section plane, filled with a rather electron dense membranous matrix composed of cristae (Fig. 3A). Similar findings were obtained when tachyzoites were treated with diclazuril solvent (DMSO) as shown by Jimenez-Melendez et al. (2017).

In *B. besnoiti* tachyzoites exposed to decoquinate for 24 h, no obvious structural alterations were evident, and they closely resembled their non-treated counterparts (data not shown). However, after 3 days of treatment, most notably the mitochondria were severely altered and lacking an electron dense matrix, and they were seemingly replaced by largely empty vacuoles that filled considerable space in the cytoplasm of these parasites (Fig.3 B-D). In addition, the cytoplasm was often filled with loose membrane residues. However, despite these alterations, after three days the parasites still retained their shape, were still within a parasitophorous vacuole (PV), but also already obviously dead parasites with distorted disorganized cytoplasm and vacuolization could be seen. After 6 days, mitochondria, were not discernible anymore, the cytoplasmic organization was completely lost and lipid droplets were formed (Fig. 3E). Also, there were parasites which were not enclosed by a parasitophorous vacuole membrane anymore. Only few seemingly still viable parasites could be found in these specimens. In cultures treated with diclazuril, (Fig. 4), small but distinct effects related to the drug action appeared already at 24 h of treatment (Fig. 4A-C). These included a widening between the nuclear membrane and the cytoplasm of the tachyzoites. At 3 d of treatment, dividing parasites were visible that were still attached to the residual body (Fig. 4D. In addition, the gap around the nuclear periphery was more evident, and a compartmentalization took place, with

occasional structures resembling amylopectin granules forming within the cytoplasm of tachyzoites, Vacuolization also took place in the residual body. However, the PV and its membrane were still evident in many cases and the mitochondria appeared still largely unaffected. After 6 days, amylopectin granules became more prominent, and complexes with largely disorganized cytoplasm were formed (Fig. 4E).

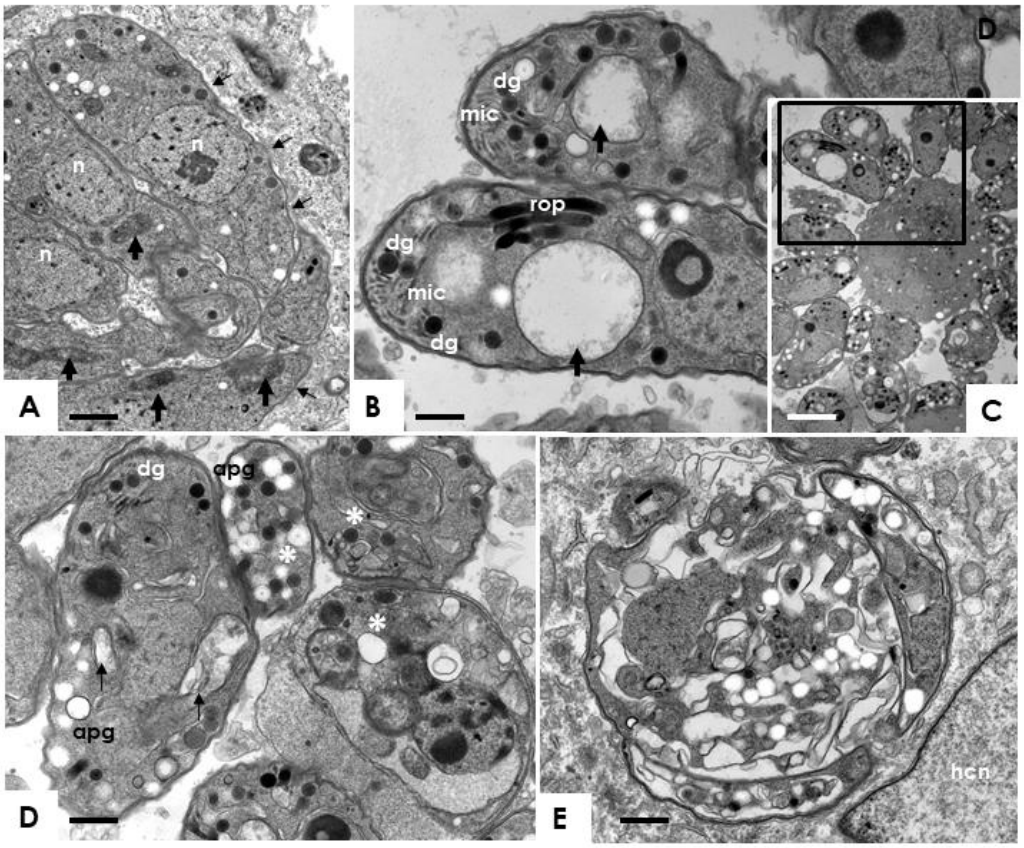

Figure 3: Representative TEM images of *B. besnoiti* tachyzoites cultured in human foreskin fibroblast cells. (A) Tachyzoites treated with NaOH/MetOH, situated within a vacuole and surrounded by a parasitophorous vacuole membrane (depicted with thin blackarrows). Note the individual nuclei and the mitochondria with an electron dense matrix (thick vertical black arrows). (B-D) Tachyzoites treated with decoquinate during 3 days, residues of mitochondria lacking any discernible matriy are indicated by black arrows. (C) is a lower magnification overview of (B), the boxed area is enlarged in (B). Note the presence of dramatically altered parasites in (D), marked with an asterisk (*). (E) Image of a *B. besnoiti* tachyzoite exposed to decoquinate during 6 days, with severely altered structural features. Rop = rhoptries, dg = dense granules, mic = micronems, n = nucleus, apg = amylopectin granules. Scale bars: A = 0.5 µm; B = 0.3 µm; C = 1 µm; D = 0.3 µm; E = 0.4 µm.

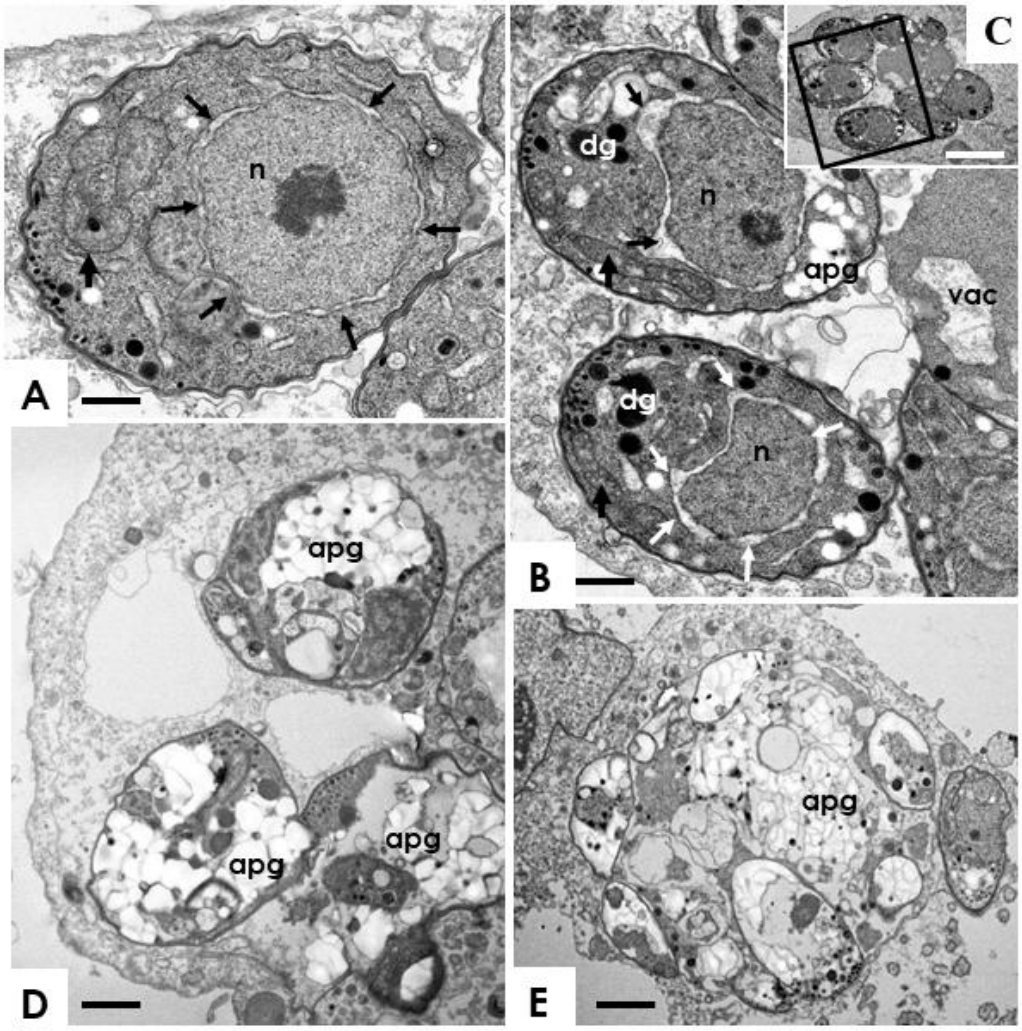

Figure 4: Representative TEM images of *B. besnoiti* tachyzoites in human foreskin fibroblast cell cultures exposed to diclazuril after 24 h of treatments (A-C, the boxed area in C is shown at larger magnification in B); 3 days of treatment (D); 6 days of treatment (E). The vertical arrows indicate mitochondria, arrows surrounding nuclei (n) point towards the separation of the nuclear membrane and the cytoplasm. dg = dense granules, apg = amylopectin granules, vac shows a vacuole in the residual body. Scale bars: A = 0.3 µm; B = 0.4 µm; C = 1.1 µm; D = 0.4 µm; E = 0.8 µm.

4. DISCUSSION

In this study, the safety and efficacy of a wide panel of commercially available compounds in Europe, namely toltrazuril, diclazuril, imidocarb, decoquinate, sulfadiazine and trimethoprim (alone or in combination with sulfadiazine) were assessed for activity against *B. besnoiti* tachyzoites for the first time. Some of these drugs had previously shown efficacy against other apicomplexan parasites and, in particular, against Toxoplasmatinae parasites, both *in vitro* (Hemphill *et al.*, 2016) and *in vivo* (Sánchez-Sánchez *et al.,* 2018). Two compounds, namely decoquinate and diclazuril, both commercialised for the treatment of various infections in cattle, inhibited *B. besnoiti* invasion and proliferation, with IC_{50} values in the nanomolar range.

Inhibition rates of decoquinate and diclazuril in terms of inhibition of parasite invasion and proliferation reached values higher or close to 90%. The *in vitro* model in Marc-145 cells employed in the present work was previously used to assess the activities of a panel of bumped kinase inhibitors (BKIs), which target calcium dependent protein kinase 1, and similar results were obtained (Jiménez-Meléndez *et al.*, 2017). In contrast, the low efficacy of imidocarb, sulfadiazine and trimethoprim (alone or in combination with sulfadiazine) against *B. besnoiti* infection may lead us to rule out their potential therapeutic activity. In addition, toltrazuril assays were aborted due to cytotoxicity exerted in the host cells.

Our results showed that decoquinate represents a safe compound in our *in vitro* model. Under the experimental settings employed, the efficacy of this compound was higher when it was administered at the time of infection, but it also interfered with proliferation in invaded tachyzoites. This result contrasts to previous studies carried out with *N. caninum* tachyzoites, where decoquinate showed a minimum effect against extracellular zoites. It is known that decoquinate affects electron transport in mitochondria so that a feasible explanation to the findings observed in *N. caninum* could be the presence of less active mitochondria in extracellular tachyzoites (Lindsay *et al.*, 1997). However, in *T. gondii* tachyzoites, it was demonstrated that decoquinate is able to affect oxygen consumption of extracellular tachyzoites (Pfefferkorn *et al.*, 1993). Accordingly, decoquinate might be more active against those parasites with higher capacity to survive extracellularly, as shown for *B. besnoiti* (Frey *et al.*, 2016). Interestingly, we obtained IC_{50} values in the low nanomolar range (10 nM), in agreement with previous studies that have shown decoquinate to have *in vitro* activity against *T. gondii* tachyzoites with IC_{50} of 0.005 µg/ml (12 nM) (Ricketts & Pfefferkorn, 1993). Although decoquinate is specifically designed to treat gastrointestinal coccidiosis in several species (e.g cattle, small ruminants and poultry) at concentrations around 0.5 mg/kg bw, it is well absorbed and reaches maximum plasma concentrations of 2 µM in milking cows (Quintero de Leonardo *et al.*, 2009). These concentrations are much higher than the IC_{50} and IC_{99} found *in vitro*. Accordingly, it may represent a valuable therapeutic tool to control acute clinical cases of bovine besnoitiosis as food additive at the recommended posology. Since remaining viable tachyzoites were able to resume proliferation once the treatment with the IC_{99} was suspended, a parasitostatic effect is suggested for this compound for at least 48h of treatment, as it has been described for hydroxiquinoxalines (Mehlhorn et al., 2008). This parasitostatic effect could be desirable since treated *Besnoitia* tachyzoites might be an antigenic stimulus and would allow the development of a strong immune response against the parasite, potentially preventing reinfection after recovering from the acute stage, as it has been postulated for other compounds such as BKIs (Winzer *et al.*, 2015). In *N. caninum*, the parasiticidal or parasitostatic effect of this drug depends on the concentration employed. A coccidiocidal effect of decoquinate was observed against intracellular tachyzoites when administered at concentrations higher than 0.01 µg/mL (24 nM (Lindsay *et al.*, 1997).

Electron microscopy showed that the mitochondrium is, as expected, the main site of action of decoquinate. However, after 6 days of treatment, mitochondrial impairment led to more dramatic alterations

and a general breakdown of the structural organization of the parasite, with deposits of amylopectin granules in the cytoplasm, all of this leading to a general loss of viability for most tachyzoites. This finding may indicate a transitional stage from tachyzoite to bradyzoite, as it has been described previously for tachyzoites from the RH strain of *T. gondii* treated with decoquinate (Lindsay *et al.*, 1998). Thus, decoquinate could represent a stressing agent to induce the differentiation from *Besnoitia* tachyzoites to bradyzoites *in vitro*.

Regarding triazinone-derivative coccidiocidals, our results showed that diclazuril is safe at the highest concentrations used in the *in vitro* model employed and effective against *B. besnoiti* tachyzoites, inhibiting both parasite invasion and proliferation. Those results are in agreement with previous *in vitro* studies with *T. gondii* (Lindsay & Blagburn, 1994) and *N. caninum* tachyzoites (Lindsay *et al.*, 1994). Indeed diclazuril inhibited *T. gondii* tachyzoite proliferation by 97% at a concentration of 0.005 µg/mL (12.2 nM). Remarkably, higher concentrations are needed for *B. besnoiti* since the IC_{50} was 135 nM. In cattle, this compound is marketed against coccidiosis and the bioavailability of the compound is low, reaching maximum plasmatic concentrations of 95.8 nM (EMEA, 2004). Thus, further pharmacokinetics studies assessing different dosages and possibly also formulations are needed to obtain a higher bioavailability of the compound in cattle. We also showed that treatments with the IC_{99} for at least 48 h are able to exert a parasiticidal effect on *B. besnoiti* tachyzoites, since lysis plaques were absent and the parasitic load was clearly diminished in those wells. These results are in agreement with TEM results, since after 6 days of treatment almost no viable parasites were present and a clear effect on the cytokinesis of daughter zoites, with the formation of multinucleated complexes was visualized. These findings are similar to those previously described for *T. gondii* tachyzoites treated with diclazuril, since an effect on endodiogeny together with the presence of multi-nucleated complexes were observed when treated at a concentration of 1 µg/mL (Lindsay *et al.*, 1995). Opposite to our results, ultra-structural effects of diclazuril were not noted until 2 days after treatment whilst in *B. besnoiti* we have observed that the first effects appeared after 24 h of treatment. *In vivo* experiments regarding mice infected with tachyzoites from the RH strain of *T. gondii* have shown that this compound is able to prevent death of up to 80-100% of the infected animals after oral administration at 1.0 or 10 mg/kg on 1 day prior to infection and then daily for 10 days (Lindsay & Blagburn, 1994).

The other triazinone derivative studied in the present work, toltrazuril, was cytotoxic at concentrations up to 30 µM. This safety concern has been also described in other cell lines, such as HFF cells, showing that concentrations of 10 µg/mL (23 µM) diminished cell viability up to 92% (Qian *et al.*, 2015). However, at the highest concentration employed here, a remarkable effect on parasitic growth inhibition was noted. This compound might present good activity against *B. besnoiti* tachyzoites considering that it is well-absorbed in cattle and is rapidly metabolized to ponazuril (toltrazuril-sulfone), which is the major metabolite (Stock *et al.*, 2017). Moreover, toltrazuril has been effective against *N. caninum* both in *in vitro* (Darius *et al.*, 2004) and *in vivo* studies (Strohbusch *et al.*, 2009; Syed-Hussain *et al.*, 2015). Thus, before ruling out its therapeutic potential for bovine besnoitiosis, further experiments should be performed.

Imidocarb dipropionate was discarded in our experimental settings, since it failed to exert more than 30 % parasite invasion and proliferation inhibition. No previous *in vitro* treatments with this compound against *T. gondii* or *N. caninum* have been reported. When similar series of compounds, diminazene aceturate and pentamidines were studied they were not effective against *B. besnoiti* in an *in vitro* model using epithelial-like Vero cells (Shkap *et al.*, 1987b). The lack of efficacy may be due to a less relevant myo-inositol synthesis pathway in *B. besnoiti*. Up to date, only glycolysis and glutamine byosinthesis metabolic routes have been reported in *B. besnoiti*-infected cells (Taubert *et al.*, 2016). Besides, it has been postulated that the activity of imidocarb may resemble that of

the trypanocidal and babesicidal berenil (diminazene aceturate) (Mehlhorn., 2008b), binding to DNA in the minor groove of the kinetoplast, which is absent in apicomplexan parasites.

Finally, regarding DHFR and DHFS inhibitors, alone or in combination, sulfadiazine failed to inhibit parasite growth by more than 50%, even when it was co-administered with trimethoprim at the time point of infection. Previous *in vitro* studies regarding Toxoplasmatinae parasites have shown variable results, since sulfadiazine is highly efficacious against *T. gondii* with IC_{50} in the range of 2.5 µg/mL (Sánchez-Sánchez *et al.*, 2018) whilst little activity was exerted against *N. caninum* at concentrations up to 100 µg/ml (400 µM) and longer treatments were needed (Lindsay *et al.*, 1994). This finding agrees with our results where low parasitic growth inhibition was observed when treatments lasted for 3 or 6 days. Besides, previous studies carried out in *Besnoitia* have also reported variable results. Sulfadiazine lacked efficacy upon *B. besnoiti* infection in gerbils (Shkap *et al.*, 1987b), whereas in other *Besnoitia* species, such as *B. darlingi,* treatment with sulfadiazine was able to diminish parasitic growth *in vitro* at concentrations higher than 4 µM in an 8 day-assay (50% growth inhibition) (Elsheikha & Mansfield, 2004). *In vivo* information regarding sulfonamide therapy in bovine besnoitiosis indicate that they are commonly used under field conditions to diminish the severity of clinical signs, but they usually fail to cure the infected cattle and recurrences are not rare, even if treatment is administered when clinical signs first appear (Jacquiet *et al.*, 2010). The lack of efficacy of sulphadiazine observed *in vitro* may explain this *in vivo* variability. Trimethoprim also failed to exert a potent inhibition *in vitro*. However, a strong inhibition of *T. gondii* growth has been observed with an IC_{50} of 2.3 µg/ml, with striking morphological changes of the parasites (Sánchez-Sánchez *et al.*, 2018). In addition, trimethoprim is also effective against *N. caninum* tachyzoites at 10 µg/ml (Lindsay *et al.*, 1994).

In summary, the present study demonstrates proof of concept for the efficacy of decoquinate and diclazuril against *B. besnoiti in vitro,* and further assessments of safety and efficacy of both drugs should be performed in the target species. Concentrations of diclazuril needed to clear the parasite *in vitro* are higher than the ones reported in the literature for this compound. Thus, prior to attempt *in vivo* treatments, further studies regarding pharmacokinetic parameters, employing other administration routes or posologies, are needed in order to achieve higher bioavailability and raise maximum plasmatic concentrations. An ideal drug against *B. besnoiti* should allow the generation of a strong humoral immune response to avoid re-infections and preventing that new entries in the herd (specifically breeding bulls) get infected. Regarding this issue, the parasitostatic effect exerted by both compounds could favor the development of a humoral immune response.

ACKNOWLEDGEMENTS

This work was financially supported through research projects from the Spanish Ministry of Economy and Competitiveness (Ref. AGL2013-04442), Community of Madrid (Ref. S2013/ABI-2906, PLATESA-CM), and by the Swiss National Science Foundation (grant No. 310030_165782). Alejandro Jiménez-Meléndez was supported by a grant from the Spanish Ministry of Education, Culture and Sports (grant nº FPU13/05481) and Laura Rico SanRomán was financially supported by SALUVET INNOVA S.L. We also would like to acknowledge members from SALUVET research group for their support.

REFERENCES:

Álvarez-García, G., 2016. From the mainland to Ireland - bovine besnoitiosis and its spread in Europe. Vet. Rec. 178 (24), 605-607.

Basso, W., Schares, G., Gollnick, N.S., Rutten, M., Deplazes, P., 2011. Exploring the life cycle of *Besnoitia besnoiti* - experimental infection of putative definitive and intermediate host species. Vet. Parasitol. 178 (3-4), 223-234.

Bessoff, K., Spangenberg, T., Foderaro, J.E., Jumani, R.S., Ward, G.E., Huston, C.D., 2014. Identification of *Cryptosporidium parvum* active chemical series by repurposing the open access Malaria Box. Antimicrob. Agents Chemother. 58 (5), 2731-2739.

Cortes, H.C., Müller, N., Esposito, M., Leitao, A., Naguleswaran, A., Hemphill, A., 2007. *In vitro* efficacy of nitro- and bromo-thiazolyl-salicylamide compounds (thiazolides) against *Besnoitia besnoiti* infection in Vero cells. Parasitology 134 (Pt 7), 975-985.

Cortes, H.C., Müller, N., Boykin, D., Stephens, C.E., Hemphill, A., 2011. *In vitro* effects of arylimidamides against *Besnoitia besnoiti* infection in Vero cells. Parasitol. 138 (5), 583-592.

Darius, A.K., Mehlhorn, H., Heydorn, A.O., 2004. Effects of toltrazuril and ponazuril on the fine structure and multiplication of tachyzoites of the NC-1 strain of *Neospora caninum* (a synonym of Hammondia heydorni) in cell cultures. Parasitol. Res. 92, 453-458.

Daugschies, A., Najdrowski, M., 2005. Eimeriosis in cattle: current understanding. J. Vet. Med. B Infect. Dis. Vet. Public Health. B 52 (10), 417-427.

Dittmar, A.J., Drozda, A.A., Blader, I.J., 2016. Drug repurposing screening identifies novel compounds that effectively inhibit *Toxoplasma gondii* growth. Msphere 1 (2), e00042-15.

Elsheikha, H.M., Mansfield, L.S., 2004. Determination of the activity of sulfadiazine against *Besnoitia darlingi* tachyzoites in cultured cells. Parasitol. Res. 93 (5), 423-426.

European Medicines Agency (EMEA). Diclazuril (Extension to all ruminants and porcine species): Summary report (2)-Committee for veterinary Medicinal Products. 2004. Available online from: http:/www.ema.europa.eu/ema/index.jsp?curl=pages/includes/document/document_detail.jsp?webContentId=WC500013730&mid=WC0b01ac058008d7ad.

European Food Safety Authority, 2010. Scientific statement on bovine besnoitiosis. , Available from <http://www.efsa.europa.eu>.

Fernández-García, A., Risco-Castillo, V., Pedraza-Díaz, S., Aguado-Martínez, A., Álvarez-García, G., Gómez-Bautista, M., Collantes-Fernández, C., Ortega-Mora, L.M., 2009. First isolation of *Besnoitia besnoiti* from a chronically infected cow in Spain. J. Parasitol. 95, 474-476.

Frey, C.F., Regidor-Cerrillo, J., Marreros, N., García-Lunar, P., Gutiérrez-Expósito, D., Schares, G., Dubey, J.P., Gentile, A., Jacquiet, P., Shkap, V., Cortes, H., Ortega-Mora, L.M., Álvarez-García, G., 2016. *Besnoitia besnoiti* lytic cycle *in vitro* and differences in invasion and intracellular proliferation among isolates. Parasit. Vectors. 9 (1), 115.

Fry, M., Williams, R.B., 1984. Effects of decoquinate and clopidol on electron transport in mitochondria of *Eimeria tenella* (Apicomplexa: Coccidia). Biochem. Pharmacol. 33 (2), 229-240.

Gutiérrez-Expósito, D., Ortega-Mora, L.M., Marco, I., Boadella, M., Gortazar, C., San Miguel-Ayanz, J.M., García-Lunar, P., Lavin, S., Álvarez-García, G., 2013. First serosurvey of *Besnoitia* spp. infection in wild European ruminants in Spain. Vet. Parasitol. 197 (3-4), 557-564.

Gutiérrez-Expósito, D., Ferre, I., Ortega-Mora, L.M., Álvarez-García, G., 2017. Advances in the diagnosis of bovine besnoitiosis: current options and applications for control. Int. J. Parasitol. 47 (12), 737-751.

Hemphill, A., Aguado-Martínez, A., Müller, J., 2016. Approaches for the vaccination and treatment of *Neospora caninum* infections in mice and ruminants models. Parasitology 143(2), 245-259.

Hoffmann, B., Depner, K., Schirrmeier, H., Beer, M., 2006. A universal heterologous internal control system for duplex real-time RT-PCR assays used in a detection system for pestiviruses. J. Virol. Methods 136 (1-2), 200-209.

Jacquiet, P., Liénard, E., Franc, M., 2010. Bovine besnoitiosis: Epidemiological and clinical aspects. Vet. Parasitol. 174 (1-2), 30-36.

Jiménez-Meléndez, A., Ojo, K.K., Wallace, A.M., Smith, T.R., Hemphill, A., Balmer, V., Regidor-Cerrillo, J., Ortega-Mora, L.M., Hehl, A.B., Fan, E., Maly, D.J., Van Voorhis, W.C., Alvarez-Garcia, G., 2017. *In vitro* efficacy of bumped kinase inhibitors against *Besnoitia besnoiti* tachyzoites. Int. J. Parasitol. 47 (12), 811-821, 10.1016/j.ijpara.2017.08.005.

Kaartinen, L., Löhönen, K., Wiese, B., Franklin, A., Pyörälä, S., 1999. Pharmacokinetics of sulphadiazine-trimethoprim in lactating dairy cows. Acta Vet. Scand. 40, 271-278.

Leonardo, Q., Rosiles, R., Bautista, J., González-Monsón, N., Sumano, H., 2009. Oral pharmacokinetics and milk residues of decoquinate in milking cows. J. Vet. Pharmacol. Ther. 32 (4), 403-406.

Lindsay, D.S., Nazir, M.M., Maqbool, A., Ellison, S.P., Strobl, J.S., 2013. Efficacy of decoquinate against *Sarcocystis neurona* in cell cultures. Vet. Parasitol. 196 (1), 21-23.

Lindsay, D.S., Rippey, N.S., Toivio-Kinnucan, M.A., Blagburn, B.L., 1995. Ultrastructural effects of diclazuril against *Toxoplasma gondii* and investigation of a diclazuril-resistant mutant. J. Parasitol. , 459-466.

Lindsay, D.S., Butler, J.M., Blagburn, B.L., 1997. Efficacy of decoquinate against *Neospora caninum* tachyzoites in cell cultures. Vet. Parasitol. 68 (1-2), 35-40.

Lindsay, D.S., Blagburn, B.L., 1994. Activity of diclazuril against *Toxoplasma gondii* in cultured cells and mice. Am. J. Vet. Res. 55 (4), 530-533.

Lindsay, D.S., Rippey, N.S., Cole, R.A., Parsons, L.C., Dubey, J.P., Tidwell, R.R., Blagburn, B.L., 1994. Examination of the activities of 43 chemotherapeutic agents against *Neospora caninum* tachyzoites in cultured cells. Am. J. Vet. Res. 55 (7), 976-981.

Lindsay, D., Toivio-Kinnucan, M., Blagburn, B., 1998. Decoquinate induces tissue cyst formation by the RH strain of *Toxoplasma gondii*. Vet. Parasitol. 77 (2-3), 75-81.

Mehlhorn, H., (Ed), 2008. Encyclopedia of parasitology: A-M. Springer, Germany, 280; 381 pp.

Müller, J., Aguado-Martínez, A., Balmer, V., Maly, D.J., Fan, E., Ortega-Mora, L., Ojo, K.K., Van Voorhis, W.C., Hemphill, A., 2017. Two novel calcium-dependent kinase 1-inhibitors interfere with vertical transmission in mice infected with *Neospora caninum* tachyzoites. Antimicrob. Agents Chemother. 61, 02324-16.

Müller, J., Aguado-Martínez, A., Manser, V., Balmer, V., Winzer, P., Ritler, D., Hostettler, I., Arranz-Solís, D., Ortega-Mora, L.M., Hemphill, A., 2015. Buparvaquone is active against *Neospora caninum in vitro* and in experimentally infected mice. Int. J. Parasitol. Drugs Drug Resist. 5, 16-25.

Pfefferkorn, E., Borotz, S.E., Nothnagel, R.F., 1993. Mutants of *Toxoplasma gondii* resistant to atovaquone (566C80) or decoquinate. J. Parasitol. , 559-564.

Pols, J.W., 1960. Studies on bovine besnoitiosis with special reference to the aetiology. Onderstepoort Jour Vet Res 28 (3), 265-356.

Qian, W., Wang, H., Shan, D., Li, B., Liu, J., Liu, Q., 2015. Activity of several kinds of drugs against *Neospora caninum*. Parasitol. Int. 64 (6), 597-602.

Ricketts, A.P., Pfefferkorn, E.R., 1993. *Toxoplasma gondii*: susceptibility and development of resistance to anticoccidial drugs *in vitro*. Antimicrob. Agents Chemother. 37 (11), 2358-2363.

Ryan, E.G., Lee, A., Carty, C., O'Shaughnessy, J., Kelly, P., Cassidy, J.P., Sheehan, M., Johnson, A., de Waal, T., 2016. Bovine besnoitiosis (*Besnoitia besnoiti*) in an Irish dairy herd. Vet. Rec. 178 (24), 608.

Sánchez-Sánchez, R., Vázquez, P., Ferre, I., Ortega-Mora, L.M., 2018. Treatment of toxoplasmosis and neosporosis in farm ruminants: state of knowledge and future trends. Curr. Top. Med. Chem. ,

Schares, G., Maksimov, A., Basso, W., More, G., Dubey, J.P., Rosenthal, B., Majzoub, M., Rostaher, A., Selmair, J., Langenmayer, M.C., Scharr, J.C., Conraths, F.J., Gollnick, N.S., 2011b. Quantitative real time polymerase chain reaction assays for the sensitive detection of *Besnoitia besnoiti* infection in cattle. Vet. Parasitol. 178 (3-4), 208-216, 10.1016/j.vetpar.2011.01.038.

Shkap, V., De Waal, D.T., Potgieter, F.T., 1985. Chemotherapy of experimental *Besnoitia besnoiti* infection in rabbits. Onderstepoort J. Vet. Res. 52 (4), 289.

Shkap, V., Pipano, E., Ungar-Waron, H., 1987. *Besnoitia besnoiti*: chemotherapeutic trials *in vivo* and *in vitro*. Rev. Elev. Med. Vet. Pays. Trop. 40 (3), 259-264.

Stock, M., Elazab, S., Hsu, W., 2017. Review of triazine antiprotozoal drugs used in veterinary medicine. J. Vet. Pharmacol. Ther. .

Strohbusch, M., Muller, N., Hemphill, A., Krebber, R., Greif, G., Gottstein, B., 2009. Toltrazuril treatment of congenitally acquired *Neospora caninum* infection in newborn mice. Parasitol. Res. , 10.1007/s00436-009-1328-x.

Syed-Hussain, S., Howe, L., Pomroy, W., West, D., Hardcastle, M., Williamson, N., 2015. Study on the use of toltrazuril to eliminate *Neospora caninum* in congenitally infected lambs born from experimentally infected ewes. Vet. Parasitol. 210 (3), 141-144.

Taubert, A., Hermosilla, C., Silva, L., Wieck, A., Failing, K., Mazurek, S., 2016. Metabolic signatures of *Besnoitia besnoiti*-infected endothelial host cells and blockage of key metabolic pathways indicate high glycolytic and glutaminolytic needs of the parasite. Parasitol. Res. 115 (5), 2023-2034.

Torre, D., Casari, S., Speranza, F., Donisi, A., Gregis, G., Poggio, A., Ranieri, S., Orani, A., Angarano, G., Chiodo, F., Fiori, G., Carosi, G., 1998. Randomized trial of trimethoprim-sulfamethoxazole versus pyrimethamine-sulfadiazine for therapy of toxoplasmic encephalitis in patients with AIDS. Italian Collaborative Study Group. Antimicrob. Agents Chemother. 42 (6), 1346-1349.

Van Voorhis, W.C., Doggett, J.S., Parsons, M., Hulverson, M.A., Choi, R., Arnold, S., Riggs, M.W., Hemphill, A., Howe, D.K., Mealey, R.H., 2017. Extended-spectrum antiprotozoal bumped kinase inhibitors: A review. Exp. Parasitol. 180, 71-83.

Vial, H.J., Gorenflot, A., 2006. Chemotherapy against babesiosis. Vet. Parasitol. 138 (1-2), 147-160.

Williams, R., 2006. Tracing the emergence of drug-resistance in coccidia (*Eimeria* spp.) of commercial broiler flocks medicated with decoquinate for the first time in the United Kingdom. Vet. Parasitol. 135 (1), 1-14.

Winzer, P., Muller, J., Aguado-Martinez, A., Rahman, M., Balmer, V., Manser, V., Ortega-Mora, L.M., Ojo, K.K., Fan, E., Maly, D.J., Van Voorhis, W.C., Hemphill, A., 2015. *In vitro* and *in vivo* effects of the Bumped Kinase Inhibitor 1294 in the related cyst-forming Apicomplexans *Toxoplasma gondii* and *Neospora caninum*. Antimicrob. Agents Chemother. 59 (10), 6361-6374.

In vitro efficacy of bumped kinase inhibitors against *Besnoitia besnoiti* tachyzoites

Alejandro Jiménez-Meléndez[1], Kayode K. Ojo[2], Alexandra M. Wallace[2], Tess R. Smith[2], Andrew Hemphill[3], Vreni Balmer[3], Javier Regidor-Cerrillo[1], Luis M. Ortega-Mora[1], Adrian B. Hehl[4], Erkang Fan[5], Dustin J. Maly[5,6], Wesley C. Van Voorhis[2], Gema Álvarez-García[1,*]

[1]*SALUVET, Animal Health Department, Faculty of Veterinary Sciences, Complutense University of Madrid, Ciudad Universitaria s/n, 28040 Madrid, Spain*

[2]*Center for Emerging and Re-emerging Infectious Diseases (CERID), Division of Allergy and Infectious Diseases, Department of Medicine, University of Washington, Seattle, Washington, USA*

[3]*Institute of Parasitology, Vetsuisse Faculty, University of Bern, Länggass-Strasse 122, CH-3012 Berne, Switzerland*

[4]*Institute of Parasitology, University of Zurich, Winterthurerstrasse 266a, CH-8057, Zurich, Switzerland*

[5]*Department of Biochemistry, University of Washington, Seattle, WA 98195-7742 USA*

[6]*Department of Chemistry, University of Washington, Seattle, WA 98195- 1700 USA*

[*] Corresponding author: Tel: +34913944095. Fax: +34913944098. *E-mail*: gemaga@vet.ucm.es.

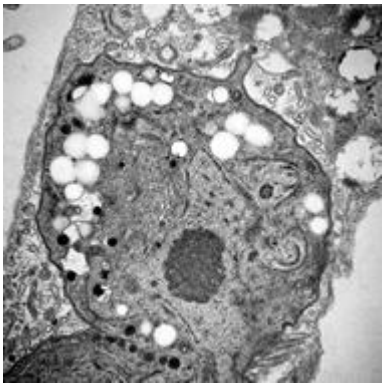

Published in *International Journal for Parasitology*. 2017 Oct;47(12):811-821. doi: 10.1016/j.ijpara.2017.08.005. Epub 2017 Sep 9.

Presented as poster communication in COST Action 1307 Congress 2016.
(5th-6th May, Porto, Portugal)

ABSTRACT

Besnoitia besnoiti is an apicomplexan parasite responsible for bovine besnoitiosis, a chronic and debilitating disease that causes systemic and skin manifestations and sterility in bulls. Neither treatments nor vaccines are currently available. In the search for therapeutic candidates, calcium-dependent protein kinases (CDPKs) have arisen as promising drug targets in other apicomplexans (e.g. *Neospora caninum*, *Toxoplasma gondii*, *Plasmodium* spp. and *Eimeria* spp.) and are effectively targeted by bumped kinase inhibitors (BKIs). In this study, we identified and cloned the gene coding for *Bb*CDPK1. The impact of a library of nine bumped kinase inhibitor (BKI) analogues on the activity of recombinant *Bb*CDPK1 was assessed by luciferase assay. Afterwards, those were further screened for efficacy against *B. besnoiti* tachyzoites grown in Marc-145 cells. Primary tests at 5 µM revealed that eight compounds exhibited more than 90% inhibition of invasion and proliferation. The compounds BKI 1294, 1517, 1553 and 1571 were further characterized, and EC_{99} (1294: 2.38 µM; 1517: 2.20 µM; 1553: 3.34 µM; 1571: 2.78 µM) were determined by quantitative real-time PCR in 3-day proliferation assays. Exposure of infected cultures with EC_{99} concentrations of these drugs for up to 48 h was not parasiticidal. The lack of parasiticidal action was confirmed by transmission electron microscopy, which showed that BKI treatment interfered with cell cycle regulation and non-disjunction of tachyzoites, resulting in the formation of large multi-nucleated complexes which co-existed with viable parasites within the parasitophorous vacuole. However, it is possible that, in the face of an active immune response, parasite clearance may occur. In summary, BKIs may be effective drug candidates to control *B. besnoiti* infection. Further in vivo experiments should be planned, as attainment and maintenance of therapeutic blood plasma levels in calves, without toxicity, has been demonstrated for BKIs 1294, 1517 and 1553.

Keywords: *Besnoitia besnoiti*, Chemotherapy, Bumped kinase inhibitors, CDPK1, *in vitro* assay.

1. Introduction

Besnoitia besnoiti is an apicomplexan parasite responsible for bovine besnoitiosis, a chronic and debilitating disease of cattle that causes systemic and skin manifestations, as well as sterility in bulls. At present, it is considered a re-emerging cattle disease in Europe. It has spread towards northern and central eastern Europe, given the absence of effective treatments or vaccines and the lack of common policies concerning animal trade (European Food Safety Authority, 2010; Álvarez-García *et al.*, 2013; Álvarez-García, 2016).

Taxonomically, *B. besnoiti* belongs to the subfamily Toxoplasmatinae, together with other cyst-forming parasites of veterinary and human health importance, such as *Neospora caninum* and *Toxoplasma gondii,* respectively. Similarly, it has a heteroxenous life cycle but the definitive host has not yet been identified (Diesing *et al.*, 1988; Basso *et al.*, 2011;). Domestic bovines and wild ruminants such as antelopes and roe deer (Arnal *et al.*, 2016) act as intermediate hosts, where two asexual infective stages of the parasite develop: initially, fast-replicating tachyzoites are found inside endothelial cells of blood vessels during the acute stage of the disease, which may go unnoticed due to the non-specific clinical signs such as fever, anorexia or swelling of lymph nodes (reviewed by Álvarez-García *et al.*, 2014). During the chronic stage of the disease, when the immune response is elicited against the parasite, tachyzoites switch into slowly dividing bradyzoites. Bradyzoites form tissue cysts are located mainly in the s.c. connective tissue and are responsible for the characteristic lesions found during the chronic stage.

In bovines, treatments attempted for besnoitiosis have included the use of formaline, sulphametazine, toltrazuril or oxytetracycline (Franc & Cardiegues, 1999). In laboratory settings, experimentally infected

rabbits were treated with formaline, pentamidines, sulphonamides, trimethoprim, pyrimethamine and oxytetracycline (Pols, 1960; Shkap *et al.*, 1985a, 1987b) and oxytetracycline was applied in gerbils (Shkap *et al.*, 1985b). Unfortunately, all these studies had been carried out under very different experimental conditions with a limited number of animals, and results were mainly based on clinical inspection and histopathology. *In vitro* studies showed that arylimidamides (Cortes *et al.*, 2011) and thiazolides (Cortes *et al.*, 2007) have activity against *B. besnoiti*, but further research with well-established and reliable experimental models, both *in vitro* and *in vivo*, is urgently needed.

Apicomplexan calcium-dependent protein kinases (CDPKs) belong to a superfamily of serine-threonine kinases. They are conserved enzymes among members of the phylum Apicomplexa but are absent in mammalian cells (Ward *et al.*, 2004; Srinivasan & Krupa, 2005; Billker *et al.*, 2009). CDPKs thus represent parasite-specific drug targets. Bumped kinase inhibitors (BKIs), namely pyrazolo-pyrimidine and 5-aminopyrazole-4-carbomidecarboxamide analogues, specifically designed to act on CDPK1 (Lourido & Moreno, 2015; Van Voorhis *et al.*, 2017) have shown efficacy against *T. gondii* (Doggett *et al.,* 2014; Ojo *et al.,* 2010); *N. caninum* (Winzer *et al.,* 2015; Ojo *et al.,* 2014); *Babesia* spp. (Pedroni *et al.*, 2016); *Cryptosporidium parvum* (Lendner *et al.*, 2015) and *Plasmodium* spp. (Ojo *et al.*, 2012; Van Voorhis *et al.*, 2017). In *T. gondii,* CDPK1 plays a crucial role in gliding motility, microneme secretion, host cell invasion and egress, and parasite differentiation by means of calcium-dependent mechanisms (Lourido *et al.*, 2010; Lourido & Moreno, 2015). Bumped kinase inhibitors (Doerig *et al.*, 2002; Greenbaum, 2008) selectively bind to a hydrophobic pocket adjacent to the ATP binding site. This hydrophobic pocket is made accessible by a small "gatekeeper" amino-acid such as glycine, a unique characteristic of some apicomplexan CDPK1s. Pharmacological inhibition of either *Tg*CDPK1 or *Nc*CDPK1 with BKIs *in vitro* blocks host cell invasion, thereby inhibiting parasitic growth (Ojo *et al.*, 2010; Winzer *et al.*, 2015;).

Currently, the exact mechanisms of host cell invasion and proliferation of *B. besnoiti* are not well understood, but Frey *et al.* (2016) demonstrated that lytic cycle events are similar to those exploited by closely related *N. caninum* and *T. gondii*. *Besnoitia besnoiti* CDPK1 has not yet been identified. However, the existence of the orthologue *Bb*CDPK1 is likely since it has been proven that members of the Toxoplasmatinae share a high degree of homology in relation to CDPK enzymes (Keyloun *et al.*, 2014; Ojo *et al.*, 2014). Recently, a standardized experimental in vitro model of infection using an epithelial-like cell line (Frey *et al.*, 2016) was developed. This model allowed a detailed study of the *B. besnoiti* lytic cycle, revealing that these parasites can survive extracellularly for extended periods of time (up to 24 h p.i.), and showed that *Besnoitia* tachyzoites generally have a low invasion rate and proliferate asynchronously. The establishment of this *in vitro* model set the basis for performance of drug screening and testing of potential therapeutic candidates against this protozoal agent.

The rational approach followed herein has been previously exploited in the closely related protozoans *T. gondii* and *N. caninum*, where CDPK orthologues were identified and a variety of compounds were screened in *in vitro* assays (Van Voorhis *et al.*, 2017). Thus, in the present study, we identified and characterized *Bb*CDPK1 and evaluated the efficacy of nine BKIs against *B. besnoiti* tachyzoites in a standardized *in vitro* assay model.

2. Materials and methods

2.1. Parasite maintenance and cell cultures

Marc-145 and Human Foreskin Fibroblast (HFF) cells were maintained in DMEM (Gibco, Thermo Fisher Scientific, Waltham, MA, USA) with phenol red supplemented with 10% heat inactivated and sterile filtrated fetal calf serum (FCS) (Gibco, Thermo Fisher Scientific, Waltham, MA, USA), 5 mM HEPES (pH 7.2), 2 mM glutamine (Lonza Group, Basel, Switzerland), and a mixture of penicillin (100 U/ml), streptomycin (100 µg/ml) and amphotericin B (Lonza Group, Basel, Switzerland) as previously published (Frey *et al.*, 2016). They were cultured at 37 °C and 5% CO_2 in 75 or 25 cm^2 tissue culture flasks. Marc-145

cell cultures were passaged twice each week, HFFs once each week. *Besnoitia besnoiti* Spain1 (Bb-Spain1) used for all *in vitro* assays and Evora (Bb-Evora) strains were maintained by serial passages in Marc-145 cells in the same culture medium with 5% FCS (Fernández-García *et al.*, 2009b). FCS used in all the experiments was previously checked for the absence of specific IgG against *B. besnoiti*, *N. caninum* and *T. gondii* by IFAT (Fernández-García *et al.*, 2009a).

Tachyzoites were harvested 3 days p.i., when the majority of them were still intracellular, by recovering the infected cell monolayer with a rubber cell scraper, followed by repeated passages through a 25 gauge needle at 4 °C and separation from cell debris on a PD-10 column (GE Healthcare, Little Chalfont, United Kingdom) (Frey *et al.*, 2016). Tachyzoite viability was confirmed by trypan blue exclusion followed by counting in a Neubauer chamber. Purified tachyzoites were used to infect Marc-145 or HFF cell monolayers as described in section 2.5.1.

2.2. BbCDPK1 identification, sequencing and cloning

2.2.1. NCBI BLAST® search and Clustal analyses

The amino acid sequence of *Nc*CDPK1 (NCLIV_011980) from ToxoDB (www.toxodb.org) was used in order to retrieve orthologous genes in apicomplexan parasites using the NCBI BLAST® tool (https://blast.ncbi.nlm.nih.gov/Blast.cgi). Nucleotide sequences coding for related sequences of CDPK1 in *T. gondii*, *N. caninum* and *Hammondia hammondi* were considered (Supplementary Fig. S1). Clustal Omega (http://www.ebi.ac.uk/Tools/msa/clustalo/) was employed to align nucleotide and protein sequences. Next, three pairs of primers (Table 1) were designed in conserved, homologous regions (BbCDPK1Fw2; BbCDPK1Fw3, BbCDPK1Rv1 and BbCDPK1FwC) (Supplementary Fig. S1).

Total RNA from the Bb-Evora strain collected from infected Marc-145 monolayers at 8 h p.i. was stored in RNA later reagent (Qiagen, Valencia, CA, USA) and cDNA was synthetized using a SuperScript Vilo® cDNA synthesis kit (Life technologies, Thermo Fisher Scientific, Waltham, MA, USA) according to the manufacturer´s instructions. cDNA was diluted 1:10 in molecular grade distilled H_20. cDNA from the Nc-Liverpool strain of *N. caninum* was also employed to test specificity of the primers used.

PCR conditions were 94 °C for 5 min, 35 cycles at 94 °C for 30 s, 60 °C for 1 min and 72 °C for 1 min 30 s and a final elongation at 72 °C for 10 min. PCRs were carried out with the Platinum® Taq DNA Polymerase High Fidelity (Invitrogen, Thermo Fisher Scientific, Waltham, MA, USA) and all primers were purchased from Sigma-Aldrich. PCR products were visualized in 1.5% agarose gel stained with ethidium bromide and next purified using the Geneclean Turbo® kit (QBiogene, Montreal, Canada) according to the manufacturer's instructions for sequencing. PCR products were directly sequenced in both directions using the Big Dye® Terminator v3.1 Cycle Sequencing Kit (Applied Biosystems, Thermo Fisher Scientific, Waltham, MA, USA) and a 3730 DNA analyser (Applied Biosystems, Thermo Fisher Scientific, Waltham, MA, USA) at the Unidad Genómica del Parque Científico de Madrid, Spain. Sequence data were analyzed using BioEdit Sequence Alignment Editor v.7.0.1 (Hall, 1999) (Copyright_ 1997–2004 Tom Hall, Ibis Therapeutics, Carlsbad, CA, USA).

The sequence obtained (see Section 3.1) was compared with the *B. besnoiti* genome (the genome sequence is the property of the University of Zurich, Switzerland and will be made freely available to the community on NCBI and EuPathDB after publication). After retrieving the coding sequence using the GeneWise-Pairwise Sequence Alignment (EMBL-EBI) tool in order to process introns, a truncated region of the Bb*CDPK1* gene was amplified from *B. besnoiti* Evora strain cDNA using primers Bb_LIC_Fw (5`-GGG TCC TGG TTC GAT GGG TCA GCA AGA AAG CAC GCT CGG C-3`) and Bb_LIC_Rev: CTT GTT CGT GCT GTT TAC TTA GTT GCC GCA GAG CTT CAG AAG-3`) (data not shown). The PCR product was cloned into the ligation-independent cloning (LIC) site of expression vector pAVA0421 and expressed and purified as previously published for *Nc*CDPK1 (Ojo et al., 2014). The purified protein was visualized by SDS-PAGE and Coomassie staining (Supplementary Fig. S2).

2.2.2. In silico analysis and prediction of N-myristoylation and palmitoylation

The predicted molecular weight of *Bb*CDPK1 was obtained using ExPasy tools for prediction of protein properties (ProtParam; http://web.expasy.org/protparam).

The Simple Modular Architecture Research Tool (SMART; http://smart.embl-heidelberg.de) was used to predict functional domains in proteins. Myristoylation prediction was carried out using Prosite PDOC00008 (http://www.expasy.ch/prosite/) as described by Etzold et al. (2014) for CDPKs from *C. parvum*.

Palmitoylation sites were predicted with CSS-Palm 2.0 (http://csspalm.biocuckoo.org).

Modeling of *Bb*CDPK1 secondary and tertiary structures was performed using the I-TASSER online tool (http://zhanglab.ccmb.med.umich.edu) (Yang *et al.*, 2015).

2.3. BbCDPK1 enzymatic activity assays and its inhibition by BKIs

Protein kinase activity of recombinant *Bb*CDPK1 (r*Bb*CDPK1) and inhibition of its kinase phosphorylation properties by a panel of BKIs (Keyloun *et al.*, 2014) was measured in a non-radioactive assay using Kinase-Glo® luciferase reagent (Promega, Madison, WI, USA) as previously described (Ojo *et al.*, 2014). Basically, this luminescence-based assay measures kinase activity in the presence or absence of inhibitors by reporting changes in initial ATP concentrations. Kinase phosphorylation reactions were performed as previously published for *Nc*CDPK1 (Ojo *et al.*, 2014) in a 25 µL buffered solution containing 20 mM HEPES (pH, 7.5), 0.1% BSA, 10 mM $MgCl_2$, 1 mM EGTA, 2 mM $CaCl_2$, 20 µM peptide substrate (Biotin-C6-PLARTLSVAGLPGKK) (BioSyntide-2) (American Peptide Company, Inc. Sunnyvale, CA, USA), 3.5 nM *Bb*CDPK1, and 2 to 0.00012207 µM inhibitor (4-fold serial dilutions). Phosphorylation reactions were initiated by the addition of 10 µM Na_2ATP (Sigma-Aldrich, St. Louis, MO, USA). After incubating for 90 min at 30°C, the reaction was terminated by adding EGTA to a final concentration of 5 mM. Changes in the initial ATP concentration were evaluated as a luminescence readout using a MicroBeta2 multilabel plate reader (Perkin Elmer, Waltham, MA, USA). Results were converted to percent inhibition and IC_{50} values (the concentration of compound that led to 50% inhibition of enzyme activity) using non-linear regression analysis in GraphPad Prism (GraphPad Software, La Jolla, CA, USA).

2.4. Mammalian cell toxicity assays

The potential toxicity of the compounds against a mammalian cell line was determined by an XTT cell viability assay (Panreac Applichem, Darmstadt, Germany) to quantify cell growth. Marc-145 cells in the exponential phase of growth were seeded in 96-well flat-bottomed plates at a density of 2×10^5 cells/mL containing compounds (20 mM stock solutions dissolved in DMSO at the maximum concentration employed in our assays (5 µM) in quadruplicate and grown for 72 h at 37°C in a 5% CO_2 humidified incubator. Afterwards, 50 µL of XTT reagent was added to each well and incubated for 4 h. Fluorescence was measured at the respective excitation and emission wavelengths of 475 nm and 660 nm in a Synergy™ H1 microplate reader (Biotek Instruments Inc, Winooski, VT, USA). The percentage of growth inhibition was computed for any BKI tested, based on the DMSO vehicle. Three independent assays were performed with nine selected BKIs employed in the screening assays.

2.5. In vitro drug efficacy

Nine BKIs previously optimized with functional groups for improved potency, selectivity and pharmacokinetic properties were selected for further studies (Supplementary Fig. S3). The purity of all compounds (>98%) was confirmed by reverse-phase HPLC and ^{1}H-Nuclear Magnetic Resonance (NMR) (Doggett *et al.*, 2014; Ojo *et al.*, 2014, 2016; Huang *et al.*, 2015; Vidadala *et al.*, 2016). BKIs were sent to Saluvet research group (Complutense University of Madrid, Spain) at a concentration of 20 mM diluted in 100% DMSO. Compounds were stored, protected from light, at -20°C.

2.5.1. Drug screening

Marc-145 cells ($5x10^4$ cells per well) were incubated in culture media at 37°C with 5% CO_2 and grown to confluence in 24-well plates. In the initial drug screening, inhibitors were added at a final concentration of 5 µM, just prior to infection with purified tachyzoites from the Bb-Spain1 strain. DMSO (as solvent)

was added to negative control wells at the same final concentration. Cultures were subsequently infected with 10^3 purified tachyzoites from the Bb-Spain1 strain. Another set of experiments adding the different compounds 6 h p.i., when 50% invasion rate is reached for the strain employed (Frey *et al.*, 2016), was also performed to address possible effects on parasite proliferation. Before administration of the compounds, infected monolayers were gently rinsed with PBS three times in order to discard non-invaded tachyzoites. In both sets of experiments, immunofluorescence assays were performed after 3 days at 37°C/5% CO_2 (see Section 2.6) to count invasion events per well. Each condition was assessed in triplicate and the experiments were carried out in three independent assays. Those compounds that showed the highest values of both parasite invasion and proliferation inhibition were selected for further experiments.

2.5.2. Short-term assays: EC_{50} and EC_{99} determination

Marc-145 cells were grown as mentioned above in 24 well plates. Just prior to infection, BKIs were added at final concentrations ranging from 5 nM to 5 µM for determination of EC_{50} and EC_{99} (the effective concentration to reduce parasite numbers 50% or 99%, respectively) values. Then, Bb-Spain1 tachyzoites were added at a parasite:host cell ratio of 1:100 (10^3 tachyzoites per well). DMSO control wells were also included in each culture plate.

A similar experiment to determine the effects of the compounds on *B. besnoiti* proliferation was also performed. Here, infection of host cell monolayers was performed as previously described and compounds 1294, 1517, 1553 or 1571 were added at a final concentration from 5 nM to 5 µM per well at 24 h p.i., when the parasite invasion is completed (Frey *et al.*, 2016). Prior to the addition of the compounds, three washes with PBS were performed in order to discard non-invaded tachyzoites.

After 72 h p.i., samples were collected using a lysis solution (100 µL of PBS, proteinase K and AL Buffer) according to the manufacturer´s instructions contained in the DNeasy® Blood and Tissue kit (Qiagen, Valencia, CA, USA), for further DNA extraction and quantitative real-time (qPCR) to quantify the number of parasites in each well. Immunofluorescence staining was also performed as stated below for each compound and concentration used at 72 days p.i. Each condition was assessed in triplicate and the experiments were carried out in three independent assays.

2.5.3. Characterization of long-term effects of BKI treatments on B. besnoiti tachyzoites

Tachyzoites from the Bb-Spain1 strain were grown as previously stated and compounds 1294 1517, 1553 and 1571 were added just prior to infection at the previously established EC_{99} concentration. Drugs were left in the cultures for 6, 24 or 48 h. Drugs containing media were discarded and fresh culture media were added. Samples were collected at 1, 3 and 5 days post treatment for subsequent qPCR analysis. IFAT was performed at 8 and 10 days post treatment to assess whether any tachyzoites were able to re-infect host cells (Winzer *et al.*, 2015). Each condition was assessed in triplicate and the experiments were carried out in three independent assays.

2.5.4. Transmission Electron Microscopy analysis of B. besnoiti- infected HFFs treated with selected BKIs

HFF cell cultures were maintained in T25 tissue culture flasks and were infected with 10^7 Bb-Spain1 tachyzoites (parasite:host cell ratio of 10:1). After allowing the tachyzoites to invade the host cells for 3 h, monolayers were washed three times with PBS and treated with BKIs at a concentration of 5 µM. Samples were processed for Transmission Electron Microscopy (TEM) analysis at different time points after infection (4, 6 and 8 days) as described earlier (Müller *et al.*, 2017; Winzer *et al.*, 2015).

2.6. Immunofluorescence staining

For immunofluorescence staining, supernatants of the cell cultures were discarded at 72 h p.i., wells were washed three times with PBS and subsequently fixated with ice-cold methanol or paraformaldehyde 3%-glutaraldehyde 0.05% for 10 min. Then, wells were washed a further three times with PBS. Afterwards, those were incubated with 300 µl/well of Triton-X 100 (0.2%) in PBS for 30 min at 37°C, followed by three additional washes with PBS. As primary antibody, a polyclonal rabbit-anti tachyzoite Bb-Spain1 (Gutiérrez-Expósito

et al., 2013) was added at a dilution of 1:1000 in PBS and incubated for 1 h at 37°C. After three additional washes with PBS, 250 µl of Alexa Fluor® 488 Goat Anti-Rabbit IgG (H+L) (Life technologies, Carlsbad, CA, USA) were added per well at a dilution of 1:1000. The plates were incubated for 45 min at room temperature in the darkness and washed three times with PBS. In the final wash, DAPI stain was included. Finally, the plates were washed with distilled water and the total number of invasion events per well was counted using an inverted fluorescence microscope (Nikon Eclipse TE200) at 200X magnification. Two categories of plaque forming tachyzoites were distinguished: parasitophorous vacuoles (PVs) and lysis plaques, as described by Frey et al. (Frey *et al.*, 2016). For the isolate employed, 80% of the invasion events consisted of lysis plaques at 72 h p.i.

2.7. DNA extraction and quantitative real-time PCR (qPCR)

The harvested cell culture samples were incubated for 10 min at 56°C. Afterwards, DNA was purified using the spin column protocol for cultured cells according to the manufacturer's instructions contained in the DNeasy®Blood and Tissue kit (Qiagen, Valencia, CA, USA). DNA was eluted in 200 µl of elution buffer. The DNA content and purity of each sample was measured by UV spectrometry (Nanophotometer®, Implen GmbH, Munich, Germany).

The BbRT2 qPCR assay for specific detection of *Besnoitia* spp. DNA from ungulates (i.e., *B. besnoiti*, *Besnoitia tarandi, Besnoitia caprae* and *Besnoitia bennetti*) was performed according to Frey et al., ((Frey *et al.*, 2016). Briefly, each 20 µl reaction contained 10 µl of Power SYBR Green master mix® (Applied Biosystems, Thermo Fisher Scientific, Foster City, CA, USA), 0.5 µl of primer Bb3 (5'-CAA CAA GAG CAT CGC CTT C-3'; 20 µM), 0.5 µl of primer Bb 6 (5'-ATT AAC CAA TCC GTG ATA GCA G-3'; 20 µM), and 4 µl of water. The qPCRs were run on a 7300 Real-Time PCR System® (Applied Biosystems). Twenty to 100 ng of DNA in a volume of 5 µl was added to each reaction. The DNA positive control was extracted from *B. besnoiti* tachyzoites cultured in vitro. The product of the DNA extraction process using water instead of cells was used as a negative control. In each qPCR, 10-fold serial dilutions of genomic DNA corresponding to 0.1–100,000 Bb-Spain1 tachyzoites were included. The cycling conditions were 10 min at 95 °C followed by 40 cycles of 95 °C for 15 s and 60 °C for 1 min. Fluorescence emission was measured during the 60°C step. A dissociation stage was added at the end of each run, and the melting curves were analyzed. BbRT2-PCR was run in duplicate for each sample. The threshold cycle values (Ct-values) obtained for positive samples in the BbRT2-PCR were also expressed as tachyzoites per reaction using the standard curve included in each run.

2.8. Data analyses

The cytotoxicity of screened BKIs was compared by a one-way ANOVA test. For the determination of the percentage of inhibition (%) in the in vitro drug screening, first the invasion rate (IR) was calculated by counting all the events per well. Then, invasion rates were related to the negative control (DMSO) to determine the relative invasion rate (RIR) of the parasite for each condition. Afterwards, the % of inhibition was determined as indicated below.

% Relative invasion rate (RIR) = (IR treated well / IR DMSO well) x 100

Table 1: List of primers used in the present study (Reference: This study).

Use	Primer sequence (5'-3')
Protein identification and sequencing	FW2: GAAGCAGAAGACGGACAAGGAGTC
	FW3: GCATCATCGACTTTGGCCTCAGCA
	FWC: GACGAGCTCCACGCGACGCCGGGGATGTTCGTT
	RV1: GGT TAA TTA ATT TCC GCA GAG CTT CAA GAG CAT
Protein cloning	Bb_LIC_Fw: GGG TCC TGG TTC GAT GGG TCA GCA AGA AAG CAC GCT CGG C
	Bb_LIC_Rev: CTT GTT CGT GCT GTT TAC TTA GTT GCC GCA GAG CTT CAG AAG

% Inhibition = 100 - %RIR

For the compounds that showed the highest percentages of inhibition in the initial drug screening at 0 and 6 h p.i., tachyzoite yields after 72 h of incubation were determined by qPCR for EC_{50} and EC_{99} calculations and adjusted to the amount of DNA quantified by spectrophotometry in each sample. The relative growth for each drug concentration was determined relative to the DMSO control, using the tachyzoite yield per ng of DNA. Afterwards, the EC_{50} and EC_{99} concentrations were determined using an ED_{50} plus sheet for Microsoft Excel after a logarithmic transformation of the data.

The Kruskal-Wallis test was performed to compare the efficacy of the nine compounds against *B. besnoiti* in the drug screening, and to search for differences among the four compounds selected for determination of EC_{50} and EC_{99} values. This test was also used to address whether there were differences among the different concentrations of BKIs tested. Finally, a two-way ANOVA test was employed to compare the different treatment durations employed. All statistical analyses were performed using the software GraphPad Prism® 6.0 (GraphPad Software, San Diego, CA, USA). For all statistical analysis, *P* values lower than 0.05 were considered significant.

3. Results

3.1. BbCDPK1 identification, sequencing and cloning

The partial sequence of *Bb*CDPK1 initially obtained consisted of a 1160 bp sequence that showed features characteristic of a CDPK1 enzyme, including the amino-acid sequence of the putative active site of the enzyme, which was identical to the one present in *Nc*CDPK1 (Fig. 1). When the whole sequence data was subjected to intron processing, the complete coding sequence obtained showed 95% identity both in nucleotide and amino acid sequences compared with *Nc*CDPK1 and *Tg*CDPK1 sequences, including the putative active site with a glycine gatekeeper (Fig. 1; GenBank® accession number N° **KY991370**). The expected molecular weight of the obtained protein was 56 kDa (Expasy ProtParam). Using

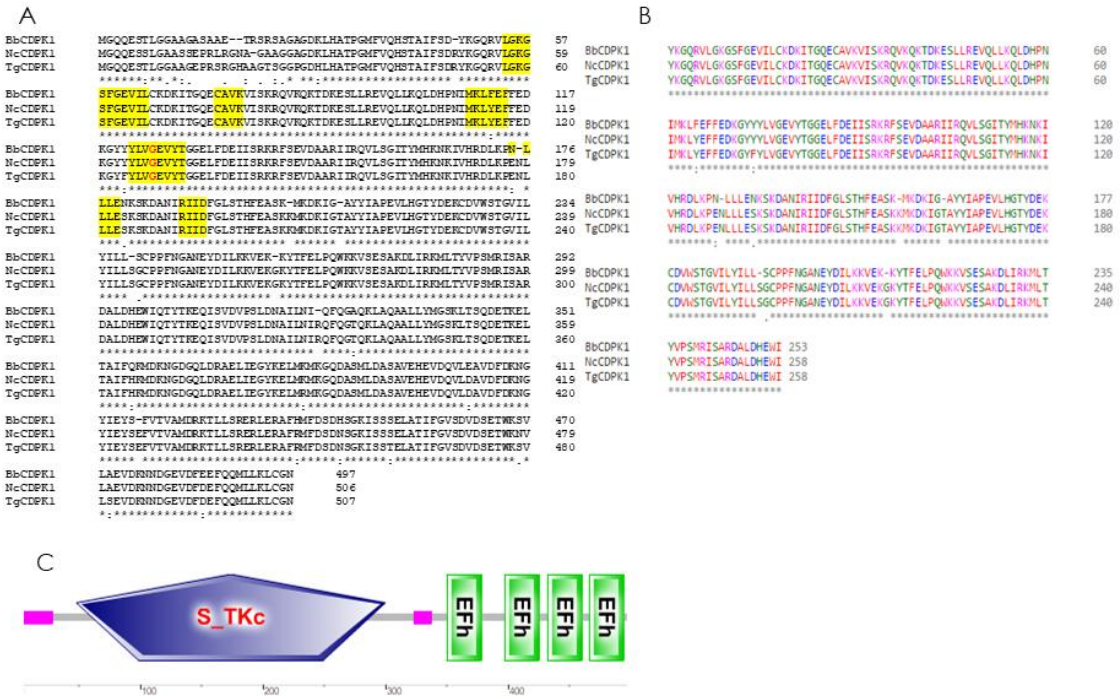

Fig. 1. Sequence features of *Bb*CDPK1 (GenBank® accession number **KY991370**). (A) Alignment of amino acids sequences of *Bb*CDPK1, *Nc*CDPK1 and *Tg*CDPK1. Yyellow highlighted amino acids were postulated by Keyloun et al. (2014) to contribute to the potential activity or resistance of CDPK1 enzymes to bumped kinase inhibitors. Gatekeeper (Gly) is marked in red. (B) Alignment of amino acid sequences of the kinase domain of *Bb*CDPK1, *Nc*CDPK1 and *Tg*CDPK1. (C) Simple Modular Architecture Research Tool (SMART) image of *Bb*CDPK1, with the serin-threonin kinase domain and four calcium-binding EF hands. *Bb*, *Besnoitia Besnoiti*, *Nc*, *Neospora caninum*, *Ta*, *Toxoplasma gondii*.

the Simple Modular Architecture Research Tool (EMBLEM, Heidelberg, Germany) for protein sequence analysis and classification, the sequence obtained showed a kinase domain with an ATP binding site and four EF hand domains for calcium binding, as described for other apicomplexan CDPK1 enzymes (Fig. 1). Moreover, putative sites of N-mirystoilation were found in the N-terminal region of the protein, as well as one site of palmytoilation. *Bb*CDPK1 showed 98 and 98.4% amino acid identity in the kinase domain with *Tg*CDPK1 and *Nc*CDPK1, respectively.

Not surprisingly, results from I-TASSER modeling showed that *Tg*CDPK1 has the closest structural similarity.

3.2. Screening of recombinant BbCDPK1 using BKI-analogues

Due to the close homology of *Bb*CDPK1 with CDPK1 in other apicomplexans, the enzyme was expressed as a recombinant protein to test the effects of BKI analogues on its activity. Upon separation by SDS-PAGE, recombinant *Bb*CDPK1 exhibited a molecular weight of 57 kDa (Fig. 1). Nine BKIs, namely BKI-1294, 1605, 1649, 1517, 1553, 1571, 1575, 1586 and 1597, inhibited *Bb*CDPK1 with IC_{50} values in the lower nanomolar range (Table 2). Thus, these compounds were further assessed in cellular assays. The activity of the recombinant enzyme was proven to be calcium-dependent, so it is highly unlikely that the activity was not associated with the recombinant enzyme itself.

Table 2: Activity of BKIs screened against *Bb*CDPK1 activity (IC_{50} values, µM)

Compound	1294	1517	1553	1571	1575	1586	1597	1605	1649
IC_{50} (r*Bb*CDPK1)	0.004	0.012	0.004	0.024	0.022	0.011	0.002	0.015	0.006

3.3. Cytotoxicity in Marc-145 cells

When the compounds were added to uninfected Marc-145 cells at the highest concentration employed in the in vitro assays (5 µM), those which did not cause significant cytotoxicity compared with DMSO (P>0.05; one-way ANOVA). Percentages of cytotoxicity of the screened BKIs compared with the DMSO-treated negative control wells were as follows: 1294: 5.2%; 1517: 5.2%; 1553: 5.8%; 1571: 2.8%; 1575: 4%; 1586: 5%; 1597: 5.1%; 1605: 3.8%; 1649:5%. Moreover, upon inspection by light microscopy, no alterations in the Marc-145 cell morphology was detected.

Table 3: Percentage of inhibition of parasite growth in the drug screening when BKIs were administered at 0 or at 6 hpi at a concentration of 5 µM

Compound		1294	1517	1553	1571	1575	1586	1597	1605	1649
Time of administration	0 hpi	99	98	98	96	95	92	95	96	63
	6 hpi	90	93	96	95	89	87	83	87	63

3.4. Initial drug screening of BKIs in B. besnoiti-infected Marc-145 cells

In the initial drug treatments carried out at the time point of infection (0 h p.i.) and 6 h p.i., eight out of nine BKIs caused more than 80% of parasite growth inhibition. Compound 1649 was the least effective (63%, Kruskall-Wallis test, $P<0.01$), whereas 1294, 1517, 1553 and 1571 were the most efficacious, and were thus selected for further studies (Table 3). Parasite growth was markedly inhibited in drug-treated wells since only parasitophorous vacuoles (PVs) were found, whilst in DMSO-treated control wells parasites were displaying the normal features of their lytic cycle at 72 h p.i. as a consequence of parasite egress (Frey et al., 2016), where most invasion events consisted of plaques lysis.

3.5. Dose-response experiments and EC_{50} and EC_{99} determination

All four selected BKIs led to a significant reduction in parasite growth when administered at concentrations higher than 0.05 µM at the time point of infection (Fig. 2A). When BKIs were added at 5 µM at 24 h p.i., parasite proliferation was still inhibited by 80%, indicating that these compounds inhibit both host cell invasion and intracellular proliferation (Fig. 2B). The EC_{50} and EC_{99} values determined at 0 h p.i. were largely in a similar range among these compounds, except for 1553, which appeared slightly less efficacious (Table 4). Treatments with compounds 1294 and 1517 showed the lowest parasite loads. Statistically significant differences in the number of parasites per well were found between compounds 1517 and 1571 at a concentration of 5 µM when administered at 0 hp.i. (Kruskal Wallis, $P<0.05$), and among the different concentrations for each BKI (Kruskal Wallis, $P<0.01$).

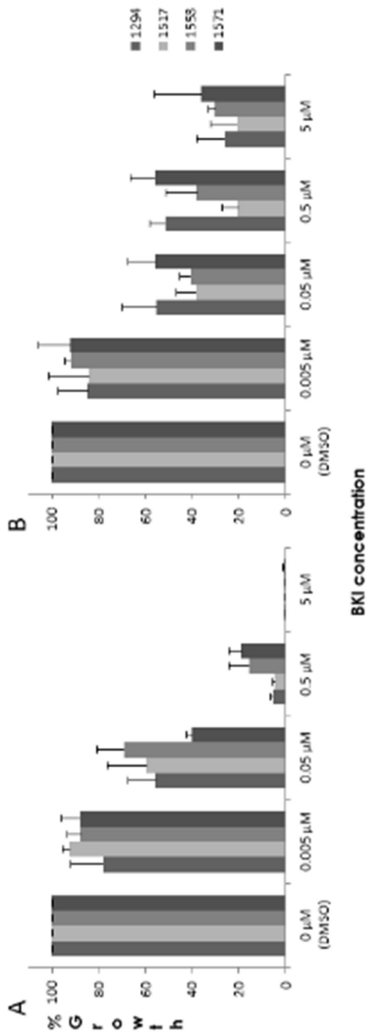

Figure 2. Percentages of *Besnoitia besnoiti* growth inhibition (related to negative control, DMSO) when bumped kinase inhibitors (BKIs) are administered at 0 h p.i. (A) and at 24 h p.i. (B) as determined by quantitative real-time PCR. Error bars in graphs represent standard deviation.

Table 4: *In vitro* activity of selected BKIs against *B. besnoiti* tachyzoites proliferation (EC_{50} & EC_{99} values, µM)

Compound	1294	1517	1553	1571
EC_{50} (*B. besnoiti*)	0.045	0.067	0.097	0.051
EC_{99} (*B. besnoiti*)	2.38	2.28	3.35	2.78

3.6. Characterization of the long-term post-treatment effects of BKI exposure on B. besnoiti tachyzoites

Following BKI treatments for various time spans, parasite growth was hardly detected until 3 days p.i., and statistically significant differences between the four BKI-treated and DMSO-treated cultures were observed at 5 days post treatment for each of that tachyzoites remained viable and were able to re-infect host cells even after 48 h post treatment. Lysis plaques were present in 6 and 24 h treated wells both at 8 and 10 days post treatment, whilst in 48 h treated wells only parasitophorous vacuoles could be found.

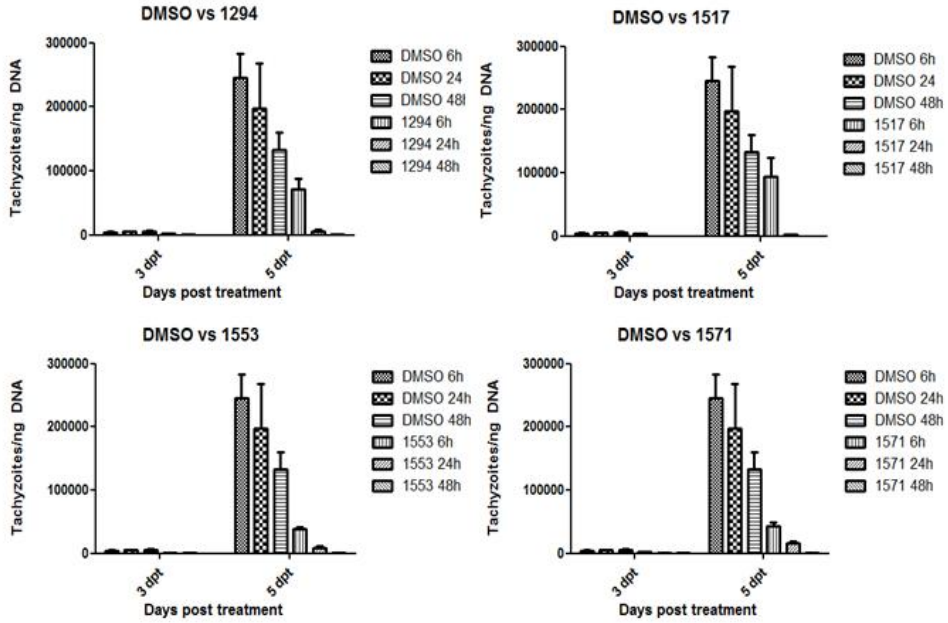

Figure 3. Tachyzoite yield expressed as tachyzoites per ng of DNA from *Besnoitia besnoiti* cell cultures infected and treated with the four bumped kinase inhibitors selected for 6, 24 or 48 h collected at 3 and 5 days post treatement (dpt). Error bars in graphs represent standard deviation.

the treatment durations (P<0.001, two-way ANOVA) (Fig. 3). Differences were also found among the different treatment durations (6, 24 and 48 h) for each BKI (P<0.001, two-way ANOVA) (Fig. 3). Upon short treatments (6 h) with the four BKIs, compounds 1553 and 1517 showed statistically significant differences (P<0.01, two-way ANOVA), and the lowest tachyzoite yield (TY) was recorded in cultures treated with compound 1553. Longer treatments for up to 24 h were more effective but failed to inhibit parasite proliferation completely, not showing statistically significant differences among the compounds. However, TYs diminished to low values after 48 h treatments with all four compounds, and this was corroborated by IFAT. Further analysis by IFAT at 8 and 10 days post treatment showed

3.7. Determination of the effects of BKIs on the ultrastructure of B. besnoiti tachyzoites: Transmission Electron Microscopy analysis

In control cultures, which were exposed to solvent but not to drugs, *B. besnoiti* tachyzoites underwent intracellular proliferation within a PV, surrounded by a PV membrane (PVM) (Fig. 4). In longitudinal sections they exhibited the typical features of apicomplexan parasites including a polar organization, apical organelles such as micronemes and rhoptries, dense granules, nucleus and mitochondrion. Individual tachyzoites were more clearly visible in smaller vacuoles (Fig. 4A, B), and appeared more tightly packed in larger vacuoles (Fig. 4C, D).

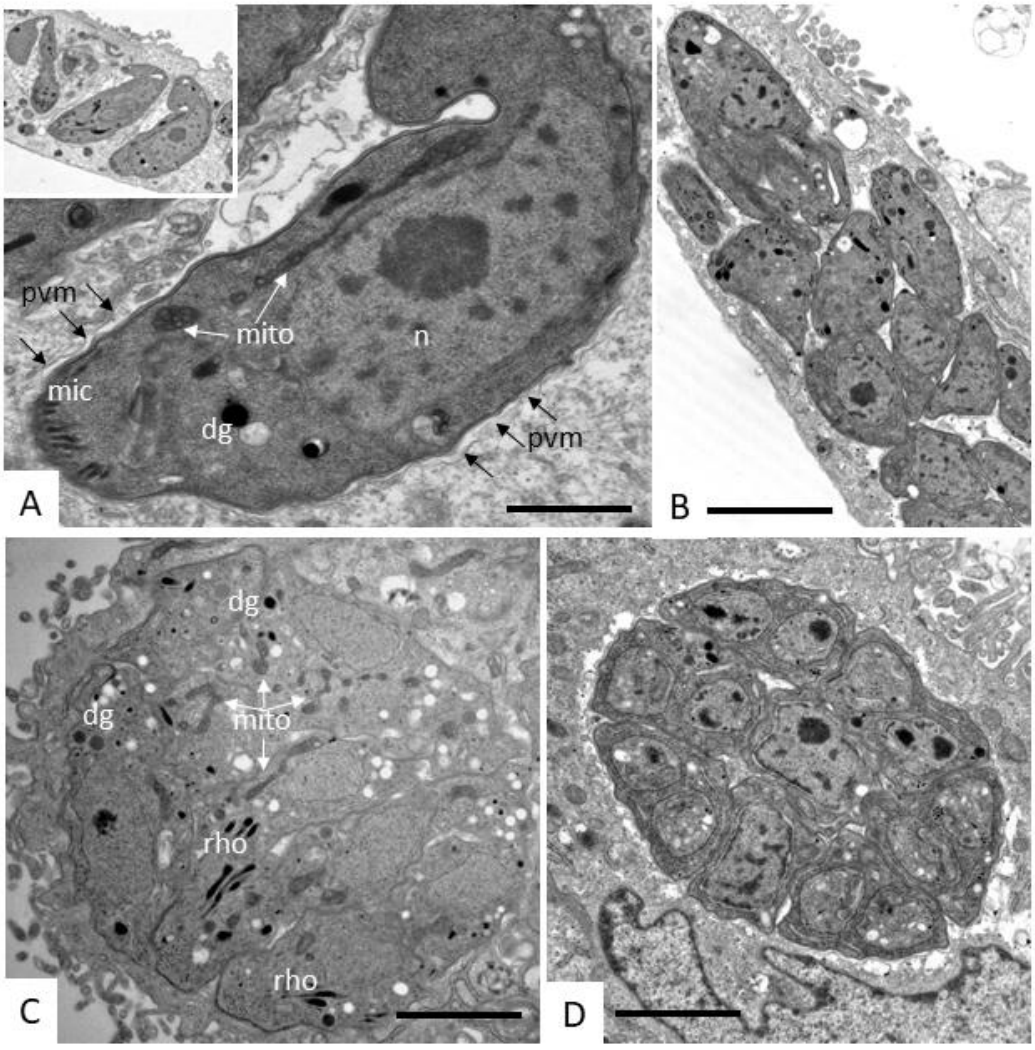

Figure 4. Representative Transmission Electron Microscopy (TEM) images of *Besnoitia besnoiti* tachyzoitesin HFF cell cultures treated with DMSO. Intact tachyzoites are observed in longitudinal (A,B,C) and transversal cut sections (C,D,E). Note that image B is a larger magnification view of A. Numerous viable tachyzoites, located within parasitophorous vacuoles surrounded by a parasitophorous vacuole membrane (PVM) (A,D,E), can be seen. Non distorted apical complexes contained typical organelles from apicomplexan parasites, such as the conoid (con), dense granules (dg), micronemes (mic) and rhoptries (rho) (B,D). Also, mitochondria (mito) and the nucleous (nuc) of the tachyzoites are clearly discernible. Scale bars: A = 3 µm; B = 0.5 µm; C = 1.2 µm; D = 1.2 µm; E = 1.2 µm

In the infected HFF cell cultures treated with the four selected BKIs, clear alterations were visible, which were mostly very similar for all four BKIs. As exemplified for BKI-1294 (Fig. 5A-D), a fraction of parasites was evidently distorted, with highly vacuolized cytoplasm and most likely non-viable, while inside the same host cell, still intact parasites formed multinucleated complexes, some of which remained viable for up to 8 days and clearly grew in size (Fig. 5D). These complexes were a large mass that contained several nuclei and apical complex precursors, already containing structural features such as conoids and secretory organelles. However, parasites appeared stuck in the cell cycle and could not complete cytokinesis. BKI-1571 and 1553 also induced the formation of such complexes (Fig. 5E, F), while compound 1517-treated cultures often exhibited already distorted tachyzoites and still viable complexes within the same host cells as shown in Fig. 5H. BKI-treated parasites, in general, often formed amylopectin granules (Fig. 5), which represent a source of energy in apicomplexan bradyzoites. Host cell mitochondria were often unaffected and

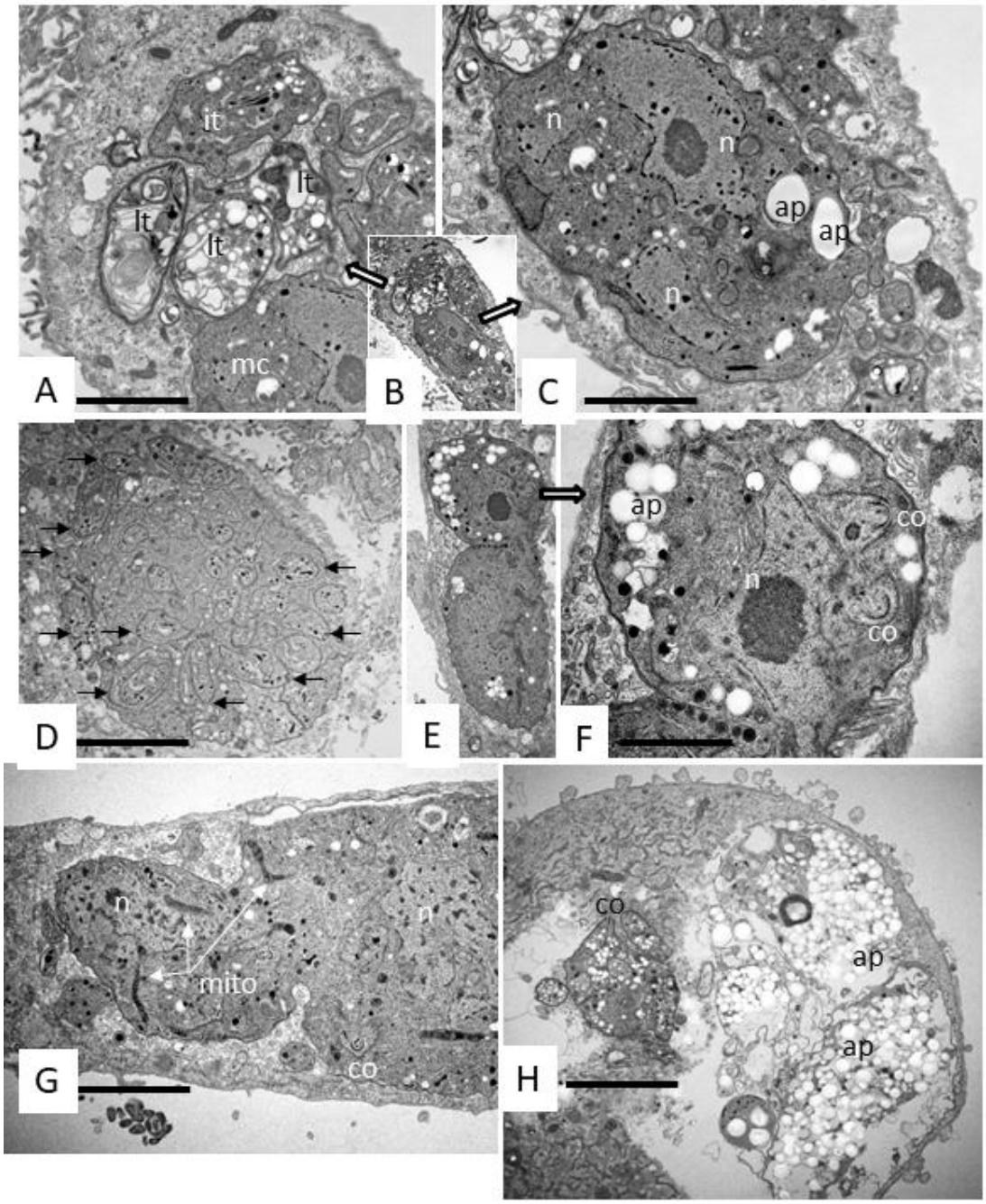

Figure. 5. Representative Transmission Electron Microscopy (TEM) images of *Besnoitia besnoitia* tachyzoites in HFF cell cultures treated with bumped kinase inhibitors such as 1294 for 4 days (A-C) or 6 days (D), 1571 for 4 days (E, F), 1553 for 6 days (G) and 1517 for 6 days (H). (A, C) Largely distorted tachyzoites (lt), intact parasites (it) and complexes (mc) can be present in a single host cell. (B). Images A and C are larger magnification views of B, showing largely distorted and intact tachyzoites (A) or a multinucleated compound (C). A low magnification view. [explain arrows] (D) A large complex generated by exposure to bumped kinase inhibitor 1294 for 6 days which contains numerous precursors of apical complexes marked with arrows. (E) A complex exhibiting numerous amylopectin granules (ap); note the two emerging conoids (co). (F) A larger magnification view of E. (G) Exposure to bumped kinase inhibitor 1553 also results in the formation of large complexes; note the intact mitochondria (mito) and emerging conoid structure (co). H: 1517 treatment results in the formation of parasites that form large cytoplasmic amylopectin granule deposits. Scale bars: A = 2 µm, C = 1.6 µm, D = 4.2 µm, F = 1.3 µm; G = 2.8 µm, H = 3.4 µm

appeared still intact, suggesting that the host cells were not extensively affected.

Compounds 1294 (Fig. 5A-D) and 1517 (Fig. 5H) showed a more dramatic effect on the ultrastructure of the tachyzoites, seemingly

being more lethal with severe alterations in the cytoplasms and membranes of the parasites.

Alterations in the ultra-structure of the tachyzoites and the morphology of the PV were suggested based to IFAT results (Fig. 6). In BKI-treated wells, seemingly distorted PVs with non-discernible tachyzoites were visualized, whilst in DMSO-treated control wells parasitophorous vacuoles showed the characteristic rossetta morphology and zoites were clearly discernible by a surface staining with the antibody employed.

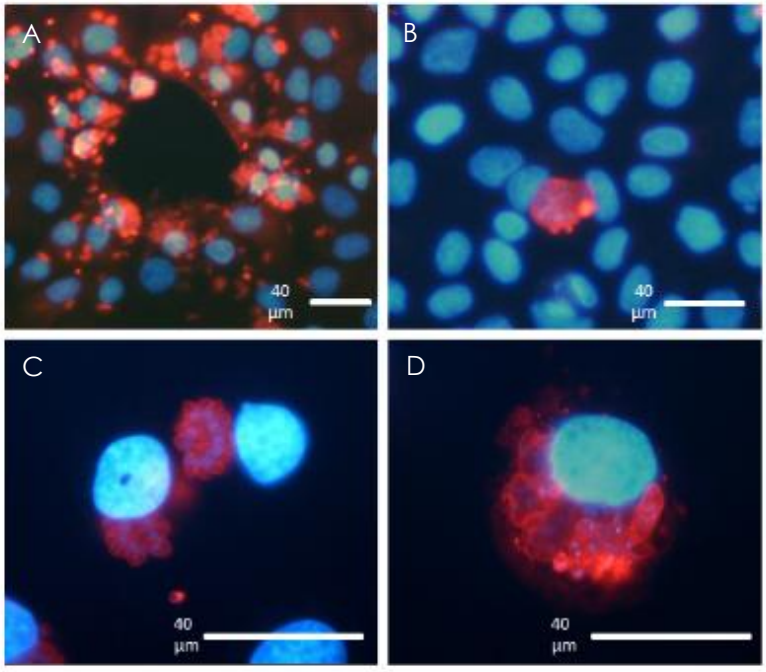

Figure 6: Marc-145 cell cultures infected with *Besnoitia besnoiti* and treated with DMSO (Fig. 5A) or bumped kinase inhibitor 1294 for 3 days. (A) Marc-145 cell culture infected with *B. besnoiti* tachyzoites and treated with DMSO. Note a lysis plaque. (B) Culture treated with bumped kinase inhibitor 1294 at 5 µM for 3 days. (C) Culture treated with bumped kinase inhibitor 1294 at 0.5 µM for 3 days. Note a seemingly viable parasitophorous vacuole (PV) with well-defined tachyzoites. (D) Culture treated with bumped kinase inhibitor 1294 at 0.5 µM for 3 days. Note a distorted PV with tachyzoites that are not well-defined. Scale bars: A = 40 µm, B = 40 µm, C = 40 µm, D = 40 µm.

4. **Discussion**

This study shows that *Bb*CDPK1 could represent a promising drug target for the treatment of bovine besnoitiosis. First, we have shown the transcription of a CDPK1 homologue in *B. besnoiti* tachyzoites, namely *Bb*CDPK1. Next, the activity of recombinant *Bb*CDPK1 was inhibited by a panel of BKIs. Thirdly, selected BKIs were shown to have a profound impact on *B. besnoiti* host cell invasion and proliferation, and these effects were visualized by immunofluorescence and TEM.

As expected, the CDPK1-type kinase identified in *B. besnoiti* showed a high degree of sequence similarities with CDPK1 enzymes from other members of the Toxoplasmatinae (*T. gondii* and *N. caninum*). Indeed, the amino acid sequence of *Bb*CDPK1 reported herein shares a high percentage of identity (95%) with orthologues *Nc*CDPK1 and *Tg*CDPK1, including a glycine in the gatekeeper position, which discriminates CDPK1 from other kinases (Ojo *et al.*, 2014). The sequence showed additional characteristic features of CDPK1 enzymes such as an N-terminal serine-threonine kinase domain, a junctional domain and a series of calcium-binding domains known as EF hands. The existence of EF hands suggest that *Bb*CDPK1 might play an important role in regulating calcium-dependent pathways (Hui *et al.*, 2015). Moreover, the sequence showed the closest structural similarity with *Tg*CDPK1. Accordingly, the newly identified orthologue was named *Bb*CDPK1. Besides, putative n-

myristoylation residues were found, similar to what has been reported for *Cryptosporidium Cp*CDPKs (Etzold *et al.*, 2014), which may be important for the association of the enzyme with lipid membranes that can influence its activity.

Kinase assays showed that selected BKIs inhibited the *Bb*CDPK1 enzyme activity even at low nanomolar range concentrations. A similar finding occurred with both *Nc*CDPK1 and *Tg*CDPK1, whose X-ray crystal structures confirmed a structural basis for BKI selectivity (Ojo *et al.*, 2010, 2014). These observations are supported by the high kinase domain sequence identity found in members of the Toxoplasmatinae, where the percentage of identity of *Bb*CDPK1 is as high as 98% and 98.4% with *Tg*CDPK1 and *Nc*CDPK1, respectively. Previously, it has been shown that the degree of sensitivity or resistance of CDPK enzymes to these inhibitors depends on the size and characteristics of the gatekeeper residue and the topology of the adjacent ATP-binding pocket (Keyloun *et al.*, 2014). Regarding this issue, *Bb*CDPK1 possesses only a single amino acid difference in the active site compared with *Tg*CDPK1 and *Nc*CDPK1 sequences (Phenylalanine in position 112 instead of Tyrosine). Consequently, a similar susceptibility pattern against BKIs was expected in all of the Toxoplasmatinae orthologues with the same atypically small glycine gatekeeper residue (Van Voorhis *et al.*, 2017). Enzymatic results indicated that BKIs may be targeting at least *Bb*CDPK1. Similar effects were observed with the four BKIs studied that effectively inhibit other CDPK1 orthologues present in *N. caninum* (Müller et al., 2017b), *T. gondii* (Winzer *et al.*, 2015) and *C. parvum* (Castellanos-González *et al.*, 2013). Further studies with a parasite line expressing a gatekeeper mutant would be needed to definitively claim that the in vivo phenotype of BKI-treated parasites is solely due to inhibition of *Bb*CDPK1. In the context of these future studies, it should be also verified whether CDPK1 inhibition *in vitro* is abolished when a large gatekeeper mutant recombinant enzyme is used for the kinase assay.

The results obtained in *in vitro* assays suggests that *Bb*CDPK1 may be a key regulator during the parasite lytic cycle, since invasion and proliferation events were severely impaired as in *N. caninum* and *T. gondii (Müller et al., 2017b)*. We included in this panel of BKIs the well-studied BKI 1294 which has been used in *in vitro* and *in vivo* assays against *Theileria equi* (Hines *et al.*, 2015), *C. parvum* (Lendner *et al.*, 2015), *T. gondii* (Winzer *et al.*, 2015; Doggett *et al.*, 2014) and *N. caninum* (Müller *et al.*, 2017a; Ojo *et al.*, 2014), together with other novel and less studied BKIs. Eight out of nine compounds effectively inhibited parasite invasion, with BKIs 1294, 1517, 1553 and 1571 being the most promising ones (inhibition of parasite invasion > 90%) when administered at 5 µM at 0 and at 6 h p.i. Moreover, these compounds lacked cytotoxicity in Marc-145 cells when applied at this concentration, as was also observed by Müller et al. (Müller *et al.*, 2017a) in human foreskin fibroblast cells.

The EC_{50} & EC_{99} values obtained for these four compounds are in the nanomolar range, which is in accordance with those published for *N. caninum* (Ojo *et al.*, 2014; Müller *et al.*, 2017) and *T. gondii* (Winzer *et al.*, 2015). Most parasite clearance was accomplished by treatments with EC_{99} concentrations only after 72 h of treatment, whereas short treatments did not completely inhibit parasite proliferation, suggesting that these BKIs are parasitostatic rather than parasiticidal. This was confirmed by visualizing cultures at 8 and 10 days post treatment, which revealed the presence of remaining viable tachyzoites in drug-treated cultures re-infecting host cells, and by TEM analyses that showed seemingly still viable tachyzoites. TEM showed that the effects of these compounds were not limited to the arrest of host cell invasion, suggesting that there may be additional targets involved (Ojo *et al.*, 2014). Thus, it is possible that secondary targets besides CDPK1 are affected. In *T. gondii* for instance, Mitogen-Activated Protein kinase (MAPK) was previously shown to be inhibited by a BKI analogue, with different pyrazolo-pyrimidine R1 and R2 groups (Sugi *et al.*, 2013, 2015). Inspection of BKI-treated *B. besnoiti* by TEM revealed similar findings for BKIs 1294, 1517, 1553 and 1571. Exposure to these BKIs led to severe ultrastructural alterations in some, but not all, tachyzoites. At later time points after 4-6 days of treatment, PVs containing large multinucleated complexes were found, some of which showed clear signs of cellular degeneration and others obviously still viable,

similar to what has been reported earlier in BKI-1294, 1517 and 1553 treated cell cultures infected with *N. caninum* or *T. gondii* (Winzer *et al.,* 2015; Müller *et al.,* 2017b). As for *N. caninum,* BKIs 1294 and 1517 showed more dramatic effects (Müller *et al.*, 2017b). These complexes result from parasites that undergo nuclear division, but not cytokinesis, resulting in the formation of tachyzoite precursors that are trapped within the host cell. Whether this effect is due to CDPK1 inhibition or whether there are other targets of BKIs which regulate parasite cytokinesis needs to be elucidated.

In addition, BKI 1294 treatment induced higher expression levels of bradyzoite-specific genes (i.e MAG1, BAG1) in drug-treated cultures infected with *N. caninum* and *T. gondii* and increased labeling intensity for anti-BAG1 and anti-CC2 bradyzoite-specific markers was noted (Winzer *et al.*, 2015). Similar increased staining with the bradyzoite marker MAG1 was observed in *N. caninum* tachyzoites treated with BKI 1517 and 1553, together with an increased presence of amylopectin granules as visualized by TEM (Müller *et al.*, 2017b). Similarly, amylopectin granules were present in BKI-treated *B. besnoiti*, a characteristic feature of *B. besnoiti* bradyzoites (Fernández-García *et al.*, 2009b). This is particularly interesting, since BKI treatments could potentially represent a convenient exogenous trigger to induce tachyzoite-to-bradyzoite conversion of *B. besnoiti in vitro*.

In conclusion, we here demonstrate the therapeutic potential of BKIs for treatment of bovine besnoitiosis. Prospectively, one could envisage BKI treatment of affected cattle at the acute stage of infection where tachyzoites replicate and disseminate, inducing vascular damage and clinical signs of respiratory disorders and orchitis. During the chronic stage, BKI therapy might be more difficult, possibly due to potentially poor drug accessibility to the interior of bradyzoite-containing tissue cysts (Álvarez-García *et al.*, 2014b). A major caveat for the development of BKIs against besnoitiosis is the absence of laboratory animal models; thus studies need to be carried out directly in the target animal (Álvarez-García *et al.*, 2014b). Plasma levels of up to 5 µM have been already achieved in cattle treated with BKI 1294, 1517 and 1553 (Huang *et al.*, 2015; Schaefer *et al.*, 2016; Hulverson *et al.*, 2017), and whether the administration of these BKIs during the acute stage of the disease is enough to avoid tissue cyst formation needs to be further investigated.

Acknowledgements

This work was financially supported through two research projects from the Spanish Ministry of Economy and Competitiveness (Ref. AGL2013-04442) and Community of Madrid, Spain (Ref. S2013/ABI-2906, PLATESA-CM), and by the Swiss National Science Foundation (grant No. 310030_165782 and CRSII3_160702). We also acknowledge support from the National Institute of Allergy and Infectious Diseases, USA and National Institute of Child Health and Human Development of the National Institutes of Health, USA under the award numbers R01AI089441, R01AI111341, and R01HD080670. The work was also supported by awards # 2014-06183 from the United States Department of Agriculture National Institute of Food and Agriculture. Alejandro Jiménez-Meléndez was supported by a grant from the Spanish Ministry of Education, Culture and Sports (grant nº FPU13/05481). In addition, we acknowledge Laura Jiménez-Pelayo and Marta García-Sánchez for their technical assistance. Conflict of Interest Disclosure: Dr. Van Voorhis is the founder of the company ParaTheraTech Inc., dedicated to bringing BKIs to market in animal health applications. He did not carry out or interpret the experiments in this paper.

Supplemental Fig. 1

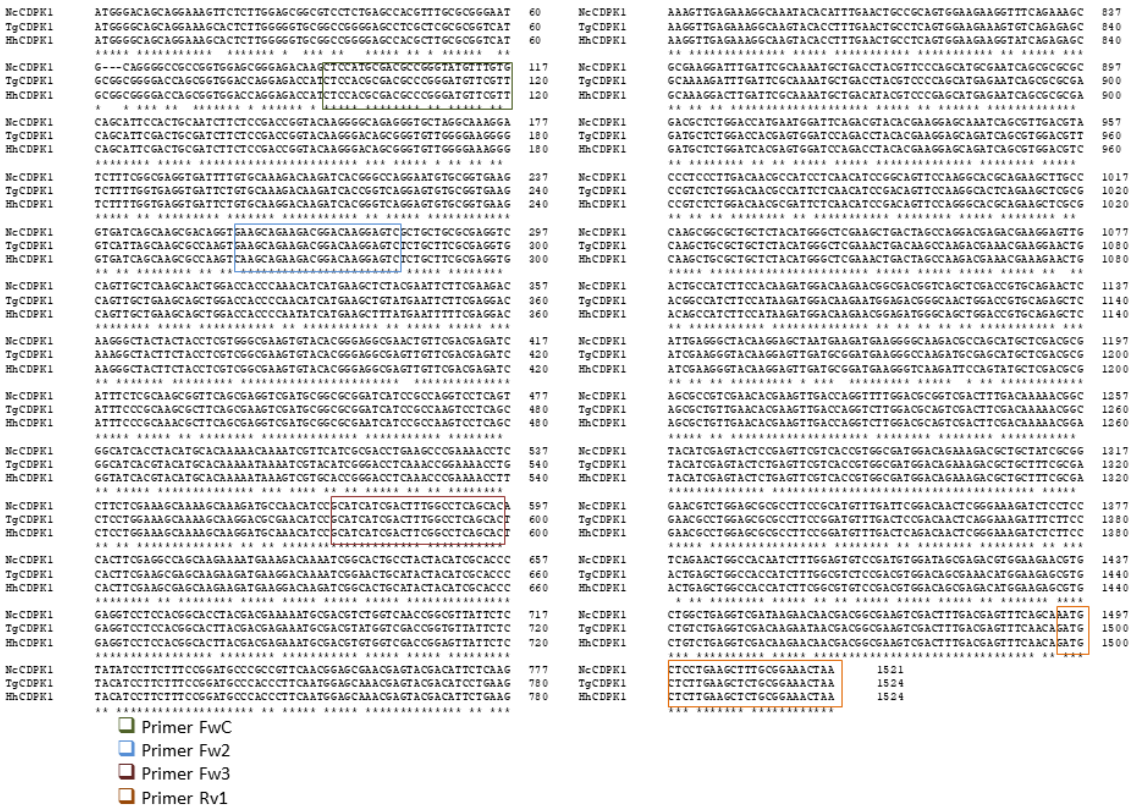

Supplemental Fig. 1: Alignments of *N. caninum*, *T. gondii* and *H. hammondi* CDPK1 sequences and primer design.

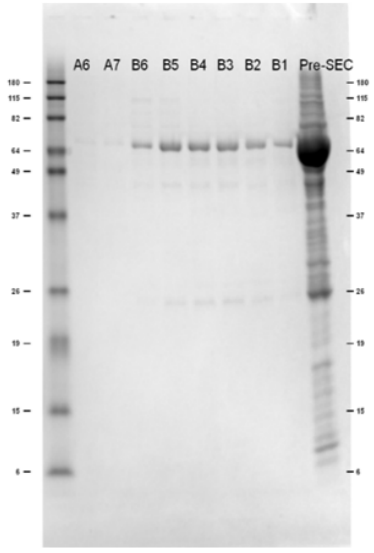

Supplemental Fig. 2: Coomassie blue stained SDS-PAGE gel of recombinant *Bb*CDPK protein purified by immobilized metal-affinity chromatography (IMAC) followed by size exclusion chromatography. Purified size exclusion chromatography fractions B1 to B6 were pooled and stored at -20°C for subsequent use in enzyme assays. The storage buffer is composed of 50% glycerol, 12.5 mM HEPES pH 7.5, 250 mM NaCl, 0.5 mM DTT, 0.0125% sodium azide, and protease inhibitor.

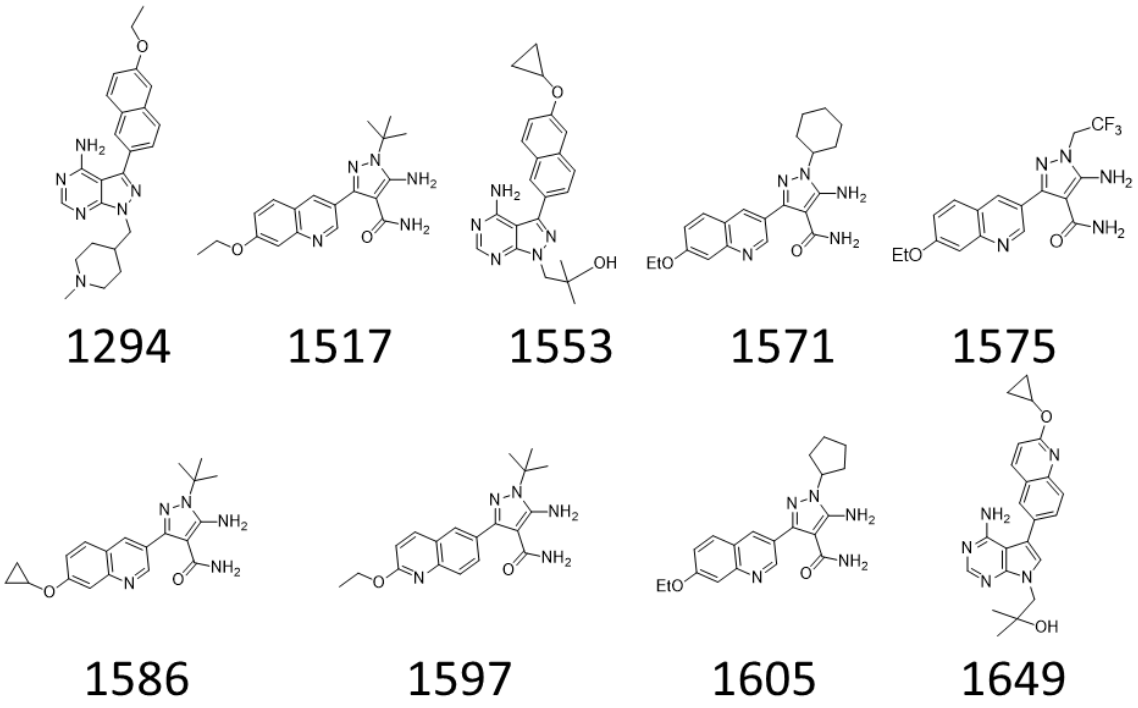

Supplemental Fig. 3: Chemical structure of the panel of 9 BKIs used in the drug screening.

REFERENCES:

Álvarez-García, G., Frey, C.F., Mora, L.M., Schares, G., 2013. A century of bovine besnoitiosis: An unknown disease re-emerging in Europe. Trends Parasitol. 29, 407-415.

Álvarez-García, G., García-Lunar, P., Gutiérrez-Expósito, D., Shkap, V., Ortega-Mora, L.M., 2014. Dynamics of *Besnoitia besnoiti* infection in cattle. Parasitology 141 (11), 1419-1435.

Álvarez-García, G., 2016. From the mainland to Ireland - bovine besnoitiosis and its spread in Europe. Vet. Rec. 178 (24), 605-607.

Arnal, M., Gutiérrez-Expósito, D., Martínez-Durán, D., Regidor-Cerrillo, J., Revilla, M., Fernández de Luco, D., Jiménez-Meléndez, A., Ortega-Mora, L., Álvarez-García, G., 2017. Systemic Besnoitiosis in a Juvenile Roe Deer (*Capreolus capreolus*). Transbound. Emerg. Dis. 64(5), e8-e14

Basso, W., Schares, G., Gollnick, N.S., Rutten, M., Deplazes, P., 2011. Exploring the life cycle of *Besnoitia besnoiti* - experimental infection of putative definitive and intermediate host species. Vet. Parasitol. 178 (3-4), 223-234.

Billker, O., Lourido, S., Sibley, L.D., 2009. Calcium-dependent signaling and kinases in apicomplexan parasites. Cell Host Microbe 5 (6), 612-622.

Castellanos-Gonzalez, A., White, A.C.,Jr, Ojo, K.K., Vidadala, R.S., Zhang, Z., Reid, M.C., Fox, A.M., Keyloun, K.R., Rivas, K., Irani, A., Dann, S.M., Fan, E., Maly, D.J., Van Voorhis, W.C., 2013. A novel calcium-dependent protein kinase inhibitor as a lead compound for treating cryptosporidiosis. J. Infect. Dis. 208 (8), 1342-1348.

Cortes, H.C., Müller, N., Esposito, M., Leitao, A., Naguleswaran, A., Hemphill, A., 2007. *In vitro* efficacy of nitro- and bromo-thiazolyl-salicylamide compounds (thiazolides) against *Besnoitia besnoiti* infection in Vero cells. Parasitology 134 (Pt 7), 975-985.

Cortes, H.C., Muller, N., Boykin, D., Stephens, C.E., Hemphill, A., 2011. *In vitro* effects of arylimidamides against *Besnoitia besnoiti* infection in Vero cells. Parasitol. 138 (5), 583-592.

Diesing, L., Heydorn, A.O., Matuschka, F.R., Bauer, C., Pipano, E., de Waal, D.T., Potgieter, F.T., 1988. *Besnoitia besnoiti*: studies on the definitive host and experimental infections in cattle. Parasitol. Res. 75 (2), 114-117.

Doerig, C., Meijer, L., Mottram, J.C., 2002. Protein kinases as drug targets in parasitic protozoa. Trends Parasitol. 18 (8), 366-371.

Doggett, J.S., Ojo, K.K., Fan, E., Maly, D.J., Van Voorhis, W.C., 2014. Bumped kinase inhibitor 1294 treats established *Toxoplasma gondii* infection. Antimicrob. Agents Chemother. 58 (6), 3547-3549.

Etzold, M., Lendner, M., Daugschies, A., Dyachenko, V., 2014. CDPKs of Cryptosporidium parvum—stage-specific expression *in vitro*. Parasitol. Res. 113 (7), 2525-2533.

European Food Safety Authority, 2010. Scientific statement on bovine besnoitiosis. , Available from <http://www.efsa.europa.eu>.

Fernández-García, A., Risco-Castillo, V., Pedraza-Díaz, S., Aguado-Martínez, A., Álvarez-García, G., Gómez-Bautista, M., Collantes-Fernández, E., Ortega-Mora, L.M., 2009a. First isolation of *Besnoitia besnoiti* from a chronically infected cow in Spain. J. Parasitol. 95 (2), 474-476.

Fernández-García, A., Álvarez-García, G., Risco-Castillo, V., Aguado-Martínez, A., Marugán-Hernández, V., Ortega-Mora, L.M., 2009b. Pattern of recognition of B*esnoitia besnoiti t*achyzoite and bradyzoite antigens by naturally infected cattle. Vet. Parasitol. 164 (2-4), 104-110.

Franc, M., Cardiegues, M., 1999. La besnoitiose bovine: attitude diagnostique et therapeutique. Bulletin des GTV. Bovins, Parasitologie , 119-124.

Frey, C.F., Regidor-Cerrillo, J., Marreros, N., García-Lunar, P., Gutiérrez-Expósito, D., Schares, G., Dubey, J.P., Gentile, A., Jacquiet, P., Shkap, V., Cortes, H., Ortega-Mora, LM., Álvarez-García, G., 2016. *Besnoitia besnoiti* lytic cycle in vitro and differences in invasion and intracellular proliferation among isolates. Parasites & vectors 9 (1), 1.

Greenbaum, D.C., 2008. Is chemical genetics the new frontier for malaria biology? Trends Pharmacol. Sci. 29 (2), 51-56.

Gutiérrez-Expósito, D., Ortega-Mora, L.M., Marco, I., Boadella, M., Gortazar, C., San Miguel-Ayanz, J.M., García-Lunar, P., Lavin, S., Álvarez-García, G., 2013. First serosurvey of *Besnoitia* spp. infection in wild European ruminants in Spain. Vet. Parasitol. 197 (3-4), 557-564.

Hines, S.A., Ramsay, J.D., Kappmeyer, L.S., Lau, A.O., Ojo, K.K., Van Voorhis, W.C., Knowles, D.P., Mealey, R.H., 2015. *Theileria equi* isolates vary in susceptibility to imidocarb dipropionate but demonstrate uniform *in vitro* susceptibility to a bumped kinase inhibitor. Parasit. Vectors 8(1), 33.

Huang, W., Ojo, K.K., Zhang, Z., Rivas, K., Vidadala, R.S.R., Scheele, S., DeRocher, A.E., Choi, R., Hulverson, M.A., Barrett, L.K., Bruzual, I., Diddaramaiah, L.K., Kerchner, L.M., Kurnick, M.D., Freiberg, G.M., Kempf, D., Hol, W.G., Merrit, E.A., Neckermann, G., de Hostos, E.I., Isoherranen, N., Maly, D.J., Parsons, M., Dogget, J.S., Van Voorhis, W.C., Fan, E., 2015. SAR studies of 5-aminopyrazole-4-carboxamide analogues as potent and selective inhibitors of *Toxoplasma gondii* CDPK1. ACS Med. Chem. Lett. 6 (12), 1184-1189.

Hui, R., El Bakkouri, M., Sibley, L.D., 2015. Designing selective inhibitors for calcium-dependent protein kinases in apicomplexans. Trends Pharmacol. Sci. 36 (7), 452-460.

Hulverson, M.A., Vinayak, S., Choi, R., Schaefer, D.A., Castellanos-Gonzalez, A., Vidadala, R.S., Brooks, C.F., Herbert, G.T., Betzer, D.P., Whitman, G.R., Sparks, H.N., Arnold, S.L.M., Rivas, K.L., Barret, L.K., White, A.C.Jr., Maly, D.J., Riggs, M.W., Striepen, B., Van Voorhis, W.C., Maly, D.J. 2017. Bumped-Kinase Inhibitors for Cryptosporidiosis Therapy. J. Infect. Dis. 215 (8), 1275-1284.

Keyloun, K.R., Reid, M.C., Choi, R., Song, Y., Fox, A.M., Hillesland, H.K., Zhang, Z., Vidadala, R., Merritt, E.A., Lau, A.O., Maly, D.J., Fan, E., Barrett, L.K., van Voorhis, W.C., Ojo, K.K., 2014. The gatekeeper residue and beyond: homologous calcium-dependent protein kinases as drug development targets for veterinarian Apicomplexa parasites. Parasitology 141 (11), 1499-1509.

Lendner, M., Böttcher, D., Delling, C., Ojo, K.K., Van Voorhis, W.C., Daugschies, A., 2015. A novel CDPK1 inhibitor—a potential treatment for cryptosporidiosis in calves? Parasitol. Res. 114 (1), 335-336.

Lourido, S., Shuman, J., Zhang, C., Shokat, K.M., Hui, R., Sibley, L.D., 2010. Calcium-dependent protein kinase 1 is an essential regulator of exocytosis in *Toxoplasma*. Nature 465 (7296), 359-362.

Lourido, S., Moreno, S.N., 2015. The calcium signaling toolkit of the Apicomplexan parasites *Toxoplasma gondii* and *Plasmodium* spp. Cell Calcium 57 (3), 186-193.

Müller, J., Aguado-Martínez, A., Balmer, V., Maly, D.J., Fan, E., Ortega-Mora, L., Ojo, K.K., Van Voorhis, W.C., Hemphill, A., 2017b. Two novel calcium-dependent kinase 1-inhibitors interfere with vertical transmission in mice infected with *Neospora caninum* tachyzoites. Antimicrob. Agents Chemother. 02324-16.

Ojo, K.K., Larson, E.T., Keyloun, K.R., Castaneda, L.J., DeRocher, A.E., Inampudi, K.K., Kim, J.E., Arakaki, T.L., Murphy, R.C., Zhang, L., 2010. *Toxoplasma gondii* calcium-dependent protein kinase 1 is a target for selective kinase inhibitors. Nature Struct. Mol. Bio. 17 (5), 602-607.

Ojo, K.K., Pfander, C., Mueller, N.R., Burstroem, C., Larson, E.T., Bryan, C.M., Fox, A.M., Reid, M.C., Johnson, S.M., Murphy, R.C., Kennedy, M., Mann, H., Leibly, D.J., Hewitt, S.N., Verlinde, C.L., Kappe, S., Merritt, E.A., Maly, D.J., Billker, O., Van Voorhis, W.C., 2012. Transmission of malaria to mosquitoes blocked by bumped kinase inhibitors. J. Clin. Invest. 122 (6), 2301-2305.

Ojo, K.K., Reid, M.C., Kallur Siddaramaiah, L., Muller, J., Winzer, P., Zhang, Z., Keyloun, K.R., Vidadala, R.S., Merritt, E.A., Hol, W.G., Maly, D.J., Fan, E., Van Voorhis, W.C., Hemphill, A., 2014. *Neospora caninum* calcium-dependent protein kinase 1 is an effective drug target for neosporosis therapy. PLoS One 9 (3), e92929.

Ojo, K.K., Dangoudoubiyam, S., Verma, S.K., Scheele, S., DeRocher, A.E., Yeargan, M., Choi, R., Smith, T.R., Rivas, K.L., Hulverson, M.A., 2016. Selective inhibition of *Sarcocystis neurona* calcium-dependent protein kinase 1 for equine protozoal myeloencephalitis therapy. Int. J. Parasitol. 46 (13), 871-880.

Pedroni, M.J., Vidadala, R.S.R., Choi, R., Keyloun, K.R., Reid, M.C., Murphy, R.C., Barrett, L.K., Van Voorhis, W.C., Maly, D.J., Ojo, K.K., 2016. Bumped kinase inhibitor prohibits egression in Babesia bovis. Vet. Parasitol. 215, 22-28.

Pols, J.W., 1960. Studies on bovine besnoitiosis with special reference to the aetiology. Onderstepoort Jour Vet Res 28 (3), 265-356.

Schaefer, D.A., Betzer, D.P., Smith, K.D., Millman, Z.G., Michalski, H.C., Menchaca, S.E., Zambriski, J.A., Ojo, K.K., Hulverson, M.A., Arnold, S.L., Rivas, K.L., Vidadala, R.S., Huang, W., Barret, L.K., Maly, D.J., Fan, E., Van Voorhis, W.C., Riggs, M.W., 2016. Novel Bumped Kinase Inhibitors are safe and effective therapeutics in the calf clinical model for cryptosporidiosis. J. Infect. Dis. 214 (12), 1856-1864.

Shkap, V., De Waal, D.T., Potgieter, F.T., 1985. Chemotherapy of experimental *Besnoitia besnoiti* infection in rabbits. Onderstepoort J. Vet. Res. 52 (4), 289.

Shkap, V., Pipano, E., Ungar-Waron, H., 1987. *Besnoitia besnoiti*: chemotherapeutic trials *in vivo* and *in vitro*. Rev. Elev. Med. Vet. Pays. Trop. 40 (3), 259-264.

Srinivasan, N., Krupa, A., 2005. A genomic perspective of protein kinases in *Plasmodium falciparum*. Proteins: Struct. Funct. Bioinf. 58 (1), 180-189.

Sugi, T., Kobayashi, K., Takemae, H., Gong, H., Ishiwa, A., Murakoshi, F., Recuenco, F.C., Iwanaga, T., Horimoto, T., Akashi, H., 2013. Identification of mutations in TgMAPK1 of *Toxoplasma gondii* conferring resistance to 1NM-PP1. Int. J. Parasitol. Drugs Drug Resist. 3, 93-101.

Sugi, T., Kawazu, S., Horimoto, T., Kato, K., 2015. A single mutation in the gatekeeper residue in TgMAPKL-1 restores the inhibitory effect of a bumped kinase inhibitor on the cell cycle. Int. J. Parasitol. Drugs Drug Resist 5 (1), 1-8.

Van Voorhis, W.C., Doggett, J.S., Parsons, M., Hulverson, M.A., Choi, R., Arnold, S., Riggs, M.W., Hemphill, A., Howe, D.K., Mealey, R.H., Lau, A.O.T., Merrit, E.A., Maly, D.J., Fan, E., Ojo, K.K., 2017. Extended-spectrum antiprotozoal bumped kinase inhibitors: A review. Exp. Parasitol. 180, 71-83.

Vidadala, R.S.R., Rivas, K.L., Ojo, K.K., Hulverson, M.A., Zambriski, J.A., Bruzual, I., Schultz, T.L., Huang, W., Zhang, Z., Scheele, S., DeRocher, A.E., Choi, R., Barrett, L.K., Siddaramaiah, L.K., Hol, W.G., Fan, E., Merritt, E.A., Parsons, M., Freiberg, G., Marsh, K., Kempf, D.J., Carruthers, V.B., Isoherranen, N., Doggett, J.S., Van Voorhis, W.C., Maly, D.J., 2016. Development of an Orally Available and Central Nervous System (CNS) Penetrant *Toxoplasma gondii* Calcium-Dependent Protein Kinase 1 (Tg CDPK1) Inhibitor with Minimal Human Ether-a-go-go-Related Gene (hERG) Activity for the Treatment of Toxoplasmosis. J. Med. Chem. 59 (13), 6531-6546.

Ward, P., Equinet, L., Packer, J., Doerig, C., 2004. Protein kinases of the human malaria parasite *Plasmodium falciparum*: the kinome of a divergent eukaryote. BMC Genomics 5 (1), 79.

Winzer, P., Muller, J., Aguado-Martinez, A., Rahman, M., Balmer, V., Manser, V., Ortega-Mora, L.M., Ojo, K.K., Fan, E., Maly, D.J., Van Voorhis, W.C., Hemphill, A., 2015. *In Vitro* and *In Vivo* Effects of the Bumped Kinase Inhibitor 1294 in the Related Cyst-Forming Apicomplexans *Toxoplasma gondii* and *Neospora caninum*. Antimicrob. Agents Chemother. 59 (10), 6361-6374.

Yang, J., Yan, R., Roy, A., Xu, D., Poisson, J., Zhang, Y., 2015. The I-TASSER Suite: protein structure and function prediction. Nat. Methods 12 (1), 7-8.

CAPÍTULO V: DISCUSIÓN GENERAL/GENERAL DISCUSSION

In view of the many gaps regarding *Besnoitia besnoiti* biology, the present doctoral thesis covers one general objective, which is the development of standardized *in vitro* models of *B. besnoiti* infection in bovine target cells and, later on, two specific objectives regarding the employment of these standardized *in vitro* models in molecular pathogenesis (Subobjective 2.1) and drug screening studies (Subobjectives 2.2.1 and 2.2.2).

For this purpose, in the first objective, key target cells of the parasite during both acute (endothelial cells, ECs) and chronic (fibroblasts) stages of bovine besnoitiosis were isolated from catle whose health status had been previously checked. Endothelial cells have been postulated to be one of the main target cells during the acute stage of bovine besnoitiosis, even though few studies have been able to demonstrate the presence and multiplication of the parasite inside ECs *in vivo* (Langenmayer *et al.*, 2015c). On the other hand, cyst formation during the chronic stage of the disease has been described in cells with a myofibroblastic origin (Basson *et al.*, 1970; Dubey *et al.*, 2013). For the isolation of the primary cultures, several key aspects have been considered. First, primary cell cultures have been chosen, since immortalized cell lines may show phenotypic modifications due to *in vitro* pressure and may lose specific functions of their original tissue (Pan *et al.*, 2009), which may influence the host-parasite interaction and thus differ from what happens under *in vivo* conditions. Second, the target host species (bovine species) and the tissue location (large vessel) origin of isolated cells have been taken into consideration. Third, the absence of frequent contaminants of mammalian cell cultures was checked in a two-step process; donor animals were carefully monitored for the absence of prevalent bovine pathogens (such as bovine viral diarrhea virus, BVDV) and all reagents employed in cell culture were proven to be free from frequent contaminants in mammalian cell culture systems such as *Mycoplasma* spp. and BVDV (Uryvaev *et al.*, 2012). Besides, BVDV is responsible for transcriptomic changes in persistently infected ECs (Neill *et al.*, 2008), so it may influence the host-parasite interaction in pathogenesis studies.

Once primary bovine aorta ECs (BAEC) and fibroblasts were isolated, morphology results, as well as surface and intracellular markers determined by flow cytometry, evidenced their endothelial and fibroblast origin, respectively. Endothelial cells under *in vitro* conditions grow in a single layer of cells with a cobblestone pattern (Wise et al., 2002), meanwhile fibroblasts presented a spindle-shaped morphology (DiPietro and Burns, 2003). In agreement with the literature, the surface marker which better discriminated between both cell cultures was CD31 (or PECAM), which is essential to maintain integrity and control permeability of the endothelial barrier (Lertkiatmongkol *et al.*, 2016). Interestingly, despite the homogeneous morphology shown by both low-passage and high-passage BAEC, changes in CD31 expression were found, being lower in high-passage BAEC. This finding strengthens the hypothesis that phenotypic changes may happen under *in vitro* conditions and the employment of low passage primary cells is desirable. Both BAEC and fibroblasts were found to be positive for vimentin, cytokeratin and CD44 markers, which was indicative of a mesenchymal origin for both cell cultures.

Next, tachyzoites from the Bb-Spain1 isolate showed similar features to those previously described in monkey kidney Marc-145 cells (Frey *et al.*, 2016; Diezma-Díaz *et al.*, 2017). Thus, this isolate behaves similarly regardless the cell line, and was again categorized as a low invader (since invasion rates -IR- were not higher than 4.5% in both cell lines) and a low proliferating isolate. Other studies addressing the invasive capabilities of *B. besnoiti* tachyzoites in bovine umbilical vein endothelial cells (BUVEC) have described IRs up to 30%, but differences in the experimental setup were found that make difficult to compare both studies: i) a higher multiplicity of infection (3 to 5) was employed and ii) the number of parasite *in vitro* passages was not specified (Taubert *et al.*, 2016). One key aspect that should be considered is that *in vitro* adaptation is a common feature in apicomplexan parasites, and it has been shown to influence both *in vitro* behavior and *in vivo* virulence

both in *N. caninum* (Bartley *et al.*, 2006) and *T. gondii* (Nischik *et al.,* 2001). Thus, a robust *in vitro* system aiming to mimic what happens under *in vivo* conditions should consider the employment of low passage isolates in order to obtain reproducible results.

For other apicomplexan parasites, a clear influence of the host cell type employed in *in vitro* assays has been previously described. For example, tachyzoite to bradyzoite switch seems to be favored in differentiated cell types, such as keratinocytes for *N. caninum* (Vonlaufen *et al.*, 2002b) or in skeletal muscle cells for *T. gondii* (da Fonseca Ferreira-da-Silva *et al.,* 2009; Guimarães *et al.,* 2008). Also, in *Eimeria* spp, the formation of meronts I has only been described in cells with a bovine origin, both in epithelial and ECs (Hermosilla *et al.*, 2002). It was also shown for *B. besnoiti* a predilection of this parasite to proliferate inside NA42/13 cells, followed by BHK21 and KH-R cell lines, irrespective of the host origin (Schares *et al.*, 2009). Thus, despite *B. besnoiti* tachyzoites displayed a similar lytic cycle in these target cells, they should be employed in studies of host-pathogen interactions.

However, the *in vitro* systems developed herein could be further optimized. BAEC come from the aorta, which is a large vessel exposed to high blood flows *in vivo*, which may influence the adhesion capabilities of *B. besnoiti* tachyzoites. However, in *T. gondii*, shear stress forces have been shown to increment their adhesion to ECsEC under *in vitro* conditions, which are accompanied by changes in the cytoskeleton of the cells (Harker *et al.*, 2014). Thus, in order to address further studies, a broader panel of ECs isolated from different locations where the parasitic growth is favoured *in vivo*, such as microvasculature from nasal turbinates and reproductive tract should be taken into consideration (Álvarez-García *et al.*, 2014b). Also, it is widely known that ECs from microvasculature present some phenotypic and functional differences when compared to ECs isolated from large vessels (Aird, 2012), and a different tropism of *B. besnoiti* alongside the circulatory system of infected animals has been described (McCully *et al.*, 1966). Similarly, fibroblasts could be isolated from bovine skin to carry out further experiments such as tachyzoite to bradyzoite switch assays.

Additionally, we addressed the possible influence of a frequent bovine pathogen such as BVDV on *B. besnoiti in vitro* infection. Our results showed that BVDV coinfection favored early tachyzoite invasion of BAEC cells, which could explain a slight increase in the tachyzoite yield observed in BVDV infected BAEC. However, the total number of invasion events remained unchanged. In this sense, epidemiological studies addressing coinfections between *B. besnoiti* and BVDV are necessary to clarify the possible synergism suggested *in vitro*. In other bovine pathogens, *in vivo* studies have shown inconclusive results, since some studies have found an association with BVDV and abortions due to *N. caninum* (Vanleeuwen *et al.*, 2009; Bjorkman *et al.*, 2000), whilst other claimed that there was no association (Mainar-Jaime *et al.*, 2001). Regarding *in vitro* coinfections, a recent study performed with the intracellular pathogen *Mycoplasma bovis* evidenced that BVDV infection did not influence on the bacteria *in vitro* behaviour assessed in bovine macrophages (Bomac) (Bürgi *et al.*, 2018).

In the second objective of the present doctoral thesis, the usefulness of *in vitro* models for the study of the biology of *B. besnoiti* has been explored. First, BAEC obtained in the objective 1 have been used to address *B. besnoiti* tachyzoites-BAEC molecular interactions by means of RNASeq in the subobjective 2.1. The results have shown an early BAEC modulation upon *B. besnoiti* invasion, characterized by a proinflammatory and procoagulant state, with a progression of endothelial activation with the upregulation of fibrosis markers along the lytic cycle. At 12 h pi, even though a low number of differentially expressed genes (DEG) were found when compared to the uninfected BAECs. Our results showed the upregulation of the tricarboxylic acid pathway in infected cells as a key source of energy for the tachyzoites, in agreement with early works performed by Fernández-

García *et al*. (2013). In addition, Taubert et al., (2016) also showed an upregulation of glycolysis and glutaminolysis in bovine umbilical vein endothelial cells (BUVEC) *in vitro*. Also, a downregulation of genes involved in ECs protection (eg. NOX5, SOD3 and Serpine5) were indicative of endothelial dysfuction. Besides, genes belonging to a disintegrin and metalloproteinase with thrombospondin motifs (ADAMTS) family were overexpressed at 12 hpi, such as ADAMTS1 and ADAMTSL2. These findings may suggest an effect on extracellular matrix organization (ECM) upon tachyzoite invasion. ADAMTS1 has been previously shown to contribute to the dissemination of *Toxoplasma* infected leukocytes into immune-privileged sites (Seipel *et al.*, 2010).

When infected BAEC at the two post-infection times assayed (12 and 32 hpi) were compared, a higher number of DEG were identified, along with numerous enriched pathways, showing a phenotype compatible with a type II endothelial activation (Gimbrone Jr & García-Cardeña, 2016). This hypothesis was supported by the upregulation of genes responsible for the loss of vascular integrity, leukocyte adhesion molecules and coagulation. First, the loss of vascular integrity was evidenced by several genes associated with ECM organization, such as ADAMTS as both pi times, and matrix metalloproteinases (such as MPP14) at 12 hpi. Those molecules have been shown to be also modulated in infections by closely related parasites, *T. gondii* and *N. caninum*, with importance for crossing biological barriers (Horcajo *et al.*, 2017). Additionally, other ECM-related molecules, such as several integrins, fibronectin, collagen and claudin 1 were modulated. Second, the expression of surface markers responsible for an increase in leukocyte adhesion was shown at 12 hpi. For example, selectins (SELE and SELP), ICAM-1, VCAM-1 were found to be upregulated at 12 hpi. Accordingly, the KEGG pathway for TNFa, a potent proinflammatory molecule, was found to be enriched in our subset of DEG. Also, IL-6 and IL-1A were found to be upregulated at 12 hpi. These molecules could establish a proinflammatory loop in the endothelium and attract distinct populations of leukocytes. In all these processes, the transcription factor NFkB seems to play a pivotal role since it coordinates the expression of effector proteins that appeared as DEG, such as E-Selectin (SELE), VCAM1, IL-6 and CCL-2. Moreover, several inhibitors and NFκB2 genes were upregulated at 12 hpi indicating that this pathway might be modulated upon parasite-infection.

Thus, our results partially agree with findings previously reported by Maksimov et al., (Maksimov *et al.*, 2016), where the transcription of several genes (*n*=12) that encode adhesion molecules, chemokines and regulatory molecules was studied by qPCR in BUVEC-infected cells. However, few statistically significant results were observed, corresponding to the upregulation of ICAM at 24 hpi, P-SELE at 6 and 12 hpi, chemokines (CXCL-1, CXCL-8 and CCL5) between 6 and 48 hpi and regulatory molecules (IL-6 and COX-2) at 48hpi. In contrast, the relevance of other molecules such as VCAM was suspected but no statistically significant differences were found. These differences might be explained by differences in the experimental design, including the host cells (BUVEC), *B. besnoiti* isolate (Bb1Evora04) and MOI employed.

Also, genes involved in fibrinolysis pathways have been found to be DE, with the upregulation of molecules with fibrinolytic properties such as plasminogen activator, urokinase receptor (PLAUR) and plasminogen activator, tissue type (PLAT). In addition, fibronectin and thrombospondin are adhesins which favour the platelet adhesion that were also upregulated at 32 hpi.

Another important phenomenon which occured after *B. besnoiti* infection is a pro-fibrotic phenotype in infected BAEC, characterized by the expression of several fibrosis markers, including chemokines responsible for the recruitment of monocytes and macrophages, such as CCL2, IL6 and IL1A, and mediators of macrophage differentiation, such as macrophage colony stimulating factor 1 (MCSF-1) at 12 hpi. This macrophage

recruitment could explain the predominance of activated macrophages among the leukocyte populations in the inflammatory foci around tissue cysts in chronic besnoitiosis (Frey *et al.*, 2013). Besides, CCL2 is able to mediate the activation of fibroblasts to produce TGF-β and thus, to stimulate collagen synthesis (Gharaee-Kermani *et al.*, 1996). Moreover, the KEGG pathway for TGF-β was enriched in our subset of DEG. Since scleroderma is commonly associated with the chronic stage of bovine besnoitiosis, CCL2 may play a key role in the pathogenesis of bovine besnoitiosis. Other relevant DEG were proheparin-binding EGF-like growth factor, which is involved in macrophage mediated cellular proliferation and has mytogenic properties for fibroblasts (Jin *et al.*, 2002), and integrins that allow the anchoring of ECs to components of ECM such as fibronectin or collagen, and regulating the TGFβ pathway (Henderson *et al.*, 2013).

Finally, angiogenesis was represented by several DEG in the present work, since DEG involved in both early (growth factors and matrix metalloproteinases) and late steps (integrins and vasohibin) were found. This multistep process involves several mechanisms, from the activation of endothelial cells leading to a degradation of the endothelial barrier mediated by proteases (such as MMP or ADAMTS), to the reorganization and migration of endothelial cells to form a capillary network.

All those findings were corroborated by qPCR, since a panel of *Bos Taurus* genes (n=16) showed a similar profile of expression as described for the RNA-Seq results.

In addition, the present work explored the transcriptome of *B. besnoiti* tachyzoites at two times pi. The results have shown that up to 106 *B. besnoiti* genes are DE, most of them (n=98) being upregulated at 32 hpi. Among these, *Besnoitia* orthologue genes involved in the lytic cycle of closely related Toxoplasmatinae parasites were identified and upregulated at 32 hpi, coding for surface proteins (e.g SRS22A), microneme proteins (e.g MIC2, MIC11), AP-2 transcription factors (A2X6), rhoptry-kinases, (ROP5B, ROP17, ROP40) rhoptry neck kinases (RON6, RON8). Those proteins have been described for the first time, since the identification of these genes in previous works using a proteomic approach was hampered by the lack of the whole genome sequence (Garcia-Lunar *et al.*, 2014; Fernandez-Garcia *et al.*, 2013; Fernandez-Garcia *et al.*, 2013). Also, several *B. besnoiti* orthologues exclusively present in apicomplexan parasites were expressed at both pi time points, such as genes encoding for dense granule proteins (GRAs) or calcium-dependent kinases (CDPKs) without differences in their expression profiles. This has been previously reported for GRA and ROP proteins in *N. caninum* (Pastor-Fernández *et al.,* 2016a, b) and *T. gondii* (Radke *et al.,* 2005), evidencing an important role of these proteins in the maturation of the parasitophorous vacuole and egress. Another important family described is calcium dependant kinases (CDPKs), which have arised as potential drug targets in apicomplexan parasites, leading to the discovery of specific specific bumped kinase inhibitors (BKIs), which are indeed effective against *B. besnoiti* tachyzoites *in vitro* (Jiménez-Meléndez et al., 2017). Also, Aspartyl proteases, another family important in the cleaving of proteins and of increasing interest in the drug design against *T. gondii,* have been detected (Dogga *et al.*, 2017). Results from the parasite transcriptome were also corroborated by qPCR validation, showing a similar profile to the RNA-Seq results.

In conclusion, this work represents the first study addressing the interaction between *B. besnoiti* tachyzoites and BAEC by using a transcriptomics approach using RNASeq. The different steps of ECs activation were progressively induced and correlated with microscopic lesions described in tissues from naturally and experimentally infected cattle. A rapid progression of a proinflammatory, procoagulant and profibrotic state was triggered upon parasite invasion. Additionally, we have identified for the first time many *B. besnoiti* genes, orthologues of other Toxoplasmatinae parasites, some of which were upregulated during proliferation. This work may help to search for potential drug and vaccine targets and

promising markers of disease and prognosis (eg. CCL2 as a fibrosis marker), that should be further studied *in vivo*.

Next, drug screening studies have been performed, assessing both commercially available drugs (subobjective 2.2.) and new generation drugs (subobjective 2.3). However, since the lytic cycle of *B. besnoiti* tachyzoites in primary bovine target cells did not show remarkable differences regarding invasion and proliferation capacities compared with Marc-145 cell line, the *in vitro* model based on Marc-145 cells was used representing a more economic approach. The employment of an immortalized cell line avoids the continuous isolation of primary cells and the inherent variability of primary cultures associated to donors. In the Subobjective 2.2., we have applied the principle of drug repurposing, since it represents an affordable strategy exploited in other apicomplexan parasites to find drugs commercially available in the short-medium run. Thus, we addressed the safety and efficacy of a panel of drugs already commercialized in cattle to treat several infectious diseases.

Among those products which are licensed in Europe, we selected decoquinate (DQ), two folate inhibitors (sulfadiazines and trimethoprim, alone or in combination with sulfadiazines), one diamidine (imidocarb) and two triazinones (diclazuril and toltrazuril). These drugs had previously shown efficacy against other coccidian parasites (Sanchez-Sanchez *et al.*, 2018).

Results obtained showed that none of the compounds exhibited cytotoxicity in the *in vitro* model employed when compared to the vehicle controls (DMSO or a mixture of NaOH/MetOH for decoquinate). When further assays were performed, the results from the drug screening by immunofluorescence showed that almost all of them were able to inhibit the invasion and growth of *B. besnoiti* tachyzoites when compared to the vehicle-treated cultures. However, toltrazuril was cytotoxic at concentrations higher than 30 µM, the efficacy of all the compounds (except for imidocarb) was higher when they were administered at the moment of infection (at 0 hpi), and decoquinate and diclazuril were the most efficacious compounds, reaching values close to 90% of parasite growth inhibition. Besides, in toltrazuril, diclazuril and decoquinate-treated wells, lysis plaques were absent, indicative of parasite growth alteration. Thus, decoquinate and diclazuril were selected for further efficacy studies.

The results obtained showed that decoquinate was able, not only to affect extracellular parasites, but it also interfered with proliferation of intracellular tachyzoites. This finding contrasts with previous studies performed in *N. caninum*, where decoquinate showed a minimum effect against extracellular zoites. This finding may be explained by a less active mitochondria in extracellular tachyzoites of *N. caninum* (Lindsay *et al.,* 1997). Moreover, it was demonstrated that decoquinate is able to affect oxygen consumption of extracellular *T. gondii* tachyzoites (Pfefferkorn *et al.*, 1993). This finding may suggest that decoquinate can present a higher activity against parasites with a longer extracellular survival capacity, such as *B. besnoiti* (Frey *et al.*, 2016). Interestingly, we obtained IC_{50} values in the low nanomolar range (10 nM), in agreement with previous studies that have shown decoquinate to have *in vitro* activity against *T. gondii* tachyzoites with IC_{50} of 0.005 µg/ml (12 nM) (Ricketts & Pfefferkorn, 1993). Although decoquinate is specifically designed to treat gastrointestinal coccidiosis in several species (e.g cattle, small ruminants and poultry) at concentrations around 0.5 mg/Kg bw, it is well absorbed and reaches maximum plasma concentrations of 2 µM in milking cows (Quintero de Leonardo *et al.*, 2009), which are higher than the IC_{50} and IC_{99} found *in vitro*. Accordingly, it may represent a valuable therapeutic tool to control acute clinical cases of bovine besnoitiosis as food additive at the recommended posology. However, this drug showed a parasitostatic effect, since tachyzoites were able to proliferate when the treatment was suspended. This finding has been described as characteristic of hydroxiquinoxalines (Mehlhorn, 2008). This parasitostatic

effect could be desirable since treated *Besnoitia* tachyzoites might be an antigenic stimulus and would allow the development of a strong immune response against the parasite, potentially preventing reinfection after recovering from the acute infection, as it has been postulated for other compounds such as BKIs (Winzer *et al.*, 2015). Electron microscopy showed that the mitochondrium is, as expected, the main site of action of decoquinate. However, after 6 days of treatment, mitochondrial impairment led to more dramatic alterations and a general breakdown of the structural organization of the parasite with deposits of amylopectin granules in the cytoplasm, maybe responsible for a loss of parasite viability. This finding may indicate a transitional stage from tachyzoite to bradyzoite, as it has been described previously for tachyzoites from the RH strain of *T. gondii* treated with decoquinate (Lindsay *et al.*, 1998). Thus, decoquinate could represent a stressing agent to induce tachyzoite to bradyzoite switch *in vitro*. However, this question needs further clarification, since the viability of those damaged tachyzoites was not assessed.

Diclazuril was able to inhibit both parasite invasion and proliferation, in agreement with previous results reported for *T. gondii* (Lindsay & Blagburn, 1994) and *N. caninum* (Lindsay *et al.*, 1994). However, our results showed that higher concentrations are needed to clear *B. besnoiti*, since the IC50 was ten times higher than the one described for *T. gondii*. However, we showed that treatments with the IC_{99} for at least 48 h are able to exert a parasiticidal effect on *B. besnoiti* tachyzoites, since lysis plaques were absent and the parasitic load was clearly diminished in those wells. These results are in agreement with TEM results, since after 6 days of treatment almost no viable parasites were present and a clear effect on the cytokinesis of daughter zoites, with the formation of multinucleated complexes was visualized. These findings are similar to those previously described for *T. gondii* tachyzoites treated with diclazuril, since an effect on endodiogeny together with the presence of multi-nucleated complexes were observed (Lindsay *et al.*, 1995). Opposite to our results, ultrastructural effects of diclazuril were not noted until 2 days after treatment whilst in *B. besnoiti* we have observed that the first effects appeared after 24 h of treatment. In cattle, this compound is marketed against gastrointestinal coccidiosis, and the bioavailability of the compound is low, reaching maximum plasmatic concentrations of 95.8 nM (EMEA, 2004), which are below the effective concentrations needed *in vitro*. Thus, further pharmacokinetics studies assessing different dosages and possibly also new formulations are needed to obtain a higher bioavailability of this compound in cattle.

Imidocarb dipropionate was discarded in our experimental settings, since it failed to exert more than 30 % parasite invasion and proliferation inhibition. No previous *in vitro* treatments with this compound against *T. gondii* or *N. caninum* have been reported. When similar series of compounds, diminazene aceturate and pentamidines were studied they were not effective against *B. besnoiti* in an *in vitro* model using epithelial-like Vero cells (Shkap *et al.*, 1987b). Besides, it has been postulated that the activity of imidocarb may resemble that of the trypanocidal and babesicidal berenil (diminazene aceturate) (Mehlhorn, 2008b), binding to DNA in the minor groove of the kinetoplast, which is absent in apicomplexan parasites. Finally, regarding DHFR and DHFS inhibitors, alone or in combination, sulfadiazine failed to inhibit parasite growth by more than 50%, even when it was co-administered with trimethoprim at the time point of infection. Previous *in vitro* studies regarding Toxoplasmatinae parasites have shown variable results, since sulfadiazine is highly efficacious against *T. gondii* with IC_{50} in the range of 2.5 µg/mL (Sanchez-Sanchez *et al.*, 2018) whilst little activity was exerted against *N. caninum* at concentrations up to 100 µg/ml (400 µM) and longer treatments were needed (Lindsay *et al.*, 1994). This finding agrees with our results where low parasitic growth inhibition was observed when treatments lasted for 3 or 6 days. Besides, previous studies carried out in *Besnoitia* have also reported variable results. Sulfadiazine lacked efficacy upon *B. besnoiti* infection in gerbils (Shkap *et al.*, 1987b), whereas in other *Besnoitia* species, such as *B. darlingi,* treatment with sulfadiazine was able

to diminish parasitic growth *in vitro* at concentrations higher than 4 µM in an 8 day-assay (50% growth inhibition) (Elsheikha & Mansfield, 2004). *In vivo* information regarding sulfonamide therapy in bovine besnoitiosis indicate that they were commonly used under field conditions to diminish the severity of clinical signs, but they usually failed to cure the infected cattle, even if the treatment was administered when first clinical signs appeared (Jacquiet *et al.*, 2010). The lack of efficacy of sulphadiazine observed *in vitro* may explain this *in vivo* variability. Trimethoprim also failed to exert a potent parasite growth inhibition *in vitro*. However, a strong inhibition of *T. gondii* growth has been observed with an IC_{50} of 2.3 µg/ml, with striking morphological changes of the parasites (Sánchez-Sánchez *et al.*, 2018). In addition, trimethoprim is also effective against *N. caninum* tachyzoites at 10 µg/ml (Lindsay *et al.*, 1994).

However, there are other commercially available compounds that may be worth trying for efficacy against *B. besnoiti* tachyzoites *in vitro*. For example, macrolide antibiotics, (e.g spiramycin), which are antimicrobial agents able to inhibit bacterial protein synthesis and effective against gram-positive, gram-negative bacteria and protozoan parasites, including *T. gondii* (Sánchez-Sánchez *et al.,* 2018). Also, polyether ionophores (e.g monensin, lasalocid), which induce ionic gradient perturbations, acting on different metabolic pathways (Couzinet *et al.*, 2000), and showing broad spectrum bioactivity, including antibacterial, antifungal, antiparasitic and antiviral effects (Rutkowski & Brzezinski, 2013). These compounds have also shown great *in vitro* activities against apicomplexan parasites (Ricketts & Pfefferkorn, 1993), as well as some promising *in vivo* results (Buxton *et al.*, 1988). Monensin has been shown to have coccidiostatic effects (Bergstrom & Maki, 1976) and growth promoting properties by favouring ruminal propionic acid production (Richardson *et al.*, 1976). However, European Union regulations on the additives for use in animal nutrition banned the use of growth promoting agents as feed additives in animals (Sánchez-Sánchez *et al.,* 2018).

In the third subobjective, a panel of new generation bumped kinase inhibitors (BKIs) has been assayed to test their safety and efficacy against *B. besnoiti* tachyzoites *in vitro*. It is widely known the key role that calcium plays as a second messenger involved in several cellular processes. A family named as calcium dependent protein kinases (CDPKs) is present in apicomplexan parasites, ciliates parasites and algae but absent in mammalian cells, which makes them attractive drug targets. They control a wide range of processes including egress (TgCDPK1 and TgCDPK3), microneme secretion (TgCDPK1), motility (TgCDPK1), or cell division (TgCDPK7) (Lourido *et al.*, 2010, 2012, 2013; Garrison *et al.*, 2012; McCoy *et al.*, 2012; Morlon-Guyot *et al.*, 2014). Besides, some key structural properties of CDPK1 have allowed the development of BKIs, a class of pyrazolopyrimidine inhibitors with bulky moieties able to block the ATP binding site, originally developed as antimalarial agents (Van Voorhis *et al.*, 2017).

First, a CDPK1 homologue in *B. besnoiti* tachyzoites, namely *Bb*CDPK1 was demonstrated. This homologue showed a high sequence identity with CDPK1 enzymes from other Toxoplasmatinae members (*T. gondii* and *N. caninum*), including a glycine in the gatekeeper position, an N-terminal serine-threonine kinase domain, a junctional domain and a series of calcium-binding domains known as EF hands. The existence of EF hands suggest that *Bb*CDPK1 might play an important role in regulating calcium-dependent pathways (Hui *et al.*, 2015). Kinase assays showed that a panel of nine selected BKIs inhibited the *Bb*CDPK1 enzyme activity even at low nanomolar range concentrations, as for NcCDPK1 and *Tg*CDPK1. This finding was explained by the high kinase domain sequence identity found with other Toxoplasmatinae members, where *Bb*CDPK1 identity was as high as 98% and 98.4% with *Tg*CDPK1 and *Nc*CDPK1, respectively. However, further studies with transgenic parasites are needed to definitively claim that the phenotype of BKI treated parasites is solely due to*Bb*CDPK1 inhibition.

The drug screening results showed that none of the compounds exhibited cytotoxicity in the *in vitro* model employed at 5µM concentration when compared to the vehicle controls (DMSO). All, except for 1649, exerted a high inhibition of parasitic growth, since lysis plaques were absent in BKI-treated wells. Those compounds that showed the best results (inhibition of parasite invasion > 90% when administered at 0 hpi) and had also showed promising results aginst infections by other apicomplexan parasites (i.e 1249, 1517, 1553, 1571) were selected for further studies.

The IC_{50} and IC_{99} values obtained for these selected compounds were in the nanomolar range, which is in accordance with those results published for *N. caninum* (Ojo *et al.*, 2014; Müller *et al.*, 2017a;) and *T. gondii* (Winzer *et al.*, 2015). However, short treatments did not completely inhibit parasite proliferation, suggesting a parasitostatic effect. Transmission electron microscopy studies showed that the effects of these compounds were not limited to the arrest of host cell invasion, suggesting that there may be additional drug targets (Ojo *et al.*, 2014). Parasitophorous vacuoles containing large multinucleated complexes were found, similar to what has been reported earlier in BKI-1294, 1517 and 1553-treated cell cultures infected with *N. caninum* or *T. gondii* (Winzer *et al.*, 2015; Müller *et al.*, 2017b). These complexes have been postulated to exert an antigenic stimulus, which may aid together with the host immune response, to clear the infection (Müller *et al.*, 2017b). Also, amylopectin granules were present in BKI-treated *B. besnoiti* tachyzoites, a characteristic feature of *B. besnoiti* bradyzoites (Fernández-García *et al.*, 2009b). This is particularly interesting, since BKI treatments could potentially represent a convenient exogenous trigger to induce tachyzoite-to-bradyzoite conversion of *B. besnoiti in vitro,* as previously observed for decoquinate.

It is already known that other prospective drugs, such as thiazolides (Cortes *et al.*, 2007a); arylimidamides (Cortes *et al.*, 2011) and imidazolopyridines (Moine *et al.*, 2015) have shown good *in vitro* properties against *B. besnoiti* tachyzoites. However, for thiazolides *in vivo* toxic effects have been described in small and large mammals, so they do not represent appropriate drugs to be tested in the target species until more safe compounds are developed (Sánchez-Sánchez *et al.*, 2018). Also, the naptoquinone buparvaquone, currently available in some regions of the world to combact cattle theileriosis has been recently demonstrated to produce a marked inhibition of tachyzoite proliferation at nanomolar concentrations, with severe mitochondrial alterations. However, after prolonged exposure to the drug, a rapid adaptation of tachyzoites to increased drug concentrations was seen, being able to resume proliferation even though they had alterations in the structure of the mitochondria and resisting concentrations up to 10 µM (Müller *et al.*, 2018). However, the mechanisms involved in this adaptation are not known. Besides, this drug is not licensed in the EU.

Among other prospective drugs which may exert interesting activities against *B. besnoiti*, it may be worth trying compounds such as artemisine and artemisine derivatives, since they present potent activities against other parasites such as *T. gondii* (Gomes *et al.*, 2012) and *N. caninum* (Qian *et al.*, 2015). Besides, other herbal extracts, such as curcumin, has been recently found to present good *in vitro* activities against *B. besnoiti* tachyzoites (Cervantes-Valencia *et al.*, 2018). Also, other examples of compounds that have been shown interesting results against apicomplexan parasites are anticancer drugs, such as miltefosine, which is highly active against extracellular *T. gondii* tachyzoites (Nyoman & Lüder, 2013). Recently, organometallic ruthenium complexes are object of great attention and have been reported to have IC50 values in the nanomolar range for both *N. caninum* and *T. gondii* (Barna *et al.*, 2013). Finally, endochin-like quinolones have been shown to present *in vitro* EC50 in the low nanomolar range against both *T. gondii* (Doggett *et al.*, 2012) and *N. caninum* (Anghel et al., 2018).

In the search for other potential targets, recently lipids have been gaining attention, given that they are commonly exploited for therapy against other obligate intracellular pathogens, such as viruses (Fernández-Oliva et al., 2019) and since Toxoplasmatinae parasites need to scavenge lipids from the host cell (Nishikawa *et al.*, 2011; Nolan *et al.*, 2015). Besides, it has been shown that *B. besnoiti* infection alters both endogenous cholesterol de novo synthesis and exogenous LDL uptake in host endothelial cells (Silva et al., 2019).

In conclusion, results obtained in the present subobjective demonstrate proof of concept for the efficacy of decoquinate, diclazuril, as well as BKIs 1294, 1517, 1553 and 1571 against *B. besnoiti in vitro*. However, further assessments of safety and efficacy of all compounds should be performed in the target species. In the case of diclazuril, new posologies should be addressed in order to increase bioavailability and achieve greater systemic exposure in cattle, which are needed to fight against the intraorganic distribution of *B. besnoiti* in infected cattle. For BKIs, plasma levels of up to 5 µM have been already achieved in cattle treated with BKI 1294, 1517 and 1553 (Huang *et al.*, 2015; Schaefer *et al.*, 2016; Hulverson *et al.*, 2017), and whether the administration of these BKIs during the acute stage of the disease is enough to avoid tissue cyst formation needs to be further investigated.

Finally, in order to facilitate drug screenings against *B. besnoiti*, new methodologies should be implemented. In other apicomplexan parasites, assays using transgenic parasites have been developed (Müller & Hemphill, 2012). The parasites employed for these screenings express reporter genes, such as beta-galactosidase (Ojo *et al.*, 2014), luciferase (Cui et al., 2008) or fluorescent proteins such as GFP or YFP (Gubbels et al., 2003) under the control of a strong promotor (Rodriguez and Tarleton, 2012), with no need to harvest infected cells and offering a higher sensitivity (Gubbels et al., 2003). However, so far no transgenic *Besnoitia* parasites have been developed. Also, standardized *in vivo* models of infection in the target species are urgently needed, and considerable efforts have been carried out in this field (Diezma-Díaz *et al.*, 2017, 2018, 2019).

CAPÍTULO VI: CONCLUSIONES/ CONCLUSIONS

<u>Objetivo 1</u>: Desarrollo de nuevos modelos *in vitro* estandarizados para el estudio de la infección por *Besnoitia besnoiti* empleando cultivos primarios bovinos – células endoteliales y fibroblastos- y estudios de la interacción del parásito con el virus de la diarrea vírica bovina en células endoteliales.

- **Primera**: Se han obtenido con éxito dos cultivos primarios de aorta bovina libres del virus de la diarrea vírica bovina (VDVB). Ambos cultivos presentaron características morfológicas y un patrón de expresión de marcadores de superficie e intracelulares compatibles con células endoteliales y fibroblastos. Además, se ha confirmado la importancia de la realización de controles de calidad exhaustivos para trabajar con reactivos y líneas de cultivo celular libres deVDVB, ya que la coinfección con este virus favorece la invasión temprana de los taquizoítos de *B. besnoiti* en las células endoteliales de aorta bovina (BAEC).

- **Segunda**: Los taquizoítos de *B. besnoiti* presentan un ciclo lítico en BAEC y fibroblastos similar al previamente descrito en células MARC-145. En base a los resultados de invasión y proliferación de *B. besnoiti* obtenidos en BAEC se han seleccionado los tiempos más adecuados para realizar estudios de transcriptómica y explorar la interacción parásito-célula hospedadora en las células endoteliales bovinas diana del parásito durante la besnoitiosis aguda: las 12 horas post-infección, representativo de invasión temprana; y las 32 hpi, cuando los taquizoítos han realizado al menos dos ciclos de replicación.

<u>Objetivo 2:</u> Empleo de modelos experimentales *in vitro* para la realización de estudios de patogenia molecular y cribado farmacológico en la infección por *B. besnoiti*.

<u>Subobjetivo 2.1.</u>: Empleo de BAEC en estudios de patogenia molecular de la infección por *B. besnoiti*.

- **<u>Primera:</u>** La infección por *B. besnoiti* modula las BAEC, desencadenando mecanismos relacionados con la activación de las células endoteliales de tipo II, que se han asociado al daño endotelial. Dicha activación de las células endoteliales transcurre progresivamente según avanza el ciclo lítico del parásito. Tanto a las 12 como a las 32 hpi se detectaron genes diferencialmente expresados compatibles con una activación del endotelio, hecho que se corroboró cuando ambos tiempos pi se compararon entre sí.

- **<u>Segunda</u>:** Las células endoteliales infectadas con *B. besnoiti* presentan un fenotipo proinflamatorio (con la sobreexpresión de citoquinas- IL6, IL1A-; quimioquinas - CXCL1, CXCL2, CXCL3, CCL2, CCl24-; marcadores de adhesión de leucocitos - SELE, SELP, ICAM1, VCAM1), fibrinolítico (destacando PLAT, PLAUR) y profibrótico (con la sobreexpresión de IL-6, CCL2, entre otros). Además, destaca la regulación de la angiogénesis, con la sobreexpresión de moléculas implicadas en fases tempranas, como factores de crecimiento y metaloproteasas de matriz, y tardías, destacando la sobreexpresión de integrinas y vasohibina. Estos hallazgos se correlaccionan con las lesiones microscópicas detectadas en tejidos de animales infectados. Además, se han identificado posibles biomarcadores de pronóstico y progresión de la infección (p.ej. CCL2) cuya utilidad deberá valorarse *in vivo*.

- **<u>Tercera:</u>** Se han identificado, por primera vez, numerosos genes de *B. besnoiti* ortólogos de protozoos Toxoplasmatinae, que codifican proteínas implicadas en el

ciclo lítico: proteínas de gránulos densos (GRA), de roptrias (ROP y RON), de micronemas (MIC) y de superficie (SRS) y que podrían ser posibles dianas terapéuticas o vacunales. En particular, destaca la sobreexpresión de genes que codifican las proteínas de roptrias (ROP5B, ROP17 y ROP40), de micronemas (MIC2 y MIC11), del glideosoma (GAP80) y de superficie (SRS22A) a medida que progresa el ciclo lítico. Este hecho parece indicar que, a las 32 hpi, los taquizoítos están preparando la maquinaria necesaria para invadir nuevas células hospedadoras tras la egresión. Por otra parte, se confirma la presencia de otros genes que codifican proteínas de gránulos densos (GRA) y las proteínas quinasas dependientes de calcio (CDPK) que no están diferencialmente expresadas, lo que sugiere un papel de estas proteínas tanto en la invasión como en la adaptación al ambiente intracelular y la replicación de los taquizoítos.

<u>Subobjetivo 2.2.</u>: Cribado farmacológico de compuestos anticoccidiales disponibles comercialmente frente a la infección por *B. besnoiti*.

- **Primera**: El decoquinato y el diclazurilo son compuestos seguros y eficaces frente a la infección por *B. besnoiti* en el modelo *in vitro* empleado. Por el contrario, se descarta el empleo de toltrazurilo, imidocarb, sulfadiazina y trimetoprim, sólo o combinado con la sulfadiazina, para el control de la besnoitiosis bovina, ya que presentaron valores de inhibición de la invasión y proliferación de *B. besnoiti in vitro* inferiores a los obtenidos en el caso del decoquinato y el diclazurilo. Además, el toltrazurilo fue citotóxico en el modelo *in vitro* empleado.

- **Segunda**: El decoquinato podría emplearse como aditivo en pienso para el control de la besnoitiosis bovina. Este fármaco presenta una actividad parasitostática frente a la infección por *B. besnoiti* alterando la mitocondria de los taquizoítos. Esta actividad parasitostática unida a la respuesta inmunitaria desarrrollada por el hospedador podrían controlar la fase aguda de la besonitiosis bovina al alcanzar el decoquinato en el ganado bovino concentraciones plasmáticas máximas superiores a la CI99 obtenida *in vitro*.

- **Tercera**: El diclazurilo es una alternativa menos atractiva que el decoquinato para combatir la infección por *B. besnoiti*, ya que presenta una actividad parasiticida interfiriendo en la citoquinesis de los parásitos en división y las concentraciones plasmáticas máximas descritas en el ganado bovino son inferiores a las CI99 obtenidas *in* vitro, por lo que serían necesarios futuros estudios para mejorar su biodisponibilidad.

<u>Subobjetivo 2.3.</u>: Cribado farmacológico de fármacos de "nueva generación" ("*bumped kinase inhibitors*") frente a la infección por *B. besnoiti*.

- **Primera:** Los taquizoítos de *B. besnoiti* presentan una de las posibles dianas de los fármacos inhibidores de las protein kinasas dependientes de calcio o "*bumped kinase inhibitors*", la enzima *Bb*CDPK1. Dicha enzima presenta una secuencia de aminoácidos con una elevada homología con sus ortólogos NcCDPK1 y TgCDPK1, incluyendo el aminoácido "*gatekeeper*" glicina en el centro activo de la misma. Además, la actividad de la enzima *Bb*CDPK1 disminuye al verse sometida a concentraciones crecientes de fármacos inhibidores de las proteínas kinasas dependientes de calcio.

- **Segunda:** Los fármacos "Bumped kinase inhibitors" son seguros y eficaces frente a la infección por *B. besnoiti in vitro*. En concreto, los compuestos 1294, 1517, 1553 y 1571 podrían emplearse a largo plazo en el tratamiento de la besnoitiosis bovina, ya que presentan CI50 en el rango nanomolar y un efecto parasitostático *in vitro*, interfiriendo en la citoquinesis de los taquizoítos dando lugar a la formación de complejos multinucleados. Por ello, son necesarios futuros estudios de eficacia en la especie de destino.

Objective 1: Development of novel standardized *in vitro* models for the study of *Besnoitia besnoiti* infection using primary bovine target cells – aorta endothelial cells and fibroblasts – and studies on the parasite - bovine viral diarrhea virus interaction.

- **First**: Primary bovine cultures, free from the bovine viral diarrhea virus (BVDV) infection, have been succesfully obtained from aorta. Both primary cultures have shown morphological and a pattern of expression of surface and intracellular markers compatible with endothelial cells and fibroblasts. Besides, it has been corroborated the importance of performing thorough quality controls to work with cell culture reagents and cell lines free from BVDV, since coinfection with this virus favours early invasion of the host cell by *B. besnoiti* tachyzoites.

- **Second**: *Besnoitia besnoiti* tachyzoites have shown a lytic cycle in BAEC and fibroblasts similar to the one described in MARC-145 cells. According to the invasion and proliferation results obtained in BAEC, the most appropriate times pi to explore the host-parasite interaction during acute besnoitiosis by means of transcriptomic analyses have been described: 12 hpi: representative of early invasion; and 32 hpi, when tachyzoites have been subjected to at least two rounds of replication.

Objective 2: Employment of *in vitro* experimental models in molecular pathogenesis and drug screening studies in *B. besnoiti* infection

Sub-objective 2.1.: Employment of BAEC in molecular pathogenesis studies of *B. besnoiti* infection

- **First:** *Besnoitia besnoiti* infection is able to modulate the endothelial cells, triggering mechanisms relating to a type II endothelial activation, associated to endothelial damage. Endothelial cell activation progresses as the lytic cycle of the parasite advances. Differentially expressed genes associated with the endothelial activation have been detected at 12 and 32 hpi, which was corroborated when both times pi were compared.

- **Segunda:** Endothelial cells infected with *B. besnoiti* tachyzoites present a proinflammatory (with the upregulation of citoquines – IL6, IL1A-; chemokines- CXCL1, CXCL2, CXCL3, CCL2, CCL24; leukocyte adhesión markers – SELE, SELP, ICAM-1, VCAM-1), fibrinolytic (PLAT, PLAUR) and profibrotic (with the upregulation of IL6 and CCL2, among others) phenotype. Besides, angiogenesis regulation predominates, with the upregulation of genes involved in early, such as growth factors and matrix metalloproteases, and late stages, such as integrins and vasohibin. Those findings correlate with the microscopic lesions found in tissues from infected animals. Besides, putative biomarkers of prognosis and disease progression (such as CCL2) have been detected, that should be further evaluated *in vivo*.

- **Third:** Numerous *B. besnoiti* genes orthologues of other Toxoplasmatinae protozoa have been described, coding for proteins involved in the lytic cycle: dense granule proteins (GRA), rhoptry proteins (ROP and RON), microneme proteins (MIC) and surface (SRS), which may be possible therapeutic and vaccinal targets. In particular, genes coding for rhoptry proteins (ROP5B, ROP17, ROP40), micronemes (MIC2, MIC11), glideosome (GAP80) and surface (SRS22A) are upregulated when the lytic cycle progresses. This finding might be due to the fact that, at 32 hpi, tachyzoites are preparing the machinery needed to invade new host cells after egress. In addition,

other non-upregulated genes which encode for dense granule proteins (GRA) and calcium dependent protein kinases (CDPKs) have been identified, suggesting a role for these genes in the invasion, intracellular adaptation and replication of tachyzoites.

Sub-objective 2.2.: Drug screening of commercially available anti-coccidials against *B. besnoiti* infection.

- **First**: Decoquinate and diclazuril are safe and effective compounds against *B. besnoiti* infection *in vitro*. On the other hand, the use of toltrazuril, imidocarb, sulfadiazin and trimethoprim, alone or in combination with sulfadiazine, against bovine besnoitiosis is ruled out, since they showed lesser invasion and proliferation inhibition values. Besides, toltrazuril was cytotoxic in the *in vitro* model employed.

- **Second**: Decoquinate can be employed as a feed additive for bovine besnoitiosis control. This drug is parasitostatic and alters the parasite mitochondria. This parasitostatic effect, together with the immune response developed by the host, might help to control the acute stage of bovine besnoitiosis, since decoquinate achieves maximum plasmatic concentrations in cattle higher than the IC99 obtained *in vitro*.

- **Third**: Diclazuril is a les attractive alternative compared to decoquinate to control *B. besnoiti* infection, since it shows a parasiticidal effect interfering in the cytokinesis of dividing parasites, and the máximum plasmatic concentrations described in cattle are below the IC99 obtained *in vitro*. Thus, further studies are needed to improve its bioavailability in cattle.

Sub-objective 2.3.: Drug screening of new generation drugs (bumped kinase inhibitors) against *B .besnoiti* infection.

- **First:** *Besnoitia besnoiti* tachyzoites have one of the targets of the inhibitors of the calcium dependent protein kinases, or bumped kinase inhibitors, the enzyme *Bb*CDPK1. This enzyme shows a great identity with its orthologues NcCDPK1 and TgCDPK1, including the gatekeeper aminoacid glycine. Besides, the activity of the recombinant enzyme r*Bb*CDPK1 diminishes when BKIs are added.

- **Second:** Bumped kinase inhibitors are safe and effective against *B. besnoiti* infection *in vitro*. In particular, compounds 1294, 1517, 1553 and 1571 could be employed in the long run for bovine besnoitiosis treatment, since they present IC50 in the nanomolar range and show a parasitostatic effect *in vitro,* interfering on the cytokinesis of tachyzoites and producing multinucleated complexes. Thus, future efficacy studies in the target species are needed.

REFERENCIAS/REFERENCES

Aguado-Martínez, A, Álvarez-García, G, Schares, G, Risco-Castillo, V, Fernández-García, A, Marugán-Hernández, V, Ortega-Mora, LM, 2010. Characterisation of NcGRA7 and NcSAG4 proteins: Immunolocalisation and their role in the host cell invasion by *Neospora caninum* tachyzoites. Acta Parasitol. 55 (4), 304-312.

Aird, W.C., 2012. Endothelial cell heterogeneity. Cold Spring Harbor perspectives in medicine 2 (1), a006429.

Ajioka, J.W., 1998. *Toxoplasma gondii*: ESTs and gene discovery. Int. J. Parasitol. 28 (7), 1025-1031.

Alexander, D.L., Mital, J., Ward, G.E., Bradley, P., Boothroyd, J.C., 2005. Identification of the moving junction complex of *Toxoplasma gondii:* a collaboration between distinct secretory organelles. PLoS Pathog. 1 (2), e17.

Alshehabat, M., Alekish, M., Talafha, A., 2016. Selected metabolic biochemical and enzyme activities associated with Besnoitia besnoiti infection in dairy cattle. Trop. Anim. Health Prod. 48, 1301-1304.

Álvarez-García, G., Pitarch, A., Zaballos, A., Fernández-García, A., Gil, C., Gómez-Bautista, M., Aguado-Martínez, A., Ortega-Mora, L.M., 2007. The NcGRA7 gene encodes the immunodominant 17 kDa antigen of *Neospora caninum* . Parasitology 134 (Pt 1), 41-50,

Álvarez-García, G., Frey, C.F., Mora, L.M.O., Schares, G., 2013. A century of bovine besnoitiosis: an unknown disease re-emerging in Europe. Trends Parasitol. 29 (8), 407-415.

Álvarez-García, G., Fernández-García, A., Gutiérrez-Expósito, D., Quiteria, J.A., Aguado-Martínez, A., Ortega-Mora, L.M., 2014a. Seroprevalence of *Besnoitia besnoiti* infection and associated risk factors in cattle from an endemic region in Europe. Vet. J. 200 (2), 328-331.

Álvarez-García, G., García-Lunar, P., Gutiérrez-Expósito, D., Shkap, V., Ortega-Mora, L.M., 2014b. Dynamics of *Besnoitia besnoiti* infection in cattle. Parasitology 141 (11), 1419-1435, 10.1017/S0031182014000729.

Álvarez-García, G., 2016. From the mainland to Ireland - bovine besnoitiosis and its spread in Europe. Vet. Rec. 178 (24), 605-607, 10.1136/vr.i3175.

Alzieu, J.P., 2007. Re-emerging cattle besnoitiosis (*Besnoitia besnoiti*) in France: update on clinical and epidemiological aspects. 21st International Conference WAAVP, Gante (Belgium) , 222.

Arnal, M., Gutiérrez-Expósito, D., Martínez-Durán, D., Regidor-Cerrillo, J., Revilla, M., Fernández de Luco, D., Jiménez-Meléndez, A., Ortega-Mora, L., Álvarez-García, G., 2017. Systemic Besnoitiosis in a Juvenile Roe Deer (*Capreolus capreolus*). Transbound. Emerg. Diseases. 64, e8-e14.

Arranz-Solís, D., Regidor-Cerrillo, J., Lourido, S., Ortega-Mora, L.M., Saeij, J.P., 2018. Toxoplasma CRISPR/Cas9 constructs are functional for gene disruption in *Neospora caninum*. Int. J. Parasitol. 48 (8), 597-600.

Asai, T., Howe, D.K., Nakajima, K., Nozaki, T., Takeuchi, T., Sibley, L.D., 1998. *Neospora caninum:* tachyzoites express a potent type-I nucleoside triphosphate hydrolase. Exp. Parasitol. 90 (3), 277-285.

Ashmawy, K.I., Abu-Akkada, S.S., 2014. Evidence for bovine besnoitiosis in Egypt-first serosurvey of *Besnoitia besnoiti* in cattle and water buffalo (Bubalus bubalis) in Egypt. Trop. Anim. Health Prod. 46 (3), 519-522.

Atkinson, R.A., Ryce, C., Miller, C.M., Balu, S., Harper, P.A., Ellis, J.T., 2001. Isolation of *Neospora caninum* genes detected during a chronic murine infection. Int. J. Parasitol. 31 (1), 67-71.

Aurrecoechea, C., Barreto, A., Basenko, E.Y., Brestelli, J., Brunk, B.P., Cade, S., Crouch, K., Doherty, R., Falke, D., Fischer, S., 2016. EuPathDB: the eukaryotic pathogen genomics database resource. Nucleic Acids Res. 45 (D1), D581-D591.

Bahl, A., Davis, P.H., Behnke, M., Dzierszinski, F., Jagalur, M., Chen, F., Shanmugam, D., White, M.W., Kulp, D., Roos, D.S., 2010. A novel multifunctional oligonucleotide microarray for *Toxoplasma gondii*. BMC Genomics 11, 603.

Bargai, U., Nobel, T., Pearl, S., 1984. Radiographic changes in testes of bulls infected with besnoitiosis: A Correlated Radiologic-Pathologic Study. Vet. Radiol. 25 (5), 235-239.

Barna, F., Debache, K., Vock, C.A., Kuster, T., Hemphill, A., 2013. *In vitro* effects of novel ruthenium complexes in *Neospora caninum* and *Toxoplasma gondii* tachyzoites. Antimicrob. Agents Chemother. 57 (11), 5747-5754.

Baroni, L., Pollo-Oliveira, L., Heck, A.J., Altelaar, A.M., Yatsuda, A.P., 2019. Actin from the apicomplexan *Neospora caninum* (NcACT) has different isoforms in 2D electrophoresis. Parasitology 146 (1), 33-41.

Barragán, A., Sibley, L.D., 2002. Transepithelial migration of *Toxoplasma gondii* is linked to parasite motility and virulence. J. Exp. Med. 195 (12), 1625-1633.

Bartley, P.M., Wright, S., Sales, J., Chianini, F., Buxton, D., Innes, E.A., 2006. Long-term passage of tachyzoites in tissue culture can attenuate virulence of *Neospora caninum in vivo*. Parasitology 133, 421-432.

Basso, W., Schares, S., Barwald, A., Herrmann, D.C., Conraths, F.J., Pantchev, N., Vrhovec, M.G., Schares, G., 2009. Molecular comparison of *Neospora caninum* oocyst isolates from naturally infected dogs with cell culture-derived tachyzoites of the same isolates using nested polymerase chain reaction to amplify microsatellite markers. Vet. Parasitol. 160 (1-2), 43-50, 10.1016/j.vetpar.2008.10.085.

Basso, W., Schares, S., Minke, L., Barwald, A., Maksimov, A., Peters, M., Schulze, C., Muller, M., Conraths, F.J., Schares, G., 2010. Microsatellite typing and avidity analysis suggest a common source of infection in herds with epidemic *Neospora caninum*-associated bovine abortion. Vet. Parasitol. 173 (1-2), 24-31.

Basso, W., Schares, G., Gollnick, N.S., Rutten, M., Deplazes, P., 2011. Exploring the life cycle of *Besnoitia besnoiti* - experimental infection of putative definitive and intermediate host species. Vet. Parasitol. 178 (3-4), 223-234.

Basso, W., Lesser, M., Grimm, F., Hilbe, M., Sydler, T., Trosch, L., Ochs, H., Braun, U., Deplazes, P., 2013. Bovine besnoitiosis in Switzerland: Imported cases and local transmission. Vet. Parasitol. 198, 265-273.

Basson, P.A., Van Niekerk, J., McCUlly, R.M., Bigalke, R.D., 1965. Besnoitiosis in South African antelopes: a preliminary note on the ocurrence of *Besnoitia* cysts in the cardio-vascular system. Jl S. Afr. vet. med. Ass. 36, 578.

Basson, P., McCully, R., Bigalke, R., 1970. Observations on the pathogenesis of bovine and antelope strains of *Besnoitia besnoiti* (Marotel, 1912) infection in cattle and rabbits.

Beck, H, Blake, D, Dardé, M, Felger, I, Pedraza-Díaz, S, Regidor-Cerrillo, J, Gómez-Bautista, M, Ortega-Mora, LM, Putignani, L, Shiels, B, Tait, A, Weir, W, 2009. Molecular approaches to diversity of populations of apicomplexan parasites. Int. J. Parasitol. 39 (2), 175-189.

Behnke, M.S., Wootton, J.C., Lehmann, M.M., Radke, J.B., Lucas, O., Nawas, J., Sibley, L.D., White, M.W., 2010. Coordinated progression through two subtranscriptomes underlies the tachyzoite cycle of *Toxoplasma gondii*. PLoS One 5 (8), e12354, 10.1371/journal.pone.0012354.

Behnke, M.S., Khan, A., Wootton, J.C., Dubey, J.P., Tang, K., Sibley, L.D., 2011. Virulence differences in *Toxoplasma* mediated by amplification of a family of polymorphic pseudokinases. Proc. Natl. Acad. Sci. U. S. A. 108 (23), 9631-9636.

Bergstrom, R.C., Maki, L.R., 1976. Coccidiostatic action of monensin fed to lambs: body weight gains and feed conversion efficacy. Am. J. Vet. Res. 37 (1), 79-81.

Bertranpetit, E., Jombart, T., Paradis, E., Pena, H., Dubey, J., Su, C., Mercier, A., Devillard, S., Ajzenberg, D., 2017. Phylogeography of *Toxoplasma gondii* points to a South American origin. Infection, Genetics and Evolution 48, 150-155.

Besnoit, C., Robin, V., 1912. Sarcosporidiose Cutanée Chez Un Vache. Rev. Vet, 649-663 pp.

Bessoff, K., Spangenberg, T., Foderaro, J.E., Jumani, R.S., Ward, G.E., Huston, C.D., 2014. Identification of *Cryptosporidium parvum* Active Chemical Series by Repurposing the Open Access Malaria Box. Antimicrob. Agents Chemother. 58 (5), 2731-2739.

Bezerra, M.A., Pereira, L.M., Bononi, A., Biella, C.A., Baroni, L., Pollo-Oliveira, L., Yatsuda, A.P., 2017. Constitutive expression and characterization of a surface SRS (NcSRS67) protein of *Neospora caninum* with no orthologue in *Toxoplasma gondii*. Parasitol. Int. 66 (2), 173-180.

Bigalke, R., Naude, T., 1962. The diagnostic value of cysts in the scleral conjunctiva in bovine besnoitiosis. JS Afr Vet Med Assoc 33 (1), 21-27.

Bigalke, R.D., 1967. The artificial transmission of *Besnoitia besnoiti* (Marotel, 1912) from chronically infected to susceptible cattle and rabbits. Onderstepoort J. Vet. Res. 34 (2), 303-316.

Bigalke, R.D., van Niekerk, J.W., Basson, P.A., McCully, R.M., 1967. Studies on the relationship between *Besnoitia* of blue wildebeest and impala, and *Besnoitia besnoiti* of cattle. Onderstepoort J. Vet. Res. 34 (1), 7-28.

Bigalke, R.D., 1968. New concepts on the epidemiological features of bovine besnoitiosis as determined by laboratory and field investigations. Onderstepoort J. Vet. Res. 35 (1), 3-137.

Bigalke, R.D., Schoeman, J.H., McCully, R.M., 1974. Immunization against bovine besnoitiosis with a live vaccine prepared from a blue wildebeest strain of Besnoitia besnoiti grown in cell cultures. 1. Studies on rabbits. Onderstepoort J. Vet. Res. 41 (1), 1-5.

Bigalke, R., 1981. Besnoitiosis and Globidiosis. Ristic, M. , McIntyre , I (Eds), Diseases of cattle in the tropics. Marunus Nijhoff, The Hague, The Netherlands , 429-442.

Bigalke, R., Prozesky, L., Coetzer, J., Tustin, R., 2004. Besnoitiosis. Infectious diseases of livestock, Volume One (Ed. 2), 351-359.

Bjorkman, C., Alenius, S., Manuelsson, U., Uggla, A., 2000. *Neospora caninum* and bovine virus diarrhoea virus infections in Swedish dairy cows in relation to abortion. Vet. J. 159 (2), 201-206.

Blader, I.J., Coleman, B.I., Chen, C., Gubbels, M., 2015. Lytic cycle of *Toxoplasma gondii*: 15 years later. Annu. Rev. Microbiol. 69, 463-485.

Boucher, L.E., Bosch, J., 2015. The apicomplexan glideosome and adhesins - Structures and function. J. Struct. Biol. 190 (2), 93-114.

Bougdour, A., Durandau, E., Brenier-Pinchart, M., Ortet, P., Barakat, M., Kieffer, S., Curt-Varesano, A., Curt-Bertini, R., Bastien, O., Coute, Y., 2013. Host cell subversion by *Toxoplasma* GRA16, an exported dense granule protein that targets the host cell nucleus and alters gene expression. Cell Host Microbe 13 (4), 489-500.

Bradley, P.J., Ward, C., Cheng, S.J., Alexander, D.L., Coller, S., Coombs, G.H., Dunn, J.D., Ferguson, D.J., Sanderson, S.J., Wastling, J.M., Boothroyd, J.C., 2005. Proteomic analysis of rhoptry organelles reveals many novel constituents for host-parasite interactions in *Toxoplasma gondii*. J. Biol. Chem. 280 (40), 34245-34258.

Braun, L., Brenier-Pinchart, M.P., Yogavel, M., Curt-Varesano, A., Curt-Bertini, R.L., Hussain, T., Kieffer-Jaquinod, S., Coute, Y., Pelloux, H., Tardieux, I., Sharma, A., Belrhali, H., Bougdour, A., Hakimi, M.A., 2013. A *Toxoplasma* dense granule protein, GRA24, modulates the early immune response to infection by promoting a direct and sustained host p38 MAPK activation. J. Exp. Med. 210 (10), 2071-2086.

Brown, W.C., Norimine, J., Knowles, D.P., Goff, W.L., 2006. Immune control of *Babesia bovis* infection. Vet. Parasitol. 138 (1-2), 75-87.

Bürgi, N., Josi, C., Bürki, S., Schweizer, M., Pilo, P., 2018. *Mycoplasma bovis* co-infection with bovine viral diarrhea virus in bovine macrophages. Vet. Res. 49 (1), 2.

Buxton, D., Blewett, D., Trees, A., McColgan, C., Finlayson, J., 1988. Further studies in the use of monensin in the control of experimental ovine toxoplasmosis. J. Comp. Pathol. 98 (2), 225-236.

Bwangamoi, O., Carles, A.B., Wandera, J.G., 1989. An epidemic of besnoitiosis in goats in Kenya. Vet. Rec. 125 (18), 461.

Cadéac, 1884. Identité de l'élèphantiasis et de l'anasarque du boeuf. Description de cette maladie. Revue vétérinaire , 521.

Calarco, L., Ellis, J., 2019. Annotating the 'hypothetical'in hypothetical proteins: *In-silico* analysis of uncharacterised proteins for the Apicomplexan parasite, *Neospora caninum*. Vet. Parasitol. 265, 29-37.

Calarco, L., Barratt, J., Ellis, J., 2018. Genome Wide Identification of Mutational Hotspots in the Apicomplexan Parasite *Neospora caninum* and the Implications for Virulence. Genome biology and evolution 10 (9), 2417-2431.

Camicia, G., de Larrañaga, G., 2013. Trampas extracelulares de neutrófilos: un mecanismo de defensa con dos caras. Medicina Clínica 140 (2), 70-75.

Cardoso, R., Wang, J., Müller, J., Rupp, S., Leitão, A., Hemphill, A., 2018. Modulation of cis-and trans-Golgi and the Rab9A-GTPase during infection by *Besnoitia besnoiti*, *Toxoplasma gondii* and *Neospora caninum*. Exp. Parasitol. 187, 75-85.

Cardoso, R., Nolasco, S., Goncalves, J., Cortes, H.C., Leitao, A., Soares, H., 2014. *Besnoitia besnoiti* and *Toxoplasma gondii*: two apicomplexan strategies to manipulate the host cell centrosome and Golgi apparatus. Parasitology 141 (11), 1436-1454.

Carruthers, V., Boothroyd, J.C., 2007. Pulling together: an integrated model of *Toxoplasma* cell invasion. Curr. Opin. Microbiol. 10 (1), 83-89.

Carruthers, V.B., Tomley, F.M., 2008. Microneme proteins in apicomplexans. Subcell. Biochem. 47, 33-45.

Carvalho, J.V., Alves, C.M., Cardoso, M.R., Mota, C.M., Barbosa, B.F., Ferro, E.A., Silva, N.M., Mineo, T.W., Mineo, J.R., Silva, D.A., 2010. Differential susceptibility of human trophoblastic (BeWo) and uterine cervical (HeLa) cells to *Neospora caninum* infection. Int. J. Parasitol. 40 (14), 1629-1637.

Castellanos-Gonzalez, A., White, A.C.,Jr, Ojo, K.K., Vidadala, R.S., Zhang, Z., Reid, M.C., Fox, A.M., Keyloun, K.R., Rivas, K., Irani, A., Dann, S.M., Fan, E., Maly, D.J., Van Voorhis, W.C., 2013. A novel calcium-dependent protein kinase inhibitor as a lead compound for treating cryptosporidiosis. J. Infect. Dis. 208 (8), 1342-1348.

Castellanos-Gonzalez, A., Sparks, H., Nava, S., Huang, W., Zhang, Z., Rivas, K., Hulverson, M.A., Barrett, L.K., Ojo, K.K., Fan, E., 2016. A novel calcium-dependent kinase inhibitor, bumped kinase inhibitor 1517, cures cryptosporidiosis in immunosuppressed mice. J. Infect. Dis. 214 (12), 1850-1855.

Cervantes-Valencia, M.E., Hermosilla, C., Alcala-Canto, Y., Tapia, G., Taubert, A., Silva, L.M., 2018. Antiparasitic efficacy of curcumin against *Besnoitia besnoiti* tachyzoites *in vitro*. Front. Vet. Science 5, 333.

Chase, C.C., 2013. The impact of BVDV infection on adaptive immunity. Biologicals 41 (1), 52-60.

Chatikobo, P., Choga, T., Ncube, C., Mutambara, J., 2013. Participatory diagnosis and prioritization of constraints to cattle production in some smallholder farming areas of Zimbabwe. Prev. Vet. Med. 109 (3-4), 327-333.

Chaussabel, D., Semnani, R.T., McDowell, M.A., Sacks, D., Sher, A., Nutman, T.B., 2003. Unique gene expression profiles of human macrophages and dendritic cells to phylogenetically distinct parasites. Blood 102 (2), 672-681.

Cheema, A.H., Toofanian, F., 1979. Besnoitiosis in wild and domestic goats in Iran. Cornell Vet. 69 (3), 159-168.

Cho, J.H., Chung, W.S., Song, K.J., Na, B.K., Kang, S.W., Song, C.Y., Kim, T.S., 2005. Protective efficacy of vaccination with *Neospora caninum* multiple recombinant antigens against experimental *Neospora caninum* infection. Korean J. Parasitol. 43 (1), 19-25.

Collantes-Fernández, E., Arrighi, R.B., Álvarez-García, G., Weidner, J.M., Regidor-Cerrillo, J., Boothroyd, J.C., Ortega-Mora, L.M., Barragán, A., 2012. Infected dendritic cells facilitate systemic dissemination and transplacental passage of the obligate intracellular parasite *Neospora caninum* in mice. PLoS One 7 (3), e32123.

Collantes-Fernández, E., López-Pérez, I., Álvarez-García, G., Ortega-Mora, L.M., 2006. Temporal distribution and parasite load kinetics in blood and tissues during *Neospora caninum* infection in mice. Infect. Immun. 74 (4), 2491-2494.

Cortes, H., Chagas-Silva, J., Baptista, M., Pereira, R., Leitao, A., Horta, A., Vasques, M., Barbas, J., Marques, C., 2006d. *Besnoitia besnoiti* impact on fertility of cattle exploited in Mediterranean pastures (Alentejo). Animal products from the Mediterranean area: EAAP publication 119, 323-329.

Cortes, H.C., Vidal, R., Reis, Y., 2004. Bovine besnoitiosis, one approach for a better understanding of its importance in Portugal. Proceedings of 23rd World Buiatrics Congress , 35-36.

Cortes, H.C., Leitão, A., Vidal, R., Vila-Viçosa, M.J., Ferreira, M.L., Caeiro, V., Hjerpe, C.A., 2005. Besnoitiosis in bulls in Portugal. Vet. Rec. 157 (9), 262-264.

Cortes, H.C., Reis, Y., Waap, H., Marcelino, E., Vaz, Y., Nunes, T., Fanzendeiro, I., Caeiro, V., Leitao, A., 2006a. Longitudinal study of *Besnoitia besnoiti* infection prevalence rates in a beef cattle herd in Alentejo, Portugal. In: Proceedings of the COST 854 Final Conference, Liege, Belgium.

Cortes, H.C., Reis, Y., Waap, H., Vidal, R., Soares, H., Marques, I., Pereira da Fonseca, I., Fazendeiro, I., Ferreira, M.L., Caeiro, V., Shkap, V., Hemphill, A., Leitao, A., 2006b. Isolation of *Besnoitia besnoiti* from infected cattle in Portugal. Vet. Parasitol. 141 (3-4), 226-233.

Cortes, H.C., Nunes, S., Reis, Y., Staubli, D., Vidal, R., Sager, H., Leitao, A., Gottstein, B., 2006c. Immunodiagnosis of *Besnoitia besnoiti* infection by ELISA and Western blot. Vet. Parasitol. 141 (3-4), 216-225, 10.1016/j.vetpar.2006.05.023.

Cortes, H.C., Mueller, N., Esposito, M., Leitao, A., Naguleswaran, A., Hemphill, A., 2007a. *In vitro* efficacy of nitro- and bromo-thiazolyl-salicylamide compounds (thiazolides) against *Besnoitia besnoiti* infection in Vero cells. Parasitology 134 (Pt 7), 975-985.

Cortes, H.C., Reis, Y., Gottstein, B., Hemphill, A., Leitao, A., Muller, N., 2007b. Application of conventional and real-time fluorescent ITS1 rDNA PCR for detection of *Besnoitia besnoiti* infections in bovine skin biopsies. Vet. Parasitol. 146 (3-4), 352-356.

Cortes, H.C., Muller, N., Boykin, D., Stephens, C.E., Hemphill, A., 2011. *In vitro* effects of arylimidamides against *Besnoitia besnoiti* infection in Vero cells. Parasitol. 138 (5), 583-592.

Cortes, H., Leitao, A., Gottstein, B., Hemphill, A., 2014. A review on bovine besnoitiosis: a disease with economic impact in herd health management, caused by *Besnoitia besnoiti* (Franco and Borges, 1915). Parasitology 141 (11), 1406-1417.

Couzinet, S., Dubremetz, J., Buzoni-Gatel, D., Jeminet, G., Prensier, G., 2000. *In vitro* activity of the polyether ionophorous antibiotic monensin against the cyst form of *Toxoplasma gondii*. Parasitology 121 (04), 359-365.

Cui, L., Miao, J., Wang, J., Li, Q., Cui, L., 2008. *Plasmodium falciparum*: development of a transgenic line for screening antimalarials using firefly luciferase as the reporter. Exp. Parasitol. 120 (1), 80-87.

da Fonseca Ferreira-da-Silva, M., Takács, A.C., Barbosa, H.S., Gross, U., Lüder, C.G., 2009. Primary skeletal muscle cells trigger spontaneous *Toxoplasma gondii* tachyzoite-to-bradyzoite conversion at higher rates than fibroblasts. Int. J. Med. Microbiol. 299 (5), 381-388.

Darius, A.K., Mehlhorn, H., Heydorn, A.O., 2004. Effects of toltrazuril and ponazuril on the fine structure and multiplication of tachyzoites of the NC-1 strain of *Neospora caninum* (a synonym of *Hammondia heydorni*) in cell cultures. Parasitol. Res. 92, 452-458.

Dellacasa-Lindberg, I., Fuks, J.M., Arrighi, R.B., Lambert, H., Wallin, R.P., Chambers, B.J., Barragan, A., 2011. Migratory activation of primary cortical microglia upon infection with *Toxoplasma gondii*. Infect. Immun. 79 (8), 3046-3052.

Dellarupe, A., Regidor-Cerrillo, J., Jiménez-Ruiz, E., Schares, G., Unzaga, J.M., Venturini, M.C., Ortega-Mora, L.M., 2014a. Clinical outcome and vertical transmission variability among canine *Neospora caninum* isolates in a pregnant mouse model of infection. Parasitology 141 (3), 356-366.

Dellarupe, A., Regidor-Cerrillo, J., Jimenez-Ruiz, E., Schares, G., Unzaga, J.M., Venturini, M.C., Ortega-Mora, L.M., 2014b. Comparison of host cell invasion and proliferation among *Neospora caninum* isolates obtained from oocysts and from clinical cases of naturally infected dogs. Exp. Parasitol. 145, 22-28.

Diesing, L., Heydorn, A.O., Matuschka, F.R., Bauer, C., Pipano, E., de Waal, D.T., Potgieter, F.T., 1988. *Besnoitia besnoiti*: studies on the definitive host and experimental infections in cattle. Parasitol. Res. 75 (2), 114-117.

Diezma-Díaz, C., Jiménez-Meléndez, A., Fernández, M., Gutiérrez-Expósito, D., García-Lunar, P., Ortega-Mora, L., Pérez-Salas, J., Blanco-Murcia, J., Ferre, I., Álvarez-García, G., 2017. Bovine chronic besnoitiosis in a calf: Characterization of a novel *B. besnoiti* isolate from an unusual case report. Vet. Parasitol. 247, 10-18.

Diezma-Díaz, C., Jiménez-Meléndez, A., Re, M.T., Ferre, I., Ferreras, M.d.C., Gutiérrez-Expósito, D., Rojo-Montejo, S., Román-Trufero, A., Benavides-Silván, J., García-Lunar, P., 2018. Effect of parasite dose and host age on the infection with *Besnoitia besnoiti* tachyzoites in cattle. Transbound. Emerg. Diseases, 65, 1979-1990.

Diezma-Díaz, C., Ferre, I., Re, M., Jiménez-Meléndez, A., Tabanera, E., González-Huecas, M., Pizarro-Díaz, M., Yanguas-Pérez, D., Brum, P., Blanco-Murcia, J., Ortega-Mora, LM., Álvarez-García, G., 2019. The route of *Besnoitia besnoiti* tachyzoites inoculation does not influence the clinical outcome of the infection in calves. Vet. Parasitol. 267, 21-25.

Diezma-Díaz, C., Ferre, I., Re, M., Jiménez-Meléndez, A., Tabanera, E., Pizarro-Díaz, M., González-Huecas, M., Alcaide-Pardo, M., Blanco-Murcia, J., Ortega-Mora, LM., Álvarez-García, G., 2019. A model for chronic bovine besnoitiosis: parasite stage and inoculation route are key factors. Transbound. Emerg. Diseases (In press).

Dittmar, A.J., Drozda, A.A., Blader, I.J., 2016. Drug Repurposing Screening Identifies Novel Compounds That Effectively Inhibit *Toxoplasma gondii* Growth. Msphere 1 (2), e00042-15.

Dogga, S.K., Mukherjee, B., Jacot, D., Kockmann, T., Molino, L., Hammoudi, P., Hartkoorn, R.C., Hehl, A.B., Soldati-Favre, D., 2017. A druggable secretory protein maturase of *Toxoplasma* essential for invasion and egress. Elife 6, e27480.

Doggett, J.S., Ojo, K.K., Fan, E., Maly, D.J., Van Voorhis, W.C., 2014. Bumped kinase inhibitor 1294 treats established *Toxoplasma gondii* infection. Antimicrob. Agents Chemother. 58 (6), 3547-3549.

Doggett, J.S., Nilsen, A., Forquer, I., Wegmann, K.W., Jones-Brando, L., Yolken, R.H., Bordon, C., Charman, S.A., Katneni, K., Schultz, T., Burrows, J.N., Hinrichs, D.J., Meunier, B., Carruthers, V.B., Riscoe, M.K., 2012. Endochin-like quinolones are highly efficacious against acute and latent experimental toxoplasmosis. Proc. Natl. Acad. Sci. U. S. A. 109 (39), 15936-15941.

Donahoe, S.L., Phalen, D.N., McAllan, B.M., O'Meally, D., McAllister, M.M., Ellis, J., Slapeta, J., 2017. Differential Gamma Interferon- and Tumor Necrosis Factor Alpha-Driven Cytokine Response Distinguishes Acute Infection of a Metatherian Host with *Toxoplasma gondii* and *Neospora caninum*. Infect. Immun. 85 (6).

Donahoe, S.L., Lindsay, S.A., Krockenberger, M., Phalen, D., Slapeta, J., 2015. A review of neosporosis and pathologic findings of *Neospora caninum* infection in wildlife. Int. J. Parasitol. Parasites Wildl. 4 (2), 216-238.

Dong, J., Li, J., Wang, J., Li, F., Yang, J., Gong, P., Li, H., Zhang, X., 2017. Identification and characterization of GRA6/GRA7 of *Neospora caninum* in MDBK cells. Acta biochimica et biophysica Sinica 49 (4), 361-366.

Driskell, R.R., Watt, F.M., 2015. Understanding fibroblast heterogeneity in the skin. Trends Cell Biol. 25 (2), 92-99.

Dubey, J.P., Lindsay, D.S., Rosenthal, B.M., Sreekumar, C., Hill, D.E., Shen, S.K., Kwok, O.C., Rickard, L.G., Black, S.S., Rashmir-Raven, A., 2002. Establishment of *Besnoitia darlingi* from opossums (*Didelphis virginiana*) in experimental intermediate and definitive hosts, propagation in cell culture, and description of ultrastructural and genetic characteristics. Int. J. Parasitol. 32 (8), 1053-1064.

Dubey, J.P., Shkap, V., Pipano, E., Fish, L., Fritz, D.L., 2003a. Ultrastructure of *Besnoitia besnoiti* tissue cysts and bradyzoites. J. Eukaryot. Microbiol. 50 (4), 240-244.

Dubey, J.P., Sreekumar, C., Lindsay, D.S., Hill, D., Rosenthal, B.M., Venturini, L., Venturini, M.C., Greiner, E.C., 2003b. *Besnoitia oryctofelisi* n. sp. (Protozoa: Apicomplexa) from domestic rabbits. Parasitol. 126 (6), 521-539.

Dubey, J.P., Sreekumar, C., Rosenthal, B.M., Lindsay, D.S., Grisard, E.C., Vitor, R.W.A., 2003c. Biological and molecular characterization of *Besnoitia akodoni* n.sp (Protozoa: Apicomplexa) from the rodent *Akodon montensis* in Brazil. Parassitologia (Rome) 45 (2), 61-70.

Dubey, J.P., Lindsay, D.S., 2003. Development and ultrastructure of *Besnoitia oryctofelisi* tachyzoites, tissue cysts, bradyzoites, schizonts and merozoites. Int. J. Parasitol. 33 (8), 807-819.

Dubey, J.P., Sreekumar, C., Rosenthal, B.M., Vianna, M.C., Nylund, M., Nikander, S., Oksanen, A., 2004. Redescription of *Besnoitia tarandi* (Protozoa: Apicomplexa) from the reindeer (*Rangifer tarandus*). Int. J. Parasitol. 34 (11), 1273-1287.

Dubey, J.P., Sreekumar, C., Donovan, T., Rozmanec, M., Rosenthal, B.M., Vianna, M.C., Davis, W.P., Belden, J.S., 2005. Redescription of *Besnoitia bennetti* (Protozoa: Apicomplexa) from the donkey (*Equus asinus*). Int. J. Parasitol. 35 (6), 659-672.

Dubey, J.P., Yabsley, M.J., 2010. *Besnoitia neotomofelis* n. sp. (Protozoa: Apicomplexa) from the southern plains woodrat (*Neotoma micropus*). Parasitology 137 (12), 1731-1747

Dubey, J.P., Jenkins, M.C., Rajendran, C., Miska, K., Ferreira, L.R., Martins, J., Kwok, O.C.H., Choudhary, S., 2011. Gray wolf (*Canis lupus*) is a natural definitive host for *Neospora caninum*. Vet. Parasitol. 181 (2–4), 382-387.

Dubey, J., Schares, G., 2011. Neosporosis in animals—the last five years. Vet. Parasitol. 180 (1), 90-108.

Dubey, J.P., van Wilpe, E., Blignaut, D.J., Schares, G., Williams, J.H., 2013. Development of early tissue cysts and associated pathology of *Besnoitia besnoiti* in a naturally infected bull (Bos taurus) from South Africa. J. Parasitol. 99 (3), 459-466.

Dubey, J.P., Jenkins, M.C., Ferreira, L.R., Choudhary, S., Verma, S.K., Kwok, O.C., Fetterer, R., Butler, E., Carstensen, M., 2014. Isolation of viable *Neospora caninum* from brains of wild gray wolves (*Canis lupus*). Vet. Parasitol. 201 (1-2), 150-153.

Dubey, J.P., 2014. The history and life cycle of Toxoplasma gondii. In: *Toxoplasma Gondii*. Elsevier, pp. 1-17.

Ellis, J.T., Holmdahl, O.J., Ryce, C., Njenga, J.M., Harper, P.A., Morrison, D.A., 2000a. Molecular phylogeny of *Besnoitia* and the genetic relationships among *Besnoitia* of cattle, wildebeest and goats. Protist 151 (4), 329-336.

Ellis, J.T., Ryce, C., Atkinson, R., Balu, S., Jones, P., Harper, P.A., 2000b. Isolation, characterization and expression of a GRA2 homologue from *Neospora caninum*. Parasitology 120 (Pt 4), 383-390.

Elsheikha, H.M., Mansfield, L.S., 2004. Determination of the activity of sulfadiazine against *Besnoitia darlingi* tachyzoites in cultured cells. Parasitol. Res. 93 (5), 423-426.

Elsheikha, H.M., Mansfield, L.S., Morsy, G.H., 2008. Studies on besnoitiosis *bennetti* in miniature donkeys. J. Egypt. Soc. Parasitol. 38 (1), 171-184.

Elsheikha, H.M., 2007. *Besnoitia bennetti* infection in miniature donkeys: an emerging protozoan of increasing concern. Vet. Parasitol. 145 (3-4), 390-391.

English, E.D., Adomako-Ankomah, Y., Boyle, J.P., 2015. Secreted effectors in *Toxoplasma gondii* and related species: determinants of host range and pathogenesis? Parasite Immunol. 37 (3), 127-140.

Esteban-Gil, A., Calvete, C., Casasús, I., Sanz, A., Ferrer, J., Peris, M.P., Marcén-Seral, J.M., Castillo, J.A., 2017. Epidemiological patterns of bovine besnoitiosis in an endemic beef cattle herd reared under extensive conditions. Vet. Parasitol. 236, 14-21.

Esteban-Gil, A., Grisez, C., Prevot, F., Florentin, S., Decaudin, A., Picard-Hagen, N., Berthelot, X., Ronsin, P., Alzieu, J.P., Marois, M., Corboz, N., Peglion, M., Vilardell, C., Lienard, E., Bouhsira, E., Castillo, J.A., Franc, M., Jacquiet, P., 2014. No detection of *Besnoitia besnoiti* DNA in the semen of chronically infected bulls. Parasitol. Res. 113 (6), 2355-2362.

European Food Safety Authority, 2010. Scientific statement on bovine besnoitiosis. Available from <http://www.efsa.europa.eu>.

Fayer, R., Hammond, D.M., Chobatar, B., Elsner, Y.Y., 1969. Cultivation of *Besnoitia jellisoni* in bovine cell cultures. J. Parasitol. 55, 645-653.

Fereig, R.M., Shimoda, N., Abdelbaky, H.H., Kuroda, Y., Nishikawa, Y., 2019. *Neospora* GRA6 possesses immune-stimulating activity and confers efficient protection against *Neospora caninum* infection in mice. Vet. Parasitol. 267, 61-68.

Fernández-García, A., Risco-Castillo, V., Pedraza-Díaz, S., Aguado-Martínez, A., Alvarez-García, G., Gómez-Bautista, M., Collantes-Fernández, E., Ortega-Mora, L.M., 2009a. First isolation of *Besnoitia besnoiti* from a chronically infected cow in Spain. J. Parasitol. 95 (2), 474-476, 10.1645/GE-1772.1.

Fernández-García, A., Álvarez-García, G., Risco-Castillo, V., Aguado-Martínez, A., Marugán-Hernández, V., Ortega-Mora, L.M., 2009b. Pattern of recognition of *Besnoitia besnoiti* tachyzoite and bradyzoite antigens by naturally infected cattle. Vet. Parasitol. 164, 104-110.

Fernández-García, A., Álvarez-García, G., Risco-Castillo, V., Aguado-Martínez, A., Marcén, J.M., Rojo-Montejo, S., Castillo, J.A., Ortega-Mora, L.M., 2010. Development and use of an indirect ELISA in an outbreak of bovine besnoitiosis in Spain. Vet. Rec. 166 (26), 818-822.

Fernández-García, A., Álvarez-García, G., Marugán-Hernández, V., García-Lunar, P., Aguado-Martínez, A., Risco-Castillo, V., Ortega-Mora, L.M., 2013. Identification of *Besnoitia besnoiti* proteins that showed differences in abundance between tachyzoite and bradyzoite stages by difference gel electrophoresis. Parasitology 140 (8), 999-1008.

Fernández-Oliva, A., Ortega-González, P., Risco, C., 2019. Targeting host lipid flows: Exploring new antiviral and antibiotic strategies. Cell. Microbiol. 21 (3), e12996.

Fouquet, CM, 2009. La besnoitiose bovine : suivi épidémiologique de l'épizootie de la région PACA. Tesis Doctoral, Facultad de Veterinaria de Lyon, Francia .

Franc, M., Cardiegues, M., 1999. La besnoitiose bovine: attitude diagnostique et therapeutique. Bulletin des GTV. Bovins, Parasitologie, 119-124.

Franco and Borges, 1915. Nota Sobre a Sarcosporidiose Bovina. Revista de Medicina Veterinária, 255-299 pp.

Frank, M., Pipano, E., Rosenberg, A., 1977. Prevalence of antibodies against *Besnoitia Besnoiti* in beef and dairy-cattle in Israel. Refuah Veterinarith 34 (3), 83-86.

Frenal, K., Polonais, V., Marq, J.B., Stratmann, R., Limenitakis, J., Soldati-Favre, D., 2010. Functional dissection of the apicomplexan glideosome molecular architecture. Cell. Host Microbe 8 (4), 343-357.

Frenkel, J., 1977. *Besnoitia wallacei* of cats and rodents: with a reclassification of other cyst-forming isosporoid coccidia. J. Parasitol. 63, 611-628.

Frenkel, J., Dubey, J., Hoff, R., 1976. Loss of stages after continuous passage of *Toxoplasma gondii* and *Besnoitia jellisoni*. J. Eukaryot. Microbiol. 23 (3), 421-424.

Frey, C.F., Gutiérrez-Expósito, D., Ortega-Mora, L.M., Benavides, J., Marcén, J.M., Castillo, J.A., Casasús, I., Sanz, A., García-Lunar, P., Esteban-Gil, A., Álvarez-García, G., 2013. Chronic bovine besnoitiosis: intra-organ parasite distribution, parasite loads and parasite-associated lesions in subclinical cases. Vet. Parasitol. 197 (1-2), 95-103.

Frey, C.F., Regidor-Cerrillo, J., Marreros, N., García-Lunar, P., Gutiérrez-Expósito, D., Schares, G., Dubey, J.P., Gentile, A., Jacquiet, P., Shkap, V., Cortes, H., Ortega-Mora, LM., Álvarez-García, G., 2016. *Besnoitia besnoiti* lytic cycle *in vitro* and differences in invasion and intracellular proliferation among isolates. Parasit. Vectors 9 (1), 115.

Friedrich, N., Santos, J.M., Liu, Y., Palma, A.S., Leon, E., Saouros, S., Kiso, M., Blackman, M.J., Matthews, S., Feizi, T., Soldati-Favre, D., 2010. Members of a novel protein family containing microneme adhesive repeat domains act as sialic acid-binding lectins during host cell invasion by apicomplexan parasites. J. Biol. Chem. 285 (3), 2064-2076.

Gagnieur, L., Cheval, J., Gratigny, M., Hébert, C., Muth, E., Dumarest, M., Eloit, M., 2014. Unbiased analysis by high throughput sequencing of the viral diversity in fetal bovine serum and trypsin used in cell culture. Biologicals 42 (3), 145-152.

Gail, M., Gross, U., Bohne, W., 2001. Transcriptional profile of *Toxoplasma gondii*-infected human fibroblasts as revealed by gene-array hybridization. Mol. Genet. Genomics 265 (5), 905-912.

Gajria, B., Bahl, A., Brestelli, J., Dommer, J., Fischer, S., Gao, X., Heiges, M., Iodice, J., Kissinger, J.C., Mackey, A.J., Pinney, D.F., Roos, D.S., Stoeckert, C.J.,Jr, Wang, H., Brunk, B.P., 2008. ToxoDB: an integrated *Toxoplasma gondii* database resource. Nucleic Acids Res. 36, D553-6, gkm981.

García-Lunar, P., Ortega-Mora, L.M., Schares, G., Gollnick, N.S., Jacquiet, P., Grisez, C., Prevot, F., Frey, C.F., Gottstein, B., Álvarez-García, G., 2013a. An inter-laboratory comparative study of serological tools employed in the diagnosis of *Besnoitia besnoiti* infection in bovines. Transbound Emerg. Dis. 60 (1), 59-68.

García-Lunar, P., Regidor-Cerrillo, J., Gutiérrez-Expósito, D., Ortega-Mora, L., Álvarez-García, G., 2013b. First 2-DE approach towards characterising the proteome and immunome of *Besnoitia besnoiti* in the tachyzoite stage. Vet. Parasitol. 195 (1-2), 24-34.

García-Lunar, P., Regidor-Cerrillo, J., Ortega-Mora, L.M., Gutiérrez-Expósito, D., Álvarez-García, G., 2014. Proteomics reveals differences in protein abundance and highly similar antigenic profiles between *Besnoitia besnoiti* and *Besnoitia tarandi*. Vet. Parasitol. 205 (3-4), 434-443.

García-Lunar, P., Ortega-Mora, L., Schares, G., Diezma-Díaz, C., Álvarez-García, G., 2017. A new lyophilized tachyzoite based ELISA to diagnose *Besnoitia* spp. infection in bovids and wild ruminants improves specificity. Vet. Parasitol. 244, 176-182.

García-Lunar, P., Schares, G., Sanz-Fernandez, A., Jiménez-Meléndez, A., García-Soto, I., Regidor-Cerrillo, J., Pastor-Fernández, I., Hemphill, A., Fernández-Álvarez, M., Ortega-Mora, L., Álvarez-García, G., 2019. Development and characterization of monoclonal antibodies against *Besnoitia besnoiti* tachyzoites. Parasitology 146 (2), 187-196.

Garrido-Castañé, I., Romero, A.O., Espuny, J.C., Hentrich, B., Basso, W., 2019. *Besnoitia besnoiti* seroprevalence in beef, dairy and bullfighting cattle in Catalonia (north-eastern Spain): A cross-sectional study. Parasitol. Int. 69, 71-74.

Garrison, E., Treeck, M., Ehret, E., Butz, H., Garbuz, T., Oswald, B.P., Settles, M., Boothroyd, J., Arrizabalaga, G., 2012. A forward genetic screen reveals that calcium-dependent protein kinase 3 regulates egress in *Toxoplasma*. PLoS Pathog. 8 (11), e1003049.

Gazzonis, A.L., Álvarez García, G., Maggioni, A., Zanzani, S.A., Olivieri, E., Compiani, R., Sironi, G., Ortega Mora, L.M., Manfredi, M.T., 2017. Serological dynamics and risk factors of *Besnoitia besnoiti* infection in breeding bulls from an endemically infected purebred beef herd. Parasitol. Res. 116 (4), 1383-1393.

Gentile, A., Militerno, G., Schares, G., Nanni, A., Testoni, S., Bassi, P., Gollnick, N.S., 2012. Evidence for bovine besnoitiosis being endemic in Italy-First *in vitro* isolation of *Besnoitia besnoiti* from cattle born in Italy. Vet. Parasitol. 184 (2-4), 10.1016/j.vetpar.2011.09.014.

Gharaee-Kermani, M., Denholm, E.M., Phan, S.H., 1996. Costimulation of fibroblast collagen and transforming growth factor beta1 gene expression by monocyte chemoattractant protein-1 via specific receptors. J. Biol. Chem. 271 (30), 17779-17784.

Gimbrone Jr, M.A., García-Cardeña, G., 2016. Endothelial cell dysfunction and the pathobiology of atherosclerosis. Circ. Res. 118 (4), 620-636.

Givens, M.D., Marley, M., 2008. Infectious causes of embryonic and fetal mortality. Theriogenology 70 (3), 270-285.

Gobel, E., Widauer, R., Reimann, M., Munz, E., 1985. Ultrastructure of the asexual multiplication of *Besnoitia besnoiti* (Marotel, 1912) in Vero- and CRFK-cell cultures. Zentralbl. Veterinarmed. B. 32 (3), 202-212.

Goldman, M., Pipano, E., 1983. Serological studies on bovine besnoitiosis in Israel. Trop. Anim. Health Prod. 15 (1), 32-38.

Gollnick, N.S., Scharr, J.C., Schares, G., Langenmayer, M.C., 2015. Natural *Besnoitia besnoiti* infections in cattle: chronology of disease progression. BMC Vet. Res. 11, 35.

Gomes, T.C., Andrade Júnior, Heitor Franco de, Lescano, S.A.Z., Amato-Neto, V., 2012. *In vitro* action of antiparasitic drugs, especially artesunate, against *Toxoplasma gondii*. Rev. Soc. Bras. Med. Trop. 45 (4), 485-490.

Gondim, L., Meyer, J., Peters, M., Rezende-Gondim, M., Vrhovec, M., Pantchev, N., Bauer, C., Conraths, F., Schares, G., 2015. In vitro cultivation of *Hammondia heydorni*: Generation of tachyzoites, stage conversion into bradyzoites, and evaluation of serologic cross-reaction with Neospora caninum. Vet. Parasitol. 210 (3-4), 131-140.

Gubbels, M.J., Li, C., Striepen, B., 2003. High-throughput growth assay for *Toxoplasma gondii* using yellow fluorescent protein. Antimicrob. Agents Chemother. 47 (1), 309-316, 10.1128/aac.47.1.309-316.2003.

Guimarães, E.V., de Carvalho, L., Santos Barbosa, H., 2008. Primary culture of skeletal muscle cells as a model for studies of *Toxoplasma gondii* cystogenesis. J. Parasitol. 94 (1), 72-83.

Guiton, P.S., Sagawa, J.M., Fritz, H.M., Boothroyd, J.C., 2017. An *in vitro* model of intestinal infection reveals a developmentally regulated transcriptome of *Toxoplasma* sporozoites and a NF-κB-like signature in infected host cells. PloS one 12 (3), e0173018.

Gutiérrez-Expósito, D., Ortega-Mora, L.M., Gajadhar, A.A., García-Lunar, P., Dubey, J.P., Álvarez-García, G., 2012. Serological evidence of *Besnoitia* spp. infection in Canadian wild ruminants and strong cross-reaction between *Besnoitia besnoiti* and *Besnoitia tarandi*. Vet. Parasitol. 190 (1–2), 19-28.

Gutiérrez-Expósito, D., Ortega-Mora, L.M., Marco, I., Boadella, M., Gortazar, C., San Miguel-Ayanz, J.M., Garcia-Lunar, P., Lavin, S., Alvarez-Garcia, G., 2013. First serosurvey of *Besnoitia* spp. infection in wild European ruminants in Spain. Vet. Parasitol. 197 (3-4), 557-564.

Gutiérrez-Expósito, D., Esteban-Gil, A., Ortega-Mora, L.M., Garcia-Lunar, P., Castillo, J.A., Marcen, J.M., Álvarez-García, G., 2014. Prevalence of *Besnoitia besnoiti* infection in beef cattle from the Spanish Pyrenees. Vet. J. 200 (3), 468-470.

Gutiérrez-Expósito, D., Arnal, M.C., Martínez-Durán, D., Regidor-Cerrillo, J., Revilla, M., de Luco, Daniel L Fernández, Jiménez-Meléndez, A., Calero-Bernal, R., Habela, M.A., García-Bocanegra, I., Arenas-Montes, A., Ortega-Mora, LM., Álvarez-García, G., 2016. The role of wild ruminants as reservoirs *of Besnoitia besnoiti* infection in cattle. Vet. Parasitol. 223, 7-13.

Gutiérrez-Expósito, D. Epidemiología de la besnoitiosis bovina en España. Doctoral thesis. Faculty of Veterinary Sciences, Complutense Univeristy of Madrid, Spain.

Gutiérrez-Expósito, D., Ferre, I., Ortega-Mora, L.M., Alvarez-Garcia, G., 2017a. Advances in the diagnosis of bovine besnoitiosis: current options and applications for control. Int. J. Parasitol. 47 (12), 737-751.

Gutiérrez-Expósito, D., García-Bocanegra, I., Howe, D.K., Arenas-Montes, A., Yeargan, M.R., Ness, S.L., Ortega-Mora, L.M., Álvarez-García, G., 2017b. A serosurvey of selected cystogenic coccidia in Spanish equids: first detection of anti-*Besnoitia* spp. specific antibodies in Europe. BMC Vet. Res. 13 (1), 128.

Gutiérrez-Expósito, D., Ortega-Mora, L.M., Ara, V., Marco, I., Lavin, S., Carvajal-Valilla, J., Morales, A., Álvarez-García, G., 2017c. Absence of antibodies specific to *Besnoitia* spp. in European sheep and goats from areas in Spain where bovine besnoitiosis is endemic. Parasitol. Res. 116 (1), 445-448.

Gutiérrez-Expósito, D., Ortega-Mora, L.M., García-Lunar, P., Rojo-Montejo, S., Zabala, J., Serrano, M., Álvarez-García, G., 2017d. Clinical and serological dynamics of *Besnoitia besnoiti* infection in three endemically infected beef cattle herds. Transbound Emerg. Dis. 64 (2), 538-546.

Habarugira, G., Nkuranga, C., Asiimwe, B., Turikumwenayo, J.B., Ojok, L., 2019. First confirmed case of bovine besnoitiosis in Rwanda. Vet. Parasitol. Regional Studies and Reports 17, 100294.

Hadween, S., 1922. Cyst-forming protozoa in reindeer and caribou, and a sarcosporidian parasite of the seal (*Phoca richardi*). 61, 282-374.

Håkansson, S., Morisaki, H., Heuser, J., Sibley, L.D., 1999. Time-lapse video microscopy of gliding motility in *Toxoplasma gondii* reveals a novel, biphasic mechanism of cell locomotion. Mol. Biol. Cell 10 (11), 3539-3547.

Hakimi, M.A., Olias, P., Sibley, L.D., 2017. *Toxoplasma* Effectors Targeting Host Signaling and Transcription. Clin. Microbiol. Rev. 30 (3), 615-645.

Harding, C.R., Egarter, S., Gow, M., Jimenez-Ruiz, E., Ferguson, D.J., Meissner, M., 2016. Gliding Associated Proteins play essential roles during the formation of the inner membrane complex of *Toxoplasma gondii*. PLoS Pathog. 12 (2), e1005403.

Harker, K.S., Jivan, E., McWhorter, F.Y., Liu, W.F., Lodoen, M.B., 2014. Shear forces enhance *Toxoplasma gondii* tachyzoite motility on vascular endothelium. MBio 5 (2), e01111-13.

Harper, J.M., Zhou, X.W., Pszenny, V., Kafsack, B.F.C., Carruthers, V.B., 2004. The novel coccidian micronemal protein MIC11 undergoes proteolytic maturation by sequential cleavage to remove an internal propeptide. Int. J. Parasitol. 34 (9), 1047-1058.

Hassan, M.A., Melo, M.B., Haas, B., Jensen, K.D., Saeij, J.P., 2012. De novo reconstruction of the *Toxoplasma gondii* transcriptome improves on the current genome annotation and reveals alternatively spliced transcripts and putative long non-coding RNAs. BMC Genomics 13, 696.

Hehl, A.B., Basso, W.U., Lippuner, C., Ramakrishnan, C., Okoniewski, M., Walker, R.A., Grigg, M.E., Smith, N.C., Deplazes, P., 2015. Asexual expansion of *Toxoplasma gondii* merozoites is distinct from tachyzoites and entails expression of non-overlapping gene families to attach, invade, and replicate within feline enterocytes. BMC Genomics 16, 66.

Hemphill, A., Anghel, N., Balmer, V., Müller, J., Winzer, P., Aguado-Martinez, A., Roozbehani, M., Pou, S., Nilsen, A., Riscoe, M., 2018. Endochin-Like Quinolones Exhibit Promising Efficacy Against *Neospora Caninum in vitro* and in Experimentally Infected Pregnant Mice. Frontiers in veterinary science 5, 285.

Hemphill, A., 1996. Subcellular localization and functional characterization of Nc-p43, a major *Neospora caninum* tachyzoite surface protein. Infect. Immun. 64 (10), 4279-4287.

Hemphill, A., Gottstein, B., 1996. Identification of a major surface protein on *Neospora caninum* tachyzoites. Parasitol. Res. 82 (6), 497-504.

Hemphill, A., Gottstein, B., Kaufmann, H., 1996. Adhesion and invasion of bovine endothelial cells by *Neospora caninum*. Parasitology 112 (Pt 2), 183-197.

Hemphill, A., Vonlaufen, N., Naguleswaran, A., Keller, N., Riesen, M., Guetg, N., Srinivasan, S., Alaeddine, F., 2004. Tissue culture and explant approaches to studying and visualizing *Neospora caninum* and its interactions with the host cell. Microscopy and Microanalysis 10 (5), 602-620.

Hemphill, A., Gottstein, B., 2006. *Neospora caninum* and neosporosis - recent achievements in host and parasite cell biology and treatment. Acta Parasitol. 51 (1), 15-25.

Henderson, N.C., Arnold, T.D., Katamura, Y., Giacomini, M.M., Rodriguez, J.D., McCarty, J.H., Pellicoro, A., Raschperger, E., Betsholtz, C., Ruminski, P.G., 2013. Targeting of a v integrin identifies a core molecular pathway that regulates fibrosis in several organs. Nat. Med. 19 (12), 1617.

Herin, V.V., 1952. Note sur le existence de la Globidiose bovine an Ruanda-Urundi. Ann. Soc. Belg. Med. Trop 32 (2), 155-160-155-160.

Hermosilla, C., Barbisch, B., Heise, A., Kowalik, S., Zahner, H., 2002. Development of *Eimeria bovis in vitro*: suitability of several bovine, human and porcine endothelial cell lines, bovine fetal gastrointestinal, Madin–Darby bovine kidney (MDBK) and African green monkey kidney (VERO) cells. Parasitol. Res. 88 (4), 301-307.

Heydorn, A.O., Senaud, J., Mehlhorn, H., Heinonen, R., 1984. *Besnoitia* spp. from goats in Kenya. Z. Parasitenkd. 70 (6), 709-713.

Hines, S.A., Ramsay, J.D., Kappmeyer, L.S., Lau, A.O., Ojo, K.K., Van Voorhis, W.C., Knowles, D.P., Mealey, R.H., 2015. *Theileria equi* isolates vary in s usceptibility to imidocarb dipropionate but demonstrate uniform in vitro susceptibility to a bumped kinase inhibitor. Parasit. Vectors 8 (1), 33.

Hofmeyr, C.F.B., 1945. Globidiosis in cattle. J. S. Afr. Vet. Med. Ass. 16, 102-109.

Horcajo, P., Xia, D., Randle, N., Collantes-Fernández, E., Wastling, J., Ortega-Mora, L., Regidor-Cerrillo, J., 2018. Integrative transcriptome and proteome analyses define marked differences between *Neospora caninum* isolates throughout the tachyzoite lytic cycle. Journal of proteomics 180, 108-119.

Horcajo, P., Regidor-Cerrillo, J., Aguado-Martínez, A., Hemphill, A., Ortega-Mora, L.M., 2016. Vaccines for bovine neosporosis: current status and key aspects for development. Parasite Immunol. 38 (12), 709-723.

Horcajo, P., Jimenez-Pelayo, L., Garcia-Sanchez, M., Regidor-Cerrillo, J., Collantes-Fernandez, E., Rozas, D., Hambruch, N., Pfarrer, C., Ortega-Mora, L.M., 2017. Transcriptome modulation of bovine trophoblast cells *in vitro* by *Neospora caninum*. Int. J. Parasitol. 47 (12), 791-799.

Hordijk, P.L., 2006. Endothelial signalling events during leukocyte transmigration. The FEBS journal 273 (19), 4408-4415.

Hornok, S., Estok, P., Kovats, D., Flaisz, B., Takacs, N., Szoke, K., Krawczyk, A., Kontschan, J., Gyuranecz, M., Fedak, A., Farkas, R., Haarsma, A.J., Sprong, H., 2015a. Screening of bat faeces for arthropod-borne apicomplexan protozoa: *Babesia canis* and *Besnoitia besnoiti*-like sequences from Chiroptera. Parasit. Vectors 8, 441.

Hornok, S., Fedak, A., Baska, F., Basso, W., Dencso, L., Toth, G., Szeredi, L., Abonyi, T., Denes, B., 2015b. Vector-borne transmission of *Besnoitia besnoiti* by blood-sucking and secretophagous flies: epidemiological and clinicopathological implications. Parasit. Vectors 8, 450-015-1058-0, 10.1186/s13071-015-1058-0.

Hornok, S., Fedak, A., Baska, F., Hofmann-Lehmann, R., Basso, W., 2014. Bovine besnoitiosis emerging in Central-Eastern Europe, Hungary. Parasit. Vectors 7.

Howe, D.K., 2001. Initiation of a *Sarcocystis neurona* expressed sequence tag (EST) sequencing project: a preliminary report. Vet. Parasitol. 95 (2-4), 233-239.

Howe, D.K., Crawford, A.C., Lindsay, D., Sibley, L.D., 1998. The p29 and p35 immunodominant antigens of *Neospora caninum* tachyzoites are homologous to the family of surface antigens of *Toxoplasma gondii*. Infect. Immun. 66 (11), 5322-5328.

Huang, W., Ojo, K.K., Zhang, Z., Rivas, K., Vidadala, R.S.R., Scheele, S., DeRocher, A.E., Choi, R., Hulverson, M.A., Barrett, L.K., 2015. SAR studies of 5-aminopyrazole-4-carboxamide analogues as potent and selective inhibitors of *Toxoplasma gondii* CDPK1. ACS Med. Chem. Lett. 6 (12), 1184-1189.

Hui, R., El Bakkouri, M., Sibley, L.D., 2015. Designing selective inhibitors for calcium-dependent protein kinases in apicomplexans. Trends Pharmacol. Sci. 36 (7), 452-460.

Hulverson, M.A., Vinayak, S., Choi, R., Schaefer, D.A., Castellanos-Gonzalez, A., Vidadala, R.S., Brooks, C.F., Herbert, G.T., Betzer, D.P., Whitman, G.R., 2017. Bumped-Kinase Inhibitors for Cryptosporidiosis Therapy. J. Infect. Dis. 215 (8), 1275-1284.

Innes, E.A., Bartley, P.M., Maley, S.W., Wright, S.E., Buxton, D., 2007. Comparative host-parasite relationships in ovine toxoplasmosis and bovine neosporosis and strategies for vaccination. Vaccine 25(30) (0264-410), 5495-5503.

Irigoien, M., Del Cacho, E., Gallego, M., Lopez-Bernad, F., Quilez, J., Sanchez-Acedo, C., 2000. Immunohistochemical study of the cyst of *Besnoitia besnoiti*. Vet. Parasitol. 91 (1-2), 1-6.

J. Cuillé, P.C., 1937. Nouvelles recherches sur la transmission experimentale de la maladie appelée "anasarque des bovides" (globidiose cutanée du boeuf). Bull. Acad. Med 118, 217-219.

Jacquiet, P., Liénard, E., Franc, M., 2010. Bovine besnoitiosis: Epidemiological and clinical aspects. Vet. Parasitol. 174 (1-2), 30-36.

Jiménez-Pelayo, L., García-Sánchez, M., Regidor-Cerrillo, J., Horcajo, P., Collantes-Fernández, E., Gómez-Bautista, M., Hambruch, N., Pfarrer, C., Ortega-Mora, L.M., 2017. Differential susceptibility of bovine caruncular and trophoblast cell lines to infection with high and low virulence isolates of *Neospora caninum*. Parasit. Vectors. 10 (1), 463.

Jin, K., Mao, X.O., Sun, Y., Xie, L., Jin, L., Nishi, E., Klagsbrun, M., Greenberg, D.A., 2002. Heparin-binding epidermal growth factor-like growth factor: hypoxia-inducible expression *in vitro* and stimulation of neurogenesis *in vitro* and *in vivo*. J. Neurosci. 22 (13), 5365-5373.

Johnson, S.M., Murphy, R.C., Geiger, J.A., DeRocher, A.E., Zhang, Z., Ojo, K.K., Larson, E.T., Perera, B.G., Dale, E.J., He, P., Reid, M.C., Fox, A.M., Mueller, N.R., Merritt, E.A., Fan, E., Parsons, M., Van Voorhis, W.C., Maly, D.J., 2012. Development of *Toxoplasma gondii* calcium-dependent protein kinase 1 (TgCDPK1) inhibitors with potent anti-toxoplasma activity. J. Med. Chem. 55 (5), 2416-2426.

Juste, R.A., Cuervo, L.A., Marco, J.C., Oregui, L.M., 1990. La besnoitiosis bovina, ¿desconocida en España? Medicina Veterinaria 7 (11), 613-618.

Keeley, A., Soldati, D., 2004. The glideosome: a molecular machine powering motility and host-cell invasion by Apicomplexa. Trends Cell Biol. 14 (10), 528-532.

Keller, N., Riesen, M., Naguleswaran, A., Vonlaufen, N., Stettler, R., Leepin, A., Wastling, J.M., Hemphill, A., 2004. Identification and characterization of a *Neospora caninum* microneme-associated protein (NcMIC4) that exhibits unique lactose-binding properties. Infect. Immun. 72 (8), 4791-4800.

Keller, N., Naguleswaran, A., Cannas, A., Vonlaufen, N., Bienz, M., Bjorkman, C., Bohne, W., Hemphill, A., 2002. Identification of a *Neospora caninum* microneme protein (NcMIC1) which interacts with sulfated host cell surface glycosaminoglycans. Infect. Immun. 70 (6), 3187-3198.

Kiehl, E., Heydorn, A.O., Schein, E., Al-Rasheid, K.A., Selmair, J., Abdel-Ghaffar, F., Mehlhorn, H., 2010. Molecular biological comparison of different *Besnoitia* species and stages from different countries. Parasitol. Res. 106 (4), 889-894.

Kim, K., Weiss, L.M., 2004. *Toxoplasma gondii:* the model apicomplexan. Int. J. Parasitol. 34 (3), 423-432.

Knight, B., Kissane, S., Falciani, F., Salmon, M., Stanford, M., Wallace, G., 2006. Expression analysis of immune response genes of Müller cells infected with *Toxoplasma gondii*. J. Neuroimmunol. 179 (1-2), 126-131.

Krishna, R., Xia, D., Sanderson, S., Shanmugasundram, A., Vermont, S., Bernal, A., Daniel-Naguib, G., Ghali, F., Brunk, B.P., Roos, D.S., Wastling, J.M., Jones, A.R., 2015. A large-scale proteogenomics study of apicomplexan pathogens-*Toxoplasma gondii* and *Neospora caninum*. Proteomics 15 (15), 2618-2628.

Kumi-Diaka, J., Wilson, S., Sanusi, A., Njoku, C.E., Osori, D.I., 1981. Bovine besnoitiosis and its effect on the male reproductive system. Theriogenology 16 (5), 523-530.

Lally, N., Jenkins, M., Liddell, S., Dubey, J.P., 1997. A dense granule protein (NCDG1) gene from *Neospora caninum*. Mol. Biochem. Parasitol. 87 (2), 239-243.

Langenmayer, M.C., Scharr, J.C., Sauter-Louis, C., Schares, G., Gollnick, N.S., 2015a. Natural *Besnoitia besnoiti* infections in cattle: hematological alterations and changes in serum chemistry and enzyme activities. BMC Vet. Res. 11 (1), 32.

Langenmayer, M., Gollnick, N., Scharr, J., Schares, G., Herrmann, D., Majzoub-Altweck, M., Hermanns, W., 2015b. *Besnoitia besnoiti* infection in cattle and mice: ultrastructural pathology in acute and chronic besnoitiosis. Parasitol. Res. 114 (3), 955-963.

Langenmayer, M.C., Gollnick, N.S., Majzoub-Altweck, M., Scharr, J.C., Schares, G., Hermanns, W., 2015c. Naturally Acquired Bovine Besnoitiosis: Histological and Immunohistochemical Findings in Acute, Subacute, and Chronic Disease. Vet. Pathol. 52 (3), 476-488,

Lau, Y., Lee, W., Gudimella, R., Zhang, G., Ching, X., Razali, R., Aziz, F., Anwar, A., Fong, M., 2016. Deciphering the draft genome of *Toxoplasma gondii* RH strain. PloS one 11 (6), e0157901.

Lee, S., Eo, K., Jung, B.Y., Kwak, D., Kwon, O., 2017. Seroprevalence and risk factors of *Besnoitia besnoiti* infection in Korean cattle–short communication. Acta Vet. Hung. 65 (4), 510-516.

Lee, E.G., Kim, J.H., Shin, Y.S., Shin, G.W., Kim, Y.H., Kim, G.S., Kim, D.Y., Jung, T.S., Suh, M.D., 2004. Two-dimensional gel electrophoresis and immunoblot analysis of *Neospora caninum* tachyzoites. J. Vet. Sci. 5 (1229-845; 2), 139-145.

Lee, E.G., Kim, J.H., Shin, Y.S., Shin, G.W., Suh, M.D., Kim, D.Y., Kim, Y.H., Kim, G.S., Jung, T.S., 2003. Establishment of a two-dimensional electrophoresis map for *Neospora caninum* tachyzoites by proteomics. Proteomics 3 (12), 2339-2350.

Lei, T., Wang, H., Liu, J., Nan, H., Liu, Q., 2014. ROP18 is a key factor responsible for virulence difference between *Toxoplasma gondii* and *Neospora caninum*. PLoS One 9 (6), e99744.

Leineweber, M., Spekker-Bosker, K., Ince, V., Schares, G., Hemphill, A., Eller, S.K., Däubener, W., 2017. First Characterization of the *Neospora caninum* Dense Granule Protein GRA9. BioMed research international 2017.

Leitao, J.L.D.S., 1949. Globidiose bovina por *Globidium besnoiti*. Rev. De Med. Vet. (Portugal) 44 (330), 152-156.

Lendner, M., Böttcher, D., Delling, C., Ojo, K.K., Van Voorhis, W.C., Daugschies, A., 2015. A novel CDPK1 inhibitor—a potential treatment for cryptosporidiosis in calves? Parasitol. Res. 114 (1), 335-336.

LEONARDO, Q., Rosiles, R., Bautista, J., GONZÁLEZ-MONSÓN, N., Sumano, H., 2009. Oral pharmacokinetics and milk residues of decoquinate in milking cows. J. Vet. Pharmacol. Ther. 32 (4), 403-406.

Lertkiatmongkol, P., Liao, D., Mei, H., Hu, Y., Newman, P.J., 2016. Endothelial functions of platelet/endothelial cell adhesion molecule-1 (CD31). Curr. Opin. Hematol. 23 (3), 253-259.

Lesage, K.M., Huot, L., Mouveaux, T., Courjol, F., Saliou, J., Gissot, M., 2018. Cooperative binding of ApiAP2 transcription factors is crucial for the expression of virulence genes in *Toxoplasma gondii*. Nucleic Acids Res. 46 (12), 6057-6068.

Levine, N.D., 1961. Protozoan Parasites of Domestic Animals and of Man. , Minneapolis, MN, 1–412 pp.

Li, L., Crabtree, J., Fischer, S., Pinney, D., Stoeckert, C.J.,Jr., Sibley, L.D., Roos, D.S., 2004. ApiEST-DB: analyzing clustered EST data of the apicomplexan parasites. Nucleic Acids Res. 32 Database issue, D326-D328.

Li, L., Brunk, B.P., Kissinger, J.C., Pape, D., Tang, K., Cole, R.H., Martin, J., Wylie, T., Dante, M., Fogarty, S.J., Howe, D.K., Liberator, P., Diaz, C., Anderson, J., White, M., Jerome, M.E., Johnson, E.A., Radke, J.A., Stoeckert, C.J.,Jr., Waterston, R.H., Clifton, S.W., Roos, D.S., Sibley, L.D., 2003. Gene discovery in the apicomplexa as revealed by EST sequencing and assembly of a comparative gene database. Genome Res. 13 (3), 443-454.

Li, W., Liu, J., Wang, J., Fu, Y., Nan, H., Liu, Q., 2015. Identification and characterization of a microneme protein (NcMIC6) in *Neospora caninum*. Parasitol. Res. 114 (8), 2893-2902.

Liddell, S., Lally, N.C., Jenkins, M.C., Dubey, J.P., 1998. Isolation of the cDNA encoding a dense granule associated antigen (NCDG2) of *Neospora caninum*. Mol. Biochem. Parasitol. 93 (1), 153-158.

Liénard, E., Nabuco, A., Vandenabeele, S., Losson, B., Tosi, I., Bouhsira, É., Prévot, F., Sharif, S., Franc, M., Vanvinckenroye, C., 2018. First evidence of *Besnoitia bennetti* infection (Protozoa: Apicomplexa) in donkeys (*Equus asinus*) in Belgium. Parasit. Vectors 11 (1), 427.

Lienard, E., Pop, L., Prevot, F., Grisez, C., Mallet, V., Raymond-Letron, I., Bouhsira, E., Franc, M., Jacquiet, P., 2015. Experimental infections of rabbits with proliferative and latent stages of *Besnoitia besnoiti*. Parasitol. Res. 114 (10), 3815-3826.

Lienard, E., Salem, A., Jacquiet, P., Grisez, C., Prevot, F., Blanchard, B., Bouhsira, E., Franc, M., 2012. Development of a protocol testing the ability of *Stomoxys calcitrans* (Linnaeus, 1758) (Diptera: Muscidae) to transmit *Besnoitia besnoiti* (Henry, 1913) (Apicomplexa: Sarcocystidae). Parasitol. Res. 112(2):479-486.

Lindsay, D.S., Blagburn, B.L., 1994. Activity of diclazuril against *Toxoplasma gondii* in cultured cells and mice. Am. J. Vet. Res. 55 (4), 530-533.

Lindsay, D.S., Rippey, N.S., Cole, R.A., Parsons, L.C., Dubey, J.P., Tidwell, R.R., Blagburn, B.L., 1994. Examination of the activities of 43 chemotherapeutic agents against *Neospora caninum* tachyzoites in cultured cells. Am. J. Vet. Res. 55 (7), 976-981.

Lindsay, D.S., Rippey, N.S., Toivio-Kinnucan, M.A., Blagburn, B.L., 1995. Ultrastructural effects of diclazuril against *Toxoplasma gondii* and investigation of a diclazuril-resistant mutant. J. Parasitol. 81, 459-466.

Lindsay, D.S., Butler, J.M., Rippey, N.S., Blagburn, B.L., 1996. Demonstration of synergistic effects of sulfonamides and dihydrofolate reductase/thymidylate synthase inhibitors against *Neospora caninum* tachyzoites in cultured cells, and characterization of mutants resistant to pyrimethamine. Am. J. Vet. Res. 57 (1), 68-72.

Lindsay, D.S., Butler, J.M., Blagburn, B.L., 1997. Efficacy of decoquinate against *Neospora caninum* tachyzoites in cell cultures. Vet. Parasitol. 68 (1-2), 35-40.

Lindsay, D., Toivio-Kinnucan, M., Blagburn, B., 1998. Decoquinate induces tissue cyst formation by the RH strain of *Toxoplasma gondii*. Vet. Parasitol. 77 (2-3), 75-81.

Liu, Q., Wang, Z., Huang, S., Zhu, X., 2015. Diagnosis of toxoplasmosis and typing of *Toxoplasma gondii*. Parasit. Vectors 8 (1), 292.

Liu, G., Cui, X., Hao, P., Yang, D., Liu, J., Liu, Q., 2013. GRA 14, a novel dense granule protein from *Neospora caninum*. Acta Biochim. Biophys. Sin. (Shanghai) 45 (7), 607-609.

Long, S., Wang, Q., Sibley, L.D., 2016. Analysis of noncanonical calcium-dependent protein kinases in *Toxoplasma gondii* by targeted gene deletion Using CRISPR/Cas9. Infect. Immun. 84 (5), 1262-1273.

Lourido, S., Shuman, J., Zhang, C., Shokat, K.M., Hui, R., Sibley, L.D., 2010. Calcium-dependent protein kinase 1 is an essential regulator of exocytosis in *Toxoplasma*. Nature 465 (7296), 359-362.

Lourido, S., Tang, K., Sibley, L.D., 2012. Distinct signalling pathways control Toxoplasma egress and host-cell invasion. EMBO J. 31 (24), 4524-4534, 10.1038/emboj.2012.299.

Lourido, S., Jeschke, G.R., Turk, B.E., Sibley, L.D., 2013. Exploiting the unique ATP-binding pocket of *Toxoplasma* calcium-dependent protein kinase 1 to identify its substrates. ACS chemical biology 8 (6), 1155-1162.

Lourido, S., Moreno, S.N., 2015. The calcium signaling toolkit of the Apicomplexan parasites *Toxoplasma gondii* and *Plasmodium* spp. Cell Calcium 57 (3), 186-193.

Lovett, J.L., Howe, D.K., Sibley, L.D., 2000. Molecular characterization of a thrombospondin-related anonymous protein homologue in *Neospora caninum*. Mol. Biochem. Parasitol. 107 (1), 33-43.

Ma, L., Liu, G., Liu, J., Li, M., Zhang, H., Tang, D., Liu, Q., 2017a. *Neospora caninum* ROP16 play an important role in the pathogenicity by phosphorylating host cell STAT3. Vet. Parasitol. 243, 135-147.

Ma, L., Liu, J., Li, M., Fu, Y., Zhang, X., Liu, Q., 2017b. Rhoptry protein 5 (ROP5) is a key virulence factor in *Neospora caninum*. Frontiers in microbiology 8, 370.

Madubata, C., Dunams-Morel, D.B., Elkin, B., Oksanen, A., Rosenthal, B.M., 2012. Evidence for a recent population bottleneck in an Apicomplexan parasite of caribou and reindeer, *Besnoitia tarandi*. Infect. Genet. Evol. 12 (8), 1605-1613.

Mainar-Jaime, R., Berzal-Herranz, B., Arias, P., Rojo-Vázquez, F., 2001. Epidemiological pattern and risk factors associated with bovine viral-diarrhoea virus (BVDV) infection in a non-vaccinated dairy-cattle population from the Asturias region of Spain. Prev. Vet. Med. 52 (1), 63-73.

Maksimov, P., Hermosilla, C., Kleinertz, S., Hirzmann, J., Taubert, A., 2016. *Besnoitia besnoiti* infections activate primary bovine endothelial cells and promote PMN adhesion and NET formation under physiological flow condition. Parasitol. Res. 115 (5), 1991-2001.

Marcelino, E., Martins, T.M., Morais, J.B., Nolasco, S., Cortes, H., Hemphill, A., Leitao, A., Novo, C., 2011. *Besnoitia besnoiti* protein disulfide isomerase (BbPDI): molecular characterization, expression and in silico modelling. Exp. Parasitol. 129 (2), 164-174.

Marcén-Seral, JM, 2011. Las especies felina y canina como potenciales hospedadores definitivos y transmisores de *Besnoitia besnoiti*: infección experimental en el gato y en el perro. Doctoral Thesis. Faculty of Veterinary Sciences, Zaragoza, Spain.

Marotel, M., 1912. Discussion of paper by Besnoit e Robin. Bull. et Mem. de la Soc. des Sciences Vet. de Lyon et de la Soc. de Med. Vet. de Lyon e du Sud-Est 15, 196-217.

Marugán-Hernández, V., Álvarez-García, G., Risco-Castillo, V., Regidor-Cerrillo, J., Ortega-Mora, L.M., 2010. Identification of *Neospora caninum* proteins regulated during the differentiation process from tachyzoite to bradyzoite stage by DIGE. Proteomics 10 (9), 1740-1750.

Marugán-Hernández, V., Álvarez-García, G., Tomley, F., Hemphill, A., Regidor-Cerrillo, J., Ortega-Mora, L.M., 2011a. Identification of novel rhoptry proteins in *Neospora caninum* by LC/MS-MS analysis of subcellular fractions. J. Proteomics 74 (5), 629-642.

Marugán-Hernández, V., Ortega-Mora, L.M., Aguado-Martínez, A., Jiménez-Ruiz, E., Álvarez-Garcia, G., 2011b. Transgenic *Neospora caninum* strains constitutively expressing the bradyzoite NcSAG4 protein proved to be safe and conferred significant levels of protection against vertical transmission when used as live vaccines in mice. Vaccine 29 (44), 7867-7874.

Mazuz, M.L., Alvarez-García, G., King, R., Savisky, I., Shkap, V., Ortega-Mora, L.M., Gutiérrez-Expósito, D., 2018. Exposure to *Neospora* spp. and *Besnoitia* spp. in wildlife from Israel. Int. J. Parasitol. Parasites Wildl. 7 (3), 317-321.

Mbuthia, P.G., Gathumbi, P.K., Bwangamoi, O., Wasike, P.N., 1993. Natural besnoitiosis in a rabbit. Vet. Parasitol. 45 (3-4), 191-198.

McCoy, J.M., Whitehead, L., van Dooren, G.G., Tonkin, C.J., 2012. TgCDPK3 regulates calcium-dependent egress of *Toxoplasma gondii* from host cells. PLoS Pathog. 8 (12), e1003066.

McCully, R.M., Basson, P.A., Van Niekerk, J.W., Bigalkie, R.D., 1966. Observations on *Besnoitia* cysts in the cardiovascular system of some wild antelopes and domestic cattle. Onderstepoort J. Vet. Res. 33 ((2)), 245-276.

Mehlhorn, H., Klimpel, S., Schein, E., Heydorn, A.O., Al-Quraishy, S., Selmair, J., 2009. Another African disease in Central Europa: Besnoitiosis of cattle. I. Light and electron microscopical study. Parasitol. Res. 104 (4), 861-868.

Meissner, M., Schluter, D., Soldati, D., 2002. Role of *Toxoplasma gondii* myosin A in powering parasite gliding and host cell invasion. Science 298 (5594), 837-840.

Millán, J., Sobrino, R., Rodríguez, A., Oleaga, Á., Gortazar, C., Schares, G., 2012. Large-scale serosurvey of *Besnoitia besnoiti* in free-living carnivores in Spain. Vet. Parasitol. 190 (1–2), 241-245.

Moine, E., Denevault-Sabourin, C., Debierre-Grockiego, F., Silpa, L., Gorgette, O., Barale, J., Jacquiet, P., Brossier, F., Gueiffier, A., Dimier-Poisson, I., 2015. A small-molecule cell-based screen led to the identification of biphenylimidazoazines with highly potent and broad-spectrum anti-apicomplexan activity. Eur. J. Med. Chem. 89, 386-400.

Mordue, D.G., Desai, N., Dustin, M., Sibley, L.D., 1999a. Invasion by *Toxoplasma gondii* establishes a moving junction that selectively excludes host cell plasma membrane proteins on the basis of their membrane anchoring. J. Exp. Med. 190 (12), 1783-1792.

Mordue, D.G., Hakansson, S., Niesman, I., Sibley, L.D., 1999b. *Toxoplasma gondii* resides in a vacuole that avoids fusion with host cell endocytic and exocytic vesicular trafficking pathways. Exp. Parasitol. 92 (2), 87-99.

Morlon-Guyot, J., Berry, L., Chen, C., Gubbels, M., Lebrun, M., Daher, W., 2014. The *Toxoplasma gondii* calcium-dependent protein kinase 7 is involved in early steps of parasite division and is crucial for parasite survival. Cell. Microbiol. 16 (1), 95-114.

Mota, C.M., Oliveira, A., Davoli-Ferreira, M., Silva, M.V., Santiago, F.M., Nadipuram, S.M., Vashisht, A.A., Wohlschlegel, J.A., Bradley, P.J., Silva, J.S., 2016. *Neospora caninum* activates p38 MAPK as an evasion mechanism against innate immunity. Frontiers in microbiology 7, 1456.

Moudy, R., Manning, T.J., Beckers, C.J., 2001. The loss of cytoplasmic potassium upon host cell breakdown triggers egress of *Toxoplasma gondii*. J. Biol. Chem. 276 (44), 41492-41501.

Müller, J., Hemphill, A., 2012. *In vitro* culture systems for the study of apicomplexan parasites in farm animals. Int. J. Parasitol. 43(2):115-24

Müller, J., Aguado-Martinez, A., Manser, V., Balmer, V., Winzer, P., Ritler, D., Hostettler, I., Arranz-Solis, D., Ortega-Mora, L., Hemphill, A., 2015. Buparvaquone is active against Neospora caninum *in vitro* and in experimentally infected mice. Int. J. Parasitol. Drugs Drug Resist 5 (1), 16-25.

Müller, J., Aguado, A., Laleu, B., Balmer, V., Ritler, D., Hemphill, A., 2017a. *In vitro* screening of the open source Pathogen Box identifies novel compounds with profound activities against *Neospora caninum*. Int. J. Parasitol. 47 (12), 801-809.

Müller, J., Aguado-Martínez, A., Balmer, V., Maly, D.J., Fan, E., Ortega-Mora, L., Ojo, K.K., Van Voorhis, W.C., Hemphill, A., 2017b. Two novel calcium-dependent kinase 1-inhibitors interfere with vertical transmission in mice infected with *Neospora caninum* tachyzoites. Antimicrob. Agents Chemother. , AAC. 02324-16.

Müller, J., Manser, V., Hemphill, A., 2018. *In vitro* treatment of *Besnoitia besnoiti* with the naphto-quinone buparvaquone results in marked inhibition of tachyzoite proliferation, mitochondrial alterations and rapid adaptation of tachyzoites to increased drug concentrations. Parasitology 146, 112-120.

Muno, R.M.d., Moura, M.A., Carvalho, L.C.d., Seabra, S.H., Barbosa, H.S., 2014. Spontaneous cystogenesis of *Toxoplasma gondii* in feline epithelial cells *in vitro*.

Muñoz-Caro, T., Silva, L.M., Ritter, C., Taubert, A., Hermosilla, C., 2014. *Besnoitia besnoiti* tachyzoites induce monocyte extracellular trap formation. Parasitol. Res. 113 (11), 4189-4197.

Muñoz-Caro, T., Hermosilla, C., Silva, L.M., Cortes, H., Taubert, A., 2014. Neutrophil extracellular traps as innate immune reaction against the emerging apicomplexan parasite *Besnoitia besnoiti*. PloS one 9 (3), e91415.

Nagamune, K., Hicks, L.M., Fux, B., Brossier, F., Chini, E.N., Sibley, L.D., 2008a. Abscisic acid controls calcium-dependent egress and development in *Toxoplasma gondii*. Nature 451 (7175), 207-210.

Nagamune, K., Moreno, S.N., Chini, E.N., Sibley, L.D., 2008b. Calcium regulation and signaling in apicomplexan parasites. In: Molecular Mechanisms of Parasite Invasion. Springer, pp. 70-81.

Naguleswaran, A., Alaeddine, F., Guionaud, C., Vonlaufen, N., Sonda, S., Jenoe, P., Mevissen, M., Hemphill, A., 2005. *Neospora caninum* protein disulfide isomerase is involved in tachyzoite-host cell interaction. Int. J. Parasitol. 35 (13), 1459-1472.

Naguleswaran, A., Muller, N., Hemphill, A., 2003. *Neospora caninum* and *Toxoplasma gondii*: a novel adhesion/invasion assay reveals distinct differences in tachyzoite-host cell interactions. Exp. Parasitol. 104 (3-4), 149-158.

Naguleswaran, A., Cannas, A., Keller, N., Vonlaufen, N., Bjorkman, C., Hemphill, A., 2002. Vero cell surface proteoglycan interaction with the microneme protein NcMIC(3) mediates adhesion of *Neospora caninum* tachyzoites to host cells unlike that in *Toxoplasma gondii*. Int. J. Parasitol. 32 (6), 695-704.

Naguleswaran, A., Cannas, A., Keller, N., Vonlaufen, N., Schares, G., Conraths, F.J., Bjorkman, C., Hemphill, A., 2001. *Neospora caninum* microneme protein NcMIC3: secretion, subcellular localization, and functional involvement in host cell interaction. Infect. Immun. 69 (10), 6483-6494.

Namavari, M., Oryan, A., Namazi, F., Kargar, M., Mansourian, M., Rahimian, A., Tahamtan, Y., 2013. Evaluation of cross immunity and histopathological findings in experimentally infected BALB/c mice with *Neospora caninum* and *Besnoitia caprae*. Iran. J. Parasitol. 8 (1), 99-106.

Neill, J.D., Ridpath, J.F., Lange, A., Zuerner, R.L., 2008. Bovine viral diarrhoea virus infection alters global transcription profiles in bovine endothelial cells. Dev. Biol. (Basel) 132, 93-98.

Nelson, M.M., Jones, A.R., Carmen, J.C., Sinai, A.P., Burchmore, R., Wastling, J.M., 2008. Modulation of the host cell proteome by the intracellular apicomplexan parasite *Toxoplasma gondii*. Infect. Immun. 76 (2), 828-844.

Ness, S.L., Peters-Kennedy, J., Schares, G., Dubey, J.P., Mittel, L.D., Mohammed, H.O., Bowman, D.D., Felippe, M.J., Wade, S.E., Shultz, N., Divers, T.J., 2012. Investigation of an outbreak of besnoitiosis in donkeys in northeastern Pennsylvania. J. Am. Vet. Med. Assoc. 240 (11), 1329-1337.

Ness, S.L., Schares, G., Peters-Kennedy, J., Mittel, L.D., Dubey, J.P., Bowman, D.D., Mohammed, H.O., Divers, T.J., 2014. Serological diagnosis of *Besnoitia bennetti* infection in donkeys (*Equus asinus*). J. Vet. Diagn. Invest. 26 (6), 778-782.

Neuman, M., 1962b. The experimental infection of the gerbil (*Meriones tristami shawii*) with *Besnoitia besnoiti*. Refuah Vet 19, 188.

Neuman, M., 1972a. Serological survey of *Besnoitia besnoiti* (Marotel 1912) infection in Israel by immunofluorescence. Zentralbl. Veterinarmed. B. 19 (5), 391-396.

Neuman, M., 1972b. Pathological changes causing sterility in bulls affected with *Besnoitia besnoiti*. 19 (J. Protozool), 54.

Neuman, M., 1974. Cultivation of *Besnoitia besnoiti* Marotel, 1912, in cell culture. Tropenmed. Parasitol. 25 (2), 243-249.

Ng, S.T., Sanusi Jangi, M., Shirley, M.W., Tomley, F.M., Wan, K.L., 2002. Comparative EST analyses provide insights into gene expression in two asexual developmental stages of *Eimeria tenella*. Exp. Parasitol. 101 (2-3), 168-173.

Nganga, C.J., Kanyari, P.W., Munyua, W.K., 1994. Isolation of *Besnoitia wallacei* in Kenya. Vet. Parasitol. 52 (3-4), 203-206.

Niedelman, W., Gold, D.A., Rosowski, E.E., Sprokholt, J.K., Lim, D., Farid Arenas, A., Melo, M.B., Spooner, E., Yaffe, M.B., Saeij, J.P., 2012. The rhoptry proteins ROP18 and ROP5 mediate *Toxoplasma gondii* evasion of the murine, but not the human, interferon-gamma response. PLoS Pathog. 8 (6), e1002784.

Nieto-Rodríguez, J.M., Calero-Bernal, R., Álvarez-García, G., Gutiérrez-Expósito, D., Redondo-García, E., Fernández-García, J.L., Martínez-Estéllez, M.Á.H., 2016. Characterization of an outbreak of emerging bovine besnoitiosis in southwestern Spain. Parasitol. Res. 115 (7), 2887-2892.

Nischik, N., Schade, B., Dytnerska, K., Dlugonska, H., Reichmann, G., Fischer, H.G., 2001. Attenuation of mouse-virulent *Toxoplasma gondii* parasites is associated with a decrease in interleukin-12-inducing tachyzoite activity and reduced expression of actin, catalase and excretory proteins. Microbes Infect. 3 (9), 689-699.

Nishikawa, Y., Shimoda, N., Fereig, R.M., Moritaka, T., Umeda, K., Nishimura, M., Ihara, F., Kobayashi, K., Himori, Y., Suzuki, Y., Furuoka, H., 2018. *Neospora caninum* dense granule protein 7 regulates the pathogenesis of neosporosis by modulating host immune response. Appl. Environ. Microbiol. 84 (18),

Nishikawa, Y., Ibrahim, H.M., Kameyama, K., Shiga, I., Hiasa, J., Xuan, X., 2011. Host cholesterol synthesis contributes to growth of intracellular *Toxoplasma gondii* in macrophages. J. Vet. Med. Sci. 73 (5), 633-639.

Nishimura, M., Tanaka, S., Ihara, F., Muroi, Y., Yamagishi, J., Furuoka, H., Suzuki, Y., Nishikawa, Y., 2015. Transcriptome and histopathological changes in mouse brain infected with *Neospora caninum*. Sci. Rep. 5:7936.

Njagi, O.N., Ndarathi, C.M., Nyaga, P.N., Munga, L.K., 1998. An epidemic of besnoitiosis in cattle in Kenya. Onderstepoort J. Vet. Res. 65 (2), 133-136.

Njenga, J., Bwangamoi, O., Mutiga, E., Kangethe, E., Mugera, G., 1993. Preliminary findings from an experimental study of caprine besnoitiosis in Kenya. Vet. Res. Commun. 17 (3), 203-208.

Njenga, J.M., Bwangamoi, O., Kangethe, E.K., Mugera, G.M., Mutiga, E.R., 1995. Comparative ultrastructural studies on *Besnoitia besnoiti* and *Besnoitia caprae*. Vet. Res. Commun. 19 (4), 295-308.

Nobel, T.A., Neumann, M., Klopper, U., Perl, S., 1981. Cysts of *Besnoitia besnoiti* in genital organs of the cow. Bull. Acad. Med. Vet. France 50, 569-574.

Nolan, S.J., Romano, J.D., Luechtefeld, T., Coppens, I., 2015. *Neospora caninum* Recruits Host Cell Structures to Its Parasitophorous Vacuole and Salvages Lipids from Organelles. Eukaryot. Cell. 14 (5), 454-473.

Nyoman, A.D.N., Lüder, C.G., 2013. Apoptosis-like cell death pathways in the unicellular parasite *Toxoplasma gondii* following treatment with apoptosis inducers and chemotherapeutic agents: a proof-of-concept study. Apoptosis 18 (6), 664-680.

Ojo, K.K., Larson, E.T., Keyloun, K.R., Castaneda, L.J., DeRocher, A.E., Inampudi, K.K., Kim, J.E., Arakaki, T.L., Murphy, R.C., Zhang, L., 2010. *Toxoplasma gondii* calcium-dependent protein kinase 1 is a target for selective kinase inhibitors. Nat. Struct. Mol. Biol.17 (5), 602-607.

Ojo, K.K., Pfander, C., Mueller, N.R., Burstroem, C., Larson, E.T., Bryan, C.M., Fox, A.M., Reid, M.C., Johnson, S.M., Murphy, R.C., Kennedy, M., Mann, H., Leibly, D.J., Hewitt, S.N., Verlinde, C.L., Kappe, S., Merritt, E.A., Maly, D.J., Billker, O., Van Voorhis, W.C., 2012. Transmission of malaria to mosquitoes blocked by bumped kinase inhibitors. J. Clin. Invest. 122 (6), 2301-2305.

Ojo, K.K., Reid, M.C., Kallur Siddaramaiah, L., Muller, J., Winzer, P., Zhang, Z., Keyloun, K.R., Vidadala, R.S., Merritt, E.A., Hol, W.G., Maly, D.J., Fan, E., Van Voorhis, W.C., Hemphill, A., 2014. *Neospora caninum* calcium-dependent protein kinase 1 is an effective drug target for neosporosis therapy. PLoS One 9 (3), e92929.

Ojo, K.K., Dangoudoubiyam, S., Verma, S.K., Scheele, S., DeRocher, A.E., Yeargan, M., Choi, R., Smith, T.R., Rivas, K.L., Hulverson, M.A., 2016. Selective inhibition of *Sarcocystis neurona* calcium-dependent protein kinase 1 for equine protozoal myeloencephalitis therapy. Int. J. Parasitol. 46 (13), 871-880.

Okada, T., Marmansari, D., Li, Z.M., Adilbish, A., Canko, S., Ueno, A., Shono, H., Furuoka, H., Igarashi, M., 2013. A novel dense granule protein, GRA22, is involved in regulating parasite egress in *Toxoplasma gondii*. Mol. Biochem. Parasitol. 189 (1-2), 5-13.

Okomo-Adhiambo, M., Beattie, C., Rink, A., 2006. cDNA microarray analysis of host-pathogen interactions in a porcine *in vitro* model for *Toxoplasma gondii* infection. Infect. Immun. 74 (7), 4254-4265.

Olafsson, E.B., Ross, E.C., Varas-Godoy, M., Barragan, A., 2019. TIMP-1 promotes hypermigration of *Toxoplasma*-infected primary dendritic cells via CD63-ITGB1-FAK signaling. J. Cell. Sci. 132 (3).

Olias, P., Schade, B., Mehlhorn, H., 2011. Molecular pathology, taxonomy and epidemiology of *Besnoitia* species (Protozoa: Sarcocystidae). Infection, Genetics and Evolution 11 (7), 1564-1576.

Oryan, A., Azizi, S., 2008. Ultrastructure and pathology of *Besnoitia caprae* in the naturally infected goats of Kerman, East of Iran. Parasitol. Res. 102 (6), 1171-1176.

Oryan, A., Namazi, F., Namavari, M., Sharifiyazdi, H., Moraveji, M., 2010. Comparison of the pathogensis of two isolates of *Besnoitia caprae* in inbred BALB/c mice. Vet. Res. Commun. 34 (5), 423-434, 10.1007/s11259-010-9415-0.

Oryan, A., Namazi, F., Silver, I.A., 2011. histopathologic and ultrastructural studies on experimental caprine besnoitiosis. Vet. Pathol. 48 (6), 10.1177/0300985811398248.

Oryan, A., Silver, I.A., Sadoughifar, R., 2014. Caprine besnoitiosis: an emerging threat and its relationship to some other infections of ungulates by *Besnoitia* species. Res. Vet. Sci. 97 (1).

Oryan, A., Sadoughifar, R., Namavari, M., 2016. Optimization of murine model for *Besnoitia caprae*. Journal of Parasitic Diseases 40 (3), 699-706.

Pan, C., Kumar, C., Bohl, S., Klingmueller, U., Mann, M., 2009. Comparative proteomic phenotyping of cell lines and primary cells to assess preservation of cell type-specific functions. Mol. Cell. Proteomics 8 (3), 443-450, 10.1074/mcp.M800258-MCP200 [doi].

Pastor-Fernández, I., 2016. Identificación y Caracterización De Las Proteínas NcROP40 y NcNTPasa, y Evaluación De Su Utilidad Vacunal Frente a La Neosporosis. Doctoral Thesis, Faculty of Veterinary Sciences, Complutense University of Madrid, Spain.

Pastor-Fernández, I., Regidor-Cerrillo, J., Álvarez-García, G., Marugán-Hernández, V., García-Lunar, P., Hemphill, A., Ortega-Mora, L.M., 2016a. The tandemly repeated NTPase (NTPDase) from *Neospora caninum* is a canonical dense granule protein whose RNA expression, protein secretion and phosphorylation coincides with the tachyzoite egress. Parasit. Vectors 9 (1), 352.

Pastor-Fernández, I., Regidor-Cerrillo, J., Jiménez-Ruiz, E., Álvarez-García, G., Marugán-Hernández, V., Hemphill, A., Ortega-Mora, L.M., 2016b. Characterization of the Neospora caninum NcROP40 and NcROP2Fam-1 rhoptry proteins during the tachyzoite lytic cycle. Parasitology 143 (1), 97-113.

Pedraza-Díaz, S., Marugán-Hernández, V., Collantes-Fernández, E., Regidor-Cerrillo, J., Rojo-Montejo, S., Gómez-Bautista, M., Ortega-Mora, L.M., 2009. Microsatellite markers for the molecular characterization of *Neospora caninum*: application to clinical samples. Vet. Parasitol. 166 (1-2), 38-46.

Pernas, L., Adomako-Ankomah, Y., Shastri, A.J., Ewald, S.E., Treeck, M., Boyle, J.P., Boothroyd, J.C., 2014. *Toxoplasma* effector MAF1 mediates recruitment of host mitochondria and impacts the host response. PLoS Biol. 12 (4), e1001845.

Persson, E.K., Agnarson, A.M., Lambert, H., Hitziger, N., Yagita, H., Chambers, B.J., Barragan, A., Grandien, A., 2007. Death receptor ligation or exposure to perforin trigger rapid egress of the intracellular parasite *Toxoplasma gondii*. J. Immunol. 179 (12), 8357-8365.

Peterhans, E., Jungi, T.W., Schweizer, M., 2003. BVDV and innate immunity. Biologicals 31 (2), 107-112.

Peteshev, V.M., Galuzo, I.G., Polomoshnov, A.P., 1974. Cats-definitive hosts of Besnoita (*Besnoitia besnoiti*) (In Russian). Azv Akad Nauk Kazakh SSR B 1, 33-38.

Pfefferkorn, E., Borotz, S.E., Nothnagel, R.F., 1993. Mutants of *Toxoplasma gondii* resistant to atovaquone (566C80) or decoquinate. J. Parasitol. 79 (4), 559-564.

Pober, J.S., Sessa, W.C., 2007. Evolving functions of endothelial cells in inflammation. Nature Reviews Immunology 7 (10), 803.

Pols, J.W., 1960. Studies on bovine besnoitiosis with special reference to the aetiology. Onderstepoort Jour Vet Res 28 ((3)), 265-356.

Qian, W., Wang, H., Shan, D., Li, B., Liu, J., Liu, Q., 2015. Activity of several kinds of drugs against *Neospora caninum*. Parasitol. Int. 64 (6), 597-602.

Radke, J.R., Behnke, M.S., Mackey, A.J., Radke, J.B., Roos, D.S., White, M.W., 2005. The transcriptome of *Toxoplasma gondii*. BMC Biol. 3, 26.

Ramaprasad, A., Mourier, T., Naeem, R., Malas, T.B., Moussa, E., Panigrahi, A., Vermont, S.J., Otto, T.D., Wastling, J., Pain, A., 2015. Comprehensive evaluation of *Toxoplasma gondii* VEG and *Neospora caninum* LIV genomes with tachyzoite stage transcriptome and proteome defines novel transcript features. PLoS One 10 (4), e0124473.

Regidor-Cerrillo, J., Pedraza-Díaz, S., Gómez-Bautista, M., Ortega-Mora, L.M., 2006. Multilocus microsatellite analysis reveals extensive genetic diversity in *Neospora caninum*. J. Parasitol. 92 (3), 517-524.

Regidor-Cerrillo, J., Gómez-Bautista, M., Pereira-Bueno, J., Adúriz, G., Navarro-Lozano, V., Risco-Castillo, V., Fernández-García, A., Pedraza-Díaz, S., Ortega-Mora, L.M., 2008. Isolation and genetic characterization of *Neospora caninum* from asymptomatic calves in Spain. Parasitology 135 (14), 1651-1659.

Regidor-Cerrillo, J., Gomez-Bautista, M., Sodupe, I., Aduriz, G., Alvarez-Garcia, G., Del Pozo, I., Ortega-Mora, L.M., 2011. *In vitro* invasion efficiency and intracellular proliferation rate comprise virulence-related phenotypic traits of *Neospora caninum*. Vet. Res. 42 (1), 41.

Regidor-Cerrillo, J., Alvarez-Garcia, G., Pastor-Fernandez, I., Marugan-Hernandez, V., Gomez-Bautista, M., Ortega-Mora, L.M., 2012. Proteome expression changes among virulent and attenuated *Neospora caninum* isolates. J. Proteomics 75 (8), 2306-2318.

Regidor-Cerrillo, J., García-Lunar, P., Pastor-Fernández, I., Álvarez-García, G., Collantes-Fernández, E., Gómez-Bautista, M., Ortega-Mora, L.M., 2015. *Neospora caninum* tachyzoite immunome study reveals differences among three biologically different isolates. Vet. Parasitol. 212 (3-4), 92-99.

Reid, A.J., 2015. Large, rapidly evolving gene families are at the forefront of host-parasite interactions in Apicomplexa. Parasitology 142 . Suppl. 1:S57-70.

Reid, A.J., Vermont, S.J., Cotton, J.A., Harris, D., Hill-Cawthorne, G.A., Konen-Waisman, S., Latham, S.M., Mourier, T., Norton, R., Quail, M.A., Sanders, M., Shanmugam, D., Sohal, A., Wasmuth, J.D., Brunk, B., Grigg, M.E., Howard, J.C., Parkinson, J., Roos, D.S., Trees, A.J., Berriman, M., Pain, A., Wastling, J.M., 2012. Comparative genomics of the apicomplexan parasites *Toxoplasma gondii* and *Neospora caninum*: Coccidia differing in host range and transmission strategy. PLoS Pathog. 8 (3), e1002567.

Reis, Y., Cortes, H., Viseu Melo, L., Fazendeiro, I., Leitao, A., Soares, H., 2006. Microtubule cytoskeleton behavior in the initial steps of host cell invasion by *Besnoitia besnoiti*. FEBS Lett. 580 (19), 4673-4682.

Relja Beck, Igor Štoković, Jelka Pleadin, Ana Beck, 2013. Bovine besnoitiosis in Croatia. Proccedings Apicompexa congress 2013, 64.

Richardson, L., Raun, A., Potter, E., Cooley, C., Rathmacher, R., 1976. Effect of monensin on rumen fermentation *in vitro* and *in vivo*. J. Anim. Sci. 43 (3), 657-664.

Ricketts, A.P., Pfefferkorn, E.R., 1993. *Toxoplasma gondii*: susceptibility and development of resistance to anticoccidial drugs *in vitro*. Antimicrob. Agents Chemother. 37 (11), 2358-2363.

Risco-Castillo, V., Fernández-García, A., Ortega-Mora, L.M., 2004. Comparative analysis of stress agents in a simplified *in vitro* system of *Neospora caninum* bradyzoite production. J. Parasitol. 90 (3), 466-470.

Rodriguez, A., Tarleton, R.L., 2012. Transgenic parasites accelerate drug discovery. Trends Parasitol. 28 (3), 90-92.

Roiko, M.S., Carruthers, V.B., 2013. Functional dissection of *Toxoplasma gondii* perforin-like protein 1 reveals a dual domain mode of membrane binding for cytolysis and parasite egress. J. Biol. Chem. 288 (12), 8712-8725.

Rojo-Montejo, S., Collantes-Fernández, E., Regidor-Cerrillo, J., Álvarez-García, G., Marugan-Hernández, V., Pedraza-Díaz, S., Blanco-Murcia, J., Prenafeta, A., Ortega-Mora, L.M., 2009a. Isolation and characterization of a bovine isolate of *Neospora caninum* with low virulence. Vet. Parasitol. 159 (1), 7-16.

Rojo-Montejo, S., Collantes-Fernández, E., Blanco-Murcia, J., Rodríguez-Bertos, A., Risco-Castillo, V., Ortega-Mora, L.M., 2009b. Experimental infection with a low virulence isolate of *Neospora caninum* at 70 days gestation in cattle did not result in foetopathy. Vet. Res. 40 (5), 49.

Rosowski, E.E., Lu, D., Julien, L., Rodda, L., Gaiser, R.A., Jensen, K.D., Saeij, J.P., 2011. Strain-specific activation of the NF-kappaB pathway by GRA15, a novel *Toxoplasma gondii* dense granule protein. J. Exp. Med. 208 (1), 195-212.

Rostaher, A., Mueller, R.S., Majzoub, M., Schares, G., Gollnick, N.S., 2010. Bovine besnoitiosis in Germany. Vet. Dermatol. 21, 329-334.

Rutkowski, J., Brzezinski, B., 2013. Structures and properties of naturally occurring polyether antibiotics. Biomed. Res. Int. 2013, 162513.

Ryan, E.G., Lee, A., Carty, C., O'Shaughnessy, J., Kelly, P., Cassidy, J.P., Sheehan, M., Johnson, A., de Waal, T., 2016. Bovine besnoitiosis (*Besnoitia besnoiti*) in an Irish dairy herd. Vet. Rec. 178 (24), 608.

Sadoughifar, R., Namavari, M., Oryan, A., 2015. Suspension culture of *Besnoitia caprae* by murine macrophage. Journal of parasitic diseases 39 (4), 624-627.

Sahun, S, 1998. La besnoitiose bovine en France: Mise aun point d´un test ELISA et enquete sur le terrain. Doctoral Thesis, Toulouse, France.

Samish, M., Shkap, V., Bin, H., Pipano, E.M., 1988. Cultivation of *Besnoitia besnoiti* in four tick cell lines. Int. J. Parasitol. 18 (3), 291-296.

Sánchez-Sánchez, R., Ferre, I., Re, M., Vázquez, P., Ferrer, L.M., Blanco-Murcia, J., Regidor-Cerrillo, J., Díaz, M.P., González-Huecas, M., Tabanera, E., 2018a. Safety and efficacy of the bumped kinase inhibitor BKI-1553 in pregnant sheep experimentally infected with *Neospora caninum* tachyzoites. Int. J. Parasitol. Drugs Drug Resist. 8(1):112-12.

Sánchez-Sánchez, R., Ferre, I., Regidor-Cerrillo, J., Gutiérrez-Expósito, D., Ferrer, L.M., Arteche-Villasol, N., Moreno-Gonzalo, J., Müller, J., Aguado-Martínez, A., Pérez, V., 2018b. Virulence in Mice of a *Toxoplasma gondii* Type II Isolate Does Not Correlate With the Outcome of Experimental Infection in Pregnant Sheep. Front. Cell. Infect. Microbiol. 8, 436.

Sánchez-Sánchez, R., Ferre, I., Re, M., Ramos, J.J., Regidor-Cerrillo, J., Pizarro Diaz, M., Gonzalez-Huecas, M., Tabanera, E., Benavides, J., Hemphill, A., Hulverson, M.A., Barrett, L.K., Choi, R., Whitman, G.R., Ojo, K.K., Van Voorhis, W.C., Ortega-Mora, L.M., 2019. Treatment with bumped kinase inhibitor 1294 is safe and leads to significant protection against abortion and vertical transmission in sheep experimentally infected with *Toxoplasma gondii* during pregnancy. Antimicrob. Agents Chemother. 63 (7).

Sánchez-Sánchez, R., Vazquez, P., Ferre, I., Ortega-Mora, L.M., 2018. Treatment of toxoplasmosis and neosporosis in farm ruminants: state of knowledge and future trends. Curr. Top. Med. Chem. 18, 1304-1323.

Schaefer, D.A., Betzer, D.P., Smith, K.D., Millman, Z.G., Michalski, H.C., Menchaca, S.E., Zambriski, J.A., Ojo, K.K., Hulverson, M.A., Arnold, S.L., Rivas, K.L., Vidadala, R.S., Huang, W., Barret, L.K., Maly, D.J., Fan, E., Van Voorhis, W.C., Riggs, M.W., 2016. Novel Bumped Kinase Inhibitors are safe and effective therapeutics in the calf clinical model for cryptosporidiosis. J. Infect. Dis. 214 (12), 1856-1864.

Schares, G., Basso, W., Majzoub, M., Cortes, H.C., Rostaher, A., Selmair, J., Hermanns, W., Conraths, F.J., Gollnick, N.S., 2009. First in vitro isolation of *Besnoitia besnoiti* from chronically infected cattle in Germany. Vet. Parasitol. 163 (4), 315-322.

Schares, G., Maksimov, A., Basso, W., More, G., Dubey, J.P., Rosenthal, B., Majzoub, M., Rostaher, A., Selmair, J., Langenmayer, M.C., Scharr, J.C., Conraths, F.J., Gollnick, N.S., 2011. Quantitative real time polymerase chain reaction assays for the sensitive detection of *Besnoitia besnoiti* infection in cattle. Vet. Parasitol. 178 (3-4), 208-216.

Schares, G., Venepally, P., Lorenzi, H.A., 2017. Draft Genome Sequence and Annotation of the Apicomplexan Parasite *Besnoitia besnoiti*. Genome Announc 5 (46).

Schares, G., Jutras, C., Bärwald, A., Basso, W., Maksimov, A., Schares, S., Tuschy, M., Conraths, F.J., Brodeur, V., 2019. *Besnoitia tarandi* in Canadian woodland caribou–Isolation, characterization and suitability for serological tests. Int. J. Parasitol. Parasites Wildl. 8, 1-9.

Schulz, K.C.A., 1960. A report on naturally acquired besnoitiosis in bovines with special reference to its pathology. 31 (J. S. Afr. Vet. Med. Assoc), 21-35.

Seipel, D., Oliveira, B.C., Resende, T.L., Schuindt, S.H., Pimentel, P.M., Kanashiro, M.M., Arnholdt, A.C., 2010. *Toxoplasma gondii* infection positively modulates the macrophages migratory molecular complex by increasing matrix metalloproteinases, CD44 and alpha v beta 3 integrin. Vet. Parasitol. 169 (3-4), 312-319.

Senaud, J., Mehlhorn, H., Scholtyseck, E., 1974. *Besnoitia jellisoni* in macrophages and cysts from experimentally infected laboratory mice. J. Protozool. 21 (5), 715-720.

Sharif, S., Jacquiet, P., Prevot, F., Grisez, C., Raymond-Letron, I., Semin, M., Geffré, A., Trumel, C., Franc, M., Bouhsira, É., 2019. *Stomoxys calcitrans*, mechanical vector of virulent *Besnoitia besnoiti* from chronically infected cattle to susceptible rabbit. Med. Vet. Entomol. 3(2), 247-255.

Shastri, A.J., Marino, N.D., Franco, M., Lodoen, M.B., Boothroyd, J.C., 2014. GRA25 is a novel virulence factor of *Toxoplasma gondii* and influences the host immune response. Infect. Immun. 82 (6), 2595-2605.

Sheffield, H.G., 1966. Electron microscope study of the proliferative form of *Besnoitia jellisoni*. J. Parasitol. , 583-594.

Shen, B., Brown, K., Long, S., Sibley, L.D., 2017. Development of CRISPR/Cas9 for efficient genome editing in *Toxoplasma gondii*. In: *In Vitro* Mutagenesis. Springer, pp. 79-103.

Shkap, V., De Waal, D.T., Potgieter, F.T., 1985. Chemotherapy of experimental *Besnoitia besnoiti* infection in rabbits. Onderstepoort J. Vet. Res. 52 (4), 289.

Shkap, V, 1986. Antigenicity of *Besnoitia besnoiti* with special reference to prophylactic immunization**.** Thesis, Hebrew University, Jerusalem.

Shkap, V., Pipano, E., Greenblatt, C., 1987a. Cultivation of *Besnoitia besnoiti* and evaluation of susceptibility of laboratory animals to cultured parasites. Vet. Parasitol. 23 (3-4), 169-178.

Shkap, V., Pipano, E., Ungar-Waron, H., 1987b. *Besnoitia besnoiti*: chemotherapeutic trials *in vivo* and *in vitro*. Rev. Elev. Med. Vet. Pays. Trop. 40 (3), 259-264.

Shkap, V., Pipano, E., Marcus, S., Krigel, Y., 1994. Bovine besnoitiosis: transfer of colostral antibodies with observations possibly relating to natural transmission of the infection. Onderstepoort J. Vet. Res. 61 (3), 273-275.

Shkap, V., Yakobson, B.A., Pipano, E., 1988. Transmission and scanning electron microscopy of *Besnoitia besnoiti*. Int. J. Parasitol. 18 (6), 761-766.

Sibley, L.D., Hakansson, S., Carruthers, V.B., 1998. Gliding motility: an efficient mechanism for cell penetration. Curr. Biol. 8 (1), R12-4.

Sidik, S.M., Huet, D., Ganesan, S.M., Huynh, M., Wang, T., Nasamu, A.S., Thiru, P., Saeij, J.P., Carruthers, V.B., Niles, J.C., 2016. A genome-wide CRISPR screen in Tox*oplasma* identifies essential apicomplexan genes. Cell 166 (6), 1423-1435. e12.

Silva, L.M., Lütjohann, D., Hamid, P., Velasquez, Z.D., Kerner, K., Larrazabal, C., Failing, K., Hermosilla, C., Taubert, A., 2019. *Besnoitia besnoiti* infection alters both endogenous cholesterol de novo synthesis and exogenous LDL uptake in host endothelial cells. Scientific reports 9 (1), 6650.

Skariah, S., McIntyre, M.K., Mordue, D.G., 2010. *Toxoplasma gondii*: determinants of tachyzoite to bradyzoite conversion. Parasitol. Res. 107 (2), 253-260.

Smith, D., Frenkel, J., 1984. *Besnoitia darlingi* (Apicomplexa, Sarcocystidae, Toxoplasmatinae): Transmission between Opossums and Cats 1. J. Protozool. 31 (4), 584-587.

Smith, D.D., Frenkel, J., 1977. Besnoitia darlingi (Protozoa: Toxoplasmatinae): cyclic transmission by cats. J. Parasitol. , 1066-1071.

Sohn, C.S., Cheng, T.T., Drummond, M.L., Peng, E.D., Vermont, S.J., Xia, D., Cheng, S.J., Wastling, J.M., Bradley, P.J., 2011b. Identification of novel proteins in *Neospora caninum* using an organelle purification and monoclonal antibody approach. PLoS One 6 (4), e18383.

Sokol, S.L., Primack, A.S., Nair, S.C., Wong, Z.S., Tembo, M., Verma, S.K., Cerqueira-Cezar, C.K., Dubey, J., Boyle, J.P., 2018. Dissection of the *in vitro* developmental program of *Hammondia hammondi* reveals a link between stress sensitivity and life cycle flexibility in *Toxoplasma gondii*. eLife 7, e36491.

Sonda, S., Fuchs, N., Connolly, B., Fernandez, P., Gottstein, B., Hemphill, A., 1998. The major 36 kDa *Neospora caninum* tachyzoite surface protein is closely related to the major *Toxoplasma gondii* surface antigen. Mol. Biochem. Parasitol. 97 (1-2), 97-108.

Sonda, S., Fuchs, N., Gottstein, B., Hemphill, A., 2000. Molecular characterization of a novel microneme antigen in *Neospora caninum*. Mol. Biochem. Parasitol. 108 (1), 39-51.

Sundermann, C.A., Estridge, B.H., 1999. Growth of and competition between *Neospora caninum* and *Toxoplasma gondii in vitro*. Int. J. Parasitol. 29 (10), 1725-1732.

Talevich, E., Kannan, N., 2013. Structural and evolutionary adaptation of rhoptry kinases and pseudokinases, a family of coccidian virulence factors. BMC Evol. Biol. 13, 117.

Taubert, A., Hermosilla, C., Silva, L., Wieck, A., Failing, K., Mazurek, S., 2016. Metabolic signatures of *Besnoitia besnoiti*-infected endothelial host cells and blockage of key metabolic pathways indicate high glycolytic and glutaminolytic needs of the parasite. Parasitol. Res. 115 (5), 2023-2034.

Taubert, A., Krull, M., Zahner, H., Hermosilla, C., 2006a. *Toxoplasma gondii* and *Neospora caninum* infections of bovine endothelial cells induce endothelial adhesion molecule gene transcription and subsequent PMN adhesion. Vet. Immunol. Immunopathol. 112 (3-4), 272-283.

Taubert, A., Zahner, H., Hermosilla, C., 2006b. Dynamics of transcription of immunomodulatory genes in endothelial cells infected with different coccidian parasites. Vet. Parasitol. 142 (3-4), 214-222.

Tenter, A.M., Barta, J.R., Beveridge, I., Duszynski, D.W., Mehlhorn, H., Morrison, D.A., Thompson, R.C., Conrad, P.A., 2002. The conceptual basis for a new classification of the coccidia. Int. J. Parasitol. 32 (5), 595-616.

Tomavo, S., 2001. The differential expression of multiple isoenzyme forms during stage conversion of *Toxoplasma gondii*: an adaptive developmental strategy. Int. J. Parasitol. 31 (10), 1023-1031.

Treeck, M., Sanders, J.L., Gaji, R.Y., LaFavers, K.A., Child, M.A., Arrizabalaga, G., Elias, J.E., Boothroyd, J.C., 2014. The calcium-dependent protein kinase 3 of *Toxoplasma* influences basal calcium levels and functions beyond egress as revealed by quantitative phosphoproteome analysis. PLoS pathogens 10 (6), e1004197.

Uryvaev, L., Dedova, A., Dedova, L., Ionova, K., Parasjuk, N., Selivanova, T., Bunkova, N., Gushina, E., Grebennikova, T., Podchernjaeva, R., 2012. Contamination of cell cultures with bovine viral diarrhea virus (BVDV). Bull. Exp. Biol. Med. 153 (1), 77-81.

Uvaliev, I.U., Baigaziev, K.K., 1979. The treatment of *Besnoitia* infection in animals. Mater respublikans , 185-190.

Uzeda, R.S., Andrade, M.R., Corbellini, L.G., Antonello, A.M., Vogel, F.S., Gondim, L.F., 2014. Frequency of antibodies against *Besnoitia besnoiti* in Brazilian cattle. Vet. Parasitol. 199 (3-4), 242-246.

Van Linthout, S., Miteva, K., Tschöpe, C., 2014. Crosstalk between fibroblasts and inflammatory cells. Cardiovasc. Res. 102 (2), 258-269.

Van Voorhis, W.C., Doggett, J.S., Parsons, M., Hulverson, M.A., Choi, R., Arnold, S., Riggs, M.W., Hemphill, A., Howe, D.K., Mealey, R.H., 2017. Extended-spectrum antiprotozoal bumped kinase inhibitors: A review. Exp. Parasitol. 80:71-83.

Vanleeuwen, J.A., Haddad, J.P., Dohoo, I.R., Keefe, G.P., Tiwari, A., Tremblay, R., 2009. Associations between reproductive performance and seropositivity for bovine leukemia virus, bovine viral-diarrhea virus, *Mycobacterium avium* subspecies *paratuberculosis*, and *Neospora caninum* in Canadian dairy cows. Prev. Vet. Med. 94, 54-64.

Vidadala, R.S.R., Rivas, K.L., Ojo, K.K., Hulverson, M.A., Zambriski, J.A., Bruzual, I., Schultz, T.L., Huang, W., Zhang, Z., Scheele, S., 2016. Development of an orally available and central nervous system (CNS) penetrant *Toxoplasma gondii* calcium-dependent protein kinase 1 (Tg CDPK1) inhibitor with minimal human ether-a-go-go-related gene (hERG) activity for the treatment of toxoplasmosis. J. Med. Chem. 59 (13), 6531-6546.

Villagra-Blanco, R., Silva, L., Aguilella-Segura, A., Arcenillas-Hernández, I., Martínez-Carrasco, C., Seipp, A., Gärtner, U., de Ybanez, R.R., Taubert, A., Hermosilla, C., 2017a. Bottlenose dolphins (*Tursiops truncatus*) do also cast neutrophil extracellular traps against the apicomplexan parasite *Neospora caninum*. Int. J. Parasitol. Parasites Wildl. 6 (3), 287-294.

Villagra-Blanco, R., Silva, L.M., Muñoz-Caro, T., Yang, Z., Li, J., Gärtner, U., Taubert, A., Zhang, X., Hermosilla, C., 2017b. Bovine polymorphonuclear neutrophils cast neutrophil extracellular traps against the abortive parasite *Neospora caninum*. Frontiers immunol. 8, 606.

Vogelsang, E.G., Gallo, P., 1941. Globidium besnoiti (Marotel, 1912) y habronemosis cutanea en bovinos de Venezuela. Rev. Med. Vet. Parasitol. 3, 1535, 153-155.

Vonlaufen, N., Guetg, N., Naguleswaran, A., Muller, N., Bjorkman, C., Schares, G., von Blumroeder, D., Ellis, J., Hemphill, A., 2004. *In vitro* induction of *Neospora caninum* bradyzoites in vero cells reveals differential antigen expression, localization, and host-cell recognition of tachyzoites and bradyzoites. Infect. Immun. 72 (1), 576-583.

Vonlaufen, N., Gianinazzi, C., Muller, N., Simon, F., Bjorkman, C., Jungi, T.W., Leib, S.L., Hemphill, A., 2002a. Infection of organotypic slice cultures from rat central nervous tissue with *Neospora caninum*: an alternative approach to study host-parasite interactions. Int. J. Parasitol. 32 (5), 533-542.

Vonlaufen, N., Muller, N., Keller, N., Naguleswaran, A., Bohne, W., McAllister, M.M., Bjorkman, C., Muller, E., Caldelari, R., Hemphill, A., 2002b. Exogenous nitric oxide triggers *Neospora caninum* tachyzoite-to-bradyzoite stage conversion in murine epidermal keratinocyte cell cultures. Int. J. Parasitol. 32 (10), 1253-1265.

Waap, H., Leitao, A., Nunes, T., Cortes, H., Vaz, Y, 2012. Bovine besnoitiosis in the Alentejo region. In: I International Meeting on Apicomplexan Parasites in Farm Animals, Lisbon, Portugal, pp. 76.

Wang, J., Huang, S., Li, T., Chen, K., Ning, H., Zhu, X., 2016. Evaluation of the basic functions of six calcium-dependent protein kinases in *Toxoplasma gondii* using CRISPR-Cas9 system. Parasitol. Res. 115 (2), 697-702.

Wang, J., Tang, D., Li, W., Xu, J., Liu, Q., Liu, J., 2017. A new microneme protein of *Neospora caninum*, NcMIC8 is involved in host cell invasion. Exp. Parasitol. 175, 21-27.

Wastling, J.M., Xia, D., Sohal, A., Chaussepied, M., Pain, A., Langsley, G., 2009. Proteomes and transcriptomes of the Apicomplexa--where's the message? Int. J. Parasitol. 39 (2), 135-143.

Wei, Z., Wang, Y., Zhang, X., Wang, X., Gong, P., Li, J., Taubert, A., Hermosilla, C., Zhang, X., Yang, Z., 2018. Bovine macrophage-derived extracellular traps act as early effectors against the abortive parasite *Neospora caninum*. Vet. Parasitol. 258, 1-7.

Wei, Z., Hermosilla, C., Taubert, A., He, X., Wang, X., Gong, P., Li, J., Yang, Z., Zhang, X., 2016. Canine neutrophil extracellular traps release induced by the apicomplexan parasite *Neospora caninum in vitro*. Front. Immunol. 7, 436.

Weidner, J.M., Kanatani, S., Hernández-Castañeda, M.A., Fuks, J.M., Rethi, B., Wallin, R.P., Barragan, A., 2013. Rapid cytoskeleton remodelling in dendritic cells following invasion by *Toxoplasma gondii* coincides with the onset of a hypermigratory phenotype. Cell. Microbiol. 15 (10), 1735-1752.

Weiss, L.M., Ma, Y.F., Halonen, S., McAllister, M.M., Zhang, Y.W., 1999. The *in vitro* development of *Neospora caninum* bradyzoites. Int. J. Parasitol. 29 (10), 1713-1723.

Wetzel, D.M., Chen, L.A., Ruiz, F.A., Moreno, S.N., Sibley, L.D., 2004. Calcium-mediated protein secretion potentiates motility in *Toxoplasma gondii*. J. Cell. Sci. 117 (Pt 24), 5739-5748.

Winzer, P., Muller, J., Aguado-Martinez, A., Rahman, M., Balmer, V., Manser, V., Ortega-Mora, L.M., Ojo, K.K., Fan, E., Maly, D.J., Van Voorhis, W.C., Hemphill, A., 2015. *In vitro* and *in vivo* effects of the bumped kinase inhibitor 1294 in the related cyst-forming apicomplexans *Toxoplasma gondii* and *Neospora caninum*. Antimicrob. Agents Chemother. 59 (10), 6361-6374.

Xia, D., Sanderson, S.J., Jones, A.R., Prieto, J.H., Yates, J.R., Bromley, E., Tomley, F.M., Lal, K., Sinden, R.E., Brunk, B.P., Roos, D.S., Wastling, J.M., 2008. The proteome of *Toxoplasma gondii*: integration with the genome provides novel insights into gene expression and annotation. Genome Biol. 9 (7), R116-2008-9-7-r116.

Yamagishi, J., Wakaguri, H., Ueno, A., Goo, Y.K., Tolba, M., Igarashi, M., Nishikawa, Y., Sugimoto, C., Sugano, S., Suzuki, Y., Watanabe, J., Xuan, X., 2010. High-resolution characterization of *Toxoplasma gondii* transcriptome with a massive parallel sequencing method. DNA Res. 17 (4), 233-243.

Yang, Z., Wei, Z., Hermosilla, C., Taubert, A., He, X., Wang, X., Gong, P., Li, J., Zhang, X., 2018. Caprine monocytes release extracellular traps against *Neospora caninum in vitro*. Front. Immunol. 8, 2016.

Zacarias, JA, 2009. Epidemiología (seroprevalencia y vectores) de la Besnoitiosis bovina de las Sierras de Urbasa y Andía. Doctoral Thesis. University of Zaragoza.

Zhang, N., Chen, J., Wang, M., Petersen, E., Zhu, X., 2013. Vaccines against *Toxoplasma gondii*: new developments and perspectives. Expert review of vaccines 12 (11), 1287-1299.

Zhang, H., Compaore, M.K., Lee, E.G., Liao, M., Zhang, G., Sugimoto, C., Fujisaki, K., Nishikawa, Y., Xuan, X., 2007. Apical membrane antigen 1 is a cross-reactive antigen between *Neospora caninum* and *Toxoplasma gondii,* and the anti-NcAMA1 antibody inhibits host cell invasion by both parasites. Mol. Biochem. Parasitol. 151 (2), 205-212.

Zhou, D.H., Wang, Z.X., Zhou, C.X., He, S., Elsheikha, H.M., Zhu, X.Q., 2017. Comparative proteomic analysis of virulent and avirulent strains of *Toxoplasma gondii* reveals strain-specific patterns. Oncotarget 8 (46), 80481-80491.

Zhou, D.H., Zhao, F.R., Nisbet, A.J., Xu, M.J., Song, H.Q., Lin, R.Q., Huang, S.Y., Zhu, X.Q., 2014. Comparative proteomic analysis of different *Toxoplasma gondii* genotypes by two-dimensional fluorescence difference gel electrophoresis combined with mass spectrometry. Electrophoresis 35 (4), 533-545.

Zhou, D.H., Yuan, Z.G., Zhao, F.R., Li, H.L., Zhou, Y., Lin, R.Q., Zou, F.C., Song, H.Q., Xu, M.J., Zhu, X.Q., 2011. Modulation of mouse macrophage proteome induced by *Toxoplasma gondii* tachyzoites *in vivo*. Parasitol. Res. 109 (6), 1637-1646.

Zhou, H., Zhao, Q., Das Singla, L., Min, J., He, S., Cong, H., Li, Y., Su, C., 2013. Differential proteomic profiles from distinct *Toxoplasma gondii* strains revealed by 2D-difference gel electrophoresis. Exp. Parasitol. 133 (4), 376-382.

ANEXO 1: RESULTADOS TRANSCRIPTOMA

- Resultados mapeados frente a *Bos taurus* 12 hpi vs C-
- Resultados mapeados frente a *Bos taurus* 32 hpi vs C-
- Resultados mapeados frente a *Bos taurus* 12 vs 32 hpi
- Resultados *gene ontology* 32 hpi vs C-
- Resultados *gene ontology* 12 hpi vs 32 hpi
- Resultados mapeados frente a *Besnoitia besnoiti* 12 hpi vs 32 hpi

Results mapped Bos taurus C-(+) over 12 hpi (-)

Identifier	description	pValue	fdr	log2 Ratio	fc
GPX3		2,03E-03	0,008496	1,817	3,523
FABP4	fatty acid-binding protein, adipocyte [Source:RefSeq peptic	0,0001568	0,04001	1,729	3,315
FBP1	Fructose-1,6-bisphosphatase 1 [Source:UniProtKB/Swiss-P	0,0001241	0,03679	1,612	3,057
OMD	osteomodulin precursor [Source:RefSeq peptide;Acc:NP_7	4,08E-03	0,008496	1,602	3,036
NOX5	NADPH oxidase 5 [Source:RefSeq peptide;Acc:NP_001094(	1,08E-05	0,01464	1,456	2,743
SOD3	extracellular superoxide dismutase [Source:RefSeq peptide	8,72E-02	0,03122	1,438	2,709
EPAS1	endothelial PAS domain-containing protein 1 [Source:RefS	2,71E-05	0,0234	1,325	2,505
SERPINA5	Plasma serine protease inhibitor [Source:UniProtKB/Swiss-	0,0002979	0,04885	1,316	2,490
ECM2	extracellular matrix protein 2 precursor [Source:RefSeq pe	5,41E-02	0,02822	1,298	2,459
PGF	Placenta growth factor [Source:UniProtKB/Swiss-Prot;Acc:	5,65E-02	0,02822	1,264	2,402
COLQ	acetylcholinesterase collagenic tail peptide [Source:RefSec	0,000218	0,04204	1,253	2,383
EHD3	EH domain-containing protein 3 [Source:RefSeq peptide;A	3,06E-03	0,008496	1,243	2,367
WDR96	WD repeat-containing protein 96 [Source:RefSeq peptide;A	0,0001172	0,03587	1,229	2,344
USH1C	harmonin [Source:RefSeq peptide;Acc:NP_001030459]	0,0001396	0,03897	1,201	2,299
SEP4	septin-4 [Source:RefSeq peptide;Acc:NP_001029823]	5,08E-02	0,02822	1,146	2,213
C1QTNF1	complement C1q tumor necrosis factor-related protein 1 p	3,97E-02	0,02693	1,071	2,101
GPR77	C5a anaphylatoxin chemotactic receptor C5L2 [Source:Ref	2,96E-02	0,0234	1,071	2,101
HEBP1	Heme-binding protein 1 [Source:UniProtKB/Swiss-Prot;Acc	4,37E-02	0,02764	1,068	2,097
CA5B	carbonic anhydrase 5B, mitochondrial [Source:RefSeq pep	0,0002156	0,04204	1,066	2,094
SELENBP1	Selenium-binding protein 1 [Source:UniProtKB/Swiss-Prot;	2,88E-02	0,0234	1,066	2,094
ASS1	Argininosuccinate synthase [Source:UniProtKB/Swiss-Prot;	8,94E-02	0,03122	1,006	2,008
FAM107A		5,37E-03	0,008496	1,780	3,434
SLC6A4	sodium-dependent serotonin transporter [Source:RefSeq p	0,0001172	0,03587	1,380	2,603
GLDC	glycine dehydrogenase [Source:RefSeq peptide;Acc:NP_00	0,0001138	0,03587	1,190	2,282
PGM5	phosphoglucomutase-like protein 5 [Source:RefSeq peptid	0,0003131	0,04951	0,981	1,973
ALDH6A1	methylmalonate-semialdehyde dehydrogenase [Source:Re	8,13E-05	0,03122	0,963	1,950
LTA4H	Leukotriene A-4 hydrolase [Source:UniProtKB/Swiss-Prot;A	6,52E-02	0,02978	0,940	1,918
CH25H	cholesterol 25-hydroxylase [Source:RefSeq peptide;Acc:NP	4,55E-03	0,008496	0,935	1,912
CFH	complement factor H precursor [Source:RefSeq peptide;Ac	0,0001959	0,04001	0,885	1,846
LOC790886	uncharacterized protein LOC790886 precursor [Source:Ref	0,0001961	0,04001	0,883	1,844
NQO1	NAD(P)H dehydrogenase [Source:RefSeq peptide;Acc:NP_(	6,87E-05	0,02978	0,883	1,844
ST6GAL1	beta-galactoside alpha-2,6-sialyltransferase 1 [Source:RefS	9,21E-02	0,03122	0,872	1,830
PPP1R9A	neurabin-1 [Source:RefSeq peptide;Acc:NP_001069621]	0,0002942	0,04885	0,868	1,826
CHN1	N-chimaerin isoform 2 [Source:RefSeq peptide;Acc:NP_00	0,0002529	0,04528	0,860	1,815
ACSF2	Acyl-CoA synthetase family member 2, mitochondrial [Sou	0,0001779	0,04001	0,786	1,724
AASS	alpha-aminoadipic semialdehyde synthase, mitochondrial p	0,0001885	0,04001	0,781	1,718
DYNC2LI1	Cytoplasmic dynein 2 light intermediate chain 1 [Source:U	2,69E-05	0,0234	0,776	1,713
TGFBR2	TGF-beta receptor type-2 precursor [Source:RefSeq peptid	0,0003069	0,04936	0,682	1,605
MUT	methylmalonyl-CoA mutase, mitochondrial precursor [Sou	8,65E-05	0,03122	0,654	1,574
MOSPD2	motile sperm domain-containing protein 2 [Source:RefSeq	0,0002806	0,04842	0,644	1,563
UTP14A	UTP14, U3 small nucleolar ribonucleoprotein, homolog A [	0,0002244	0,04204	0,620	1,537
LGALS9	galectin-9 isoform 1 [Source:RefSeq peptide;Acc:NP_0010	6,91E-02	0,02978	0,618	1,535
SGK1	Serine/threonine-protein kinase Sgk1 [Source:UniProtKB/S	8,82E-02	0,03122	-0,653	-1,572
LAP3	Cytosol aminopeptidase [Source:UniProtKB/Swiss-Prot;Acc	5,54E-02	0,02822	-0,655	-1,575
TSR1		0,0001614	0,04001	-0,744	-1,675
ANXA1	annexin A1 [Source:RefSeq peptide;Acc:NP_786978]	0,000197	0,04001	-0,783	-1,721
COTL1	Coactosin-like protein [Source:UniProtKB/Swiss-Prot;Acc:C	0,000184	0,04001	-0,837	-1,786
GPATCH4	G patch domain-containing protein 4 [Source:UniProtKB/S	0,0002655	0,04665	-0,851	-1,804
ARID3A	AT-rich interactive domain-containing protein 3A [Source:I	0,0001473	0,03995	-1,109	-2,157
ITGB3	integrin beta-3 precursor [Source:RefSeq peptide;Acc:NP_(	0,0001356	0,03897	-1,126	-2,183
CXCL12	stromal cell-derived factor 1 precursor [Source:RefSeq pep	0,0001775	0,04001	-1,271	-2,413
CD200	OX-2 membrane glycoprotein precursor [Source:RefSeq pe	0,0001958	0,04001	-1,393	-2,626
ULBP15		0,0002986	0,04885	-1,409	-2,656
ADAMTSL2	ADAMTS-like protein 2 precursor [Source:RefSeq peptide;A	0,000251	0,04528	-1,646	-3,130
RPRM	Protein reprimo [Source:UniProtKB/Swiss-Prot;Acc:Q1RMT	3,68E-02	0,02685	-2,397	-5,267
NPTX1	neuronal pentraxin-1 precursor [Source:RefSeq peptide;Ac	1,90E-03	0,008496	-2,625	-6,169
ADAMTS1	A disintegrin and metalloproteinase with thrombospondin	1,31E-05	0,01554	-3,863	-14,551

Results mapped against *Bos taurus* 32 hpi vs C-

Identifier	transcript_id	description	pValue	fdr	log2 Ratio	Fold change
MT1A	NM_001040492	Metallothionein-1A [Source:UniProtKB/Swiss-Prot;Acc:P67983]	1,97E-02	0.00389	-2,640	-6,233
RPRM	NM_001080739	Protein reprimo [Source:UniProtKB/Swiss-Prot;Acc:Q1RMT2]	1,85E-02	0.003745	-2,582	-5,988
ADAMTS1	NM_001101080	A disintegrin and metalloproteinase with thrombospondin motifs 1 [Source:RefSeq peptide;Acc:NP_001094	0.0003034	0.01405	-2,562	-5,905
AQP1	NM_174702	Aquaporin-1 [Source:UniProtKB/Swiss-Prot;Acc:P47865]	0.001016	0.02858	-2,558	-5,889
ADAMTSL2	NM_001205934	ADAMTS-like protein 2 precursor [Source:RefSeq peptide;Acc:NP_001192863]	5,78E-03	0.001829	-2,461	-5,506
SEMA3C	NM_001101082	Semaphorin-3C [Source:UniProtKB/Swiss-Prot;Acc:A7MB70]	6,55E-02	0.006215	-2,426	-5,374
LOXL4	NM_174384	Lysyl oxidase homolog 4 [Source:UniProtKB/Swiss-Prot;Acc:Q8MJ24]	3,21E-02	0.004633	-2,404	-5,293
FOSB	NM_001102248	protein fosB [Source:RefSeq peptide;Acc:NP_001095718]	6,88E-02	0.006403	-2,400	-5,278
GRIN3A	NM_001191535		0.001101	0.03012	-2,349	-5,095
ATP8A2	NM_001163802		7.28e-05	0.006646	-2,140	-4,408
FN1	NM_001163778	fibronectin precursor [Source:RefSeq peptide;Acc:NP_001157250]	9,11E-02	0.007395	-2,088	-4,252
NPTX1	NM_001192354	neuronal pentraxin-1 precursor [Source:RefSeq peptide;Acc:NP_001179283]	0.0001066	0.007971	-2,060	-4,170
NTNG2	NM_001099025	netrin-G2 precursor [Source:RefSeq peptide;Acc:NP_001092495]	0.001268	0.03246	-2,038	-4,107
EFEMP1	NM_001081717	EGF-containing fibulin-like extracellular matrix protein 1 precursor [Source:RefSeq peptide;Acc:NP_001075	0.0001051	0.007917	-1,949	-3,861
RBP4	NM_001040475	Retinol-binding protein 4 [Source:UniProtKB/Swiss-Prot;Acc:P18902]	0.0002447	0.01283	-1,913	-3,766
MTUS1	NM_001075692	Microtubule-associated tumor suppressor 1 homolog [Source:UniProtKB/Swiss-Prot;Acc:Q17QT2]	2,91E-02	0.004458	-1,897	-3,724
TGFBI	NM_001205402	transforming growth factor-beta-induced protein ig-h3 precursor [Source:RefSeq peptide;Acc:NP_001192	0.0001019	0.0078	-1,873	-3,663
CLCA3	NM_181018	Voltage-dependent calcium channel gamma-like subunit [Source:RefSeq peptide;Acc:NP_001029916]	4,35E-04	0.0004126	-1,823	-3,538
INHBE	NM_001205842	inhibin beta E chain precursor [Source:RefSeq peptide;Acc:NP_001192771]	6,51E-03	0.001931	-1,817	-3,523
F2RL1	NM_001046283	proteinase-activated receptor 2 precursor [Source:RefSeq peptide;Acc:NP_001039748]	0.0001644	0.01055	-1,798	-3,477
HGF	NM_001031751; NM	hepatocyte growth factor precursor [Source:RefSeq peptide;Acc:NP_001026921]	0.0007432	0.02485	-1,753	-3,371
MEDAG	NM_001083660	Uncharacterized protein C13orf33 homolog [Source:UniProtKB/Swiss-Prot;Acc:A4IFN2]	0.000854	0.02649	-1,743	-3,347
SLC8A1	NM_176632	sodium/calcium exchanger 1 precursor [Source:RefSeq peptide;Acc:NP_788805]	0.0001538	0.01021	-1,741	-3,343
CHAC1	NM_001098882	cation transport regulator-like protein 1 [Source:RefSeq peptide;Acc:NP_001092352]	0.002252	0.04373	-1,704	-3,258
TMEM26	NM_001103163	transmembrane protein 26 [Source:RefSeq peptide;Acc:NP_001096633]	0.002612	0.04777	-1,656	-3,151
SNX10	NM_001075375	Sorting nexin-10 [Source:UniProtKB/Swiss-Prot;Acc:Q0IIL5]	0.0005017	0.01898	-1,648	-3,134
PAMR1	NM_001015591	inactive serine protease PAMR1 precursor [Source:RefSeq peptide;Acc:NP_001015591]	0.001777	0.03837	-1,630	-3,095
GJA1	NM_174068	Gap junction alpha-1 protein [Source:UniProtKB/Swiss-Prot;Acc:P18246]	1,70E-03	0.0008958	-1,586	-3,002
ROBO1	NM_001192888	roundabout homolog 1 precursor [Source:RefSeq peptide;Acc:NP_001179817]	7,54E-03	0.002031	-1,583	-2,996
TAGLN	NM_001046149	Transgelin [Source:UniProtKB/Swiss-Prot;Acc:Q9TS87]	0.002235	0.04366	-1,560	-2,949
SLC1A3	NM_174600	Excitatory amino acid transporter 1 [Source:UniProtKB/Swiss-Prot;Acc:P46411]	1,02E-02	0.002488	-1,537	-2,902
PDGFRA	NM_001192345	alpha-type platelet-derived growth factor receptor precursor [Source:RefSeq peptide;Acc:NP_001179274	5.84e-05	0.005802	-1,470	-2,770
LAP3	NM_174098	Cytosol aminopeptidase [Source:UniProtKB/Swiss-Prot;Acc:P00727]	2,26E-03	0.001129	-1,452	-2,736
ANXA8L1	NM_174241	Annexin A8 [Source:UniProtKB/Swiss-Prot;Acc:Q95L54]	7,98E-02	0.006767	-1,434	-2,702
SRPX2	NM_001014926	sushi repeat-containing protein SRPX2 precursor [Source:RefSeq peptide;Acc:NP_001014926]	2,43E-02	0.004354	-1,424	-2,683
TMEM37	NM_001034744	voltage-dependent calcium channel gamma-like subunit [Source:RefSeq peptide;Acc:NP_001029916]	6,05E-02	0.005876	-1,419	-2,674
GJB3	NM_001104995	Gap junction beta-3 protein [Source:UniProtKB/Swiss-Prot;Acc:Q58D78]	0.002725	0.04917	-1,407	-2,652
DDIT4	NM_001075922	DNA damage-inducible transcript 4 protein [Source:UniProtKB/Swiss-Prot;Acc:Q08E62]	0.0002206	0.01197	-1,402	-2,643
ERC2	NM_001102195	ERC protein 2 [Source:RefSeq peptide;Acc:NP_001095665]	0.0001492	0.01004	-1	-2,630

PRSS12	NM_001193222	neurotrypsin precursor [Source:RefSeq peptide;Acc:NP_001180151]	0.0003277	0.01475	-1,390	-2,621
CKMT1B	NM_174275	Creatine kinase U-type, mitochondrial [Source:UniProtKB/Swiss-Prot;Acc:Q9TTK8]	0.001638	0.03698	-1,388	-2,617
FLRT3	NM_001192674	leucine-rich repeat transmembrane protein FLRT3 precursor [Source:RefSeq peptide;Acc:NP_001179603]	3,81E-02	0.004753	-1,386	-2,614
MAP1LC3C	NM_001101058	microtubule-associated proteins 1A/1B light chain 3C [Source:RefSeq peptide;Acc:NP_001094528]	0.0005048	0.01902	-1,379	-2,601
THBS1	NM_174196	thrombospondin-1 precursor [Source:RefSeq peptide;Acc:NP_776621]	0.0009419	0.02752	-1,364	-2,574
TPPP3	NM_001034774	Tubulin polymerization-promoting protein family member 3 [Source:UniProtKB/Swiss-Prot;Acc:Q3ZCC8]	0.0005348	0.01999	-1,353	-2,554
FAM13C	NM_001078029	protein FAM13C [Source:RefSeq peptide;Acc:NP_001071497]	5,25E-02	0.005624	-1,310	-2,479
SEMA7A	NM_001206185	semaphorin-7A precursor [Source:RefSeq peptide;Acc:NP_001193114]	0.0004086	0.01672	-1,294	-2,452
ANGPTL2	NM_001109814	angiopoietin-related protein 2 precursor [Source:RefSeq peptide;Acc:NP_001103284]	0.0006249	0.02222	-1,288	-2,442
CLDN1	NM_001001854	Claudin-1 [Source:UniProtKB/Swiss-Prot;Acc:Q6L708]	0.0002661	0.01323	-1,272	-2,415
TMEM150A	NM_001193030	transmembrane protein 150A precursor [Source:RefSeq peptide;Acc:NP_001179959]	0.0001561	0.01022	-1,257	-2,390
DECR1	NM_001075423	2,4-dienoyl-CoA reductase, mitochondrial [Source:RefSeq peptide;Acc:NP_001068891]	5,27E-02	0.005624	-1,251	-2,380
PAK7	NM_001206594	serine/threonine-protein kinase PAK 7 [Source:RefSeq peptide;Acc:NP_001193523]	6,07E-02	0.005876	-1,247	-2,373
COL3A1	NM_001076831		1,11E-02	0.002625	-1,243	-2,367
TRIB3	NM_001076103	Tribbles homolog 3 [Source:UniProtKB/Swiss-Prot;Acc:Q0VCE3]	0.001915	0.03978	-1,221	-2,331
TP53I11	NM_001075725		0.0007992	0.02575	-1,214	-2,320
GAS2	NM_001105001	growth arrest-specific protein 2 [Source:RefSeq peptide;Acc:NP_001098471]	5,83E-02	0.005802	-1,209	-2,312
KRT18	NM_001192095	keratin, type I cytoskeletal 18 [Source:RefSeq peptide;Acc:NP_001179024]	0.0009018	0.02709	-1,207	-2,309
CDH23	NM_001191206	cadherin-23 precursor [Source:RefSeq peptide;Acc:NP_001178135]	0.0002206	0.01197	-1,204	-2,304
TF	NM_177484	serotransferrin precursor [Source:RefSeq peptide;Acc:NP_803450]	0.0004745	0.01828	-1,183	-2,270
CBLB	NM_001205923	E3 ubiquitin-protein ligase CBL-B [Source:RefSeq peptide;Acc:NP_001192852]	5,31E-03	0.001829	-1,176	-2,259
GLI1	NM_001099000	zinc finger protein GLI1 [Source:RefSeq peptide;Acc:NP_001092470]	0.002601	0.04777	-1,174	-2,256
LAMP5	NM_001083418	Lysosome-associated membrane glycoprotein 5 [Source:UniProtKB/Swiss-Prot;Acc:A4FV27]	7,53E-04	0.0005953	-1,169	-2,249
MYO1B	NM_001102199	myosin-Ib [Source:RefSeq peptide;Acc:NP_001095669]	2,90E-02	0.004458	-1,167	-2,245
MRC2	NM_001192670	C-type mannose receptor 2 precursor [Source:RefSeq peptide;Acc:NP_001179599]	4,84E-02	0.00541	-1,167	-2,245
AK4	NM_001077933	Adenylate kinase isoenzyme 4, mitochondrial [Source:UniProtKB/Swiss-Prot;Acc:Q0VCP1]	0.001961	0.04029	-1,152	-2,222
TXK	NM_001206148	tyrosine-protein kinase TXK [Source:RefSeq peptide;Acc:NP_001193077]	0.001427	0.03437	-1,149	-2,218
SMOC2	NM_001098134; NM	SPARC-related modular calcium-binding protein 2 precursor [Source:RefSeq peptide;Acc:NP_001091603]	0.00202	0.04116	-1,137	-2,199
FBLN5	NM_001014946	fibulin-5 precursor [Source:RefSeq peptide;Acc:NP_001014946]	9,44E-02	0.007466	-1,129	-2,187
EPB49	NM_001034431	Dematin [Source:UniProtKB/Swiss-Prot;Acc:Q08DM1]	5,07E-02	0.005593	-1,123	-2,178
LOC784768	NM_001242583	epithelial chloride channel protein precursor [Source:RefSeq peptide;Acc:NP_001229512]	0.0004019	0.01654	-1,121	-2,175
LTBP1	NM_001103091	latent-transforming growth factor beta-binding protein 1 precursor [Source:RefSeq peptide;Acc:NP_00109	0.0007032	0.02433	-1,118	-2,170
SLC39A8	NM_001205630	zinc transporter ZIP8 precursor [Source:RefSeq peptide;Acc:NP_001192559]	0.0002582	0.01301	-1,110	-2,158
PROM1	NM_001245952	prominin-1 precursor [Source:RefSeq peptide;Acc:NP_001232881]	0.0003768	0.01597	-1,097	-2,139
DDR2	NM_001083720	discoidin domain-containing receptor 2 precursor [Source:RefSeq peptide;Acc:NP_001077189]	0.000306	0.01406	-1,094	-2,135
CCDC3	NM_001172375_2; N	coiled-coil domain-containing protein 3 precursor [Source:RefSeq peptide;Acc:NP_001165846]	3.13e-05	0.004633	-1,092	-2,132
RAB20	NM_001193089	ras-related protein Rab-20 [Source:RefSeq peptide;Acc:NP_001180018]	0.00275	0.04945	-1,090	-2,129
SYT12	NM_001192890	synaptotagmin-12 [Source:RefSeq peptide;Acc:NP_001179819]	0.001011	0.02858	-1,066	-2,094
TPM2	NM_001010995	Tropomyosin beta chain [Source:UniProtKB/Swiss-Prot;Acc:Q5KR48]	0.0005463	0.02026	-1,063	-2,089
FUT1	NM_177499	galactoside 2-alpha-L-fucosyltransferase 1 [Source:RefSeq peptide;Acc:NP_803465]	0.0006971	0.02424	-1,054	-2,076
DKK2	NM_001082615	dickkopf-related protein 2 precursor [Source:RefSeq peptide;Acc:NP_001076084]	0.001596	0.03636	-1,045	-2,063

NUAK1	NM_001205496	NUAK family SNF1-like kinase 1 [Source:RefSeq peptide;Acc:NP_001192425]	0.0002765	0.01346	-1,038	-2,053
FEZ1	NM_001024522	fasciculation and elongation protein zeta-1 [Source:RefSeq peptide;Acc:NP_001019693]	0.001004	0.02858	-1,029	-2,041
PRSS54	NM_001099044	inactive serine protease 54 precursor [Source:RefSeq peptide;Acc:NP_001092514]	0.0003933	0.0163	-1,023	-2,032
COL1A1	NM_001034039	Collagen alpha-1(I) chain [Source:UniProtKB/Swiss-Prot;Acc:P02453]	0.001013	0.02858	-1,023	-2,032
SSBP3	NM_001104986	single-stranded DNA-binding protein 3 [Source:RefSeq peptide;Acc:NP_001098456]	0.0004364	0.01756	-1,015	-2,021
CDH2	NM_001166492	Cadherin-2 [Source:UniProtKB/Swiss-Prot;Acc:P19534]	0.00223	0.04365	-1,015	-2,021
CYP3A4	NM_001099367	cytochrome P450, family 3, subfamily A, polypeptide 4 [Source:RefSeq peptide;Acc:NP_001092837]	0.001958	0.04029	-1,013	-2,018
CYP3A5	NM_001075888; NM	cytochrome P450, family 3, subfamily A, polypeptide 5 [Source:RefSeq peptide;Acc:NP_001069356]; cytoc	0.001983	0.04066	-1,010	-2,014
MEIS3	NM_001193152	homeobox protein Meis3 [Source:RefSeq peptide;Acc:NP_001180081]	0.001014	0.02858	-0,976	-1,967
PTGS1	NM_001105323	Prostaglandin G/H synthase 1 [Source:UniProtKB/Swiss-Prot;Acc:O62664]	3,92E-04	0.0004126	-0,975	-1,966
CSPG4	NM_001192782	chondroitin sulfate proteoglycan 4 precursor [Source:RefSeq peptide;Acc:NP_001179711]	0.001778	0.03837	-0,974	-1,964
MAGED4B	NM_001103311	melanoma-associated antigen D4 [Source:RefSeq peptide;Acc:NP_001096781]	5,66E-02	0.005783	-0,973	-1,963
MDFI	NM_001205537	myoD family inhibitor [Source:RefSeq peptide;Acc:NP_001192466]	0.001219	0.03177	-0,972	-1,961
CHST2	NM_001113769	carbohydrate sulfotransferase 2 [Source:RefSeq peptide;Acc:NP_001107241]	3,19E-02	0.004633	-0,969	-1,957
AQP9	NM_001205833	aquaporin 9 [Source:HGNC Symbol;Acc:643]	0.0004169	0.01691	-0,967	-1,955
THSD7A	NM_001206743	thrombospondin type-1 domain-containing protein 7A precursor [Source:RefSeq peptide;Acc:NP_0011936	0.0008156	0.0259	-0,961	-1,947
FLNC	NM_001206990		0.001878	0.03928	-0,955	-1,939
TMEM151A	NM_001083782	transmembrane protein 151B [Source:RefSeq peptide;Acc:NP_001077251]	0.0007215	0.02463	-0,946	-1,927
WNT11	NM_001082456	protein Wnt-11 [Source:RefSeq peptide;Acc:NP_001075925]	0.0007536	0.02506	-0,946	-1,927
TRIM44	NM_001105014; NM	Tripartite motif-containing protein 44 [Source:UniProtKB/Swiss-Prot;Acc:A6QQX5]	0.001197	0.03158	-0,943	-1,922
BGN	NM_178318	Biglycan [Source:UniProtKB/Swiss-Prot;Acc:P21809]	2,16E-02	0.004017	-0,942	-1,921
SLC1A4	NM_001081577	Neutral amino acid transporter A [Source:UniProtKB/Swiss-Prot;Acc:A2VDL4]	0.00149	0.03511	-0,936	-1,913
BEX2	NM_001077087; NM	protein BEX2 [Source:RefSeq peptide;Acc:NP_001070555]; Protein BEX2 [Source:UniProtKB/Swiss-Prot;Acc:(	0.001274	0.03251	-0,927	-1,902
ANKRD50	NM_001205949	ankyrin repeat domain-containing protein 50 [Source:RefSeq peptide;Acc:NP_001192878]	3,48E-03	0.001376	-0,917	-1,888
ITGB7	NM_001105365	integrin beta-7 precursor [Source:RefSeq peptide;Acc:NP_001098835]	0.001776	0.03837	-0,907	-1,875
PTCH1	NM_001205879	protein patched homolog 1 [Source:RefSeq peptide;Acc:NP_001192808]	4.16e-05	0.005004	-0,875	-1,834
TM4SF20	NM_001076981	transmembrane 4 L6 family member 20 [Source:RefSeq peptide;Acc:NP_001070449]	0.0008493	0.02644	-0,867	-1,824
ADRBK2	NM_174500	Beta-adrenergic receptor kinase 2 [Source:UniProtKB/Swiss-Prot;Acc:P26818]	0.0004137	0.01686	-0,858	-1,813
PTAFR	NM_001040538	Platelet-activating factor receptor [Source:UniProtKB/Swiss-Prot;Acc:Q9TTY5]	0.0009129	0.02726	-0,852	-1,805
ADAM19	NM_001075475	disintegrin and metalloproteinase domain-containing protein 19 precursor [Source:RefSeq peptide;Acc:NI	0.0001205	0.008734	-0,846	-1,797
VEGFA	NM_174216		0.0006858	0.02402	-0,839	-1,788
DPF1	NM_001076855		0.0001191	0.008734	-0,836	-1,785
ARID3A	NM_001205695	AT-rich interactive domain-containing protein 3A [Source:RefSeq peptide;Acc:NP_001192624]	0.000803	0.02575	-0,835	-1,784
CACNA1G	NM_001193140	voltage-dependent T-type calcium channel subunit alpha-1G [Source:RefSeq peptide;Acc:NP_001180069	0.002523	0.04696	-0,828	-1,776
NLGN3	NM_001075504	neuroligin-3 precursor [Source:RefSeq peptide;Acc:NP_001068972]	0.001295	0.0327	-0,826	-1,772
ZP2	NM_173973	zona pellucida sperm-binding protein 2 precursor [Source:RefSeq peptide;Acc:NP_776398]	0.002042	0.04142	-0,821	-1,766
CXCR4	NM_174301	C-X-C chemokine receptor type 4 [Source:UniProtKB/Swiss-Prot;Acc:P25930]	0.0001817	0.01113	-0,814	-1,758
CAMKK1	NM_001192251	calcium/calmodulin-dependent protein kinase kinase 1 [Source:RefSeq peptide;Acc:NP_001179180]	0.002295	0.04408	-0,807	-1,749
FGD3	NM_001024527	FYVE, RhoGEF and PH domain-containing protein 3 [Source:RefSeq peptide;Acc:NP_001019698]	0.002081	0.04193	-0,803	-1,745
TBX18	NM_001192462	T-box transcription factor TBX18 [Source:RefSeq peptide;Acc:NP_001179391]	0.0002539	0.013	-0,802	-1,744
MYC	NM_001046074	Myc proto-oncogene protein [Source:UniProtKB/Swiss-Prot;Acc:Q2HJ27]	0.002633	0.04808	-0,801	-1,742

TC2N	NM_001193204	tandem C2 domains nuclear protein [Source:RefSeq peptide;Acc:NP_001180133]	0.001015	0.02858	-0,786	-1,724
MX1	NM_173940	Interferon-induced GTP-binding protein Mx1 Interferon-induced GTP-binding protein Mx1, N-terminally proc	0.001554	0.03596	-0,779	-1,716
ENO3	NM_001034702	Beta-enolase [Source:UniProtKB/Swiss-Prot;Acc:Q3ZC09]	0.001441	0.03462	-0,777	-1,713
MYB	NM_175050	transcriptional activator Myb [Source:RefSeq peptide;Acc:NP_778220]	0.001136	0.03041	-0,770	-1,705
THSD1	NM_001014967	thrombospondin type-1 domain-containing protein 1 precursor [Source:RefSeq peptide;Acc:NP_00101496	0.001829	0.03895	-0,754	-1,687
COTL1	NM_001046593	Coactosin-like protein [Source:UniProtKB/Swiss-Prot;Acc:Q2HJ57]	4,46E-02	0.005159	-0,751	-1,683
TBXAS1	NM_001046027	thromboxane-A synthase [Source:RefSeq peptide;Acc:NP_001039492]	0.001306	0.03285	-0,748	-1,680
HMGCS1	NM_001206578	hydroxymethylglutaryl-CoA synthase, cytoplasmic [Source:RefSeq peptide;Acc:NP_001193507]	0.002011	0.04107	-0,727	-1,655
SLC25A30	NM_001098895	kidney mitochondrial carrier protein 1 [Source:RefSeq peptide;Acc:NP_001092365]	0.0002017	0.01157	-0,720	-1,647
FSTL1	NM_001017950	Follistatin-related protein 1 [Source:UniProtKB/Swiss-Prot;Acc:Q58D84]	2.7e-05	0.004458	-0,716	-1,643
NDRG1	NM_001035009	protein NDRG1 [Source:RefSeq peptide;Acc:NP_001030181]	0.0001941	0.01137	-0,714	-1,640
CYP51A1	NM_001025319	Lanosterol 14-alpha demethylase [Source:UniProtKB/Swiss-Prot;Acc:Q4PJW3]	4,75E-02	0.005367	-0,703	-1,628
SLC22A17	NM_001130755	Solute carrier family 22 member 17 [Source:UniProtKB/Swiss-Prot;Acc:Q3SZQ2]	0.002497	0.04667	-0,702	-1,627
GTDC1	NM_001076035	Glycosyltransferase-like domain-containing protein 1 [Source:UniProtKB/Swiss-Prot;Acc:Q08DA7]	0.0002982	0.01395	-0,700	-1,625
CELF2	NM_001078165		0.0004484	0.01784	-0,694	-1,618
MTMR7	NM_001075641	myotubularin-related protein 7 [Source:RefSeq peptide;Acc:NP_001069109]	0.0002341	0.01248	-0,689	-1,613
SDC3	NM_001206531	syndecan-3 precursor [Source:RefSeq peptide;Acc:NP_001193460]	0.0004872	0.01857	-0,689	-1,613
DPYSL3	NM_001101068	dihydropyrimidinase-related protein 3 [Source:RefSeq peptide;Acc:NP_001094538]	7,85E-02	0.006767	-0,688	-1,611
UCP2	NM_001033611	Mitochondrial uncoupling protein 2 [Source:UniProtKB/Swiss-Prot;Acc:Q3SZI5]	0.002432	0.0458	-0,681	-1,603
PRKAR2B	NM_174649	cAMP-dependent protein kinase type II-beta regulatory subunit [Source:RefSeq peptide;Acc:NP_777074]	0.001448	0.03463	-0,678	-1,600
WDR59	NM_001101130	WD repeat-containing protein 59 [Source:RefSeq peptide;Acc:NP_001094600]	0.0002604	0.01301	-0,671	-1,592
OLFML2B	NM_001100354	Olfactomedin-like protein 2B [Source:UniProtKB/Swiss-Prot;Acc:A6QLD2]	0.001776	0.03837	-0,661	-1,581
BDKRB1	NM_001109999	B1 bradykinin receptor [Source:RefSeq peptide;Acc:NP_001103469]	0.002227	0.04365	-0,659	-1,578
FKBP11	NM_001045932	peptidyl-prolyl cis-trans isomerase FKBP11 precursor [Source:RefSeq peptide;Acc:NP_001039397]	0.00183	0.03895	-0,656	-1,576
CCDC8	NM_001035485		0.002444	0.0458	-0,652	-1,572
TUFT1	NM_174479	tuftelin [Source:RefSeq peptide;Acc:NP_776904]	0.001515	0.03552	-0,652	-1,571
SKIL	NM_001205947	ski-like protein [Source:RefSeq peptide;Acc:NP_001192876]	0.0006342	0.02247	-0,640	-1,558
DBT	NM_173905	Lipoamide acyltransferase component of branched-chain alpha-keto acid dehydrogenase complex, mitc	0.001697	0.03748	-0,638	-1,556
CTDSPL	NM_001193081		0.0001558	0.01022	-0,630	-1,547
HEY1	NM_001001172	Hairy/enhancer-of-split related with YRPW motif protein 1 [Source:UniProtKB/Swiss-Prot;Acc:Q2KIN4]	0.001588	0.03636	-0,624	-1,541
CAMKMT	NM_001105641	calmodulin-lysine N-methyltransferase [Source:RefSeq peptide;Acc:NP_001099111]	0.002691	0.04867	-0,620	-1,537
IARS	NM_001101069	isoleucyl-tRNA synthetase, cytoplasmic [Source:RefSeq peptide;Acc:NP_001094539]	0.001549	0.03596	-0,620	-1,536
DAAM1	NM_001081588	disheveled-associated activator of morphogenesis 1 [Source:RefSeq peptide;Acc:NP_001075057]	0.0008916	0.02697	-0,612	-1,528
IGF1R	NM_001244612	Insulin-like growth factor 1 receptor Insulin-like growth factor 1 receptor alpha chain Insulin-like growth fact	0.0009336	0.02745	-0,608	-1,524
MAGED1	NM_001046125	melanoma-associated antigen D1 [Source:RefSeq peptide;Acc:NP_001039590]	0.0001182	0.008734	-0,606	-1,522
F2RL2	NM_001038533	proteinase-activated receptor 3 precursor [Source:RefSeq peptide;Acc:NP_001033622]	8.81e-05	0.00721	-0,601	-1,516
SLC6A9	NM_001102032; NM	sodium- and chloride-dependent glycine transporter 1-like [Source:RefSeq peptide;Acc:NP_001095502]; sc	0.0008781	0.02697	-0,597	-1,513
SH3KBP1	NM_001128500	SH3 domain-containing kinase-binding protein 1 [Source:RefSeq peptide;Acc:NP_001121972]	0.0009337	0.02745	-0,594	-1,509
LGR4	NM_001205511	leucine-rich repeat-containing G-protein coupled receptor 4 precursor [Source:RefSeq peptide;Acc:NP_0	8,50E-02	0.00702	-0,592	-1,507
JAG1	NM_001191178	protein jagged-1 precursor [Source:RefSeq peptide;Acc:NP_001178107]	0.0002896	0.01368	-0,588	-1,503
LMCD1	NM_001076222	LIM and cysteine-rich domains protein 1 [Source:UniProtKB/Swiss-Prot;Acc:Q17QE2]	0.0008478	0.02644	0,585	1,500

STARD8	NM_001102517		4,19E-02	0.005004	0,588	1,503
TNFAIP1	NM_001192290	BTB/POZ domain-containing adapter for CUL3-mediated RhoA degradation protein 2 [Source:RefSeq pep	2.39e-05	0.004354	0,593	1,509
ARHGEF15	NM_001205712		0.001358	0.03358	0,595	1,510
ATP6V1E1	NM_174810	V-type proton ATPase subunit E 1 [Source:RefSeq peptide;Acc:NP_777235]	2,59E-02	0.004458	0,598	1,514
SORBS2	NM_001079787	sorbin and SH3 domain-containing protein 2 [Source:RefSeq peptide;Acc:NP_001073255]	0.002329	0.04448	0,600	1,515
PIM2	NM_001206378	serine/threonine-protein kinase pim-2 [Source:RefSeq peptide;Acc:NP_001193307]	0.002046	0.04142	0,603	1,519
PDCD4	NM_001083647	programmed cell death protein 4 [Source:RefSeq peptide;Acc:NP_001077116]	0.0002696	0.01333	0,603	1,519
NEU1	NM_001083642	Sialidase-1 [Source:UniProtKB/Swiss-Prot;Acc:A6BMK7]	0.0003561	0.01544	0,606	1,522
IRAK3	NM_001190299	interleukin-1 receptor-associated kinase 3 [Source:RefSeq peptide;Acc:NP_001177228]	0.001849	0.03909	0,608	1,524
ASRGL1	NM_001077035	L-asparaginase [Source:UniProtKB/Swiss-Prot;Acc:Q32LE5]	0.0001655	0.01055	0,608	1,524
GLS	NM_001077964	glutaminase kidney isoform, mitochondrial [Source:RefSeq peptide;Acc:NP_001071432]	0.000134	0.009284	0,609	1,525
TANK	NM_001192264	TRAF family member-associated NF-kappa-B activator [Source:RefSeq peptide;Acc:NP_001179193]	0.0001429	0.009692	0,610	1,526
CD302	NM_001110191	CD302 antigen [Source:UniProtKB/Swiss-Prot;Acc:A8WH74]	0.001556	0.03596	0,610	1,527
GLB1	NM_001035043	beta-galactosidase precursor [Source:RefSeq peptide;Acc:NP_001030215]	0.002582	0.0477	0,612	1,528
M6PR	NM_175779	Cation-dependent mannose-6-phosphate receptor [Source:UniProtKB/Swiss-Prot;Acc:P11456]	0.0002958	0.0139	0,614	1,530
TYMS	NM_001037816	thymidylate synthase [Source:RefSeq peptide;Acc:NP_001032905]	0.0003528	0.01544	0,616	1,532
C7H5orf54	NM_001098107	Transposon-derived Buster3 transposase-like protein [Source:UniProtKB/Swiss-Prot;Acc:A4Z945]	0.001694	0.03748	0,622	1,538
ERO1L	NM_001103348	ERO1-like protein alpha [Source:UniProtKB/Swiss-Prot;Acc:A5PJN2]	0.0004756	0.01828	0,625	1,542
FANCI	NM_001191454	Fanconi anemia group I protein [Source:RefSeq peptide;Acc:NP_001178383]	0.0001848	0.01113	0,625	1,542
RRAGC	NM_001076456_2; N	ras-related GTP-binding protein C [Source:RefSeq peptide;Acc:NP_001069924]	0.002796	0.0498	0,626	1,543
RABGGTA	NM_001015614	Geranylgeranyl transferase type-2 subunit alpha [Source:UniProtKB/Swiss-Prot;Acc:Q5EA80]	0.001209	0.03177	0,626	1,544
FAM54A	NM_001017948	Protein FAM54A [Source:UniProtKB/Swiss-Prot;Acc:Q58CR1]	0.0006171	0.02203	0,628	1,545
PIK3CD	NM_001205548		0.0002815	0.01364	0,628	1,546
RPH3AL	NM_001035494; NM	Rab effector Noc2 [Source:UniProtKB/Swiss-Prot;Acc:Q58D79]	0.001426	0.03437	0,630	1,548
RAPGEF1	NM_001205872		6,80E-02	0.00639	0,632	1,549
STOM	NM_001105473	erythrocyte band 7 integral membrane protein [Source:RefSeq peptide;Acc:NP_001098943]	0.001321	0.03306	0,632	1,549
DDB2	NM_001075788	DNA damage-binding protein 2 [Source:UniProtKB/Swiss-Prot;Acc:Q0VBY8]	0.000176	0.01092	0,633	1,551
LSR	NM_001083394	lipolysis-stimulated lipoprotein receptor [Source:RefSeq peptide;Acc:NP_001076863]	0.00273	0.04917	0,635	1,553
BCL2L1	NM_001077486	bcl-2-like protein 1 [Source:RefSeq peptide;Acc:NP_001070954]	0.0008289	0.02623	0,637	1,555
TRPC1	NM_174476	short transient receptor potential channel 1 [Source:RefSeq peptide;Acc:NP_776901]	0.00164	0.03698	0,640	1,559
ZNF706	NM_001199073; NM	zinc finger protein 706 [Source:RefSeq peptide;Acc:NP_001186002]	0.0009934	0.02858	0,641	1,559
NPAS2	NM_001083763	neuronal PAS domain-containing protein 2 [Source:RefSeq peptide;Acc:NP_001077232]	0.001022	0.02858	0,643	1,562
DCK	NM_001034573	Deoxycytidine kinase [Source:UniProtKB/Swiss-Prot;Acc:Q3MHR2]	0.0002533	0.013	0,644	1,562
C1QTNF5	NM_001099138	complement C1q tumor necrosis factor-related protein 5 precursor [Source:RefSeq peptide;Acc:NP_0010	2,03E-02	0.00389	0,644	1,563
LDLRAP1	NM_001083668	low density lipoprotein receptor adapter protein 1 [Source:RefSeq peptide;Acc:NP_001077137]	0.0006944	0.02424	0,646	1,564
TSPAN5	NM_001076119	Tetraspanin-5 [Source:UniProtKB/Swiss-Prot;Acc:Q17QJ5]	7,62E-02	0.006759	0,647	1,565
RNF157	NM_001205618	RING finger protein 157 [Source:RefSeq peptide;Acc:NP_001192547]	0.0001228	0.008767	0,651	1,570
ETS1	NM_001099106	protein C-ets-1 [Source:RefSeq peptide;Acc:NP_001092576]	0.0004024	0.01654	0,652	1,571
EFHD2	NM_001103245	EF-hand domain-containing protein D2 [Source:UniProtKB/Swiss-Prot;Acc:A5D7A0]	0.00278	0.04971	0,652	1,572
BAX	NM_173894_2; NM_	Apoptosis regulator BAX [Source:UniProtKB/Swiss-Prot;Acc:O02703]	0.0004531	0.01785	0,653	1,573
RAD18	NM_001035295	E3 ubiquitin-protein ligase RAD18 [Source:RefSeq peptide;Acc:NP_001030372]	0.0003011	0.01401	0,653	1,573

CDK1	NM_174016	Cyclin-dependent kinase 1 [Source:UniProtKB/Swiss-Prot;Acc:P48734]	0.0001779	0.01097	0,658	1,578
TCF4	NM_001034621	transcription factor 4 [Source:RefSeq peptide;Acc:NP_001029793]	0.0001532	0.01021	0,662	1,582
SLC20A2	NM_001080280	sodium-dependent phosphate transporter 2 [Source:RefSeq peptide;Acc:NP_001073749]	0.000717	0.02463	0,663	1,583
VLDLR	NM_174489	very low-density lipoprotein receptor precursor [Source:RefSeq peptide;Acc:NP_776914]	0.001782	0.03837	0,668	1,588
MMP15	NM_001191434	matrix metalloproteinase-15 precursor [Source:RefSeq peptide;Acc:NP_001178363]	0.001717	0.03764	0,670	1,591
UBE2C	NM_001037449	Ubiquitin-conjugating enzyme E2 C [Source:UniProtKB/Swiss-Prot;Acc:Q32PA5]	0.001397	0.0339	0,673	1,594
C19H17orf61	NM_001045957	UPF0451 protein C17orf61 homolog [Source:UniProtKB/Swiss-Prot;Acc:Q2KI29]	0.000165	0.01055	0,674	1,596
MOSPD2	NM_001101896_2; N	motile sperm domain-containing protein 2 [Source:RefSeq peptide;Acc:NP_001095366]	0.0003568	0.01544	0,677	1,598
KANK2	NM_001076531	KN motif and ankyrin repeat domain-containing protein 2 [Source:RefSeq peptide;Acc:NP_001069999]	8,05E-02	0.006767	0,679	1,601
TMEM251	NM_001077132	UPF0694 transmembrane protein C14orf109 homolog [Source:UniProtKB/Swiss-Prot;Acc:Q2HJ69]	0.0008316	0.02623	0,681	1,603
MSH2	NM_001034584	DNA mismatch repair protein Msh2 [Source:UniProtKB/Swiss-Prot;Acc:Q3MHE4]	0.002638	0.04808	0,684	1,606
PTPRE	NM_001205531	receptor-type tyrosine-protein phosphatase epsilon [Source:RefSeq peptide;Acc:NP_001192460]	0.00138	0.03373	0,684	1,606
TNIP1	NM_001024554	TNFAIP3-interacting protein 1 [Source:RefSeq peptide;Acc:NP_001019725]	0.0001036	0.007869	0,689	1,612
CDKN3	NM_001040582	cyclin-dependent kinase inhibitor 3 [Source:RefSeq peptide;Acc:NP_001035672]	0.0001378	0.009414	0,691	1,615
PDE7B	NM_001102068	cAMP-specific 3,5-cyclic phosphodiesterase 7B [Source:RefSeq peptide;Acc:NP_001095538]	0.001098	0.03012	0,693	1,617
LRRC2	NM_001080311	leucine-rich repeat-containing protein 2 [Source:RefSeq peptide;Acc:NP_001073780]	0.001179	0.03119	0,695	1,619
SPRED1	NM_001192516	sprouty-related, EVH1 domain-containing protein 1 [Source:RefSeq peptide;Acc:NP_001179445]	0.0001912	0.01134	0,695	1,619
ADORA2B	NM_001075925	Adenosine receptor A2b [Source:UniProtKB/Swiss-Prot;Acc:Q1LZD0]	0.001919	0.03978	0,696	1,619
TMBIM1	NM_205798	transmembrane BAX inhibitor motif-containing protein 1 [Source:RefSeq peptide;Acc:NP_991367]	1,17E-02	0.00272	0,696	1,620
KIAA0317	NM_001076165	protein KIAA0317 homolog [Source:RefSeq peptide;Acc:NP_001069633]	0.000389	0.01623	0,702	1,626
PSRC1	NM_001046501	Proline/serine-rich coiled-coil protein 1 [Source:UniProtKB/Swiss-Prot;Acc:Q29RJ9]	0.002539	0.04718	0,709	1,635
AOX1	NM_176668	aldehyde oxidase [Source:RefSeq peptide;Acc:NP_788841]	0.001061	0.02946	0,711	1,637
MYBL1	NM_176635	myb-related protein A [Source:RefSeq peptide;Acc:NP_788808]	0.0007676	0.02522	0,713	1,639
PLA2G15	NM_174560	Group XV phospholipase A2 [Source:UniProtKB/Swiss-Prot;Acc:Q8WMP9]	0.0003301	0.01478	0,722	1,649
CHST1	NM_001083648	carbohydrate sulfotransferase 1 precursor [Source:RefSeq peptide;Acc:NP_001077117]	0.0002047	0.01157	0,732	1,661
C11H2orf28	NM_001105505_2; NM_001105505		0.002161	0.04296	0,737	1,667
PFKFB3	NM_001077837	6-phosphofructo-2-kinase/fructose-2,6-biphosphatase 3 [Source:RefSeq peptide;Acc:NP_001071305]	0.001449	0.03463	0,738	1,667
DKK3	NM_001100306	dickkopf-related protein 3 precursor [Source:RefSeq peptide;Acc:NP_001093776]	0.0001897	0.01133	0,739	1,669
LAMTOR1	NM_001034769	Ragulator complex protein LAMTOR1 [Source:UniProtKB/Swiss-Prot;Acc:Q3T0D8]	0.0003225	0.01465	0,741	1,671
CALCRL	NM_001102107	calcitonin gene-related peptide type 1 receptor precursor [Source:RefSeq peptide;Acc:NP_001095577]	0.001291	0.03269	0,743	1,674
PROCR	NM_174437	Endothelial protein C receptor [Source:UniProtKB/Swiss-Prot;Acc:Q28105]	0.001533	0.03575	0,748	1,679
GPRC5B	NM_001075741	G-protein coupled receptor family C group 5 member B precursor [Source:RefSeq peptide;Acc:NP_00106	0.001657	0.03719	0,748	1,680
TMEM194A	NM_001102161	Transmembrane protein 194A [Source:UniProtKB/Swiss-Prot;Acc:A7MBC7]	0.0004531	0.01785	0,754	1,687
SCN3B	NM_001046495; NM	Sodium channel subunit beta-3 [Source:UniProtKB/Swiss-Prot;Acc:Q2KI11]	0.0002593	0.01301	0,756	1,689
CYBASC3	NM_001099149	Cytochrome b ascorbate-dependent protein 3 [Source:UniProtKB/Swiss-Prot;Acc:A5D9A7]	0.000584	0.02133	0,761	1,694
GNPTAB	NM_001192228	N-acetylglucosamine-1-phosphotransferase subunits alpha/beta [Source:RefSeq peptide;Acc:NP_001179	0.001372	0.03373	0,761	1,695
CCNG1	NM_001013364	Cyclin-G1 [Source:UniProtKB/Swiss-Prot;Acc:Q5E9I1]	0.0006604	0.02322	0,766	1,700
SPDYA	NM_001191147		0.002247	0.04373	0,768	1,703
KRT80	NM_001077952	Keratin, type II cytoskeletal 80 [Source:UniProtKB/Swiss-Prot;Acc:A0JND2]	0.0007048	0.02433	0,770	1,705
PTGIS	NM_174444	Prostacyclin synthase [Source:UniProtKB/Swiss-Prot;Acc:Q29626]	0.0004433	0.01776	0,772	1,707
FAM110B	NM_001077018		0.0002459	0.01283	0,772	1,708

TLR4	NM_174198	toll-like receptor 4 precursor [Source:RefSeq peptide;Acc:NP_776623]	1.59e-05	0.00343	0,773	1,708
PKIG	NM_205812	cAMP-dependent protein kinase inhibitor gamma [Source:RefSeq peptide;Acc:NP_991381]	2,82E-02	0.004458	0,773	1,709
LGALS3	NM_001102341	galectin-3 [Source:RefSeq peptide;Acc:NP_001095811]	0.0001721	0.01075	0,777	1,714
DNASE2	NM_001075127	deoxyribonuclease-2-alpha precursor [Source:RefSeq peptide;Acc:NP_001068595]	5,87E-02	0.005802	0,777	1,714
DNALI1	NM_001191299	axonemal dynein light intermediate polypeptide 1 [Source:RefSeq peptide;Acc:NP_001178228]	0.001258	0.03238	0,782	1,720
CD9	NM_173900	CD9 antigen [Source:UniProtKB/Swiss-Prot;Acc:P30932]	0.0007881	0.02571	0,785	1,723
HDAC5	NM_001038025	histone deacetylase 5 [Source:RefSeq peptide;Acc:NP_001033114]	3,70E-02	0.004753	0,788	1,727
FRY	NM_001205616	protein furry homolog [Source:RefSeq peptide;Acc:NP_001192545]	0.0001631	0.01055	0,792	1,732
DDAH2	NM_001034704	N(G),N(G)-dimethylarginine dimethylaminohydrolase 2 [Source:UniProtKB/Swiss-Prot;Acc:Q3SX44]	0.0003899	0.01623	0,795	1,735
CD14	NM_174008	monocyte differentiation antigen CD14 precursor [Source:RefSeq peptide;Acc:NP_776433]	0.0004788	0.01833	0,798	1,739
GUSB	NM_001083436	beta-glucuronidase precursor [Source:RefSeq peptide;Acc:NP_001076905]	7,98E-02	0.006767	0,801	1,742
CD40	NM_001105611	tumor necrosis factor receptor superfamily member 5 precursor [Source:RefSeq peptide;Acc:NP_00109908	0.0009687	0.02816	0,802	1,744
STK38L	NM_001101092	serine/threonine-protein kinase 38-like [Source:RefSeq peptide;Acc:NP_001094562]	0.0001932	0.01137	0,805	1,747
AXIN2	NM_001192299	axin-2 [Source:RefSeq peptide;Acc:NP_001179228]	0.001122	0.03034	0,822	1,768
KCNJ2	NM_174373	Inward rectifier potassium channel 2 [Source:UniProtKB/Swiss-Prot;Acc:O19182]	8,23E-02	0.006857	0,823	1,768
TTC9B	NM_001105507	tetratricopeptide repeat protein 9B [Source:RefSeq peptide;Acc:NP_001098977]	0.002158	0.04296	0,825	1,771
TNFAIP8	NM_001083711	Tumor necrosis factor alpha-induced protein 8 [Source:UniProtKB/Swiss-Prot;Acc:A4IF78]	0.0007968	0.02575	0,827	1,774
FAM3C	NM_001099147	Protein FAM3C [Source:UniProtKB/Swiss-Prot;Acc:A5PKI3]	1,51E-02	0.003336	0,834	1,783
LDB2	NM_001046611	LIM domain binding 2 [Source:RefSeq peptide;Acc:NP_001040076]	0.002506	0.04675	0,836	1,785
ABI3	NM_001083454	ABI gene family member 3 [Source:RefSeq peptide;Acc:NP_001076923]	2.77e-05	0.004458	0,840	1,791
PAM	NM_173948	peptidyl-glycine alpha-amidating monooxygenase precursor [Source:RefSeq peptide;Acc:NP_776373]	0.0001009	0.007789	0,841	1,791
CDKN1A	NM_001098958	cyclin-dependent kinase inhibitor 1 [Source:RefSeq peptide;Acc:NP_001092428]	0.0005516	0.02038	0,851	1,804
TEX2	NM_001101970	testis-expressed sequence 2 protein [Source:RefSeq peptide;Acc:NP_001095440]	0.0004649	0.01809	0,852	1,804
ZDHHC14	NM_001191179	probable palmitoyltransferase ZDHHC14 [Source:RefSeq peptide;Acc:NP_001178108]	0.0001299	0.00907	0,857	1,811
SMAD9	NM_001076928	mothers against decapentaplegic homolog 9 [Source:RefSeq peptide;Acc:NP_001070396]	0.001816	0.03883	0,858	1,813
MALL	NM_001046115	MAL-like protein [Source:RefSeq peptide;Acc:NP_001039580]	7,22E-02	0.006646	0,868	1,825
ITGA2	NM_001166499	integrin alpha-2 precursor [Source:RefSeq peptide;Acc:NP_001159971]	0.001867	0.03916	0,871	1,829
GLDC	NM_001192951	glycine dehydrogenase [Source:RefSeq peptide;Acc:NP_001179880]	0.0007349	0.02465	0,888	1,851
LEPREL1	NM_001100345	prolyl 3-hydroxylase 2 precursor [Source:RefSeq peptide;Acc:NP_001093815]	0.0003066	0.01406	0,890	1,853
CEBPD	NM_174267		3,85E-02	0.004753	0,892	1,856
ZC3H12A	NM_001102187	Ribonuclease ZC3H12A [Source:UniProtKB/Swiss-Prot;Acc:A6QQJ8]	9,95E-02	0.007745	0,893	1,857
TMEM70	NM_001099126	Transmembrane protein 70, mitochondrial [Source:UniProtKB/Swiss-Prot;Acc:A6H773]	2,74E-02	0.004458	0,895	1,859
ADAMTSL4	NM_001101061	ADAMTS-like protein 4 precursor [Source:RefSeq peptide;Acc:NP_001094531]	0.0002301	0.01241	0,896	1,861
CA5B	NM_001080908	carbonic anhydrase 5B, mitochondrial [Source:RefSeq peptide;Acc:NP_001074377]	0.001855	0.03913	0,903	1,870
CLSTN2	NM_001206757	calsyntenin-2 precursor [Source:RefSeq peptide;Acc:NP_001193686]	0.002057	0.04154	0,906	1,873
ASS1	NM_173892	Argininosuccinate synthase [Source:UniProtKB/Swiss-Prot;Acc:P14568]	1,78E-02	0.003663	0,907	1,875
ICAM3	NM_174349	intercellular adhesion molecule 3 precursor [Source:RefSeq peptide;Acc:NP_776774]	0.0003485	0.01539	0,907	1,876
MAP3K8	NM_001099071	mitogen-activated protein kinase kinase kinase 8 [Source:RefSeq peptide;Acc:NP_001092541]	0.0008851	0.02697	0,909	1,877
BSPRY	NM_001206723		0.001644	0.03698	0,910	1,879
CSF2	NM_174027	Granulocyte-macrophage colony-stimulating factor [Source:UniProtKB/Swiss-Prot;Acc:P11052]	3,78E-02	0.004753	0,913	1,883
PLEKHF1	NM_001082468	bta-mir-2901 [Source:miRBase;Acc:MI0013076]	0.0007876	0.02571	0,915	1,886

PPP1R3C	NM_001076164	Protein phosphatase 1 regulatory subunit 3C [Source:UniProtKB/Swiss-Prot;Acc:Q0VCR4]	0.0002119	0.01176	0,917	1,888
FRMD4A	NM_001192267	FERM domain-containing protein 4A [Source:RefSeq peptide;Acc:NP_001179196]	1,72E-02	0.003632	0,928	1,903
KIAA1274	NM_001206604		3,60E-02	0.004753	0,934	1,910
PARM1	NM_001075771	prostate androgen-regulated mucin-like protein 1 precursor [Source:RefSeq peptide;Acc:NP_001069239]	0.002113	0.04241	0,938	1,916
HMHA1	NM_001205741		0.0002003	0.01157	0,949	1,930
PPP1R9A	NM_001076153	neurabin-1 [Source:RefSeq peptide;Acc:NP_001069621]	0.001219	0.03177	0,953	1,936
APOLD1	NM_001101180	apolipoprotein L domain-containing protein 1 [Source:RefSeq peptide;Acc:NP_001094650]	6,54E-02	0.006215	0,958	1,942
NDRG2	NM_001035304		0.0002522	0.013	0,959	1,945
IGFBP6	NM_001040495	insulin-like growth factor-binding protein 6 precursor [Source:RefSeq peptide;Acc:NP_001035585]	0.000755	0.02506	0,960	1,945
SAO	NM_001130764	Primary amine oxidase, liver isozyme [Source:UniProtKB/Swiss-Prot;Acc:Q29437]	0.00178	0.03837	0,960	1,945
HEBP1	NM_001075985	Heme-binding protein 1 [Source:UniProtKB/Swiss-Prot;Acc:Q148C9]	7,92E-03	0.002031	0,972	1,961
ENKUR	NM_001192445	enkurin [Source:RefSeq peptide;Acc:NP_001179374]	7,55E-02	0.006759	0,975	1,966
ID2	NM_001034231	DNA-binding protein inhibitor ID-2 [Source:UniProtKB/Swiss-Prot;Acc:Q3ZC46]	8,32E-04	0.0006073	0,976	1,966
CD46	NM_001242564; NM	membrane cofactor protein isoform 5 precursor [Source:RefSeq peptide;Acc:NP_001229494]	0.001085	0.03004	0,985	1,980
SLC39A10	NM_001205880	zinc transporter ZIP10 precursor [Source:RefSeq peptide;Acc:NP_001192809]	0.000892	0.02697	0,986	1,981
HDHD3	NM_001014896	Haloacid dehalogenase-like hydrolase domain-containing protein 3 [Source:UniProtKB/Swiss-Prot;Acc:Q5E	0.0002161	0.01189	0,991	1,987
NR4A1	NM_001075911	Nuclear receptor subfamily 4 group A member 1 [Source:UniProtKB/Swiss-Prot;Acc:Q0V8F0]	0.0009698	0.02816	0,996	1,995
HPCAL1	NM_001098964	Hippocalcin-like protein 1 [Source:UniProtKB/Swiss-Prot;Acc:P29105]	6,11E-03	0.001871	0,997	1,996
ACVR1C	NM_001192879	activin receptor type-1C precursor [Source:RefSeq peptide;Acc:NP_001179808]	0.002181	0.04296	1,007	2,010
HMMR	NM_001206621		8,05E-02	0.006767	1,023	2,032
EMILIN2	NM_001143869	EMILIN-2 precursor [Source:RefSeq peptide;Acc:NP_001137341]	0.001378	0.03373	1,038	2,053
DYRK3	NM_001100298	dual specificity tyrosine-phosphorylation-regulated kinase 3 [Source:RefSeq peptide;Acc:NP_001093768]	3,47E-03	0.001376	1,039	2,055
PTX3	NM_001076259	pentraxin-related protein PTX3 precursor [Source:RefSeq peptide;Acc:NP_001069727]	0.001113	0.03029	1,041	2,058
ID1	NM_001097568	DNA-binding protein inhibitor ID-1 [Source:RefSeq peptide;Acc:NP_001091037]	0.0004492	0.01784	1,065	2,092
KCNJ16	NM_001076294	inward rectifier potassium channel 16 [Source:RefSeq peptide;Acc:NP_001069762]	0.002432	0.0458	1,068	2,097
SULT1B1	NM_001075823	Sulfotransferase family cytosolic 1B member 1 [Source:UniProtKB/Swiss-Prot;Acc:Q3T0Y3]	4,71E-03	0.001719	1,075	2,107
ID3	NM_001014950	DNA-binding protein inhibitor ID-3 [Source:UniProtKB/Swiss-Prot;Acc:Q5E981]	0.0001998	0.01157	1,086	2,123
OSBPL11	NM_001193008	oxysterol-binding protein-related protein 11 [Source:RefSeq peptide;Acc:NP_001179937]	3,22E-02	0.004633	1,101	2,145
LBH	NM_001099152	Protein LBH [Source:UniProtKB/Swiss-Prot;Acc:A5PJU8]	2,05E-02	0.00389	1,102	2,147
TBC1D16	NM_001206271	TBC1 domain family member 16 [Source:RefSeq peptide;Acc:NP_001193200]	7,14E-05	0.0002323	1,107	2,154
FABP5	NM_174315		0.002173	0.04296	1,111	2,160
IL4R	NM_001075142	interleukin-4 receptor subunit alpha precursor [Source:RefSeq peptide;Acc:NP_001068610]	4,61E-02	0.005268	1,122	2,176
CEACAM1	NM_205788	carcinoembryonic antigen-related cell adhesion molecule 1 precursor [Source:RefSeq peptide;Acc:NP_99	0.0001852	0.01113	1,133	2,193
CXCL3	NM_001046513	chemokine (C-X-C motif) ligand 2 precursor [Source:RefSeq peptide;Acc:NP_001039978]	0.0007956	0.02575	1,137	2,199
FAM107A	NM_001083488		0.001278	0.03253	1,143	2,208
KANK4	NM_001102053		9,50E-04	0.0006445	1,151	2,221
CNKSR3	NM_001192112	connector enhancer of kinase suppressor of ras 3 [Source:RefSeq peptide;Acc:NP_001179041]	1,11E-03	0.0007037	1,161	2,236
NFKBIZ	NM_174726	NF-kappa-B inhibitor zeta [Source:UniProtKB/Swiss-Prot;Acc:Q9BE45]	0.001308	0.03285	1,164	2,241
LY6G6E	NM_001081520	lymphocyte antigen 6 complex, locus G6E precursor [Source:RefSeq peptide;Acc:NP_001074989]	0.0002548	0.013	1,169	2,249
SLC31A2	NM_001034556	probable low affinity copper uptake protein 2 [Source:RefSeq peptide;Acc:NP_001029728]	0.0002583	0.01301	1,174	2,256
C23H6orf25	NM_001078081	protein G6b precursor [Source:RefSeq peptide;Acc:NP_001071549]	0.0003575	0.01544	1,175	2,258

SDCBP	NM_001075483	syntenin-1 [Source:RefSeq peptide;Acc:NP_001068951]	2.79e-07	0.0003783	1,176	2,259
SAT2	NM_203323	Diamine acetyltransferase 2 [Source:UniProtKB/Swiss-Prot;Acc:Q7PCJ8]	0.002294	0.04408	1,180	2,266
ALPL	NM_176858	Alkaline phosphatase, tissue-nonspecific isozyme [Source:UniProtKB/Swiss-Prot;Acc:P09487]	0.0002724	0.0134	1,184	2,272
SGSH	NM_001102189	N-sulphoglucosamine sulphohydrolase precursor [Source:RefSeq peptide;Acc:NP_001095659]	0.0003205	0.01463	1,198	2,294
RENBP	NM_001046223		0.0004754	0.01828	1,230	2,346
NAV3	NM_001192669	neuron navigator 3 [Source:RefSeq peptide;Acc:NP_001179598]	2,48E-03	0.001176	1,233	2,351
SLC9A3R2	NM_001077065	Na(+)/H(+) exchange regulatory cofactor NHE-RF2 [Source:RefSeq peptide;Acc:NP_001070533]	4,27E-02	0.005004	1,236	2,355
ECM1	NM_001099706	extracellular matrix protein 1 precursor [Source:RefSeq peptide;Acc:NP_001093176]	0.0003579	0.01544	1,247	2,373
CH25H	NM_001075243	cholesterol 25-hydroxylase [Source:RefSeq peptide;Acc:NP_001068711]	0.0009181	0.02727	1,254	2,385
BHLHE40	NM_001024929	Class E basic helix-loop-helix protein 40 [Source:UniProtKB/Swiss-Prot;Acc:Q5EA15]	3,24E-03	0.001376	1,256	2,388
SYTL2	NM_001102278	synaptotagmin-like protein 2 [Source:RefSeq peptide;Acc:NP_001095748]	3,86E-02	0.004753	1,281	2,430
TM4SF18	NM_001034287; NM	Transmembrane 4 L6 family member 18 [Source:UniProtKB/Swiss-Prot;Acc:Q3T110]	5,62E-03	0.001829	1,284	2,435
SPRY1	NM_001099366	protein sprouty homolog 1 [Source:RefSeq peptide;Acc:NP_001092836]	3,75E-02	0.004753	1,287	2,440
LY6G6C	NM_001077856	Lymphocyte antigen 6 complex locus protein G6c [Source:UniProtKB/Swiss-Prot;Acc:A0JNL5]	0.0003437	0.01525	1,298	2,459
SNN	NM_001113722	Stannin [Source:UniProtKB/Swiss-Prot;Acc:Q17Q87]	5,63E-03	0.001829	1,304	2,469
GPR158	NM_001206442	Probable G-protein coupled receptor 158 [Source:UniProtKB/Swiss-Prot;Acc:E1BBQ2]	0.002207	0.04339	1,316	2,490
HCRTR1	NM_001048182	Orexin receptor type 1 [Source:UniProtKB/Swiss-Prot;Acc:Q0GBZ5]	0.001024	0.02858	1,322	2,500
CHRM4	NM_001103243	muscarinic acetylcholine receptor M4 [Source:RefSeq peptide;Acc:NP_001096713]	0.0002383	0.01264	1,335	2,523
CFB	NM_001040526	Complement factor B Complement factor B Ba fragment Complement factor B Bb fragment [Source:UniPr	0.0002046	0.01157	1,340	2,532
GPR77	NM_001077947	C5a anaphylatoxin chemotactic receptor C5L2 [Source:RefSeq peptide;Acc:NP_001071415]	0.0002061	0.01158	1,340	2,532
RAMP3	NM_001083505	receptor activity-modifying protein 3 precursor [Source:RefSeq peptide;Acc:NP_001076974]	0.0007644	0.0252	1,340	2,532
EPAS1	NM_174725	endothelial PAS domain-containing protein 1 [Source:RefSeq peptide;Acc:NP_777150]	0.001046	0.02912	1,346	2,542
FAM71F1	NM_001046457	Protein FAM71F1 [Source:UniProtKB/Swiss-Prot;Acc:Q2KIP3]	3,59E-02	0.004753	1,353	2,554
CSF1	NM_174026	macrophage colony-stimulating factor 1 precursor [Source:RefSeq peptide;Acc:NP_776451]	7,11E-03	0.001987	1,359	2,565
NT5E	NM_174129	5-nucleotidase precursor [Source:RefSeq peptide;Acc:NP_776554]	5,47E-02	0.005653	1,362	2,570
FBP1	NM_001034447	Fructose-1,6-bisphosphatase 1 [Source:UniProtKB/Swiss-Prot;Acc:Q3SZB7]	0.001002	0.02858	1,383	2,608
OSTN	NM_001098935	osteocrin precursor [Source:RefSeq peptide;Acc:NP_001092405]	0.0008565	0.02649	1,415	2,667
ARNT2	NM_001206705		3,84E-02	0.004753	1,438	2,709
LOC510193	NM_001100333	apolipoprotein L, 3-like [Source:RefSeq peptide;Acc:NP_001093803]	0.002004	0.04101	1,438	2,709
FCGR2	NM_174539	Low affinity immunoglobulin gamma Fc region receptor II [Source:UniProtKB/Swiss-Prot;Acc:Q28110]	0.0001269	0.008979	1,453	2,738
NTN1	NM_001192566	netrin-1 precursor [Source:RefSeq peptide;Acc:NP_001179495]	0.0001199	0.008734	1,462	2,755
SOD2	NM_201527	Superoxide dismutase [Mn], mitochondrial [Source:UniProtKB/Swiss-Prot;Acc:P41976]	5,24E-02	0.005624	1,463	2,757
SPRY4	NM_001081512	Protein sprouty homolog 4 [Source:UniProtKB/Swiss-Prot;Acc:A2VDU1]	5,47E-02	0.005653	1,471	2,772
GMPR	NM_001075977	GMP reductase 1 [Source:RefSeq peptide;Acc:NP_001069445]	3,49E-02	0.004753	1,516	2,860
COL15A1	NM_001191285	collagen alpha-1(XV) chain precursor [Source:RefSeq peptide;Acc:NP_001178214]	0.0007584	0.02509	1,545	2,918
PCDH12	NM_001098111	protocadherin-12 precursor [Source:RefSeq peptide;Acc:NP_001091580]	7,05E-03	0.001987	1,593	3,017
STOML3	NM_001080909		7,49E-02	0.006759	1,614	3,061
ITGA10	NM_001205590	integrin alpha-10 precursor [Source:RefSeq peptide;Acc:NP_001192519]	4,25E-02	0.005004	1,628	3,091
RGS16	NM_174450	Regulator of G-protein signaling 16 [Source:UniProtKB/Swiss-Prot;Acc:O46471]	9.74e-05	0.007642	1,648	3,134
IL21R	NM_001193179	interleukin-21 receptor precursor [Source:RefSeq peptide;Acc:NP_001180108]	8,03E-02	0.006767	1,656	3,151
SLAMF8	NM_001205794	SLAM family member 8 precursor [Source:RefSeq peptide;Acc:NP_001192723]	0.002569	0.04764	1,830	3,555

EHD3	NM_001098004	EH domain-containing protein 3 [Source:RefSeq peptide;Acc:NP_001091473]	2,81E-05	0.0002323	1,852	3,610
RUNDC3B	NM_001076874_2; N	RUN domain-containing protein 3B [Source:UniProtKB/Swiss-Prot;Acc:Q08E29]	9,88E-03	0.002468	1,876	3,671
SLC6A4	NM_174609	sodium-dependent serotonin transporter [Source:RefSeq peptide;Acc:NP_777034]	1,22E-02	0.002759	1,880	3,681
LDOC1	NM_001081544		2,22E-04	0.0003515	1,886	3,696
OXTR	NM_174134	Oxytocin receptor [Source:UniProtKB/Swiss-Prot;Acc:P56449]	9,32E-02	0.007466	1,903	3,740
SELE	NM_174181	E-selectin [Source:UniProtKB/Swiss-Prot;Acc:P98107]	0.002144	0.04285	1,910	3,758
C2CD4B	NM_001046307	C2 calcium-dependent domain-containing protein 4A [Source:UniProtKB/Swiss-Prot;Acc:Q2KJ18]	5,48E-02	0.005653	1,933	3,818
SECTM1	NM_001102326; NM	secreted and transmembrane 1 precursor [Source:RefSeq peptide;Acc:NP_001095796]; secreted and tran	0.0008763	0.02697	1,933	3,818
GRO1	NM_175700	Growth-regulated protein homolog beta [Source:UniProtKB/Swiss-Prot;Acc:O46677]	0.0002317	0.01243	1,945	3,850
IL1A	NM_174092	Interleukin-1 alpha [Source:UniProtKB/Swiss-Prot;Acc:P08831]	0.001323	0.03306	1,945	3,850
CRYAB	NM_174290	Alpha-crystallin B chain [Source:UniProtKB/Swiss-Prot;Acc:P02510]	3,99E-04	0.0004126	1,948	3,858
RND1	NM_001046016	Rho-related GTP-binding protein Rho6 [Source:UniProtKB/Swiss-Prot;Acc:Q2HJ68]	3,58E-02	0.004753	1,972	3,923
CD274	NM_001163412	programmed cell death 1 ligand 1 precursor [Source:RefSeq peptide;Acc:NP_001156884]	0.0001706	0.01072	2,034	4,095
HCAR1	NM_001145234	hydroxycarboxylic acid receptor 1 [Source:RefSeq peptide;Acc:NP_001138706]	2.7e-05	0.004458	2,039	4,110
CXCL2	NM_001048165; NM	Growth-regulated protein homolog gamma [Source:UniProtKB/Swiss-Prot;Acc:O46675]	0.0001214	0.008734	2,074	4,211
RBM20	NM_001192613	probable RNA-binding protein 20 [Source:RefSeq peptide;Acc:NP_001179542]	1.88e-07	0.0003515	2,076	4,216
IGFBP5	NM_001105327	Insulin-like growth factor-binding protein 5 [Source:UniProtKB/Swiss-Prot;Acc:Q05717]	0.0002102	0.01174	2,118	4,341
FABP4	NM_174314	fatty acid-binding protein, adipocyte [Source:RefSeq peptide;Acc:NP_776739]	0.0001705	0.01072	2,129	4,374
FNDC4	NM_001102324	fibronectin type III domain-containing protein 4 precursor [Source:RefSeq peptide;Acc:NP_001095794]	1.48e-06	0.0008441	2,162	4,475
ZBTB32	NM_001191224	zinc finger and BTB domain-containing protein 32 [Source:RefSeq peptide;Acc:NP_001178153]	4,00E-03	0.001517	2,237	4,714
FCGR1A	NM_174538	high affinity immunoglobulin gamma Fc receptor I precursor [Source:RefSeq peptide;Acc:NP_776963]	2,94E-03	0.001327	2,283	4,867
GPX3	NM_174077		7.71e-06	0.002031	2,335	5,046
HLX	NM_001101097	H2.0-like homeobox protein [Source:UniProtKB/Swiss-Prot;Acc:A7MB54]	0.0008054	0.02575	2,426	5,374
IL1RL1	NM_001206302		0.0004636	0.01809	2,497	5,645
MYLK	NM_176636_2; NM_176636		1,51E-03	0.0008441	2,507	5,684
MRAP2	NM_001099393	melanocortin-2 receptor accessory protein 2 [Source:RefSeq peptide;Acc:NP_001092863]	5,32E-04	0.0004589	2,532	5,784
SEMA6D	NM_001191133	semaphorin-6D precursor [Source:RefSeq peptide;Acc:NP_001178062]	2,69E-02	0.004458	2,594	6,038
RCAN1	NM_001034679	Calcipressin-1 [Source:UniProtKB/Swiss-Prot;Acc:Q3ZBP4]	1,30E-04	0.0003092	3,097	8,556
KCNJ15	NM_001099018	ATP-sensitive inward rectifier potassium channel 15 [Source:RefSeq peptide;Acc:NP_001092488]	0,0+D1:E397(	0.0002323	3,234	9,409

RESULTS 12 vs 32 hpi

Identifier	transcript_id	description	pValue	fdr	log2 Ratio	FC
CXCL2	NM_001048165; NM_174299	Growth-regulated protein homolog gamma [Source:UniProtKB/Swiss-Prot;Acc:O46675]	9,22E-03	0.001748	3,502	11,32940351
IL6	NM_001015617; NM_173923	interferon beta-2 precursor [Source:RefSeq peptide;Acc:NP_001015617]; Interleukin-6 [Source:UniProtKB/Swiss-Prot;Acc:P26892]	0.002083	0.04193	3,495	11,27456604
GRO1	NM_175700	Growth-regulated protein homolog beta [Source:UniProtKB/Swiss-Prot;Acc:O46677]	8,23E-03	0.001661	3,234	9,408730002
CD274	NM_001163412	programmed cell death 1 ligand 1 precursor [Source:RefSeq peptide;Acc:NP_001156884]	9,60E-03	0.001766	3,179	9,056791217
CCL24	NM_001046596	C-C motif chemokine 24 precursor [Source:RefSeq peptide;Acc:NP_001040061]	7,72E-02	0.006096	3,03	8,168097006
SELE	NM_174181	E-selectin [Source:UniProtKB/Swiss-Prot;Acc:P98107]	4,91E-02	0.00461	2,907	7,500568772
FCGR1A	NM_174538	high affinity immunoglobulin gamma Fc receptor I precursor [Source:RefSeq peptide;Acc:NP_776963]	8,52E-04	0.0005049	2,814	7,032316487
IL1A	NM_174092	Interleukin-1 alpha [Source:UniProtKB/Swiss-Prot;Acc:P08831]	4,60E-02	0.004447	2,629	6,1859707
RCAN1	NM_001034679	Calcipressin-1 [Source:UniProtKB/Swiss-Prot;Acc:Q3ZBP4]	1,61E-05	7,63E-02	2,609	6,100806613
C2CD4B	NM_001046307	C2 calcium-dependent domain-containing protein 4A [Source:UniProtKB/Swiss-Prot;Acc:Q2KJ18]	1,93E-02	0.002552	2,595	6,041890342
IL1RL1	NM_001206302		3,41E-02	0.003587	2,572	5,946331938
KCNJ15	NM_001099018	ATP-sensitive inward rectifier potassium channel 15 [Source:RefSeq peptide;Acc:NP_001092488]	1,60E-05	7,63E-02	2,458	5,494544934
OXTR	NM_174134	Oxytocin receptor [Source:UniProtKB/Swiss-Prot;Acc:P56449]	2,75E-03	0.0009037	2,396	5,2634181
ID1	NM_001097568	DNA-binding protein inhibitor ID-1 [Source:RefSeq peptide;Acc:NP_001091037]	5,90E-03	0.001364	2,391	5,245208057
PTX3	NM_001076259	pentraxin-related protein PTX3 precursor [Source:RefSeq peptide;Acc:NP_001069727]	0.001495	0.03482	2,377	5,194554411
SOD2	NM_201527	Superoxide dismutase [Mn], mitochondrial [Source:UniProtKB/Swiss-Prot;Acc:P41976]	1,91E-02	0.002552	2,233	4,701105314
CHRM4	NM_001103243	muscarinic acetylcholine receptor M4 [Source:RefSeq peptide;Acc:NP_001096713]	5,36E-02	0.004748	2,163	4,478451555
MRAP2	NM_001099393	melanocortin-2 receptor accessory protein 2 [Source:RefSeq peptide;Acc:NP_001092863]	3,47E-04	0.0003482	2,127	4,368082183
FNDC4	NM_001102324	fibronectin type III domain-containing protein 4 precursor [Source:RefSeq peptide;Acc:NP_001095794]	4,10E-03	0.001064	2,092	4,263386944
CCL2	NM_174006	C-C motif chemokine 2 [Source:UniProtKB/Swiss-Prot;Acc:P28291]	0.0001369	0.00843	2,088	4,251582697
RND1	NM_001046016	Rho-related GTP-binding protein Rho6 [Source:UniProtKB/Swiss-Prot;Acc:Q2HJ68]	4,27E-03	0.001064	2,06	4,169863043
RGS16	NM_174450	Regulator of G-protein signaling 16 [Source:UniProtKB/Swiss-Prot;Acc:O46471]	2,95E-02	0.003375	2,047	4,132457551
SERPINB2	NM_001192079; NM_001192051	serpin peptidase inhibitor, clade B (ovalbumin), member 2 [Source:RefSeq peptide;Acc:NP_001179008]; serpin peptidase inhibitor	0.0005175	0.0174	2,039	4,109605758
SPRY4	NM_001081512	Protein sprouty homolog 4 [Source:UniProtKB/Swiss-Prot;Acc:A2VDU1]	9,06E-03	0.001748	2,01	4,0278222
ADAMTS4	NM_181667	A disintegrin and metalloproteinase with thrombospondin motifs 4 precursor [Source:RefSeq peptide;Acc:NP_858053]	0.00169	0.03718	1,931	3,813194181
NFKBIZ	NM_174726	NF-kappa-B inhibitor zeta [Source:UniProtKB/Swiss-Prot;Acc:Q9BE45]	2.24e-05	0.002722	1,911	3,76069681
SELP	NM_174183	P-selectin precursor [Source:RefSeq peptide;Acc:NP_776608]	3,11E-02	0.003473	1,89	3,706352248
SLC46A2	NM_001024519	thymic stromal cotransporter homolog [Source:RefSeq peptide;Acc:NP_001019690]	0.0004954	0.0172	1,878	3,675651534
RBM20	NM_001192613	probable RNA-binding protein 20 [Source:RefSeq peptide;Acc:NP_001179542]	8,50E-04	0.0005049	1,785	3,446184639
NT5E	NM_174129	5-nucleotidase precursor [Source:RefSeq peptide;Acc:NP_776554]	2,51E-03	0.0009037	1,758	3,38228915
HCAR1	NM_001145234	hydroxycarboxylic acid receptor 1 [Source:RefSeq peptide;Acc:NP_001138706]	4,82E-02	0.004568	1,744	3,34962595
SEMA6D	NM_001191133	semaphorin-6D precursor [Source:RefSeq peptide;Acc:NP_001178062]	0.0008911	0.02514	1,735	3,328794939
PLAT	NM_174146	Tissue-type plasminogen activator Tissue-type plasminogen activator chain A Tissue-type plasminogen activator chain B [Source:Un	0.0007996	0.02333	1,698	3,244508622
MYLK	NM_176636_2; NM_176636		1.19e-05	0.002015	1,683	3,210949555
COL15A1	NM_001191285	collagen alpha-1(XV) chain precursor [Source:RefSeq peptide;Acc:NP_001178214]	0.0004748	0.01692	1,627	3,088700532
CXCL3	NM_001046513	chemokine (C-X-C motif) ligand 2 precursor [Source:RefSeq peptide;Acc:NP_001039978]	0.0002496	0.01266	1,617	3,067365319
ZBTB32	NM_001191224	zinc finger and BTB domain-containing protein 32 [Source:RefSeq peptide;Acc:NP_001178153]	1,66E-02	0.002544	1,616	3,06523992
RGS2	NM_001075596	regulator of G-protein signaling 2 [Source:RefSeq peptide;Acc:NP_001069064]	0.0001552	0.009314	1,606	3,044066762
ESM1	NM_001098101	endothelial cell-specific molecule 1 precursor [Source:RefSeq peptide;Acc:NP_001091570]	0.0004177	0.01623	1,594	3,018851937
CRYAB	NM_174290	Alpha-crystallin B chain [Source:UniProtKB/Swiss-Prot;Acc:P02510]	7,82E-03	0.001612	1,533	2,893869772
PLAUR	NM_174423	Urokinase plasminogen activator surface receptor [Source:UniProtKB/Swiss-Prot;Acc:Q05588]	2.35e-05	0.00282	1,519	2,865923301
TRIB1	NM_001101105	tribbles homolog 1 [Source:RefSeq peptide;Acc:NP_001094575]	6,93E-02	0.00566	1,503	2,834314793
IGFBP5	NM_001105327	Insulin-like growth factor-binding protein 5 [Source:UniProtKB/Swiss-Prot;Acc:Q05717]	0.000427	0.01623	1,472	2,774061938
OSTN	NM_001098935	osteocrin precursor [Source:RefSeq peptide;Acc:NP_001092405]	3,19E-02	0.003474	1,432	2,698205069
ZC3H12A	NM_001102187	Ribonuclease ZC3H12A [Source:UniProtKB/Swiss-Prot;Acc:A6QQJ8]	0.000279	0.01322	1,392	2,624422509
CEBPD	NM_174267		0.0002052	0.01093	1,387	2,615342697
NR4A1	NM_001075911	Nuclear receptor subfamily 4 group A member 1 [Source:UniProtKB/Swiss-Prot;Acc:Q0V8F0]	0.0003291	0.01425	1,381	2,604488379
NAV3	NM_001192669	neuron navigator 3 [Source:RefSeq peptide;Acc:NP_001179598]	3,67E-04	0.0003482	1,368	2,581124981
ULBP13	NM_001168604		0.0002288	0.01186	1,367	2,579336501
TM4SF18	NM_001034287; NM_001184724	Transmembrane 4 L6 family member 18 [Source:UniProtKB/Swiss-Prot;Acc:Q3T110]	3.23e-07	0.0003482	1,361	2,568631618
DOK5	NM_001075939; NM_001075939_2	docking protein 5 [Source:RefSeq peptide;Acc:NP_001069407]	0.0001813	0.01029	1,341	2,533268507
ULBP15	NM_001168611_2; NM_001168611		0.0001436	0.008673	1,336	2,524504064
ID2	NM_001034231	DNA-binding protein inhibitor ID-2 [Source:UniProtKB/Swiss-Prot;Acc:Q3ZC46]	7,12E-03	0.001534	1,327	2,508804409

CD46	NM_001242564; NM_001242565; NM	membrane cofactor protein isoform 5 precursor [Source:RefSeq peptide;Acc:NP_001229494]	3,06E-02	0.003459	1,325	2,505328877	
PROCR	NM_174437	Endothelial protein C receptor [Source:UniProtKB/Swiss-Prot;Acc:Q28105]	2,20E-02	0.002722	1,322	2,500124605	
IL21R	NM_001193179	interleukin-21 receptor precursor [Source:RefSeq peptide;Acc:NP_001180108]	0.0009072	0.02522	1,305	2,470837274	
ITGA2	NM_001166499	integrin alpha-2 precursor [Source:RefSeq peptide;Acc:NP_001159971]	0.0002591	0.013	1,298	2,458877735	
ICAM1	NM_174348	intercellular adhesion molecule 1 precursor [Source:RefSeq peptide;Acc:NP_776773]	0.002095	0.042	1,257	2,38998241	
MAFF	NM_001103300	Transcription factor MafF [Source:UniProtKB/Swiss-Prot;Acc:A7YY73]	0.001603	0.03626	1,255	2,386671486	
VCAM1	NM_001101158; NM_174484	vascular cell adhesion molecule 1 precursor [Source:RefSeq peptide;Acc:NP_001094628]; vascular cell adhesion molecule 1 precur	0.001186	0.03048	1,249	2,37676621	
OLR1	NM_174132	oxidized low-density lipoprotein receptor 1 [Source:RefSeq peptide;Acc:NP_776557]	0.0001158	0.007715	1,244	2,368543224	
FRMD4A	NM_001192267	FERM domain-containing protein 4A [Source:RefSeq peptide;Acc:NP_001179196]	2.58e-06	0.0009037	1,242	2,365262	
RUNDC3B	NM_001076874_2; NM_001076874	RUN domain-containing protein 3B [Source:UniProtKB/Swiss-Prot;Acc:Q08E29]	0.0005707	0.01878	1,241	2,363623094	
PCDH12	NM_001098111	protocadherin-12 precursor [Source:RefSeq peptide;Acc:NP_001091580]	0.0001788	0.01021	1,237	2,357078816	
ID3	NM_001014950	DNA-binding protein inhibitor ID-3 [Source:UniProtKB/Swiss-Prot;Acc:Q5E981]	0.0004714	0.01687	1,212	2,316585612	
SLC4A7	NM_001098926	sodium bicarbonate cotransporter 3 [Source:RefSeq peptide;Acc:NP_001092396]	0.0004652	0.01671	1,211	2,314980434	
NTN1	NM_001192566	netrin-1 precursor [Source:RefSeq peptide;Acc:NP_001179495]	0.001923	0.0398	1,202	2,300583787	
PLAU	NM_174147	Urokinase-type plasminogen activator Urokinase-type plasminogen activator long chain A Urokinase-type plasminogen activator sh	0.001286	0.03199	1,19	2,281527432	
NDRG2	NM_001035304		5,55E-02	0.004829	1,187	2,276788058	
RAMP3	NM_001083505	receptor activity-modifying protein 3 precursor [Source:RefSeq peptide;Acc:NP_001076974]	0.001714	0.03732	1,186	2,275210456	
MALL	NM_001046115	MAL-like protein [Source:RefSeq peptide;Acc:NP_001039580]	5,86E-04	0.000397	1,168	2,246999806	
ARNT2	NM_001206705		1,83E-02	0.002552	1,154	2,225300241	
SYTL2	NM_001102278	synaptotagmin-like protein 2 [Source:RefSeq peptide;Acc:NP_001095748]	8,66E-02	0.006462	1,143	2,208397694	
PKIG	NM_205812	cAMP-dependent protein kinase inhibitor gamma [Source:RefSeq peptide;Acc:NP_991381]	3,04E-03	0.0009037	1,14	2,203810232	
NFKBIE	NM_001130746	NF-kappa-B inhibitor epsilon [Source:RefSeq peptide;Acc:NP_001124218]	0.000131	0.008281	1,14	2,203810232	
RRP15	NM_001040506	RRP15-like protein [Source:UniProtKB/Swiss-Prot;Acc:Q3T062]	3,58E-02	0.003685	1,134	2,194663875	
ADRA2B	NM_001206628	Alpha-2B adrenergic receptor [Source:UniProtKB/Swiss-Prot;Acc:O77700]	0.0003238	0.01423	1,129	2,187070915	
SLCO4A1	NM_001192727	solute carrier organic anion transporter family member 4A1 [Source:RefSeq peptide;Acc:NP_001179656]	0.001338	0.03259	1,127	2,184041091	
ITGA10	NM_001205590	integrin alpha-10 precursor [Source:RefSeq peptide;Acc:NP_001192519]	0.001959	0.04014	1,126	2,182527754	
SPRY1	NM_001099366	protein sprouty homolog 1 [Source:RefSeq peptide;Acc:NP_001092836]	1,80E-02	0.002552	1,112	2,161450804	
EPB42	NM_174312		0.0003725	0.01535	1,103	2,148008943	
TTC9B	NM_001105507	tetratricopeptide repeat protein 9B [Source:RefSeq peptide;Acc:NP_001098977]	0.0004025	0.01577	1,098	2,140577397	
FCGR2	NM_174539	Low affinity immunoglobulin gamma Fc region receptor II [Source:UniProtKB/Swiss-Prot;Acc:Q28110]	0.00037	0.01532	1,092	2,131693472	
SLC39A10	NM_001205880	zinc transporter ZIP10 precursor [Source:RefSeq peptide;Acc:NP_001192809]	0.0002737	0.01311	1,089	2,127265346	
CELF4	NM_001099068	CUGBP Elav-like family member 4 [Source:RefSeq peptide;Acc:NP_001092538]	0.001475	0.03462	1,085	2,121375483	
HBEGF	NM_001144090	proheparin-binding EGF-like growth factor precursor [Source:RefSeq peptide;Acc:NP_001137562]	0.001027	0.02796	1,082	2,11696879	
CYP27B1	NM_001192284	25-hydroxyvitamin D-1 alpha hydroxylase, mitochondrial [Source:RefSeq peptide;Acc:NP_001179213]	0.002673	0.04839	1,069	2,097978655	
CNKSR3	NM_001192112	connector enhancer of kinase suppressor of ras 3 [Source:RefSeq peptide;Acc:NP_001179041]	1,55E-04	0.0002451	1,068	2,096524951	
LDOC1	NM_001081544		2,02E-02	0.002583	1,061	2,086377187	
KCNJ2	NM_174373	Inward rectifier potassium channel 2 [Source:UniProtKB/Swiss-Prot;Acc:O19182]	7,01E-02	0.00568	1,057	2,080600533	
MGLL	NM_001206681	monoglyceride lipase [Source:RefSeq peptide;Acc:NP_001193610]	0.001071	0.02878	1,051	2,071965527	
SULT1B1	NM_001075823	Sulfotransferase family cytosolic 1B member 1 [Source:UniProtKB/Swiss-Prot;Acc:Q3T0Y3]	1,94E-02	0.002552	1,044	2,061936638	
FSD1L	NM_001192260	FSD1-like protein [Source:RefSeq peptide;Acc:NP_001179189]	0.0002683	0.01304	1,037	2,051956291	
FAM107B	NM_001046393	protein FAM107B [Source:RefSeq peptide;Acc:NP_001039858]	0.0001251	0.008066	1,034	2,047693801	
CSF1	NM_174026	macrophage colony-stimulating factor 1 precursor [Source:RefSeq peptide;Acc:NP_776451]	0.0002992	0.01397	1,032	2,044857061	
HCRTR1	NM_001048182	Orexin receptor type 1 [Source:UniProtKB/Swiss-Prot;Acc:Q0GBZ5]	0.001158	0.03016	1,027	2,037782393	
TNIP1	NM_001024554	TNFAIP3-interacting protein 1 [Source:RefSeq peptide;Acc:NP_001019725]	0.0002824	0.01332	1,025	2,034959384	
TMEM204	NM_001076377	Transmembrane protein 204 [Source:UniProtKB/Swiss-Prot;Acc:Q0IIE5]	0.000353	0.01497	1,019	2,0265138	
EAF2	NM_001046507	ELL-associated factor 2 [Source:RefSeq peptide;Acc:NP_001039972]	0.002512	0.04679	1	2	
DRD1	NM_174042	D(1A) dopamine receptor [Source:UniProtKB/Swiss-Prot;Acc:Q95136]	0.002819	0.04994	1	2	
CD40	NM_001105611	tumor necrosis factor receptor superfamily member 5 precursor [Source:RefSeq peptide;Acc:NP_001099081]	0.0001035	0.007218	0,9914	1,988113332	
EFHD2	NM_001103245	EF-hand domain-containing protein D2 [Source:UniProtKB/Swiss-Prot;Acc:A5D7A0]	0.0003609	0.01507	0,9914	1,988113332	
PLAC8	NM_001025325; NM_001076987	placenta-specific 8 [Source:RefSeq peptide;Acc:NP_001020496]; Placenta-specific gene 8 protein [Source:UniProtKB/Swiss-Prot;Ac	0.002369	0.04528	0,9672	1,95504254	
METTL11B	NM_001192536	alpha N-terminal protein methyltransferase 1B [Source:RefSeq peptide;Acc:NP_001179465]	0.001628	0.03656	0,9628	1,949089042	
MARCH3	NM_001077941	E3 ubiquitin-protein ligase MARCH3 [Source:UniProtKB/Swiss-Prot;Acc:A0JN69]	0.0002685	0.01304	0,9546	1,93804222	
SDCBP	NM_001075483	syntenin-1 [Source:RefSeq peptide;Acc:NP_001068951]	9,25E-04	0.0005083	0,9507	1,932810236	
C1QTNF5	NM_001099138	complement C1q tumor necrosis factor-related protein 5 precursor [Source:RefSeq peptide;Acc:NP_001092608]	4,78E-02	0.004568	0,9476	1,928661557	
SNN	NM_001113722	Stannin [Source:UniProtKB/Swiss-Prot;Acc:Q17Q87]	0.0005404	0.01811	0,9467	1,92745877	
VLDLR	NM_174489	very low-density lipoprotein receptor precursor [Source:RefSeq peptide;Acc:NP_776914]	0.0001322	0.008301	0,9455	1,925856221	

GNPTAB	NM_001192228	N-acetylglucosamine-1-phosphotransferase subunits alpha/beta [Source:RefSeq peptide;Acc:NP_001179157]	5,03E-02	0.004676	0,9441	1,923988265
LRRC8A	NM_001076807	leucine-rich repeat-containing protein 8A [Source:RefSeq peptide;Acc:NP_001070275]	0.0006759	0.02108	0,9359	1,913083707
TSPAN18	NM_001080920	tetraspanin 18 [Source:HGNC Symbol;Acc:20660]	0.0006898	0.02123	0,933	1,909242028
IL4R	NM_001075142	interleukin-4 receptor subunit alpha precursor [Source:RefSeq peptide;Acc:NP_001068610]	0.000305	0.01414	0,917	1,888184838
APOLD1	NM_001101180	apolipoprotein L domain-containing protein 1 [Source:RefSeq peptide;Acc:NP_001094650]	0.0002304	0.01187	0,9151	1,885699774
NFKBIA	NM_001045868	NF-kappa-B inhibitor alpha [Source:RefSeq peptide;Acc:NP_001039333]	0.001267	0.03189	0,9136	1,883740192
LBH	NM_001099152	Protein LBH [Source:UniProtKB/Swiss-Prot;Acc:A5PJU8]	0.001302	0.03223	0,9052	1,872804103
SLC20A2	NM_001080280	sodium-dependent phosphate transporter 2 [Source:RefSeq peptide;Acc:NP_001073749]	0.0003657	0.01521	0,9022	1,868913762
ECM1	NM_001099706	extracellular matrix protein 1 precursor [Source:RefSeq peptide;Acc:NP_001093176]	0.002685	0.04839	0,8946	1,859094363
SLC9A3R2	NM_001077065	Na(+)/H(+) exchange regulatory cofactor NHE-RF2 [Source:RefSeq peptide;Acc:NP_001070533]	0.001175	0.03037	0,891	1,854461093
ZDHHC14	NM_001191179	probable palmitoyltransferase ZDHHC14 [Source:RefSeq peptide;Acc:NP_001178108]	0.0001345	0.008387	0,8847	1,846380637
IHH	NM_001076870	indian hedgehog protein [Source:RefSeq peptide;Acc:NP_001070338]	0.0001215	0.007925	0,8823	1,843311638
CDC20B	NM_001206982	cell division cycle protein 20 homolog B [Source:RefSeq peptide;Acc:NP_001193911]	0.002443	0.04604	0,8795	1,839737586
BIRC3	NM_001035293; NM_001035293_2		0.0007268	0.02201	0,8758	1,835025358
DUSP23	NM_001082609	dual specificity protein phosphatase 23 [Source:RefSeq peptide;Acc:NP_001076078]	0.0004298	0.01623	0,8694	1,826902955
ITGAV	NM_174367	integrin alpha-V precursor [Source:RefSeq peptide;Acc:NP_776792]	0.0002141	0.01122	0,8691	1,826523101
SMAD9	NM_001076928	mothers against decapentaplegic homolog 9 [Source:RefSeq peptide;Acc:NP_001070396]	0.001345	0.03259	0,8688	1,826143325
ETS1	NM_001099106	protein C-ets-1 [Source:RefSeq peptide;Acc:NP_001092576]	3.61e-06	0.000978	0,8634	1,819320857
DYRK3	NM_001100298	dual specificity tyrosine-phosphorylation-regulated kinase 3 [Source:RefSeq peptide;Acc:NP_001093768]	1,12E-02	0.001938	0,8569	1,811142423
PTGIS	NM_174444	Prostacyclin synthase [Source:UniProtKB/Swiss-Prot;Acc:Q29626]	0.001329	0.03256	0,8551	1,808884133
TSPAN13	NM_001035362	Tetraspanin-13 [Source:UniProtKB/Swiss-Prot;Acc:Q3ZBV0]	0.0001771	0.01017	0,8518	1,804751246
MCAM	NM_001110062	cell surface glycoprotein MUC18 precursor [Source:RefSeq peptide;Acc:NP_001103532]	0.001785	0.03821	0,8481	1,800128631
MSX1	NM_174798	homeobox protein MSX-1 [Source:RefSeq peptide;Acc:NP_777223]	0.0003541	0.01497	0,84	1,790050142
DPYSL5	NM_001109964	dihydropyrimidinase-related protein 5 [Source:RefSeq peptide;Acc:NP_001103434]	0.000564	0.01863	0,8398	1,789802005
RASL12	NM_001076933	ras-like protein family member 12 [Source:RefSeq peptide;Acc:NP_001070401]	0.0006117	0.01966	0,8328	1,781138866
ZFP36	NM_174493	tristetraprolin [Source:RefSeq peptide;Acc:NP_776918]	0.002615	0.04787	0,8248	1,771289468
KLF4	NM_001105385	Krueppel-like factor 4 [Source:RefSeq peptide;Acc:NP_001098855]	0.001402	0.03346	0,8133	1,757226303
FAM110B	NM_001077018		0.0004527	0.01645	0,8121	1,755765291
MANF	NM_001101211	Mesencephalic astrocyte-derived neurotrophic factor [Source:UniProtKB/Swiss-Prot;Acc:P80513]	0.0006965	0.02137	0,8005	1,741704651
ANXA1	NM_175784	annexin A1 [Source:RefSeq peptide;Acc:NP_786978]	0.001035	0.02796	0,7971	1,737604808
BHLHE40	NM_001024929	Class E basic helix-loop-helix protein 40 [Source:UniProtKB/Swiss-Prot;Acc:Q5EA15]	0.0001124	0.007611	0,7946	1,734596375
TBC1D16	NM_001206271	TBC1 domain family member 16 [Source:RefSeq peptide;Acc:NP_001193200]	1,29E-02	0.002142	0,7838	1,721659687
NPAS2	NM_001083763	neuronal PAS domain-containing protein 2 [Source:RefSeq peptide;Acc:NP_001077232]	0.0002707	0.01304	0,7781	1,714870935
ZNF706	NM_001199073; NM_001199074	zinc finger protein 706 [Source:RefSeq peptide;Acc:NP_001186002]	1,12E-02	0.001938	0,7774	1,714039076
TCF4	NM_001034621	transcription factor 4 [Source:RefSeq peptide;Acc:NP_001029793]	5,34E-02	0.004748	0,7737	1,709648807
C5H12orf39	NM_001075407	Spexin [Source:UniProtKB/Swiss-Prot;Acc:Q0VC44]	0.001908	0.03971	0,7713	1,70680708
YOD1	NM_001080309	Ubiquitin thioesterase OTU1 [Source:UniProtKB/Swiss-Prot;Acc:Q05B57]	0.001582	0.03615	0,7625	1,696427764
SMOX	NM_001205439	spermine oxidase [Source:RefSeq peptide;Acc:NP_001192368]	0.0005167	0.0174	0,7547	1,687280696
HPCAL1	NM_001098964	Hippocalcin-like protein 1 [Source:UniProtKB/Swiss-Prot;Acc:P29105]	0.0002679	0.01304	0,7531	1,685410479
KANK4	NM_001102053		7,31E-02	0.005872	0,7507	1,682609039
CEACAM1	NM_205788	carcinoembryonic antigen-related cell adhesion molecule 1 precursor [Source:RefSeq peptide;Acc:NP_991357]	0.001265	0.03189	0,7495	1,681210067
IRAK3	NM_001190299	interleukin-1 receptor-associated kinase 3 [Source:RefSeq peptide;Acc:NP_001177228]	0.0005024	0.01732	0,7471	1,678415609
ENO2	NM_001101125	gamma-enolase [Source:RefSeq peptide;Acc:NP_001094595]	0.001321	0.03247	0,7468	1,678066629
RIPK2	NM_001034610	Receptor-interacting serine/threonine-protein kinase 2 [Source:UniProtKB/Swiss-Prot;Acc:Q3SZJ2]	0.0002029	0.01087	0,7374	1,667168588
CHP1	NM_001075576	Calcium-binding protein p22 [Source:UniProtKB/Swiss-Prot;Acc:Q3SYS6]	0.0003819	0.01561	0,7227	1,650267618
MMP14	NM_174390	matrix metalloproteinase-14 precursor [Source:RefSeq peptide;Acc:NP_776815]	0.002233	0.04374	0,7225	1,650038858
CXCR7	NM_001098381	C-X-C chemokine receptor type 7 [Source:RefSeq peptide;Acc:NP_001091851]	0.001821	0.03871	0,7182	1,645128185
ADORA2B	NM_001075925	Adenosine receptor A2b [Source:UniProtKB/Swiss-Prot;Acc:Q1LZD0]	0.002263	0.04414	0,7171	1,643874315
RPIA	NM_001035433	Ribose-5-phosphate isomerase [Source:UniProtKB/Swiss-Prot;Acc:Q3T186]	0.0003553	0.01497	0,7154	1,641938397
CD9	NM_173900	CD9 antigen [Source:UniProtKB/Swiss-Prot;Acc:P30932]	0.0002118	0.01122	0,7145	1,640914421
ARHGEF15	NM_001205712		0.0003241	0.01423	0,7103	1,636144308
ODC1	NM_174130	Ornithine decarboxylase [Source:UniProtKB/Swiss-Prot;Acc:P27117]	0.0001693	0.009816	0,7087	1,634330772
NEU1	NM_001083642	Sialidase-1 [Source:UniProtKB/Swiss-Prot;Acc:A6BMK7]	0.0004286	0.01623	0,7079	1,633424758
CCRN4L	NM_001082454	nocturnin [Source:RefSeq peptide;Acc:NP_001075923]	0.002004	0.04086	0,7067	1,632066678
SLC31A1	NM_001100381	high affinity copper uptake protein 1 [Source:RefSeq peptide;Acc:NP_001093851]	0.0003283	0.01425	0,7048	1,629918694
OSBPL11	NM_001193008	oxysterol-binding protein-related protein 11 [Source:RefSeq peptide;Acc:NP_001179937]	0.0005147	0.0174	0,7021	1,626871158

FAM3C	NM_001099147	Protein FAM3C [Source:UniProtKB/Swiss-Prot;Acc:A5PKI3]	0.0001827	0.01031	0,7001	1,624617399	
GPRC5B	NM_001075741	G-protein coupled receptor family C group 5 member B precursor [Source:RefSeq peptide;Acc:NP_001069209]	0.002216	0.04358	0,6893	1,612500938	
LIMD2	NM_001040512	LIM domain-containing protein 2 [Source:UniProtKB/Swiss-Prot;Acc:Q1LZA7]	0.001094	0.02913	0,6805	1,602695111	
DGKD	NM_001035282	diacylglycerol kinase delta [Source:RefSeq peptide;Acc:NP_001030359]	0.001356	0.03264	0,6733	1,594716531	
KIAA0317	NM_001076165	protein KIAA0317 homolog [Source:RefSeq peptide;Acc:NP_001069633]	0.0003954	0.01575	0,6712	1,592396935	
PLA2G15	NM_174560	Group XV phospholipase A2 [Source:UniProtKB/Swiss-Prot;Acc:Q8WMP9]	0.001242	0.03156	0,6649	1,585458374	
CHST1	NM_001083648	carbohydrate sulfotransferase 1 precursor [Source:RefSeq peptide;Acc:NP_001077117]	0.001289	0.03199	0,664	1,584469622	
TSPAN5	NM_001076119	Tetraspanin-5 [Source:UniProtKB/Swiss-Prot;Acc:Q17QJ5]	2,57E-02	0.003011	0,6599	1,579973105	
GPATCH4	NM_001078129	G patch domain-containing protein 4 [Source:UniProtKB/Swiss-Prot;Acc:Q2KJE1]	0.00209	0.04198	0,6538	1,573306769	
DNAJB11	NM_001034268	DnaJ homolog subfamily B member 11 [Source:UniProtKB/Swiss-Prot;Acc:Q3ZBA6]	0.0006521	0.02068	0,6433	1,561897739	
FBXL14	NM_001075947	F-box/LRR-repeat protein 14 [Source:UniProtKB/Swiss-Prot;Acc:Q17R01]	0.0003132	0.01423	0,6421	1,560599129	
TRMT6	NM_001038040	tRNA (adenine(58)-N(1))-methyltransferase non-catalytic subunit TRM6 [Source:UniProtKB/Swiss-Prot;Acc:Q2T9V5]	0.001876	0.03917	0,6408	1,55919352	
SLC2A3	NM_174603	solute carrier family 2, facilitated glucose transporter member 3 [Source:RefSeq peptide;Acc:NP_777028]	0.001717	0.03732	0,6399	1,558221148	
COQ10B	NM_001075654	coenzyme Q-binding protein COQ10 homolog B, mitochondrial [Source:RefSeq peptide;Acc:NP_001069122]	0.001851	0.03901	0,6375	1,555631119	
CD44	NM_174013	CD44 antigen precursor [Source:RefSeq peptide;Acc:NP_776438]	0.001555	0.03578	0,631	1,548638056	
ANKH	NM_001109793	progressive ankylosis protein homolog [Source:RefSeq peptide;Acc:NP_001103263]	0.001973	0.04031	0,6288	1,5462783	
PLS3	NM_001045923	Plastin-3 [Source:UniProtKB/Swiss-Prot;Acc:A7E3Q8]	0.0001361	0.00843	0,627	1,544350266	
SORBS2	NM_001079787	sorbin and SH3 domain-containing protein 2 [Source:RefSeq peptide;Acc:NP_001073255]	0.0007726	0.02282	0,626	1,543280175	
TNFAIP1	NM_001192290	BTB/POZ domain-containing adapter for CUL3-mediated RhoA degradation protein 2 [Source:RefSeq peptide;Acc:NP_001179219]	3,32E-02	0.003542	0,6179	1,534639719	
NFKB2	NM_001102101	nuclear factor NF-kappa-B p100 subunit [Source:RefSeq peptide;Acc:NP_001095571]	0.001555	0.03578	0,6151	1,53166416	
SPRED1	NM_001192516	sprouty-related, EVH1 domain-containing protein 1 [Source:RefSeq peptide;Acc:NP_001179445]	0.0008022	0.02333	0,6112	1,527529244	
DEPDC1B	NM_001191451	DEP domain-containing protein 1B [Source:RefSeq peptide;Acc:NP_001178380]	0.001598	0.03626	0,6082	1,524356136	
SPIRE2	NM_001205387	spire homolog 2 (Drosophila) [Source:HGNC Symbol;Acc:30623]	0.002681	0.04839	0,6081	1,52425048	
EHD3	NM_001098004	EH domain-containing protein 3 [Source:RefSeq peptide;Acc:NP_001091473]	0.000122	0.007925	0,6067	1,522772055	
STK38L	NM_001101092	serine/threonine-protein kinase 38-like [Source:RefSeq peptide;Acc:NP_001094562]	0.0002278	0.01186	0,6053	1,521295065	
TFPI2	NM_182788	Tissue factor pathway inhibitor 2 [Source:UniProtKB/Swiss-Prot;Acc:Q7YRQ8]	0.000194	0.01069	0,605	1,520978753	
FAM206A	NM_001045956	Protein FAM206A [Source:UniProtKB/Swiss-Prot;Acc:Q29S16]	0.0007676	0.02274	0,602	1,517819253	
ESAM	NM_001078066	endothelial cell-selective adhesion molecule precursor [Source:RefSeq peptide;Acc:NP_001071534]	0.0004509	0.01645	0,5981	1,513721713	
ST3GAL4	NM_205806	CMP-N-acetylneuraminate-beta-galactosamide-alpha-2, 3-sialyltransferase 4 precursor [Source:RefSeq peptide;Acc:NP_991375]	0.0004972	0.0172	0,5887	1,503890994	
MBOAT1	NM_001192857	lysophospholipid acyltransferase 1 [Source:RefSeq peptide;Acc:NP_001179786]	0.001201	0.03077	0,5883	1,503474084	
C8H9orf3	NM_001206980; NM_001206980_2		0.0004247	0.01623	0,5845	1,499519205	
ZNF462	NM_001205811	zinc finger protein 462 [Source:RefSeq peptide;Acc:NP_001192740]	0.0003889	0.01563	-0,5866	-1,50170351	
SLC25A30	NM_001098895	kidney mitochondrial carrier protein 1 [Source:RefSeq peptide;Acc:NP_001092365]	0.001105	0.02934	-0,5871	-1,50222405	
IL31RA	NM_001192563	interleukin-31 receptor subunit alpha precursor [Source:RefSeq peptide;Acc:NP_001179492]	0.00118	0.03041	-0,589	-1,50420375	
TNFRSF1B	NM_001040490	tumor necrosis factor receptor superfamily member 1B precursor [Source:RefSeq peptide;Acc:NP_001035580]	0.002349	0.04508	-0,5928	-1,50817099	
TRIM34	NM_001046461	tripartite motif-containing protein 6 [Source:RefSeq peptide;Acc:NP_001192118]	0.001135	0.02987	-0,5999	-1,51561151	
ACSF2	NM_001078112	Acyl-CoA synthetase family member 2, mitochondrial [Source:UniProtKB/Swiss-Prot;Acc:Q17QJ1]	0.0001146	0.007708	-0,6051	-1,52108418	
ADA	NM_173887	adenosine deaminase [Source:RefSeq peptide;Acc:NP_776312]	0.0001014	0.007164	-0,6096	-1,5258361	
IARS	NM_001101069	isoleucyl-tRNA synthetase, cytoplasmic [Source:RefSeq peptide;Acc:NP_001094539]	0.0003204	0.01423	-0,6147	-1,53123955	
CELF2	NM_001078165		0.0007925	0.02326	-0,6177	-1,53442699	
TTC21B	NM_001102108	tetratricopeptide repeat protein 21B [Source:RefSeq peptide;Acc:NP_001095578]	0.0002016	0.01086	-0,6198	-1,53666214	
OSBPL3	NM_001192901	oxysterol-binding protein-related protein 3 [Source:RefSeq peptide;Acc:NP_001179830]	4,27E-02	0.004264	-0,6224	-1,53943398	
NGFRAP1	NM_001163777	Protein BEX3 [Source:UniProtKB/Swiss-Prot;Acc:Q3ZBJ6]	0.0005075	0.0174	-0,6249	-1,54210393	
RAPGEF2	NM_001191326	rap guanine nucleotide exchange factor 2 [Source:RefSeq peptide;Acc:NP_001178255]	0.0003213	0.01423	-0,6298	-1,54735047	
SMARCA2	NM_001099115	probable global transcription activator SNF2L2 [Source:RefSeq peptide;Acc:NP_001092585]	0.0004265	0.01623	-0,6301	-1,54767227	
PCCA	NM_001083509	propionyl-CoA carboxylase alpha chain, mitochondrial [Source:RefSeq peptide;Acc:NP_001076978]	0.001035	0.02796	-0,6309	-1,54853072	
PCCB	NM_001038548	Propionyl-CoA carboxylase beta chain, mitochondrial [Source:UniProtKB/Swiss-Prot;Acc:Q2TBR0]	0.0003852	0.01561	-0,6376	-1,55573895	
PLCB4	NM_001166510		0.001351	0.03259	-0,6405	-1,55886933	
TNS1	NM_174766	tensin-1 [Source:RefSeq peptide;Acc:NP_777191]	0.0008372	0.02405	-0,6407	-1,55908545	
JUB	NM_001192517	LIM domain-containing protein ajuba [Source:UniProtKB/Swiss-Prot;Acc:E1BKA3]	0.0003236	0.01423	-0,6439	-1,56254745	
TLE1	NM_001098020		6,74E-02	0.005559	-0,6451	-1,56384768	
DAK	NM_001024524	bifunctional ATP-dependent dihydroxyacetone kinase/FAD-AMP lyase (cyclizing) [Source:RefSeq peptide;Acc:NP_001019695]	0.002436	0.04604	-0,6463	-1,56514899	
NEK6	NM_001098988	serine/threonine-protein kinase Nek6 [Source:RefSeq peptide;Acc:NP_001092458]	0.0001118	0.007611	-0,651	-1,57025624	
JAG1	NM_001191178	protein jagged-1 precursor [Source:RefSeq peptide;Acc:NP_001178107]	4,48E-02	0.004395	-0,6541	-1,57363396	
SYNM	NM_001191453	synemin [Source:RefSeq peptide;Acc:NP_001178382]	0.001093	0.02913	-0,6596	-1,57964459	
WSCD1	NM_001206900	WSC domain-containing protein 1 [Source:RefSeq peptide;Acc:NP_001193829]	0.0005158	0.0174	-0,6608	-1,58095905	

ST6GAL1	NM_177517	beta-galactoside alpha-2,6-sialyltransferase 1 [Source:RefSeq peptide;Acc:NP_803483]	0.000453	0.01645	-0,6609	-1,58106864
XDH	NM_173972	xanthine dehydrogenase/oxidase [Source:RefSeq peptide;Acc:NP_776397]	0.001168	0.03028	-0,6614	-1,58161669
DBI	NM_001113321	Acyl-CoA-binding protein [Source:UniProtKB/Swiss-Prot;Acc:P07107]	0.002738	0.04915	-0,668	-1,5888688
PTCH1	NM_001205879	protein patched homolog 1 [Source:RefSeq peptide;Acc:NP_001192808]	0.0005171	0.0174	-0,674	-1,59549048
TM6SF1	NM_001102295	transmembrane 6 superfamily member 1 [Source:RefSeq peptide;Acc:NP_001095765]	0.002111	0.04205	-0,6744	-1,5959329
MTMR10	NM_001193073	myotubularin-related protein 10 [Source:RefSeq peptide;Acc:NP_001180002]	0.0003238	0.01423	-0,6789	-1,60091865
IDH1	NM_181012	Isocitrate dehydrogenase [NADP] cytoplasmic [Source:UniProtKB/Swiss-Prot;Acc:Q9XSG3]	0.002797	0.04975	-0,6822	-1,60458476
MTMR7	NM_001075641	myotubularin-related protein 7 [Source:RefSeq peptide;Acc:NP_001069109]	0.0004359	0.01627	-0,6843	-1,60692211
CYP27A1	NM_001083413	sterol 26-hydroxylase, mitochondrial [Source:RefSeq peptide;Acc:NP_001076882]	0.0005625	0.01863	-0,6869	-1,60982069
ALDOC	NM_001097984	fructose-bisphosphate aldolase C [Source:RefSeq peptide;Acc:NP_001091453]	0.00232	0.04479	-0,6891	-1,61227741
LTA4H	NM_001034280	Leukotriene A-4 hydrolase [Source:UniProtKB/Swiss-Prot;Acc:Q3SZH7]	0.001841	0.03887	-0,6913	-1,61473789
DPYSL3	NM_001101068	dihydropyrimidinase-related protein 3 [Source:RefSeq peptide;Acc:NP_001094538]	0.0001636	0.009688	-0,6954	-1,61933335
FLNB	NM_001191460	filamin-B [Source:RefSeq peptide;Acc:NP_001178389]	0.0004019	0.01577	-0,6963	-1,62034385
CHST2	NM_001113769	carbohydrate sulfotransferase 2 [Source:RefSeq peptide;Acc:NP_001107241]	0.0004904	0.01719	-0,6985	-1,62281664
CBR1	NM_001034513	carbonyl reductase [Source:RefSeq peptide;Acc:NP_001029685]	0.001376	0.03294	-0,702	-1,6267584
GRK5	NM_174331	G protein-coupled receptor kinase 5 [Source:UniProtKB/Swiss-Prot;Acc:P43249]	0.002247	0.04392	-0,7049	-1,63003168
ZMYM3	NM_001193249	zinc finger MYM-type protein 3 [Source:RefSeq peptide;Acc:NP_001180178]	0.0001645	0.009688	-0,7074	-1,63285875
LOC514257	NM_001075657	uncharacterized protein LOC514257 [Source:RefSeq peptide;Acc:NP_001069125]	0.001643	0.03666	-0,7101	-1,63591751
TMEM38A	NM_001083463	Trimeric intracellular cation channel type A [Source:UniProtKB/Swiss-Prot;Acc:A4FV75]	0.001341	0.03259	-0,7104	-1,63625772
CMBL	NM_001192983	carboxymethylenebutenolidase homolog [Source:RefSeq peptide;Acc:NP_001179912]	0.00035	0.01495	-0,7117	-1,6377328
IDS	NM_001192851		0.001034	0.02796	-0,7117	-1,6377328
EHHADH	NM_001075780	peroxisomal bifunctional enzyme [Source:RefSeq peptide;Acc:NP_001069248]	0.0008977	0.02522	-0,7137	-1,64000476
GLIPR2	NM_001076112	Golgi-associated plant pathogenesis-related protein 1 [Source:RefSeq peptide;Acc:NP_001069580]	0.001724	0.03732	-0,716	-1,6426214
DHCR7	NM_001014927	7-dehydrocholesterol reductase [Source:RefSeq peptide;Acc:NP_001014927]	0.0001989	0.01084	-0,721	-1,64832417
CYBRD1	NM_001206049	cytochrome b reductase 1 [Source:RefSeq peptide;Acc:NP_001192978]	0.000418	0.01623	-0,7227	-1,65026762
RNPEP	NM_001097563		0.0009068	0.02522	-0,7231	-1,65072523
VASH1	NM_001206803	vasohibin-1 [Source:RefSeq peptide;Acc:NP_001193732]	0.0005885	0.01917	-0,7244	-1,65221336
MGARP	NM_001166611	Protein MGARP [Source:UniProtKB/Swiss-Prot;Acc:A6QLZ1]	0.0009481	0.02621	-0,7321	-1,66105518
HOXA3	NM_001076825	Homeobox protein Hox-A3 [Source:UniProtKB/Swiss-Prot;Acc:Q08DG7]	0.001791	0.03824	-0,7321	-1,66105518
MAGED1	NM_001046125	melanoma-associated antigen D1 [Source:RefSeq peptide;Acc:NP_001039590]	1,86E-02	0.002552	-0,7422	-1,67272467
ADH5	NM_001034249	Alcohol dehydrogenase class-3 [Source:UniProtKB/Swiss-Prot;Acc:Q3ZC42]	0.0009589	0.02643	-0,7433	-1,67400055
EPB41L4A	NM_001105384		0.0001015	0.007164	-0,7444	-1,6752774
BGN	NM_178318	Biglycan [Source:UniProtKB/Swiss-Prot;Acc:P21809]	0.0001953	0.0107	-0,7447	-1,6756258
BTBD19	NM_001101241	BTB/POZ domain-containing protein 19 [Source:UniProtKB/Swiss-Prot;Acc:A6QPA3]	0.001502	0.03484	-0,7458	-1,67690388
TMCC3	NM_001038063	transmembrane and coiled-coil domains protein 3 [Source:RefSeq peptide;Acc:NP_001033152]	0.0003974	0.01576	-0,7494	-1,68109354
LRTOMT	NM_001024545	Leucine-rich repeat-containing protein 51 [Source:UniProtKB/Swiss-Prot;Acc:Q5EAD8]	0.00261	0.04787	-0,7526	-1,68482646
LSAMP	NM_001205368		0.0002677	0.01304	-0,7575	-1,69055857
ADRBK2	NM_174500	Beta-adrenergic receptor kinase 2 [Source:UniProtKB/Swiss-Prot;Acc:P26818]	0.001417	0.03359	-0,7623	-1,69619261
DPF1	NM_001076855		5,16E-02	0.004741	-0,7679	-1,70278938
IGF1R	NM_001244612	Insulin-like growth factor 1 receptor Insulin-like growth factor 1 receptor alpha chain Insulin-like growth factor 1 receptor beta chai	0.0007604	0.0227	-0,7707	-1,70609739
OLFML2B	NM_001100354	Olfactomedin-like protein 2B [Source:UniProtKB/Swiss-Prot;Acc:A6QLD2]	0.001005	0.02747	-0,7733	-1,70917486
KIAA0754	NM_001206988	bta-mir-2416 [Source:miRBase;Acc:MI0011462]	0.0004479	0.01645	-0,7744	-1,71047854
ZNF521	NM_001105419	zinc finger protein 521 [Source:RefSeq peptide;Acc:NP_001098889]	0.002677	0.04839	-0,7753	-1,71154592
C7H5orf45	NM_001167943	UPF0544 protein C5orf45 homolog [Source:RefSeq peptide;Acc:NP_001161415]	0.002668	0.04839	-0,7791	-1,71606
PTAFR	NM_001040538	Platelet-activating factor receptor [Source:UniProtKB/Swiss-Prot;Acc:Q9TTY5]	0.001486	0.03479	-0,7945	-1,73447615
THBS3	NM_001101839	thrombospondin-3 precursor [Source:RefSeq peptide;Acc:NP_001095309]	0.000857	0.02433	-0,7946	-1,73459638
LAP3	NM_174098	Cytosol aminopeptidase [Source:UniProtKB/Swiss-Prot;Acc:P00727]	0.0007847	0.0231	-0,7969	-1,73736394
BCAT2	NM_001013593	Branched-chain-amino-acid aminotransferase, mitochondrial [Source:UniProtKB/Swiss-Prot;Acc:Q5EA40]	0.001285	0.03199	-0,7983	-1,73905071
SORD	NM_001037320	Sorbitol dehydrogenase [Source:UniProtKB/Swiss-Prot;Acc:Q58D31]	0.00244	0.04604	-0,8029	-1,74460448
CCDC8	NM_001035485		0.0001406	0.008547	-0,8035	-1,74533019
ADAM19	NM_001075475	disintegrin and metalloproteinase domain-containing protein 19 precursor [Source:RefSeq peptide;Acc:NP_001068943]	0.0003599	0.01507	-0,8051	-1,7472669
ANKRD50	NM_001205949	ankyrin repeat domain-containing protein 50 [Source:RefSeq peptide;Acc:NP_001192878]	1,61E-02	0.002539	-0,8055	-1,74775141
PRKAR2B	NM_174649	cAMP-dependent protein kinase type II-beta regulatory subunit [Source:RefSeq peptide;Acc:NP_777074]	0.0004914	0.01719	-0,8063	-1,74872084
FRMD6	NM_001102133	FERM domain-containing protein 6 [Source:RefSeq peptide;Acc:NP_001095603]	0.0003891	0.01563	-0,8078	-1,75053997
CAV1	NM_174004	Caveolin-1 [Source:UniProtKB/Swiss-Prot;Acc:P79132]	0.001827	0.03875	-0,8085	-1,75138954
RAB30	NM_001076229	Ras-related protein Rab-30 [Source:UniProtKB/Swiss-Prot;Acc:Q17QB7]	0.002597	0.04781	-0,8118	-1,75540023

LOC512486	NM_001244229	interferon-induced guanylate-binding protein 1 [Source:RefSeq peptide;Acc:NP_001231158]	0.0006871	0.02123	-0,8134	-1,75734811	
CTDSPL	NM_001193081		2,43E-02	0.002884	-0,8141	-1,75820099	
SCN9A	NM_001110787	sodium channel protein type 9 subunit alpha [Source:RefSeq peptide;Acc:NP_001104257]	0.001361	0.03268	-0,8181	-1,76308252	
ANKS1B	NM_001102291	ankyrin repeat and sterile alpha motif domain-containing protein 1B [Source:RefSeq peptide;Acc:NP_001095761]	0.002357	0.04514	-0,8186	-1,76369366	
PJA1	NM_001080366; NM_001080366_2		8,35E-02	0.006437	-0,8231	-1,7692035	
IL7R	NM_001205887	interleukin-7 receptor subunit alpha precursor [Source:RefSeq peptide;Acc:NP_001192816]	0.0004419	0.0163	-0,8236	-1,76981676	
LOXL2	NM_001099053		3,53E-03	0.000978	-0,8254	-1,77202628	
FOXP2	NM_001205569		0.0002776	0.01322	-0,8285	-1,77583803	
ADCK3	NM_001046419	Chaperone activity of bc1 complex-like, mitochondrial [Source:UniProtKB/Swiss-Prot;Acc:Q29RI0]	0.0006459	0.02062	-0,8297	-1,77731574	
MAGED4B	NM_001103311	melanoma-associated antigen D4 [Source:RefSeq peptide;Acc:NP_001096781]	0.0002556	0.01289	-0,8341	-1,78274456	
TSPAN6	NM_001038109	Tetraspanin-6 [Source:UniProtKB/Swiss-Prot;Acc:Q32KU6]	8,80E-03	0.001737	-0,8345	-1,78323891	
ECHDC2	NM_001038536	Enoyl-CoA hydratase domain-containing protein 2, mitochondrial [Source:UniProtKB/Swiss-Prot;Acc:Q2TBT3]	0.0004316	0.01624	-0,8357	-1,78472278	
PCED1B	NM_001101207	Protein FAM113B [Source:UniProtKB/Swiss-Prot;Acc:A6QL70]	0.001309	0.03231	-0,8402	-1,79029831	
COLQ	NM_001035297	acetylcholinesterase collagenic tail peptide [Source:RefSeq peptide;Acc:NP_001030374]	0.0008453	0.02421	-0,8495	-1,80187633	
TMEM187	NM_001075355	Transmembrane protein 187 [Source:UniProtKB/Swiss-Prot;Acc:Q0VCM2]	0.001587	0.03618	-0,8554	-1,80926032	
GJA1	NM_174068	Gap junction alpha-1 protein [Source:UniProtKB/Swiss-Prot;Acc:P18246]	4,11E-02	0.004147	-0,8701	-1,82778959	
DYNC2LI1	NM_001038051	Cytoplasmic dynein 2 light intermediate chain 1 [Source:UniProtKB/Swiss-Prot;Acc:Q32KV4]	8,85E-02	0.006501	-0,8717	-1,8298178	
PRSS54	NM_001099044	inactive serine protease 54 precursor [Source:RefSeq peptide;Acc:NP_001092514]	0.001696	0.03722	-0,8718	-1,82994463	
IFI6	NM_001075588	Interferon alpha-inducible protein 6 [Source:UniProtKB/Swiss-Prot;Acc:Q6IED8]	0.0007615	0.0227	-0,8824	-1,84343941	
WDR59	NM_001101130	WD repeat-containing protein 59 [Source:RefSeq peptide;Acc:NP_001094600]	3,53E-02	0.00368	-0,8828	-1,84395059	
DBT	NM_173905	Lipoamide acyltransferase component of branched-chain alpha-keto acid dehydrogenase complex, mitochondrial [Source:UniProtK	0.0005573	0.01854	-0,8906	-1,853947	
PHF17	NM_001015559		0.0001215	0.007925	-0,8913	-1,85484676	
FGD3	NM_001024527	FYVE, RhoGEF and PH domain-containing protein 3 [Source:RefSeq peptide;Acc:NP_001019698]	0.001503	0.03484	-0,892	-1,85574695	
RP2	NM_001035403	protein XRP2 [Source:RefSeq peptide;Acc:NP_001030480]	0.0002709	0.01304	-0,8955	-1,86025449	
FSTL1	NM_001017950	Follistatin-related protein 1 [Source:UniProtKB/Swiss-Prot;Acc:Q58D84]	5,73E-03	0.001361	-0,8989	-1,86464372	
FDFT1	NM_001013004	squalene synthase [Source:RefSeq peptide;Acc:NP_001013022]	0.002411	0.04581	-0,8993	-1,86516078	
FAM115A	NM_001099054	protein FAM115A [Source:RefSeq peptide;Acc:NP_001092524]	0.0008996	0.02522	-0,9	-1,86606598	
CBLB	NM_001205923	E3 ubiquitin-protein ligase CBL-B [Source:RefSeq peptide;Acc:NP_001192852]	5,28E-02	0.004748	-0,9039	-1,8711173	
NFATC4	NM_001102536		0.0006698	0.02096	-0,9076	-1,8759222	
USH1C	NM_001035382	harmonin [Source:RefSeq peptide;Acc:NP_001030459]	0.001652	0.03677	-0,9125	-1,88230446	
PCK2	NM_001205594	phosphoenolpyruvate carboxykinase [Source:RefSeq peptide;Acc:NP_001192523]	0.002392	0.04553	-0,9144	-1,88478505	
GHR	NM_176608	growth hormone receptor precursor [Source:RefSeq peptide;Acc:NP_788781]	9,20E-02	0.006684	-0,9161	-1,88700729	
MYH7	NM_174727; NM_174727_2		0.001675	0.03711	-0,9167	-1,88779224	
ACSL6	NM_001038042	long-chain-fatty-acid--CoA ligase 6 [Source:RefSeq peptide;Acc:NP_001033131]	8,60E-02	0.006462	-0,9221	-1,89487148	
BASP1	NM_174780		0.001348	0.03259	-0,9225	-1,89539692	
CADM1	NM_001038558	cell adhesion molecule 1 precursor [Source:RefSeq peptide;Acc:NP_001033647]	1,32E-03	0.0006603	-0,9301	-1,90540806	
PSAT1	NM_001102150	phosphoserine aminotransferase [Source:RefSeq peptide;Acc:NP_001095620]	0.001474	0.03462	-0,9313	-1,9069936	
NNAT	NM_178323; NM_001201324	Neuronatin [Source:UniProtKB/Swiss-Prot;Acc:Q3ZBS9]	0.000756	0.02268	-0,932	-1,9079191	
WARS	NM_174218	Tryptophan--tRNA ligase, cytoplasmic T1-TrpRS T2-TrpRS [Source:UniProtKB/Swiss-Prot;Acc:P17248]	0.0009664	0.02656	-0,9381	-1,91600324	
PGF	NM_173950	Placenta growth factor [Source:UniProtKB/Swiss-Prot;Acc:Q9XS47]	0.002485	0.04661	-0,9445	-1,92452178	
ZNF423	NM_001101893_2; NM_001101893	zinc finger protein 423 [Source:RefSeq peptide;Acc:NP_001095363]	0.001268	0.03189	-0,9492	-1,9308017	
FLRT3	NM_001192674	leucine-rich repeat transmembrane protein FLRT3 precursor [Source:RefSeq peptide;Acc:NP_001179603]	0.00108	0.02892	-0,9503	-1,93227442	
ACOX2	NM_001102015	peroxisomal acyl-coenzyme A oxidase 2 [Source:RefSeq peptide;Acc:NP_001095485]	0.001333	0.03257	-0,9528	-1,9356257	
GJB1	NM_174069	Gap junction beta-1 protein [Source:UniProtKB/Swiss-Prot;Acc:O18968]	0.0005905	0.01917	-0,9582	-1,94288431	
APOBEC3B	NM_001077845	apolipoprotein B mRNA editing enzyme, catalytic polypeptide-like 3B [Source:RefSeq peptide;Acc:NP_001071313]	0.0004554	0.01648	-0,9592	-1,94423148	
ALDH6A1	NM_175811	methylmalonate-semialdehyde dehydrogenase [Source:RefSeq peptide;Acc:NP_787005]	8,42E-02	0.006439	-0,9613	-1,94706359	
CYP51A1	NM_001025319	Lanosterol 14-alpha demethylase [Source:UniProtKB/Swiss-Prot;Acc:Q4PJW3]	0.0001298	0.008281	-0,9685	-1,95680501	
CADPS2	NM_001102055	calcium-dependent secretion activator 2 [Source:RefSeq peptide;Acc:NP_001095525]	8,13E-02	0.006372	-0,9806	-1,9732859	
PROM1	NM_001245952	prominin-1 precursor [Source:RefSeq peptide;Acc:NP_001232881]	0.0005725	0.01878	-0,9837	-1,97753057	
SLC22A17	NM_001130755	Solute carrier family 22 member 17 [Source:UniProtKB/Swiss-Prot;Acc:Q3SZQ2]	7,42E-02	0.005908	-0,9838	-1,97766765	
C4H7orf57	NM_001079785	uncharacterized protein C7orf57 homolog [Source:RefSeq peptide;Acc:NP_001073253]	0.0001099	0.007603	-0,9873	-1,98247133	
NTRK2	NM_001075225	BDNF/NT-3 growth factors receptor precursor [Source:RefSeq peptide;Acc:NP_001068693]	0.0006579	0.02068	-0,992	-1,98894034	
THSD1	NM_001014967	thrombospondin type-1 domain-containing protein 1 precursor [Source:RefSeq peptide;Acc:NP_001014967]	3,33E-02	0.003542	-0,9966	-1,99529215	
SALL2	NM_001102112	sal-like protein 2 [Source:RefSeq peptide;Acc:NP_001095582]	0.002306	0.04464	-1	-2	
TRPV2	NM_001024493	transient receptor potential cation channel subfamily V member 2 [Source:RefSeq peptide;Acc:NP_001019664]	0.002377	0.04534	-1	-2	
MEOX1	NM_001035376	homeobox protein MOX-1 [Source:RefSeq peptide;Acc:NP_001030453]	0.002663	0.04839	-1	-2	

PHYHD1	NM_001076243	phytanoyl-CoA dioxygenase domain-containing protein 1 [Source:RefSeq peptide;Acc:NP_001069711]	0.001111	0.02942	-1,002	-2,00277451
ARMCX1	NM_001075167	armadillo repeat-containing X-linked protein 1 [Source:RefSeq peptide;Acc:NP_001068635]	0.001868	0.03912	-1,006	-2,00833509
WNT11	NM_001082456	protein Wnt-11 [Source:RefSeq peptide;Acc:NP_001075925]	0.0006571	0.02068	-1,011	-2,01530752
LAPTM4B	NM_205802	lysosomal-associated transmembrane protein 4B [Source:RefSeq peptide;Acc:NP_991371]	0.001628	0.03656	-1,015	-2,02090289
CREG1	NM_001075942	protein CREG1 precursor [Source:RefSeq peptide;Acc:NP_001069410]	0.0006835	0.02123	-1,022	-2,0307322
AQP9	NM_001205833	aquaporin 9 [Source:HGNC Symbol;Acc:643]	0.0004645	0.01671	-1,032	-2,04485706
CELF6	NM_001205644	CUGBP Elav-like family member 6 [Source:RefSeq peptide;Acc:NP_001192573]	0.001628	0.03656	-1,067	-2,09507225
CXCR4	NM_174301	C-X-C chemokine receptor type 4 [Source:UniProtKB/Swiss-Prot;Acc:P25930]	5,81E-02	0.004965	-1,072	-2,10234582
ITGB8	NM_001192875	integrin beta-8 precursor [Source:RefSeq peptide;Acc:NP_001179804]	5,55E-04	0.000397	-1,083	-2,11843667
ARMCX2	NM_001076960	armadillo repeat-containing X-linked protein 2 [Source:RefSeq peptide;Acc:NP_001070428]	8,27E-02	0.006429	-1,084	-2,11990557
SH3KBP1	NM_001128500	SH3 domain-containing kinase-binding protein 1 [Source:RefSeq peptide;Acc:NP_001121972]	1.76e-05	0.002552	-1,085	-2,12137548
ADSSL1	NM_001099192	Adenylosuccinate synthetase isozyme 1 [Source:UniProtKB/Swiss-Prot;Acc:A5PJR4]	0.001953	0.04014	-1,088	-2,12579135
TF	NM_177484	serotransferrin precursor [Source:RefSeq peptide;Acc:NP_803450]	0.0005873	0.01917	-1,093	-2,13317156
UBE2L6	NM_001098917	Ubiquitin/ISG15-conjugating enzyme E2 L6 [Source:UniProtKB/Swiss-Prot;Acc:A5PJC4]	0.0017	0.03722	-1,103	-2,14800894
THSD7A	NM_001206743	thrombospondin type-1 domain-containing protein 7A precursor [Source:RefSeq peptide;Acc:NP_001193672]	0.0003921	0.01569	-1,111	-2,15995312
EPB49	NM_001034431	Dematin [Source:UniProtKB/Swiss-Prot;Acc:Q08DM1]	1,67E-02	0.002544	-1,112	-2,1614508
FUT1	NM_177499	galactoside 2-alpha-L-fucosyltransferase 1 [Source:RefSeq peptide;Acc:NP_803465]	0.0004012	0.01577	-1,118	-2,17045874
ALDH1L2	NM_001191391	aldehyde dehydrogenase family 1 member L2, mitochondrial [Source:RefSeq peptide;Acc:NP_001178320]	0.0004873	0.01718	-1,118	-2,17045874
JAKMIP2	NM_001075897	janus kinase and microtubule-interacting protein 2 [Source:RefSeq peptide;Acc:NP_001069365]	0.0009167	0.02541	-1,122	-2,17648488
DGAT2	NM_205793	Diacylglycerol O-acyltransferase 2 [Source:UniProtKB/Swiss-Prot;Acc:Q70VZ8]	0.001322	0.03247	-1,122	-2,17648488
TBXAS1	NM_001046027	thromboxane-A synthase [Source:RefSeq peptide;Acc:NP_001039492]	2.96e-06	0.0009037	-1,123	-2,17799403
FNDC5	NM_001105421	fibronectin type III domain-containing protein 5 [Source:RefSeq peptide;Acc:NP_001098891]	0.002134	0.04242	-1,124	-2,17950422
PTGS1	NM_001105323	Prostaglandin G/H synthase 1 [Source:UniProtKB/Swiss-Prot;Acc:O62664]	4,40E-04	0.000378	-1,132	-2,19162353
SLC4A11	NM_001191314	sodium bicarbonate transporter-like protein 11 [Source:RefSeq peptide;Acc:NP_001178243]	0.0001405	0.008547	-1,142	-2,20686748
DDR2	NM_001083720	discoidin domain-containing receptor 2 precursor [Source:RefSeq peptide;Acc:NP_001077189]	5,96E-02	0.005043	-1,146	-2,21299471
MAP1LC3C	NM_001101058	microtubule-associated proteins 1A/1B light chain 3C [Source:RefSeq peptide;Acc:NP_001094528]	0.0004932	0.01719	-1,157	-2,22993244
EFHC1	NM_001192244	EF-hand domain-containing protein 1 [Source:RefSeq peptide;Acc:NP_001179173]	3,17E-02	0.003474	-1,162	-2,2376742
SSBP3	NM_001104986	single-stranded DNA-binding protein 3 [Source:RefSeq peptide;Acc:NP_001098456]	4,50E-02	0.004395	-1,162	-2,2376742
CLDN1	NM_001001854	Claudin-1 [Source:UniProtKB/Swiss-Prot;Acc:Q6L708]	0.0003763	0.01544	-1,163	-2,23922578
TC2N	NM_001193204	tandem C2 domains nuclear protein [Source:RefSeq peptide;Acc:NP_001180133]	0.000102	0.007164	-1,165	-2,24233216
PTPLAD2	NM_001076522	3-hydroxyacyl-CoA dehydratase 4 [Source:RefSeq peptide;Acc:NP_001069990]	0.0007975	0.02333	-1,185	-2,27363395
SLC1A3	NM_174600	Excitatory amino acid transporter 1 [Source:UniProtKB/Swiss-Prot;Acc:P46411]	0.001723	0.03732	-1,194	-2,28786195
HMGCS1	NM_001206578	hydroxymethylglutaryl-CoA synthase, cytoplasmic [Source:RefSeq peptide;Acc:NP_001193507]	0.0007328	0.02209	-1,224	-2,33593479
RASSF4	NM_001075454	ras association domain-containing protein 4 [Source:RefSeq peptide;Acc:NP_001068922]	0.0007089	0.02161	-1,228	-2,34242036
KRT18	NM_001192095	keratin, type I cytoskeletal 18 [Source:RefSeq peptide;Acc:NP_001179024]	0.0004818	0.0171	-1,23	-2,3456699
SERINC2	NM_001035285_2; NM_001035285	serine incorporator 2 [Source:RefSeq peptide;Acc:NP_001030362]	5,20E-02	0.004741	-1,233	-2,35055266
TRH	NM_001101221; NM_001101221_2	prothyroliberin precursor [Source:RefSeq peptide;Acc:NP_001094691]	0.0006875	0.02123	-1,233	-2,35055266
PAMR1	NM_001015591	inactive serine protease PAMR1 precursor [Source:RefSeq peptide;Acc:NP_001015591]	0.00191	0.03971	-1,234	-2,3521825
PTGR1	NM_001035281	prostaglandin reductase 1 [Source:RefSeq peptide;Acc:NP_001030358]	0.0003071	0.01414	-1,251	-2,38006339
KCNAB1	NM_001025336	Voltage-gated potassium channel subunit beta-1 [Source:UniProtKB/Swiss-Prot;Acc:Q4PJK1]	0.000288	0.01352	-1,256	-2,38832637
NUAK1	NM_001205496	NUAK family SNF1-like kinase 1 [Source:RefSeq peptide;Acc:NP_001192425]	2,70E-03	0.0009037	-1,257	-2,38998241
DHX58	NM_001015545	probable ATP-dependent RNA helicase DHX58 [Source:RefSeq peptide;Acc:NP_001015545]	0.00128	0.03199	-1,262	-2,39827983
FGF7	NM_001193131	keratinocyte growth factor precursor [Source:RefSeq peptide;Acc:NP_001180060]	0.001929	0.03984	-1,266	-2,4049385
MYO1B	NM_001102199	myosin-Ib [Source:RefSeq peptide;Acc:NP_001095669]	3,09E-03	0.0009037	-1,268	-2,40827476
CLCA3	NM_181018	epithelial chloride channel protein precursor [Source:RefSeq peptide;Acc:NP_851361]	2,84E-04	0.0003482	-1,276	-2,42166617
HMCN1	NM_001192537	hemicentin-1 precursor [Source:RefSeq peptide;Acc:NP_001179466]	0.001474	0.03462	-1,294	-2,45206972
CCDC3	NM_001172375_2; NM_001172375	coiled-coil domain-containing protein 3 precursor [Source:RefSeq peptide;Acc:NP_001165846]	1,97E-02	0.002552	-1,297	-2,45717396
DECR1	NM_001075423	2,4-dienoyl-CoA reductase, mitochondrial [Source:RefSeq peptide;Acc:NP_001068891]	2,23E-02	0.002722	-1,298	-2,45887773
ENC1	NM_001078067	ectoderm-neural cortex protein 1 [Source:RefSeq peptide;Acc:NP_001071535]	3,15E-03	0.0009037	-1,321	-2,49839225
ROBO1	NM_001192888	roundabout homolog 1 precursor [Source:RefSeq peptide;Acc:NP_001179817]	0.0002647	0.01304	-1,342	-2,53502504
ANGPTL2	NM_001109814	angiopoietin-related protein 2 precursor [Source:RefSeq peptide;Acc:NP_001103284]	0.0006223	0.01993	-1,344	-2,53854177
SGCD	NM_001191263	delta-sarcoglycan [Source:RefSeq peptide;Acc:NP_001178192]	0.0003271	0.01425	-1,352	-2,55265754
BEX2	NM_001077087; NM_001077034	protein BEX2 [Source:RefSeq peptide;Acc:NP_001070555]; Protein BEX2 [Source:UniProtKB/Swiss-Prot;Acc:Q2TBV0]	0.0006588	0.02068	-1,366	-2,57754926
GALNTL1	NM_001101127	putative polypeptide N-acetylgalactosaminyltransferase-like protein 1 [Source:RefSeq peptide;Acc:NP_001094597]	0.0002482	0.01265	-1,385	-2,61171957
FAM129A	NM_001191282	protein Niban [Source:RefSeq peptide;Acc:NP_001178211]	7,50E-03	0.00158	-1,388	-2,61715614
PAK7	NM_001206594	serine/threonine-protein kinase PAK 7 [Source:RefSeq peptide;Acc:NP_001193523]	5,66E-02	0.004881	-1,394	-2,62806325

TIMP3	NM_174473	metalloproteinase inhibitor 3 precursor [Source:RefSeq peptide;Acc:NP_776898]	6.25e-06	0.001411	-1,407	-2,65185152
LTC4S	NM_001046098	Leukotriene C4 synthase [Source:UniProtKB/Swiss-Prot;Acc:Q2NKS0]	0.0001164	0.007715	-1,409	-2,65553032
FMOD	NM_174058	Fibromodulin [Source:UniProtKB/Swiss-Prot;Acc:P13605]	0.000191	0.0106	-1,419	-2,67400099
GLI1	NM_001099000	zinc finger protein GLI1 [Source:RefSeq peptide;Acc:NP_001092470]	0.0003176	0.01423	-1,419	-2,67400099
SCN1A	NM_001193218	sodium channel protein type 1 subunit alpha [Source:RefSeq peptide;Acc:NP_001180147]	0.0006536	0.02068	-1,434	-2,70194817
ANXA8L1	NM_174241	Annexin A8 [Source:UniProtKB/Swiss-Prot;Acc:Q95L54]	0.0002133	0.01122	-1,45	-2,73208051
WNT5A	NM_001205971	protein Wnt-5a [Source:RefSeq peptide;Acc:NP_001192900]	0.0001688	0.009816	-1,452	-2,73587061
EPHX2	NM_001075534	epoxide hydrolase 2 [Source:RefSeq peptide;Acc:NP_001069002]	0.0003221	0.01423	-1,464	-2,75872184
SNX10	NM_001075375	Sorting nexin-10 [Source:UniProtKB/Swiss-Prot;Acc:Q0IIL5]	0.0003104	0.01422	-1,48	-2,78948733
SCARA5	NM_001102499	Scavenger receptor class A member 5 [Source:UniProtKB/Swiss-Prot;Acc:A5PJQ2]	6,82E-03	0.001503	-1,499	-2,82646729
GPR75	NM_001205061	probable G-protein coupled receptor 75 [Source:RefSeq peptide;Acc:NP_001191990]	6,07E-02	0.005097	-1,512	-2,85205143
SELENBP1	NM_001046048	Selenium-binding protein 1 [Source:UniProtKB/Swiss-Prot;Acc:Q2KJ32]	2,55E-05	8,04E-02	-1,514	-2,85600796
SAMD9	NM_001205781	sterile alpha motif domain-containing protein 9 [Source:RefSeq peptide;Acc:NP_001192710]	2,07E-03	0.0009037	-1,538	-2,90391656
SULT1A1	NM_177521	Sulfotransferase 1A1 [Source:UniProtKB/Swiss-Prot;Acc:P50227]	0.001688	0.03718	-1,543	-2,91399823
F2RL1	NM_001046283	proteinase-activated receptor 2 precursor [Source:RefSeq peptide;Acc:NP_001039748]	9,54E-02	0.006852	-1,546	-2,92006402
TXK	NM_001206148	tyrosine-protein kinase TXK [Source:RefSeq peptide;Acc:NP_001193077]	1,72E-02	0.002544	-1,557	-2,94241349
NYNRIN	NM_001192459	protein NYNRIN [Source:RefSeq peptide;Acc:NP_001179388]	0.0007663	0.02274	-1,557	-2,94241349
TPPP3	NM_001034774	Tubulin polymerization-promoting protein family member 3 [Source:UniProtKB/Swiss-Prot;Acc:Q3ZCC8]	0.000517	0.0174	-1,571	-2,97110584
SERPINA5	NM_176646	Plasma serine protease inhibitor [Source:UniProtKB/Swiss-Prot;Acc:Q9N2I2]	1,47E-02	0.002366	-1,574	-2,97729051
CRISP2	NM_001038089	cysteine-rich secretory protein 2 precursor [Source:RefSeq peptide;Acc:NP_001033178]	0.000609	0.01964	-1,58	-2,9896985
TNFRSF19	NM_001077096	tumor necrosis factor receptor superfamily member 19 precursor [Source:RefSeq peptide;Acc:NP_001070564]	8,63E-02	0.006462	-1,589	-3,0084075
ASB9	NM_001191166	ankyrin repeat and SOCS box protein 9 [Source:RefSeq peptide;Acc:NP_001178095]	0.0002395	0.01228	-1,607	-3,04617748
ENO3	NM_001034702	Beta-enolase [Source:UniProtKB/Swiss-Prot;Acc:Q3ZC09]	4,23E-03	0.001064	-1,611	-3,054635
APOA1	NM_174242	Apolipoprotein A-I Truncated apolipoprotein A-I [Source:UniProtKB/Swiss-Prot;Acc:P15497]	1,43E-02	0.002341	-1,636	-3,10802908
COL3A1	NM_001076831		2,28E-03	0.0009037	-1,65	-3,13833639
FAM115C	NM_001101924	protein FAM115C [Source:RefSeq peptide;Acc:NP_001095394]	2,21E-02	0.002722	-1,658	-3,15578736
FBLN5	NM_001014946	fibulin-5 precursor [Source:RefSeq peptide;Acc:NP_001014946]	4,75E-05	9,01E-02	-1,674	-3,19098096
C10H5orf13	NM_001105045	neuronal protein 3.1 [Source:RefSeq peptide;Acc:NP_001098515]	0.000855	0.02433	-1,687	-3,21986455
SLC9A9	NM_001076068	sodium/hydrogen exchanger 9 [Source:RefSeq peptide;Acc:NP_001069536]	0.001492	0.03482	-1,717	-3,28752075
RTP4	NM_001075961	28kD interferon responsive protein [Source:RefSeq peptide;Acc:NP_001069429]	0.0008269	0.02383	-1,734	-3,32648839
NTS	NM_173945	Neurotensin/neuromedin N Large neuromedin N Neuromedin N Neurotensin Tail peptide [Source:UniProtKB/Swiss-Prot;Acc:P0115	0.001169	0.03028	-1,755	-3,37526318
MEDAG	NM_001083660	Uncharacterized protein C13orf33 homolog [Source:UniProtKB/Swiss-Prot;Acc:A4IFN2]	0.0001571	0.009368	-1,758	-3,38228915
NOX5	NM_001101137	NADPH oxidase 5 [Source:RefSeq peptide;Acc:NP_001094607]	2,18E-03	0.0009037	-1,766	-3,40109664
LAMP5	NM_001083418	Lysosome-associated membrane glycoprotein 5 [Source:UniProtKB/Swiss-Prot;Acc:A4FV27]	2,80E-03	0.0009037	-1,769	-3,40817638
ERC2	NM_001102195	ERC protein 2 [Source:RefSeq peptide;Acc:NP_001095665]	0.0001307	0.008281	-1,779	-3,43188212
FN1	NM_001163778	fibronectin precursor [Source:RefSeq peptide;Acc:NP_001157250]	2,90E-02	0.003351	-1,809	-3,50399326
INHBE	NM_001205842	inhibin beta E chain precursor [Source:RefSeq peptide;Acc:NP_001192771]	9,24E-02	0.006684	-1,839	-3,57761961
STRA6	NM_001075730	stimulated by retinoic acid gene 6 protein homolog [Source:RefSeq peptide;Acc:NP_001069198]	8,80E-02	0.006501	-1,866	-3,64520512
CKMT1B	NM_174275	Creatine kinase U-type, mitochondrial [Source:UniProtKB/Swiss-Prot;Acc:Q9TTK8]	5,42E-02	0.004755	-1,905	-3,74508899
FAM13C	NM_001078029	protein FAM13C [Source:RefSeq peptide;Acc:NP_001071497]	2,29E-03	0.0009037	-1,919	-3,78160847
WISP2	NM_001102176	WNT1-inducible-signaling pathway protein 2 precursor [Source:RefSeq peptide;Acc:NP_001095646]	1,71E-02	0.002544	-1,946	-3,85304758
TMEM37	NM_001034744	voltage-dependent calcium channel gamma-like subunit [Source:RefSeq peptide;Acc:NP_001029916]	1,70E-03	0.0008038	-2,095	-4,27226163
GJA4	NM_001083738	Gap junction alpha-4 protein [Source:UniProtKB/Swiss-Prot;Acc:A4IFL1]	0.002703	0.04864	-2,158	-4,46295729
ATP8A2	NM_001163802		5.74e-06	0.001361	-2,198	-4,5884281
SEMA3C	NM_001101082	Semaphorin-3C [Source:UniProtKB/Swiss-Prot;Acc:A7MB70]	0.0001116	0.007611	-2,216	-4,64603493
SRPX2	NM_001014926	sushi repeat-containing protein SRPX2 precursor [Source:RefSeq peptide;Acc:NP_001014926]	4,78E-04	0.000378	-2,218	-4,65248017
OMD	NM_173947	osteomodulin precursor [Source:RefSeq peptide;Acc:NP_776372]	1,84E-02	0.002552	-2,224	-4,67186958
MT1A	NM_001040492	Metallothionein-1A [Source:UniProtKB/Swiss-Prot;Acc:P67983]	6,35E-02	0.005279	-2,275	-4,83997636
SLC8A1	NM_176632	sodium/calcium exchanger 1 precursor [Source:RefSeq peptide;Acc:NP_788805]	3,41E-05	8,07E-02	-2,354	-5,11239745
SLCO2B1	NM_174843	solute carrier organic anion transporter family member 2B1 [Source:RefSeq peptide;Acc:NP_777268]	0.0001847	0.01036	-2,46	-5,50216727
IGFBP3	NM_174556	Insulin-like growth factor-binding protein 3 [Source:UniProtKB/Swiss-Prot;Acc:P20959]	0.0001913	0.0106	-2,559	-5,89299074
AQP1	NM_174702	Aquaporin-1 [Source:UniProtKB/Swiss-Prot;Acc:P47865]	0.0006987	0.02137	-2,669	-6,35988201
OLFML3	NM_001075197	Olfactomedin-like protein 3 [Source:UniProtKB/Swiss-Prot;Acc:Q0VCP3]	3,89E-02	0.00396	-2,67	-6,36429187
LOXL4	NM_174384	Lysyl oxidase homolog 4 [Source:UniProtKB/Swiss-Prot;Acc:Q8MJ24]	9,98E-03	0.001785	-2,68	-6,40855902
EFEMP1	NM_001081717	EGF-containing fibulin-like extracellular matrix protein 1 precursor [Source:RefSeq peptide;Acc:NP_001075186]	9,69E-03	0.001766	-2,822	-7,07142025
UPK1B	NM_174482	Uroplakin-1b [Source:UniProtKB/Swiss-Prot;Acc:P38573]	9.65e-07	0.0005083	-2,883	-7,37682494

GO enrichment 32 hpi vs C-

GO biological process complete	Bos taurus - REFLIST (21987)	32 hpi vs C-	Expected hits	Hits (over/under)	32 hpi vs C- (fold Enrichment)	raw P-value	FDR
positive regulation of protein deubiquitination (GO:1903003)	6	3	.12	+	25.69	5.33E-04	3.41E-02
regulation of atrial cardiac muscle cell membrane depolarization (GO:0060371)	7	3	.14	+	22.02	7.51E-04	4.46E-02
interleukin-1 beta secretion (GO:0050702)	10	4	.19	+	20.55	1.13E-04	9.78E-03
thrombin-activated receptor signaling pathway (GO:0070493)	11	4	.21	+	18.68	1.51E-04	1.27E-02
interleukin-1 secretion (GO:0050701)	12	4	.23	+	17.12	1.99E-04	1.58E-02
interleukin-1 beta production (GO:0032611)	15	4	.29	+	13.70	4.05E-04	2.79E-02
interleukin-1 production (GO:0032612)	16	4	.31	+	12.84	4.98E-04	3.25E-02
toll-like receptor 4 signaling pathway (GO:0034142)	17	4	.33	+	12.09	6.06E-04	3.74E-02
regulation of interleukin-8 secretion (GO:2000482)	19	4	.37	+	10.82	8.70E-04	5.00E-02
regulation of execution phase of apoptosis (GO:1900117)	19	4	.37	+	10.82	8.70E-04	4.98E-02
regulation of platelet activation (GO:0010543)	29	6	.56	+	10.63	4.75E-05	4.80E-03
regulation of nitric oxide biosynthetic process (GO:0045428)	30	6	.58	+	10.27	5.61E-05	5.54E-03
positive regulation of Rho protein signal transduction (GO:0035025)	27	5	.53	+	9.51	3.26E-04	2.34E-02
positive regulation of reactive oxygen species metabolic process (GO:2000379)	52	9	1.01	+	8.89	2.23E-06	3.72E-04
cellular response to cAMP (GO:0071320)	30	5	.58	+	8.56	5.02E-04	3.25E-02
negative regulation of osteoblast differentiation (GO:0045668)	37	6	.72	+	8.33	1.57E-04	1.30E-02
negative regulation of ERK1 and ERK2 cascade (GO:0070373)	52	8	1.01	+	7.90	1.78E-05	2.13E-03
regulation of cell migration involved in sprouting angiogenesis (GO:0090049)	33	5	.64	+	7.78	7.41E-04	4.45E-02
lipopolysaccharide-mediated signaling pathway (GO:0031663)	33	5	.64	+	7.78	7.41E-04	4.44E-02
positive regulation of fibroblast proliferation (GO:0048146)	40	6	.78	+	7.71	2.30E-04	1.76E-02
regulation of reactive oxygen species biosynthetic process (GO:1903426)	40	6	.78	+	7.71	2.30E-04	1.75E-02
negative regulation of cytokine secretion (GO:0050710)	41	6	.80	+	7.52	2.59E-04	1.96E-02
biomineral tissue development (GO:0031214)	55	8	1.07	+	7.47	2.56E-05	2.85E-03
positive regulation of Ras protein signal transduction (GO:0046579)	42	6	.82	+	7.34	2.91E-04	2.13E-02
positive regulation of small GTPase mediated signal transduction (GO:0051057)	47	6	.91	+	6.56	5.03E-04	3.25E-02
cellular response to amino acid stimulus (GO:0071230)	48	6	.93	+	6.42	5.57E-04	3.51E-02
regulation of coagulation (GO:0050818)	74	9	1.44	+	6.25	2.93E-05	3.18E-03
regulation of fibroblast proliferation (GO:0048145)	59	7	1.15	+	6.09	2.60E-04	1.96E-02
regulation of hemostasis (GO:1900046)	69	8	1.34	+	5.96	1.10E-04	9.67E-03
regulation of blood coagulation (GO:0030193)	69	8	1.34	+	5.96	1.10E-04	9.61E-03
response to amino acid (GO:0043200)	61	7	1.19	+	5.90	3.13E-04	2.27E-02
regulation of osteoblast differentiation (GO:0045667)	88	10	1.71	+	5.84	1.82E-05	2.16E-03
negative regulation of ossification (GO:0030279)	62	7	1.21	+	5.80	3.43E-04	2.45E-02
tissue remodeling (GO:0048771)	82	9	1.60	+	5.64	6.10E-05	5.99E-03
positive regulation of inflammatory response (GO:0050729)	77	8	1.50	+	5.34	2.21E-04	1.71E-02
regulation of reactive oxygen species metabolic process (GO:2000377)	107	11	2.08	+	5.28	1.66E-05	2.02E-03
regulation of smooth muscle cell proliferation (GO:0048660)	70	7	1.36	+	5.14	6.71E-04	4.09E-02
integrin-mediated signaling pathway (GO:0007229)	72	7	1.40	+	4.99	7.83E-04	4.59E-02
negative regulation of MAPK cascade (GO:0043409)	124	12	2.41	+	4.97	1.21E-05	1.58E-03
positive regulation of angiogenesis (GO:0045766)	129	12	2.51	+	4.78	1.75E-05	2.11E-03
cellular response to metal ion (GO:0071248)	98	9	1.91	+	4.72	2.14E-04	1.68E-02
regulation of cytokine secretion (GO:0050707)	131	12	2.55	+	4.71	2.01E-05	2.29E-03
regulation of interleukin-6 production (GO:0032675)	92	8	1.79	+	4.47	6.66E-04	4.08E-02
response to metal ion (GO:0010038)	162	14	3.15	+	4.44	7.72E-06	1.05E-03
extracellular matrix organization (GO:0030198)	162	14	3.15	+	4.44	7.72E-06	1.04E-03
positive regulation of vasculature development (GO:1904018)	140	12	2.73	+	4.40	3.69E-05	3.89E-03
regulation of ossification (GO:0030278)	153	13	2.98	+	4.36	1.92E-05	2.24E-03
circadian rhythm (GO:0007623)	96	8	1.87	+	4.28	8.63E-04	4.98E-02

cellular response to inorganic substance (GO:0071241)	109	9	2.12	+	4.24	4.43E-04	3.01E-02
positive regulation of immune effector process (GO:0002699)	137	11	2.67	+	4.12	1.33E-04	1.13E-02
negative regulation of protein phosphorylation (GO:0001933)	352	28	6.85	+	4.09	1.31E-09	6.19E-07
negative regulation of cytokine production (GO:0001818)	177	14	3.45	+	4.06	1.96E-05	2.25E-03
cellular response to acid chemical (GO:0071229)	114	9	2.22	+	4.06	6.00E-04	3.72E-02
positive regulation of cell migration (GO:0030335)	349	27	6.79	+	3.97	4.54E-09	1.64E-06
cytokine production (GO:0001816)	117	9	2.28	+	3.95	7.14E-04	4.33E-02
regulation of ERK1 and ERK2 cascade (GO:0070372)	209	16	4.07	+	3.93	7.42E-06	1.02E-03
negative regulation of phosphorylation (GO:0042326)	381	29	7.42	+	3.91	1.70E-09	6.85E-07
protein localization to plasma membrane (GO:0072659)	133	10	2.59	+	3.86	4.34E-04	2.96E-02
regulation of body fluid levels (GO:0050878)	254	19	4.94	+	3.84	1.44E-06	2.49E-04
positive regulation of cell motility (GO:2000147)	362	27	7.05	+	3.83	9.35E-09	3.07E-06
response to inorganic substance (GO:0010035)	243	18	4.73	+	3.81	3.10E-06	4.82E-04
positive regulation of cellular component movement (GO:0051272)	368	27	7.16	+	3.77	1.29E-08	3.80E-06
negative regulation of response to external stimulus (GO:0032102)	219	16	4.26	+	3.75	1.28E-05	1.66E-03
extracellular structure organization (GO:0043062)	192	14	3.74	+	3.75	4.51E-05	4.62E-03
inflammatory response (GO:0006954)	307	22	5.98	+	3.68	4.25E-07	8.83E-05
regulation of angiogenesis (GO:0045765)	227	16	4.42	+	3.62	1.94E-05	2.25E-03
regulation of organ morphogenesis (GO:2000027)	143	10	2.78	+	3.59	7.37E-04	4.45E-02
positive regulation of locomotion (GO:0040017)	387	27	7.53	+	3.58	3.43E-08	9.51E-06
response to wounding (GO:0009611)	259	18	5.04	+	3.57	7.10E-06	9.84E-04
regulation of inflammatory response (GO:0050727)	217	15	4.22	+	3.55	4.33E-05	4.50E-03
regulation of vasculature development (GO:1901342)	247	17	4.81	+	3.54	1.43E-05	1.79E-03
negative regulation of protein kinase activity (GO:0006469)	219	15	4.26	+	3.52	4.78E-05	4.79E-03
rhythmic process (GO:0048511)	146	10	2.84	+	3.52	8.56E-04	4.96E-02
response to acid chemical (GO:0001101)	161	11	3.13	+	3.51	4.89E-04	3.23E-02
positive regulation of defense response (GO:0031349)	205	14	3.99	+	3.51	8.74E-05	7.87E-03
receptor-mediated endocytosis (GO:0006898)	163	11	3.17	+	3.47	5.38E-04	3.43E-02
positive regulation of response to external stimulus (GO:0032103)	208	14	4.05	+	3.46	1.01E-04	8.92E-03
negative regulation of phosphorus metabolic process (GO:0010563)	468	31	9.11	+	3.40	1.01E-08	3.25E-06
negative regulation of phosphate metabolic process (GO:0045936)	468	31	9.11	+	3.40	1.01E-08	3.18E-06
negative regulation of cell migration (GO:0030336)	197	13	3.83	+	3.39	2.13E-04	1.68E-02
regulation of cell migration (GO:0030334)	612	40	11.91	+	3.36	9.62E-11	6.80E-08
wound healing (GO:0042060)	216	14	4.20	+	3.33	1.47E-04	1.23E-02
regulation of Ras protein signal transduction (GO:0046578)	201	13	3.91	+	3.32	2.56E-04	1.94E-02
negative regulation of kinase activity (GO:0033673)	233	15	4.54	+	3.31	9.21E-05	8.24E-03
immune response-regulating signaling pathway (GO:0002764)	171	11	3.33	+	3.30	7.82E-04	4.61E-02
negative regulation of cellular component movement (GO:0051271)	219	14	4.26	+	3.28	1.68E-04	1.35E-02
negative regulation of cell motility (GO:2000146)	206	13	4.01	+	3.24	3.20E-04	2.31E-02
vasculature development (GO:0001944)	398	25	7.75	+	3.23	7.04E-07	1.29E-04
regulation of response to external stimulus (GO:0032101)	528	33	10.28	+	3.21	1.27E-08	3.81E-06
regulation of cell motility (GO:2000145)	642	40	12.50	+	3.20	3.65E-10	2.06E-07
regulation of locomotion (GO:0040012)	700	43	13.63	+	3.16	1.16E-10	7.81E-08
cardiovascular system development (GO:0072358)	407	25	7.92	+	3.16	1.03E-06	1.85E-04
blood vessel development (GO:0001568)	378	23	7.36	+	3.13	3.25E-06	4.99E-04
negative regulation of protein modification process (GO:0031400)	494	30	9.62	+	3.12	1.07E-07	2.75E-05
cell-cell adhesion (GO:0098609)	314	19	6.11	+	3.11	2.49E-05	2.79E-03
positive regulation of immune response (GO:0050778)	365	22	7.11	+	3.10	6.12E-06	8.65E-04
blood vessel morphogenesis (GO:0048514)	299	18	5.82	+	3.09	4.32E-05	4.52E-03
kidney development (GO:0001822)	200	12	3.89	+	3.08	8.18E-04	4.76E-02

renal system development (GO:0072001)	219	13	4.26	+	3.05	5.54E-04	3.51E-02
negative regulation of transferase activity (GO:0051348)	253	15	4.92	+	3.05	2.16E-04	1.69E-02
regulation of cellular component movement (GO:0051270)	696	41	13.55	+	3.03	1.04E-09	5.08E-07
negative regulation of signal transduction (GO:0009968)	931	54	18.12	+	2.98	3.21E-12	5.67E-09
negative regulation of intracellular signal transduction (GO:1902532)	434	25	8.45	+	2.96	3.06E-06	4.80E-04
regulation of small GTPase mediated signal transduction (GO:0051056)	227	13	4.42	+	2.94	7.59E-04	4.49E-02
negative regulation of locomotion (GO:0040013)	228	13	4.44	+	2.93	7.89E-04	4.61E-02
import into cell (GO:0098657)	423	24	8.23	+	2.91	6.14E-06	8.59E-04
regulation of MAPK cascade (GO:0043408)	549	31	10.69	+	2.90	2.97E-07	6.57E-05
negative regulation of response to stimulus (GO:0048585)	1178	66	22.93	+	2.88	4.14E-14	2.93E-10
negative regulation of cell communication (GO:0010648)	987	55	19.21	+	2.86	8.66E-12	1.11E-08
protein complex oligomerization (GO:0051259)	359	20	6.99	+	2.86	4.63E-05	4.71E-03
negative regulation of signaling (GO:0023057)	990	55	19.27	+	2.85	9.68E-12	1.05E-08
regulation of defense response (GO:0031347)	415	23	8.08	+	2.85	1.37E-05	1.73E-03
positive regulation of cell death (GO:0010942)	417	23	8.12	+	2.83	1.47E-05	1.82E-03
positive regulation of intracellular signal transduction (GO:1902533)	691	38	13.45	+	2.83	2.51E-08	7.23E-06
positive regulation of immune system process (GO:0002684)	620	34	12.07	+	2.82	1.50E-07	3.59E-05
cell adhesion (GO:0007155)	589	32	11.47	+	2.79	4.28E-07	8.77E-05
biological adhesion (GO:0022610)	593	32	11.54	+	2.77	4.93E-07	9.81E-05
regulation of immune response (GO:0050776)	521	28	10.14	+	2.76	2.79E-06	4.48E-04
regulation of protein secretion (GO:0050708)	280	15	5.45	+	2.75	5.94E-04	3.70E-02
regulation of protein serine/threonine kinase activity (GO:0071900)	356	19	6.93	+	2.74	1.22E-04	1.04E-02
cellular response to oxygen-containing compound (GO:1901701)	573	30	11.15	+	2.69	2.03E-06	3.41E-04
regulation of protein kinase activity (GO:0045859)	617	32	12.01	+	2.66	1.11E-06	1.97E-04
regulation of kinase activity (GO:0043549)	668	34	13.00	+	2.61	7.64E-07	1.38E-04
regulation of cell activation (GO:0050865)	394	20	7.67	+	2.61	1.54E-04	1.28E-02
negative regulation of cell proliferation (GO:0008285)	473	24	9.21	+	2.61	3.48E-05	3.70E-03
cellular metal ion homeostasis (GO:0006875)	359	18	6.99	+	2.58	3.74E-04	2.62E-02
regulation of phosphorylation (GO:0042325)	1237	62	24.08	+	2.57	3.10E-11	2.92E-08
response to oxygen-containing compound (GO:1901700)	859	43	16.72	+	2.57	5.77E-08	1.57E-05
regulation of cell proliferation (GO:0042127)	1200	60	23.36	+	2.57	7.34E-11	5.77E-08
regulation of cytokine production (GO:0001817)	481	24	9.36	+	2.56	4.48E-05	4.62E-03
circulatory system development (GO:0072359)	643	32	12.52	+	2.56	2.56E-06	4.21E-04
regulation of phosphate metabolic process (GO:0019220)	1415	70	27.54	+	2.54	1.98E-12	4.67E-09
regulation of protein phosphorylation (GO:0001932)	1154	57	22.46	+	2.54	3.34E-10	1.97E-07
regulation of phosphorus metabolic process (GO:0051174)	1420	70	27.64	+	2.53	2.28E-12	4.61E-09
positive regulation of multicellular organismal process (GO:0051240)	1187	58	23.11	+	2.51	3.19E-10	1.96E-07
negative regulation of multicellular organismal process (GO:0051241)	840	41	16.35	+	2.51	1.84E-07	4.26E-05
endocytosis (GO:0006897)	370	18	7.20	+	2.50	5.25E-04	3.37E-02
tube development (GO:0035295)	659	32	12.83	+	2.49	5.49E-06	7.92E-04
metal ion homeostasis (GO:0055065)	413	20	8.04	+	2.49	2.77E-04	2.06E-02
positive regulation of cell proliferation (GO:0008284)	642	31	12.50	+	2.48	8.46E-06	1.13E-03
positive regulation of signal transduction (GO:0009967)	1101	53	21.43	+	2.47	3.25E-09	1.24E-06
positive regulation of developmental process (GO:0051094)	980	47	19.08	+	2.46	3.11E-08	8.80E-06
positive regulation of programmed cell death (GO:0043068)	397	19	7.73	+	2.46	4.49E-04	3.04E-02
carbohydrate metabolic process (GO:0005975)	377	18	7.34	+	2.45	6.46E-04	3.97E-02
positive regulation of cell communication (GO:0010647)	1194	57	23.24	+	2.45	1.44E-09	6.35E-07
tube morphogenesis (GO:0035239)	503	24	9.79	+	2.45	1.21E-04	1.04E-02
positive regulation of signaling (GO:0023056)	1200	57	23.36	+	2.44	1.58E-09	6.57E-07
positive regulation of response to stimulus (GO:0048584)	1520	72	29.59	+	2.43	6.50E-12	9.19E-09

regulation of intracellular signal transduction (GO:1902531)	1363	63	26.53	+	2.37	6.15E-10	3.22E-07
enzyme linked receptor protein signaling pathway (GO:0007167)	484	22	9.42	+	2.34	3.75E-04	2.61E-02
regulation of transferase activity (GO:0051338)	749	34	14.58	+	2.33	1.18E-05	1.56E-03
regulation of anatomical structure morphogenesis (GO:0022603)	758	34	14.76	+	2.30	1.35E-05	1.72E-03
cell surface receptor signaling pathway (GO:0007166)	1524	68	29.67	+	2.29	4.04E-10	2.20E-07
regulation of protein modification process (GO:0031399)	1482	66	28.85	+	2.29	8.53E-10	4.31E-07
chemical homeostasis (GO:0048878)	765	34	14.89	+	2.28	1.52E-05	1.87E-03
cell migration (GO:0016477)	610	27	11.87	+	2.27	1.59E-04	1.30E-02
negative regulation of cellular protein metabolic process (GO:0032269)	906	40	17.64	+	2.27	2.61E-06	4.25E-04
regulation of secretion (GO:0051046)	505	22	9.83	+	2.24	5.93E-04	3.71E-02
regulation of localization (GO:0032879)	1975	86	38.45	+	2.24	3.92E-12	6.16E-09
ion homeostasis (GO:0050801)	553	24	10.76	+	2.23	4.94E-04	3.25E-02
localization of cell (GO:0051674)	692	30	13.47	+	2.23	7.44E-05	7.06E-03
cell motility (GO:0048870)	692	30	13.47	+	2.23	7.44E-05	7.01E-03
regulation of immune system process (GO:0002682)	946	41	18.41	+	2.23	3.61E-06	5.49E-04
negative regulation of protein metabolic process (GO:0051248)	951	41	18.51	+	2.21	3.92E-06	5.89E-04
regulation of response to stress (GO:0080134)	932	40	18.14	+	2.20	5.74E-06	8.19E-04
cellular response to chemical stimulus (GO:0070887)	1859	79	36.19	+	2.18	9.21E-11	6.85E-08
response to abiotic stimulus (GO:0009628)	683	29	13.30	+	2.18	1.32E-04	1.12E-02
epithelium development (GO:0060429)	756	32	14.72	+	2.17	8.31E-05	7.53E-03
response to cytokine (GO:0034097)	652	27	12.69	+	2.13	4.76E-04	3.16E-02
regulation of transport (GO:0051049)	1257	52	24.47	+	2.13	5.96E-07	1.12E-04
regulation of multicellular organismal development (GO:2000026)	1415	58	27.54	+	2.11	1.72E-07	4.05E-05
regulation of signal transduction (GO:0009966)	2442	100	47.54	+	2.10	1.39E-12	3.93E-09
negative regulation of developmental process (GO:0051093)	710	29	13.82	+	2.10	2.86E-04	2.11E-02
positive regulation of protein phosphorylation (GO:0001934)	764	31	14.87	+	2.08	1.75E-04	1.40E-02
regulation of multicellular organismal process (GO:0051239)	2170	88	42.24	+	2.08	6.54E-11	5.44E-08
cellular response to organic substance (GO:0071310)	1505	61	29.30	+	2.08	1.34E-07	3.39E-05
locomotion (GO:0040011)	864	35	16.82	+	2.08	8.31E-05	7.68E-03
positive regulation of phosphorus metabolic process (GO:0010562)	864	35	16.82	+	2.08	8.31E-05	7.63E-03
positive regulation of phosphate metabolic process (GO:0045937)	864	35	16.82	+	2.08	8.31E-05	7.58E-03
homeostatic process (GO:0042592)	1188	48	23.13	+	2.08	2.97E-06	4.71E-04
regulation of cell communication (GO:0010646)	2661	107	51.80	+	2.07	5.96E-13	2.11E-09
regulation of signaling (GO:0023051)	2688	108	52.32	+	2.06	4.28E-13	2.02E-09
positive regulation of phosphorylation (GO:0042327)	797	32	15.51	+	2.06	2.21E-04	1.71E-02
regulation of response to stimulus (GO:0048583)	3065	123	59.66	+	2.06	4.03E-15	5.70E-11
response to organic substance (GO:0010033)	1882	75	36.64	+	2.05	6.00E-09	2.12E-06
positive regulation of protein modification process (GO:0031401)	935	37	18.20	+	2.03	9.44E-05	8.39E-03
positive regulation of cellular component organization (GO:0051130)	867	34	16.88	+	2.01	1.59E-04	1.31E-02
response to external stimulus (GO:0009605)	1313	51	25.56	+	2.00	4.91E-06	7.16E-04
defense response (GO:0006952)	855	33	16.64	+	1.98	3.65E-04	2.58E-02
tissue development (GO:0009888)	1220	46	23.75	+	1.94	2.91E-05	3.19E-03
negative regulation of molecular function (GO:0044092)	930	35	18.10	+	1.93	2.71E-04	2.03E-02
response to endogenous stimulus (GO:0009719)	838	31	16.31	+	1.90	8.75E-04	4.99E-02
regulation of developmental process (GO:0050793)	1885	69	36.69	+	1.88	5.87E-07	1.14E-04
regulation of cell death (GO:0010941)	1235	45	24.04	+	1.87	8.14E-05	7.57E-03
regulation of cellular protein metabolic process (GO:0032268)	2147	77	41.79	+	1.84	2.92E-07	6.54E-05
anatomical structure morphogenesis (GO:0009653)	1668	59	32.47	+	1.82	1.35E-05	1.73E-03
positive regulation of cellular protein metabolic process (GO:0032270)	1198	42	23.32	+	1.80	3.63E-04	2.58E-02
regulation of protein metabolic process (GO:0051246)	2290	80	44.58	+	1.79	4.21E-07	9.01E-05

positive regulation of protein metabolic process (GO:0051247)	1278	44	24.88	+	1.77	3.69E-04	2.60E-02
negative regulation of biological process (GO:0048519)	3995	137	77.77	+	1.76	9.17E-12	1.08E-08
negative regulation of cellular process (GO:0048523)	3643	124	70.91	+	1.75	2.39E-10	1.53E-07
cellular developmental process (GO:0048869)	2722	92	52.99	+	1.74	1.88E-07	4.28E-05
positive regulation of cellular process (GO:0048522)	4026	136	78.37	+	1.74	3.83E-11	3.38E-08
immune system process (GO:0002376)	1466	49	28.54	+	1.72	2.89E-04	2.13E-02
regulation of catalytic activity (GO:0050790)	1845	61	35.91	+	1.70	7.07E-05	6.75E-03
nervous system development (GO:0007399)	1574	52	30.64	+	1.70	3.07E-04	2.24E-02
regulation of biological quality (GO:0065008)	2881	95	56.08	+	1.69	3.68E-07	8.00E-05
positive regulation of biological process (GO:0048518)	4501	148	87.62	+	1.69	2.10E-11	2.12E-08
cell differentiation (GO:0030154)	2646	87	51.51	+	1.69	1.45E-06	2.46E-04
negative regulation of nitrogen compound metabolic process (GO:0051172)	1930	63	37.57	+	1.68	7.01E-05	6.74E-03
developmental process (GO:0032502)	4084	132	79.50	+	1.66	1.44E-09	6.18E-07
regulation of molecular function (GO:0065009)	2639	85	51.37	+	1.65	4.35E-06	6.41E-04
system development (GO:0048731)	3107	100	60.48	+	1.65	4.23E-07	8.92E-05
negative regulation of cellular metabolic process (GO:0031324)	2059	66	40.08	+	1.65	7.96E-05	7.45E-03
response to stress (GO:0006950)	2362	75	45.98	+	1.63	2.89E-05	3.19E-03
animal organ development (GO:0048513)	2215	70	43.12	+	1.62	6.91E-05	6.69E-03
multicellular organism development (GO:0007275)	3483	109	67.80	+	1.61	4.87E-07	9.84E-05
anatomical structure development (GO:0048856)	3839	120	74.73	+	1.61	8.59E-08	2.25E-05
negative regulation of macromolecule metabolic process (GO:0010605)	2072	63	40.33	+	1.56	4.59E-04	3.06E-02
negative regulation of metabolic process (GO:0009892)	2230	67	43.41	+	1.54	4.98E-04	3.26E-02
positive regulation of nitrogen compound metabolic process (GO:0051173)	2435	72	47.40	+	1.52	4.57E-04	3.08E-02
positive regulation of metabolic process (GO:0009893)	2691	78	52.38	+	1.49	4.58E-04	3.07E-02
positive regulation of cellular metabolic process (GO:0031325)	2524	73	49.13	+	1.49	7.46E-04	4.45E-02
response to chemical (GO:0042221)	3604	104	70.16	+	1.48	3.23E-05	3.46E-03
cellular response to stimulus (GO:0051716)	5669	158	110.35	+	1.43	4.93E-07	9.67E-05
localization (GO:0051179)	4170	116	81.17	+	1.43	5.08E-05	5.06E-03
cell communication (GO:0007154)	4743	128	92.33	+	1.39	6.89E-05	6.71E-03
signaling (GO:0023052)	4642	124	90.36	+	1.37	1.62E-04	1.31E-02
response to stimulus (GO:0050896)	6867	183	133.67	+	1.37	7.02E-07	1.30E-04
signal transduction (GO:0007165)	4380	116	85.26	+	1.36	3.92E-04	2.72E-02
regulation of cellular metabolic process (GO:0031323)	5061	133	98.52	+	1.35	1.62E-04	1.31E-02
regulation of metabolic process (GO:0019222)	5366	137	104.45	+	1.31	4.26E-04	2.93E-02
regulation of biological process (GO:0050789)	10422	254	202.88	+	1.25	1.19E-06	2.07E-04
regulation of cellular process (GO:0050794)	9867	237	192.07	+	1.23	1.87E-05	2.20E-03
biological regulation (GO:0065007)	11094	264	215.96	+	1.22	4.16E-06	6.19E-04
cellular process (GO:0009987)	13729	302	267.25	+	1.13	5.89E-04	3.70E-02
biological_process (GO:0008150)	17363	380	337.99	+	1.12	1.46E-07	3.55E-05
Unclassified (UNCLASSIFIED)	4624	48	90.01	-	.53	1.46E-07	3.62E-05
nervous system process (GO:0050877)	1646	11	32.04	-	.34	2.20E-05	2.49E-03
sensory perception (GO:0007600)	1355	5	26.38	-	.19	5.88E-07	1.12E-04
RNA processing (GO:0006396)	702	1	13.67	-	.07	3.13E-05	3.37E-03
detection of chemical stimulus (GO:0009593)	1024	1	19.93	-	.05	6.37E-08	1.70E-05
detection of stimulus (GO:0051606)	1120	1	21.80	-	.05	8.81E-09	2.97E-06
detection of chemical stimulus involved in sensory perception of smell (GO:0050	973	0	18.94	-	< 0.01	1.03E-08	3.16E-06
detection of chemical stimulus involved in sensory perception (GO:0050907)	1003	0	19.52	-	< 0.01	4.33E-09	1.61E-06
detection of stimulus involved in sensory perception (GO:0050906)	1044	0	20.32	-	< 0.01	1.92E-09	7.53E-07
sensory perception of smell (GO:0007608)	997	0	19.41	-	< 0.01	7.11E-09	2.45E-06
sensory perception of chemical stimulus (GO:0007606)	1072	0	20.87	-	< 0.01	1.32E-09	6.03E-07

GO enrichment 12 vs 32 hpi

GO biological process complete	Bos taurus - REFLIST (21987	12 vs 32 hpi	Expected hits	Hits (over/u	12 vs 32 hpi (	raw P-value	FDR
regulation of growth (GO:0040008)	461	24	10.04	+	2.39	1.58E-04	1.02E-02
regulation of I-kappaB kinase/NF-kappaB signaling (GO:0043122)	147	12	3.20	+	3.75	1.62E-04	1.04E-02
circulatory system development (GO:0072359)	643	41	14.01	+	2.93	3.06E-09	1.05E-06
sensory perception of chemical stimulus (GO:0007606)	1072	1	23.35	-	.04	3.01E-09	1.06E-06
wound healing (GO:0042060)	216	19	4.71	+	4.04	7.81E-07	1.09E-04
regulation of immune system process (GO:0002682)	946	46	20.61	+	2.23	8.03E-07	1.11E-04
positive regulation of protein metabolic process (GO:0051247)	1278	49	27.84	+	1.76	1.75E-04	1.12E-02
negative regulation of protein phosphorylation (GO:0001933)	352	27	7.67	+	3.52	5.36E-08	1.13E-05
regulation of adaptive immune response (GO:0002819)	105	10	2.29	+	4.37	1.79E-04	1.14E-02
localization (GO:0051179)	4170	131	90.85	+	1.44	9.83E-06	1.16E-03
response to abiotic stimulus (GO:0009628)	683	31	14.88	+	2.08	1.85E-04	1.17E-02
anatomical structure development (GO:0048856)	3839	141	83.63	+	1.69	2.07E-10	1.17E-07
regulation of lymphocyte differentiation (GO:0045619)	127	11	2.77	+	3.98	1.87E-04	1.18E-02
positive regulation of alpha-beta T cell differentiation (GO:0046638)	34	6	.74	+	8.10	1.89E-04	1.19E-02
regulation of cell differentiation (GO:0045595)	1255	56	27.34	+	2.05	8.78E-07	1.20E-04
regulation of protein phosphorylation (GO:0001932)	1154	62	25.14	+	2.47	2.30E-10	1.20E-07
positive regulation of intracellular signal transduction (GO:1902533)	691	40	15.05	+	2.66	5.87E-08	1.22E-05
cell motility (GO:0048870)	692	40	15.08	+	2.65	6.08E-08	1.23E-05
tissue development (GO:0009888)	1220	64	26.58	+	2.41	2.27E-10	1.24E-07
negative regulation of macromolecule metabolic process (GO:0010605)	2072	71	45.14	+	1.57	2.00E-04	1.25E-02
localization of cell (GO:0051674)	692	40	15.08	+	2.65	6.08E-08	1.25E-05
sensory perception (GO:0007600)	1355	7	29.52	-	.24	9.28E-07	1.26E-04
negative regulation of response to external stimulus (GO:0032102)	219	19	4.77	+	3.98	9.47E-07	1.27E-04
detection of stimulus involved in sensory perception (GO:0050906)	1044	2	22.74	-	.09	6.46E-08	1.29E-05
positive regulation of hemopoiesis (GO:1903708)	149	14	3.25	+	4.31	1.11E-05	1.30E-03
regulation of biomineral tissue development (GO:0070167)	68	8	1.48	+	5.40	2.13E-04	1.33E-02
negative chemotaxis (GO:0050919)	35	6	.76	+	7.87	2.17E-04	1.35E-02
regulation of hydrolase activity (GO:0051336)	1041	46	22.68	+	2.03	1.17E-05	1.36E-03
small molecule catabolic process (GO:0044282)	252	16	5.49	+	2.91	2.24E-04	1.38E-02
negative regulation of phosphorylation (GO:0042326)	381	28	8.30	+	3.37	7.02E-08	1.38E-05
regulation of tube diameter (GO:0035296)	88	9	1.92	+	4.69	2.30E-04	1.40E-02
regulation of blood vessel diameter (GO:0097746)	88	9	1.92	+	4.69	2.30E-04	1.41E-02
regulation of hemostasis (GO:1900046)	69	8	1.50	+	5.32	2.34E-04	1.42E-02
regulation of blood coagulation (GO:0030193)	69	8	1.50	+	5.32	2.34E-04	1.42E-02
regulation of protein kinase activity (GO:0045859)	617	29	13.44	+	2.16	2.37E-04	1.43E-02
nervous system process (GO:0050877)	1646	13	35.86	-	.36	1.27E-05	1.43E-03
regulation of cytokine secretion (GO:0050707)	131	11	2.85	+	3.85	2.40E-04	1.44E-02
regulation of cell activation (GO:0050865)	394	24	8.58	+	2.80	1.26E-05	1.44E-03
cytokine-mediated signaling pathway (GO:0019221)	341	22	7.43	+	2.96	1.26E-05	1.45E-03
regulation of epithelial cell migration (GO:0010632)	178	13	3.88	+	3.35	2.45E-04	1.46E-02
regulation of biological process (GO:0050789)	10422	268	227.05	+	1.18	2.52E-04	1.49E-02
negative regulation of ERK1 and ERK2 cascade (GO:0070373)	52	7	1.13	+	6.18	2.51E-04	1.50E-02
positive regulation of epithelial cell migration (GO:0010634)	110	10	2.40	+	4.17	2.53E-04	1.50E-02
mammary gland development (GO:0030879)	93	11	2.03	+	5.43	1.38E-05	1.50E-03
epithelial cell proliferation (GO:0050673)	70	8	1.52	+	5.25	2.56E-04	1.51E-02

response to inorganic substance (GO:0010035)	243	18	5.29	+	3.40	1.40E-05	1.51E-03
cellular developmental process (GO:0048869)	2722	93	59.30	+	1.57	1.38E-05	1.51E-03
regulation of defense response (GO:0031347)	415	27	9.04	+	2.99	1.13E-06	1.51E-04
negative regulation of hydrolase activity (GO:0051346)	413	22	9.00	+	2.45	2.61E-04	1.52E-02
cell communication (GO:0007154)	4743	138	103.33	+	1.34	2.61E-04	1.52E-02
circulatory system process (GO:0003013)	267	19	5.82	+	3.27	1.38E-05	1.52E-03
positive regulation of MAPK cascade (GO:0043410)	369	23	8.04	+	2.86	1.35E-05	1.52E-03
multicellular organismal process (GO:0032501)	5631	159	122.67	+	1.30	2.60E-04	1.53E-02
negative regulation of cellular component movement (GO:0051271)	219	17	4.77	+	3.56	1.38E-05	1.53E-03
negative regulation of inflammatory response (GO:0050728)	90	9	1.96	+	4.59	2.68E-04	1.55E-02
positive regulation of cell adhesion (GO:0045785)	283	17	6.17	+	2.76	2.67E-04	1.55E-02
regulation of immune effector process (GO:0002697)	244	18	5.32	+	3.39	1.47E-05	1.58E-03
negative regulation of cellular process (GO:0048523)	3643	131	79.36	+	1.65	4.68E-09	1.58E-06
positive regulation of cell death (GO:0010942)	417	22	9.08	+	2.42	2.79E-04	1.61E-02
negative regulation of osteoblast differentiation (GO:0045668)	37	6	.81	+	7.44	2.84E-04	1.63E-02
RNA processing (GO:0006396)	702	3	15.29	-	.20	2.87E-04	1.63E-02
regulation of catalytic activity (GO:0050790)	1845	73	40.19	+	1.82	1.23E-06	1.63E-04
negative regulation of intracellular signal transduction (GO:1902532)	434	30	9.45	+	3.17	8.42E-08	1.63E-05
negative regulation of signal transduction (GO:0009968)	931	51	20.28	+	2.51	4.96E-09	1.63E-06
regulation of vasculature development (GO:1901342)	247	22	5.38	+	4.09	8.64E-08	1.65E-05
positive regulation of angiogenesis (GO:0045766)	129	16	2.81	+	5.69	8.83E-08	1.66E-05
cellular response to lipid (GO:0071396)	313	18	6.82	+	2.64	2.94E-04	1.67E-02
response to copper ion (GO:0046688)	12	4	.26	+	15.30	3.03E-04	1.70E-02
tissue morphogenesis (GO:0048729)	455	23	9.91	+	2.32	3.01E-04	1.70E-02
notochord development (GO:0030903)	12	4	.26	+	15.30	3.03E-04	1.71E-02
phytosteroid metabolic process (GO:0016128)	4	3	.09	+	34.43	3.16E-04	1.74E-02
import into cell (GO:0098657)	423	22	9.22	+	2.39	3.14E-04	1.74E-02
defense response (GO:0006952)	855	36	18.63	+	1.93	3.11E-04	1.74E-02
positive regulation of cell motility (GO:2000147)	362	35	7.89	+	4.44	1.48E-12	1.74E-09
phytosteroid biosynthetic process (GO:0016129)	4	3	.09	+	34.43	3.16E-04	1.75E-02
positive regulation of response to external stimulus (GO:0032103)	208	14	4.53	+	3.09	3.14E-04	1.75E-02
organic hydroxy compound metabolic process (GO:1901615)	288	17	6.27	+	2.71	3.23E-04	1.77E-02
vascular process in circulatory system (GO:0003018)	114	10	2.48	+	4.03	3.30E-04	1.80E-02
regulation of T-helper cell differentiation (GO:0045622)	24	5	.52	+	9.56	3.36E-04	1.82E-02
developmental process (GO:0032502)	4084	151	88.97	+	1.70	2.22E-11	1.85E-08
lipid metabolic process (GO:0006629)	930	38	20.26	+	1.88	3.50E-04	1.89E-02
positive regulation of cellular protein metabolic process (GO:0032270)	1198	46	26.10	+	1.76	3.54E-04	1.91E-02
tube development (GO:0035295)	659	41	14.36	+	2.86	5.93E-09	1.91E-06
anatomical structure morphogenesis (GO:0009653)	1668	64	36.34	+	1.76	1.80E-05	1.92E-03
regulation of blood vessel endothelial cell migration (GO:0043535)	74	8	1.61	+	4.96	3.61E-04	1.93E-02
alcohol biosynthetic process (GO:0046165)	74	8	1.61	+	4.96	3.61E-04	1.94E-02
epithelium development (GO:0060429)	756	42	16.47	+	2.55	1.04E-07	1.94E-05
negative regulation of response to cytokine stimulus (GO:0060761)	39	6	.85	+	7.06	3.66E-04	1.95E-02
cellular response to cytokine stimulus (GO:0071345)	585	33	12.74	+	2.59	1.50E-06	1.96E-04
response to cytokine (GO:0034097)	652	38	14.20	+	2.68	1.08E-07	1.96E-05
detection of stimulus (GO:0051606)	1120	3	24.40	-	.12	1.07E-07	1.96E-05
detection of chemical stimulus (GO:0009593)	1024	1	22.31	-	.04	6.25E-09	1.96E-06
regulation of signal transduction (GO:0009966)	2442	105	53.20	+	1.97	2.52E-11	1.98E-08

regulation of cellular protein metabolic process (GO:0032268)	2147	85	46.77	+	1.82	1.11E-07	1.99E-05
regulation of ERK1 and ERK2 cascade (GO:0070372)	209	20	4.55	+	4.39	1.15E-07	2.03E-05
tube morphogenesis (GO:0035239)	503	30	10.96	+	2.74	1.57E-06	2.04E-04
response to lipid (GO:0033993)	461	26	10.04	+	2.59	1.96E-05	2.06E-03
cellular response to oxygen-containing compound (GO:1901701)	573	30	12.48	+	2.40	1.96E-05	2.07E-03
regulation of cell-cell adhesion (GO:0022407)	275	19	5.99	+	3.17	2.03E-05	2.11E-03
response to stress (GO:0006950)	2362	83	51.46	+	1.61	2.05E-05	2.12E-03
positive regulation of response to stimulus (GO:0048584)	1520	70	33.11	+	2.11	7.11E-09	2.18E-06
nucleobase metabolic process (GO:0009112)	40	6	.87	+	6.89	4.14E-04	2.19E-02
regulation of smooth muscle contraction (GO:0006940)	40	6	.87	+	6.89	4.14E-04	2.20E-02
small molecule metabolic process (GO:0044281)	1433	64	31.22	+	2.05	1.28E-07	2.22E-05
positive regulation of biological process (GO:0048518)	4501	148	98.06	+	1.51	1.29E-07	2.23E-05
lung development (GO:0030324)	138	13	3.01	+	4.32	2.22E-05	2.27E-03
regulation of system process (GO:0044057)	324	18	7.06	+	2.55	4.34E-04	2.28E-02
response to endogenous stimulus (GO:0009719)	838	35	18.26	+	1.92	4.33E-04	2.28E-02
positive regulation of leukocyte differentiation (GO:1902107)	118	12	2.57	+	4.67	2.28E-05	2.32E-03
negative regulation of transferase activity (GO:0051348)	253	18	5.51	+	3.27	2.32E-05	2.34E-03
regulation of anatomical structure morphogenesis (GO:0022603)	758	47	16.51	+	2.85	4.74E-10	2.39E-07
positive regulation of cell proliferation (GO:0008284)	642	35	13.99	+	2.50	1.87E-06	2.40E-04
regulation of intracellular signal transduction (GO:1902531)	1363	68	29.69	+	2.29	5.13E-10	2.42E-07
regulation of phosphorylation (GO:0042325)	1237	64	26.95	+	2.37	5.03E-10	2.45E-07
positive regulation of leukocyte activation (GO:0002696)	230	17	5.01	+	3.39	2.48E-05	2.48E-03
positive regulation of cellular component movement (GO:0051272)	368	35	8.02	+	4.37	2.28E-12	2.48E-09
regulation of organ morphogenesis (GO:2000027)	143	11	3.12	+	3.53	4.81E-04	2.52E-02
epithelial cell differentiation (GO:0030855)	385	23	8.39	+	2.74	2.54E-05	2.53E-03
regulation of multicellular organismal process (GO:0051239)	2170	107	47.27	+	2.26	3.57E-15	2.53E-11
cellular alcohol metabolic process (GO:0044107)	5	3	.11	+	27.54	4.98E-04	2.56E-02
cellular alcohol biosynthetic process (GO:0044108)	5	3	.11	+	27.54	4.98E-04	2.57E-02
regulation of cytokine secretion involved in immune response (GO:0002739)	14	4	.30	+	13.11	4.92E-04	2.57E-02
positive regulation of protein kinase C signaling (GO:0090037)	5	3	.11	+	27.54	4.98E-04	2.58E-02
positive regulation of T-helper 1 cell differentiation (GO:0045627)	5	3	.11	+	27.54	4.98E-04	2.59E-02
negative regulation of cellular metabolic process (GO:0031324)	2059	74	44.86	+	1.65	2.64E-05	2.59E-03
positive regulation of leukocyte cell-cell adhesion (GO:1903039)	144	11	3.14	+	3.51	5.08E-04	2.60E-02
regulation of blood circulation (GO:1903522)	162	14	3.53	+	3.97	2.64E-05	2.61E-03
respiratory tube development (GO:0030323)	141	13	3.07	+	4.23	2.73E-05	2.64E-03
regulation of leukocyte migration (GO:0002685)	147	15	3.20	+	4.68	2.13E-06	2.64E-04
positive regulation of protein phosphorylation (GO:0001934)	764	36	16.64	+	2.16	2.72E-05	2.65E-03
positive regulation of Ras protein signal transduction (GO:0046579)	42	6	.91	+	6.56	5.23E-04	2.66E-02
Unclassified (UNCLASSIFIED)	4624	60	100.74	-	.60	2.13E-06	2.66E-04
positive regulation of alpha-beta T cell activation (GO:0046635)	42	6	.91	+	6.56	5.23E-04	2.67E-02
signal transduction (GO:0007165)	4380	127	95.42	+	1.33	5.29E-04	2.68E-02
biological_process (GO:0008150)	17363	419	378.26	+	1.11	2.13E-06	2.68E-04
cell surface receptor signaling pathway (GO:0007166)	1524	76	33.20	+	2.29	3.60E-11	2.68E-08
regulation of immune response (GO:0050776)	521	28	11.35	+	2.47	2.79E-05	2.69E-03
negative regulation of developmental process (GO:0051093)	710	37	15.47	+	2.39	2.12E-06	2.70E-04
positive regulation of Rho protein signal transduction (GO:0035025)	27	5	.59	+	8.50	5.40E-04	2.71E-02
steroid biosynthetic process (GO:0006694)	79	8	1.72	+	4.65	5.40E-04	2.71E-02
regulation of transferase activity (GO:0051338)	749	32	16.32	+	1.96	5.36E-04	2.71E-02

regulation of endothelial cell proliferation (GO:0001936)	100	9	2.18	+	4.13	5.47E-04	2.73E-02
angiogenesis (GO:0001525)	209	16	4.55	+	3.51	2.87E-05	2.74E-03
negative regulation of kinase activity (GO:0033673)	233	17	5.08	+	3.35	2.89E-05	2.74E-03
regulation of alpha-beta T cell activation (GO:0046634)	60	7	1.31	+	5.36	5.53E-04	2.75E-02
negative regulation of transport (GO:0051051)	303	17	6.60	+	2.58	5.59E-04	2.77E-02
detection of chemical stimulus involved in sensory perception (GO:0050907)	1003	1	21.85	-	.05	9.28E-09	2.79E-06
positive regulation of phosphate metabolic process (GO:0045937)	864	39	18.82	+	2.07	3.00E-05	2.81E-03
positive regulation of phosphorus metabolic process (GO:0010562)	864	39	18.82	+	2.07	3.00E-05	2.83E-03
response to lipopolysaccharide (GO:0032496)	187	15	4.07	+	3.68	3.08E-05	2.86E-03
sensory perception of smell (GO:0007608)	997	0	21.72	-	< 0.01	6.27E-10	2.86E-07
morphogenesis of an epithelial sheet (GO:0002011)	43	6	.94	+	6.40	5.86E-04	2.87E-02
negative regulation of immune effector process (GO:0002698)	80	8	1.74	+	4.59	5.83E-04	2.88E-02
regulation of muscle contraction (GO:0006937)	101	9	2.20	+	4.09	5.85E-04	2.88E-02
regulation of T-helper 1 type immune response (GO:0002825)	15	4	.33	+	12.24	6.13E-04	2.95E-02
positive regulation of interleukin-6 production (GO:0032755)	61	7	1.33	+	5.27	6.05E-04	2.95E-02
chromosome organization (GO:0051276)	911	6	19.85	-	.30	6.03E-04	2.95E-02
negative regulation of smooth muscle cell migration (GO:0014912)	15	4	.33	+	12.24	6.13E-04	2.96E-02
regulation of anatomical structure size (GO:0090066)	383	20	8.34	+	2.40	6.09E-04	2.96E-02
positive regulation of T-helper cell differentiation (GO:0045624)	15	4	.33	+	12.24	6.13E-04	2.97E-02
regulation of response to wounding (GO:1903034)	123	12	2.68	+	4.48	3.33E-05	3.03E-03
cell migration (GO:0016477)	610	36	13.29	+	2.71	1.78E-07	3.03E-05
oxoacid metabolic process (GO:0043436)	737	35	16.06	+	2.18	3.31E-05	3.04E-03
regulation of wound healing (GO:0061041)	103	11	2.24	+	4.90	3.30E-05	3.05E-03
regulation of response to external stimulus (GO:0032101)	528	40	11.50	+	3.48	4.31E-11	3.05E-08
heart development (GO:0007507)	386	20	8.41	+	2.38	6.43E-04	3.08E-02
blood circulation (GO:0008015)	261	18	5.69	+	3.17	3.41E-05	3.09E-03
regulation of locomotion (GO:0040012)	700	54	15.25	+	3.54	6.57E-15	3.09E-11
regulation of cell morphogenesis (GO:0022604)	336	18	7.32	+	2.46	6.50E-04	3.10E-02
negative regulation of protein modification process (GO:0031400)	494	27	10.76	+	2.51	3.46E-05	3.10E-03
response to oxygen-containing compound (GO:1901700)	859	42	18.71	+	2.24	2.52E-06	3.10E-04
actin filament bundle assembly (GO:0051017)	44	6	.96	+	6.26	6.54E-04	3.11E-02
alcohol metabolic process (GO:0006066)	189	15	4.12	+	3.64	3.45E-05	3.11E-03
negative regulation of ossification (GO:0030279)	62	7	1.35	+	5.18	6.61E-04	3.14E-02
response to hypoxia (GO:0001666)	145	13	3.16	+	4.12	3.58E-05	3.16E-03
positive regulation of protein modification process (GO:0031401)	935	41	20.37	+	2.01	3.60E-05	3.16E-03
nervous system development (GO:0007399)	1574	55	34.29	+	1.60	6.73E-04	3.18E-02
negative regulation of MAPK cascade (GO:0043409)	124	12	2.70	+	4.44	3.58E-05	3.18E-03
negative regulation of growth (GO:0045926)	174	12	3.79	+	3.17	6.77E-04	3.19E-02
regulation of plasma membrane bounded cell projection organization (GO:0120035)	423	21	9.22	+	2.28	6.79E-04	3.19E-02
signaling (GO:0023052)	4642	133	101.13	+	1.32	6.83E-04	3.20E-02
positive regulation of cellular process (GO:0048522)	4026	135	87.71	+	1.54	1.91E-07	3.21E-05
regulation of hemopoiesis (GO:1903706)	281	16	6.12	+	2.61	6.93E-04	3.23E-02
DNA repair (GO:0006281)	361	0	7.86	-	< 0.01	6.96E-04	3.23E-02
positive regulation of cell activation (GO:0050867)	236	19	5.14	+	3.70	2.65E-06	3.23E-04
sterol biosynthetic process (GO:0016126)	37	7	.81	+	8.68	3.71E-05	3.24E-03
regulation of kinase activity (GO:0043549)	668	29	14.55	+	1.99	7.02E-04	3.26E-02
response to wounding (GO:0009611)	259	24	5.64	+	4.25	1.11E-08	3.26E-06
negative regulation of biological process (GO:0048519)	3995	139	87.03	+	1.60	1.13E-08	3.27E-06

regulation of cell migration (GO:0030334)	612	51	13.33	+	3.83	2.31E-15	3.27E-11
positive regulation of T cell differentiation (GO:0045582)	63	7	1.37	+	5.10	7.22E-04	3.32E-02
small molecule biosynthetic process (GO:0044283)	452	25	9.85	+	2.54	3.83E-05	3.32E-03
regulation of platelet activation (GO:0010543)	29	5	.63	+	7.91	7.21E-04	3.33E-02
regulation of T-helper 1 cell differentiation (GO:0045625)	6	3	.13	+	22.95	7.35E-04	3.34E-02
positive regulation of chemokine production (GO:0032722)	45	6	.98	+	6.12	7.28E-04	3.34E-02
cellular response to stimulus (GO:0051716)	5669	157	123.50	+	1.27	7.31E-04	3.34E-02
regulation of response to cytokine stimulus (GO:0060759)	86	10	1.87	+	5.34	3.88E-05	3.34E-03
xanthine metabolic process (GO:0046110)	6	3	.13	+	22.95	7.35E-04	3.35E-02
regulation of transport (GO:0051049)	1257	46	27.38	+	1.68	7.39E-04	3.35E-02
positive regulation of signal transduction (GO:0009967)	1101	56	23.99	+	2.33	1.21E-08	3.35E-06
negative regulation of immune system process (GO:0002683)	312	17	6.80	+	2.50	7.61E-04	3.39E-02
negative regulation of alpha-beta T cell differentiation (GO:0046639)	16	4	.35	+	11.48	7.54E-04	3.40E-02
cellular response to lipopolysaccharide (GO:0071222)	105	9	2.29	+	3.93	7.58E-04	3.40E-02
anatomical structure formation involved in morphogenesis (GO:0048646)	674	29	14.68	+	1.98	7.59E-04	3.40E-02
negative regulation of molecular function (GO:0044092)	930	50	20.26	+	2.47	1.20E-08	3.40E-06
positive regulation of apoptotic process (GO:0043065)	394	20	8.58	+	2.33	7.57E-04	3.41E-02
regulation of cell projection organization (GO:0031344)	428	21	9.32	+	2.25	7.67E-04	3.41E-02
negative regulation of cytokine production (GO:0001818)	177	12	3.86	+	3.11	7.79E-04	3.45E-02
taxis (GO:0042330)	357	19	7.78	+	2.44	7.83E-04	3.46E-02
response to decreased oxygen levels (GO:0036293)	147	13	3.20	+	4.06	4.08E-05	3.50E-03
mammary gland epithelium development (GO:0061180)	46	6	1.00	+	5.99	8.08E-04	3.52E-02
positive regulation of programmed cell death (GO:0043068)	397	20	8.65	+	2.31	8.08E-04	3.52E-02
icosanoid biosynthetic process (GO:0046456)	30	5	.65	+	7.65	8.26E-04	3.54E-02
actin filament bundle organization (GO:0061572)	46	6	1.00	+	5.99	8.08E-04	3.54E-02
morphogenesis of an epithelium (GO:0002009)	359	19	7.82	+	2.43	8.05E-04	3.54E-02
regulation of smooth muscle cell migration (GO:0014910)	30	5	.65	+	7.65	8.26E-04	3.55E-02
regulation of interleukin-1 production (GO:0032652)	46	6	1.00	+	5.99	8.08E-04	3.55E-02
regulation of CD4-positive, alpha-beta T cell differentiation (GO:0043370)	30	5	.65	+	7.65	8.26E-04	3.56E-02
cellular response to cAMP (GO:0071320)	30	5	.65	+	7.65	8.26E-04	3.57E-02
gland development (GO:0048732)	291	19	6.34	+	3.00	4.19E-05	3.57E-03
regulation of nitric oxide biosynthetic process (GO:0045428)	30	5	.65	+	7.65	8.26E-04	3.58E-02
regulation of cell growth (GO:0001558)	266	18	5.79	+	3.11	4.30E-05	3.64E-03
organic acid metabolic process (GO:0006082)	752	35	16.38	+	2.14	4.35E-05	3.64E-03
negative regulation of nitrogen compound metabolic process (GO:0051172)	1930	70	42.05	+	1.66	4.32E-05	3.64E-03
regulation of reactive oxygen species metabolic process (GO:2000377)	107	9	2.33	+	3.86	8.59E-04	3.65E-02
positive regulation of defense response (GO:0031349)	205	13	4.47	+	2.91	8.58E-04	3.65E-02
negative regulation of protein metabolic process (GO:0051248)	951	48	20.72	+	2.32	2.20E-07	3.65E-05
regulation of leukocyte cell-cell adhesion (GO:1903037)	205	13	4.47	+	2.91	8.58E-04	3.66E-02
regulation of peptidase activity (GO:0052547)	400	20	8.71	+	2.30	8.65E-04	3.66E-02
negative regulation of multicellular organismal process (GO:0051241)	840	47	18.30	+	2.57	1.37E-08	3.66E-06
positive regulation of multicellular organismal process (GO:0051240)	1187	70	25.86	+	2.71	1.55E-13	3.66E-10
negative regulation of response to stimulus (GO:0048585)	1178	67	25.66	+	2.61	3.64E-12	3.68E-09
negative regulation of cell differentiation (GO:0045596)	508	27	11.07	+	2.44	4.49E-05	3.71E-03
negative regulation of cell communication (GO:0010648)	987	52	21.50	+	2.42	1.37E-08	3.72E-06
regulation of leukocyte activation (GO:0002694)	365	19	7.95	+	2.39	8.83E-04	3.73E-02
oxidation-reduction process (GO:0055114)	968	42	21.09	+	1.99	4.48E-05	3.73E-03
cell adhesion (GO:0007155)	589	35	12.83	+	2.73	2.27E-07	3.73E-05

negative regulation of apoptotic process (GO:0043066)	662	32	14.42	+	2.22	4.55E-05	3.74E-03
regulation of apoptotic process (GO:0042981)	1141	47	24.86	+	1.89	4.63E-05	3.74E-03
positive regulation of small GTPase mediated signal transduction (GO:0051057)	47	6	1.02	+	5.86	8.95E-04	3.76E-02
regulation of osteoblast differentiation (GO:0045667)	88	10	1.92	+	5.22	4.63E-05	3.76E-03
biological regulation (GO:0065007)	11094	287	241.69	+	1.19	4.60E-05	3.76E-03
fatty acid derivative metabolic process (GO:1901568)	86	8	1.87	+	4.27	9.03E-04	3.79E-02
regulation of endothelial cell migration (GO:0010594)	131	10	2.85	+	3.50	9.08E-04	3.80E-02
smooth muscle tissue development (GO:0048745)	17	4	.37	+	10.80	9.16E-04	3.82E-02
negative regulation of signaling (GO:0023057)	990	52	21.57	+	2.41	1.46E-08	3.82E-06
positive regulation of metabolic process (GO:0009893)	2691	84	58.63	+	1.43	9.25E-04	3.84E-02
inflammatory response (GO:0006954)	307	26	6.69	+	3.89	1.50E-08	3.86E-06
system development (GO:0048731)	3107	115	67.69	+	1.70	1.53E-08	3.86E-06
negative regulation of protein kinase activity (GO:0006469)	219	16	4.77	+	3.35	4.86E-05	3.88E-03
negative regulation of cell proliferation (GO:0008285)	473	26	10.30	+	2.52	4.86E-05	3.90E-03
zymogen activation (GO:0031638)	31	5	.68	+	7.40	9.43E-04	3.91E-02
animal organ development (GO:0048513)	2215	86	48.26	+	1.78	2.44E-07	3.93E-05
negative regulation of cellular protein metabolic process (GO:0032269)	906	46	19.74	+	2.33	2.43E-07	3.95E-05
regulation of cell communication (GO:0010646)	2661	110	57.97	+	1.90	5.88E-11	3.96E-08
regulation of inflammatory response (GO:0050727)	217	18	4.73	+	3.81	3.29E-06	3.97E-04
detection of chemical stimulus involved in sensory perception of smell (GO:0050911)	973	0	21.20	-	< 0.01	9.03E-10	3.99E-07
positive regulation of lymphocyte activation (GO:0051251)	208	13	4.53	+	2.87	9.73E-04	4.01E-02
regulation of leukocyte differentiation (GO:1902105)	208	13	4.53	+	2.87	9.73E-04	4.02E-02
response to organic substance (GO:0010033)	1882	80	41.00	+	1.95	1.62E-08	4.02E-06
cell differentiation (GO:0030154)	2646	89	57.64	+	1.54	5.10E-05	4.05E-03
regulation of interleukin-2 production (GO:0032663)	48	6	1.05	+	5.74	9.89E-04	4.06E-02
regulation of signaling (GO:0023051)	2688	111	58.56	+	1.90	6.40E-11	4.11E-08
cellular response to organic substance (GO:0071310)	1505	65	32.79	+	1.98	2.60E-07	4.13E-05
biological adhesion (GO:0022610)	593	35	12.92	+	2.71	2.64E-07	4.15E-05
blood vessel development (GO:0001568)	378	29	8.23	+	3.52	1.70E-08	4.15E-06
positive regulation of cytokine secretion involved in immune response (GO:0002741)	7	3	.15	+	19.67	1.03E-03	4.24E-02
ion homeostasis (GO:0050801)	553	25	12.05	+	2.08	1.04E-03	4.25E-02
negative regulation of cell migration (GO:0030336)	197	15	4.29	+	3.50	5.38E-05	4.25E-03
regulation of cytokine production (GO:0001817)	481	26	10.48	+	2.48	5.46E-05	4.29E-03
integrin-mediated signaling pathway (GO:0007229)	72	9	1.57	+	5.74	5.66E-05	4.42E-03
negative regulation of cell death (GO:0060548)	730	34	15.90	+	2.14	5.71E-05	4.43E-03
endothelial cell proliferation (GO:0001935)	18	4	.39	+	10.20	1.10E-03	4.44E-02
positive regulation of blood circulation (GO:1903524)	49	6	1.07	+	5.62	1.09E-03	4.44E-02
regulation of response to stimulus (GO:0048583)	3065	129	66.77	+	1.93	2.20E-13	4.44E-10
acute inflammatory response (GO:0002526)	40	7	.87	+	8.03	5.77E-05	4.45E-03
cell adhesion mediated by integrin (GO:0033627)	18	4	.39	+	10.20	1.10E-03	4.46E-02
alditol metabolic process (GO:0019400)	18	4	.39	+	10.20	1.10E-03	4.47E-02
multicellular organism development (GO:0007275)	3483	129	75.88	+	1.70	1.07E-09	4.47E-07
carbohydrate metabolic process (GO:0005975)	377	19	8.21	+	2.31	1.11E-03	4.48E-02
vasculature development (GO:0001944)	398	32	8.67	+	3.69	1.05E-09	4.50E-07
epithelial cell development (GO:0002064)	160	11	3.49	+	3.16	1.15E-03	4.60E-02
cellular process (GO:0009987)	13729	334	299.09	+	1.12	1.15E-03	4.61E-02
positive regulation of developmental process (GO:0051094)	980	62	21.35	+	2.90	2.61E-13	4.61E-10
cellular response to molecule of bacterial origin (GO:0071219)	112	9	2.44	+	3.69	1.16E-03	4.63E-02

response to external stimulus (GO:0009605)	1313	52	28.60	+	1.82	6.03E-05	4.63E-03
positive regulation of adaptive immune response based on somatic recombination of immune re	69	7	1.50	+	4.66	1.18E-03	4.68E-02
negative regulation of cysteine-type endopeptidase activity involved in apoptotic process (GO:00	69	7	1.50	+	4.66	1.18E-03	4.70E-02
positive regulation of cell differentiation (GO:0045597)	662	40	14.42	+	2.77	1.96E-08	4.70E-06
positive regulation of fat cell differentiation (GO:0045600)	50	6	1.09	+	5.51	1.20E-03	4.75E-02
regulation of cell motility (GO:2000145)	642	51	13.99	+	3.65	1.35E-14	4.77E-11
regulation of cell migration involved in sprouting angiogenesis (GO:0090049)	33	5	.72	+	6.95	1.21E-03	4.79E-02
regulation of epithelial cell proliferation (GO:0050678)	249	17	5.42	+	3.13	6.29E-05	4.81E-03
regulation of phosphate metabolic process (GO:0019220)	1415	72	30.83	+	2.34	8.02E-11	4.93E-08
extracellular matrix organization (GO:0030198)	162	11	3.53	+	3.12	1.26E-03	4.96E-02
positive regulation of adaptive immune response (GO:0002821)	70	7	1.52	+	4.59	1.27E-03	4.98E-02
polyol metabolic process (GO:0019751)	70	7	1.52	+	4.59	1.27E-03	4.99E-02
regulation of smooth muscle cell proliferation (GO:0048660)	70	7	1.52	+	4.59	1.27E-03	5.00E-02
regulation of cell adhesion (GO:0030155)	491	26	10.70	+	2.43	6.63E-05	5.04E-03
regulation of phosphorus metabolic process (GO:0051174)	1420	72	30.94	+	2.33	8.55E-11	5.04E-08
DNA metabolic process (GO:0006259)	592	1	12.90	-	.08	6.72E-05	5.05E-03
positive regulation of phosphorylation (GO:0042327)	797	36	17.36	+	2.07	6.77E-05	5.06E-03
negative regulation of defense response (GO:0031348)	133	12	2.90	+	4.14	6.71E-05	5.07E-03
regulation of coagulation (GO:0050818)	74	9	1.61	+	5.58	6.86E-05	5.11E-03
negative regulation of metabolic process (GO:0009892)	2230	77	48.58	+	1.58	6.92E-05	5.12E-03
negative regulation of catalytic activity (GO:0043086)	705	39	15.36	+	2.54	3.44E-07	5.34E-05
movement of cell or subcellular component (GO:0006928)	1029	50	22.42	+	2.23	3.57E-07	5.49E-05
regulation of cellular component movement (GO:0051270)	696	53	15.16	+	3.50	1.95E-14	5.50E-11
negative regulation of locomotion (GO:0040013)	228	16	4.97	+	3.22	7.60E-05	5.59E-03
cellular response to chemical stimulus (GO:0070887)	1859	75	40.50	+	1.85	3.73E-07	5.67E-05
negative regulation of phosphate metabolic process (GO:0045936)	468	30	10.20	+	2.94	3.84E-07	5.72E-05
regulation of angiogenesis (GO:0045765)	227	20	4.95	+	4.04	3.92E-07	5.77E-05
regulation of programmed cell death (GO:0043067)	1158	47	25.23	+	1.86	7.90E-05	5.78E-03
negative regulation of phosphorus metabolic process (GO:0010563)	468	30	10.20	+	2.94	3.84E-07	5.78E-05
regulation of MAPK cascade (GO:0043408)	549	38	11.96	+	3.18	1.46E-09	5.89E-07
respiratory system development (GO:0060541)	158	13	3.44	+	3.78	8.10E-05	5.91E-03
locomotion (GO:0040011)	864	47	18.82	+	2.50	2.55E-08	6.00E-06
regulation of cell proliferation (GO:0042127)	1200	67	26.14	+	2.56	6.37E-12	6.00E-09
regulation of biological quality (GO:0065008)	2881	108	62.76	+	1.72	2.60E-08	6.02E-06
peptide cross-linking (GO:0018149)	29	6	.63	+	9.50	8.74E-05	6.21E-03
negative regulation of cell motility (GO:2000146)	206	15	4.49	+	3.34	8.61E-05	6.21E-03
regulation of alpha-beta T cell differentiation (GO:0046637)	43	7	.94	+	7.47	8.67E-05	6.22E-03
positive regulation of immune effector process (GO:0002699)	137	12	2.98	+	4.02	8.73E-05	6.23E-03
response to oxygen levels (GO:0070482)	159	13	3.46	+	3.75	8.60E-05	6.23E-03
regulation of cytokine-mediated signaling pathway (GO:0001959)	77	9	1.68	+	5.37	9.08E-05	6.29E-03
positive regulation of lymphocyte differentiation (GO:0045621)	77	9	1.68	+	5.37	9.08E-05	6.32E-03
response to molecule of bacterial origin (GO:0002237)	207	15	4.51	+	3.33	9.05E-05	6.34E-03
negative regulation of programmed cell death (GO:0043069)	679	32	14.79	+	2.16	9.01E-05	6.34E-03
regulation of cellular component organization (GO:0051128)	1844	66	40.17	+	1.64	9.01E-05	6.36E-03
regulation of protein modification process (GO:0031399)	1482	67	32.29	+	2.08	2.80E-08	6.38E-06
regulation of ossification (GO:0030278)	153	18	3.33	+	5.40	2.90E-08	6.51E-06
regulation of cell death (GO:0010941)	1235	53	26.91	+	1.97	5.55E-06	6.64E-04
regulation of protein metabolic process (GO:0051246)	2290	91	49.89	+	1.82	3.01E-08	6.64E-06

regulation of localization (GO:0032879)	1975	86	43.03	+	2.00	1.70E-09	6.68E-07
cardiovascular system development (GO:0072358)	407	32	8.87	+	3.61	1.75E-09	6.69E-07
response to metal ion (GO:0010038)	162	13	3.53	+	3.68	1.02E-04	7.07E-03
positive regulation of leukocyte migration (GO:0002687)	98	10	2.13	+	4.68	1.06E-04	7.21E-03
positive regulation of cell communication (GO:0010647)	1194	61	26.01	+	2.35	1.94E-09	7.23E-07
regulation of adaptive immune response based on somatic recombination of immune receptors b	98	10	2.13	+	4.68	1.06E-04	7.24E-03
regulation of blood vessel size (GO:0050880)	98	10	2.13	+	4.68	1.06E-04	7.28E-03
blood vessel morphogenesis (GO:0048514)	299	23	6.51	+	3.53	5.00E-07	7.29E-05
cell-cell adhesion (GO:0098609)	314	19	6.84	+	2.78	1.08E-04	7.33E-03
positive regulation of locomotion (GO:0040017)	387	35	8.43	+	4.15	8.44E-12	7.46E-09
regulation of body fluid levels (GO:0050878)	254	21	5.53	+	3.80	5.31E-07	7.66E-05
positive regulation of cell-cell adhesion (GO:0022409)	164	13	3.57	+	3.64	1.15E-04	7.70E-03
regulation of tube size (GO:0035150)	99	10	2.16	+	4.64	1.15E-04	7.71E-03
regulation of bone mineralization (GO:0030500)	62	8	1.35	+	5.92	1.19E-04	7.96E-03
positive regulation of cell migration (GO:0030335)	349	35	7.60	+	4.60	5.64E-13	7.98E-10
cholesterol biosynthetic process (GO:0006695)	31	6	.68	+	8.88	1.21E-04	8.01E-03
positive regulation of signaling (GO:0023056)	1200	61	26.14	+	2.33	2.22E-09	8.03E-07
regulation of multicellular organismal development (GO:2000026)	1415	77	30.83	+	2.50	5.27E-13	8.27E-10
response to stimulus (GO:0050896)	6867	197	149.60	+	1.32	7.03E-06	8.35E-04
carboxylic acid metabolic process (GO:0019752)	700	32	15.25	+	2.10	1.28E-04	8.47E-03
regulation of developmental process (GO:0050793)	1885	92	41.07	+	2.24	6.62E-13	8.50E-10
regulation of chemokine production (GO:0032642)	63	8	1.37	+	5.83	1.32E-04	8.69E-03
regulation of response to stress (GO:0080134)	932	49	20.30	+	2.41	4.15E-08	9.01E-06
tissue remodeling (GO:0048771)	82	9	1.79	+	5.04	1.41E-04	9.18E-03
regulation of molecular function (GO:0065009)	2639	96	57.49	+	1.67	6.44E-07	9.19E-05
secondary alcohol biosynthetic process (GO:1902653)	32	6	.70	+	8.61	1.41E-04	9.22E-03
positive regulation of ERK1 and ERK2 cascade (GO:0070374)	146	12	3.18	+	3.77	1.53E-04	9.89E-03
positive regulation of vasculature development (GO:1904018)	140	17	3.05	+	5.57	4.63E-08	9.91E-06
positive regulation of immune system process (GO:0002684)	620	35	13.51	+	2.59	7.05E-07	9.97E-05

RESULTS MAPPED Besnoitia besnoiti 12 vs 32 hpi

Identifier	Blast2GO description	GO Names	gc	width	pValue	fdr	FC
augustus_masked-19-processed-gene-1.1-	GMC oxidoreductase	F:oxidoreductase activity, acting on CH-OH group of donors; F:flavin adenine dinucleotide binding; P:oxidation-r	0,5251	1377	4,93E-02	0,004883	8,17
augustus_masked-74-processed-gene-1.43-	SRS domain-containing	C:membrane	0,5435	1047	0,0008579	0,03744	7,44
augustus_masked-38-processed-gene-3.7-	SRS domain-containing	C:membrane	0,5354	1272	1,26E-02	0,002285	6,90
maker-68-augustus-gene-0.65-	SAG-related sequence SRS22A	C:membrane	0,5615	837	6,71E-02	0,005925	6,46
augustus_masked-54-processed-gene-0.17-	SRS domain-containing	C:membrane	0,5523	1110	4,94E-02	0,004883	6,00
maker-54-augustus-gene-0.44-	SRS domain-containing	C:membrane	0,5392	1545	1,54E-08	1,22E-02	5,01
maker-68-augustus-gene-0.51-	SRS domain-containing	C:membrane	0,5804	1182	1,27E-02	0,002285	4,91
augustus_masked-38-processed-gene-3.20-	SRS domain-containing	C:membrane	0,5303	1137	0,0003837	0,02117	4,59
maker-1-augustus-gene-6.28-	---NA---		0,5234	384	6,26E-10	2,49E-06	3,54
augustus_masked-74-processed-gene-1.12-	SRS domain-containing	C:membrane	0,5595	1185	0,0003199	0,01815	3,41
augustus_masked-74-processed-gene-1.30-	SRS domain-containing	C:membrane	0,5297	1533	1,97E-02	0,002788	3,00
augustus_masked-4-processed-gene-4.24-	---NA---		0,5765	654	2,18E-02	0,002872	2,96
augustus_masked-38-processed-gene-3.4-	SRS domain-containing	C:membrane	0,5149	1140	4,77E-02	0,004883	2,87
augustus_masked-99-processed-gene-0.31-	SAG-related sequence SRS38C	C:membrane	0,5414	1110	2,28E-02	0,002872	2,80
maker-42-augustus-gene-0.52-	transmembrane	C:integral component of membrane	0,5583	5268	1,60E-03	0,0005361	2,70
augustus_masked-15-processed-gene-3.1-	rhoptry kinase family ROP40 (incomplete catalytic triad)	F:ATP binding; P:entry into host; C:rhoptry; C:membrane; F:protein kinase activity; P:phosphorylation; F:transferase	0,5577	1551	1,89E-02	0,002775	2,65
augustus_masked-4-processed-gene-3.7-	SAG-related sequence SRS40F	C:membrane	0,5427	1113	1,49E-02	0,002372	2,57
augustus_masked-99-processed-gene-0.14-	SRS domain-containing	C:membrane	0,5399	978	0,0001064	0,00845	2,53
maker-37-augustus-gene-0.43-	hypothetical protein TGMAS_315750		0,5406	960	4,86E-02	0,004883	2,47
maker-32-augustus-gene-1.44-	phosphatase 2C domain-containing	F:protein serine/threonine phosphatase activity; C:protein serine/threonine phosphatase complex; P:protein dep	0,5269	1452	1,35E-05	1,22E-02	2,44
augustus_masked-33-processed-gene-1.6-	transmembrane	C:integral component of membrane	0,5278	648	0,001245	0,04756	2,44
maker-13-augustus-gene-2.38-	hypothetical protein TGME49_211030		0,544	579	5,54E-02	0,00524	2,40
maker-22-augustus-gene-2.52-	SCP family extracellular subfamily	C:extracellular region	0,5645	822	1,75E-02	0,002666	2,38
augustus_masked-67-processed-gene-0.16-	rhoptry kinase family ROP37 (incomplete catalytic triad)	F:ATP binding; F:protein kinase activity; P:protein phosphorylation	0,5468	1944	4,78E-03	0,001186	2,34
augustus_masked-74-processed-gene-1.38-	SRS domain-containing	C:membrane	0,5163	1044	1,35E-05	0,002331	2,33
augustus_masked-1-processed-gene-0.17-	rhoptry 5B	F:ATP binding; F:protein kinase activity; P:protein phosphorylation	0,5782	1989	1,62E-06	0,0005361	2,29
maker-2-augustus-gene-2.36-	phosphorylase family	P:nicotinamide metabolic process; P:pyrimidine nucleobase metabolic process; P:nicotinate nucleotide metab	0,5658	912	1,09E-02	0,00216	2,29
augustus_masked-64-processed-gene-0.27-	photosensitized INA-labeled PHIL1		0,5887	654	2,77E-02	0,00323	2,26
augustus_masked-20-processed-gene-1.3-	PAP2 superfamily	F:phosphatidate phosphatase activity; P:glycerolipid metabolic process; C:membrane; P:phospholipid catabolic	0,5147	750	6,68E-05	0,005925	2,25
augustus_masked-99-processed-gene-0.12-	rhoptry kinase family ROP39	F:ATP binding; F:protein kinase activity; P:protein phosphorylation	0,5654	1698	0,0001011	0,008364	2,25
augustus_masked-34-processed-gene-0.20-	hypothetical protein TGGT1_202200		0,533	2105	4,53E-04	0,0001798	2,23
maker-19-augustus-gene-5.93-	alanine dehydrogenase	F:alanine dehydrogenase activity; P:electron transport; P:reductive tricarboxylic acid cycle; P:L-alanine catabolic	0,5659	963	6,80E-03	0,0015	2,21
maker-43-augustus-gene-3.31-	rhoptry ROP12		0,5874	681	2,67E-02	0,00321	2,19
augustus_masked-25-processed-gene-1.28-	rhoptry kinase family ROP11 (incomplete catalytic triad)	F:ATP binding; F:protein kinase activity; P:protein phosphorylation	0,5785	1485	3,52E-05	0,003994	2,18
augustus_masked-38-processed-gene-3.40-	SRS domain-containing	C:membrane	0,5695	1115	0,0002742	0,01729	2,18
augustus_masked-17-processed-gene-0.3-	alpha-galactosidase	P:carbohydrate metabolic process; F:hydrolase activity, hydrolyzing O-glycosyl compounds	0,6131	2313	0,0001665	0,0116	2,18
maker-18-augustus-gene-4.90-	RNA recognition motif (or RNP domain)	F:nucleotide binding; F:nucleic acid binding	0,5975	405	5,04E-02	0,004883	2,17
maker-104-augustus-gene-0.27-	microneme MIC2		0,5958	2244	2,38E-04	0,0001184	2,16
augustus_masked-74-processed-gene-1.32-	SRS domain-containing	C:membrane	0,5565	1071	0,001167	0,04591	2,15
maker-41-augustus-gene-1.29-	tryptophanyl-tRNA synthetase (2)	F:ATP binding; C:cytoplasm; P:tryptophanyl-tRNA aminoacylation; P:tryptophan metabolic process; F:tryptophan-	0,5691	2295	6,40E-06	8,47E-03	2,13
maker-34-augustus-gene-0.55-	transmembrane	C:integral component of membrane	0,5541	462	0,0001701	0,01165	2,13
maker-18-augustus-gene-1.41-	2OG-Fe(II) oxygenase family	F:L-ascorbic acid binding; F:iron ion binding; F:oxidoreductase activity, acting on paired donors, with incorporati	0,5747	1218	0,0001478	0,01048	2,12
maker-86-augustus-gene-0.75-	microneme MIC11		0,5143	630	3,15E-06	0,000834	2,12
maker-31-augustus-gene-2.69-	conserved hypothetical protein		0,5461	1203	2,14E-03	0,0006062	2,11
augustus_masked-38-processed-gene-0.8-	rhoptry kinase family ROP41	F:ATP binding; F:protein kinase activity; P:protein phosphorylation	0,5222	1350	0,0001286	0,009637	2,11
maker-3-augustus-gene-0.30-	zinc finger (CCCH type) motif-containing	F:metal ion binding	0,5436	447	5,57E-03	0,0013	2,11
maker-37-augustus-gene-1.74-	inner membrane complex 22		0,5931	720	5,85E-02	0,005399	2,09
augustus_masked-57-processed-gene-0.27-	---NA---		0,5407	984	3,79E-02	0,004177	2,08
maker-64-augustus-gene-0.58-	rhoptry ROP6		0,5929	1518	1,48E-02	0,002372	2,08
maker-58-augustus-gene-0.51-	TPA: Translation initiation factor IF-2		0,5853	1695	0,0001879	0,01265	2,08
maker-18-augustus-gene-4.75-	rhoptry neck RON3		0,5372	5907	1,67E-04	9,46E-05	2,07
augustus_masked-20-processed-gene-2.19-	gliding-associated 80		0,621	1095	7,08E-02	0,005979	2,06
maker-39-augustus-gene-4.42-	conserved *Plasmodium* protein		0,5614	1092	0,000307	0,01793	2,05

augustus_masked-12-processed-gene-0.17-	kinase domain	F:ATP binding; F:protein kinase activity; P:protein phosphorylation	0,5651	3753	0,0007652	0,03454	2,02
augustus_masked-91-processed-gene-0.1-	rhoptry kinase family	F:ATP binding; F:protein kinase activity; P:protein phosphorylation	0,5691	1736	7,01E-02	0,005979	2,02
maker-89-augustus-gene-0.50-	inner membrane complex 18		0,6291	1092	0,0009643	0,03991	2,01
augustus_masked-1-processed-gene-4.20-	microneme MIC6	F:protein binding; F:calcium ion binding	0,5552	924	3,55E-04	0,0001565	2,01
augustus_masked-74-processed-gene-1.36-	SRS domain-containing	C:membrane	0,5299	1004	0,0002475	0,01586	2,00
maker-39-augustus-gene-3.32-	hypothetical protein HHA_225560		0,5742	3088	0,0002271	0,01478	1,99
maker-64-augustus-gene-0.67-	inner membrane complex 24		0,5131	267	0,0003007	0,01792	1,99
augustus_masked-39-processed-gene-3.15-	transmembrane	C:integral component of membrane	0,5607	1434	8,30E-03	0,001736	1,98
maker-77-augustus-gene-4.38-	major facilitator family	P:transmembrane transport; C:integral component of membrane	0,5647	1539	0,0001275	0,009637	1,96
maker-20-augustus-gene-0.30-	tubulin-tyrosine ligase family	P:tyrosine metabolic process; F:tubulin-tyrosine ligase activity; P:cellular protein modification process	0,5895	5832	0,0009931	0,04067	1,96
maker-100-augustus-gene-0.56-	TPA: hypothetical protein BN1204_015380		0,5349	1047	0,0001323	0,009674	1,95
maker-35-augustus-gene-0.35-	small heat shock		0,5423	579	0,0005548	0,02687	1,94
maker-83-augustus-gene-0.18-	rhoptry neck RON5		0,5669	5931	1,77E-03	0,0005398	1,94
maker-31-augustus-gene-1.32-	microtubule associated SPM2		0,5612	1479	0,0003324	0,0186	1,93
augustus_masked-63-processed-gene-0.28-	rhoptry kinase family ROP37 (incomplete catalytic triad)	F:ATP binding; F:protein kinase activity; P:protein phosphorylation	0,5434	1807	0,0009646	0,03991	1,92
augustus_masked-24-processed-gene-1.27-	rhoptry ROP17	F:ATP binding; F:protein kinase activity; P:protein phosphorylation	0,5286	1716	0,0009238	0,03946	1,91
maker-92-augustus-gene-1.39-	rhoptry metalloprotease toxolysin TLN1	F:metal ion binding; P:metabolic process; F:peptidase activity	0,5553	4500	0,0001055	0,00845	1,91
maker-29-augustus-gene-0.63-	G2		0,5648	825	0,0006637	0,03102	1,91
augustus_masked-95-processed-gene-2.52-	rhoptry kinase family ROP32	F:ATP binding; F:protein kinase activity; P:protein phosphorylation	0,5582	1752	0,0004921	0,02506	1,90
augustus_masked-9-processed-gene-0.20-	RNA helicase-1	P:metabolic process; F:helicase activity	0,5369	1017	0,0009512	0,03991	1,90
maker-52-augustus-gene-0.20-	rhoptry neck RON4	C:membrane; C:extracellular region; C:symbiont-containing vacuole membrane	0,5621	3279	0,0003165	0,01815	1,89
augustus_masked-5-processed-gene-1.3-	leucine rich repeat-containing	F:protein binding	0,5398	804	0,0005651	0,02704	1,89
augustus_masked-99-processed-gene-0.23-	SRS domain-containing	C:membrane	0,5485	1134	0,001009	0,04091	1,87
maker-95-augustus-gene-2.58-	p25-alpha family		0,5342	483	0,0004665	0,02406	1,87
augustus_masked-91-processed-gene-0.2-	rhoptry kinase family	F:ATP binding; F:protein kinase activity; P:protein phosphorylation	0,5684	1740	0,0001118	0,008705	1,87
augustus_masked-16-processed-gene-0.22-	rhoptry neck RON8		0,5848	9258	2,31E-02	0,002872	1,85
maker-24-augustus-gene-1.38-	rhoptry neck RON10		0,5724	2706	0,0004464	0,02336	1,84
maker-11-augustus-gene-1.40-	conserved hypothetical protein		0,6023	709	0,0006562	0,03102	1,83
augustus_masked-95-processed-gene-0.5-	transmembrane	C:integral component of membrane	0,5444	2592	2,24E-02	0,002872	1,83
augustus_masked-23-processed-gene-2.4-	---NA---		0,599	1182	0,0004452	0,02336	1,83
maker-35-augustus-gene-1.42-	thioredoxin	F:protein-disulfide reductase activity; P:oxidation-reduction process; C:microtubule associated complex	0,5991	666	0,0005033	0,02531	1,81
augustus_masked-14-processed-gene-0.13-	Tsp1 domain-containing TSP12 (Precursor) related		0,539	4002	0,001305	0,04938	1,80
maker-19-augustus-gene-0.31-	GPI-anchored micronemal	F:calcium ion binding; C:extracellular region	0,6166	2856	0,0007979	0,03561	1,79
augustus_masked-74-processed-gene-1.40-	SRS domain-containing	C:membrane	0,5211	1113	0,0005098	0,02531	1,77
maker-24-augustus-gene-3.71-	conserved hypothetical protein		0,5443	948	0,000447	0,02336	1,77
maker-39-augustus-gene-4.47-	major facilitator family	C:integral component of membrane	0,5429	1770	0,0005441	0,02668	1,77
augustus_masked-1-processed-gene-8.17-	SAG-related sequence SRS23	C:membrane	0,5403	981	0,0002933	0,01792	1,76
augustus_masked-40-processed-gene-0.12-	SAG-related sequence SRS23	C:membrane	0,5604	1110	0,0008834	0,03814	1,76
maker-57-augustus-gene-0.46-	rhoptry neck RON6		0,5873	3492	0,0007477	0,03453	1,74
augustus_masked-99-processed-gene-0.21-	SRS domain-containing	C:membrane	0,5632	1140	0,001234	0,04756	1,73
maker-80-augustus-gene-0.32-	conserved hypothetical protein		0,548	1188	0,001047	0,042	1,72
augustus_masked-15-processed-gene-2.24-	microneme MIC1	F:protein binding	0,5411	2031	0,000134	0,009674	1,64
augustus_masked-2-processed-gene-6.14-	microneme MIC10		0,5635	591	0,0002962	0,01792	1,63
maker-36-augustus-gene-3.26-	D-3-phosphoglycerate dehydrogenase	F:NAD binding; F:phosphoglycerate dehydrogenase activity; P:L-serine biosynthetic process; P:oxidation-reductio	0,5338	1821	0,001159	0,04591	1,58
maker-20-augustus-gene-0.33-	nucleoside transporter	F:nucleoside transmembrane transporter activity; C:integral component of membrane; P:nucleoside transport	0,6092	2221	0,0004273	0,02325	-1,86
maker-10-augustus-gene-1.53-	chaperonin mitochondrial precursor	F:ATP binding; C:cytoplasm; P:protein refolding	0,5141	1770	0,0003022	0,01792	-1,99
augustus_masked-99-processed-gene-0.18-	SRS domain-containing	C:membrane	0,5629	1128	0,0002189	0,01449	-2,15
augustus_masked-4-processed-gene-2.29-	major facilitator family	P:transmembrane transport; C:integral component of membrane	0,6347	3129	0,001218	0,04744	-2,28
augustus_masked-32-processed-gene-0.24-	GDA1 CD39 (nucleoside phosphatase) family	P:metabolic process; F:nucleoside-triphosphatase activity; C:extracellular region	0,5274	201	4,53E-06	8,47E-03	-3,19
augustus_masked-38-processed-gene-1.6-	hypothetical protein HHA_266380		0,6586	3492	0,0008444	0,03727	-3,58
maker-4-augustus-gene-5.34-	WD G-beta repeat-containing	F:protein binding	0,66	3735	0,0007609	0,03454	-4,04
maker-42-augustus-gene-1.23-	ATP-dependent metallopeptidase subfamily	F:ATP binding; C:membrane; P:proteolysis; F:metalloendopeptidase activity; F:microtubule-severing ATPase activ	0,6677	3274	3,34E-05	2,21E-02	-6,38

ANEXO 2: ARTÍCULOS PUBLICADOS/PUBLISHED MANUSCRIPTS

- *In vitro* efficacy of bumped kinase inhibitors against *Besnoitia besnoiti* tachyzoites.

- Repurposing of commercially available anti-coccidials identifies diclazuril and decoquinate as potential therapeutic candidates against *Besnoitia besnoiti* infection.-

International Journal for Parasitology xxx (2017) xxx–xxx

Contents lists available at ScienceDirect

International Journal for Parasitology

journal homepage: www.elsevier.com/locate/ijpara

In vitro efficacy of bumped kinase inhibitors against *Besnoitia besnoiti* tachyzoites

Alejandro Jiménez-Meléndez [a], Kayode K. Ojo [b], Alexandra M. Wallace [b], Tess R. Smith [b], Andrew Hemphill [c], Vreni Balmer [c], Javier Regidor-Cerrillo [a], Luis M. Ortega-Mora [a], Adrian B. Hehl [d], Erkang Fan [e], Dustin J. Maly [e,f], Wesley C. Van Voorhis [b], Gema Álvarez-García [a,*]

[a] *SALUVET, Animal Health Department, Faculty of Veterinary Sciences, Complutense University of Madrid, Ciudad Universitaria s/n, 28040 Madrid, Spain*
[b] *Center for Emerging and Re-emerging Infectious Diseases (CERID), Division of Allergy and Infectious Diseases, Department of Medicine, University of Washington, Seattle, WA, USA*
[c] *Institute of Parasitology, Vetsuisse Faculty, University of Berne, Länggass-Strasse 122, CH-3012 Berne, Switzerland*
[d] *Institute of Parasitology, University of Zurich, Winterthurerstrasse 266a, Zurich CH-8057, Switzerland*
[e] *Department of Biochemistry, University of Washington, Seattle, WA 98195-7742, USA*
[f] *Department of Chemistry, University of Washington, Seattle, WA 98195-1700, USA*

ARTICLE INFO

Article history:
Received 27 April 2017
Received in revised form 25 August 2017
Accepted 29 August 2017
Available online xxxx

Keywords:
Besnoitia besnoiti
Chemotherapy
Bumped kinase inhibitors
CDPK1
In vitro assay

ABSTRACT

Besnoitia besnoiti is an apicomplexan parasite responsible for bovine besnoitiosis, a chronic and debilitating disease that causes systemic and skin manifestations and sterility in bulls. Neither treatments nor vaccines are currently available. In the search for therapeutic candidates, calcium-dependent protein kinases have arisen as promising drug targets in other apicomplexans (e.g. *Neospora caninum*, *Toxoplasma gondii*, *Plasmodium* spp. and *Eimeria* spp.) and are effectively targeted by bumped kinase inhibitors. In this study, we identified and cloned the gene coding for *Bb*CDPK1. The impact of a library of nine bumped kinase inhibitor analogues on the activity of recombinant *Bb*CDPK1 was assessed by luciferase assay. Afterwards, those were further screened for efficacy against *Besnoitiabesnoiti* tachyzoites grown in Marc-145 cells. Primary tests at 5 μM revealed that eight compounds exhibited more than 90% inhibition of invasion and proliferation. The compounds BKI 1294, 1517, 1553 and 1571 were further characterised, and EC_{99} (1294: 2.38 μM; 1517: 2.20 μM; 1553: 3.34 μM; 1571: 2.78 μM) were determined by quantitative real-time polymerase chain reaction in 3-day proliferation assays. Exposure of infected cultures with EC_{99} concentrations of these drugs for up to 48 h was not parasiticidal. The lack of parasiticidal action was confirmed by transmission electron microscopy, which showed that bumped kinase inhibitor treatment interfered with cell cycle regulation and non-disjunction of tachyzoites, resulting in the formation of large multi-nucleated complexes which co-existed with viable parasites within the parasitophorous vacuole. However, it is possible that, in the face of an active immune response, parasite clearance may occur. In summary, bumped kinase inhibitors may be effective drug candidates to control *Besnoitiabesnoiti* infection. Further in vivo experiments should be planned, as attainment and maintenance of therapeutic blood plasma levels in calves, without toxicity, has been demonstrated for BKIs 1294, 1517 and 1553.

1. Introduction

Besnoitia besnoiti is an apicomplexan parasite responsible for bovine besnoitiosis, a chronic and debilitating disease of cattle that causes systemic and skin manifestations, as well as sterility in bulls. At present, it is considered a re-emerging cattle disease in Europe. It has spread towards northern and central eastern Europe, given the absence of effective treatments or vaccines and the lack of common policies concerning animal trade (European Food Safety Authority, 2010; Álvarez-García et al., 2013; Álvarez-García, 2016).

Taxonomically, *B. besnoiti* belongs to the subfamily Toxoplasmatinae, together with other cyst-forming parasites of veterinary and human health importance, such as *Neospora caninum* and *Toxoplasma gondii*, respectively. Similarly, it has a heteroxenous life cycle but the definitive host has not yet been identified (Diesing et al., 1988; Basso et al., 2011). Domestic bovines and wild ruminants such as antelopes and roe deer (Arnal et al., 2017) act as

* Corresponding author.
E-mail address: gemaga@ucm.es (G. Álvarez-García).

http://dx.doi.org/10.1016/j.ijpara.2017.08.005
0020-7519/

intermediate hosts, where two asexual infective stages of the parasite develop: initially, fast-replicating tachyzoites are found inside endothelial cells of blood vessels during the acute stage of the disease, which may go unnoticed due to the non-specific clinical signs such as fever, anorexia or swelling of lymph nodes (reviewed by Álvarez-García et al., 2014). During the chronic stage of the disease, when the immune response is elicited against the parasite, tachyzoites switch into slowly dividing bradyzoites. Bradyzoites form tissue cysts are located mainly in the subcutaneous (s.c.) connective tissue and are responsible for the characteristic lesions found during the chronic stage.

In bovines, treatments attempted for besnoitiosis have included the use of formalin, sulphametazine, toltrazuril or oxytetracycline (Franc and Cardiegues, 1999). In laboratory settings, experimentally infected rabbits were treated with formalin, pentamidines, sulphonamides, trimethoprim, pyrimethamine and oxytetracycline (Pols, 1960; Shkap et al., 1985, 1987) and oxytetracycline was applied in gerbils (Shkap et al., 1985). Unfortunately, all these studies had been carried out under very different experimental conditions with a limited number of animals, and results were mainly based on clinical inspection and histopathology. In vitro studies showed that arylimidamides (Cortes et al., 2011) and thiazolides (Cortes et al., 2007) have activity against *B. besnoiti*, but further research with well-established and reliable experimental models, both in vitro and in vivo, is urgently needed.

Apicomplexan calcium-dependent protein kinases (CDPKs) belong to a superfamily of serine-threonine kinases. They are conserved enzymes among members of the phylum Apicomplexa, but are absent in mammalian cells (Ward et al., 2004; Srinivasan and Krupa, 2005; Billker et al., 2009). CDPKs thus represent parasite-specific drug targets. Bumped kinase inhibitors (BKIs), namely pyrazolo-pyrimidine and 5-aminopyrazole-4-carbomidecarboxa mide analogues, specifically designed to act on CDPK1 (Lourido and Moreno, 2015; Van Voorhis et al., 2017) have shown efficacy against *T. gondii* (Ojo et al., 2010; Doggett et al., 2014); *N. caninum* (Ojo et al., 2014; Winzer et al., 2015); *Babesia* spp. (Pedroni et al., 2016), *Cryptosporidium parvum* (Lendner et al., 2015) and *Plasmodium* spp. (Ojo et al., 2012; Van Voorhis et al., 2017). In *T. gondii*, CDPK1 plays a crucial role in gliding motility, microneme secretion, host cell invasion and egress, and parasite differentiation by means of calcium-dependent mechanisms (Lourido et al., 2010; Lourido and Moreno, 2015). Bumped kinase inhibitors (Doerig et al., 2002; Greenbaum, 2008) selectively bind to a hydrophobic pocket adjacent to the ATP binding site. This hydrophobic pocket is made accessible by a small "gatekeeper" amino-acid such as glycine, a unique characteristic of some apicomplexan CDPK1 s. Pharmacological inhibition of either *Tg*CDPK1 or *Nc*CDPK1 with BKIs in vitro blocks host cell invasion, thereby inhibiting parasitic growth (Ojo et al., 2010; Winzer et al., 2015).

Currently, the exact mechanisms of host cell invasion and proliferation of *B. besnoiti* are not well understood, but Frey et al. (2016) demonstrated that lytic cycle events are similar to those exploited by closely related *N. caninum* and *T. gondii*. *Besnoitia besnoiti* CDPK1 has not yet been identified. However, the existence of the orthologue *Bb*CDPK1 is likely since it has been proven that members of the Toxoplasmatinae share a high degree of homology in relation to CDPK enzymes (Keyloun et al., 2014; Ojo et al., 2014). Recently, a standardised experimental in vitro model of infection using an epithelial-like cell line (Frey et al., 2016) was developed. This model allowed a detailed study of the *B. besnoiti* lytic cycle, revealing that these parasites can survive extracellularly for extended periods of time (up to 24 h p.i.), and showed that *Besnoitia* tachyzoites generally have a low invasion rate and proliferate asynchronously. The establishment of this in vitro model set the basis for performance of drug screening and testing of potential therapeutic candidates against this protozoal agent.

The rational approach followed herein has been previously exploited in the closely related protozoans *T. gondii* and *N. caninum*, where CDPK orthologues were identified and a variety of compounds were screened in in vitro assays (Van Voorhis et al., 2017). Thus, in the present study, we identified and characterised *Bb*CDPK1 and evaluated the efficacy of nine BKIs against *B. besnoiti* tachyzoites in a standardized in vitro assay model.

2. Materials and methods

2.1. Parasite maintenance and cell cultures

Marc-145 and Human Foreskin Fibroblast (HFF) cells were maintained in DMEM (Gibco, Thermo Fisher Scientific, Waltham, MA, USA) with phenol red supplemented with 10% heat inactivated and sterile filtrated faetal calf serum (FCS) (Gibco, Thermo Fisher Scientific, Waltham, MA, USA), 5 mM HEPES (pH 7.2), 2 mM glutamine (Lonza Group, Basel, Switzerland), and a mixture of penicillin (100 U/ml), streptomycin (100 µg/ml) and amphotericin B (Lonza Group, Basel, Switzerland) as previously published (Frey et al., 2016). They were cultured at 37 °C and 5% CO_2 in 75 or 25 cm^2 tissue culture flasks. Marc-145 cell cultures were passaged twice each week, HFFs once each week. *Besnoitia besnoiti* Spain1 (Bb-Spain1) used for all in vitro assays and Evora (Bb-Evora) strains were maintained by serial passages in Marc-145 cells in the same culture medium with 5% FCS (Fernández-García et al., 2009a). FCS used in all the experiments was previously checked for the absence of specific IgG against *B. besnoiti*, *N. caninum* and *T. gondii* by IFAT (Fernández-García et al., 2009b).

Tachyzoites were harvested 3 days p.i., when the majority of them were still intracellular, by recovering the infected cell monolayer with a rubber cell scraper, followed by repeated passages through a 25 gauge needle at 4 °C and separation from cell debris on a PD-10 column (GE Healthcare, Little Chalfont, United Kingdom) (Frey et al., 2016). Tachyzoite viability was confirmed by trypan blue exclusion followed by counting in a Neubauer chamber. Purified tachyzoites were used to infect Marc-145 or HFF cell monolayers as described in Section 2.5.1.

2.2. BbCDPK1 identification, sequencing and cloning

2.2.1. NCBI BLAST® search and Clustal analyses

The amino acid sequence of *Nc*CDPK1 (NCLIV_011980) from ToxoDB (www.toxodb.org) was used in order to retrieve orthologous genes in apicomplexan parasites using the NCBI BLAST® tool (https://blast.ncbi.nlm.nih.gov/Blast.cgi). Nucleotide sequences coding for related sequences of CDPK1 in *T. gondii*, *N. caninum* and *Hammondia hammondi* were considered (Supplementary Fig. S1). Clustal Omega (http://www.ebi.ac.uk/Tools/msa/clustalo/) was employed to align nucleotide and protein sequences. Next, three pairs of primers (Table 1) were designed in conserved, homologous regions (BbCDPK1Fw2; BbCDPK1Fw3, BbCDPK1Rv1 and BbCDPK1FwC) (Supplementary Fig. S1).

Total RNA from the Bb-Evora strain collected from infected Marc-145 monolayers at 8 h p.i. was stored in RNA later reagent (Qiagen, Valencia, CA, USA) and cDNA was synthetized using a SuperScript Vilo® cDNA synthesis kit (Life technologies, Thermo Fisher Scientific, Waltham, MA, USA) according to the manufacturer's instructions. cDNA was diluted 1:10 in molecular grade distiled H_2O. cDNA from the Nc-Liverpool strain of *N. caninum* was also employed to test specificity of the primers used.

polymerase chain reaction (PCR) conditions were 94 °C for 5 min, 35 cycles at 94 °C for 30 s, 60 °C for 1 min and 72 °C for 1 min 30 s and a final elongation at 72 °C for 10 min. PCRs were carried out with the Platinum® Taq DNA Polymerase High Fidelity

Please cite this article in press as: Jiménez-Meléndez, A., et al. In vitro efficacy of bumped kinase inhibitors against *Besnoitia besnoiti* tachyzoites. Int. J. Parasitol. (2017), http://dx.doi.org/10.1016/j.ijpara.2017.08.005

Table 1
List of primers used in the present study.

Use	Primer sequence (5′–3′)
Protein identification and sequencing	FW2: GAAGCAGAAGACGGACAAGGAGTC FW3: GCATCATCGACTTTGGCCTCAGCA FWC: GACGAGCTCCACGCGACGCCGGGGATGTTCGTT RV1: GGT TAA TTA ATT TCC GCA GAG CTT CAA GAG CAT
Protein cloning	Bb_LIC_Fw: GGG TCC TGG TTC GAT GGG TCA GCA AGA AAG CAC GCT CGG C Bb_LIC_Rev: CTT GTT CGT GCT GTT TAC TTA GTT GCC GCA GAG CTT CAG AAG

(Invitrogen, Thermo Fisher Scientific, Waltham, MA, USA) and all primers were purchased from Sigma–Aldrich. PCR products were visualised in 1.5% agarose gel stained with ethidium bromide and next purified using the Geneclean Turbo® kit (QBiogene, Montreal, Canada) according to the manufacturer's instructions for sequencing. PCR products were directly sequenced in both directions using the Big Dye® Terminator v3.1 Cycle Sequencing Kit (Applied Biosystems, Thermo Fisher Scientific, Waltham, MA, USA) and a 3730 DNA analyser (Applied Biosystems, Thermo Fisher Scientific, Waltham, MA, USA) at the Unidad Genómica del Parque Científico de Madrid, Spain. Sequence data were analysed using BioEdit Sequence Alignment Editor v.7.0.1 (Hall, 1999) (Copyright_ 1997–2004 Tom Hall, Ibis Therapeutics, Carlsbad, CA, USA).

The sequence obtained (see Section 3.1) was compared with the *B. besnoiti* genome (the genome sequence is the property of the University of Zurich, Switzerland and will be made freely available to the community on NCBI and EuPathDB after publication). After retrieving the coding sequence using the GeneWise-Pairwise Sequence Alignment (EMBL-EBI) tool in order to process introns, a truncated region of the Bb*CDPK1* gene was amplified from *B. besnoiti* Evora strain cDNA using primers Bb_LIC_Fw (5′-GGG TCC TGG TTC GAT GGG TCA GCA AGA AAG CAC GCT CGG C-3′) and Bb_LIC_Rev (CTT GTT CGT GCT GTT TAC TTA GTT GCC GCA GAG CTT CAG AAG-3′) (data not shown). The PCR product was cloned into the ligation-independent cloning (LIC) site of expression vector pAVA0421 and expressed and purified as previously published for *Nc*CDPK1 (Ojo et al., 2014). The purified protein was visualised by SDS–PAGE and Coomassie staining (Supplementary Fig. S2).

2.2.2. In silico analysis and prediction of N-myristoylation and palmitoylation

The predicted molecular weight of *Bb*CDPK1 was obtained using ExPasy tools for prediction of protein properties (ProtParam; http://web.expasy.org/protparam). The Simple Modular Architecture Research Tool (SMART; http://smart.embl-heidelberg.de) was used to predict functional domains in proteins. Myristoylation prediction was carried out using Prosite PDOC00008 (http://www.expasy.ch/prosite/) as described by Etzold et al. (2014) for CDPKs from *C. parvum*. Palmitoylation sites were predicted with CSS-Palm 2.0 (http://csspalm.biocuckoo.org).

Modelling of *Bb*CDPK1 secondary and tertiary structures was performed using the I-TASSER online tool (http://zhanglab.ccmb.med.umich.edu) (Yang et al., 2015).

2.3. BbCDPK1 enzymatic activity assays and its inhibition by BKIs

Protein kinase activity of recombinant *Bb*CDPK1 (r*Bb*CDPK1) and inhibition of its kinase phosphorylation properties by a panel of BKIs (Keyloun et al., 2014) was measured in a non-radioactive assay using Kinase-Glo® luciferase reagent (Promega, Madison, WI, USA) as previously described (Ojo et al., 2014). Basically, this luminescence-based assay measures kinase activity in the presence or absence of inhibitors by reporting changes in initial ATP concentrations. Kinase phosphorylation reactions were performed as previously published for *Nc*CDPK1 (Ojo et al., 2014) in a 25 μL buffered solution containing 20 mM HEPES (pH, 7.5), 0.1% BSA, 10 mM $MgCl_2$, 1 mM EGTA, 2 mM $CaCl_2$, 20 μM peptide substrate (Biotin-C6-PLARTLSVAGLPGKK) (BioSyntide-2) (American Peptide Company, Inc. Sunnyvale, CA, USA), 3.5 nM *Bb*CDPK1, and 2 to 0.00012207 μM inhibitor (4-fold serial dilutions). Phosphorylation reactions were initiated by the addition of 10 μM Na_2ATP (Sigma–Aldrich, St. Louis, MO, USA). After incubating for 90 min at 30 °C, the reaction was terminated by adding EGTA to a final concentration of 5 mM. Changes in the initial ATP concentration were evaluated as a luminescence readout using a MicroBeta2 multilabel plate reader (Perkin Elmer, Waltham, MA, USA). Results were converted to percent inhibition and IC_{50} values (the concentration of compound that led to 50% inhibition of enzyme activity) using non-linear regression analysis in GraphPad Prism (GraphPad Software, La Jolla, CA, USA).

2.4. Mammalian cell toxicity assays

The potential toxicity of the compounds against a mammalian cell line was determined by an XTT cell viability assay (Panreac Applichem, Darmstadt, Germany) to quantify cell growth. Marc-145 cells in the exponential phase of growth were seeded in 96-well flat-bottomed plates at a density of 2×10^5 cells/mL containing compounds (20 mM stock solutions dissolved in dimethyl sulfoxide (DMSO) at the maximum concentration employed in our assays (5 μM) in quadruplicate and grown for 72 h at 37 °C in a 5% CO_2 humidified incubator. Afterwards, 50 μL of XTT reagent was added to each well and incubated for 4 h. Fluorescence was measured at the respective excitation and emission wavelengths of 475 nm and 660 nm in a Synergy™ H1 microplate reader (Biotek Instruments Inc, Winooski, VT, USA). The percentage of growth inhibition was computed for any BKI tested, based on the DMSO vehicle. Three independent assays were performed with nine selected BKIs employed in the screening assays.

2.5. In vitro drug efficacy

Nine BKIs previously optimised with functional groups for improved potency, selectivity and pharmacokinetic properties were selected for further studies (Supplementary Fig. S3). The purity of all compounds (>98%) was confirmed by reverse-phase HPLC and ^{1}H-Nuclear Magnetic Resonance (NMR). (Doggett et al., 2014; Ojo et al., 2014, 2016; Huang et al., 2015; Vidadala et al., 2016). BKIs were sent to Saluvet research group (Complutense University of Madrid, Spain) at a concentration of 20 mM diluted in 100% DMSO. Compounds were stored, protected from light, at -20 °C.

2.5.1. Drug screening

Marc-145 cells (5×10^4 cells per well) were incubated in culture media at 37 °C with 5% CO_2 and grown to confluence in 24-well plates. In the initial drug screening, inhibitors were added at a final concentration of 5 μM, just prior to infection with purified tachyzoites from the Bb-Spain1 strain. DMSO (as solvent) was added to negative control wells at the same final concentration. Cultures were subsequently infected with 10^3 purified tachyzoites from the Bb-Spain1 strain. Another set of experiments adding the different compounds 6 h p.i., when 50% invasion rate is reached for the strain employed (Frey et al., 2016), was also performed to address possible effects on parasite proliferation. Before

administration of the compounds, infected monolayers were gently rinsed with PBS three times in order to discard non-invaded tachyzoites. In both sets of experiments, immunofluorescence assays were performed after 3 days at 37 °C/5% CO_2 (see Section 2.6) to count invasion events per well. Each condition was assessed in triplicate and the experiments were carried out in three independent assays. Those compounds that showed the highest values of both parasite invasion and proliferation inhibition were selected for further experiments.

2.5.2. Short-term assays: EC_{50} and EC_{99} determination

Marc-145 cells were grown as mentioned above in 24 well plates. Just prior to infection, BKIs were added at final concentrations ranging from 5 nM to 5 μM for determination of EC_{50} and EC_{99} (the effective concentration to reduce parasite numbers 50% or 99%, respectively) values. Then, Bb-Spain1 tachyzoites were added at a parasite:host cell ratio of 1:100 (10^3 tachyzoites per well). DMSO control wells were also included in each culture plate.

A similar experiment to determine the effects of the compounds on *B. besnoiti* proliferation was also performed. Here, infection of host cell monolayers was performed as previously described and compounds 1294, 1517, 1553 or 1571 were added at a final concentration from 5 nM to 5 μM per well at 24 h p.i., when the parasite invasion is completed (Frey et al., 2016). Prior to the addition of the compounds, three washes with PBS were performed in order to discard non-invaded tachyzoites.

After 72 h p.i., samples were collected using a lysis solution (100 μL of PBS, proteinase K and AL Buffer) according to the manufacturer's instructions contained in the DNeasy® Blood and Tissue kit (Qiagen, Valencia, CA, USA), for further DNA extraction and quantitative real-time (qPCR) to quantify the number of parasites in each well. Immunofluorescence staining was also performed as stated below for each compound and concentration used at 72 days p.i. Each condition was assessed in triplicate and the experiments were carried out in three independent assays.

2.5.3. Characterisation of long-term effects of BKI treatments on B. besnoiti tachyzoites

Tachyzoites from the Bb-Spain1 strain were grown as previously stated and compounds 1294 1517, 1553 and 1571 were added just prior to infection at the previously established EC_{99} concentration. Drugs were left in the cultures for 6, 24 or 48 h. Drugs containing media were discarded and fresh culture media were added. Samples were collected at 1, 3 and 5 days post treatment for subsequent qPCR analysis. IFAT was performed at 8 and 10 days post treatment to assess whether any tachyzoites were able to re-infect host cells (Winzer et al., 2015). Each condition was assessed in triplicate and the experiments were carried out in three independent assays.

2.5.4. Transmission Electron Microscopy analysis of B. besnoiti – infected HFFs treated with selected BKIs

HFF cell cultures were maintained in T25 tissue culture flasks and were infected with 10^7 Bb-Spain1 tachyzoites (parasite:host cell ratio of 10:1). After allowing the tachyzoites to invade the host cells for 3 h, monolayers were washed three times with PBS and treated with BKIs at a concentration of 5 μM. Samples were processed for Transmission Electron Microscopy (TEM) analysis at different time points after infection (4, 6 and 8 days) as described earlier (Winzer et al., 2015; Müller et al., 2017).

2.6. Immunofluorescence staining

For immunofluorescence staining, supernatants of the cell cultures were discarded at 72 h p.i., wells were washed three times with PBS and subsequently fixated with ice-cold methanol or paraformaldehyde 3%- glutaraldehyde 0.05% for 10 min. Then, wells were washed a further three times with PBS. Afterwards, those were incubated with 300 μL/well of Triton-X 100 (0.2%) in PBS for 30 min at 37 °C, followed by three additional washes with PBS. As primary antibody, a polyclonal rabbit-anti tachyzoite Bb-Spain1 (Gutiérrez-Expósito et al., 2013) was added at a dilution of 1:1000 in PBS and incubated for 1 h at 37 °C. After three additional washes with PBS, 250 μL of Alexa Fluor® 488 Goat Anti-Rabbit IgG (H + L) (Life technologies, Carlsbad, CA, USA) were added per well at a dilution of 1:1000. The plates were incubated for 45 min at room temperature in the darkness and washed three times with PBS. In the final wash, DAPI stain was included. Finally, the plates were washed with distiled water and the total number of invasion events per well was counted using an inverted fluorescence microscope (Nikon Eclipse TE200) at 200× magnification. Two categories of plaque forming tachyzoites were distinguished: parasitophorous vacuoles (PVs) and lysis plaques, as described by Frey et al. (2016). For the isolate employed, 80% of the invasion events consisted of lysis plaques at 72 h p.i.

2.7. DNA extraction and quantitative real-time PCR (qPCR)

The harvested cell culture samples were incubated for 10 min at 56°C. Afterwards, DNA was purified using the spin column protocol for cultured cells according to the manufacturer's instructions contained in the DNeasy®Blood and Tissue kit (Qiagen, Valencia, CA, USA). DNA was eluted in 200 μL of elution buffer. The DNA content and purity of each sample was measured by UV spectrometry (Nanophotometer®, Implen GmbH, Munich, Germany).

The BbRT2 qPCR assay for specific detection of *Besnoitia* spp. DNA from ungulates (i.e., *B. besnoiti*, *Besnoitia tarandi, Besnoitia caprae* and *Besnoitia bennetti*) was performed according to Frey et al. (2016). Briefly, each 20 μL reaction contained 10 μl of Power SYBR Green master mix® (Applied Biosystems, Thermo Fisher Scientific, Foster City, CA, USA), 0.5 μl of primer Bb3 (5′-CAA CAA GAG CAT CGC CTT C-3′; 20 μM), 0.5 μl of primer Bb 6 (5′-ATT AAC CAA TCC GTG ATA GCA G-3′; 20 μM), and 4 μl of water. The qPCRs were run on a 7300 Real-Time PCR System® (Applied Biosystems). Twenty to 100 ng of DNA in a volume of 5 μl was added to each reaction. The DNA positive control was extracted from *B. besnoiti* tachyzoites cultured in vitro. The product of the DNA extraction process using water instead of cells was used as a negative control. In each qPCR, 10-fold serial dilutions of genomic DNA corresponding to 0.1–100,000 Bb-Spain1 tachyzoites were included. The cycling conditions were 10 min at 95 °C followed by 40 cycles of 95 °C for 15 s and 60 °C for 1 min. Fluorescence emission was measured during the 60 °C step. A dissociation stage was added at the end of each run, and the melting curves were analysed. BbRT2-PCR was run in duplicate for each sample. The threshold cycle values (Ct-values) obtained for positive samples in the BbRT2-PCR were also expressed as tachyzoites per reaction using the standard curve included in each run.

2.8. Data analyses

The cytotoxicity of screened BKIs was compared by a one-way ANOVA test. For the determination of the percentage of inhibition (%) in the in vitro drug screening, first the invasion rate (IR) was calculated by counting all the events per well. Then, invasion rates were related to the negative control (DMSO) to determine the relative invasion rate (RIR) of the parasite for each condition. Afterwards, the% of inhibition was determined as indicated below.

$$\%\text{RIR} = (\text{IR treated well}/\text{IR DMSO well}) \times 100$$

$$\%\text{Inhibition} = 100 - \%\text{RIR}$$

For the compounds that showed the highest percentages of inhibition in the initial drug screening at 0 and 6 h p.i., tachyzoite yields after 72 h of incubation were determined by qPCR for EC_{50} and EC_{99} calculations, and adjusted to the amount of DNA quantified by spectrophotometry in each sample. The relative growth for each drug concentration was determined relative to the DMSO control, using the tachyzoite yield per ng of DNA. Afterwards, the EC_{50} and EC_{99} concentrations were determined using an ED_{50} plus sheet for Microsoft Excel after a logarithmic transformation of the data.

The Kruskal–Wallis test was performed to compare the efficacy of the nine compounds against *B. besnoiti* in the drug screening, and to search for differences among the four compounds selected for determination of EC_{50} and EC_{99} values. This test was also used to address whether there were differences among the different concentrations of BKIs tested. Finally, a two-way ANOVA test was employed to compare the different treatment durations employed. All statistical analyses were performed using the software GraphPad Prism® 6.0 (GraphPad Software, San Diego, CA, USA). For all statistical analyses, $P < 0.05$ was considered significant.

3. Results

3.1. BbCDPK1 identification, sequencing and cloning

The partial sequence of *Bb*CDPK1 initially obtained consisted of a 1160 bp sequence that showed features characteristic of a CDPK1 enzyme, including the amino-acid sequence of the putative active site of the enzyme, which was identical to the one present in *Nc*CDPK1 (Fig. 1). When the whole sequence data were subjected to intron processing, the complete coding sequence obtained showed 95% identity both in nucleotide and amino acid sequences compared with *Nc*CDPK1 and *Tg*CDPK1 sequences, including the putative active site with a glycine gatekeeper (Fig. 1; GenBank® accession number N° **KY991370**). The expected molecular weight of the obtained protein was 56 kDa (Expasy ProtParam). Using the Simple Modular Architecture Research Tool (EMBLEM, Heidelberg, Germany) for protein sequence analysis and classification, the sequence obtained showed a kinase domain with an ATP binding site and four EF hand domains for calcium binding, as described for other apicomplexan CDPK1 enzymes (Fig. 1). Moreover, putative sites of N-mirystoilation were found in the N-terminal region of the protein, as well as one site of palmytoilation. *Bb*CDPK1 showed 98 and 98.4% amino acid identity in the kinase domain with *Tg*CDPK1 and *Nc*CDPK1, respectively.

Not surprisingly, results from I-TASSER modelling showed that *Tg*CDPK1 has the closest structural similarity.

3.2. Screening of recombinant BbCDPK1 using BKI-analogues

Due to the close homology of *Bb*CDPK1 with CDPK1 in other apicomplexans, the enzyme was expressed as a recombinant protein to test the effects of BKI analogues on its activity. Upon separation by SDS–PAGE, recombinant *Bb*CDPK1 exhibited a molecular weight of 57 kDa (Fig. 1). Nine BKIs, namely BKI-1294, 1605, 1649, 1517, 1553, 1571, 1575, 1586 and 1597, inhibited *Bb*CDPK1 with IC_{50} values in the lower nanomolar range (Table 2). Thus, these compounds were further assessed in cellular assays. The activity of the recombinant enzyme was proven to be calcium-dependent, so it is highly unlikely that the activity was not associated with the recombinant enzyme itself.

3.3. Cytotoxicity in Marc-145 cells

When the compounds were added to uninfected Marc-145 cells at the highest concentration employed in the in vitro assays

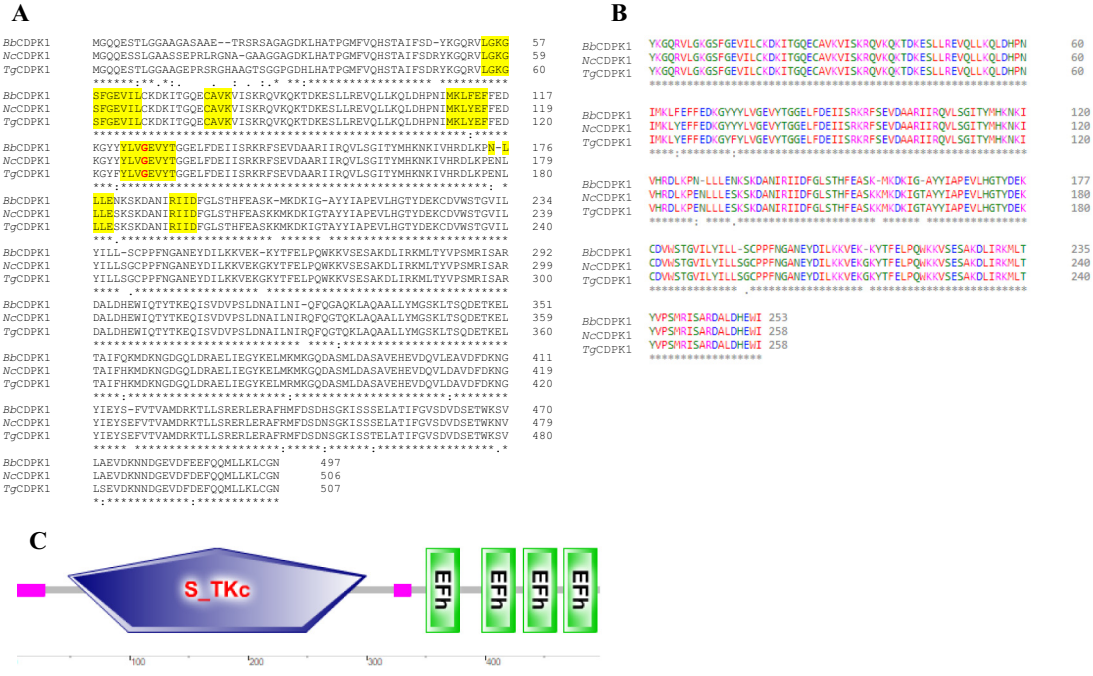

Fig. 1. Sequence features of *Bb*CDPK1 (GenBank® accession number **KY991370**). (A) Alignment of amino acids sequences of *Bb*CDPK1, *Nc*CDPK1 and *Tg*CDPK1. Yyellow highlighted amino acids were postulated by Keyloun et al. (2014) to contribute to the potential activity or resistance of CDPK1 enzymes to bumped kinase inhibitors. Gatekeeper (Gly) is marked in red. (B) Alignment of amino acid sequences of the kinase domain of *Bb*CDPK1, *Nc*CDPK1 and *Tg*CDPK1. (C) Simple Modular Architecture Research Tool (SMART) image of *Bb*CDPK1, with the serin-threonin kinase domain and four calcium-binding EF hands. *Bb*, *Besnoitia Besnoiti*, *Nc*, *Neospora caninum*, *Tg*, *Toxoplasma gondii*.

Please cite this article in press as: Jiménez-Meléndez, A., et al. In vitro efficacy of bumped kinase inhibitors against *Besnoitia besnoiti* tachyzoites. Int. J. Parasitol. (2017), http://dx.doi.org/10.1016/j.ijpara.2017.08.005

Table 2
Activity of bumped kinase inhibitors screened against *Besnoitia besnoiti* CDPK1 activity (IC_{50} values (μM)).

Compound	1294	1517	1553	1571	1575	1586	1597	1605	1649
IC_{50} (r*Bb*CDPK1)	0.004	0.012	0.004	0.024	0.022	0.011	0.002	0.015	0.006

(5 μM), those did not cause significant cytotoxicity compared with DMSO ($P > 0.05$; one-way ANOVA). Percentages of cytotoxicity of the screened BKIs compared with the DMSO-treated negative control wells were as follows: 1294: 5.2%; 1517: 5.2%; 1553: 5.8%; 1571: 2.8%; 1575: 4%; 1586: 5%; 1597: 5.1%; 1605: 3.8%; 1649:5%. Moreover, upon inspection by light microscopy, no alterations in the Marc-145 cell morphology were detected.

3.4. Initial drug screening of BKIs in B. besnoiti-infected Marc-145 cells

In the initial drug treatments carried out at the time point of infection (0 h p.i.) and 6 h p.i., eight out of nine BKIs caused more than 80% of parasite growth inhibition. Compound 1649 was the least effective (63%, Kruskal–Wallis test, $P < 0.01$), whereas 1294, 1517, 1553 and 1571 were the most efficacious, and were thus selected for further studies (Table 3). Parasite growth was markedly inhibited in drug-treated wells since only parasitophorous vacuoles (PVs) were found, whilst in DMSO-treated control wells parasites were displaying the normal features of their lytic cycle at 72 h p.i. as a consequence of parasite egress (Frey et al., 2016), where most invasion events consisted of plaques lysis.

3.5. Dose–response experiments and EC_{50} and EC_{99} determination

All four selected BKIs led to a significant reduction in parasite growth when administered at concentrations higher than 0.05 μM at the time point of infection (Fig. 2A). When BKIs were added at 5 μM at 24 h p.i., parasite proliferation was still inhibited by 80%, indicating that these compounds inhibit both host cell invasion and intracellular proliferation (Fig. 2B). The EC_{50} and EC_{99} values determined at 0 h p.i. were largely in a similar range among these compounds, except for 1553, which appeared slightly less efficacious (Table 4). Treatments with compounds 1294 and 1517 showed the lowest parasite loads. Statistically significant differences in the number of parasites per well were found between compounds 1517 and 1571 at a concentration of 5 μM when administered at 0 h p.i. (Kruskal–Wallis, $P < 0.05$), and among the different concentrations for each BKI (Kruskal–Wallis, $P < 0.01$).

3.6. Characterisation of the long-term post-treatment effects of BKI exposure on B. besnoiti tachyzoites

Following BKI treatments for various time spans, parasite growth was hardly detected until 3 days p.i., and statistically significant differences between the four BKI-treated and DMSO-treated cultures were observed at 5 days post treatment for each of the treatment durations ($P < 0.001$, two-way ANOVA) (Fig. 3). Differences were also found among the different treatment durations (6, 24 and 48 h) for each BKI ($P < 0.001$, two-way ANOVA) (Fig. 3). Upon short treatments (6 h) with the four BKIs, compounds 1553 and 1517 showed statistically significant differences ($P < 0.01$, two-way ANOVA), and the lowest tachyzoite yield (TY) was recorded in cultures treated with compound 1553. Longer treatments for up to 24 h were more effective but failed to inhibit parasite proliferation completely, not showing statistically significant differences among the compounds. However, TYs diminished to low values after 48 h treatments with all four compounds, and this was corroborated by IFAT. Further analysis by IFAT at 8 and 10 days post treatment showed that tachyzoites remained viable and were able to re-infect host cells even after 48 h post treatment.

Table 3
Percentage of inhibition of parasite growth in the drug screening when bumped kinase inhibitors were administered at 0 or at 6 h p.i. at a concentration of 5 μM.

	Compound	1294	1517	1553	1571	1575	1586	1597	1605	1649
Time of administration	0 h p.i.	99	98	98	96	95	92	95	96	63
	6 h p.i.	90	93	96	95	89	87	83	87	63

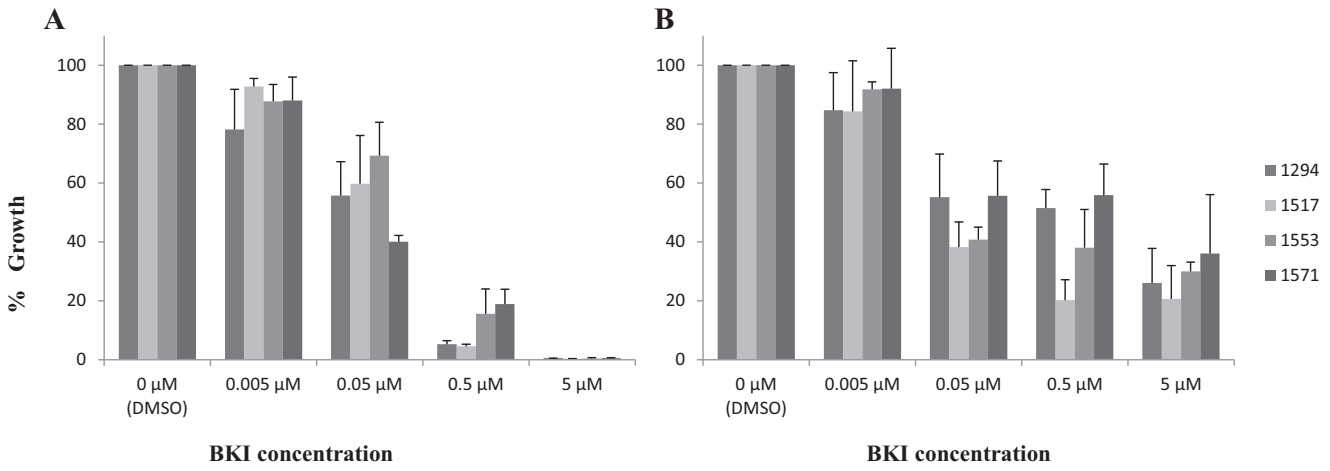

Fig. 2. Percentages of *Besnoitia besnoiti* growth inhibition (related to negative control, dimethyl sulfoxide) when bumped kinase inhibitors are administered at 0 h p.i. (A) and at 24 h p.i. (B) as determined by quantitative real-time PCR. Error bars in graphs represent the S.D.

Please cite this article in press as: Jiménez-Meléndez, A., et al. In vitro efficacy of bumped kinase inhibitors against *Besnoitia besnoiti* tachyzoites. Int. J. Parasitol. (2017), http://dx.doi.org/10.1016/j.ijpara.2017.08.005

Table 4
In vitro activity of selected bumped kinase inhibitors against *Besnoitia besnoiti* tachyzoite proliferation (EC_{50} and EC_{99} values (μM)).

Compound	1294	1517	1553	1571
EC_{50} (*B. besnoiti*)	0.045	0.067	0.097	0.051
EC_{99} (*B. besnoiti*)	2.38	2.28	3.35	2.78

Lysis plaques were present in 6 and 24 h treated wells both at 8 and 10 days post treatment, whilst in 48 h treated wells only parasitophorous vacuoles could be found.

3.7. Determination of the effects of BKIs on the ultrastructure of *B. besnoiti* tachyzoites: Transmission Electron Microscopy analysis

In control cultures, which were exposed to solvent but not to drugs, *B. besnoiti* tachyzoites underwent intracellular proliferation within a PV, surrounded by a PV membrane (PVM) (Fig. 4). In longitudinal sections they exhibited the typical features of apicomplexan parasites including a polar organisation, apical organelles such as micronemes and rhoptries, dense granules, nucleus and mitochondrion. Individual tachyzoites were more clearly visible in smaller vacuoles (Fig. 4A, B), and appeared more tightly packed in larger vacuoles (Fig. 4C, D). In the infected HFF cell cultures treated with the four selected BKIs, clear alterations were visible, which were mostly very similar for all four BKIs. As exemplified for BKI-1294 (Fig. 5A–D), a fraction of parasites was evidently distorted, with highly vacuolized cytoplasm and most likely non-viable, while inside the same host cell, still intact parasites formed multinucleated complexes, some of which remained viable for up to 8 days and clearly grew in size (Fig. 5D). These complexes were a large mass that contained several nuclei and apical complex precursors, already containing structural features such as conoids and secretory organelles. However, parasites appeared stuck in the cell cycle and could not complete cytokinesis. BKI-1571 and 1553 also induced the formation of such complexes (Fig. 5E, F), while compound 1517-treated cultures often exhibited already distorted tachyzoites and still viable complexes within the same host cells as shown in Fig. 5H. BKI-treated parasites, in general, often formed amylopectin granules (Fig. 5), which represent a source of energy in apicomplexan bradyzoites. Host cell mitochondria were often unaffected and appeared still intact, suggesting that the host cells were not extensively affected.

Compounds 1294 (Fig. 5A–D) and 1517 (Fig. 5H) showed a more dramatic effect on the ultrastructure of the tachyzoites, seemingly being more lethal with severe alterations in the cytoplasms and membranes of the parasites.

Alterations in the ultra-structure of the tachyzoites and the morphology of the PV were suggested based to IFAT results (Fig. 6). In BKI-treated wells, seemingly distorted PVs with non-discernible tachyzoites were visualised, whilst in DMSO-treated control wells parasitophorous vacuoles showed the characteristic rossetta morphology and zoites were clearly discernible by a surface staining with the antibody employed.

4. Discussion

This study shows that *Bb*CDPK1 could represent a promising drug target for the treatment of bovine besnoitiosis. First, we have shown the transcription of a CDPK1 homologue in *B. besnoiti* tachyzoites, namely *Bb*CDPK1. Next, the activity of recombinant *Bb*CDPK1 was inhibited by a panel of BKIs. Thirdly, selected BKIs were shown to have a profound impact on *B. besnoiti* host cell invasion and proliferation, and these effects were visualised by immunofluorescence and TEM.

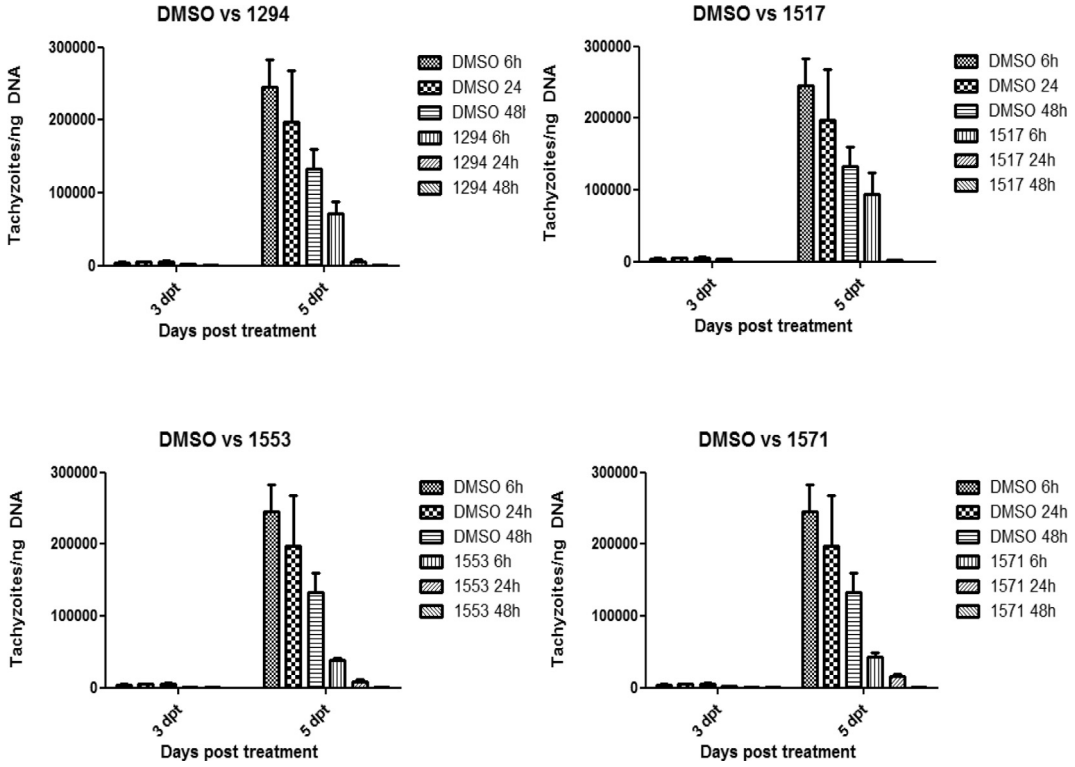

Fig. 3. Tachyzoite yield expressed as tachyzoites per ng of DNA from *Besnoitia besnoiti* cell cultures infected and treated with the four bumped kinase inhibitors selected for 6, 24 or 48 h collected at 3 and 5 days post treatment. Error bars in graphs represent the standard deviation

Please cite this article in press as: Jiménez-Meléndez, A., et al. In vitro efficacy of bumped kinase inhibitors against *Besnoitia besnoiti* tachyzoites. Int. J. Parasitol. (2017), http://dx.doi.org/10.1016/j.ijpara.2017.08.005

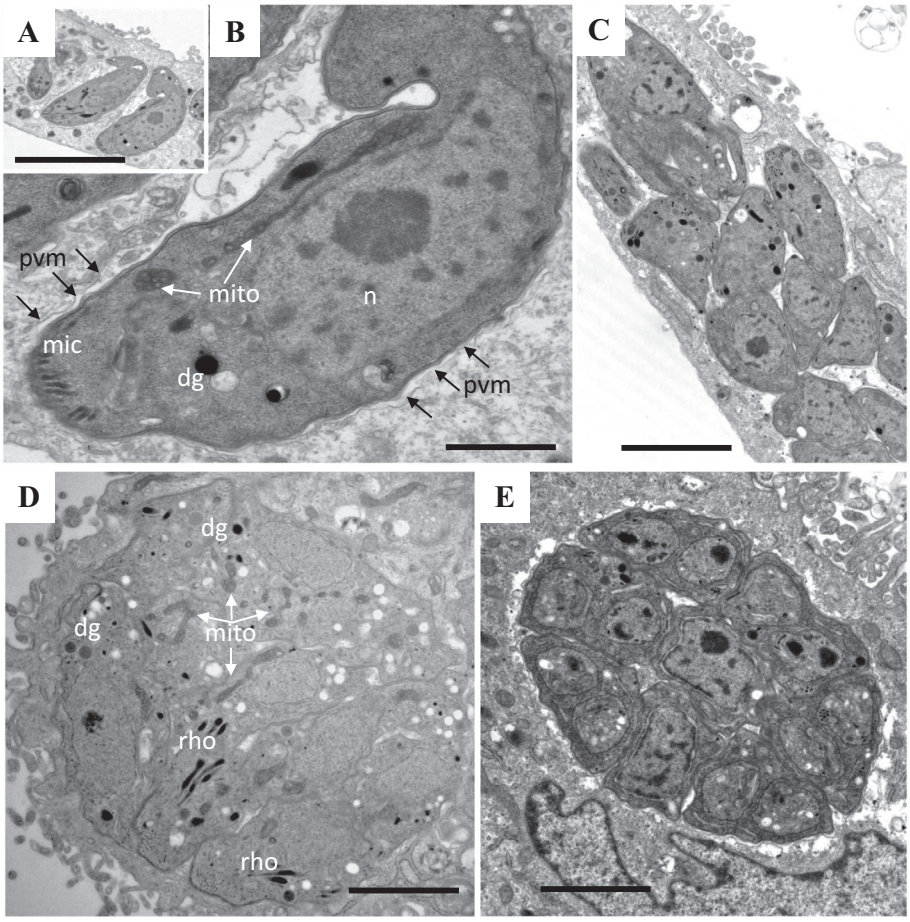

Fig. 4. Representative Transmission Electron Microscopy images of *Besnoitia besnoiti* tachyzoites in human foreskin fibroblast cell cultures treated with DMSO. Intact tachyzoites are observed in longitudinal (A, B, C) and transversal cut sections (C, D, E). Note B is a larger magnification view of A. Numerous viable tachyzoites, located within parasitophorous vacuoles surrounded by a parasitophorous vacuole membrane (A, D, E), can be seen. Non-distorted apical complexes contained typical organelles of apicomplexan parasites, such as the conoid (con), dense granules (dg), micronemes (mic) and rhoptries (rho) (B, D). Also, mitochondria (mito) and the nucleous (nuc) of the tachyzoites are clearly discernible. Scale bars: A = 3 μm; B = 0.5 μm; C = 1.2 μm; D = 1.2 μm; E = 1.2 μm.

As expected, the CDPK1-type kinase identified in *B. besnoiti* showed a high degree of sequence similarities with CDPK1 enzymes from other members of the Toxoplasmatinae (*T. gondii* and *N. caninum*). Indeed, the amino acid sequence of *Bb*CDPK1 reported herein shares a high percentage of identity (95%) with orthologues *Nc*CDPK1 and *Tg*CDPK1, including a glycine in the gatekeeper position, which discriminates CDPK1 from other kinases (Ojo et al., 2014). The sequence showed additional characteristic features of CDPK1 enzymes such as an N-terminal serine-threonine kinase domain, a junctional domain and a series of calcium-binding domains known as EF hands. The existence of EF hands suggest that *Bb*CDPK1 might play an important role in regulating calcium-dependent pathways (Hui et al., 2015). Moreover, the sequence showed the closest structural similarity with *Tg*CDPK1. Accordingly, the newly identified orthologue was named *Bb*CDPK1. Besides, putative n-myristoylation residues were found, similar to what has been reported for *Cryptosporidium Cp*CDPKs (Etzold et al., 2014), which may be important for the association of the enzyme with lipid membranes that can influence its activity.

Kinase assays showed that selected BKIs inhibited the *Bb*CDPK1 enzyme activity even at low nanomolar range concentrations. A similar finding occurred with both *Nc*CDPK1 and *Tg*CDPK1, whose X-ray crystal structures confirmed a structural basis for BKI selectivity (Ojo et al., 2010, 2014). These observations are supported by the high kinase domain sequence identity found in members of the Toxoplasmatinae, where the percentage of identity of *Bb*CDPK1 is as high as 98% and 98.4% with *Tg*CDPK1 and *Nc*CDPK1, respectively. Previously, it has been shown that the degree of sensitivity or resistance of CDPK enzymes to these inhibitors depends on the size and characteristics of the gatekeeper residue and the topology of the adjacent ATP-binding pocket (Keyloun et al., 2014). Regarding this issue, *Bb*CDPK1 possesses only a single amino acid difference in the active site compared with *Tg*CDPK1 and *Nc*CDPK1 sequences (Phenylalanine in position 112 instead of Tyrosine). Consequently, a similar susceptibility pattern against BKIs was expected in all of the Toxoplasmatinae orthologues with the same atypically small glycine gatekeeper residue (Van Voorhis et al., 2017). Enzymatic results indicated that BKIs may be targeting at least *Bb*CDPK1. Similar effects were observed with the four BKIs studied that effectively inhibit other CDPK1 orthologues present in *N. caninum* (Müller et al., 2017), *T. gondii* (Winzer et al., 2015) and *C. parvum* (Castellanos-Gonzalez et al., 2013). Further studies with a parasite line expressing a gatekeeper mutant would be needed to definitively claim that the in vivo phenotype of BKI-treated parasites is solely due to inhibition of *Bb*CDPK1. In the context of these future studies, it should be also verified whether CDPK1 inhibition in vitro is abolished when a large gatekeeper mutant recombinant enzyme is used for the kinase assay.

The results obtained in in vitro assays suggests that *Bb*CDPK1 may be a key regulator during the parasite lytic cycle, since invasion and proliferation events were severely impaired as in *N. caninum* and *T. gondii* (Müller et al., 2017). We included in this panel

Please cite this article in press as: Jiménez-Meléndez, A., et al. In vitro efficacy of bumped kinase inhibitors against *Besnoitia besnoiti* tachyzoites. Int. J. Parasitol. (2017), http://dx.doi.org/10.1016/j.ijpara.2017.08.005

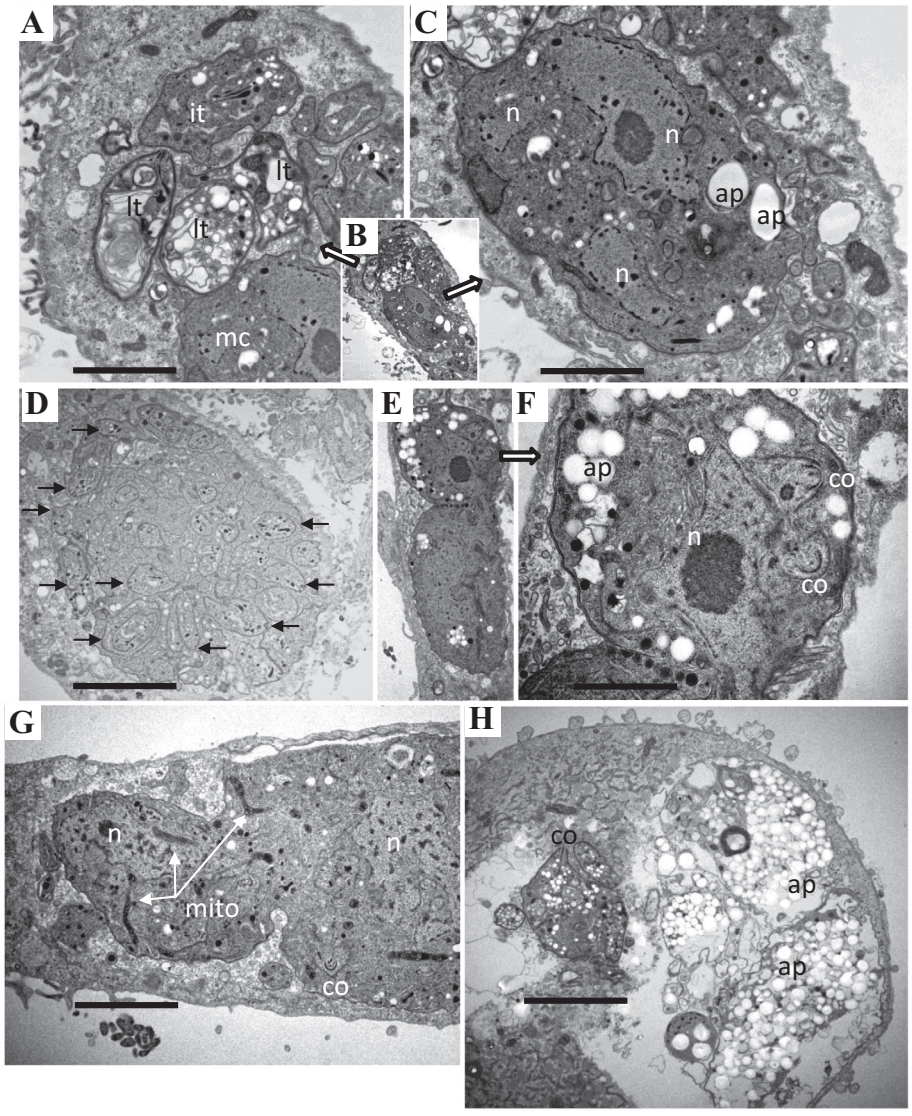

Fig. 5. Representative Transmission Electron Microscopy images of *Besnoitia besnoiti* tachyzoites in human foreskin fibroblast cell cultures treated with bumped kinase inhibitors such as 1294 for 4 days (A–C) or 6 days (D), 1571 for 4 days (E, F), 1553 for 6 days (G) and 1517 for 6 days (H). (A, C) Largely distorted tachyzoites (lt), intact parasites (it) and complexes (mc) can be present in a single host cell. (B) A and C are larger magnification views of B, showing largely distorted and intact tachyzoites (A) or a multinucleated compound (C). A low magnification view. (D) A large complex generated by exposure to bumped kinase inhibitor 1294 for 6 days which contains numerous precursors of apical complexes marked with arrows. (E) A complex exhibiting numerous amylopectin granules (ap); note the two emerging conoids (co). (F) A larger magnification view of E. (G) Exposure to bumped kinase inhibitor 1553 also results in the formation of large complexes; note the intact mitochondria (mito) and emerging conoid structure (co). H: 1517 treatment results in the formation of parasites that form large cytoplasmic amylopectin granule deposits. Scale bars: A = 2 μm, C = 1.6 μm, D = 4.2 μm, F = 1.3 μm; G = 2.8 μm, H = 3.4 μm.

of BKIs the well-studied BKI 1294 which has been used in in vitro and in vivo assays against *Theileria equi* (Hines et al., 2015), *C. parvum* (Lendner et al., 2015), *T. gondii* (Doggett et al., 2014; Winzer et al., 2015) and *N. caninum* (Ojo et al., 2014; Müller et al., 2017), together with other novel and less studied BKIs. Eight out of nine compounds effectively inhibited parasite invasion, with BKIs 1294, 1517, 1553 and 1571 being the most promising ones (inhibition of parasite invasion > 90%) when administered at 5 μM at 0 and at 6 h p.i. Moreover, these compounds lacked cytotoxicity in Marc-145 cells when applied at this concentration, as was also observed by Müller et al. (2017) in human foreskin fibroblast cells.

The EC_{50} and EC_{99} values obtained for these four compounds are in the nanomolar range, which is in accordance with those published for *N. caninum* (Ojo et al., 2014; Müller et al., 2017) and *T. gondii* (Winzer et al., 2015). Most parasite clearance was accomplished by treatments with EC_{99} concentrations only after 72 h of treatment, whereas short treatments did not completely inhibit parasite proliferation, suggesting that these BKIs are parasitostatic rather than parasiticidal. This was confirmed by visualising cultures at 8 and 10 days post treatment, which revealed the presence of remaining viable tachyzoites in drug-treated cultures re-infecting host cells, and by TEM analyses that showed seemingly still viable tachyzoites. TEM showed that the effects of these compounds were not limited to the arrest of host cell invasion, suggesting that there may be additional targets involved (Ojo et al., 2014). Thus, it is possible that secondary targets besides CDPK1 are affected. In *T. gondii* for instance, Mitogen-Activated Protein kinase (MAPK) was previously shown to be inhibited by a BKI analogue, with different pyrazolo-pyrimidine R1 and R2 groups (Sugi et al., 2013, 2015). Inspection of BKI-treated *B. besnoiti* by TEM revealed similar findings for BKIs 1294, 1517, 1553 and 1571. Exposure to these BKIs led to severe ultrastructural alterations in some, but not all, tachyzoites. At later time points after 4–6 days of treatment, PVs containing large multinucleated complexes were found,

Please cite this article in press as: Jiménez-Meléndez, A., et al. In vitro efficacy of bumped kinase inhibitors against *Besnoitia besnoiti* tachyzoites. Int. J. Parasitol. (2017), http://dx.doi.org/10.1016/j.ijpara.2017.08.005

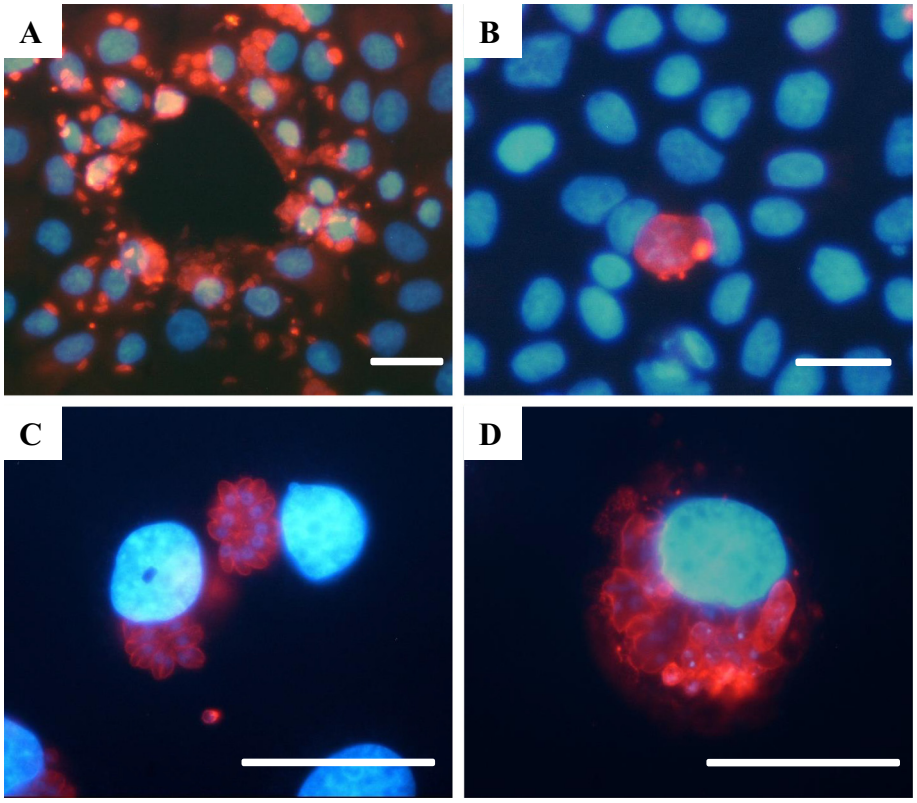

Fig. 6. Marc-145 cell cultures infected with *Besnoitia besnoiti* and treated with DMSO or bumped kinase inhibitor 1294 for 3 days. (A) Marc-145 cell culture infected with *B. besnoiti* tachyzoites and treated with DMSO. Note a lysis plaque. (B) Culture treated with bumped kinase inhibitor 1294 at 5 μM for 3 days. (C) Culture treated with bumped kinase inhibitor 1294 at 0.5 μM for 3 days. Note a seemingly viable parasitophorous vacuole (PV) with well-defined tachyzoites. (D) Culture treated with bumped kinase inhibitor 1294 at 0.5 μM for 3 days. Note a distorted PV with tachyzoites that are not well-defined. Scale bars: A = 40 μm, B = 40 μm, C = 40 μm, D = 40 μm.

some of which showed clear signs of cellular degeneration and others obviously still viable, similar to what has been reported earlier in BKI-1294, 1517 and 1553 treated cell cultures infected with *N. caninum* or *T. gondii* (Winzer et al., 2015; Müller et al., 2017). As for *N. caninum,* BKIs 1294 and 1517 showed more dramatic effects (Müller et al., 2017). These complexes result from parasites that undergo nuclear division, but not cytokinesis, resulting in the formation of tachyzoite precursors that are trapped within the host cell. Whether this effect is due to CDPK1 inhibition or whether there are other targets of BKIs which regulate parasite cytokinesis needs to be elucidated.

In addition, BKI 1294 treatment induced higher expression levels of bradyzoite-specific genes (i.e. MAG1, BAG1) in drug-treated cultures infected with *N. caninum* and *T. gondii,* and increased labelling intensity for anti-BAG1 and anti-CC2 bradyzoite-specific markers was noted (Winzer et al., 2015). Similar increased staining with the bradyzoite marker MAG1 was observed in *N. caninum* tachyzoites treated with BKI 1517 and 1553, together with an increased presence of amylopectin granules as visualised by TEM (Müller et al., 2017). Similarly, amylopectin granules were present in BKI-treated *B. besnoiti*, a characteristic feature of *B. besnoiti* bradyzoites (Fernández-García et al., 2009). This is particularly interesting, since BKI treatments could potentially represent a convenient exogenous trigger to induce tachyzoite-to-bradyzoite conversion of *B. besnoiti* in vitro.

In conclusion, we here demonstrate the therapeutic potential of BKIs for treatment of bovine besnoitiosis. Prospectively, one could envisage BKI treatment of affected cattle at the acute stage of infection where tachyzoites replicate and disseminate, inducing vascular damage and clinical signs of respiratory disorders and orchitis. During the chronic stage, BKI therapy might be more difficult, possibly due to potentially poor drug accessibility to the interior of bradyzoite-containing tissue cysts (Álvarez-García et al., 2014). A major caveat for the development of BKIs against besnoitiosis is the absence of laboratory animal models; thus studies need to be carried out directly in the target animal (Álvarez-García et al., 2014). Plasma levels of up to 5 μM have been already achieved in cattle treated with BKI 1294, 1517 and 1553 (Huang et al., 2015; Schaefer et al., 2016; Hulverson et al., 2017), and whether the administration of these BKIs during the acute stage of the disease is enough to avoid tissue cyst formation needs to be further investigated.

Acknowledgements

This work was financially supported through two research projects from the Spanish Ministry of Economy and Competitiveness (Ref. AGL2013-04442) and Community of Madrid, Spain (Ref. S2013/ABI-2906, PLATESA-CM), and by the Swiss National Science Foundation (grant No. 310030_165782 and CRSII3_160702). We also acknowledge support from the National Institute of Allergy and Infectious Diseases, USA and National Institute of Child Health and Human Development of the National Institutes of Health, USA under the award numbers R01AI089441, R01AI111341, and R01HD080670. The work was also supported by awards # 2014-06183 from the United States Department of Agriculture National Institute of Food and Agriculture. Alejandro Jiménez-Meléndez was supported by a grant from the Spanish Ministry of Education, Culture and Sports (grant n° FPU13/05481). In addition, we acknowledge Laura Jiménez-Pelayo and Marta García-Sánchez for their technical assistance. Conflict of Interest Disclosure: Dr. Van Voorhis is the founder of the company ParaTheraTech Inc., dedicated to bringing BKIs to market in animal health applications. He did not carry out or interpret the experiments in this paper.

Appendix A. Supplementary data

Supplementary data associated with this article can be found, in the online version, at http://dx.doi.org/10.1016/j.ijpara.2017.08.005.

References

Álvarez-García, G., Frey, C.F., Mora, L.M., Schares, G., 2013. A century of bovine besnoitiosis: an unknown disease re-emerging in Europe. Trends Parasitol. 29, 407–415.

Álvarez-García, G., García-Lunar, P., Gutiérrez-Expósito, D., Shkap, V., Ortega-Mora, L.M., 2014. Dynamics of *Besnoitia besnoiti* infection in cattle. Parasitology 141, 1419–1435.

Álvarez-García, G., 2016. From the mainland to Ireland – bovine besnoitiosis and its spread in Europe. Vet. Rec. 178, 605–607.

Arnal, M., Gutiérrez-Expósito, D., Martínez-Durán, D., Regidor-Cerrillo, J., Revilla, M., Fernández-de-Luco, D., Jiménez-Meléndez, A., Ortega-Mora, L.M., Álvarez-García, G., 2017. Systemic besnoitiosis in a juvenile roe deer (*Capreolus capreolus*). Transbound. Emerg. Dis. (in press)

Basso, W., Schares, G., Gollnick, N.S., Rutten, M., Deplazes, P., 2011. Exploring the life cycle of *Besnoitia besnoiti* – experimental infection of putative definitive and intermediate host species. Vet. Parasitol. 178, 223–234.

Billker, O., Lourido, S., Sibley, L.D., 2009. Calcium-dependent signaling and kinases in apicomplexan parasites. Cell Host Microbe 5, 612–622.

Castellanos-Gonzalez, A., White Jr, A.C., Ojo, K.K., Vidadala, R.S., Zhang, Z., Reid, M.C., Fox, A.M., Keyloun, K.R., Rivas, K., Irani, A., Dann, S.M., Fan, E., Maly, D.J., Van Voorhis, W.C., 2013. A novel calcium-dependent protein kinase inhibitor as a lead compound for treating cryptosporidiosis. J. Infect. Dis. 208, 1342–1348.

Cortes, H.C., Muller, N., Esposito, M., Leitao, A., Naguleswaran, A., Hemphill, A., 2007. *In vitro* efficacy of nitro- and bromo-thiazolyl-salicylamide compounds (thiazolides) against *Besnoitia besnoiti* infection in Vero cells. Parasitology 134, 975–985.

Cortes, H.C., Muller, N., Boykin, D., Stephens, C.E., Hemphill, A., 2011. *In vitro* effects of arylimidamides against *Besnoitia besnoiti* infection in Vero cells. Parasitology 138, 583–592.

Diesing, L., Heydorn, A.O., Matuschka, F.R., Bauer, C., Pipano, E., de Waal, D.T., Potgieter, F.T., 1988. *Besnoitia besnoiti*: Studies on the definitive host and experimental infections in cattle. Parasitol. Res. 75, 114–117.

Doerig, C., Meijer, L., Mottram, J.C., 2002. Protein kinases as drug targets in parasitic protozoa. Trends Parasitol. 18, 366–371.

Doggett, J.S., Ojo, K.K., Fan, E., Maly, D.J., Van Voorhis, W.C., 2014. Bumped kinase inhibitor 1294 treats established *Toxoplasma gondii* infection. Antimicrob. Agents Chemother. 58, 3547–3549.

Etzold, M., Lendner, M., Daugschies, A., Dyachenko, V., 2014. CDPKs of *Cryptosporidium parvum*—stage-specific expression *in vitro*. Parasitol. Res. 113, 2525–2533.

EFSA European Food Safety Authority, 2010. Bovine besnoitiosis: an emerging disease in Europe. Scientific statement on bovine besnoitiosis. EFSA J 8, 1499.

Fernández-García, A., Risco-Castillo, V., Pedraza-Díaz, S., Aguado-Martínez, A., Álvarez-García, G., Gómez-Bautista, M., Collantes-Fernández, E., Ortega-Mora, L., 2009a. First isolation of *Besnoitia besnoiti* from a chronically infected cow in Spain. J. Parasitol. 95, 474–476.

Fernández-García, A., Álvarez-García, G., Risco-Castillo, V., Aguado-Martínez, A., Marugán-Hernández, V., Ortega-Mora, L.M., 2009b. Pattern of recognition of *Besnoitia besnoiti* tachyzoite and bradyzoite antigens by naturally infected cattle. Vet. Parasitol. 164, 104–110.

Franc, M., Cardiegues, M., 1999. La besnoitiose bovine: attitude diagnostique et therapeutique. Bulletin des GTV. Bovins, Parasitologie, 119–124.

Frey, C.F., Regidor-Cerrillo, J., Marreros, N., García-Lunar, P., Gutiérrez-Expósito, D., Schares, G., Dubey, J.P., Gentile, A., Jacquiet, P., Shkap, V., Cortes, H., Ortega-Mora, L.M., Álvarez-Garcia, G., 2016. *Besnoitia besnoiti* lytic cycle *in vitro* and differences in invasion and intracellular proliferation among isolates. Parasit. Vectors 9, 1.

Greenbaum, D.C., 2008. Is chemical genetics the new frontier for malaria biology? Trends Pharmacol Sci. 29, 51–56.

Gutiérrez-Expósito, D., Ortega-Mora, L.M., Marco, I., Boadella, M., Gortázar, C., San Miguel-Ayanz, J.M., García-Lunar, P., Lavin, S., Álvarez-García, G., 2013. First serosurvey of *Besnoitia* spp. infection in wild european ruminants in Spain. Vet. Parasitol. 197, 557–564.

Hines, S.A., Ramsay, J.D., Kappmeyer, L.S., Lau, A.O.T., Ojo, K.K., Van Voorhis, W.C., Knowles, D.P., Mealey, R.H., 2015. *Theileria equi* isolates vary in susceptibility to imidocarb dipropionate but demonstrate uniform *in vitro* susceptibility to a bumped kinase inhibitor. Parasit. Vectors 8, 33.

Huang, W., Ojo, K.K., Zhang, Z., Rivas, K., Vidadala, R.S.R., Scheele, S., DeRocher, A.E., Choi, R., Hulverson, M.A., Barrett, L.K., Bruzual, I., Diddaramaiah, L.K., Kerchner, L.M., Kurnick, M.D., Freiberg, G.M., Kempf, D., Hol, W.G., Merrit, E.A., Neckermann, G., de Hostos, E.I., Isoherranen, N., Maly, D.J., Parsons, M., Doggett, J.S., Van Voorhis, W.C., Fan, E., 2015. SAR studies of 5-aminopyrazole-4-carboxamide analogues as potent and selective inhibitors of *Toxoplasma gondii* CDPK1. ACS Med. Chem. Lett. 6, 1184–1189.

Hui, R., El Bakkouri, M., Sibley, L.D., 2015. Designing selective inhibitors for calcium-dependent protein kinases in apicomplexans. Trends Pharmacol. Sci. 36, 452–460.

Hulverson, M.A., Vinayak, S., Choi, R., Schaefer, D.A., Castellanos-Gonzalez, A., Vidadala, R.S.R., Brooks, C.F., Herbert, G.T., Betzer, D.P., Whitman, G.R., Sparks, H. N., Arnold, S.L.M., Rivas, K.L., Barre, L.K., White Jr., A.C., Maly, D.J., Riggs, M.W., Striepen, B., Van Voorhis, W.C.,, Maly, D.J., 2017. Bumped-kinase inhibitors for cryptosporidiosis therapy. J. Infect. Dis. 215, 1275–1284.

Keyloun, K.R., Reid, M.C., Choi, R., Song, Y., Fox, A.M., Hillesland, H.K., Zhang, Z., Vidadala, R., Merritt, E.A., Lau, A.O.T., Maly, D.J., Fan, E., Barrett, L.K., Van Voorhis, W.C., Ojo, K.K., 2014. The gatekeeper residue and beyond: homologous calcium-dependent protein kinases as drug development targets for veterinarian apicomplexa parasites. Parasitology 141, 1499–1509.

Lendner, M., Böttcher, D., Delling, C., Ojo, K.K., Van Voorhis, W.C., Daugschies, A., 2015. A novel CDPK1 inhibitor—a potential treatment for cryptosporidiosis in calves? Parasitol. Res. 114, 335–336.

Lourido, S., Shuman, J., Zhang, C., Shokat, K.M., Hui, R., Sibley, L.D., 2010. Calcium-dependent protein kinase 1 is an essential regulator of exocytosis in *Toxoplasma gondii*. Nature 465, 359–362.

Lourido, S., Moreno, S.N., 2015. The calcium signaling toolkit of the apicomplexan parasites *Toxoplasma gondii* and *Plasmodium* spp. Cell Calcium 57, 186–193.

Müller, J., Aguado-Martínez, A., Balmer, V., Maly, D.J., Fan, E., Ortega-Mora, L.M., Ojo, K.K., Van Voorhis, W.C., Hemphill, A., 2017. Two novel calcium-dependent kinase 1-inhibitors interfere with vertical transmission in mice infected with *Neospora caninum* tachyzoites. Antimicrob. Agents Chemother., 02324–2416

Ojo, K.K., Larson, E.T., Keyloun, K.R., Castaneda, L.J., DeRocher, A.E., Inampudi, K.K., Kim, J.E., Arakaki, T.L., Murphy, R.C., Zhang, L., 2010. *Toxoplasma gondii* calcium-dependent protein kinase 1 is a target for selective kinase inhibitors. Nat. Struct. Mol. Biol. 17, 602–607.

Ojo, K.K., Pfander, C., Mueller, N.R., Burstroem, C., Larson, E.T., Bryan, C.M., Fox, A.M., Reid, M.C., Johnson, S.M., Murphy, R.C., Kennedy, M., Mann, H., Leibly, D.J., Hewitt, S.N., Verlinde, C.L., Kappe, S., Merritt, E.A., Maly, D.J., Billker, O., Van Voorhis, W.C., 2012. Transmission of malaria to mosquitoes blocked by bumped kinase inhibitors. J. Clin. Invest. 122, 2301–2305.

Ojo, K.K., Reid, M.C., Kallur Siddaramaiah, L., Muller, J., Winzer, P., Zhang, Z., Keyloun, K.R., Vidadala, R.S., Merritt, E.A., Hol, W.G., Maly, D.J., Fan, E., Van Voorhis, W.C., Hemphill, A., 2014. *Neospora caninum* calcium-dependent protein kinase 1 is an effective drug target for neosporosis therapy. PLoS One 9, e92929.

Ojo, K.K., Dangoudoubiyam, S., Verma, S.K., Scheele, S., DeRocher, A.E., Yeargan, M., Choi, R., Smith, T.R., Rivas, K.L., Hulverson, M.A., 2016. Selective inhibition of *Sarcocystis neurona* calcium-dependent protein kinase 1 for equine protozoal myeloencephalitis therapy. Int. J. Parasitol. 46, 871–880.

Pedroni, M.J., Vidadala, R.S.R., Choi, R., Keyloun, K.R., Reid, M.C., Murphy, R.C., Barrett, L.K., Van Voorhis, W.C., Maly, D.J., Ojo, K.K., 2016. Bumped kinase inhibitor prohibits egression in *Babesia bovis*. Vet. Parasitol. 215, 22–28.

Pols, J.W., 1960. Studies on bovine besnoitiosis with special reference to the aetiology. Onderstepoort J. Vet. Res. 28, 265–356.

Schaefer, D.A., Betzer, D.P., Smith, K.D., Millman, Z.G., Michalski, H.C., Menchaca, S. E., Zambriski, J.A., Ojo, K.K., Hulverson, M.A., Arnold, S.L., Rivas, K.L., Vidadala, R. S., Huang, W., Barrett, L.K., Maly, D.J., Fan, E., Van Voorhis, W.C., Riggs, M.W., 2016. Novel Bumped Kinase Inhibitors are safe and effective therapeutics in the calf clinical model for cryptosporidiosis. J. Infect. Dis. 214, 1856–1864.

Shkap, V., De Waal, D.T., Potgieter, F.T., 1985. Chemotherapy of experimental *Besnoitia besnoiti* infection in rabbits. Onderstepoort J. Vet. Res. 52, 289.

Shkap, V., Pipano, E., Ungar-Waron, H., 1987. Besnoitia besnoiti: Chemotherapeutic trials in vivo and in vitro. Rev. Elev. Med. Vet. Pays. Trop. 40, 259–264.

Srinivasan, N., Krupa, A., 2005. A genomic perspective of protein kinases in Plasmodium falciparum. Proteins. Struct Funct. Bioinf. 58, 180–189.

Sugi, T., Kobayashi, K., Takemae, H., Gong, H., Ishiwa, A., Murakoshi, F., Recuenco, F. C., Iwanaga, T., Horimoto, T., Akashi, H., 2013. Identification of mutations in TgMAPK1 of *Toxoplasma gondii* conferring resistance to 1NM-PP1. Int. J. Parasitol. Drugs Drug Resist. 3, 93–101.

Sugi, T., Kawazu, S., Horimoto, T., Kato, K., 2015. A single mutation in the gatekeeper residue in TgMAPKL-1 restores the inhibitory effect of a bumped kinase inhibitor on the cell cycle. Int. J. Parasitol. Drugs Drug Resist. 5, 1–8.

Van Voorhis, W.C., Doggett, J.S., Parsons, M., Hulverson, M.A., Choi, R., Arnold, S., Riggs, M.W., Hemphill, A., Howe, D.K., Mealey, R.H., Lau, A.O.T., Merrit, E.A., Maly, D.J., Fan, E., Ojo, K.K., 2017. Extended-spectrum antiprotozoal bumped kinase inhibitors: A review. Exp. Parasitol. 180, 71–83.

Vidadala, R.S.R., Rivas, K.L., Ojo, K.K., Hulverson, M.A., Zambriski, J.A., Bruzual, I., Schultz, T.L., Huang, W., Zhang, Z., Scheele, S., DeRocher, A.E., Choi, R., Barrett, L. K., Siddaramaiah, L.K., Hol, W.G., Fan, E., Merritt, E.A., Parsons, M., Freiberg, G., Marsh, K., Kempf, D.J., Carruthers, V.B., Isoherranen, N., Doggett, J.S., Van Voorhis, W.C., Maly, D.J., 2016. Development of an orally available and central nervous system (CNS) penetrant *Toxoplasma gondii* calcium-dependent protein kinase 1 (tg CDPK1) inhibitor with minimal human ether-a-go-go-related gene (hERG) activity for the treatment of toxoplasmosis. J. Med. Chem. 59, 6531–6546.

Ward, P., Equinet, L., Packer, J., Doerig, C., 2004. Protein kinases of the human malaria parasite *Plasmodium falciparum*: The kinome of a divergent eukaryote. BMC Genomics 5, 79.

Winzer, P., Muller, J., Aguado-Martínez, A., Rahman, M., Balmer, V., Manser, V., Ortega-Mora, L.M., Ojo, K.K., Fan, E., Maly, D.J., Van Voorhis, W.C., Hemphill, A., 2015. *In vitro* and *in vivo* effects of the bumped kinase inhibitor 1294 in the related cyst-forming apicomplexans *Toxoplasma gondii* and *Neospora caninum*. Antimicrob. Agents Chemother. 59, 6361–6374.

Yang, J., Yan, R., Roy, A., Xu, D., Poisson, J., Zhang, Y., 2015. The I-TASSER suite: protein structure and function prediction. Nat. Methods 12, 7–8.

Please cite this article in press as: Jiménez-Meléndez, A., et al. In vitro efficacy of bumped kinase inhibitors against *Besnoitia besnoiti* tachyzoites. Int. J. Parasitol. (2017), http://dx.doi.org/10.1016/j.ijpara.2017.08.005

Veterinary Parasitology 261 (2018) 77–85

Contents lists available at ScienceDirect

Veterinary Parasitology

journal homepage: www.elsevier.com/locate/vetpar

Research paper

Repurposing of commercially available anti-coccidials identifies diclazuril and decoquinate as potential therapeutic candidates against *Besnoitia besnoiti* infection

Alejandro Jiménez-Meléndez[a], Laura Rico-San Román[a], Andrew Hemphill[b], Vreni Balmer[b], Luis Miguel Ortega-Mora[a], Gema Álvarez-García[a,*]

[a] SALUVET, Animal Health Department, Faculty of Veterinary Sciences, Complutense University of Madrid, Ciudad Universitaria s/n, 28040, Madrid, Spain
[b] Institute of Parasitology, Vetsuisse Faculty, University of Bern, Länggass-Strasse 122, CH-3012, Bern, Switzerland

ARTICLE INFO

Keywords:
Besnoitia besnoiti
Tachyzoite
Commercial drugs
Decoquinate
Diclazuril
In vitro assays

ABSTRACT

Repurposing of currently marketed compounds with proven efficacy against apicomplexan parasites was used as an approach to define novel candidate therapeutics for bovine besnoitiosis. *Besnoitia besnoiti* tachyzoites grown in MARC-145 cells were exposed to different concentrations of toltrazuril, diclazuril, imidocarb, decoquinate, sulfadiazine and trimethoprim alone or in combination with sulfadiazine. Drugs were added either just prior to infection of MARC-145 cells (0 h post infection, hpi) or at 6 hpi. A primary evaluation of drug effects was done by direct immunofluorescence staining and counting. Potential effects on the host cells were assessed using a XTT kit for cell proliferation. Compounds displaying promising efficacy were selected for IC_{50} and IC_{99} determination by qPCR. In addition, the impact of drugs on the tachyzoite ultrastructure was assessed by TEM and long-term treatment assays were performed. Cytotoxicity assays confirmed that none of the compounds affected the host cells. Decoquinate and diclazuril displayed invasion inhibition rates of 90 and 83% at 0 h pi and 73 and 72% at 6 h pi, respectively. The remaining drugs showed lower efficacy and were not further studied. Decoquinate and diclazuril exhibited IC_{99} values of 100 nM and 29.9 μM, respectively. TEM showed that decoquinate primarily affected the parasite mitochondrium, whilst diclazuril interfered in cytokinesis of daughter zoites. The present study demonstrates the efficacy of diclazuril and decoquinate against *B. besnoiti in vitro* and further assessments of safety and efficacy of both drugs should be performed in the target species.

1. Introduction

Besnoitia besnoiti is a cyst-forming apicomplexan protozoan belonging to the Toxoplasmatinae subfamily and closely related to *Neospora caninum* and *Toxoplasma gondii*. *B. besnoiti* causes bovine besnoitiosis, a debilitating disease of cattle characterized by non-specific clinical signs such as fever or oedemas at the acute stage and skin manifestations during the chronic stage that may end up with sterility in bulls (Gutiérrez-Expósito et al., 2017). In the absence of effective treatments or vaccines for disease control, the last 20 years have witnessed a steady increase in the number of infected herds, and the disease appeared in countries where it had not been described before. Thus, the European Food and Safety Authority (EFSA) has considered bovine besnoitiosis as re-emerging in Europe (European Food Safety Authority, 2010). Recent outbreaks have been described in Central Europe or even Ireland (Álvarez-García, 2016; Ryan et al., 2016).

Due to assumed similarities with other Toxoplasmatinae parasites, *B. besnoiti* is suspected to have a heteroxenous life cycle, but the definitive host is still elusive (Basso et al., 2011). In Europe, cattle act as the main intermediate host, where two asexual and infective stages of the parasite develop: tachyzoites, responsible for the acute stage of the disease, and bradyzoites, found inside tissue cysts and responsible for the characteristic skin lesions during the chronic stage.

Currently, there are no effective therapeutics for the treatment of bovine besnoitiosis. An effective drug should target the tachyzoite stage and affect the dissemination of the parasite into different organs during the acute disease stage, and should preferentially also impact on the tissue cysts that contain bradyzoites. In the past, the effects of a wide range of compounds were assessed in naturally infected bovines, as well as in experimentally infected rabbits and gerbils (Pols, 1960; Shkap

* Corresponding author at: Animal Health Department, Faculty of Veterinary Sciences, Complutense University of Madrid, Ciudad Universitaria s/n, 28040, Madrid, Spain.
E-mail address: gemaga@vet.ucm.es (G. Álvarez-García).

https://doi.org/10.1016/j.vetpar.2018.08.015
Received 30 May 2018; Received in revised form 20 August 2018; Accepted 30 August 2018

et al., 1985; Shkap et al., 1987). However, results have remained inconclusive due to fact that these assays were performed under variable experimental conditions, and there was a lack of well-established and reproducible *in vivo* models to study bovine besnoitiosis.

Previous *in vitro* studies demonstrated that thiazolides (Cortes et al., 2007), arylimidamides (Cortes et al., 2011), and bumped kinase inhibitors (BKIs) (Jiménez-Meléndez et al., 2017) exhibited promising *in vitro* activities against *B. besnoiti*. However, arylimidamides and thiazolides are not commercially available for ruminants in Europe and BKIs are "new generation drugs" in a pre-clinical stage of development (Van Voorhis et al., 2017). Thus, they may represent valuable therapeutical tools only in the long run. In contrast, repurposing of drugs with well characterized activities, and which are already on the market for other indications, might be a valuable strategy for a speedier implementation of novel treatments against besnoitiosis. The same approach has also been exploited for other closely related parasites such as *N. caninum* (Muller et al., 2015), *T. gondii* (Dittmar et al., 2016) or *Cryptosporidium parvum* (Bessoff et al. 2014). Thus, in this study decoquinate, diclazuril, toltrazuril, imidocarb, sulfadiazine and trimethoprim, were assessed for *in vitro* activity against *B. besnoiti*, as these drugs are commercialised in cattle for the treatment of relevant diseases caused by apicomplexan parasites.

Decoquinate is an anticoccidial quinolone initially developed for poultry in 1967 (Williams, 2006) and approved as an additive in feed to prevent intestinal coccidiosis in cattle and goats. Decoquinate affects the parasite mitochondrium and acts as a cytochrome *bc1* inhibitor, thus it impairs the transfer of electrons from ubiquinone to cytochrome C (Fry and Williams, 1984). The compound is also active against *N. caninum* tachyzoites (Lindsay et al., 1997) and also affects the proliferation of *T. gondii* (Lindsay et al., 1998). The coccidicides toltrazuril and diclazuril are triazinone derivatives and are effective against intracellular stages of *Eimeria* and *Isospora* spp. The exact mechanism of action is not well understood, but several studies have shown that these drugs affect enzymes of the respiratory chain, and also target other enzymes such as dihydrofolate reductase (DHFR) (Stock et al., 2017). Imidocarb is a dicationic diamidine of the carbanilide series of antiprotozoal compounds and currently the drug of choice for the treatment of bovine babesiosis caused by *Babesia* spp. (Vial and Gorenflot, 2006). The mode of action is uncertain, but it is supposed to interfere with the production and/or utilization of polyamines or the prevention of the entry of inositol into the erythrocytes. The antibiotics sulfadiazine and trimethoprim are used in cattle for the treatment of colibacillosis, metritis and pneumonia (Kaartinen et al., 1999), and they are also commonly applied for prophylaxis and treatment of toxoplasmosis in humans (Torre et al., 1998). They act synergistically by sequentially blocking dihydropteroate synthase (DHPS) and dihydrofolate reductase (DHFR), both of which are crucially involved in the folate biosynthesis pathway and essential for nucleoside biosynthesis and nucleic acid formation. Moreover, sulfadiazine can be used to treat coccidiosis (Daugschies and Najdrowski, 2005).

Thus, the objective of the present study was to evaluate the safety and efficacy of these six commercially available drugs against *B. besnoiti* tachyzoites *in vitro*.

2. Materials and methods

2.1. Parasite maintenance and cell cultures

The monkey kidney cell line MARC-145 and human foreskin fibroblasts (HFF), as well as tachyzoites from the *B. besnoiti* Spain1 (Bb Spain 1) isolate, were maintained according to previously published procedures (Jiménez-Meléndez et al., 2017). MARC-145 cell cultures were passaged twice a week, whilst HFF cultures only once a week. The *B. besnoiti* isolate used for all *in vitro* assays was tested negative to *Mycoplasma* spp. infection by PCR (Mycoplasma Gel Form Kit®, Biotools, Spain) following the manufacturer´s instructions and bovine viral diarrhea virus (BVDV) by quantitative real-time PCR (qPCR) (Hoffmann et al., 2006). The fetal calf serum (FCS) used in all the experiments was previously checked for the absence of IgGs against *B. besnoiti*, *N. caninum* and *T. gondii* by IFAT (Fernández-García et al., 2009). For drug assays, tachyzoites were harvested three days post infection (dpi), when most of them were still intracellular, by recovering the infected cell monolayer with a cell scraper, followed by repeated passages through a 25-gauge needle at 4 °C and separation from cell debris on a PD-10 column (Frey et al., 2016). Tachyzoite viability was confirmed by trypan blue exclusion followed by counting in a Neubauer chamber. Purified viable tachyzoites were used to infect Marc-145 cell monolayers.

2.2. Cytotoxicity in MARC-145 cells

The potential toxicity of the compounds against MARC-145 cells was assessed by a XTT cell viability assay (Panreac-AppliChem, Barcelona, Spain). MARC-145 cells in the exponential phase of growth were seeded in 96-well flat-bottom plates at a density of 2×10^4cells/well containing compounds at the maximum concentration employed in our assays and grown for 72 h at 37 °C in a 5% CO_2 humidified incubator. Afterwards, 50 µL of XTT reagent was added to each well and further incubated for 4 h. Fluorescence was measured at the respective excitation and emission wavelengths of 475 nm and 660 nm in a Biotek Multiplate Reader (Biotek, Winooski, VT, USA) and specific OD values were determined according to the instructions from the manufacturer. The compounds were tested in quadruplicate in three independent assays.

2.3. Primary drug assays on B. besnoiti-infected MARC-145 cells

In preliminary experiments, dose-finding studies were carried out with at least 4 concentrations for each drug, following the procedure described by Jiménez-Meléndez et al. (2017). Each concentration was tested in triplicate in two or more independent assays. Briefly, monolayers of MARC-145 cells (5×10^4 cells per well) were incubated in culture medium at 37 °C / 5% CO_2 and grown to confluence in 24-well plates. Treatments were initiated by adding the compounds to the cell cultures just prior to infection (0 h post infection, hpi) or 6 h after cells were infected (6 hpi). The drug concentrations employed in these experiments are outlined in Table 1, and were selected based on previous *in vitro* studies on *N. caninum*, *T. gondii* or other apicomplexan parasites (e.g *Babesia* spp., *Theileria* spp.). Depending on the compound, the solvents Dimethyl Sulfoxide or a mixture of NaOH/MetOH (Lindsay et al., 2013) were added to negative control wells at equal volumes (see Table 1). Cultures were infected with 10^3 purified tachyzoites of *B. besnoiti* Bb Spain-1 when the compounds were already present, or compounds were administered 6 hpi. In the latter case, infected monolayers were gently rinsed 3 times with Phosphate Buffered Saline (PBS) prior to the addition of the compounds in order to remove non-invaded tachyzoites. Drugs were kept in the medium of cell culture until immunofluorescence staining was performed at 72 hpi. Once the optimal concentrations for each compound were identified, the assays were repeated employing the same procedure under optimized conditions. In some experiments employing sulfadiazine and trimethoprim, alone or in combination, longer treatments of 6 days, involving at least two lytic cycles of the parasite, were carried out (Lindsay et al., 1994). Each condition was assessed in triplicate and all experiments were carried out in three independent assays.

2.4. Immunofluorescence staining

For immunofluorescence staining, supernatants of the cell cultures were discarded at 72 hpi, cells were washed 3 times with PBS and were fixed by the addition of ice-cold methanol for 10 min. After another wash in PBS, cells were permeabilized with 300 µl/ well of 0.2% Triton-

Table 1
Compounds tested in all *in vitro* assays and results obtained in the preliminary experiments carried out to determine the best concentrations for the subsequent drug screening.

Compound (Company)	Solvent	Drug Stock Solution	Drug Concentration used in assays			References[b]
			Previous trials (Effect observed in treated cell cultures)	Subsequent experiments	IC_{50} and IC_{99} determinations	
Decoquinate (Zoetis™)	NaOH 0.1N–MetOH 90%	2.4 mM	240, 200, 100, 50 nM (No lysis plaques, PV[a])	240 nM	240 nM – 0.24 nM	Lindsay et al. (2013)
Diclazuril (Elanco-Lilly™)	DMSO	10 mM	100 µM (Cytotoxicity) 70, 50 µM (No lysis plaques or PV) 30 µM (No lysis plaques, PV) 10 µM (PV)	30 µM	40 µM – 0.04 µM	Lindsay et al. (1995)
Toltrazuril (Bayer™)	DMSO	10 mM	100, 70, 50 µM (Cytotoxicity) 30 µM (No lysis plaques, PV) 10 µM (Lysis plaques and PV)	30 µM		Darius et al. (2004)
Imidocarb (MSD Animal Health™)	DMSO	10 mM	70, 50, 30, 10 µM (Lysis plaques and PV)	30 µM		Hines et al. (2015)
Sulfadiazine (CZV™)	DMSO	50 mM	200, 100, 70, 50 µM (Lysis plaques and PV)	100 µM		Lindsay et al. (1994)
Trimethoprim (CZV™)	DMSO	50 mM	200, 100, 70, 50 µM (Lysis plaques and PV)	100 µM		Lindsay et al. (1994)
Sulfadiazine + Trimethoprim (CZV™)	DMSO		100-100; 100-50; 100-30; 100-10 (Lysis plaques and PV)	100 µM – 10 µM		Lindsay et al. (1994)

[a] PV: parasitophorous vacuoles.
[b] Previous studies done with these compounds and other apicomplexan parasites in order to select appropriate doses to be tested.

X 100 in PBS for 30 min at 37 °C, followed by 3 additional washes with PBS. A primary polyclonal rabbit-anti tachyzoite Bb-Spain1 polyclonal antiserum (Gutiérrez-Expósito et al., 2013) was added at a dilution of 1:1000 in PBS and incubated for 1 h at 37 °C. After 3 additional washes with PBS, Alexa Fluor® 488 Goat Anti-Rabbit IgG (H + L), (Life technologies, Thermo Fisher Scientific, USA) were added per well at a dilution of 1:1000. The plates were incubated for 45 min at room temperature in the dark, and washed 3 times with PBS. In the final wash, DAPI stain was included to stain the nuclei. Finally, the plates were washed with distilled water and the total number of invasion events per well was counted using an inverted fluorescence microscope (Nikon eclipse TE200) at 200X magnification. Two categories of plaque forming tachyzoites were distinguished: parasitophorous vacuoles (PVs) and lysis plaques, as described by Frey et al. (2016).

2.5. IC_{50} and IC_{99} determination

Those compounds that showed the highest values of both parasite invasion and proliferation inhibition were selected for IC_{50} and IC_{99} determination (the effective concentrations to reduce proliferation by 50% or 99%, respectively). MARC-145 cells were grown to confluency in 24 well plates. Just prior to infection, drugs were added at final concentrations ranging between 40 µM and 4 nM for diclazuril and 240 nM and 0.24 nM for decoquinate. Bb-Spain 1 tachyzoites were added at a parasite: host cell ratio of 1:100 (10^3 tachyzoites per well). Control wells containing the drug solvents were also included in each culture plate. After 72 hpi, samples were collected using a lysis solution (100 µL PBS, proteinase K and AL Buffer) and stored at -80 °C until further DNA extraction according to the manufacturer´s instructions (DNeasy Blood and Tissue, Qiagen, Valencia, CA, USA). Each condition was assessed in triplicate and the experiments were carried out in three independent assays.

2.6. DNA extraction and quantitative real-time PCR (qPCR)

The harvested cell culture samples were incubated for 10 min at 56 °C, and DNA was purified using the spin column protocol for cultured cells according to the manufacturer's instructions contained in the DNeasy Blood and Tissue kit (Qiagen, Valencia, CA, USA). DNA was eluted in 200 µl elution buffer. DNA content and purity of each sample was measured by UV spectrometry using a Biotek Multiplate Reader (Biotek, Winooski, VT, USA).

The BbRT2 qPCR assay for the specific detection of *Besnoitia* spp. DNA from ungulates (i.e., *B. besnoiti*, *B. tarandi, B. caprae*, and *B. bennetti*) was performed according to Frey et al. (2016). Herein the SYBR Green system was used. Briefly, each 20 µl reaction contained 10 µl of Power SYBR Green master mix® (Applied Biosystems, Foster City, CA, USA), 0.5 µl of primer Bb3 (5′-CAA CAA GAG CAT CGC CTT C-3′; 20 µM), 0.5 µl of primer Bb 6 (5′-ATT AAC CAA TCC GTG ATA GCA G-3′; 20 µM), and 4 µl water. The qPCRs were run on a 7500 Fast Real-Time PCR System® (Applied Biosystems, Thermo Fisher Scientific, USA). 20–100 ng of DNA in a volume of 5 µl was added to each reaction. The DNA positive control was extracted from *B. besnoiti* tachyzoites cultured *in vitro*. The product of the DNA extraction process using water instead of cells was used as a negative control. In each qPCR, 10-fold serial dilutions of genomic DNA corresponding to 0.1–100,000 Bb-Spain1 tachyzoites were included. The cycling conditions were 10 min at 95 °C followed by 40 cycles of 95 °C for 15 s and 60 °C for 1 min. Fluorescence emission was measured during the 60 °C step. A dissociation stage was added at the end of each run, and the melting curves were analysed. BbRT2-PCR was run in duplicate for each sample. The threshold cycle values (Ct-values) obtained for positive samples in the BbRT2-PCR were also expressed as tachyzoites per reaction using the standard curve included in each run.

2.7. Studies on the impact of decoquinate and diclazuril on the viability of *B. besnoiti* tachyzoites

Tachyzoites from Bb-Spain 1 strain were grown as previously stated and decoquinate or diclazuril were added just prior to infection at the previously established IC_{99} concentrations. Drugs were kept for 6, 24 or 48 h. Drug containing medium was discarded and fresh culture medium was added. Cell cultures were evaluated until 10 days post treatment (dpt), by daily visual inspection by light microscopy. Samples were collected at 1, 3 and 5 dpt for subsequent qPCR analysis. IFAT at 8 and 10 dpt were also performed to assess whether any tachyzoites were able to re-infect host cells (Winzer et al., 2015). Each assay was done in triplicate and at least three independent experiments were carried out.

2.8. Transmission electron microscopy

HFF cell cultures were maintained in T25 tissue culture flasks and were infected with 10^7 Bb-Spain1 tachyzoites (parasite: host cell ratio of 10:1). After allowing the tachyzoites to invade the host cells for 3 h, monolayers were washed three times with PBS and treated with decoquinate or diclazuril at the previously stated EC_{99} for each compound. Control flasks without drugs contained the corresponding amounts of either DMSO or NaOH/MetOH. Samples were processed for TEM analysis at different time points of treatment (1, 3 and 6 days) as described elsewhere (Müller et al., 2017).

2.9. Data analyses

Values for cytotoxicity of compounds are depicted in percentage (%) in relation to the respective vehicle, and were statistically evaluated using Student's-*t*- test using the raw data from the specific ODs calculated as explained in section 2.2.

To determine the percentage of inhibition of parasite growth, the invasion rates (IRs) were calculated by counting all the events per well, IRs were then related to the respective negative vehicle control to determine the relative growth (RG) of the parasite for each drug experiment. The percentage of inhibition was determined as follows:

$$\% \text{ RG} = (\text{IR drug} / \text{IR vehicle}) \times 100$$

$$\% \text{ Inhibition} = 100 - \%\text{RG}$$

For IC_{50} and IC_{99} calculations based on qPCR, the amount of DNA was quantified by spectrophotometry in each sample and adjusted. The RG in each drug concentration was determined relative to the vehicle control using the tachyzoite yield per ng of DNA. IC_{50} and IC_{99} values were calculated using the ED50 plus sheet for Microsoft Excel after a logarithmic transformation of the data.

Kruskal-Wallis test was performed to compare the efficacy of the 6 compounds against *B. besnoiti* in the drug screening, and a two-way ANOVA test followed by a Tukey post-test for multiple comparisons was employed to compare the different treatment durations. All statistical analyses were performed using the software GraphPad Prism 6.0 (GraphPad Software, San Diego, CA, USA).

3. Results

3.1. Cytotoxicity assessments in uninfected MARC-145 cells

At the concentrations used here, none of the compounds exhibited significant cytotoxicity when compared to their respective vehicle controls (DMSO or NaOH/MetOH) as shown by the results from the XTT assay ($p > 0.05$; *t*-test). Percentages of cytotoxicity of the screened compounds compared to the solvent-treated negative control wells were as follows: diclazuril: 3.2%; toltrazuril: 6%; imidocarb: 2.8%; decoquinate: 2.3%; sulfadiazine: 3%; trimethoprim: 3.1%; sulfadiazine + trimethoprim: 3.3%. Moreover, upon inspection by light microscopy, no alterations in the Marc-145 cells morphology were detected.

3.2. Primary drug assessments using immunofluorescence-based read-outs

The criteria employed to select the drug concentrations for the screening assays were the absence of cytotoxicity and the presence of an effect on *B. besnoiti* growth on the preliminary assays performed. In those assays, we found that toltrazuril was cytotoxic in the *in vitro* system employed for concentrations higher than 30 μM (50, 70 and 100 μM), leading to the detachment of the hosts cells (Table 1). In the initial drug treatments, initiated either during invasion (0 hpi) or at 6 hpi, decoquinate, diclazuril and toltrazuril were the most efficient drugs and inhibited parasite growth by more than 65% (Table 2). In general, the efficacy was higher when compounds were administered concomitantly to infection at 0 h pi, except for imidocarb (Kruskal-Wallis test, $p < 0.05$).

Parasitic growth was markedly inhibited in wells treated with decoquinate, diclazuril and toltrazuril, since only PVs but not lysis plaques were found. In contrast, in cultures treated with the other compounds and in the control wells, distinct lysis plaques were clearly visible, indicating that parasites had completed the lytic cycle. Decoquinate and diclazuril were the most efficacious, and were consequently selected for further studies (Table 2). In contrast, sulfadiazine administered at 6 h pi was the least effective compound (19% of parasite growth inhibition, Kruskall-Wallis test, $p < 0.01$) (Table 2). When sulfadiazine or trimethoprim, alone or in combination, were kept in the cultures for up to 6 days, tachyzoites were still able to replicate and proliferate, as seen by the presence of confluent lysis plaques visualized by immunofluorescence, similar to non-treated control wells (data not shown).

As previously published for the isolate employed, 80% of the invasion events observed at 72 hpi consisted of lysis plaques in non-treated wells (Frey et al., 2016).

3.3. IC_{50} & IC_{99} determinations of decoquinate and diclazuril

For both, decoquinate and diclazuril, dose-dependent effects on parasite proliferation were observed (Kruskal Wallis, $p < 0.01$). When administered concomitantly to infection at concentrations higher than 0.24 nM, exposure of infected cells to decoquinate led to a significant reduction in parasite growth, and the IC_{50} was calculated to be 10 nM. For diclazuril, higher concentrations were needed: parasitic growth was markedly inhibited when the compound was administered at concentrations higher than 40 nM, and the IC_{50} was 135 nM (Fig.1). To reach 99% inhibition, 120 nM of decoquinate and 29.5 μM of diclazuril were required.

3.4. Decoquinate and diclazuril treatments do not act parasiticidal

Infected cultures were treated with decoquinate or diclazuril with concentrations corresponding to the IC_{99} for a maximum period of 48 h, and drugs were removed and the culture continued, this in order to study the long term effects of the treatments. Parasitic growth was hardly detected until 3 dpt, regardless which drug was used and how long the treatment had lasted. Subsequently, higher inhibition rates corresponded to longer treatments of up to 48 h (Fig. 2). Statistically significant differences between treated wells and their corresponding control wells were observed at 3 and at 5 dpt for any treatment durations ($p < 0.001$, Two-Way ANOVA), with a lowest parasitic load in treated wells. Differences were also found among the different treatment durations (6, 24 and 48 h) for both drugs at 5 dpt and higher inhibition rates corresponded to longer treatments ($p < 0.001$, Two-Way ANOVA) (Fig. 2).

Short treatments for 6 and 24 h with decoquinate were more effective since the tachyzoite yields obtained at 3 dpt in decoquinate treated wells were significantly lower than in diclazuril-treated wells. Further analysis by IF at 8 and 10 dpt showed that tachyzoites remained viable and were able to re-infect host cells even after treatments of 48 h with decoquinate. Lysis plaques were present at 10 dpt in all treated wells. However, in wells treated with diclazuril for 48 h, the parasitic load was clearly diminished both at 3 d pt and at 5 dpt, showing the lowest tachyzoite yield. Shorter treatments for up to 24 h were less effective and failed to inhibit parasite proliferation completely. This finding was also corroborated upon inspection in the light microscope and by IF, since lysis plaques were absent in wells treated with diclazuril for 48 h at 7 or 10 d pt, but present in wells treated for 6 h or 24 h at both post-infection time points (7 and 10 d pt) (data not shown).

Table 2
Percentage of inhibition of parasite growth in the drug screening when compounds were administered at 0 h post infection (hpi) or at 6 hpi.

	Drugs	Decoquinate	Diclazuril	Toltrazuril	Imidocarb	Sulfadiazine	Trimethoprim	SDZ + TM
Time of administration	**0 hpi**	90	83.2	82.3	40	43	41	50
	6 hpi	74	72,8	69	36	19	31	35

3.5. Ultrastructural alterations in B. besnoiti tachyzoites induced by decoquinate and diclazuril treatments

B besnoiti tachyzoites obtained from drug solvent treated controls exhibited the hallmarks of apicomplexan parasites and closely resembled *T. gondii* and *N. caninum* tachyzoites. A negative control culture treated with decoquinate solvent (NaOH/MetOH) is shown in Fig. 3A. Tachyzoites were located within a PV that was filled with a granular matrix, and the apically located secretory organelles such as micronemes, rhoptries, as well as dense granules were evident. In addition, tachyzoites contained one mitochondrium, of which only segments were seen on a given section plane, filled with a rather electron dense membranous matrix composed of cristae (Fig. 3A). Similar findings were obtained when tachyzoites were treated with diclazuril solvent (DMSO) as shown by Jiménez-Meléndez et al. (2017).

In *B. besnoiti* tachyzoites exposed to decoquinate for 24 h, no obvious structural alterations were evident, and they closely resembled their non-treated counterparts (data not shown). However, after 3 days of treatment, most notably the mitochondria were severely altered and lacking an electron dense matrix, and they were seemingly replaced by largely empty vacuoles that filled considerable space in the cytoplasm of these parasites (Fig. 3B–D). In addition, the cytoplasm was often filled with loose membrane residues. However, despite these alterations, after three days the parasites still retained their shape, were still within a parasitophorous vacuole (PV), but also already obviously dead parasites with distorted disorganized cytoplasm and vacuolization could be seen. After 6 days, mitochondria, were not discernible anymore, the cytoplasmic organization was completely lost and lipid droplets were formed (Fig. 3E). Also, there were parasites which were not enclosed by a parasitophorous vacuole membrane anymore. Only few seemingly still viable parasites could be found in these specimens.

In cultures treated with diclazuril, (Fig. 4), small but distinct effects related to the drug action appeared already at 24 h of treatment (Fig. 4A–C). These included a widening between the nuclear membrane and the cytoplasm of the tachyzoites. At 3 d of treatment, dividing parasites were visible that were still attached to the residual body (Fig. 4D. In addition, the gap around the nuclear periphery was more evident, and a compartmentalization took place, with occasional structures resembling amylopectin granules forming within the

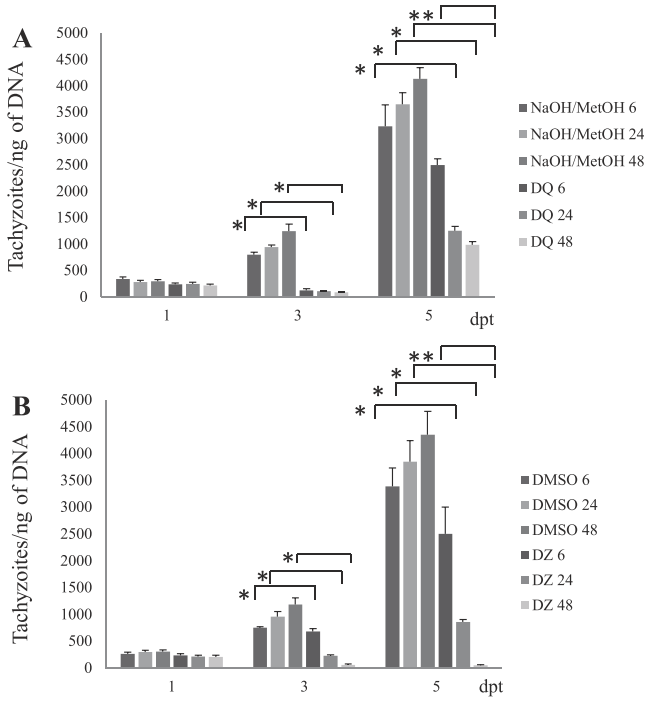

Fig. 2. Tachyzoite yield expressed as tachyzoites per ng of DNA from *Besnoitia besnoiti* infected MARC-145 cells, which were treated with decoquinate (A) or diclazuril (B) for 6, 24 or 48 h, and further cultured without drugs. Samples were collected at 1, 3 & 5 days post treatment (dpt).
*Statistically significant differences between treated wells and their corresponding control wells at 3 and at 5 dpt for any treatment durations ($p < 0.001$).
**Statistically significant differences among the different treatment durations (6, 24 and 48 h) for both drugs at 5 dpt ($p < 0.001$).

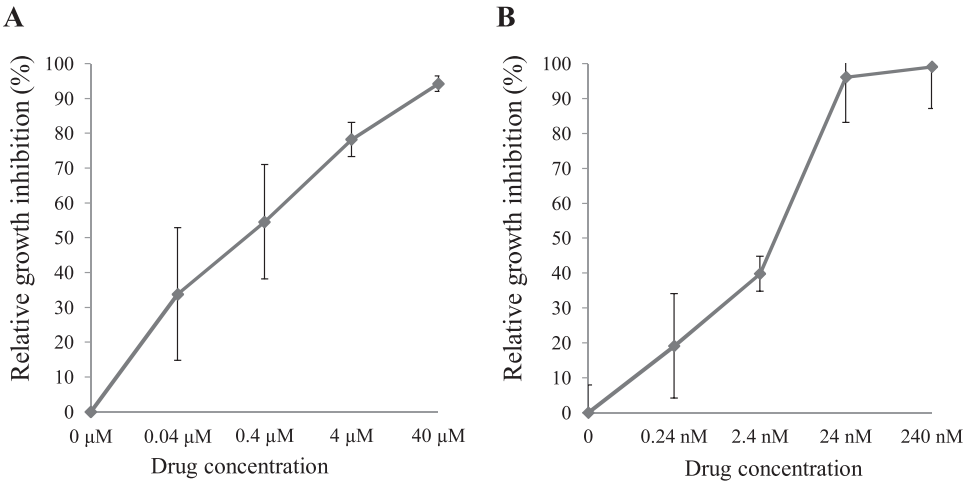

Fig. 1. Relative inhibition of *Besnoitia besnoiti* tachyzoite proliferation (in & with respect to the vehicle negative control). Decoquinate (A) and diclazuril (B) were administered at 0 h pi. Tachyzoite proliferation was assessed by qPCR.

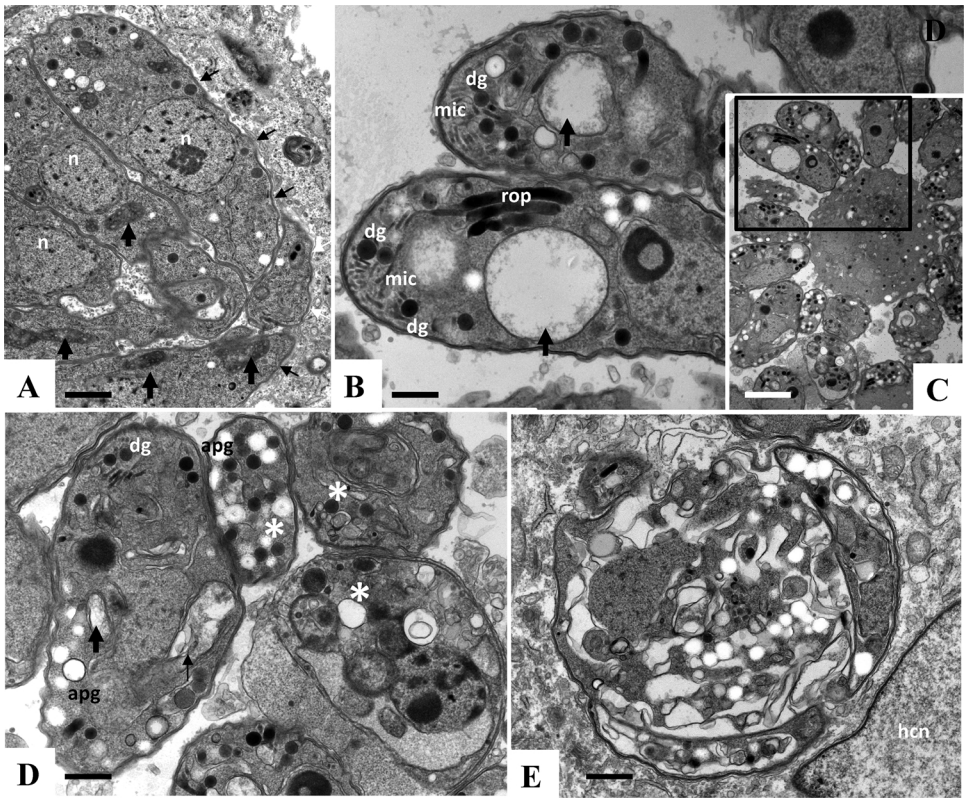

Fig. 3. Representative TEM images of *Besnoitia besnoiti* tachyzoites cultured in human foreskin fibroblast cells. (A) Tachyzoites treated with NaOH/MetOH, situated within a vacuole and surrounded by a parasitophorous vacuole membrane (depicted with thin blackarrows). Note the individual nuclei and the mitochondria with an electron dense matrix (thick vertical black arrows). (B–D) Tachyzoites treated with decoquinate during 3 days, residues of mitochondria lacking any discernible matriy are indicated by black arrows. (C) is a lower magnification overview of (B), the boxed area is enlarged in (B). Note the presence of dramatically altered parasites in (D), marked with an asterisk (*). (E) Image of a *B. besnoiti* tachyzoite exposed to decoquinate during 6 days, with severely altered structural features. Rop = rhoptries, dg = dense granules, mic = micronemes, n = nucleus, apg = amylopectin granules. Scale bars: A = 0.5 µm; B = 0.3 µm; C = 1 µm; D = 0.3 µm; E = 0.4 µm.

cytoplasm of tachyzoites, Vacuolization also took place in the residual body. However, the PV and its membrane were still evident in many cases and the mitochondria appeared still largely unaffected. After 6 day, amylopectin granules became more prominent, and complexes with largely disorganized cytoplasm were formed (Fig. 4E).

4. Discussion

In this study, the safety and efficacy of a wide panel of commercially available compounds in Europe, namely toltrazuril, diclazuril, imidocarb, decoquinate, sulfadiazine and trimethoprim (alone or in combination with sulfadiazine) were assessed for activity against *B. besnoiti* tachyzoites for the first time. Some of these drugs had previously shown efficacy against other apicomplexan parasites and, in particular, against Toxoplasmatinae parasites, both *in vitro* (Hemphill et al., 2016) and *in vivo* (Sánchez-Sánchez et al., 2018). Two compounds, namely decoquinate and diclazuril, both commercialised for the treatment of various infections in cattle, inhibited *B. besnoiti* invasion and proliferation, with IC_{50} values in the nanomolar range.

Inhibition rates of decoquinate and diclazuril in terms of inhibition of parasite invasion and proliferation reached values higher or close to 90%. The *in vitro* model in Marc-145 cells employed in the present work was previously used to assess the activities of a panel of bumped kinase inhibitors (BKIs), which target calcium dependent protein kinase 1, and similar results were obtained (Jiménez-Meléndez et al., 2017). In contrast, the low efficacy of imidocarb, sulfadiazine and trimethoprim (alone or in combination with sulfadiazine) against *B. besnoiti* infection may lead us to rule out their potential therapeutic activity. In addition, toltrazuril assays were aborted due to cytotoxicity exerted in the host cells.

Our results showed that decoquinate represents a safe compound in our *in vitro* model. Under the experimental settings employed, the efficacy of this compound was higher when it was administered at the time of infection, but it also interfered with proliferation in invaded tachyzoites. This result contrasts to previous studies carried out with *N. caninum* tachyzoites, where decoquinate showed a minimum effect against extracellular zoites. It is known that decoquinate affects electron transport in mitochondria so that a feasible explanation to the findings observed in *N. caninum* could be the presence of less active mitochondria in extracellular tachyzoites (Lindsay et al., 1997). However, in *T. gondii* tachyzoites, it was demonstrated that decoquinate is able to affect oxygen consumption of extracellular tachyzoites (Pfefferkorn et al., 1993). Accordingly, decoquinate might be more active against those parasites with higher capacity to survive extracellularly, as shown for *B. besnoiti* (Frey et al., 2016). Interestingly, we obtained IC_{50} values in the low nanomolar range (10 nM), in agreement with previous studies that have shown decoquinate to have *in vitro* activity against *T. gondii* tachyzoites with IC_{50} of 0.005 µg/ml (12 nM) (Ricketts and Pfefferkorn, 1993). Although decoquinate is specifically designed to treat gastrointestinal coccidiosis in several species (e.g cattle, small ruminants and poultry) at concentrations around 0.5 mg/kg bw, it is well absorbed and reaches maximum plasma concentrations of 2 µM in milking cows (Leonardo et al., 2009). These concentrations are much higher than the IC_{50} and IC_{99} found *in vitro*. Accordingly, it may represent a valuable therapeutic tool to control acute clinical cases of bovine besnoitiosis as food additive at the recommended posology. Since remaining viable tachyzoites were able to resume proliferation once the treatment with the IC_{99} was suspended, a parasitostatic effect is suggested for this compound for at least 48 h of treatment, as it has been described for hydroxiquinoxalines (Mehlhorn, 2008). This parasitostatic effect could be desirable since treated *Besnoitia* tachyzoites might be an antigenic stimulus and would allow the development of a strong immune response against the parasite, potentially preventing reinfection after recovering from the acute stage, as it has been postulated for other compounds such as BKIs (Winzer et al., 2015). In *N. caninum*, the parasiticidal or parasitostatic effect of this drug depends on the concentration employed. A coccidiocidal effect of decoquinate was observed against intracellular tachyzoites when administered at concentrations higher than 0.01 µg/mL (24 nM (Lindsay et al., 1997).

Electron microscopy showed that the mitochondrium is, as

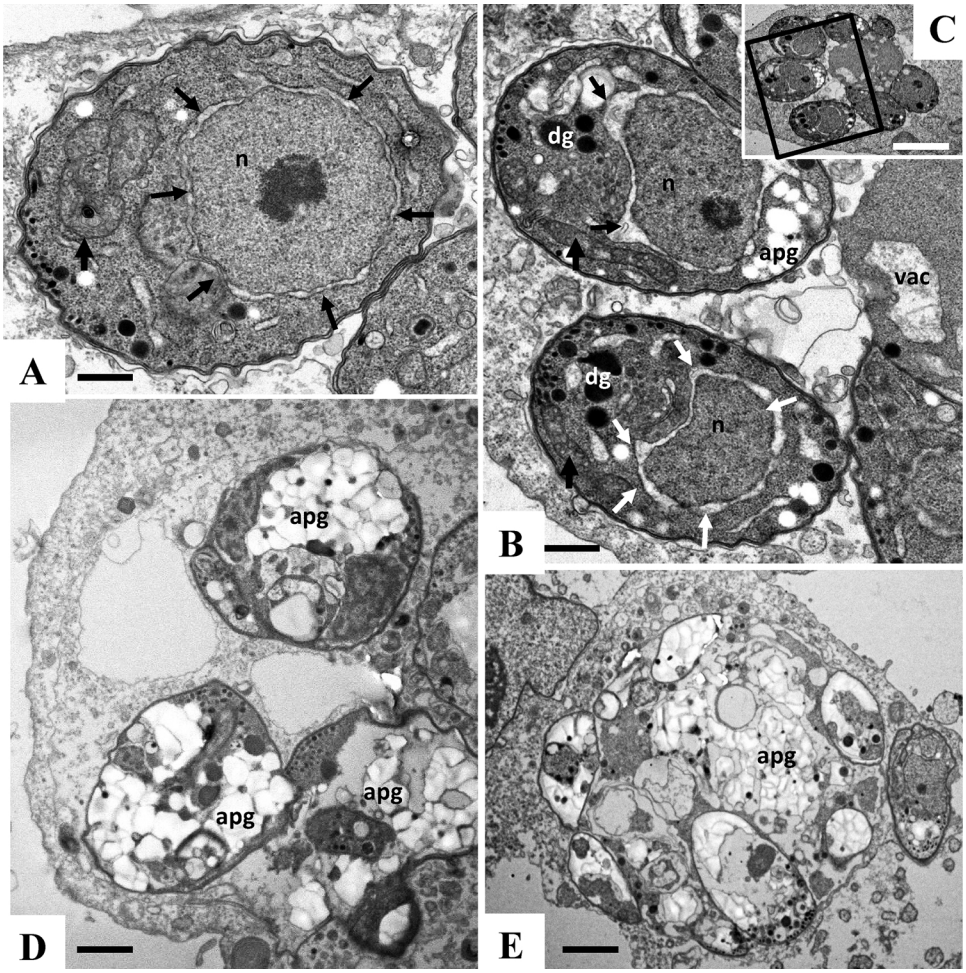

Fig. 4. Representative TEM images of *Besnoitia besnoiti* tachyzoites in human foreskin fibroblast cell cultures exposed to diclazuril after 24 h of treatments (A–C, the boxed area in C is shown at larger magnification in B); 3 days of treatment (D); 6 days of treatment (E). The vertical arrows indicate mitochondria, arrows surrounding nuclei (n) point towards the separation of the nuclear membrane and the cytoplasm. dg = dense granules, apg = amylopectin granules, vac shows a vacuole in the residual body. Scale bars: A = 0.3 μm; B = 0.4 μm; C = 1.1 μm; D = 0.4 μm; E = 0.8 μm.

expected, the main site of action of decoquinate. However, after 6 days of treatment, mitochondrial impairment led to more dramatic alterations and a general breakdown of the structural organization of the parasite, with deposits of amylopectin granules in the cytoplasm, all of this leading to a general loss of viability for most tachyzoites. This finding may indicate a transitional stage from tachyzoite to bradyzoite, as it has been described previously for tachyzoites from the RH strain of *T. gondii* treated with decoquinate (Lindsay et al., 1998). Thus, decoquinate could represent a stressing agent to induce the differentiation from *Besnoitia* tachyzoites to bradyzoites *in vitro*.

Regarding triazinone-derivative coccidiocidals, our results showed that diclazuril is safe at the highest concentrations used in the *in vitro* model employed and effective against *B. besnoiti* tachyzoites, inhibiting both parasite invasion and proliferation. Those results are in agreement with previous *in vitro* studies with *T. gondii* (Lindsay and Blagburn, 1994) and *N. caninum* tachyzoites (Lindsay et al., 1994). Indeed diclazuril inhibited *T. gondii* tachyzoite proliferation by 97% at a concentration of 0.005 μg/mL (12.2 nM). Remarkably, higher concentrations are needed for *B. besnoiti* since the IC_{50} was 135 nM. In cattle, this compound is marketed against coccidiosis and the bioavailability of the compound is low, reaching maximum plasmatic concentrations of 95.8 nM (European Medicines Agency (EMEA), 2004). Thus, further pharmacokinetics studies assessing different dosages and possibly also formulations are needed to obtain a higher bioavailability of the compound in cattle. We also showed that treatments with the IC_{99} for at least 48 h are able to exert a parasiticidal effect on *B. besnoiti* tachyzoites, since lysis plaques were absent and the parasitic load was clearly diminished in those wells. These results are in agreement with TEM results, since after 6 days of treatment almost no viable parasites were present and a clear effect on the cytokinesis of daughter zoites, with the formation of multinucleated complexes was visualized. These findings are similar to those previously described for *T. gondii* tachyzoites treated with diclazuril, since an effect on endodiogeny together with the presence of multi-nucleated complexes were observed when treated at a concentration of 1 μg/mL (Lindsay et al., 1995). Opposite to our results, ultra-structural effects of diclazuril were not noted until 2 days after treatment whilst in *B. besnoiti* we have observed that the first effects appeared after 24 h of treatment. *In vivo* experiments regarding mice infected with tachyzoites from the RH strain of *T. gondii* have shown that this compound is able to prevent death of up to 80–100% of the infected animals after oral administration at 1.0 or 10 mg/kg on 1 day prior to infection and then daily for 10 days (Lindsay and Blagburn, 1994).

The other triazinone derivative studied in the present work, toltrazuril, was cytotoxic at concentrations up to 30 μM. This safety concern has been also described in other cell lines, such as HFF cells, showing that concentrations of 10 μg/mL (23 μM) diminished cell viability up to 92% (Qian et al., 2015). However, at the highest concentration employed here, a remarkable effect on parasitic growth inhibition was noted. This compound might present good activity against

B. besnoiti tachyzoites considering that it is well-absorbed in cattle and is rapidly metabolized to ponazuril (toltrazuril-sulfone), which is the major metabolite (Stock et al., 2017). Moreover, toltrazuril has been effective against *N. caninum* both in *in vitro* (Darius et al., 2004) and *in vivo* studies (Syed-Hussain et al., 2015; Strohbusch et al., 2009). Thus, before ruling out its therapeutic potential for bovine besnoitiosis, further experiments should be performed.

Imidocarb dipropionate was discarded in our experimental settings, since it failed to exert more than 30% parasite invasion and proliferation inhibition. No previous *in vitro* treatments with this compound against *T. gondii* or *N. caninum* have been reported. When similar series of compounds, diminazene aceturate and pentamidines were studied they were not effective against *B. besnoiti* in an *in vitro* model using epithelial-like Vero cells (Shkap et al., 1987). The lack of efficacy may be due to a less relevant myo-inositol synthesis pathway in *B. besnoiti*. Up to date, only glycolysis and glutamine byosinthesis metabolic routes have been reported in *B. besnoiti*-infected cells (Taubert et al., 2016). Besides, it has been postulated that the activity of imidocarb may resemble that of the trypanocidal and babesicidal berenil (diminazene aceturate) (Mehlhorn., 2008b), binding to DNA in the minor groove of the kinetoplast, which is absent in apicomplexan parasites.

Finally, regarding DHFR and DHFS inhibitors, alone or in combination, sulfadiazine failed to inhibit parasite growth by more than 50%, even when it was co-administered with trimethoprim at the time point of infection. Previous *in vitro* studies regarding Toxoplasmatinae parasites have shown variable results, since sulfadiazine is highly efficacious against *T. gondii* with IC_{50} in the range of 2.5 µg/mL (Sánchez-Sánchez et al., 2018) whilst little activity was exerted against *N. caninum* at concentrations up to 100 µg/ml (400 µM) and longer treatments were needed (Lindsay et al., 1994). This finding agrees with our results where low parasitic growth inhibition was observed when treatments lasted for 3 or 6 days. Besides, previous studies carried out in *Besnoitia* have also reported variable results. Sulfadiazine lacked efficacy upon *B. besnoiti* infection in gerbils (Shkap et al., 1987), whereas in other *Besnoitia* species, such as *B. darlingi,* treatment with sulfadiazine was able to diminish parasitic growth *in vitro* at concentrations higher than 4 µM in a 8 day-assay (50% growth inhibition) (Elsheikha and Mansfield, 2004). *In vivo* information regarding sulfonamide therapy in bovine besnoitiosis indicate that they are commonly used under field conditions to diminish the severity of clinical signs, but they usually fail to cure the infected cattle and recurrences are not rare, even if treatment is administered when clinical signs first appear (Jacquiet et al., 2010). The lack of efficacy of sulphadiazine observed *in vitro* may explain this *in vivo* variability. Trimethoprim also failed to exert a potent inhibition *in vitro*. However, a strong inhibition of *T. gondii* growth has been observed with an IC_{50} of 2.3 µg/ml, with striking morphological changes of the parasites (Sánchez-Sánchez et al., 2018). In addition, trimethoprim is also effective against *N. caninum* tachyzoites at 10 µg/ml (Lindsay et al., 1994).

In summary, the present study demonstrates proof of concept for the efficacy of decoquinate and diclazuril against *B. besnoiti in vitro,* and further assessments of safety and efficacy of both drugs should be performed in the target species. Concentrations of diclazuril needed to clear the parasite *in vitro* are higher than the ones reported in the literature for this compound. Thus, prior to attempt *in vivo* treatments, further studies regarding pharmacokinetic parameters, employing other administration routes or posologies, are needed in order to achieve higher bioavailability and raise maximum plasmatic concentrations. An ideal drug against *B. besnoiti* should allow the generation of a strong humoral immune response to avoid re-infections and preventing that new entries in the herd (specifically breeding bulls) get infected. Regarding this issue, the parasitostatic effect exerted by both compounds could favor the development of a humoral immune response.

Acknowledgements

This work was financially supported through research projects from the Spanish Ministry of Economy and Competitiveness (Ref. AGL2013-04442), Community of Madrid (Ref. S2013/ABI-2906, PLATESA-CM), and by the Swiss National Science Foundation (grant No. 310030_165782). Alejandro Jiménez-Meléndez was supported by a grant from the Spanish Ministry of Education, Culture and Sports (grant nº FPU13/05481) and Laura Rico SanRomán was financially supported by SALUVET INNOVA S.L. We also would like to acknowledge members from SALUVET research group for their support.

References

Álvarez-García, G., 2016. From the mainland to Ireland - bovine besnoitiosis and its spread in Europe. Vet. Rec. 178, 605–607.
Basso, W., Schares, G., Gollnick, N.S., Rutten, M., Deplazes, P., 2011. Exploring the life cycle of *Besnoitia besnoiti* - experimental infection of putative definitive and intermediate host species. Vet. Parasitol. 178, 223–234.
Bessoff, K., Spangenberg, T., Foderaro, J.E., Jumani, R.S., Ward, G.E., Huston, C.D., 2014. Identification of *Cryptosporidium parvum* active chemical series by repurposing the open access malaria box. Antimicrob. Agents Chemother. 58, 2731–2739.
Cortes, H.C., Mueller, N., Esposito, M., Leitao, A., Naguleswaran, A., Hemphill, A., 2007. *In vitro* efficacy of nitro- and bromo-thiazolyl-salicylamide compounds (thiazolides) against *Besnoitia besnoiti* infection in Vero cells. Parasitology 134, 975–985.
Cortes, H.C., Muller, N., Boykin, D., Stephens, C.E., Hemphill, A., 2011. *In vitro* effects of arylimidamides against *Besnoitia besnoiti* infection in Vero cells. Parasitology 138, 583–592.
Darius, A.K., Mehlhorn, H., Heydorn, A.O., 2004. Effects of toltrazuril and ponazuril on the fine structure and multiplication of tachyzoites of the NC-1 strain of *Neospora caninum* (a synonym of *Hammondia heydorni*) in cell cultures. Parasitol. Res. 92, 453–458.
Daugschies, A., Najdrowski, M., 2005. Eimeriosis in cattle: current understanding. J. Vet. Med. B Infect. Dis. Vet. Public Health 52, 417–427.
Dittmar, A.J., Drozda, A.A., Blader, I.J., 2016. Drug repurposing screening identifies novel compounds that effectively inhibit *Toxoplasma gondii* growth. mSphere 1, e00042–15.
Elsheikha, H.M., Mansfield, L.S., 2004. Determination of the activity of sulfadiazine against *Besnoitia darlingi* tachyzoites in cultured cells. Parasitol. Res. 93, 423–426.
European Food Safety Authority, 2010. Scientific Statement on Bovine Besnoitiosis. Available from. http://www.efsa.europa.eu.
European Medicines Agency (EMEA), 2004. Diclazuril (Extension to All Ruminants and Porcine Species): Summary Report (2) - Committee for Veterinary Medicinal Products. Avalaible online 29th May 2018 from. . http://www.ema.europa.eu/ema/index.jsp?curl=pages/includes/document/document_detail.jsp?webContentId=WC500013730&mid=WC0b01ac058008d7ad.
Fernández-García, A., Risco-Castillo, V., Pedraza-Díaz, S., Aguado-Martínez, A., Álvarez-García, G., Gómez-Bautista, M., Collantes-Fernández, E., Ortega-Mora, L.M., 2009. First isolation of *Besnoitia besnoiti* from a chronically infected cow in Spain. J. Parasitol. 95, 474–476.
Frey, C.F., Regidor-Cerrillo, J., Marreros, N., García-Lunar, P., Gutiérrez-Expósito, D., Schares, G., Dubey, J.P., Gentile, A., Jacquiet, P., Shkap, V., Cortes, H., Ortega-Mora, L.M., Álvarez-García, G., 2016. *Besnoitia besnoiti* lytic cycle *in vitro* and differences in invasion and intracellular proliferation among isolates. Parasit. Vectors 9, 115.
Fry, M., Williams, R.B., 1984. Effects of decoquinate and clopidol on electron transport in mitochondria of *Eimeria tenella* (apicomplexa: Coccidia). Biochem. Pharmacol. 33, 229–240.
Gutiérrez-Expósito, D., Ortega-Mora, L.M., Marco, I., Boadella, M., Gortazar, C., San Miguel-Ayanz, J.M., García-Lunar, P., Lavin, S., Álvarez-García, G., 2013. First serosurvey of*Besnoitia* spp. infection in wild european ruminants in Spain. Vet. Parasitol. 197, 557–564.
Gutiérrez-Expósito, D., Ferre, I., Ortega-Mora, L.M., Álvarez-García, G., 2017. Advances in the diagnosis of bovine besnoitiosis: Current options and applications for control. Int. J. Parasitol. 47, 737–751.
Hemphill, A., Aguado-Martínez, A., Müller, J., 2016. Approaches for the vaccination and treatment of *Neospora caninum* infections in mice and ruminants models. Parasitology 143, 245–259.
Hines, S.A., Ramsay, J.D., Kappmeyer, L.S., Lau, A.O.T., Ojo, K.K., Van Voorhis, W.C., Knowles, D.P., Mealey, R.H., 2015. *Theileria equi* isolates vary in susceptibility to imidocarb dipropionate but demonstrate uniform *in vitro* susceptibility to a bumped kinase inhibitor. Parasites Vectors 8, 33.
Hoffmann, B., Depner, K., Schirrmeier, H., Beer, M., 2006. A universal heterologous internal control system for duplex real-time RT-PCR assays used in a detection system for pestiviruses. J. Virol. Methods 136, 200–209.
Jacquiet, P., Liénard, E., Franc, M., 2010. Bovine besnoitiosis: Epidemiological and clinical aspects. Vet. Parasitol. 174, 30–36.
Jiménez-Meléndez, A., Ojo, K.K., Wallace, A.M., Smith, T.R., Hemphill, A., Balmer, V., Regidor-Cerrillo, J., Ortega-Mora, L.M., Hehl, A.B., Fan, E., Maly, D.J., Van Voorhis, W.C., Alvarez-Garcia, G., 2017. *In vitro* efficacy of bumped kinase inhibitors against *Besnoitia besnoiti* tachyzoites. Int. J. Parasitol. 47, 811–821.
Kaartinen, L., Löhönen, K., Wiese, B., Franklin, A., Pyörälä, S., 1999. Pharmacokinetics of

sulphadiazine-trimethoprim in lactating dairy cows. Acta Vet. Scand. 40, 271–278.
Leonardo, Q., Rosiles, R., Bautista, J., González-Monsón, N., Sumano, H., 2009. Oral pharmacokinetics and milk residues of decoquinate in milking cows. J. Vet. Pharmacol. Ther. 32, 403–406.
Lindsay, D.S., Blagburn, B.L., 1994. Activity of diclazuril against *Toxoplasma gondii* in cultured cells and mice. Am. J. Vet. Res. 55, 530–533.
Lindsay, D.S., Rippey, N.S., Cole, R.A., Parsons, L.C., Dubey, J.P., Tidwell, R.R., Blagburn, B.L., 1994. Examination of the activities of 43 chemotherapeutic agents against *Neospora caninum* tachyzoites in cultured cells. Am. J. Vet. Res. 55, 976–981.
Lindsay, D.S., Rippey, N.S., Toivio-Kinnucan, M.A., Blagburn, B.L., 1995. Ultrastructural effects of diclazuril against *Toxoplasma gondii* and investigation of a diclazuril-resistant mutant. J. Parasitol. 81, 459–466.
Lindsay, D.S., Butler, J.M., Blagburn, B.L., 1997. Efficacy of decoquinate against N*eospora caninum* tachyzoites in cell cultures. Vet. Parasitol. 68, 35–40.
Lindsay, D., Toivio-Kinnucan, M., Blagburn, B., 1998. Decoquinate induces tissue cyst formation by the RH strain of Toxoplasma gondii. Vet. Parasitol. 77, 75–81.
Lindsay, D.S., Nazir, M.M., Maqbool, A., Ellison, S.P., Strobl, J.S., 2013. Efficacy of decoquinate against *Sarcocystis neurona* in cell cultures. Vet. Parasitol. 196, 21–23.
Mehlhorn, H. (Ed.), 2008. Encyclopedia of Parasitology: A-M 280 Springer, Germany 381 pp.
Muller, J., Aguado-Martinez, A., Manser, V., Balmer, V., Winzer, P., Ritler, D., Hostettler, I., Arranz-Solis, D., Ortega-Mora, L., Hemphill, A., 2015. Buparvaquone is active against *Neospora caninum in vitro* and in experimentally infected mice. Int. J. Parasitol. Drugs Drug Resist. 5, 16–25.
Müller, J., Aguado-Martínez, A., Balmer, V., Maly, D.J., Fan, E., Ortega-Mora, L., Ojo, K.K., Van Voorhis, W.C., Hemphill, A., 2017. Two novel calcium-dependent kinase 1-inhibitors interfere with vertical transmission in mice infected with *Neospora caninum* tachyzoites. Antimicrob. Agents Chemother. AAC 61 02324-16.
Pfefferkorn, E., Borotz, S.E., Nothnagel, R.F., 1993. Mutants of *Toxoplasma gondii* resistant to atovaquone (566C80) or decoquinate. J. Parasitol. 559–564.
Pols, J.W., 1960. Studies on bovine besnoitiosis with special reference to the aetiology. Onderstepoort J. Vet. Res. 28, 265–356.
Qian, W., Wang, H., Shan, D., Li, B., Liu, J., Liu, Q., 2015. Activity of several kinds of drugs against Neospora caninum. Parasitol. Int. 64, 597–602.
Ricketts, A.P., Pfefferkorn, E.R., 1993. *Toxoplasma gondii*: Susceptibility and development of resistance to anticoccidial drugs*in vitro*. Antimicrob. Agents Chemother. 37, 2358–2363.
Ryan, E.G., Lee, A., Carty, C., O'Shaughnessy, J., Kelly, P., Cassidy, J.P., Sheehan, M., Johnson, A., de Waal, T., 2016. Bovine besnoitiosis (*Besnoitia besnoiti*) in an irish dairy herd. Vet. Rec. 178, 608.
Sánchez-Sánchez, R., Vázquez, P., Ferre, I., Ortega-Mora, L.M., 2018. Treatment of toxoplasmosis and neosporosis in farm ruminants: state of knowledge and future trends. Curr. Top. Med. Chem Accepted.
Shkap, V., De Waal, D.T., Potgieter, F.T., 1985. Chemotherapy of experimental *Besnoitia besnoiti* infection in rabbits. Onderstepoort J. Vet. Res. 52, 289.
Shkap, V., Pipano, E., Ungar-Waron, H., 1987. *Besnoitia besnoiti*: Chemotherapeutic trials *in vivo*and in vitro. Rev. Elev. Med. Vet. Pays Trop. 40, 259–264.
Stock, M., Elazab, S., Hsu, W., 2017. Review of triazine antiprotozoal drugs used in veterinary medicine. J. Vet. Pharmacol. Ther. 41, 184–194.
Strohbusch, M., Muller, N., Hemphill, A., Krebber, R., Greif, G., Gottstein, B., 2009. Toltrazuril treatment of congenitally acquired *Neospora caninum* infection in newborn mice. Parasitol. Res. 104, 1335–1343.
Syed-Hussain, S.S., Howe, L., Pomroy, W.E., West, D.M., Hardcastle, M., Williamson, N.B., 2015. Study on the use of toltrazuril to eliminate *Neospora caninum* in congenitally infected lambs born from experimentally infected ewes. Vet. Parasitol. 210, 141–144.
Taubert, A., Hermosilla, C., Silva, L., Wieck, A., Failing, K., Mazurek, S., 2016. Metabolic signatures of *Besnoitia besnoiti*-infected endothelial host cells and blockage of key metabolic pathways indicate high glycolytic and glutaminolytic needs of the parasite. Parasitol. Res. 115, 2023–2034.
Torre, D., Casari, S., Speranza, F., Donisi, A., Gregis, G., Poggio, A., Ranieri, S., Orani, A., Angarano, G., Chiodo, F., Fiori, G., Carosi, G., 1998. Randomized trial of trimethoprim-sulfamethoxazole versus pyrimethamine-sulfadiazine for therapy of toxoplasmic encephalitis in patients with AIDS. italian collaborative study group. Antimicrob. Agents Chemother. 42, 1346–1349.
Van Voorhis, W.C., Doggett, J.S., Parsons, M., Hulverson, M.A., Choi, R., Arnold, S., Riggs, M.W., Hemphill, A., Howe, D.K., Mealey, R.H., 2017. Extended-spectrum antiprotozoal bumped kinase inhibitors: a review. Exp. Parasitol. 180, 71–83.
Vial, H.J., Gorenflot, A., 2006. Chemotherapy against babesiosis. Vet. Parasitol. 138, 147–160.
Williams, R., 2006. Tracing the emergence of drug-resistance in coccidia (*Eimeria* spp.) of commercial broiler flocks medicated with decoquinate for the first time in the United Kingdom. Vet. Parasitol. 135, 1–14.
Winzer, P., Muller, J., Aguado-Martinez, A., Rahman, M., Balmer, V., Manser, V., Ortega-Mora, L.M., Ojo, K.K., Fan, E., Maly, D.J., Van Voorhis, W.C., Hemphill, A., 2015. *In vitro* and *in vivo* effects of the bumped kinase inhibitor 1294 in the related cyst-forming apicomplexans *Toxoplasma gondii* and *Neospora caninum*. Antimicrob. Agents Chemother. 59, 6361–6374.